Malat1 is a Sex-Specific Determinant of Th Cell Differentiation

Mags Gwynne

Doctor of Philosophy (PhD)

The University of Hull and the University of York

Hull-York Medical School

September 2025

Abstract

Understanding cell intrinsic mediators of sexual dimorphism in lymphocytes is critical to addressing differences in incidence and severity of immunopathologies between females and males. Here, we demonstrate that the nuclear speckle-associated lincRNA *Malat1*, one of the most highly abundant transcripts in mammalian cells, exerts a sex-specific function in Th2 differentiation by controlling early differentiation and endpoint cytokine expression in female cells. *Malat1* deficiency impairs *in vitro* Th2 differentiation only in female mice, characterised by transcriptome-wide suppression of differentiation associated gene expression and cytokine expression, with particularly strong effects on IL10. Using an *in vivo* model of lung inflammation, we validated the sex-specific effects of *Malat1* loss, demonstrating altered Th2 differentiation in both the lung and spleen for only female mice. Mechanistically, naïve T helper cells from *Malat1*$^{-/-}$ female mice demonstrate impaired early differentiation in the gene expression programme, along with upregulation of an interferon stimulated gene module associated with naïve CD4^{+} T cells. This is followed by suppression of the IL2 receptor, which in turn inhibits IL2 mediated differentiation. Male Th2 differentiation was less sensitive to effects of *Malat1* loss due to stronger early activation, higher constitutive interferon responsive gene expression, and lower sensitivity to exogenous levels of IL2. *Malat1* deficiency during early Th2 differentiation suppressed differentiation-associated changes in nuclear architecture in a sex-specific manner, with effects on nuclear speckle biogenesis, Xi complex localisation, and H3K27me3 deposition. Overall, this suggests that, despite neither being X/Y linked nor sex hormone responsive, *Malat1* is a critical sex-specific regulator of Th cell differentiation, with profound implications in our understanding of how non-coding RNA drives immune sexual dimorphism.

Contents

Abstract 1

Acknowledgements 18

Author's declaration 20

1. Introduction 21

1.1. Non-coding RNA 22

1.1.1 Coding and non-coding RNA 22

1.1.2 Long non-coding RNAs 23

1.1.3 Long non-coding RNA function 26

1.2. The immune system and $CD4^+$ T helper cells 31

1.2.1 Innate and adaptive immunity 31

1.2.2 Cells of the immune system 32

1.2.3 $CD4^+$ T helper cells 35

1.2.4 CD4+ T cell activation 36

1.2.5 CD4+ T cell differentiation 37

1.2.6 Th cells and the Response to IL2 40

1.2.7 Th cell Production of IL10 44

1.2.8 LncRNAs in $CD4^+$ T cells 45

1.3. Type 2 Immunity 49

1.3.1 Type 1, 2 and 3 immune responses 49

1.3.2 Helminth infection 50

1.3.3 Type 2 immunopathologies 51

1.3.4 Murine models of type 2 inflammation....54

1.4. The role of lincRNA *Malat1* in $CD4^+$ T cells....57

1.4.1 Overview of *Malat1*....57

1.4.2 *Malat1* in nuclear speckles and splicing....59

1.4.3 The role of *Malat1* in gene expression regulation....60

1.4.4 *Malat1* in $CD4^+$ T cells....63

1.5. Sexual dimorphism in the immune system....65

1.5.1 Sexual dimorphism in Immunity....65

1.5.2 Sex hormones....66

1.5.3 X chromosome inactivation and Xi escape....68

1.5.4 Sexual dimorphism in $CD4^+$ T cells....71

1.6. Hypothesis and aims....73

1.6.1 Hypothesis....73

1.6.2 Aims....73

2. Materials and Methods....74

2.1 Animals and cell lines....75

2.1.1 Mice....75

2.1.2 Cell lines....76

2.1.3 Cell counts....76

2.1.4 Freezing cells....76

2.1.5 Thawing cells....77

2.2 *In vitro* Th2 differentiation....78

2.2.1 Naïve $CD4^+$ T cell isolation 78

2.2.2 *In vitro* Th2 differentiation 79

2.2.3 Anti-CD3 titration assays 82

2.2.4 rIL2 titration assays 84

2.2.5 IFNβ treatment 86

2.2.6 GapmeR treatments 86

2.2.7 Blocking antibody treatment 88

2.2.8 Human Th cell differentiation 88

2.2.9 Recombinant cytokine storage 88

2.3 Quantitative real-time PCR 89

2.3.1 RNA extraction 89

2.3.2 cDNA synthesis 90

2.3.3 qRTPCR 90

2.3.4 qRTPCR primer validation 91

2.4 Flow cytometry 95

2.4.1 Buffers and antibodies 95

2.4.2 Surface staining 98

2.4.3 Intracellular cytokine staining 98

2.4.4 Transcription factor staining 99

2.4.5 Data acquisition and gating strategy 99

2.5 Western blotting 102

2.5.1 Buffers 102

2.5.2 Cell lysate generation 102

2.5.3 Bicinchoninic assay (BCA) 102

2.5.4 PAGE gel protein separation 103

2.5.5 Transfer to membranes 103

2.5.6 Membrane imaging 104

2.6 Microscopy and cell imaging 105

2.6.1 Buffers and antibodies 105

2.6.2 Cytospinning cells 107

2.6.3 Cell fixing and permeabilization 107

2.6.4 Staining protocol 107

2.6.5 Image acquisition and analysis 108

2.7 *In vivo* mouse models 111

2.7.1 *S. mansoni* egg injection 111

2.7.2 Tissue preparation 113

2.7.3 Flow cytometry analysis 113

2.8 RNA sequencing 116

2.8.1 Sample validation and preparation 116

2.8.2 Library preparation and long-read ONT sequencing 116

2.8.3 RNAseq data analysis 117

2.9 Data availability 117

2.10 Diagrams and schematics 118

2.11 Statistical analyses 118

3. *Malat1* Regulates End-Stage Th2 Differentiation in a Sex-Specific Manner 120

3.1 Introduction 121

3.1.1 Statement 121

3.1.2 *Malat1* and IL10 expression 121

3.1.3 Chapter hypothesis and aims 123

3.2 Results 124

3.2.1 *Malat1* loss downregulates Th2 cell cytokine expression in females 124

3.2.2 The effect of *Malat1* loss on cytokine expression is enhanced upon inhibiting IL10 signalling 129

3.2.3 *Malat1* causes a transcriptional blunting of the Th2 differentiation programme. 131

3.2.4 The sex-specific effect of *Malat1* loss is activation strength independent 139

3.2.5 *Malat1* loss is required during early Th2 differentiation 142

3.2.6 Differentiating Th2 cells respond to IL2 in a sex-specific manner *in vitro* 146

3.2.7 *Malat1* loss suppresses expression of the IL2 receptor 148

3.2.8 Male differentiating Th2 cells are less sensitive to IL2 treatment 151

3.2.9 *Malat1* loss causes a sex-specific decrease in IL10 expression in an *in vivo* model of lung inflammation 153

3.3 Discussion 173

4. *Malat1* Regulates the Th2 Gene Programme During Early Differentiation via Repression of a Type-I Interferon Inducible Geneset 183

4.1 Introduction 184

4.1.1 Statement 184

4.1.2 $CD4^+$ T cell activation (markers CD69, IL2Rα, CD44) 184

4.1.3 Type-I IFN signalling in $CD4^+$ T cells 185

4.1.4 Nanopore long-read RNA sequencing 187

4.1.5 Hypothesis and aims 189

4.2 Results 190

4.2.1 *Malat1* loss causes a sex-specific increase in the early activation marker CD69 190

4.2.2 Time course experiments of Th2 differentiation identifies disruption of key Th2 genes at 2 days post-activation 194

4.2.3 GATA3 expression is disrupted following *Malat1* loss in both females and males 198

4.2.4 *Malat1* loss suppresses the downregulation of a type-I interferon responsive geneset 200

4.2.5 DEGs resulting from *Malat1* loss are enriched on chromosome 19 212

4.2.6 Upregulation of the type-I IFN responsive geneset can be validated by qRTPCR 215

4.2.7 Type-I Interferon treatment disrupts Th2 differentiation in a sex-specific manner 218

4.2.8 *Malat1* loss does not affect type-I IFN expression during Th2 differentiation 224

4.2.9 *Malat1* loss has limited effects on alternative splicing 227

4.3 Discussion 230

5. *Malat1* Regulates Nuclear Speckle Function and X Chromosome Inactivation During Th Cell Differentiation 239

5.1 Introduction 240

5.1.1 Nuclear speckle function and their role in Th cell differentiation 240

5.1.2 X chromosome inactivation during Th cell differentiation 241

5.1. Chapter aims 243

5.2 Results 244

5.2.1 Nuclear speckles increase in both number and size during T cell differentiation 244

5.2.2 *Malat1* loss disrupts nuclear speckle numbers during differentiation 247

5.2.3 *Malat1* loss affects SR protein phosphorylation during differentiation 252

5.2.4 *Malat1* loss affects Xi complex formation in females 255

5.2.5 *Malat1* affects X-linked gene expression during Th2 differentiation 262

5.2.6 Inhibition of Xi formation may disrupt Th2 differentiation 266

5.2.7 *Malat1* loss affects H3K27me3 deposition during early Th cell differentiation .. 268

5.2.7 *MALAT1* is downregulated during human T cell *in vitro* differentiation 272

5.2.8 Nuclear speckles increase in numbers and size during human *in vitro* differentiation 277

5.3 Discussion 280

6 Concluding Discussion 287

6.1 *Malat1* in Th cell differentiation 288

6.2 Nuclear architecture in T cell/lymphocyte development 292

6.3 Nuclear speckle function in T cells 297

6.4 Future work 301

6.4.1 Investigating *Malat1* interacting RBPs during Th cell differentiation 301

6.4.2 Further characterising the effects of *Malat1* loss in type 2 immunity and Th cell differentiation 302

6.4.3 Investigating sex-differences in Th cell differentiation 303

6.5 Concluding remarks 304

Acronyms 305

References 309

Appendix 377

Table of figures

Figure 1.1 Schematic representation of the categorisation of lncRNAs by genomic location and orientation 25

Figure 1.2 Schematic representation of the categorisation of lncRNAs by cis or trans function 27

Figure 1.3 Schematic representation of cellular lncRNA functions 30

Figure 1.4 Schematic of the CD4+ T cell differentiation pathway 38

Figure 1.5 Schematic of the response to exogenous IL2 during $CD4^+$ T cell differentiation 43

Figure 1.6 Structure and function of lincRNA Malat1 62

Figure 1.7 Schematic of X chromosome inactivation and Xist function 69

Figure 2.1 Schematic for the Th2 differentiation assay 81

Figure 2.2 Schematic of the Th2 differentiation assay with anti-CD3 titration 83

Figure 2.3 Th2 differentiation assay with rIL2 titration 85

Figure 2.4 Gating strategy for determining $CD4^+$ $TCR\beta^+$ cells via flow cytometry 101

Figure 2.5 Schematic of image analysis performed using ImageJ 110

Figure 2.6 Overview of S. mansoni egg injection experiment 112

Figure 2.7 Gating strategy used for flow cytometry analysis of the *S. mansoni* egg injection model. 114

Figure 3.1 *In vitro* Th cell differentiation schematic 125

Figure 3.2 LacZ *Malat1* knock-out model and *Malat1* knock-out efficiency 126

Figure 3.3 *Malat1* loss suppresses cytokine expression during Th2 differentiation 128

Figure 3.4 IL10R blockade enhances the effects of *Malat1* loss on pro-inflammatory cytokine expression 130

Figure 3.5 Similar numbers of DEGs occur during Th2 differentiation following *Malat1* loss 133
Figure 3.6 *Malat1* loss in females blunts transcriptional changes that occur during Th2 differentiation 136
Figure 3.7 GSEA analysis of DEGs during Th2 differentiation in *WT* and *Malat1*$^{-/-}$ females 137
Figure 3.8 GSEA analysis of DEGs during Th2 differentiation in *WT* and *Malat1*$^{-/-}$ males 138
Figure 3.9 *Malat1* loss affects IL10 expression in females independent of differentiation strength 140
Figure 3.10 IL10R blockade during weaker T cell activation does not enhance the effects of *Malat1* loss on IL4 and IL13 141
Figure 3.11 The effect of *Malat1* depletion on IL10 expression occurs during early stages of differentiation 144
Figure 3.12 Anti-IL10R blockade enhances the effects of *Malat1* GapmeR treatment on IL4 but not IL13 145
Figure 3.13 Cytokine expression in response to rIL2 is disrupted following *Malat1* loss in females 147
Figure 3.14 *Malat1* loss disrupts expression of the IL2R 149
Figure 3.15 *Il2ra* and *Il2rg* transcript levels are not disrupted at day 4 following *Malat1* loss 150
Figure 3.16 Male CD4^{+} T cells display lower sensitivity to exogenous IL2 levels 152
Figure 3.17 *S. mansoni* egg-injection triggered immune responses in both the lung and the spleen 154
Figure 3.18 Egg-injection generates robust eosinophil responses in the lung 157

Figure 3.19 Egg-injection triggers monocyte alternative activation 158
Figure 3.20 B cells are unaffected by *Malat1* loss 159
Figure 3.21 *Malat1* loss may impact $CD4^+$ T cell activation in the lung 160
Figure 3.22 *In vivo* loss of *Malat1* disrupts IL10 expression in females 162
Figure 3.23 *Malat1* loss does not affect IL4 or IFNγ expression *in vivo* 164
Figure 3.24 *Malat1* loss disrupts $IL10^+$ $IL4^+$ and $IL10^+$ $IFN\gamma^+$ cells *in vivo* 166
Figure 3.25 The repeated egg-injection experiment generated a weaker type 2 response 168
Figure 3.26 *Malat1* loss impacts the expression of the IL2R *in vivo* 170
Figure 3.27 *Malat1* loss impacts the expression of the IL2R in activated $CD4^+$ T cells *in vivo* 171
Figure 3.28 *Malat1* loss in females affects IL10 expression in $IL4^+$ $IL13^+$ Th2 cells 172
Figure 4.1 *Malat1* loss affects CD69 expression and kinetics 192
Figure 4.2 *Malat1* loss affects CD69 mRNA levels 193
Figure 4.3 *Malat1* loss impairs *Il2* receptor and cytokine transcript expression during early differentiation 195
Figure 4.4 *Malat1* loss impairs *Gata3* transcript expression during early differentiation 196
Figure 4.5 *Malat1* loss impairs early Th2 differentiation at day 2 of *in vitro* differentiation 197
Figure 4.6 *Malat1* loss suppresses GATA3 expression at day 2 of *in vitro* Th2 differentiation 199
Figure 4.7 Long-read sequencing sample validation 201
Figure 4.8 *Malat1* loss triggers upregulation of a large number of transcripts during early differentiation 203

Figure 4.9 *Malat1* loss upregulates expression of IFN stimulated genes 205
Figure 4.10 STRING analysis identifies a cluster of type-I ISGs and transcription factors resulting from *Malat1* loss 207
Figure 4.11 *Malat1* loss suppresses downregulation of an IFN-stimulated geneset 211
Figure 4.12 DEGs resultant from *Malat1* loss are enriched on chromosome 19 213
Figure 4.13 qRTPCR validates downregulation of IFN-stimulated genes during Th2 differentiation 216
Figure 4.14 qRTPCR confirms significant upregulation of IFN-stimulated genes at day 2 of differentiation from *Malat1* loss 217
Figure 4.15 IFNβ treatment upregulates IFN-stimulated genes in females 220
Figure 4.16 IFNβ treatment phenocopies the sex-specific impacts of *Malat1* loss on IL10 expression 221
Figure 4.17 IL10R blockade reveals IFNβ treatment suppresses IL10 and IL13 expression in females 222
Figure 4.18 IFNβ treatment impacts IL2R levels in females 223
Figure 4.19 *Malat1* loss during Th2 differentiation does not affect type-I IFN cytokine or receptor transcript expression 225
Figure 4.20 *Malat1* loss during Th2 differentiation does not affect IFNAR1 expression 226
Figure 4.21 *Malat1* loss has modest effects on differential transcript usage 229
Figure 5.1 Nuclear speckle numbers and size increase during Th differentiation 246
Figure 5.2 Nuclear speckle numbers and size increase during Th2 differentiation 248
Figure 5.3 Nuclear speckle numbers and size increase during Th2 differentiation 249
Figure 5.4 *Son* and *Srrm2* transcript levels are not significantly affected by *Malat1* loss 251

Figure 5.5 SR protein phosphorylation is disrupted following *Malat1* loss 254

Figure 5.6 Isolation of total $CD4^+$ T cells from human blood 255

Figure 5.7 Human Th0 cell cytokine expression following *in vitro* differentiation..... 255

Figure 5.8 *Malat1* levels decrease following human T cell activation 255

Figure 5.9 SON staining of human $CD4^+$ T cells..... 255

Figure 5.10 Speckle numbers and size increase during human $CD4^+$ T cell differentiation 255

Figure 5.6 CIZ1 localises to the X chromosome during $CD4^+$ T cell differentiation ... 257

Figure 5.7 *Malat1* loss affects Xi patch formation during differentiation 259

Figure 5.8 *Malat1* loss impacts CIZ1 intensity during T cell differentiation..... 261

Figure 5.9 *Malat1* loss affects expression of X-linked genes 264

Figure 5.10 *Ciz1* loss may disrupt $CD4^+$ T cell differentiation..... 267

Figure 5.11 *Malat1* loss impacts nuclear H3K27me3 intensity during differentiation. 269

Figure 5.12 *Malat1* loss does not change overall H3K27me3 levels..... 271

Figure 5.13 Isolation of total $CD4^+$ T cells from human blood 274

Figure 5.14 Human Th0 cell cytokine expression following *in vitro* differentiation.... 275

Figure 5.15 *Malat1* levels decrease following human T cell activation 276

Figure 5.16 SON staining of human $CD4^+$ T cells..... 278

Figure 5.17 Speckle numbers and size increase during human $CD4^+$ T cell differentiation 279

Supplementary Figure 1 Representative Isotype and FMO Control FACS Plots 378

Supplementary Figure 2 Representative Isotype and FMO Control FACS Plots 379

Supplementary Table 1. Significantly differentially expressed genes between *WT* and *Malat1*$^{-/-}$ female and males in naïve and Th2 cells 380

Supplementary Figure 3 *S. mansoni* egg-injection repeat responses in both the lung and the spleen.....381
Supplementary Figure 4 *S. mansoni* egg-injection repeat monocyte responses 382
Supplementary Figure 5 *S. mansoni* egg-injection repeat B cell responses.....383
Supplementary Figure 6 *S. mansoni* egg-injection repeat Neutrophil responses.....384
Supplementary Figure 7 *S. mansoni* egg-injection repeat T cell activation.....385
Supplementary Figure 8 *S. mansoni* egg-injection repeat lung T cell IL4, IL13 and IFNγ responses 386
Supplementary Figure 9 *S. mansoni* egg-injection repeat spleen T cell IL4, IL13 and IFNγ responses 387
Supplementary Figure 10 *S. mansoni* egg-injection repeat lung T cell double positive cytokine responses 388
Supplementary Figure 11 *S. mansoni* egg-injection repeat spleen T cell double positive responses 389
Supplementary Figure 12 *S. mansoni* egg-injection repeat lung T cell IL4 IL13 double positive responses.....390
Supplementary Figure 13 391
Representative 63x images from SON and DAPI staining naïve *WT* female $CD4^+$ T cells. Brightness and contrast were increased by 20%.....391
Supplementary Figure 14 392
Supplementary Figure 15 393
Supplementary Figure 16 394
Supplementary Figure 17 395
Supplementary Figure 18 396
Supplementary Figure 19 397

Supplementary Figure 20 398
Supplementary Figure 21 399
Supplementary Figure 22 400
Supplementary Figure 23 401
Supplementary Figure 24 402
Supplementary Figure 25 403
Supplementary Figure 26 404
Supplementary Figure 27 405
Supplementary Figure 28 406
Supplementary Figure 29 407
Supplementary Figure 30 408
Supplementary Figure 31 409
Supplementary Figure 32 410
Supplementary Figure 33 411
Supplementary Figure 34 412
Supplementary Figure 35 413
Supplementary Figure 36 414

Table of tables

Table 1.1 Examples of lincRNAs in Th cell differentiation....48

Table 2.1 GapmeR antisense oligonucleotide sequences....87

Table 2.2 Primer sequences used for qRTPCR....93

Table 2.3 Antibodies used in flow cytometry experiments....96

Table 2.4 Antibodies used for immunofluorescence staining....106

Table 2.5 Antibody panels used for flow cytometry analysis of the *S. mansoni* egg injection experiment....115

Table 3.1 Differentially expressed Th2 genes between *WT* and *Malat1*$^{-/-}$ female and males in Th2 cells....132

Table 3.2 Core Th2 genes are significantly upregulated during Th2 differentiation, and to a lesser degree in *Malat1*$^{-/-}$ females and males....134

Table 4.1 Differentially expressed genes (FDR<0.1) between WT and Malat1$^{-/-}$ naïve CD4+ T cells from Nanopore long-read RNA-seq....204

Table 4.2 Gene clusters and genes identified by K-means clustering among up-regulated DEGs in day 2 *Malat1*$^{-/-}$ cells....208

Table 4.3 Significantly enriched genes and corresponding chromosome bands in *Malat1*$^{-/-}$ DEGs at day 2 of differentiation....214

Table 4.4 Genes demonstrating DTU (FDR<0.05) between WT and Malat1$^{-/-}$ cells on day 2 of CD4+ T cell differentiation....228

Table 5.1 Table of X chromosome inactivation lncRNAs and *Xist* interacting RBPs between day 0 and day 2 of *in vitro* Th2 differentiation....265

Acknowledgements

Firstly, I would like to thank HYMS, the University of York, and the University of Hull, for funding and supporting my research. Next, I would like to thank my supervisors Professor Dimitris Lagos and Dr. Ioannis Kourtzelis, for their constant support and guidance throughout my PhD project, and for their help in developing my skills as a researcher. Thanks in particular to Dimitris for all his encouragement, mentorship, and music recommendations throughout the past four years. I would also like to thank my thesis advisory panel, Dr. Nathalie Signoret and Professor Dawn Coverley, for all the valuable insight into my project and pastoral support during the PhD.

Thanks to Dr. James Hewitson, Dr. Shinjini Chakraborty and Dr. Joanna Greenman, for the work on the *in vivo* models, for sharing your expert flow cytometry knowledge, and for keeping me sane during some extremely long days in the lab. Thanks to Professor Dawn Coverley, Dr. Justin Ainscough and Elena Guglielmi, for the help with the immunofluorescence staining and analysis. Thanks to Dr. Dave Boucher for the help with the human *in vivo* work, and for all the free snacks that have kept me going throughout the PhD. Thanks to the technology facility here at York, specifically Dr. Karen Hogg, Dr. Karen Hodgkinson, Dr. Graeme Park, Dr. Sally James and Dr. Fabiano Pais, for their training in flow cytometry and microscopy, and their help in performing RNA sequencing and analysis.

Next, I would like to thank all the past and present members of the Lagos lab, including Dr, Katie West, Dr. Josh Lee, Dr. Alina Capatina, Charlotte Booth, Ali Deghany, Lottie Plunkett-Jones, Molly Cartwright and Jack Greaves, for helping to make the work environment such a friendly and supportive place. I would particularly like to thank Dr. Katie West for her prior work on the project, and for the guidance and support during the

first two years of my PhD. Thanks to all the current and past members of Q2, who have all helped to create an incredibly welcoming environment.

Thanks to my friends in and around the country for all their support throughout this PhD, it means the world to me. I cannot name everyone here, but I would like to specifically thank Imran Khan, Isaac Reynolds, Jack Stenning, Sabina Musial, Charlie Head, Callum Room, Maud de Kinderen, Sophie James, M Holmes, Katie Lee, Alice Grahame, Charlie Mathews, Kieran Newton, Lucy Stevens, Helen Mylne, Lizzie Stevens and Siobhan Vickerstaff. I would also like to particularly thank Gemma Banister for being a huge support on Q2 through the ups and downs of my PhD. You are all wonderful friends, and I am so grateful for your support.

Thanks to my parents and my siblings for all their endless encouragement and love, and a massive thank you to my partner Eileen Xu. I could not have done this without you. I am so grateful for your love and all the effort put into keeping me sane during these past 4 years.

Finally, just in case she ever learns how to read, thanks to my dog Rosa for the support and company while writing.

Thank you all,

Mags

Author's declaration

I confirm that this work is original and that if any passages or diagrams have been copied from academic papers, books, the internet or any other sources these are clearly identified by the use of quotation marks, and the references is fully cited. I certify that, other than where indicated, this is my own work and does not breach the regulations of HYMS, the University of Hull or the University of York regarding plagiarism or academic conduct in examinations. I have read the HYMS Code of Practice on Academic Misconduct, and state that this piece of work is my own and does not contain any unacknowledged work from any other sources. This work has not previously been presented for an award at HYMS, the University of York, the University of Hull, or elsewhere. All collaborators on this project have been acknowledged, and any work that is not my own is included in the references section.

1. Introduction

1.1. Non-coding RNA

1.1.1 Coding and non-coding RNA

Despite initial characterisation as a messenger intermediate between DNA and proteins, more recent research has shown that RNA plays many significant roles outside of just coding for protein. Non-coding RNAs (ncRNA) in fact represent a significantly larger portion of the mammalian transcriptome than all protein coding transcripts. ENCODE (the ENCyclopedia Of DNA Elements) suggests that around 80% of the human genome is transcribed, which stands in stark contrast to the 2% of the genome known to code for proteins (Djebali et al., 2012). NcRNAs are involved in physiological and homeostatic critical cell functions, and also contribute to disease development and progression. However, despite their important roles, the majority of drug targets are of protein coding genes over ncRNAs. Increased research into the cellular roles of ncRNA could prove crucial in understanding how their dysregulation leads to disease and could help with identifying novel targets and treatments.

NcRNAs are split into two main categories based on size: small and long ncRNAs. Small ncRNAs are shorter than 200 nucleotides (nt) in length. Small ncRNA cellular functions include regulating gene expression via microRNAs (miRNAs), carrying amino acids via transfer RNAs (tRNAs), regulating splicing via small nuclear RNAs (snRNAs), and protecting the genome via PIWI-interacting RNAs (piRNAs) (L. L. Chen & Kim, 2024). Meanwhile, long ncRNAs (lncRNAs) are greater than 200 nt in length, and will be the focus of this thesis (Statello et al., 2020).

1.1.2 Long non-coding RNAs

LncRNAs are abundant in mammalian genomes. Initial estimates of the number of lncRNA genes suggested there were around 16,000 in the human genome (Ezkurdia et al., 2014), however more recent estimates from NONCODE (a knowledge database dedicated to non-coding RNAs) suggest that there are hundreds of thousands of lncRNA transcripts (Statello et al., 2020), greatly outnumbering protein coding genes. In terms of transcript generation, many lncRNAs are transcribed by RNA polymerase II, then capped and polyadenylated in a similar way to mRNAs, contain no open reading frame (Ruan et al., 2020). However, some lncRNAs lack a poly-A tail and can undergo alternative 3' end processing instead (Naganuma et al., 2012).

LncRNA expression is often tissue specific, and lncRNAs are not well conserved between species (Johnsson et al., 2014), displaying increased mutation rates compared to protein coding genes (Statello et al., 2020). However, this is not indicative of a lack of functionality. LncRNAs often interact with other proteins and RNAs only with a portion of their total length, meaning that only small parts of lncRNAs require conservation (Diederichs, 2014). As an additional explanation, LncRNAs are also seen to be more conserved in structure rather than sequence (Johnsson et al., 2014). LncRNAs with low sequence homology form extremely similar secondary and tertiary structures between species, which could suggest they are more tolerant of mutations than protein coding genes (Johnsson et al., 2014). Furthermore, lncRNAs with similar k-mer (sub-sequences of length k within the RNA transcript sequence) content have been shown to display functional conservation despite their lack of homology, supporting the structural conservation hypothesis. (Kirk et al., 2018). The transcriptional locus of lncRNAs can also be conserved between species, with this act of transcription keeping the surrounding

genomic area accessible and affecting the expression of neighbouring genes (Diederichs, 2014).

Categorisation of lncRNAs is done via a number of methods, as shown in *Figure 1.1*. LncRNAs that overlap with protein coding genes are further defined by their orientation or placement within the gene, as sense, anti-sense, bi-directional and intronic (Tsagakis et al., 2020). Sense lncRNAs are expressed from the sense strand of a known coding gene and can overlap with the coding sequence of genes, while anti-sense lncRNAs, are expressed from the anti-sense strand. Anti-sense genes are the second most common lncRNA, typically binding to the transcript they are complimentary to, or impacting their expression. Bi-directional lncRNAs are transcribed in the opposing direction to the coding gene, while intronic lncRNAs are transcribed from intronic regions. LncRNAs that do not overlap with protein coding genes are termed long intergenic ncRNAs (lincRNAs). LincRNAs do not overlap with any known protein coding genes and are typically located around 1kb away from neighbouring genes. LincRNAs are the most common lncRNAs, predicted to comprise around 50% of lncRNAs in humans (Eldash et al., 2023).

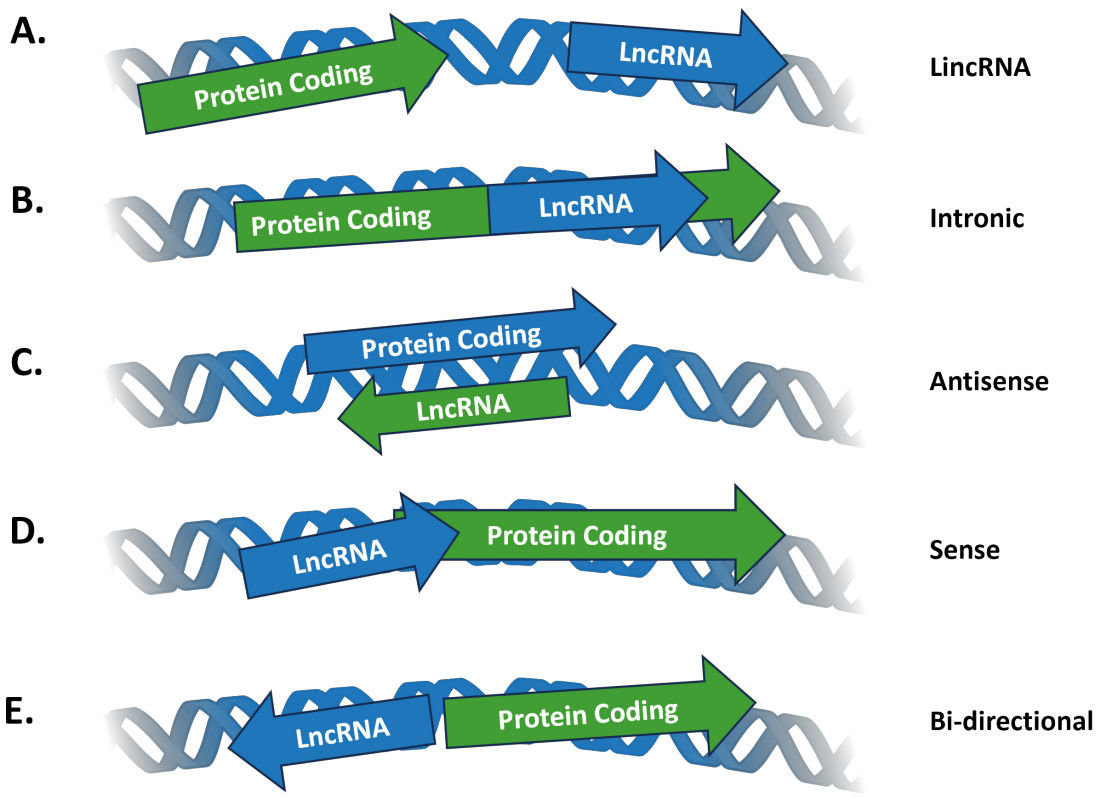

Figure 1.1 Schematic representation of the categorisation of lncRNAs by genomic location and orientation

A. long intergenic ncRNA. **B.** Intronic lncRNA. **C.** Antisense lncRNA. **D.** Sense RNA. **E.** Bi-directional lncRNA.

1.1.3 Long non-coding RNA function

LncRNAs can be further classified based on their functionality. Dependent on whether lncRNAs interact within or outside their genomic location, they are classified as cis- (*Figure 1.2 A*) or trans-acting (*Figure 1.2 B*) (Kopp & Mendell, 2018). However, these classes are not separate, as some lincRNAs can have functionality with both nearby and distant targets, and can therefore be classified as having both cis- and trans-acting effects (Statello et al., 2020).

LncRNA function can be mediated via RNA-RNA-binding protein (RBP) interaction, RNA-RNA interactions, and RNA-DNA interactions. LncRNAs have roles in many different cellular processes, from regulating gene expression, to chromosomal maintenance, and forming the core of cellular bodies. Examples of some of these roles are shown in *Figure 1.3*. LncRNAs involved in gene expression regulation can act on both on the pre- and post-transcriptional level. In terms of transcriptional regulation, many lncRNAs can affect chromatin structure and gene expression, via association with complexes such as polycomb repressive complex (PRC) 1 and 2 (Trotman et al., 2021). PRC2 tri-methylates histone H3 on lysine 27 (H3K27), causing heterochromatin formation and transcriptional repression. An example of this is lincRNA *HOTAIR*, which is able to negatively regulate HOX protein expression via this interaction, resulting in inhibitory H3K27 methylation and activation-associated H3K4 demethylation over HOX genes, to repress transcription (Raju et al., 2023). LincRNAs can more directly regulate transcription factor activity as well. LncRNA *PANDA* affects transcription factor NF-YA, inhibiting the expression of pro-apoptotic genes (Hung et al., 2011). LncRNAs also exert their function on gene expression via direct interactions with DNA. *TARID* generates an R loop at the promoter region of TCF21 to aid in recruitment of GADD45A, leading to promoter demethylation, and increased *TCF21* expression (Arab et al., 2019).

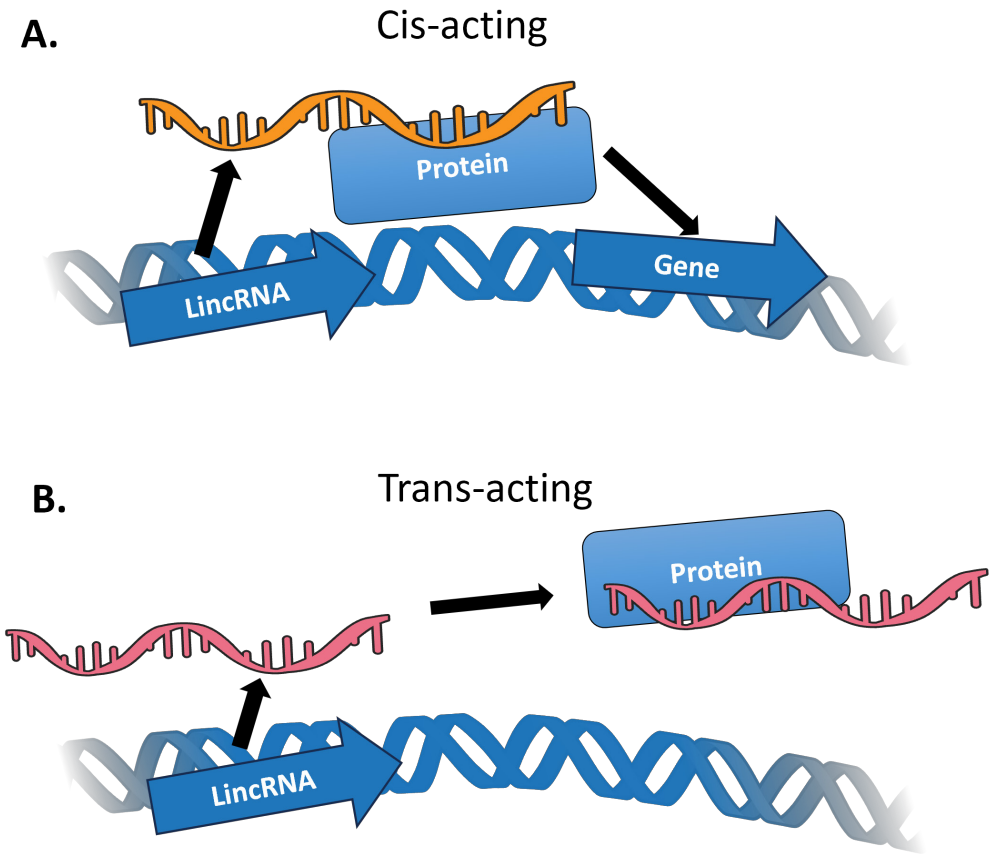

Figure 1.2 Schematic representation of the categorisation of lncRNAs by cis or trans function

A. Cis-acting lncRNAs act within their genomic loci, affecting the expression of nearby genes. **B.** Trans-acting lncRNA interact with proteins or RNA outside their genomic loci.

On the post-transcriptional level, lncRNAs are known to be able to affect transcript stability. LncRNA *LAST* promotes binding of CNDP to Cyclin D1 mRNA, helping to stabilise the transcript and enhance expression levels (Karakas & Ozpolat, 2021). LncRNAs can also directly affect translation, binding and interacting directly with the translation machinery. LncRNAs such as *GAS5* and *LINCRNA-p21* can bind directly to the translation initiation complex to inhibit the expression of key target genes C-MYC and JUNB respectively (G. Hu et al., 2014; Yoon et al., 2012).

LncRNAs often localise to specific sub-cellular areas as part of their function, with many enriched in the nucleus. LncRNA *TERC* localises to the telomere region and acts as a scaffold and template for the TERT complex to maintain telomere length (Cao et al., 2025). Another example of this is lincRNA *NEAT1*, a core component paraspeckles. Paraspeckles are nuclear non-membrane structures involved in responding to cell stress, sequestering RNA-binding proteins, enhancing miRNA processing, and regulating the DNA damage response (Hsu et al., 2025; Krol, 2017; Pisani & Baron, 2019; Taiana et al., 2020). *NEAT1* acts as a scaffold, allowing other core paraspeckle proteins NONO and SFPQ to oligomerise around it and recruit further paraspeckle components (Taiana et al., 2020).

LncRNAs are also known to localise to cytoplasmic areas as part of their function. *CEROX1* localises specifically to mitochondria, where it affects mRNA stability of proteins involved in oxidative phosphorylation (Sirey et al., 2019). Cytoplasmic lncRNAs can regulate gene expression via a process known as miRNA sponging. Here, lncRNAs sequester miRNAs by binding directly to them, and while this does not directly affect miRNA function it reduces the available free miRNAs in the cell. As an example of this, lncRNA *TRPM2* sponges *miR-612*, affecting the progression of gastric cancer (Xiao et al., 2020). Finally, lncRNAs may also be involved in cell-to-cell communication, with

enrichment in exosomes used for cell-to-cell signalling. A number of lncRNAs, such as *UCA1*, *ZFAS1* and *HOTTIP*, have been found in extracellular vesicles from many different cancers, suggesting that lncRNAs may play an important role here (Kołat et al., 2019). Overall, these examples collectively demonstrate the importance of lncRNAs in vital cellular processes.

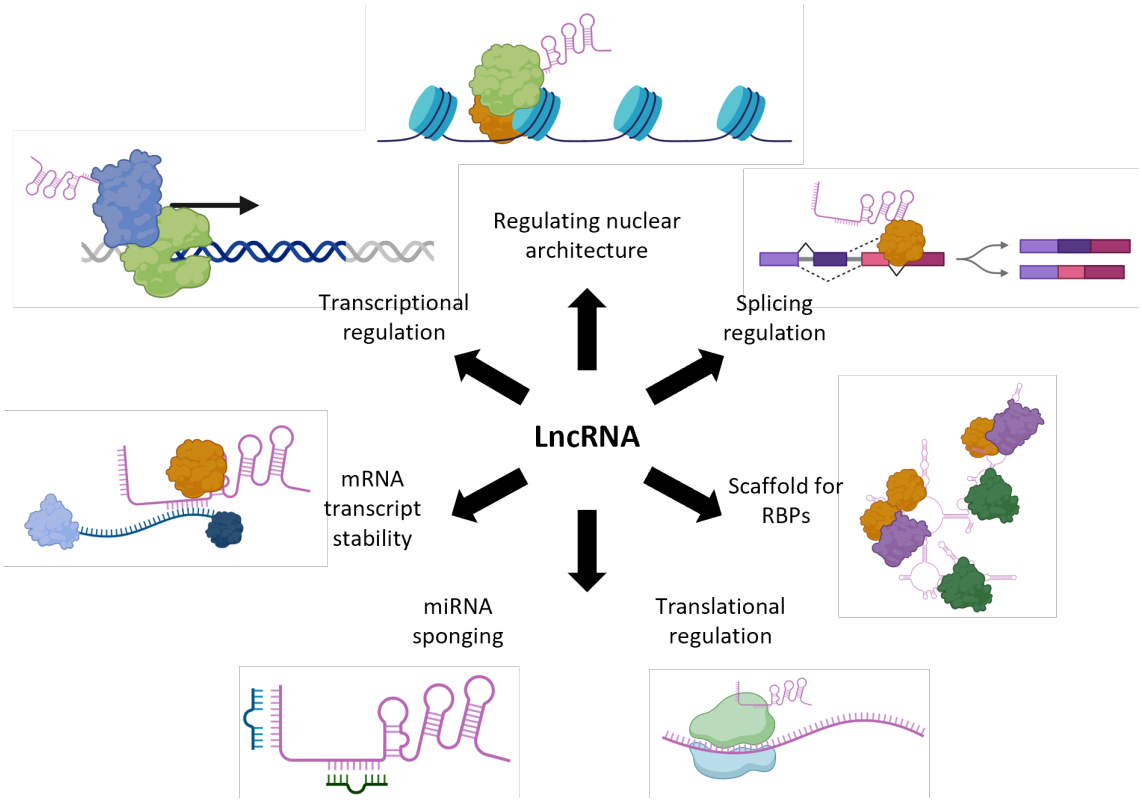

Figure 1.3 Schematic representation of cellular lncRNA functions

Schematic displaying a number of lncRNA functions, including transcriptional regulation, nuclear architecture regulation, splicing regulation, acting as a structural component, translational regulation, miRNA sponging, affecting transcript stability, and transcriptional regulation.

1.2. The immune system and $CD4^+$ T helper cells

1.2.1 Innate and adaptive immunity

In response to pathogenic infection, the immune system mounts response regulated at multiple levels, featuring an initial fast acting and non-specific response, termed the innate immune response, which then gives way to a more delayed but pathogen specific response, termed the adaptive response. The innate immune response acts as the first line of defence against invading pathogens, responding to common molecular features of pathogens not present in the host, and bridging the gap between the initial infection and the activation of the adaptive immune response (Marshall et al., 2018). Pathogen recognition leads to a signalling cascade causing the release of cytokines and chemokines, which help to recruit immune cells to the site of infection, and triggers the activation and maturation of certain immune cell types (Kubelkova & Macela, 2019). Innate immune cells can be descended from both myeloid and lymphoid lineages, producing a wide number of phenotypically distinct immune cell types involved in the innate immune system, although separate local tissue resident populations of these cells can also exist.

Adaptive immune cells are typically descended from the lymphoid lineage, including T and B lymphocytes providing a targeted response via antigen-specific receptors. These receptors are assembled by somatic recombination of DNA elements to allow for specific recognition of pathogens (Chaplin, 2010). A core feature of the adaptive response is the ability to create memory cells, which allow for a faster and more effective response against repeated infection.

1.2.2 Cells of the immune system

Cell types comprising the innate immune system include phagocytes (which phagocytose and break down pathogens), granulocytes (which release toxic granules to site of infection) and innate lymphoid cells (ILCs). Granulocytes are the most abundant type of white blood cell, characterised by their ability to release cytosolic granules containing antimicrobial agents to fight infection. Granulocytes are divided into four main subtypes: neutrophils, eosinophils, basophils, and mast cells. Of these, neutrophils are the most common, and the most abundant white blood cell in humans and mice (A. Lin & Loré, 2017). Neutrophils respond to infection via a number of different methods, including phagocytosis of pathogens, release of cytotoxic granules, and the formation of neutrophil extracellular traps (NETs) (Gierlikowska et al., 2021). Mast cells are long lived granulocytes located at mucosal surfaces. These cells contain granules rich in histamine, which are released to trigger local inflammation and immune activation. However, mast cells are also involved in tissue remodelling and wound healing (Krystel-Whittemore et al., 2016). Eosinophils, despite forming only 1-3% of total white blood cells, are critical in response to parasitic nematode infection and responses to allergens. Eosinophils regulate a type 2 immune response, releasing cytotoxic eosinophil granules, extracellular mitochondrial DNA traps, and regulating airway inflammation as part of their function (Kanda et al., 2021). Basophils are the least common type of granulocyte and also play a role in defence from parasitic infection (Min et al., 2012).

Monocytes are a branch of the innate immune system involved in phagocytosis, antigen presentation and cytokine expression. In mice, monocytes can be categorised into two main types based on the level of Ly6C expression. These are tissue resident monocytes, identified by low Ly6C expression, which patrol their respective tissues looking for signs of infection. $Ly6C^{lo}$ monocytes are involved in early inflammatory

responses to infection. Bone marrow derived monocytes, identified by high Ly6C expression, are produced in large quantities upon infection, and are capable of tissue infiltration. As well as being generally more pro-inflammatory, $Ly6C^{hi}$ monocytes are also capable of antigen presentation to T and B cells (Kratofil et al., 2017). In response to infection, monocytes can differentiate into macrophages, although some local macrophage populations produced from embryonic progenitor cells also exist (De Kleer et al., 2014; Yáñez, Bono and Goodridge, 2022). Macrophages can activate via two different pathways. M1 or classically activated macrophages are generally pro-inflammatory, produce cytokines such as interleukin (IL) 1β and tumour necrosis factor (TNF) α, and upregulate inducible nitric oxide synthase (iNOS) in response to infection. M2 or alternatively activated macrophages instead produce resistin-like alpha (RELMα) and arginase 1 (ARG1) as well as anti-inflammatory cytokines such as IL10. M2 macrophages are involved in infection clearing via phagocytosis, wound repair and tissue remodelling (Martinez & Gordon, 2014). These are not mutually exclusive responses, macrophage activation exists as a continuum between M1 and M2 responses.

Dendritic cells (DCs) are another branch of the innate immune system, and are the most efficient antigen presenting cells. DCs are characterised by their expression of CD11c and high levels of major histocompatibility complex (MHC) class II. DCs constantly patrol and sample local tissue environment for signs of infection. In response to antigen recognition, DCs migrate to lymph nodes and present these antigens to the adaptive immune system. Antigen recognition allows for guiding of the overall immune response by T helper (Th) cells, killing of infected cells by cytotoxic T cells, and the release of antigen-specific antibodies by B cells (Chaplin, 2010).

The final branch of the innate immune system are ILCs, which are split into NK cells, ILC1, ILC2 and ILC3 cells. NK cells patrol the blood and peripheral tissues, and

are known for their cytotoxic effects and cytokine release (Mace, 2022). NK cells express a number of receptors to recognise infected cells, including those for non-self ligands and stress markers, and in response release lytic granules to lyse infected cells (Mace, 2022). ILC1, 2 and 3 cells meanwhile are primarily involved in innate cytokine expression in response to initial infections (Tsymala & Kuchler, 2023). ILC1s respond to bacterial and viral infections, while ILC2s respond to parasitic infection in mucosal tissue, and ILC3s help to prevent infection in intestinal tissues (Tsymala & Kuchler, 2023).

Adaptive immune cells are derived from lymphoid lineages and differentiate into T and B cells via maturation in either the thymus (T cells) or bone marrow (B cells). B cells are identified by the expression of a B cell receptor, and produce antibodies which are involved in neutralising invading pathogen proteins, activating macrophages by binding to their Fc receptors, and activating the complement system (Hoffman et al., 2016).

T cells are identified by expression of their T cell receptor (TCR) and originate in the bone marrow but migrate to the thymus for maturation. Here, these precursor T cells undergo somatic recombination of their TCRs, specifically recombination of their variable (V), diversity (D), joining (J) and constant (C) elements of the TCR a and b chains. This leads to each T cell expressing a unique TCR that can recognise a unique antigen (Roth, 2014). T cells are split into two major branches, $CD4^+$ and $CD8^+$ T cells. $CD8^+$ T cells, also known as cytotoxic T cells, interact via their TCR with MHC class I molecules, which are present on all nucleated cells, and use this to identify and kill infected cells. In response to TCR stimulation $CD8^+$ T cells produce cytokines such as interferon gamma (IFNγ) and TNFα, and release cytotoxic granules containing perforin and granzymes to tear holes in infected cell membranes and cleave proteins inside. $CD8^+$ T cells are also able to activate apoptotic pathways via their expression of FASL,

which binds to FAS receptor on target cells to initiate a caspase signalling cascade (N. Zhang & Bevan, 2011). This thesis will primarily focus on $CD4^+$ cells, which are explored in the next section in greater detail.

1.2.3 $CD4^+$ T helper cells

$CD4^+$ T cells in response to infection can differentiate into T helper (Th) cells, which support the immune response via the generation of both cytokines and chemokines to help combat infection and recruit other immune cells (Luckheeram et al., 2012). Naïve $CD4^+$ T cells are generally found in secondary lymphoid tissues such as the spleen and lymph nodes. However, local tissue resident T cell populations exist that are involved in homeostasis (Hirahara et al., 2021). As well as producing cytokines and chemokines for guiding the immune response, $CD4^+$ T cells are involved in maturation and activation of B cell responses and can also induce Immunoglobulin (Ig) G class switching in activated B cells (Luckheeram et al., 2012). In response to different pathogens, naïve CD4+ T cells activate and differentiate into different Th cell subsets, each with distinct chemokine and cytokine expression profiles, to deal with specific infections.

A core part of $CD4^+$ T cell response is long term memory cell formation. Following infection resolution, the majority of T cells undergo apoptosis and the surviving T cells differentiate into long lived memory cells which retain antigen specificity and can rapidly respond to re-infection (Gray et al., 2018). Memory cells can be generally split into T effector memory (Tem) and T central memory (Tcm) cells. Tem cells retain their capacity for cytokine expression in response to infection, and circulate throughout the bloodstream, allowing for rapid recruitment and cytokine responses upon reinfection (Sallusto et al., 2004). Tcm cells instead localise back to the spleen and lymph nodes, and are involved in T cell expansion and B cell activation during re-infection (Sallusto et al., 2004). While Tem cells retain their Th subset specific responses, Tcm cells

can differentiate into different Th cell subsets and regain more naïve cell like properties such as increased CD62L and CCR7 receptor expression (Gasper et al., 2014).

1.2.4 CD4+ T cell activation

Two signals are required for activation of naïve T cells to occur. The primary signal involves engagement of the TCR by binding MHC class II carrying an antigen. The co-stimulatory signal involves recognition of CD80 and CD86 on an antigen presenting cell by CD28 on the T cell surface. Engagement of the TCR alone is not sufficient to generate a full T cell response, and further modulation of differentiation can occur based on the engagement strength of the TCR interaction (Hwang et al., 2020). TCR engagement triggers phosphorylation of the cytoplasmic tail of the TCR by protein tyrosine kinases. This allows other effector molecules to recognise and continue signalling. These activation signals lead to several different intracellular signals, including a massive influx of intracellular calcium in the cell, which in turn activates transcription factor Nuclear Factor of Activated T cells (NFAT). Many other transcription factor pathways are also activated in response to TCR stimulation, including NF-kB, and MAPK pathways (Conley et al., 2016).

Activation of these pathways causes a transcriptional and translational burst, with increased expression of thousands of genes (Conley et al., 2016). Major epigenetic changes also occur alongside this, with deposition of acetylation marks to allow for better expression of genes involved in T cell activation and development (Cuddapah et al., 2010). Activated T cells are notable for the production of cytokine IL2, a potent cytokine involved in stimulating T cell proliferation and invoking B cell responses.

1.2.5 CD4+ T cell differentiation

Following activation, surviving Th cells differentiate further into effector subsets to help respond to different types of infection, influenced by the cytokine profile of the surrounding environment. In general, cytokine signalling leads to increased expression of Th subset specific transcription factors, which in turn activate subset specific signal transducer and activator of transcription (STAT) protein expression, upregulating expression of subset specific cytokines. This forms a positive feedback loop, reinforcing said Th cell subset differentiation. This process involves major rewiring of gene expression pathways, and as part of this transcription factors of alternative subsets and naïve T cells are epigenetically repressed, while transcription machinery is localised to genes in the selected Th cell subset to reinforce expression (Sanders, 2006). A diagram displaying differentiation into major Th cell subsets is shown in *Figure 1.4*.

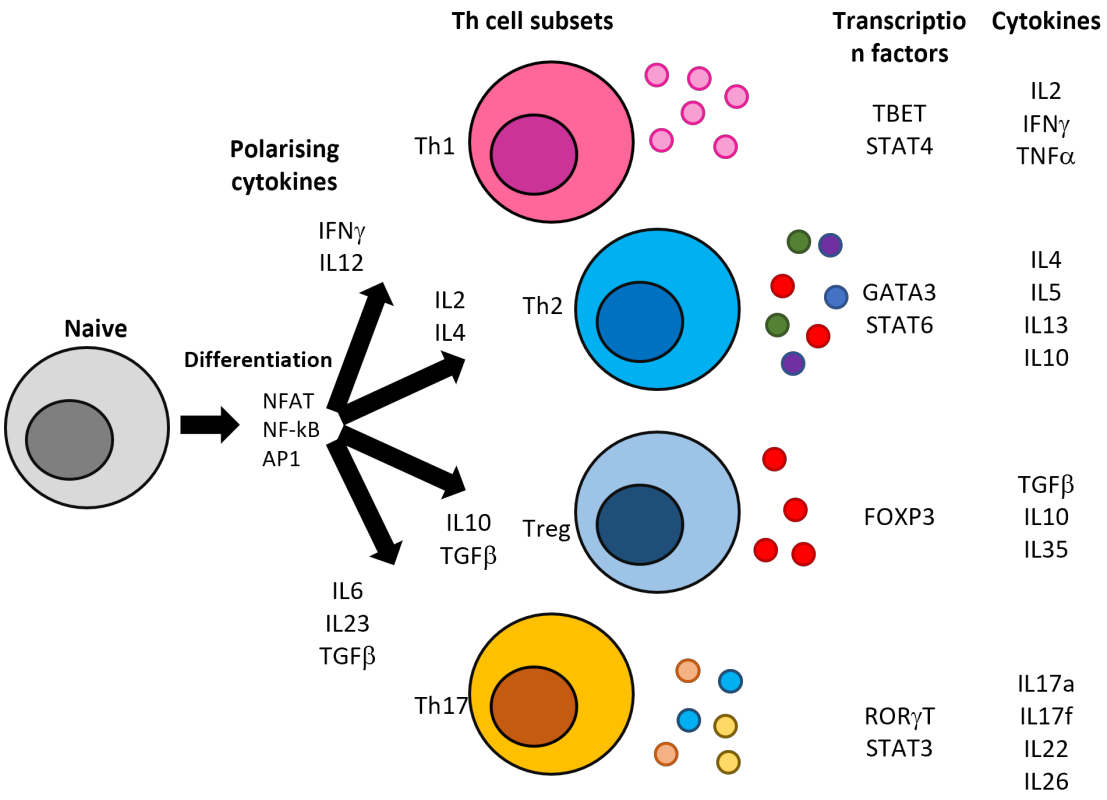

Figure 1.4 Schematic of the CD4+ T cell differentiation pathway

Schematic representation of Th cell differentiation pathways, including transcription factors involved in T cell activation, polarising cytokines for each subset, and the transcription factors and cytokines produced in each Th cell subset.

Initially, two distinct populations of effector $CD4^+$ T cells were identified with distinct cytokine expression profiles. These were termed Th1 and Th2 cells (Mosmann & Coffman, 1989). Th1 cells differentiate in response to IL12 signalling from macrophages and NK cells. This stimulates expression of core Th1 transcription factor T-box transcription factor (TBET) to form a positive feedback look via activation of STAT4, and expression of pro-inflammatory cytokine IFNγ. Th1 cells guide the response to intracellular bacteria and viruses (Luckheeram et al., 2012). IFNγ is generally pro-inflammatory and has functions such as activating macrophages, inducing antiviral states and B cell activation and class switching (Kak et al., 2018). Despite being generally pro-inflammatory cells, terminally differentiated Th1 cells can begin expressing IL10 and become Treg cells, termed T regulatory 1 (Tr1) cells (Edwards et al., 2023).

Th2 cells respond to IL4 signalling from mast cells and macrophages, which stimulates expression of GATA binding protein (GATA) 3 and activation of STAT6. Th2 differentiation leads to the expression of a number of cytokines, such as IL4, IL5, IL13 and IL10. Th2 cells help to guide the immune response to parasitic nematodes (Luckheeram et al., 2012). In terms of cytokine function, IL4 enhances T cell and macrophage responses and induces B cell differentiation (Keegan et al., 2021), IL5 stimulates antibody secretion in B cells and is involved in activating eosinophils (Pelaia et al., 2019), and IL13 stimulates IgE class switching as well as causing the physiological changes from Type 2 inflammation (De Vries, 1998).

Since the discovery of Th1 and Th2 cells, additional subsets of Th cells have been discovered, each with unique cytokine expression profiles. Th17 cells are known respond to IL6, transforming growth factor (TGF) β and IL23, which stimulates STAT3 and retinoid-related orphan receptor gamma T (RORγT) expression and activation within the

cells. Th17 cells produce IL17, IL22 and IL21, and stimulate neutrophil production. Th17 cells respond to extracellular bacteria and fungi (Luckheeram et al., 2012). Treg cells can differentiate in a few differing ways. Peripherally induced Tregs (pTregs) develop in peripheral lymphoid organs after antigen presentation, while thymic derived Tregs (nTregs) are released directly from the thymus. Tregs are generally categorised by expression of transcription factor forkhead box protein P3 (FOXP3), which induces the expression of anti-inflammatory cytokines TGFβ and IL10. Tregs are known for their roles in resolving inflammation and immune tolerance, with involvement in clearing of inflammatory responses post-infection in and wound healing (Shevyrev & Tereshchenko, 2020).

Other discrete Th cell subsets exist, such as Th9 and Th22 cells, which are characterised by the expression of IL9 and IL22 respectively (J. Chen et al., 2019; K. Zhang et al., 2023), and T follicular helper (Tfh) cells. Tfh cells are induced by IL6 signalling, express transcription factor Bcl6, and are involved in helping B cell differentiation and antibody production in the spleen and lymph nodes (Crotty, 2019). Th differentiation is also inherently plastic, and subset-specific cytokine and transcription factors can be expressed in other Th cell subsets. As an example of this, during *Schistosoma* infection, around 5% of total T cells express both IL4 and IFNγ, despite the repressive nature of these cytokines towards each other (Deaton et al., 2014).

1.2.6 Th cells and the Response to IL2

Cytokine IL2 is produced by T cells rapidly after TCR engagement, and acts as a pan-Th cell activator cytokine. IL2 signalling primarily leads to the phosphorylation and activation of STAT5 (*Figure 1.5 A*), but is also involved in activation of other intracellular

signalling pathways such as the mTOR and PI3K pathways (Ross & Cantrell, 2018). IL2 signalling in Th cells is important for late-stage differentiation, upregulating cell proliferation and subset specific cytokine and transcription factor expression (*Figure 1.5 B*).

IL2 signalling has differing effects on Th cell differentiation, highly dependent on Th cell subset (*Figure 1.5 C*). Generally, IL2 promotes both Th1 and Th2 differentiation, but inhibits Th17 differentiation. In Th1 cells IL2 drives expression of the IL12 receptor, enhancing responses to IL12, and causes increased induction of TBET. IL2 signalling also remodels Th cell metabolism, enhancing HIF-1A and C-MYC expression, which in turn enhances IFNγ expression (Shouse et al., 2024). Meanwhile, in Th2 cells IL2 signalling upregulates the expression of IL4 receptor α (IL4Rα) to enhance IL4 signalling (Liao et al., 2011). STAT5 is also able to bind to the IL4 promoter, enhancing its expression in response to IL2 (Zhu et al., 2003). IL2 is critical for immune self-tolerance and Treg development, as STAT5 binds to a conserved non-coding sequence downstream of the FOXP3 promoter. This allows for an alternate STAT5 based induction of FOXP3, and is involved in aiding Treg development in the thymus (Shouse et al., 2024). However, IL2 signalling is inhibitory for some other Th cell subsets, such as Th17 cells. Here, STAT5 binding to the IL17 promoter has an inhibitory effect on transcription, outcompeting STAT3 while not triggering transcriptional activity (Shouse et al., 2024).

IL2 signals via the tripartite IL2 receptor (IL2R), composed of chains IL2Rα, IL2Rβ and IL2Rγ. IL2Rγ, also known as the common gamma chain (γc), is a component of numerous cytokine receptors, including IL4R, IL7R, IL9R, IL15R and IL21R. IL2Rβ can also form part of the IL15R, while IL2Rα is specific only to the IL2R. IL2Rβ and IL2Rγ form the base form of the IL2R, which is capable of intracellular signalling but

displays only low affinity for IL2. IL2Rα association with IL2Rβ and IL2Rγ forms the high affinity IL2R, which mediates the majority of the biological function of IL2 (Ross & Cantrell, 2018). While IL2Rβ and IL2Rγ are expressed constitutively, IL2Rα is only expressed following T cell activation (Belot et al., 2018).

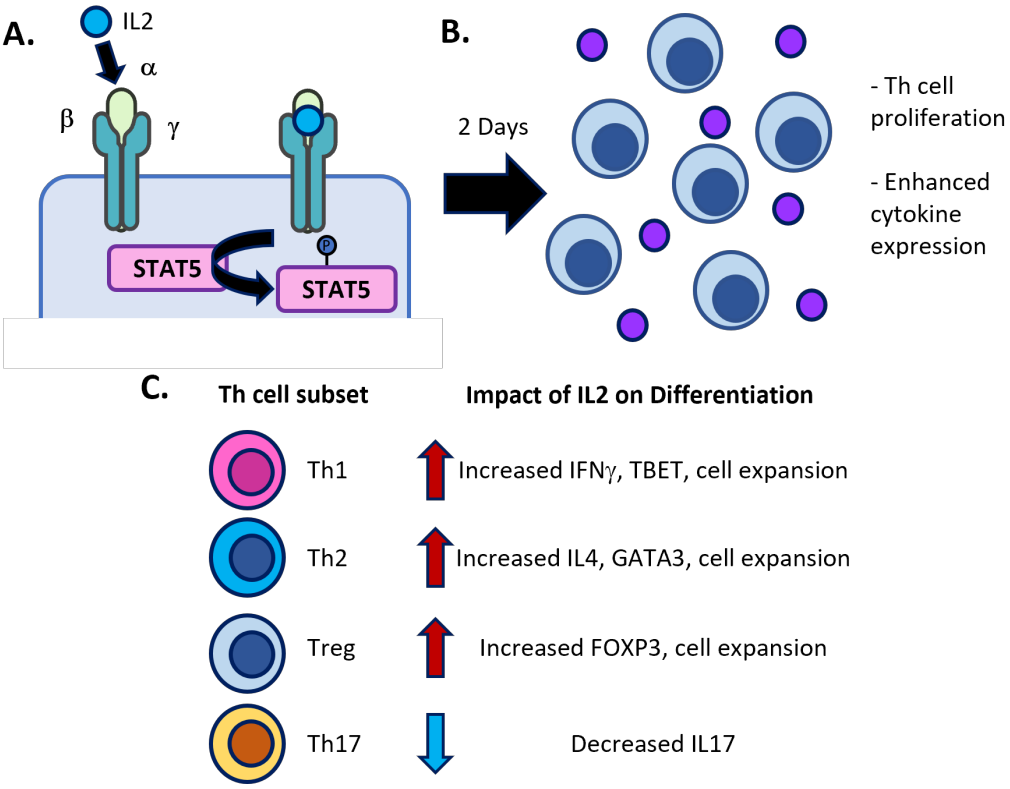

Figure 1.5 Schematic of the response to exogenous IL2 during CD4$^+$ T cell differentiation

A. Schematic of IL2 binding by the tripartite high affinity IL2 receptor. The receptor, composed of IL2Rα, β and γ, binds to IL2 and triggers phosphorylation of STAT5. **B.** The impacts of IL2 signalling in Th1/2 cells. IL2 signalling leads to increased Th cell proliferation and enhanced cytokine expression. **C.** The impact of IL2 signalling in different CD4$^+$ T cell subsets.

1.2.7 Th cell Production of IL10

IL10 is an anti-inflammatory cytokine produced by a number of different immune cells, with involvement in reducing inflammation, wrapping up the immune response following infection, and in wound healing (Saraiva et al., 2019). IL10 was initially classified as a Th2 cell cytokine with effects on inhibiting cytokine expression in Th1 cells, however it is now generally understood to be a cytokine that is expressed from all Th cell subsets (Jankovic et al., 2010). While Treg cells are defined by an anti-inflammatory cytokine profile including IL10 promoted by FOXP3 expression, other subsets such as Th2 cells constitutively produce high amounts of this IL10, and both Th1 and Th17 cells are able to express IL10 at low levels under specific conditions (Jankovic, Kugler and Shesr, 2010). Alongside its production in T cells, IL10 is primarily produced by a subset of regulatory B cells (Bregs) involved in suppression of inflammation and development of immune tolerance (Zheremyan et al., 2025). Breg cells are a highly heterogenous population defined by their expression of anti-inflammatory cytokines such as IL10, TGFβ IL35, with roles in the promotion of Treg cell development, inhibition of inflammatory cytokine signalling from dendritic cells, and promotion of $CD4^+$ T cell apoptosis (Rosser & Mauri, 2015).

IL10 in Th cells is also thought to be regulated via temporal means, as expression often occurs later than expression of other subset specific cytokines (Yssel et al., 1992). Th1 cells in particular are able to differentiate into IL10 expressing Tr1 cells following the initial Th1 response (Jankovic et al., 2010). IL10 acts via the IL10R on a number of different immune cells, including Th cells, macrophages and NK cells, where it generally reduces inflammatory cytokine expression and inhibits immune cell function (Saraiva et al., 2019).

Generally, IL10 expression in effector Th cell subsets (Th1, Th2 and Th17 cells) can be triggered downstream of their respective STAT proteins (Saraiva et al., 2019). This triggers expression of transcription factor avian musculoaponeurotic fibrosarcoma oncogene homolog (MAF), which is the master regulator of IL10 expression (Gabryšová et al., 2018; Saraiva & O'Garra, 2010; Trinchieri, 2007). However, other transcription factors in Th cell differentiation are also able to induce IL10 expression directly via different pathways as well. In Th2 cells transcription factor GATA3 can directly trigger IL10 expression via remodelling the gene locus (Shoemaker et al., 2006), while in Th1 cells IL12 signalling induces expression of transcription factor B lymphocyte-induced maturation protein-1 (BLIMP-1) which itself upregulates IL10 expression. (Neumann et al., 2014). BLIMP-1 is also involved in IL10 expression in Tr1 cells, and may play a role in Tr1 cell differentiation (Montes de Oca et al., 2016).

1.2.8 LncRNAs in $CD4^+$ T cells

LncRNAs are important regulators of T cell immunity, affecting activation, differentiation and cytokine expression through both *in cis* and *in trans* functions. T cell activation was discovered to be regulated by lncRNA *NRON*, which affects NFAT activity. *NRON* acts to repress T cell activation, where it binds and sequesters NFAT in the cytoplasm during T cell activation. This inhibits NFAT, helping to limit excessive T cell activation and NFAT- dependent cytokine production (S. Sharma et al., 2011).

Many lncRNAs also affect the balance of T cell differentiation into the different Th cell subtypes, often via affecting the subset specific transcription factors. *Linc-MAF4* was initially discovered via RNA sequencing experiments as a Th1 specific lincRNA. *Linc-MAF4* interacts with EZH2 (from PRC2) and LSD1 (a histone demethylase) to

deposit repressive H3K27me3 marks on the promoter region of the gene *Maf*. This in turn suppresses IL10 expression, and enhances Th1 differentiation (Ranzani et al., 2015). IL10 expression is also downregulated by other lncRNAs, such as *AW112010*, which interacts with histone demethylase KDM5a, removing activating H3K4 marks from the *IL10* gene (X. Yang et al., 2020). Th cell subset specific cytokine expression is also strongly regulated by lncRNAs. LncRNA *NeST* was originally identified in Th1 cells, with further experiments identifying it interacts with WDR5 to induce activating H3K4 methylation marks at the IFNγ gene locus (Collier et al., 2014).

Th2 differentiation is strongly influenced by lncRNAs, which affect expression of core Th2 transcription factors and cytokines. *GATA3* is known to be tightly regulated by a number of lncRNAs, such as antisense lncRNA *GATA3-AS1*. *GATA3-AS1* interacts *in cis* with methyltransferase WDR5, binding to an R loop formed in the intron of the *Gata3* gene. WDR5 deposits activating H3K4 marks on the *Gata3* locus, helping to promote GATA3 expression (Gibbons et al., 2018). *GATA3-AS1* has also been linked to the expression of Th2 cytokines, such as IL5 and IL13, and may help regulate them as well. Other lncRNAs have also been associated with GATA3 expression, including lncRNA *Dreg1*. *Dreg1* is highly correlated with *Gata3* in Th2 cells, and aids in establishing *Gata3* expression in Th2 cells (Chan et al., 2021). Th2 cytokines are also known to be regulated by lncRNAs. Expression of major Th2 cytokines is regulated by the *Th2-LCR* lncRNA cluster. *Th2-LCR* contains four lncRNAs expressed during Th2 differentiation, that promote H3K4 methylation and H3 acteylation of the IL4, IL5 and IL13 genes, helping to keep the chromatin open and promote their expression (Koh et al., 2010). LincRNA *FR215775* was further shown to promote expression of both IL4 and IL5 in a murine model of allergic rhinitis, also promoting Th2 cell expansion (Y. Ma et al., 2022).

In Th17 cells, *lncRNA-Gas5* directly targets transcription factor STAT3 for ubiquitination, preventing its signalling and inhibiting Th17 differentiation (J. Li et al., 2020). *LncRNA-GM* also inhibits Th17 differentiation, binding to and preventing dephosphorylation of FOXO1, which in turn enhances the expression of IL17 and IL23r (YaliChe et al., 2022). Interestingly, previously mentioned paraspeckle lincRNA *Neat1* is also known to positively regulate Th17 differentiation via a few different methods. Nuclear *Neat1* binds to and inhibits expression of NONO, preventing repression of *Il17* and *Il23r* genes (S. Chen et al., 2023). However, cytoplasmic *Neat1* can also bind and sponge miR-128-3p, preventing it from repressing transcription factor *Nfat5*, which eventually leads to increased expression of RORγT and IL17 (S. Chen et al., 2023).

During Treg differentiation, transcription factor FOXP3 expression is directly modulated by lncRNAs. *Flicr* acts *in cis* to inhibit FOXP3 expression, influencing the chromatin structure of the *FoxP3* locus to decrease expression (Zemmour et al., 2017). Meanwhile, lincRNA *Flatr* is known to promote the expression of FOXP3 in a subset of Treg cells, enhancing their immunosuppressive functions (Brajic et al., 2018). LncRNAs are also known to target other factors involved in Treg differentiation. *Lnc-EGFR* works *in cis* to target EGFR, binding to it and preventing its ubiquitination, thus preventing EGFR degradation, promoting expression of transcription factor AP-1, which in turn promotes FOXP3 expression (Jiang et al., 2017). Meanwhile, lncRNA *Snhg1* has previously been shown to affect miR-448 and IDO expression, enhancing Treg activation and inhibiting Th17 differentiation (Baban et al., 2009). Overall, the ability of lncRNAs to regulate many different parts of Th cell differentiation provides clear evidence that they are core to Th cell function.

Table 1.1 Examples of lincRNAs in Th cell differentiation

LncRNA	Type	Function	Reference
NRON	Intronic	Sequesters NFAT, limits T cell activation	(Sharma et al., 2011)
Linc-Maf4	Intergenic	Targets PRC2 to deposit H3K27me3 on the MAF promoter	(Ranzani et al., 2015)
AW112010	Intergenic	Targets KDM5a to remove H3K4 marks from the IL10 gene	(Yang et al., 2020)
NeST	Antisense	Interacts with WDR5 to place activatory H3K4 marks on IFNγ	(Collier et al., 2014)
GATA3-AS1	Antisense	Interacts with WDR5 to place activatory H3K4 marks on GATA3	(Gibbons et al., 2018)
Dreg1	Intergenic	Aids in establishing GATA3 expression in Th2 cells	(Chan et al., 2021)
Th2-LCR	Sense	Promotes H3K4 and H3 acetylation of IL4, IL5 and IL13	(Koh et al., 2010)
FR215775	Intergenic	Promotes expression of IL4 and IL5, as well as cell expansion of Th2 cells	(Ma et al., 2022)
lncRNA-Gas5	Antisense	Targets STAT3 for ubiquitination, inhibiting Th17 differentiation	(Li et al., 2020)
lncRNA-GM	Antisense	Prevents dephosphorylation of FOXO1, enahcning IL17 and IL23r expression	(YaliChe et al., 2022)
Neat1	Intergenic	Inhibits NONO and NFAT5, upregulating IL17, IL23r and RORγT	(Chen et al., 2023)
Flicr	Sense	Acts *in cis* to deposit inhibitory chromatin marks on *FoxP3*	(Zemmour et al., 2017)
Flatr	Intronic	Promotes FOXP3 expression in a subset of Treg cells	(Brajic et al., 2018)
Lnc-EGFR	Antisense	Prevents ubiquitination of EGFR, promoting AP-1 and eventual FOXP3 expression	(Jiang et al., 2017)
Snhg1	Antisense	Downregulates miR-448 and IDO expression, enhancing Treg differentiation	(Baban et al., 2009)

1.3. Type 2 Immunity

1.3.1 Type 1, 2 and 3 immune responses

The immune response is generally split into type 1, 2 or 3 responses, regulated by Th1, Th2, and Th17 differentiation respectively, in response to infection or immune challenge. Type 1 immune responses occur during infection of intracellular bacteria and parasites and are typically inflammatory in nature, involving Th1 differentiation, IFNγ expression, increased neutrophil production and activation, and iNOS mediated macrophage responses to infection (Spellberg & Edwards, 2001). Type 1 immune responses trigger increased activation of $CD8^+$ T cells to kill infected cells, and the induction of inflammatory cytokine and chemokine expression from non-immune cell types, including endothelial cells and fibroblasts (Annunziato et al., 2015).

Type 2 or allergic immune responses are driven by Th2 cells, and in the context of infection predominantly occur in response to parasitic worm infection. Type 2 responses typically produce allergic inflammation and tissue remodelling via increased production of Th2 cytokines, however can also be mounted to resolve high levels of inflammation (Spellberg & Edwards, 2001). As part of type 2 responses Th2 cells express cytokines IL4, IL5, IL13 and IL10. This triggers arginase mediated macrophage responses, eosinophil production, and B cell antibody class switching to IgE production. IL5 here triggers eosinophil generation in the bone marrow, which play a role in tissue remodelling and granuloma formation in response to infection. IL13 is also involved in mediating B cell responses via promoting class switching to IgE antibodies, and mediates the majority of physiological changes involved in type 2 inflammation (Ogulur et al., 2025).

Finally, Type 3 responses occur in response to infection with extracellular bacteria and fungi, and are driven by Th17 cells. These responses typically occur at epithelial barriers, and are categorised by high levels of neutrophil recruitment, as well as CD8 T cell activation (Rainard et al., 2020).

1.3.2 Helminth infection

In the context of infection, helminth parasites consist of a wide variety of differing parasitic worm species including blood flukes (*Schistosoma mansoni, Schistosoma japonicum*), nematodes (*Ancylostoma duodenale, Ascaris lumbricoides*) and cestodes (*Taenia solium, Echinococcus granulosus*). However, despite the differences between species all trigger type 2 responses upon host infection (Gazzinelli-Guimaraes & Nutman, 2018). Helminths often have complex lifecycles involving multiple hosts, multiple parasite development stages, and distinct effects on different organs dependent on infecting species. Helminth infections are also widespread, and thought to infect around 2 billion people worldwide (Nelwan, 2019). In terms of the lifecycle of schistosome *S. mansoni*, which infects around 250 million people, freshwater living miracidia stage parasites, are able to seek out and infect snails. Inside snails the parasites develop into sporocysts, which produce and shed infectious cercariae. Cercariae are then able to infect humans via burrowing through the skin, traveling around the body via the lungs and liver and triggering immune responses there, eventually colonising the small and large intestine where they then produce eggs (Nelwan, 2019). Helminths produce strong type 2 immune responses, with consistent production of Th2 cytokines, IgE class switching and production from B cells, mast cell degranulation, and strong eosinophil and basophil recruitment (Maizels et al., 2004). Eosinophil and basophil signalling lead to enhanced

M2 macrophage polarisation, aiding in granuloma formation in an attempt to trap parasites and inhibit migration (Maizels & Gause, 2023).

There are two main phases to helminth infection. The acute phase occurs shortly after initial infection, with symptoms consisting of fevers, headaches, myalgia, rashes, and respiratory symptoms caused via migration of parasites through the lungs (Nelwan, 2019; G. Y. Wu & Halim, 2000). Following this the infection enters the chronic stage, and the immune response becomes more anti-inflammatory, with increased IL10 expression, and the majority of patients are asymptomatic. A small proportion of patients can progress to severe chronic disease, defined by an overactive immune response, series of chronic inflammatory lesions in or around eggs lodged in blood vessels, hepatosplenomegaly, and intestinal polyp formation (McSorley & Maizels, 2012; G. Y. Wu & Halim, 2000). Praziquantel is typically used for treating helminth infections due to its cost effectiveness and lack of significant side effects. However, praziquantel does not kill immature parasites, and therefore treatment requires repetition after 2-4 weeks, and does not prevent against re-infection (Wright et al., 2018).

1.3.3 Type 2 immunopathologies

While type 2 responses are protective in regard to helminth infection, dysregulation can trigger the onset of different allergic immune conditions, including allergic respiratory disorders such as allergic rhinitis or asthma, and cutaneous disorders such as atopic dermatitis (Hassoun et al., 2021). Type 2 immunopathologies generally display typical type 2 immune cell responses, such as Th2 differentiation, cytokine expression, IgE antibody production, and infiltration of eosinophil and mast cells,

however the conditions are heterogenous and may display differences in immune cell contribution and pathology (Hassoun et al., 2021).

Recent estimates have suggested that ~9% of the world's population are diagnosed with asthma (Song et al., 2022). Asthma is often caused by chronic type 2 inflammation of the airways and lungs, with typical symptoms such as breathlessness, coughing, a tight chest, and airflow obstruction. If left untreated this can lead to recurrent asthma attacks and irreversible lung function decline. This often develops during adolescence, and can be either allergic or non-allergic, dependent on if an allergic immune cascade can be triggered (Howell et al., 2023). Lung immune cell infiltrates in asthma are primarily eosinophil driven but may also contain some neutrophils and lymphocytes. Eosinophil infiltration into airways triggers tissue remodelling, causing airway narrowing, airway mucous plugging, goblet cell hyperplasia, and hypertrophy of airway smooth muscle cells (Howell et al., 2023; Hussain & Liu, 2024). While the majority of asthma is eosinophilic, some cases display increased neutrophil infiltration instead, which is typically more aggressive and difficult to treat (Ray & Kolls, 2017). In allergic asthma, the allergic cascade is driven by B cell and Th2 responses. Recognition of antigen crosslinking to IgE triggers rapid release of histamine, tryptase, and PGD2 from mast cells, causing the typical allergic reaction (Howell et al., 2023).

Allergic rhinitis affects 500 million people worldwide and is often comorbid with asthma (Bousquet et al., 2020). Allergic rhinitis is triggered by allergen penetration of the mucosal epithelium in nasal passages, causing localised Th2 differentiation, generation of a type 2 inflammatory response, and production of allergen specific IgE antibodies (Bernstein et al., 2024). Similar to asthma, allergen recognition by IgE triggers mast cell activation and release of bioactive mediators, leading to vasodilation, mucous production and inflammation. The type 2 inflammation here is the cause of the typical symptoms

such as rhinorrea, nasal congestion, sneezing and itching of eyes and throat (Bernstein et al., 2024).

Atopic dermatitis, more commonly known as atopic eczema, is suggested to affect ~2% of individuals worldwide (J. Tian et al., 2023). Atopic dermatitis is a chronic relapsing skin disorder with symptoms of dry skin, localised rash and disrupted skin barrier. This condition is triggered by irritants such as allergens or microbes, which upregulate the type 2 immune response (Jeskey et al., 2024). Atopic dermatitis is also often diagnosed much earlier in children than asthma, and often presents as recurrent flares. While increased type 2 inflammation is still a major characteristic of atopic dermatitis, the response typically differs slightly to that of asthma and allergic rhinitis, displaying an increased role for Th2 cells in disease pathology, a preference for IL13 and IL33 cytokine expression, and reduced roles for B cell and eosinophils (Akdis et al., 2020).

Treatment of severe asthma, defined when conventional therapies do not work to reduce symptoms, often requires the use of biologics. A range of monoclonal antibody inhibitors of cytokine and antibody signalling are used to inhibit lung type 2 immune responses. B cell responses can be disrupted via inhibition of IgE-crosslinking from drugs such as omalizumab, which binds to the Fc region of the IgE antibody. Th2 cytokine signalling can also be targeted, with treatments such as mepolizumab preventing eosinophil recruitment via targeting IL5, and dupilumab inhibiting both IL4 and IL13 signalling via targeting of shared receptor IL4Rα (Gyawali et al., 2025). While some of these biologics such as dupilumab can be used for treatment of atopic dermatitis, the decreased role for B cells and differing cytokine signalling means that other drugs such as lebrikizumab (inhibits IL13 signalling) and nemolizumab (inhibits IL31 signalling) can be used as treatments instead (Ratchataswan et al., 2021).

1.3.4 Murine models of type 2 inflammation

In vitro models of immune cell differentiation may exclude several factors, including hormones, antigen presentation, cytokines, chemokines and cell-surface receptor signalling from other immune cells, that are present in *in vivo* type 2 inflammatory conditions. Therefore, a number of differing mouse models of type 2 inflammation have been developed in mice to investigate type 2 immune responses *in vivo*.

Allergic inflammation and Th2 differentiation in the lung or nasal passages can be triggered by exposure to antigens in mice. These include house dust mite (HDM) antigen, ovalbumin, or mold antigens. The HDM model is one of the more commonly used models, and the antigen is the major source of allergen seen in house dust. In these models, mice are sensitised via intranasal instillation with HDM, then re-challenged over time to generate a chronic response (Woo et al., 2018). The length of time that the mice are challenged for varies dependent on the experiment, but is typically between 2 and 8 weeks, with more acute inflammation seen during earlier time points, and allergic inflammation and airway remodelling seen during later time points (Woo et al., 2018). This model causes robust Th2 cell generation, but is primarily used to assess asthma and allergy *in vivo,* as the antigens trigger significant airway remodelling, with effects such as goblet cell hyperplasia, collagen deposition and fibrosis (Radhouani & Starkl, 2024).

Atopic dermatitis mouse models are also used for *in vivo* generation of Th2 cells. There are a number of ways of causing atopic dermatitis, with methods such as repeated epicutaneous sensitization of tape stripped skin with allergens such as ovalbumin or HDM, prolonged treatment with Haptens such as oxazolone, the MC903 mouse model which triggers pathogenic ILC2 expression, or transgenic IL4 expression in skin tissue (Jin et al., 2009). As part of these models, the mouse skin develops lesions, with both

epidermal and dermal thickening, and significant infiltration of Th2 cells and eosinophils (Jin et al., 2009). Th2 cytokines, as well as IL31 are also upregulated. However, the time period for these experiments is relatively long, requiring a minimum 7-week period (Gilhar et al., 2021). Furthermore, none of the current atopic dermatitis mouse models also fully mimic all key characteristics of human atopic dermatitis, and results are known to vary between independent studies (Gilhar et al., 2021).

Type 2 inflammation can also be triggered via helminth (parasitic nematode) infection models, including model species *S. mansoni*. Characteristics of *S. mansoni* cercariae infection of mice involve splenomegaly, liver fibrosis and granulomas in the liver, intestines and lungs. In terms of Th2 cell generation, infection typically generates a mixed Th1/Th2 response (Zhong et al., 2022). The initial acute phase of infection generates a strong Th1 response in affected tissue, produced in response to the parasites migrating throughout the body. Following this the worms begin mating and egg production in the intestines, and this shifts the immune response towards a Th2 response (Femoe et al., 2022). In terms of immune cell responses, the chronic phase generates Th2 cells with increased production of IL4 and IL13. Other characteristics include high IgE expression, eosinophil generation and activation (RELMα expression), and alternate activation of monocytes in direct sites of inflammation such as the liver, intestines and lungs (Voehringer et al., 2006). However, as worms are still present during this phase of the infection, some level of Th1 responses remain.

Interestingly the response to parasite eggs during *S. mansoni* infection is the main driver of Th2 responses *in vivo*, as the parasite eggs trigger the formation of granulomas with eosinophil and T cell infiltrates (Femoe et al., 2022). Therefore, injection of dead *S. mansoni* eggs can generate a localised and rapid type 2 immune response *in vivo*. This model involves initial intraperitoneal injection of eggs to sensitize mice, then after one-

week intravenous injection of eggs via the tail vein. The IV injection leads to egg migration to the lungs via the pulmonary artery, where the eggs are then deposited and trapped in the lung parenchyma, triggering granuloma formation. After another week mice are then sacrificed, and responses analysed in the lungs (Joyce et al., 2012). In comparison to full helminth infection, there is less risk involved as the dead *S. mansoni* eggs are non-infectious, and the timeline of the infection is relatively short, allowing for rapid analysis of type 2 responses *in vivo*. However, this model still generates some partial Th1 responses, leading to $CD4^+$ T cells production of IFNγ, which can partially suppress some Th2 cell responses. In terms of its applications this model also misses some context of a full worm infection as there is no acute phase and there are no live *S. mansoni* worms to cause pathology, and therefore this may be less applicable to direct study of diseases (Joyce et al., 2012).

1.4. The role of lincRNA *Malat1* in CD4$^+$ T cells

1.4.1 Overview of *Malat1*

Metastasis associated lung adenocarcinoma transcript 1 (*Malat1*), also known as Nuclear enriched abundant transcript 2 (*Neat2*), is one of the most extensively researched lincRNAs. *Malat1* defies many conventional lincRNA characteristics, as it as highly expressed as some housekeeping genes (Arun et al., 2020), is expressed in a wide variety of tissues, and exhibits strong sequence conservation, with >50% overall sequence conservation throughout vertebrates. This conservation increases to >80% at the 3' end (Arun et al., 2020). In humans, *Malat1* is present on chromosome 11q13.1 and is about 8.7kb in length, and in mice is present on chromosome 19qA and about 6.7kb. *Malat1* is transcribed, capped and polyadenylated similar to most mRNA transcripts, however following this *Malat1* is cleaved near the 3' end, to form a smaller 61nt long transcript, termed the *Malat1*-associated small cytoplasmic RNA (*mascRNA*). The larger transcript forms a triple helical tertiary structure at the 3' end to prevent degradation. This structure consists of two upstream poly-U rich sequences looped out, with a downstream poly-A tract inserted between them. The triple helix protects the transcript from exonuclease degradation, potentially contributing to the high expression level (Wilusz et al., 2012). As a structural feature, the triple helix is rare in humans, only found in a few other lncRNAs such as neighbouring lincRNA *NEAT1* and telomerase lncRNA *TERC* (Matveishina et al., 2020; Wilusz et al., 2012). Following processing, the long *Malat1* transcript localises to sub-nuclear compartments known as nuclear speckles, while the shorter *mascRNA* transcript instead localises to the cytoplasm (Wilusz et al., 2008).

Malat1 has shown a significant amount of clinical relevance, making it an attractive lincRNA for research. In its initial discovery, *MALAT1* was found to be upregulated in non-small cell lung carcinomas with increased likelihood to metastasise (Ji et al., 2003), while a germline single nucleotide polymorphism (SNP) of *MALAT1* is associated with improved survival outcomes in non-small cell lung carcinomas (J. Z. Wang et al., 2017). Further research identified *MALAT1* as playing a major role in multiple other cancers including prostate, breast and pancreatic cancer, with repression generally proven to decrease cell migration, invasion, and metastasis (Arun et al., 2016; Chatterjee et al., 2020; Gutschner et al., 2013; L. Li et al., 2016; H. Yang et al., 2017). It has also been implicated in autoimmune disorders, with upregulation affecting splicing in multiple sclerosis (Cardamone et al., 2019), cytokine expression in systemic lupus erythematosus (SLE) (H. Yang et al., 2017), and disease severity in rheumatoid arthritis (Chatterjee et al., 2020). Combined with the aforementioned high expression and conservation, research suggests that *Malat1* has a critical cellular function, and this provides a strong case for furthering our understanding of its role in disease.

Despite its disease relevance, high expression and conservation, generation of three knock-out models in mice initially demonstrated that *Malat1* is dispensable for normal mouse development. These models displayed no obvious homeostatic phenotypes or developmental defects (Eißmann et al., 2012; Nakagawa et al., 2012; B. Zhang et al., 2012), suggesting a redundant cellular role. However, research since then has identified a number of cellular roles of *Malat1*, particularly in terms of splicing and gene expression regulation, with important roles in immune cell function and in disease progression. Alongside these knock-out models, overexpression and rescue experiments have been performed to investigate *Malat1* function. This has been performed previously in melanoma cells using lentiviral vectors to demonstrate that *Malat1*

negatively regulate expression of miR-34a (F. Li et al., 2019), and has also been achieved previously via CRISPR activation in patient derived lung adenocarcinoma to demonstrate that *Malat1* affects tumour progression and metastasis (Martinez-Terroba et al., 2024). However, the relatively high expression of *Malat1* in the majority of tissues can complicate separating overexpression results from experimental noise (Arun et al., 2020). Alternate *Malat1* knock-down has also been performed to downregulate *Malat1* levels without disrupting the genomic locus. While this has been performed using siRNA and shRNA previously (Tripathi et al., 2013; Y. Zhao et al., 2024), the knockdown efficiency was relatively low with only a 2-4 fold decrease (Eißmann et al., 2012), potentially due to localisation of the RISC complex to the cytoplasm while *Malat1* is a primarily nuclear RNA (Pratt & MacRae, 2009).

1.4.2 *Malat1* in nuclear speckles and splicing

Malat1 localises to nuclear speckles, which are sub-nuclear membrane-less compartments (Lamond & Earnshaw, 1998; Lamond & Spector, 2003). Nuclear speckles are hubs of RNA, splicing, and mRNA transcript processing factors, and are predicted to be involved in regulating alternative splicing events and are involved in promoting high levels of transcription in specific gene compartments. While initial research involving depletion of *Malat1* suggested that *Malat1* is not an integral part of nuclear speckles (Nakagawa et al., 2012), more recent research has identified that *Malat1* loss affects the intra-speckle organisation of RNA and splicing factors (Fei et al., 2017). Typically, organised speckle structure consists of core speckle proteins SON and serine/arginine repetitive matrix protein 2 (SRRM2) at the centre of the speckle, with RNA processing factors and mRNA transcripts present at the outside. When *Malat1* is lost, this

organisation is lost and the components are instead mixed throughout the speckle (Fei et al., 2017).

Malat1 is known to interact with and affect serine/arginine rich (SR) protein and heterogenous nuclear ribonuclear proteins (HNRNP) protein activity, which often reside within nuclear speckles. Co-immunoprecipitation of *MALAT1* in HeLa cells revealed binding to serine and arginine-rich splicing factor (SRSF) 1-3, and *MALAT1* depletion was shown to affect alternative splicing events via modulating SR protein localisation to nuclear speckles and their activation via their phosphorylation (Tripathi et al., 2010). The interaction between *MALAT1* and SRSF1 has been particularly well studied. In hepatocellular carcinoma, *MALAT1* was shown to affect SRSF1 expression levels which in turn affected splicing events (Malakar et al., 2016). Further exploration in HEK 293 cells revealed that PTBP1, also known as HNRNPI, and PSF splicing factors are stabilised by *Malat1* binding (Miao et al., 2022), helping to direct them to pre-mRNAs, and affecting different alternative splicing events. Furthermore, *MALAT1* was also able to facilitate PTBP1 and PSF interactions with proteins HNRNPA1, HNRNPF and HNRNPU, affecting hepatocellular carcinoma progression (Miao et al., 2022).

1.4.3 The role of *Malat1* in gene expression regulation

Malat1 is also closely linked to the transcriptional regulation of different genes. CHART-seq experiments (a method for identifying RNA-DNA interactions) in MCF-7 cells showed that both *MALAT1* and neighbouring lincRNA *NEAT1* bind near the transcriptional start sites of hundreds of actively transcribed genes (West et al., 2014). This was further confirmed by RAP-RNA experiments (a method for identifying RNA-RNA interactions) which showed interactions between *MALAT1* and 5’ ends of nascent

pre-mRNAs during transcription (Engreitz et al., 2014). These RNA-RNA interactions were primarily between genes encoding RNA-binding proteins. *Malat1* has also been shown to regulate transcription, through interaction with previous mentioned histone methylation complex PRC2. *MALAT1* has previously been shown to associate with EZH2 and PRC2 in several different cell lines, such as MCF-7 breast cancer cells (Arratia et al., 2023), T and NK cell lymphomas (S. H. Kim et al., 2017), mantle cell lymphoma (X. Wang et al., 2016), and prostate cancer (D. Wang et al., 2015). Knock-down in prostate cancer was also shown to dysregulate H3K27 methylation patterns, suggesting that *MALAT1* may regulate PRC2 targeting (D. Wang et al., 2015).

Malat1 is also thought to regulate targets via acting as a miRNA sponge. *MALAT1* has been suggested to sponge miRNAs such as miR-3064-5p (Shih et al., 2021), miR-30b (Ahmad et al., 2023), and miR-663a (W. Tian et al., 2018) in different contexts of cancers, normally with pro-oncogenic effects. However, it is unclear on how this sponging effect occurs as miRNAs are cytoplasmic while *Malat1* is primarily nuclear, although *Malat1* could sequester miRNAs during pre-miRNA processing. Interestingly, the *mascRNA* has also been shown to affect gene expression, primarily impacting translation. *mascRNA* positively regulates QARS protein levels in the cytoplasm, which promotes global protein translation and cell proliferation (X. Lu et al., 2020).

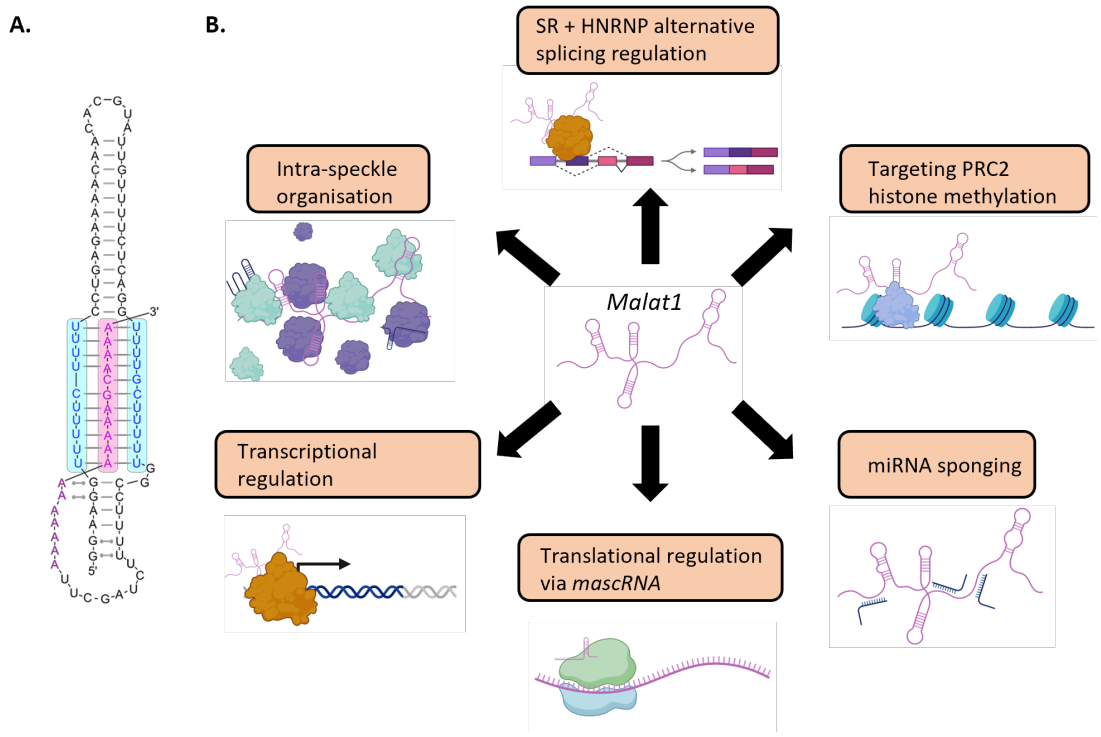

Figure 1.6 Structure and function of lincRNA Malat1

A. Secondary structure of the *Malat1* triple-helix at the 3' end. **B.** Schematic depicting the potential functions of *Malat1*, including SR + HNRNP protein alternative splicing regulation, targeting of PRC complex for epigenetic repression, miRNA sponging, translational regulation, transcriptional regulation via association with transcription factors, and intra-speckle RNA + protein organisation.

1.4.4 *Malat1* in CD4$^+$ T cells

Malat1 has been previously implicated as a regulator of multiple different branches of the immune system. In myeloid cells, *MALAT1* expression in dendritic cells was shown to promote a tolerogenic phenotype (J. Wu et al., 2018), while in macrophages *Malat1* has also been shown to differentially regulate macrophage polarisation in response to LPS or IL4 (H. Cui et al., 2019), and is downregulated in response to viral infection to induce antiviral immunity (W. Liu et al., 2020). *Malat1* is also known to play a major role in regulating CD8$^+$ T cell memory formation. *Malat1* here is thought to interact with PRC2 component EZH2 to methylate memory cell genes, and promote differentiation to terminal effector cells, with *Malat1* knock-down causing an increase in memory cells (Kanbar et al., 2022).

There are conflicting reports on the function of *Malat1* in CD4$^+$ T cells. *Malat1* loss did not affect CD4$^+$ T cells, T follicular helper cells or CD8$^+$ T cells in response to lymphocytic choriomeningitis virus infection, with the authors suggesting it was dispensable for T cell function and development (Yao et al., 2018). However, siRNA knock-down of *Malat1* in the context of multiple sclerosis and mice with experimental autoimmune encephalitis was shown to promote both Th1 and Th17 polarisation (Masoumi et al., 2019). Contrasting this, knockdown of *Malat1* has also been observed to impair Th17 differentiation in the context of acute viral myocarditis in mice (Xue et al., 2022). *Malat1* has also been shown to promote Th2 cell differentiation, where *in vitro* knock-down of *Malat1* was shown to inhibit ovalbumin-induced CD4$^+$ T cell Th2 differentiation, increasing expression of miR-135b-5p and inhibiting expression of GATA3 and IL4 (X. H. Wu et al., 2022).

Previous work from Dr. Katie West and Dr. James Hewitson demonstrated that *Malat1* plays a critical role in regulating Th1 cell differentiation (Hewitson et al., 2020)..

Downregulation of *Malat1* was shown to be a hallmark of $CD4^+$ T cell activation, in both mouse and human cells (Dey et al., 2023; Hewitson et al., 2020). However, complete loss of *Malat1* was shown to impact MAF protein and RNA expression, which in turn impacted the expression of immune regulatory cytokine IL10 in both Th1 and Th2 differentiation. *Malat1* loss was shown to impair generation of Tr1 cells *in vivo* in *Leishmania donovani* and *Plasmodium chabaudi chabaudi AS* infection models. *Malat1*$^{-/-}$ $CD4^+$ T cells displayed reduced IL10 expression, resulting in significantly reduced parasite burden in the leishmaniasis model and significantly more severe disease pathology in the malaria model (Hewitson et al., 2020). Overall, this evidence implicated *Malat1* as a key regulator of $CD4^+$ T cell activation and differentiation, and suggests that further research is required to truly understand how *Malat1* affects Th cell differentiation, and the cellular mechanisms behind this.

1.5. Sexual dimorphism in the immune system

1.5.1 Sexual dimorphism in Immunity

Biological sex is a known determinant of immune function, both in humans and mice (Klein and Flanagan, 2016; Dunn, Perry and Klein, 2024; Forsyth et al., 2024). In general, it is thought that female immune systems respond stronger than males, and may include a slight bias towards type 2 responses. This difference in immune function has a number of consequences, with wide ranging effects on diseases (Klein & Flanagan, 2016). In general, the majority of autoimmune disorders are known to affect females over males, with diagnosis rates in the UK between 2000 and 2019 generally skewed to females over males at a 2/3 to 1/3 ratio (Conrad et al., 2023). This increased female to male ratio is particularly pronounced in the diagnosis rates of autoimmune disorders such as SLE, rheumatoid arthritis and multiple sclerosis. However, some autoimmune disorders such as inflammatory bowel diseases do not show any bias, and a few such as ankylosing spondylitis show a bias toward males (Voruganti & Bowness, 2020).

Outside of autoimmune disorders, atopic allergies, including eczema and asthma, also display sex differences with a general bias in adulthood towards females over males (Gutiérrez-Brito et al., 2024). Asthma prevalence in children is in fact higher in males than females. However, in adults this trend reverses, and prevalence and mortality are both higher in females (Chowdhury et al., 2021).

Immune sexual dimorphism is also known to affect disease susceptibility, more generally with males displaying increased susceptibility to infection. This was highlighted recently by SARS-CoV-2, in which older males were more likely to suffer from severe infection, however is also seen in response to other viruses such as influenza

(Bunders & Altfeld, 2020). In terms of parasitic infections, males worldwide are more likely to be infected with parasitic worms, and often present with higher parasite burden (Zuk & McKean, 1996). However, males often have higher rates of exposure to these pathogens due to environmental factors, which could act as a cause for these differences. Sexual dimorphism also extends to vaccine efficacy, as generally, vaccines have been shown to be more effective in females, with stronger induction of antibody responses when compared to males (Fischinger et al., 2018).

Cell-intrinsic and extrinsic mediators of immune sexual dimorphism have been identified in recent years. These are mainly be split between the impact of sex hormones on immune cells, and the X and Y chromosomes, with a particular focus on the effect of X chromosome inactivation. However, research in this area is relatively novel, further research into identifying drivers of immune sex dimorphism will be essential for improving treatment of immunopathologies and vaccine efficacy.

1.5.2 Sex hormones

Sex hormones, such as testosterone, oestrogen and progesterone, are all important cell extrinsic mediators of immune sexual dimorphism. Many immune cells can respond to sex hormones via expression of oestrogen, androgen and progesterone receptors, modulating their responses to infection. Oestrogen is generally pro-inflammatory (Chakraborty et al., 2023), although the effects can vary between different cell types. For example, oestrogen is known to increase baseline neutrophil numbers but may have an inhibitory effect on NK cell cytotoxicity. Oestrogen is strongly linked to the expression of inflammatory cytokines, with oestrogen treatment in mice shown to significantly increase both IFNγ and IL2 expression in lymphoid cells (Karpuzoglu-Sahin et al., 2001).

Testosterone, meanwhile, provides an anti-inflammatory effect on immune responses, although again this is thought to vary between different cell types (Bupp & Jorgensen, 2018). Testosterone suppresses immune cell activation, for example reducing NK cell activity, and inhibiting M1 macrophage differentiation (Klein & Flanagan, 2016). *In vivo* data from a cohort undergoing hormone replacement therapy also suggests that testosterone may also cause a general attenuation of viral type-I IFN responses, particularly affecting DCs (Lakshmikanth et al., 2024). In terms of cytokine production, testosterone is strongly linked to increased expression of anti-inflammatory cytokine IL10, and has previously been shown to upregulate its expression in mouse splenocytes (Liva & Voskuhl, 2001).

Progesterone displays a more mixed impact on immune cells, with both pro- and anti-inflammatory roles. In terms of its anti-inflammatory impacts, progesterone inhibits activation of different cells, such as DCs, macrophages, NK cells and $CD4^+$ T cells (Raghupathy & Szekeres-Bartho, 2022). Progesterone can also signal to affect cytokine and chemokine secretion, reducing expression of cytokines such as IL1β and IL12, macrophage inflammatory proteins 1a and 1b, and RANTES, mostly via suppression of the NF-kB pathway (L. Cui et al., 2022). However, differing levels of progesterone have been suggested to have differing immunomodulatory effects, with high levels triggering the previously mentioned anti-inflammatory effects, while lower levels were more generally pro-inflammatory. In $CD4^+$ T cells, lower serum levels of progesterone were able to enhance T cell activation (Papapavlou et al., 2021). Furthermore, progesterone in the context of hormone replacement therapy was shown to increase pro-inflammatory cytokines IL6 and TNFα levels (Brooks-Asplund et al., 2002), and increased progesterone levels in males is linked to increased background levels of inflammation (Zitzmann et al., 2005).

1.5.3 X chromosome inactivation and Xi escape

One of the major cell intrinsic mediators of immune sexual dimorphism are genes located on the X chromosome. To avoid differences in gene dosage between females and males, one X chromosome is epigenetically silenced in females, and is referred to as the inactive X (Xi). X inactivation is epigenetic and occurs randomly in one X chromosome during embryo development. This inactivation state is inherited during all future cell divisions (Loda et al., 2022).

The process of X inactivation is primarily mediated by the X-inactive specific transcript (*XIST*) lincRNA. *XIST* is transcribed during early embryogenesis, and spreads from its gene locus to cover the entire Xi, interacting with Cip1-interacting zinc finger protein (CIZ1) and HNRNPU to recruit transcriptionally repressive elements to the Xi (Panning, 2008). Here, complexes such as SPEN, which is involved in histone deacetylation, PRC2, which forms heterochromatin via H3K27me3 deposition, and DNMT3b, which causes DNA methylation at CpG islands, are all recruited and contribute to generating an epigenetically repressed Xi state (Augui et al., 2011; Loda et al., 2022). Meanwhile, *XIST* expression in the active X chromosome (Xa) is repressed to prevent accidental transcriptional silencing, via the expression of lncRNA *TSIX*. *TSIX* runs antisense to *XIST*, and transcription of *TSIX* over the *XIST* promoter prevents its expression (Gayen et al., 2015). A third X-linked lncRNA, functional intergenic repeating RNA element (*FIRRE*), is also involved in X inactivation, specifically the nuclear organisation of the Xi. *FIRRE* forms interchromosomal contacts to aid in physical compression of the Xi and prevent physical access to transcription factors, helping to anchor the Xi in the perinucleolar region and contributing to its epigenetic repression (Fang et al., 2020).

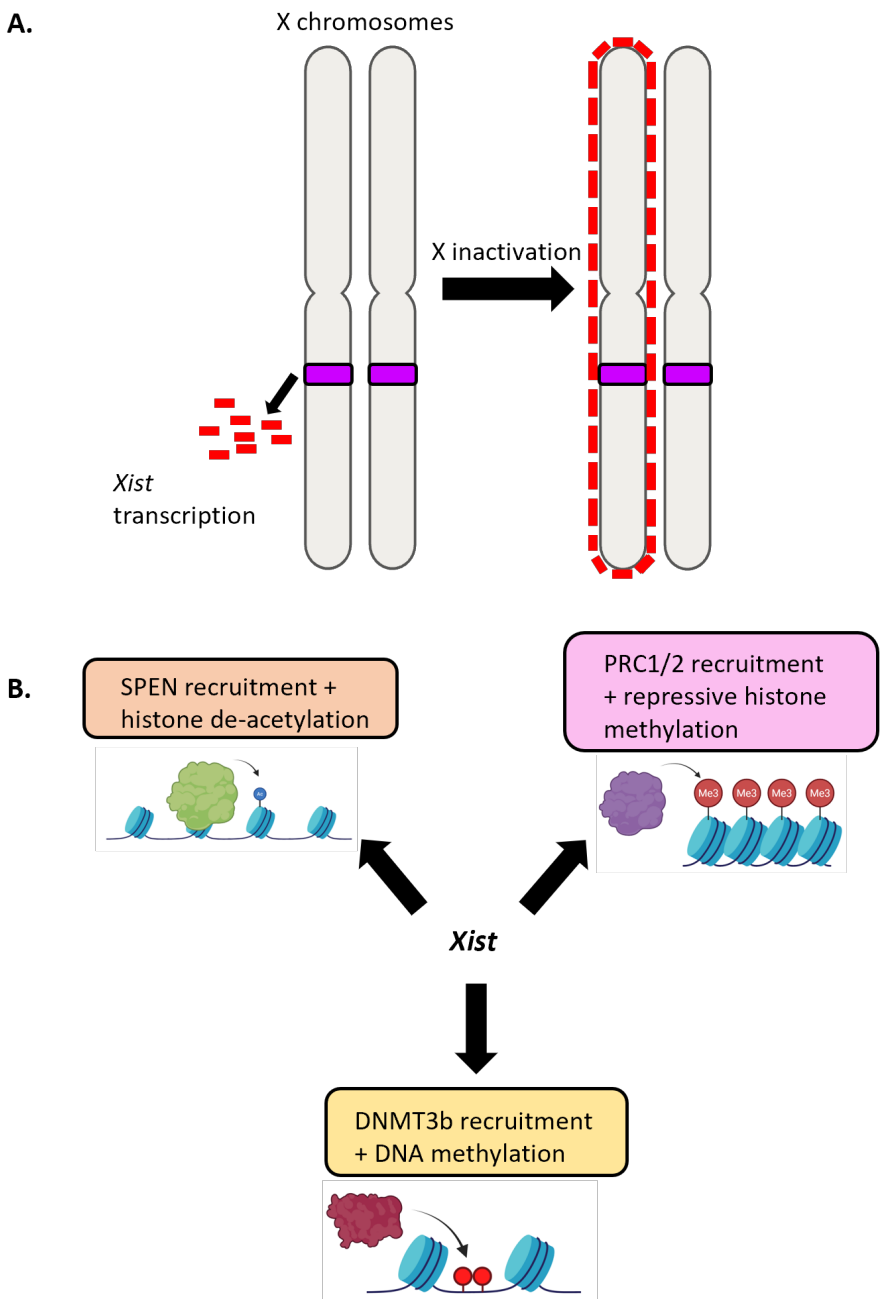

Figure 1.7 Schematic of X chromosome inactivation and Xist function

A. LncRNA *Xist* is transcribed from one X chromosome at random. Following transcription, *Xist* coats the Xi, preventing access from transcriptional machinery.

B. *Xist* recruits protein complexes for transcriptional repression of the Xi, including SPEN for histone de-acetylation, PRC1 and 2 for repressive histone methylation, and DNMT3b for DNA methylation at CpG islands.

Many genes on the X chromosome are involved in regulating the immune system, including genes for core cytokine receptor genes (*IL2Rγ, IL13R* and *IL9R*), innate immune pathogen recognition receptors (toll-like receptor (*TLR) 7* and *TLR8)*, and immune cell specific transcription factors (*FOXP3, GATA1* and *BTK*). Some X-linked genes have been shown to escape their epigenetic repression and continue transcription in a limited subset of cells. The rate of escape can vary between species; in humans, around 15% of X-linked genes are known to escape inactivation, while in mice this number is present at around 3% (Berletch et al., 2011). The distribution of genes able to escape is also not random with pockets of genes able to escape at higher rates than others typically on the short arm of the X chromosome in humans or near the centromere, although the escape genes vary between tissues.

Escape of these genes in immune cells is thought to be linked to the increased immune response strength and the increased development of autoimmune disorders in females (Wainer Katsir & Linial, 2019). Important immune genes such as *TLR7* are known to escape in human monocyte, B cells, and pDCs. Increased *TLR7* leads to increased activation and to higher expression of type-I IFNs (Youness et al., 2021). Furthermore, experimental ablation of Xi in mice is capable of causing splenomegaly and development of SLE-like symptoms, with specific impacts identified from X-linked genes such as *Tlr7*, *Cxcr3*, *Tasl* and *Tlr8* (Huret et al., 2024). As well as immune escape, the *XIST*-RBP X inactivation complex itself has been shown to promote autoimmune responses. The *XIST*-RBP complex is thought to be highly antigenic, as autoantibodies targeting the RBP components have been identified in human diseases such as SLE, multiple sclerosis and rheumatoid arthritis. Further confirming this, experimental transgenic *Xist* expression in male mice was then shown to cause significantly more severe pathology in a model of lupus (Dou et al., 2024).

1.5.4 Sexual dimorphism in $CD4^+$ T cells

$CD4^+$ T cell differentiation and function is influenced by biological sex. Females generally present higher numbers of $CD4^+$ T cells, which are more responsive to infection and display increased production of inflammatory cytokines such as IFNγ and IL2. Female $CD4^+$ T cells have also been noted to have a slight bias towards Th2 differentiation (Girón-González et al., 2000), while male $CD4^+$ T cells appear to produce more IL17, suggesting a potential bias towards Th17 differentiation (Manuel & Liang, 2021).

T cells express both androgen and oestrogen receptors. Oestrogen signalling in $CD4^+$ T cells has been shown to promote T cell activation, expression of pro-inflammatory cytokines, and differentiation to effector T cells. Oestrogen has also been linked to a general suppression of core Treg transcription factor FOXP3 (Mohammad et al., 2018). Interestingly, pregnancy-associated hormones such as progesterone are known to affect Th cell differentiation, promoting Th2 responses in foetal tissue (H. Lin et al., 1993). This is thought to have a protective effect, helping to prevent miscarriage. Meanwhile, testosterone, likely due to its ability to induce IL10 expression, promotes Treg differentiation, with other general anti-inflammatory impacts on Th cell differentiation such as increased rates of apoptosis in activated cells (Page et al., 2006). In a study on transgender men receiving testosterone therapy, testosterone caused an overall decrease in inflammatory Th1 and Th17 responses from $CD4^+$ T cells, along with increased expression of Tregs (Henze et al., 2025). Testosterone has also been shown to particularly affect IL10 expression in T cells. Male splenocytes stimulated with anti-CD3 produce higher levels of IL10, and stimulation of female splenocytes with anti-CD3 and dihydrotestosterone increased IL10 expression (Liva & Voskuhl, 2001).

X-linked genes and their escape have also been shown to impact $CD4^+$ T cell function, and may also be linked to autoimmune disease progression. X-linked genes CXCR3 and CD40LG were shown to escape inactivation in activated T cells in SLE, while in B cells the *Xist* cloud over the Xi was shown to have an altered distribution, potentially playing a role in disease progression and contributing to the sex bias in SLE (J. Wang et al., 2016). X-linked gene KDM6a is often known to be significantly upregulated in female $CD4^+$ T cells, and this has been shown to impact the expression of cytokines such as IFNγ, IL2, IL17 and IL5. This may also play a role in the development of autoimmune diseases, as deletion of KDM6a from CD4+ T cells in mice was protective against experimental autoimmune encephalitis (EAE) (Itoh et al., 2019). *Xist* and Xi dynamics are also affected in $CD4^+$ T cells, potentially allowing for greater immune escape. In naive $CD4^+$ T cells *Xist* does not localise to the Xi, and only re-localises during T cell activation (J. Wang et al., 2016). This less repressive state is thought to allow for partial Xi reactivation and easier gene escape, with escape of genes including *Cxcr3*, *Il2rg* and *Kdm6a* (Forsyth, Toothacre, et al., 2024).

1.6. Hypothesis and aims

1.6.1 Hypothesis

Our previous work focused on Th1 cells. Here, we tested the hypothesis that *Malat1* controls Th2 differentiation. Driven by early results during the project, we refined our hypothesis to test that *Malat1* is a sex-specific determinant of Th2 cell differentiation. We aimed to explore the differences in the *Malat1* effects on female and male T cell differentiation and investigate the molecular mechanisms underpinning these effects.

1.6.2 Aims

1. To determine the role of sex and *Malat1* on end-stage Th2 differentiation, using both *in vitro* and *in vivo* models of Th2 differentiation – Chapter 3.
2. To investigate the role of *Malat1* during early Th2 differentiation – Chapter 4.
3. To investigate nuclear speckle function and X chromosome inactivation during Th2 differentiation, and whether *Malat1* affects these processes – Chapter 5.

2. Materials and Methods

2.1 Animals and cell lines

2.1.1 Mice

Animal care and experimental procedures were regulated under the Animals (Scientific Procedures) Act 1986 (revised under European Directive 2010/63/EU) and were performed under U.K. Home Office License (project license number PP0841992 for breeding and PP9423191 for *S. mansoni* egg injections) with approval from the University of York Animal Welfare and Ethical Review Body. Animal experiments conformed to Animal Research: Reporting of In Vivo Experiments guidelines (du Sert et al., 2020). C57BL/6 CD45.2 mice were obtained from Charles River laboratories (UK). *Malat1*$^{-/-}$ mice were obtained from the Riken Institute (Nakagawa et al., 2012). *Ciz1*$^{-/-}$ mice were provided by Dawn Coverley. These mice were initially generated from C57BL/6 ES clone IST13830B6 (TIGM), with a neomycin resistance gene trap inserted downstream from exon 1 (Ridings-Figueroa et al., 2017). These mice also contained an inducible Ciz1 transgene via random integration transgene injected into (C57B6/CBA-F1 x C57B6/CBA-F1) F2 eggs, and an activator transgene via targeted integration at the ROSA26 locus in R1 ES cells (C57BL/6), however transgenic Ciz1 expression was not utilised in this thesis. Each of these transgenic lines were backcrossed onto C57BL/6 for 4-5 generations, then crossbred. They were then interbred without further backcrossing.

All mice were housed under specific pathogen free conditions and bred internally in the York University BSF facility as a homozygous line. In all experiments (*in vitro* CD4+ T cell differentiation and *in vivo* egg-injections) mice used were all between 6 and 12 weeks of age. Mice were euthanised via increasing concentrations of CO_2, followed by cervical dislocation.

2.1.2 Cell lines

Cell lines used were a murine T lymphocyte line (EL4), and a human T lymphocyte line (Jurkat). Cells were cultured under sterile conditions in complete Roswell Park Memorial Institute (RPMI) 1640 media (Gibco), supplemented with 10% heat inactivated Foetal Bovine Serum FBS (Gibco), 1x Glutamax (Gibco) and 1x penicillin + streptomycin (Gibco). Cells were kept in T-25 or T-75 flasks in a humidified incubator at 37ºC in 5% CO_2, and were passaged at a 1:10 split 2-3 times a week.

2.1.3 Cell counts

Cell counts were performed using trypan blue staining. 10 µl cell suspension was mixed with 10 µl 0.4% trypan blue solution (Cytiva). 10 µl of this was then loaded onto a haemocytometer chamber. Using a benchtop microscope, live cells were counted within a 16 square set. Multiplying this number by 2 x 10^4 gave the number of viable cells per 1 ml.

2.1.4 Freezing cells

For long term storage, cells were first counted, then pelleted by centrifugation at 250 x g, then suspended in 1 ml heat-inactivated FBS supplemented with 10% dimethyl sulphoxide (DMSO) (Sigma). Cells were then transferred to a cryovial, placed inside a Mr. Frosty Freezing Container (Thermo Scientific) and placed at -80ºC for up to a week. Cells were then transferred to liquid nitrogen tanks for longer term storage.

2.1.5 Thawing cells

Cell line cells were recovered from liquid nitrogen and thawed in a 37ºC waterbath. Cells were then added to 9 ml pre-warmed media, and pelleted via centrifugation at 250 x g. Cells were then resuspended in RPMI and cultured in a T-25 flask in a humidified incubator at 37ºC in 5% CO_2.

2.2 *In vitro* Th2 differentiation

2.2.1 Naïve $CD4^+$ T cell isolation

Spleens and axillary, brachial, mesenteric, and inguinal lymph nodes were collected from females and males of *WT* or *Malat1*$^{-/-}$ mice. These were homogenised through a 70 μm filter (Falcon) into a 50 ml Falcon tube using a syringe plunger, then flushed with 10-15 ml of complete RPMI media. Resulting cell filtrate was then pelleted and washed twice in 10 ml RPMI, with centrifugation at 450 x g for 5 minutes at 4 ºC. Cells were then gently suspended by pipetting in 3 ml Ammonium-Chloride-Potassium (ACK) lysis buffer (Gibco) for 10 minutes, pelleted, and washed again once with 10 ml of RPMI. Resulting pellets were then visually inspected to ensure the red blood cells had lysed. Following this, cells were suspended in 1 ml of complete RPMI and counted using a haemocytometer and trypan blue staining.

Cells were next stained for Magnetic-Activated Cell Sorting (MACS) column isolation using the Miltenyi Mouse Naive CD4+ T Cell Isolation Kit (130-104-453). Per 10^7 cells- 40 μl MACS buffer (2 mM Ethylenediaminetetraacetic acid (EDTA), 0.5% Bovine Serum Albumin (BSA), 1x Phosphate-Buffered Saline (PBS), made in-house) containing 3 μl of isolation kit biotinylated antibody cocktail was then added to each sample. This cocktail contains antibodies raised against CD8a, CD11b, CD11c, CD19, CD25, CD45R, CD49b, CD105, MHC II, Ter-119 and TCRγ/δ, to allow for negative selection of $CD4^+$ T cells. Samples were mixed well by pipetting and incubated at 4ºC for 10 minutes. 20 μl more of MACS buffer was then added along with 6 μl of anti-biotin microbeads and 3 μl of anti-CD44 microbeads. Samples were mixed well again by pipetting, then incubated at 4ºC for 15 more minutes.

Following staining, samples were washed in 5 ml MACS buffer, then pelleted and resuspended in 1 ml MACS buffer. LS columns (Miltenyi Biotec, 130-042-401) were then loaded onto a QuadroMACS separator pre-cooled to 4ºC, and washed with 3 ml of MACS buffer to equilibrate the columns. Samples were then loaded into the LS columns. The columns were rinsed with 3 ml MACS buffer, and the total eluate from the column was collected. Samples were then washed with 10 ml RPMI, pelleted and resuspended in 1 ml RPMI. Sample purity was assessed further by taking a small portion of sample (~10 µl) and performing flow cytometry staining, assessing CD4 and TCRβ expression (example purity and gating strategy shown in section 2.4.5). This typically resulted in a purity of ~95%.

2.2.2 *In vitro* Th2 differentiation

An overview of the Th2 differentiation assay is shown in *Figure 2.1*. Flat-bottom 96-well TC-treated plates (Costar) were incubated at 37ºC with 10 µg/ml anti-CD3ε activating antibody (clone 145-2C11, hereafter referred to as anti-CD3) in 100 µl PBS for 4 hours. After this incubation, the excess anti-CD3 was removed, leaving the majority of the anti-CD3 plate-bound. Purified naïve CD4+ T cells were then counted and resuspended at 5 x 10^6 cells per ml of complete RPMI (supplemented with 15% instead of 10% FBS). 100 µl of cell suspension (5 x 10^5 cells) was then added per well, and stimulated via addition of 100 µl of complete RPMI containing a cytokine and antibody activation mix. The final well (200 µl total volume) concentrations of the activation mix were as follows: 4 µg/ml soluble anti-CD28 (Biolegend, clone 37.51), 30 ng/ml mouse rIL4 (PeproTech), and 5 µg/ml anti–IFNγ (Biolegend, XMG1.2). Cells were then placed in a humidified incubator at 37ºC with 5% CO2. After 4 days, the cells were removed and

washed with 10 ml RPMI. Cells were then re-plated in flat-bottom 96 well plates in 200 µl complete RPMI containing 10 U/ml human recombinant IL2 (PeproTech), which causes late-stage cytokine expression and cell expansion. Cells were placed in a humidified incubator for 2 more days.

When investigating different stages of differentiation, samples were taken at the indicated time or day following addition of the initial activation cocktail, from day 0 (naïve cells) to day 6 (end-point differentiation). To assess end-stage differentiation efficacy, whole wells were taken as samples at the end-point of differentiation to assess for cytokine and receptor expression by flow cytometry, or transcript expression by qRTPCR (both detailed later in the methods).

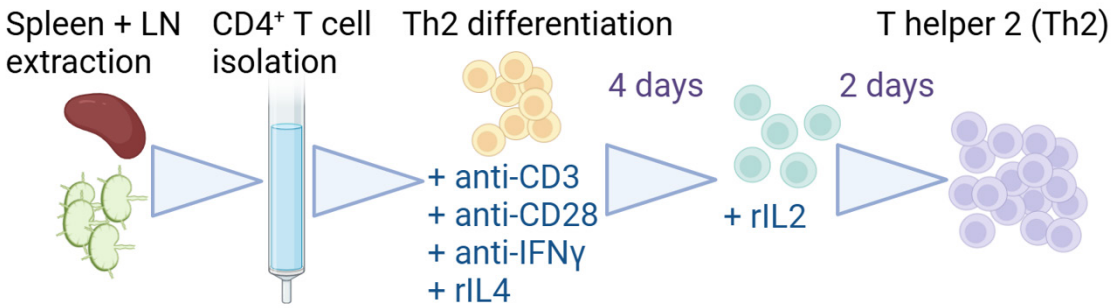

Figure 2.1 Schematic for the Th2 differentiation assay

Spleens and lymph nodes were extracted, and naïve $CD4^+$ T cells were obtained by MACS column isolation. Cells were differentiated towards a Th2 phenotype via addition of anti-CD3, anti-CD28, anti-IFNγ and rIL4. After 4 days, cells were resuspended in rIL2 for 2 more days, resulting in differentiated Th2 cells. Figure created in Biorender.

2.2.3 Anti-CD3 titration assays

To assess the effect of differing activation strength on Th2 differentiation, flat-bottom 96-well plates were incubated for 4 hours at 37ºC with 100 µl anti-CD3ε in PBS, with anti-CD3ε concentrations varied at 2, 5, 10 and 20 µg/ml. Volumes added were kept consistent via supplementing with PBS. Following this, excess anti-CD3ε was removed, and then the Th2 differentiation proceeded as normal, with analysis of cytokine expression by flow cytometry at end-point differentiation. An overview of this is shown in *Figure 2.2*.

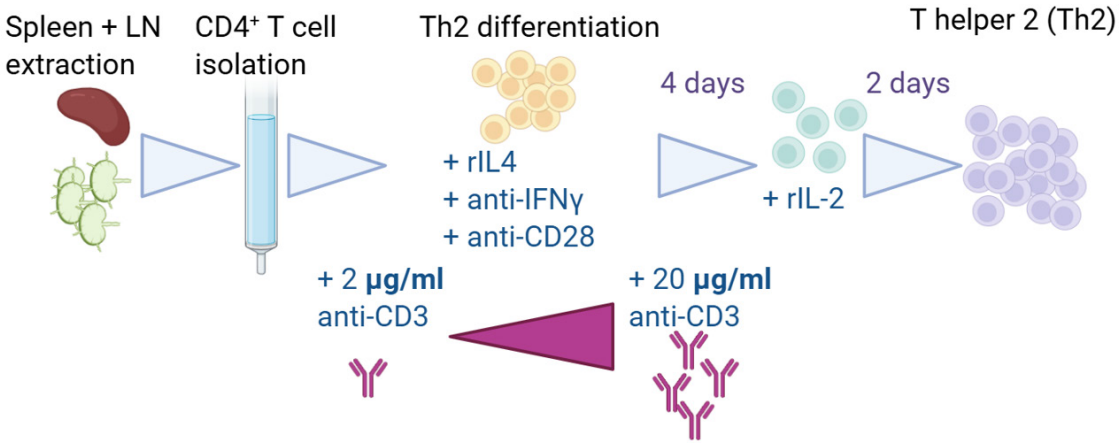

Figure 2.2 Schematic of the Th2 differentiation assay with anti-CD3 titration

Schematic for Th2 differentiation with anti-CD3 titration. Differentiation was performed as shown in Figure 2.1, but with plate-bound anti-CD3 levels varied between 2 and 20 µg/ml. Figure created in Biorender.

2.2.4 rIL2 titration assays

To assess the effect of differing IL2 levels on Th2 differentiation, after the first 4 days of Th2 differentiation cells were removed from the plate and washed with 10 ml RPMI 1640. Cells were then replated in flat-bottom 96 well plates in 200 µl RPMI containing human rIL2, with concentrations varied at 2, 5, 10 and 20 U/ml. Volumes of rIL2 added were kept consistent via supplementing with PBS. Following this, Th2 differentiation proceeded as normal, with cytokine expression assessed at end-point differentiation via flow cytometry. An overview of this experiment is shown in *Figure 2.3*.

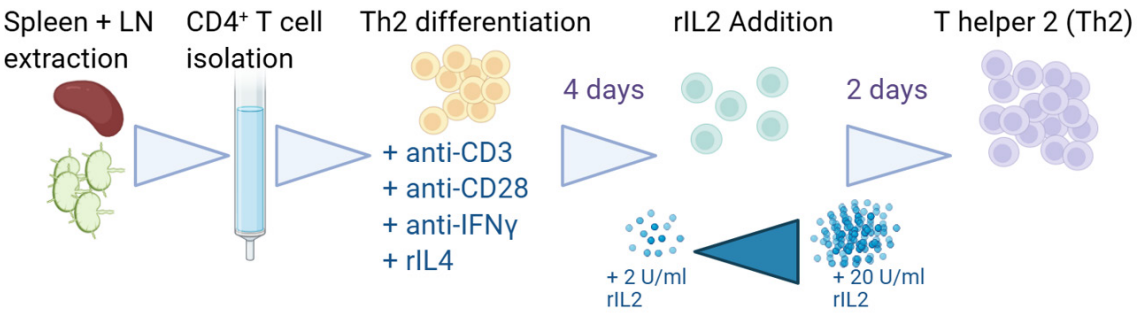

Figure 2.3 Th2 differentiation assay with rIL2 titration

Schematic for Th2 differentiation with rIL2 titration. Differentiation was performed as shown in Figure 2.1, but with resuspension at day 4 in rIL2 concentrations varied between 2 and 20 μg/ml. Figure created in Biorender.

2.2.5 IFNβ treatment

To assess the impact of type-I IFNs on Th2 differentiation, the Th2 activation mix was supplemented so the final well volume contained 5000 U/ml mouse IFNβ (Prospec, CYT-651). An equivalent volume of PBS as the IFNβ added was used as a control. Following this, Th2 differentiation proceeded as normal, with RNA extracted on day 2 for analysis of type-I IFN genes by qRTPCR, and cytokine expression assessed at end-point differentiation by flow cytometry.

2.2.6 GapmeR treatments

For *Malat1* knock-down experiments, Non-Targeting Control (NTC) or Malat1-targeting antisense oligonucleotide GapmeRs from QIAGEN (Hilden, Germany; LG00000002-DDA and LG00000008-DDA, respectively) were used. GapmeRs enter the cells via gymnosis, where they then bind to the target RNA and trigger RNase H-mediated degradation. GapmeR sequences are listed below in *Table 2.1*. Prior to use, GapmeRs were re-suspended at 50 μM in nuclease free water, gently mixed, then aliquoted under sterile conditions and stored at 20ºC. Freeze thawing of GapmeRs was avoided.

GapmeRs were added to naïve *WT* CD4+ T cells either on day 0 alongside the activation mix, or on day 4 alongside rIL2, at a final well concentration of 100 nM. Cytokine expression was then assessed at end-point differentiation by flow cytometry, and the efficacy of *Malat1* knock-down and the effect of this on other transcript levels was assessed at different days throughout differentiation by qRTPCR.

Table 2.1 GapmeR antisense oligonucleotide sequences

Target	**Sequence (5'-3')**
Antisense LNA GapmeR Control: Negative control A	A*A*C*A*C*G*T*C*T*A*T*A*C*G*C
Antisense LNA GapmeR control: *Malat1* (mouse) positive control	G*T*C*A*C*A*A*T*G*C*A*T*T*C*T*A

2.2.7 Blocking antibody treatment

Both the activation mix on day 0 and the rIL2 mix at day 4 were supplemented with either an anti-IL10R blocking antibody (1B1.3A, Bio X Cell) with final well concentrations of 10 μg/ml of antibody. Rat IgG at 10 μg/ml was used as a control. End-point activation of samples was assessed by flow cytometry.

2.2.8 Human Th cell differentiation

Human Th cells were provided by Dr. Dave Boucher, and extracted from 10ml whole blood using the EasySep™ Direct Human T Cell Isolation Kit (Stemcell Technologies). 100,000 $CD4^+$ T cells were plated in a 96 well TC treated plate, in 200 μl RPMI 1640 containing 30 U/ml human recombinant IL2 (PeproTech) and 5μl ImmunoCult Human CD3/CD28 T Cell Activator (Stemcell Technologies). For Th2 differentiation, 1 ug/ml anti-IFNγ (Biolegend, MD-1), 1 ug/ml anti-IL12 (Biolegend, C8.6) and 50 ng/ml rIL4 (Biolegend) were added to the activation mix. After 3 days, cells were either collected for immunofluorescence staining and qRTPCR, or resuspended in 200 μl RPMI containing 30 U/ml IL2 and expanded for 4 days.

2.2.9 Recombinant cytokine storage

All cytokines used in these experiments were purchased as sterile lyophilised powders, from indicated suppliers. Cytokines were resuspended at desired concentrations under sterile conditions in PBS containing 0.1% BSA, as indicated by the manufacturer. Cytokines were then aliquoted and stored at -80ºC until required. Cytokines were not re-used after thawing, to avoid degradation of activity by freeze-thaw cycles.

2.3 Quantitative real-time PCR

2.3.1 RNA extraction

Cells were washed with 1 ml of PBS, then pelleted by centrifugation at 450 x g. The supernatant was discarded, and the cells were lysed by the addition of 700 µl Qiazol (Qiagen) and mixed well. Once in Qiazol, samples could be frozen at -80ºC for short-term storage.

RNA was next extracted using the Qiagen RNeasy mini kits. Frozen samples in Qiazol were thawed at room temperature, then mixed thoroughly with 140 µl chloroform and incubated at room temperature for 2 minutes. Samples were then centrifuged for 15 minutes at 12,000 x g and 4ºC. The clear upper aqueous phase was transferred to a new tube containing 1.5x the volume of 100% ethanol, and mixed thoroughly. Samples were loaded into silica columns with 2 ml collection tubes (Qiagen) and spun at >8000 x g for 15 seconds at room temperature, and the flow-through was discarded. The columns were washed once with 650 µl buffer RWT, and twice with 450 µl buffer RPE, with 15 second centrifuge spins and discarding of the flow-through between each wash. Columns were spun for an extra 2 to remove all excess buffer, transferred to a new collection tube, and spun again for 1 minute to dry the membrane. The columns were then transferred to a new RNase free 1.5 ml Eppendorf tube, and 30 µl nuclease free water was added directly onto the membrane. RNA was then eluted from the columns via centrifugation for another minute. RNA yield and quality were assessed using the nanodrop 2000 (ThermoFisher), and RNA was kept at -80ºC for long term storage.

If RNA samples were to be sent for sequencing, on-column DNase I digestion was performed to remove any contaminating genomic DNA. The RWT wash step was split in

two, and columns were first washed with 350 µl buffer RWT, spun for 15 seconds, then incubated with 80 µl DNase I solution (Qiagen RNeasy on-column DNase digestion kit) at room temperature for 15 minutes. Following this, columns were washed again with 350 µl buffer RWT and spun for 15 seconds. RNA extraction then continued as normal.

2.3.2 cDNA synthesis

The isolated RNA was converted to its complimentary DNA (cDNA), for use in qRTPCR reactions. Per sample, 50-500ng of RNA (typically around 5 µl) was mixed with 1 µl of 50 ng/µl random hexamer primers (ThermoFisher), 1 µl 10 mM dNTP mix (Qiagen), and nuclease free DEPC treated water to take the total volume up to 13 µl (ThermoFisher). Samples were incubated at 65 ºC for 5 minutes to denature the RNA, then at 4ºC for 1 minute. Following this, 4 µl of 5x First Strand Synthesis Buffer (Invitrogen), 2 µl DTT (Invitrogen), 0.5 µl RNase OUT (Invitrogen) and 0.5 µl SuperScript II (Invitrogen) were added to each sample. Samples were then incubated at 25ºC for 10 minutes, 50ºC for 50 minutes, and 85ºC for 5 minutes, then held at 4ºC. The incubations were carried out using a VeritiPro 96 well thermal cycler (Applied Biosystems). Resultant cDNA was diluted 1:2 with nuclease free water, then stored at -20ºC.

2.3.3 qRTPCR

Transcript expression from cDNA was determined using quantitative real-time PCR (qRTPCR) assays. For primers designed in-house, 20 µl reactions were performed containing 1 µl of cDNA produced from Methods section 2.3.2, 10 µl SYBR green 2x mastermix (Invitrogen), and 0.6 µl of both forward and reverse primer 10 µM stocks to

give 0.3 nM final concentration. Reactions were loaded into a well of a MicroAmp Optical 96-Well Reaction Plate (Applied Biosystems). For Quantitect primer assays (Qiagen), per well 1 µl cDNA was mixed with 10 µl fast SYBR green master-mix, 7 µl nuclease free water and 2 µl Quantitect primer assay.

Where possible, each reaction was performed in duplicate. Plates were loaded into either a StepOnePlus Real Time PCR System (Applied Biosystems) or a QuantStudio 3 PCR system (ThermoFisher) for analysis. Relative transcript levels were determined using the ΔΔCt method, with U6 as a reference transcript. In short- average Ct values (the cycle at which fluorescence appears above background levels) of reference U6 were subtracted from average Ct values of genes of interest, to create ΔCt values. The average ΔCt value was then determined from a control group (typically *WT* female samples), and subtracted from all samples, to generate ΔΔCt values. Finally, fold change was determined by the equation below.

Fold change = $2^{-\Delta\Delta Ct}$

2.3.4 qRTPCR primer validation

All in house qRTPCR primers were validated prior to use, to ensure they displayed a single melt curve, and had primer efficiencies of 90-110%. Some in-house primers had been optimised previously by other lab members. To determine primer efficiency of new primers, 5 point standard curves were generated by serially diluting cDNA known to contain expression of the target gene. The qRTPCR reaction was then performed including the new primer pair on the serial dilution of cDNA. Using Excel, Ct values were plot against a log of the serial dilution, and the slope was determined. The following equation was then used to calculate efficiency.

Efficiency (%) = $(-1/(10^{slope}-1)) \times 100$

For transcripts proving difficult to validate primers for, such as those for some transcription factors and cytokines, Quantitect primer assays were purchased from Qiagen. All primers used in this thesis are listed in *Table 2.2*.

Table 2.2 Primer sequences used for qRTPCR

Transcript	Forward Primer	Reverse Primer
Malat1	TGCAGTGTGCCAATGTTTCG	GGCCAGCTGCAAACATTCAA
Il2ra	GCATAGACTGTGTTGGCTTCTGC	GCGTTGCTTAGGAAACTCCTGG
Il2rg	GGAGCAACAGAGATCGAAGCTG	CCACAGATTGGGTTATAGCGGC
Il2	CCAATTCGATGATGAGTCAGC	CTTATGTGTTGTAAGCAGGAGG
Cd69	CCCTTGGGCTGTGTTAATA	AACTTCTCGTACAAGCCTG
U6	CGCTTCGGCAGCACATATAG	TTCACGAATTTGGCTGCTAT
Il4	AACGAAGAACACCACAGAGAGTGAG	CGATGAATCCAGGCATCGAAAAG
Ifit1bl1	GAGATGGACTGTGAGGAAGGCT	ATCCAGGCGATAGGCTACGACT
Ifit1	GCAGAGAGTCAAGGCAGGTT	TTGTGCATCCCCAATGGGTT
Ifit3b	GCTCAGGCTTACGTTGACAAGG	CTTTAGGCGTGTCCATCCTTCC
Ifnar1	TGTGCTTCCCACCACTCAAG	AGGCGCGTGCTTTACTTCTA
Ifnar2	TGGGTATCCAGATGAACCTTG	GCCCTCCAACCACTTATCTG
Iigp1	GAGAACCAAGGTGGACTCTGAC	GAGAGCAGGAAGATTGGTGGCT
Irf1	CCCACAGAAGAGCATAGCAC	AGCAGTTCTTTGGGAATAGG
Irf7	GCATTTCGGTCGTAGGGATCTGGATGAAGA	CGTACACCTTATGCGGATCAACTGGA
Son	TTCCGGGAAATACAACAGGA	GGGTGGATTTGTTTCACCAT
Srrm2	CTGCAAGAATGTCCCAGGTT	ATGCCGGAATAGCAGATGTC

Stat1	TACGGAAAAGCAAGCGTAATCT	TGCACATGACTTGATCCTTCAC
Ifna(1+13)	TGCCCAGCAGATCAAGAAGG	TCAGGGGAAATTCCTGCACC
Ifnb	GTACAACAGCTACGCCTGGA	GAGTCCGCCTCTGATGCTTA
Ifna4	CAATGATTGAACCCACATCCCCA	CCTTGCTTTCCAATTCTCTTTTCA
Xist	CTACTGCTCCTCCGTTACATCA	AGGAGCACAAAACAGACTCCA
Gata3	Mm_Gata3_1_SG QuantiTect Primer Assay	
Tbet	Mm_Tbx21_1_SG Quantitect Primer Assay	
Maf	Mm_Maf_1_SG Quantitect Primer Assay	
Il10	Mm_Il10_1_SG QuantiTect Primer Assay	

2.4 Flow cytometry

2.4.1 Buffers and antibodies

*Antibodies***-** Antibodies used for flow cytometry, including their target, conjugated tag, company purchased from, clone and dilution are listed in ***Table 2.3***. Appropriate isotype controls as recommended by the manufacturer were used for intracellular cytokine or transcription factor staining, while fluorescence minus one (FMO) controls were used for surface receptors.

FACS buffer- PBS containing 0.5% BSA and 0.05% sodium azide

ICC staining- performed using Fixation/Permeabilisation solution, and 1x Perm/Wash Buffer (BD Bioscience).

Transcription factor staining- performed using FoxP3 Fixation/Permeabilisation solution and 1x Permeabilisation buffer (eBioscience).

Table 2.3 Antibodies used in flow cytometry experiments

Antibody target	Fluorophore/ Conjugate	Company	Clone	Dilution
TCRβ	PE-Cy7	Biolegend	H57-597	1/250
CD19	APC-Cy7	Biolegend	6D5	1/250
MHC class II	Alexa Fluor 700	Biolegend	M5/114.15.2	1/250
Ly6G	APC-Cy7	Biolegend	1A8	1/250
Ly6C	BV605	Biolegend	HK1.4	1/250
CD64	PE	Biolegend	X54-5/7.1	1/250
CD11b	PB	Biolegend	M1/70	1/250
CD44	FITC	Biolegend	IM7	1/250
CD62L	PE	Biolegend	MEL-14	1/250
CD8α	PB	Biolegend	53-6.7	1/250
CD4	PerCP/Cy5.5	Biolegend	RM4-5	1/250
IFNγ	FITC	Biolegend	XMG1.2	1/100
IL10	PE	Biolegend	JES5-16E3	1/100
IL4	PE-Dazzle or APC	Biolegend	11B11	1/100
IL2Rα	PerCP/Cy5.5 or APC	Biolegend	PC6.1	1/250
CD69	APC	Biolegend	H1.2F3	1/250
IL2Rγ	PE	Biolegend	TUGm2	1/250
GATA3	PE-Dazzle 594	Biolegend	16E10A23	1/100
IL13	PB	eBioscience	eBio13A	1/100
IFNAR1	PE	Biolegend	MAR1-5A3	1/250
streptavidin	PE-Cy7	Biolegend	405206	1/400

SIGLECF	PerCP-eFluor 710	ThermoFisher	1RNM44N	1/250
iNOS	PE-eFluor 610	ThermoFisher	CXNET	1/125
goat anti-rabbit	A647	ThermoFisher	A27040	1/400
YM1	Biotin	R&D systems	BAF2446	1/200
anti-murine RELMα	Unconjugated	Invitrogen	H1717	1/200
CD45.2	BV786	BD Bioscience	Clone 104	1/250

2.4.2 Surface staining

Cells were pelleted by centrifugation at 450 x g at 4ºC, the supernatant was discarded, and the cells were washed twice in 800 µl ice cold 1x PBS. Cells were then stained with 0.1 µl Zombie Aqua live/dead stain (BioLegend) in 100 µl PBS, for 10 minutes at 4ºC in the dark. Following this, cells were washed with 800 µl fluorescence activated cell sorting (FACS) buffer, then the supernatant was discard and Fc receptors were blocked with 3 µg/ml rat IgG (Sigma-Aldrich) for 5 min at 4°C in the dark. Cells were then stained with the required antibodies in 50 µl FACS buffer, for 30 min at 4°C in the dark. Samples were washed twice more in 800 µl FACS buffer, and resuspended in 200 µl FACS buffer for flow cytometry analysis.

If fixing was required, following surface staining cells were instead washed with 800 µl PBS, then fixed in 150 µl of 4% paraformaldehyde (Fisher bioreagents) at 4ºC for 20 minutes in the dark. Following this, cells were pelleted and washed twice more with 800 µl FACS buffer, then resuspended in 200 µl FACS buffer for flow cytometry analysis.

2.4.3 Intracellular cytokine staining

Prior to flow staining, cells were stimulated in wells via addition of 500 ng/ml PMA, 1 µg/ml ionomycin, and 10 µg/ml brefeldin A (all Sigma-Aldrich). Cells were incubated with these reagents in a humidified incubator for 4 hours at 37°C with 5% CO_2. Live dead and surface staining then proceeded as normal following this.

Following surface staining, cells were instead pelleted and washed twice with 800 µl FACS buffer, and resuspended in 150 µl Fixation/Permeabilisation solution for 20 minutes at 4ºC in the dark. Cells were then pelleted and washed twice with 500 µl of 1x Perm/Wash buffer, at which point cells could be left overnight in Perm/Wash buffer. Cells

were then resuspended in 50 µl Perm/Wash buffer containing required antibodies targeting intracellular cytokines for 30 minutes at 4ºC. Cells were then pelleted, washed twice more with 500 µl Perm/Wash buffer, then resuspended in 200 µl FACS buffer for flow cytometry analysis.

2.4.4 Transcription factor staining

Following surface staining, cells were washed twice with 800 µl FACS buffer, then fixed and permeabilized (either for 1 hour or overnight, both at 4°C in the dark) in 150 µl of the eBioscience FoxP3/Transcription Factor Fixation/Permeabilization solution (ThermoFisher). Cells were then washed twice in 800 µl of 1x eBioscience Permeabilization Buffer (ThermoFisher), then stained by resuspension in 50 µl 1x Permeabilisation Buffer containing antibodies targeting transcription factors. Cells were then washed twice more in 800 µl 1x Permeabilisation Buffer and resuspended in 200 µl FACS buffer for flow cytometry analysis.

2.4.5 Data acquisition and gating strategy

Samples were run and data was acquired on either a LSRFortessa (BD Biosciences) or a Cytoflex LX (Beckman Coulter). Compensation was carried out using single stained cells per each experiment, and appropriate isotype or fluorescence-minus-one (FMO) controls were used to identify positive and negative populations. At the cytometer, samples were gated for Live cells against SSC, then with FSC vs SSC to identify the cell population, followed by FSC-A vs FSC-H and SSC-A vs SSC-H to identify singlet events. This gating was standard for all experiments performed. For all *in vitro* Th2 differentiation experiments, a $TCR\beta^+$ vs $CD4^+$ gate was then created to identify

the $CD4^+$ T cell population within. An example of this is shown in *Figure 2.4*. Samples were run for a further 2 minutes, with minimum 10,000 events collected in the $CD4^+$ $TCR\beta^+$ gate. Further analysis was then performed using FlowJo V10.6.1 (FlowJo) for analysing data from the LSRFortessa, or CytExpert 2.6 (Beckman Coulter) for analysing data from the Cytoflex LX, typically looking at receptor or cytokine expression as a percentage of $CD4^+$ $TCR\beta^+$ cells. Gating was performed using appropriate isotype or FMO controls (*Supplementary Figures 1+2*) to identify negative populations.

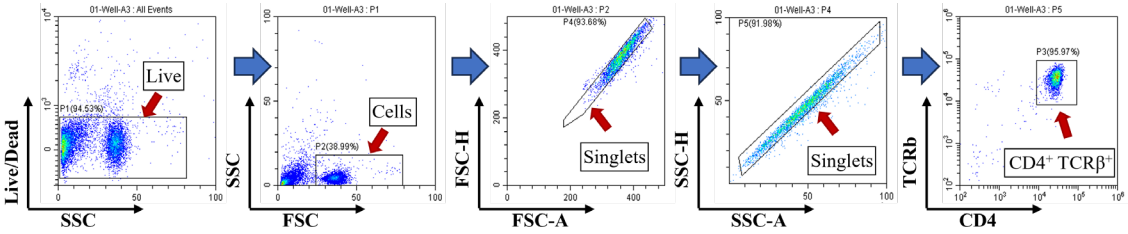

Figure 2.4 Gating strategy for determining $CD4^+$ $TCR\beta^+$ cells via flow cytometry

Example gating strategy for identifying live cells, singlets, and $CD4^+$ $TCR\beta^+$ cells.

2.5 Western blotting

2.5.1 Buffers

Transfer buffer- 1 x Trans-Blot Turbo Transfer Buffer (Bio-Rad).

1x Running buffer- 100 ml 10x Tris/Glycine/SDS stock (0.25 M Tris, 1.92 M Glycine, 1% SDS) (Geneflow) 900 ml ddH20.

1 x TBST- 100 ml 10x TBS, 900 ml H2O and 1 ml Tween.

Blocking buffer- 2% BSA TBST (0.1%) pH 8.0.

RIPA buffer- 150 nm NaCl, 10mM Tris pH7.4, 1mM PMSF, 1% Triton X-100, 1% sodium deoxycholate, 0.1% SDS.

2.5.2 Cell lysate generation

Cells were isolated and resuspended in radioassay immunoprecipitation (RIPA) buffer containing 1 µl of protease and phosphatase inhibitors (Protease Inhibitor Cocktail p8340, Phosphatase Inhibitor Cocktail II p5726, Phosphatase Inhibitor Cocktail III p0044, all from Sigma-Aldrich) per 100 µl of RIPA, at a density of ~$1x10^6$ cells per 30 µl of buffer. Samples were then centrifuged at 10,000 x g for 15 minutes at 4ºC, and the soluble fraction was isolated and stored at -20ºC.

2.5.3 Bicinchoninic assay (BCA)

Where appropriate, protein sample concentration was determined by Pierce BCA Protein Assay Kit (ThermoFisher). Protein samples in RIPA buffer were diluted 1 in 6

with PBS (2 µl protein sample in 10 µl PBS), and 5 µl of this mix was then added to a flat bottomed 96 well plate in duplicate. 95 µl of assay reagents (93.1 µl Buffer A + 1.9 µl Buffer B) was added to the samples, and the plate was incubated at 37ºC for 30 minutes. Calibration curves were generated from known concentration recombinant BSA protein standards using step-wise dilutions. Plates were read at 562 nm, and protein concentration was determined by comparing sample absorbance against the calibration curve.

2.5.4 PAGE gel protein separation

10 µg of sample was diluted with H_2O to make a volume of 15 µl, then mixed with 5 µl 4x western blot loading buffer and denatured by boiling at 95ºC for 10 minutes with regular vortexing. Proteins were then separated by size via sodium dodecyl sulfate polyacrylamide gel electrophoresis (SDS-PAGE), using gels of 15% polyacrylamide, 1.5mm width and 12 wells made in house. Samples were loaded into the well and then gels were run for 1 hour and 30 minutes at 120 volts/300 watts.

2.5.5 Transfer to membranes

Proteins were transferred to PVDF or nitrocellulose membranes using the Trans-Blot Turbo transfer system (Bio-Rad). Prior to use, PVDF membranes were immersed for 1 minute each in methanol, water and 1x transfer buffer, in that order. Whattman filter paper and the PAGE gel were also immersed in 1x transfer buffer prior to use. The filter paper, membrane, PAGE gel and filter paper sandwich was then assembled and loaded into the Trans-Blot Turbo system, and bubbles were removed via use of a roller. The transfer took place at 2.5 amps, 25 volts for 10 minutes. Once completed successful

transfer was validated by visual inspection of the ladder. The membrane was rinsed briefly in TBS, then blocked in blocking buffer for 1 hour at room temperature with rotation.

2.5.6 Membrane imaging

Membranes were transferred from blocking buffer to a 50 ml falcon containing the desired antibody in 5 ml TBST with 5% BSA. These were then incubated overnight at 4ºC with rotation. The following morning, membranes were washed three times for 10 minutes at room temperature in TBST, then transferred to a 5 ml falcon containing the required secondary antibody in 5 ml of TBST with 5% BSA. Membranes were then incubated for an hour and a half at room temperature with rotation, then washed 3 more times with TBST.

As secondary antibodies were HRP linked, ECL reagents A + B (Amersham) were mixed together at a 1:1 ratio and then spread evenly over the surface of the membrane. The membrane was then loaded into an iBright 1000 (Invitrogen) and imaged for an appropriate amount of time to identify but not overexpose bands. Membranes were then stripped by placing them in a 50 ml falcon tube with 5 ml Restore PLUS Western Blot Stripping Buffer (Thermo Scientific) and then incubated for 15 minutes at room temperature. Membranes were then quickly washed with TBS, at which point they could be blocked and probed again with new antibodies. As well as probing for proteins of interest, all blots were also probed for a loading control protein (histone H3) to ensure similar amounts of protein were loaded in each well.

2.6 Microscopy and cell imaging

2.6.1 Buffers and antibodies

CSK buffer- 10 mM PIPES pH 6.8, 100 mM NaCl, 300 mM sucrose, 1 mM MgCl2, 1 mM EGTA

Antibody Buffer- 1x PBS, 10 mg/ml BSA, 0.02% SDS, and 0.1% Triton X-100

Antibodies- Antibodies used for imaging are listed in *Table 2.4*, with information on target protein, whether the antibody is rabbit, mouse or goat, the clone, and company purchased from.

Table 2.4 Antibodies used for immunofluorescence staining

Antibody	**Rabbit/Mouse/Goat**	**Clone/Catalogue Number**	**Company**
Anti-H3K27me3	Rabbit	MA5-11198	ThermoFisher
Anti-CIZ1 C-terminus	Mouse	87	Cizzle Biotech
Anti-CIZ1 N-terminus	Rabbit	1794	Cizzle Biotech
Anti-SON	Rabbit	28046-1-AP	Proteintech
Anti-phosphoepitope-SR protein	Mouse	1H4	Merck
Goat anti-Rabbit IgG, Alexa Fluor 568 Red Secondary	Goat	A-11011	ThermoFisher
Goat anti-Mouse IgG, Alexa Fluor 488 Green Secondary	Goat	A-11001	ThermoFisher

2.6.2 Cytospinning cells

Prior to immunofluorescence staining, T cells were cytospun to ensure adherence to microscope slides. Cells were first pelleted by centrifugation at 450 x g for 5 minutes. Cells were then resuspended in complete RPMI at a density of $1x10^5$ cells per 250 µl. 250ul of cell suspension was then loaded into a cytofunnel EZ with white filter paper (Thermo Scientific) and a SuperFrost Plus slide (Thermo Scientific). Cells were spun at 1000rpm for 5 minutes with low acceleration using a Cytospin 3 centrifuge (Thermo Shandon). Slides were then removed and inspected via light microscopy to ensure cell transfer.

2.6.3 Cell fixing and permeabilization

A hydrophobic barrier was drawn around cytospun cells with a PAP pen. 40 µl CSK buffer supplemented with 0.1% Triton X-100 was then added to the cells followed by an incubation for 2 minutes at room temperature. CSK buffer was removed, and 50 µl 4% PFA in PBS was then added, followed by another incubation at room temperature for 10 minutes. Slides were then washed three times in PBS for 5 minutes, and 50 µl antibody buffer was then added to the cells. Following a 10-minute incubation at room temperature, slides were then frozen with cells in the antibody buffer, and stored at -80ºC ready for staining.

2.6.4 Staining protocol

Slides were thawed, the antibody buffer was removed, and the cells were left to incubate with 50 µl fresh antibody buffer for 15 minutes. Cells were then stained with primary antibodies (mouse anti-Ciz1 87 Ab, 1:20 dilution, rabbit anti-Ciz1 1794 Ab

1:1000 dilution and rabbit anti-SON Ab 1:1000) in 30 µl antibody buffer, for 90 minutes at 37°C in a humidified chamber to ensure evaporation was kept at a minimum. Following this, cells were washed 3x with 50 µl antibody buffer, then stained with secondary fluorescent antibodies (goat anti-rabbit alexa-fluor 568 and goat anti-rabbit alexa fluor 488) in 30 µl antibody buffer, for another 90 minutes at 37°C in a humidified chamber. Slides were then washed 3 times in PBS. One drop of vectashield plus antifade mounting medium with DAPI (Vector Laboratories) was then added to the slides, followed by a coverslip. Slides were sealed with clear nail polish and stored at 4°C.

2.6.5 Image acquisition and analysis

For CIZ1 and H3K27me3 staining investigating X chromosome inactivation, images were acquired on the Zeiss Axiovert 200M at 63x magnification using Zen Blue (Zeiss), with consistent exposure times used between samples. SON and phosphoepitope-SR staining required higher definition imaging, and images were acquired on the Zeiss LSM 880 confocal with airyscan using Zen Black (Zeiss). 16-bit images were acquired as Z-stacks of total 4.31 µm in height, consisting of 28 slices 0.16 µm apart. Tilescans were used to take 4 neighbouring images stitched together in a 2x2 grid, of total 149 by 149 µm size. Images were then processed with Zen Black. Cells were selected based on the DAPI layer with the aim to avoid bias, and minimum 15 cells were collected in each 2x2 tilescan. As two technical replicate slides were stained and imaged, this lead to a minimum of 30 cells imaged per biological replicate.

Following image acquisition, analysis was performed via ImageJ. An overview of this is shown in *Figure 2.5*. Colour channels were split, then channels of interest (SON, phospho-SR, CIZ1, H3K27me3) were maximum intensity projected, while the DAPI

channel was median intensity projected with the aim to remove background staining from cells sheared by cytospinning. A mask of the DAPI channel was then generated via auto-thresholding, binary image conversion, and use of the particle analysis setting. The mask was then applied to the channels of interest (SON, phospho-SR, Ciz1, H3K27me3) to allow for a per-cell nucleus analysis. For measuring staining intensity, the measure tool in the region of interest manager was used to automatically identify maximum and mean intensity within each nucleus. For measuring speckle size, auto-thresholding, binary conversion and the watershed tool were applied to the SON layer, and particle analysis was then iterated through each nucleus in the image to estimate the number and average size of speckles on a per-cell basis. An example image of the nucleus masks generated from the DAPI channel, and an example of the SON particle analysis is shown in *Figure 2.5*. All analysis was performed on the raw image files with no adjustment of brightness and contrast. However, brightness and contrast were increased as stated for images shown in this thesis, for ease of viewing.

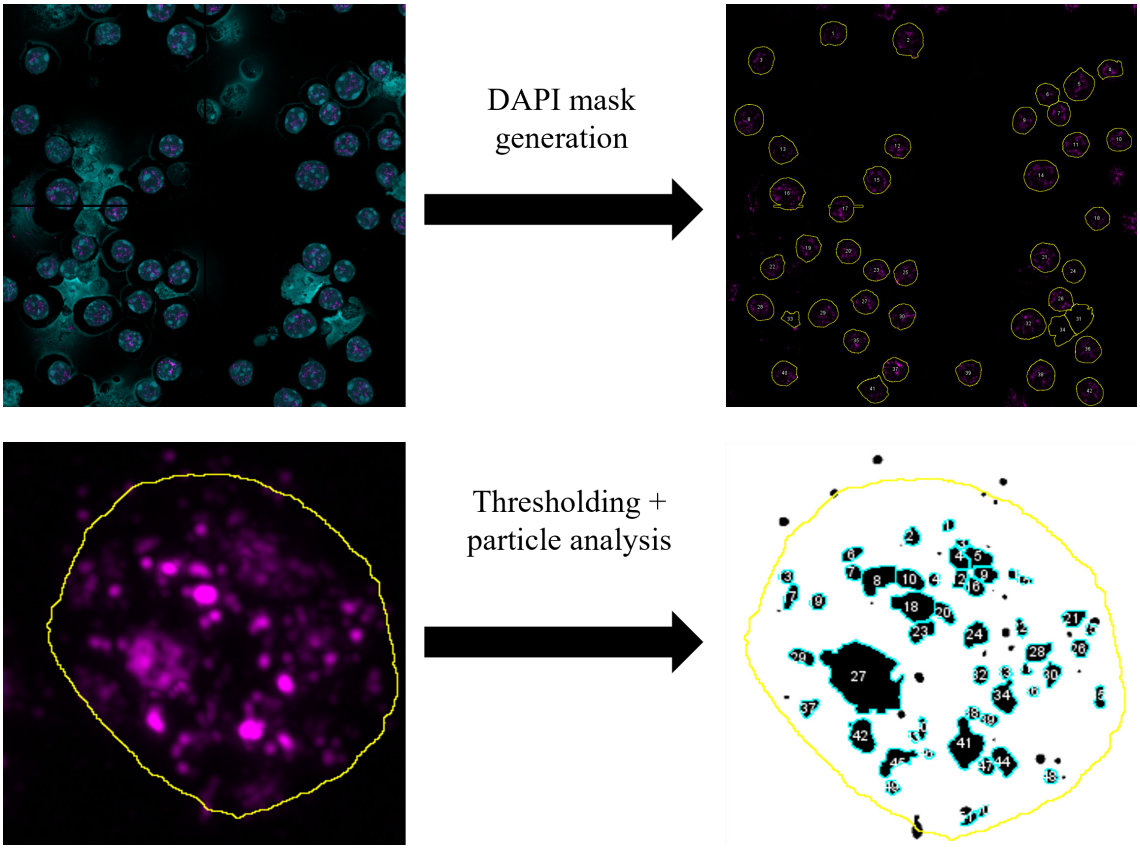

Figure 2.5 Schematic of image analysis performed using ImageJ

An overview of Image analysis performed via ImageJ. Example used is from *WT* female $CD4^+$ T cells at day 2 of differentiation, with staining for DAPI (cyan) and SON (pink). A mask of the DAPI channel was generated and applied to the channel of interest to identify each nucleus. From this intensity per nucleus could be identified. Automated thresholding and particle analysis was then iterated through each nucleus, allowing for determination of speckle size and area.

2.7 *In vivo* mouse models

2.7.1 *S. mansoni* egg injection

An overview of the experiment and tissue analysis is shown in *Figure 2.6*. Procedures were performed by Dr James Hewitson. Schistosome eggs were recovered from the livers of C57BL/6 mice at week 7 post-infection following exposure to 100 *S. mansoni* cercariae. Cercariae were obtained from schistosome-infected *Biomphalaria glabrata* snails provided by the Barrett Centre for Helminth Control (Aberystwyth University, UK). Livers were digested overnight at 37ºC with shaking with 0.2U/ml collagenase D (Roche) in the presence of 5000U/ml polymyxin B (Merck). Eggs were purified by centrifugation through 10 ml percoll (GE Healthcare) / 20ml 0.25M sucrose (450 xg, 5min, room temperature), washed in PBS and stored at -20ºC before usage. 5000 of these dead *S. mansoni* eggs in 200 µl PBS were delivered via intraperitoneal (IP) injection into females and males of *WT* or *Malat1*$^{-/-}$ mice. Two weeks later, the mice were intravenously (IV) challenged with another 5000 eggs in 200 µl PBS. Following intravenous challenge, *S. mansoni* eggs are transported to the lung by the pulmonary artery and become lodged in the lung parenchyma, causing localised type 2 inflammation. After another week tissues were harvested for analysis.

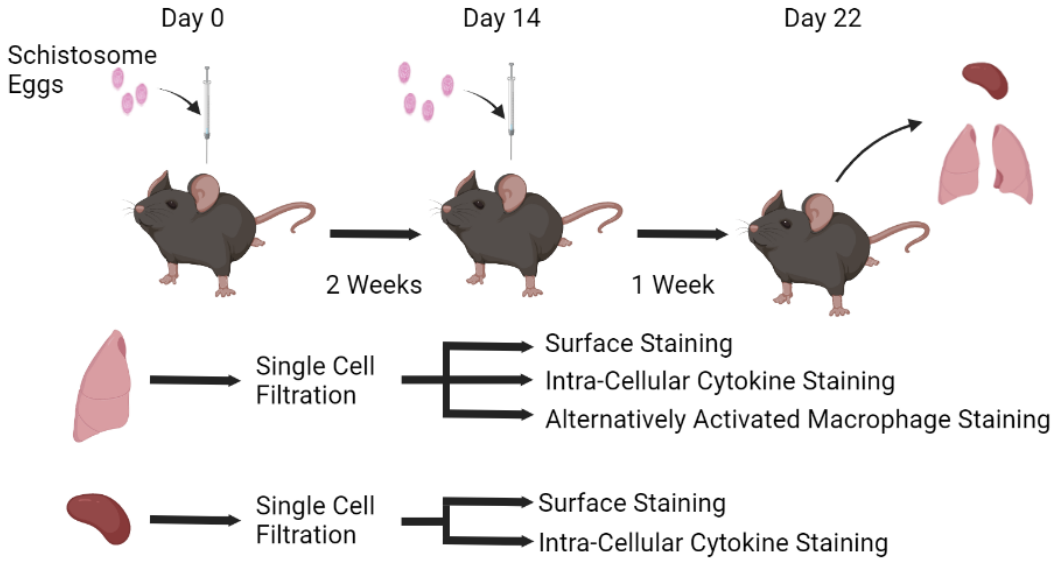

Figure 2.6 Overview of S. mansoni egg injection experiment

A schematic of the *S. mansoni* egg-injection model including the egg-injection procedure, tissue extraction, and the flow cytometry panels were performed on each tissue.

2.7.2 Tissue preparation

All samples were extracted and processed by myself, James Hewitson, Katie West, Joanna Greenman and Shinjini Chakraborty. Lungs were cut into 2mm sized pieces and digested with 0.4 U/ml Liberase TL (Roche) and 80 U/ml DNase I type IV in 2 ml HBSS (both Sigma-Aldrich) for 45 min at 37°C. Enzyme activity was inhibited with addition of EDTA of final concentration of 10 mM (pH 7.5). Single-cell suspensions were created via passing digests through 100-μm nylon filters (Falcon) in complete RPMI 1640. Immune cells were enriched via a Percoll gradient. Cells were washed twice with RPMI, then re-suspended in 8 ml of 33% isotonic Percoll (GE Healthcare) in PBS. Samples were centrifuged at 700 x g at room temperature for 12 minutes on the lowest brake and acceleration settings, and the supernatant was then removed. Finally, pellets were resuspended in 3 ml ACK red blood cell lysis buffer. Spleen single cell suspensions were generated via passing spleen suspensions through a 70 μm filter and treatment with 3 ml ACK buffer.

2.7.3 Flow cytometry analysis

Following immune cell extraction, immune cells from the lungs and the spleen were stained for analysis via flow cytometry. Three panels were used for analysis of the *in vivo* model: a myeloid cell panel, a T cell surface receptor panel investigating proportions of activated and naïve cells, and a T cell intra-cellular cytokine (ICC) panel. The overall gating strategy for these panels is shown in *Figure 2.7*, and antibodies used in each panel are shown in *Table 2.5*.

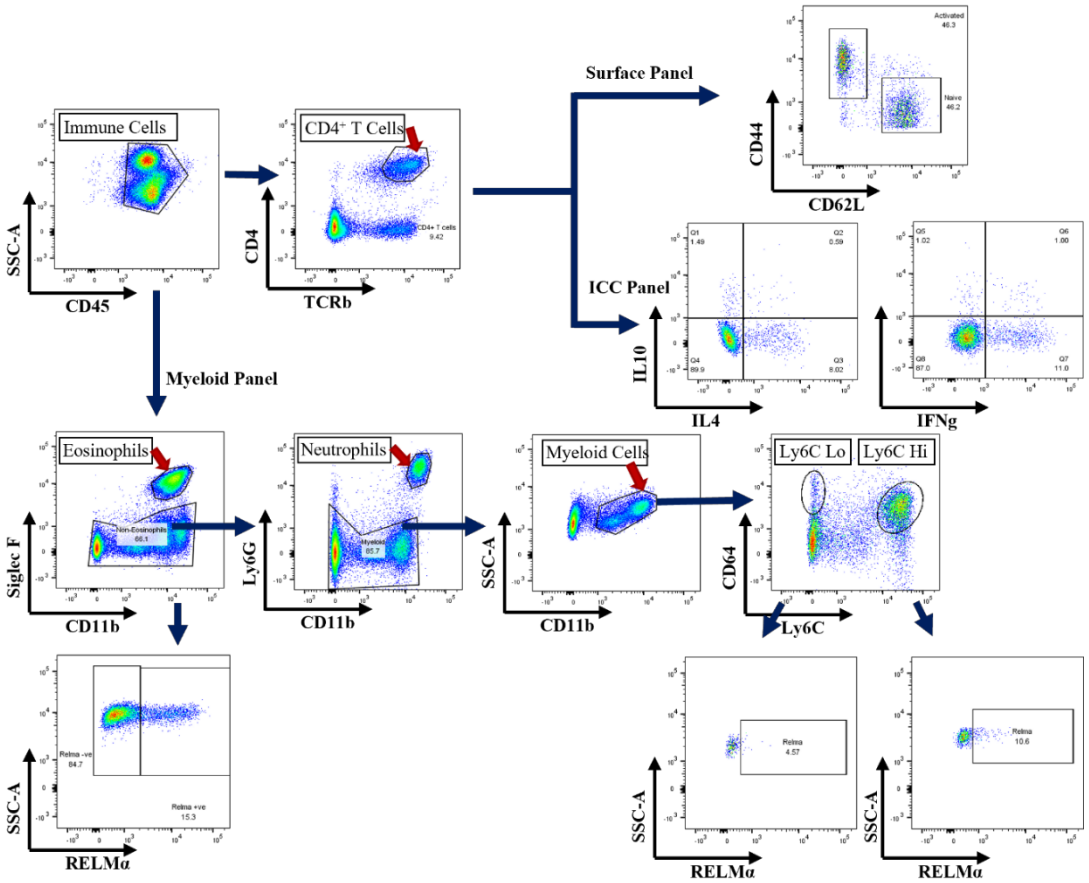

Figure 2.7 Gating strategy used for flow cytometry analysis of the *S. mansoni* egg injection model.

Overview of the gating strategy for flow cytometry analysis of the *S. mansoni* egg injection model. This example is from an injected *WT* female mouse lung. For all panels, $CD45^+$ cells were selected following live/dead, cell selection and singlet gating. For the T cell surface panel, $CD4^+$ $TCR\beta^+$ cells were selected, and the proportions of $CD44^{hi}$ $CD62L^{lo}$ cells were analysed. For the ICC panel, $CD4^+$ $TCR\beta^+$ cells were selected, then quadrants were drawn to identify $IL10^+$ $IL4^+$ and $IFN\gamma^+$ cells. For the myeloid panel, Eosinophils were identified via $SIGLECF^+$ and $CD11b^+$ expression, and RELMα expression was investigated within this population. Neutrophils were identified as $CD11b^+$ and $Ly6G^+$. $CD11b^+$ cells were investigated for $CD64^+$ and Ly6C expression. Both $CD64^+$ Ly6C low and $CD64^+$ Ly6C high monocytes were selected here, and were investigated for RELMα expression.

Table 2.5 Antibody panels used for flow cytometry analysis of the *S. mansoni* egg injection experiment

Surface Panel:	**ICC Panel:**	**Myeloid Cell Panel:**
Live/Dead (Zombie Aqua)	Live/Dead (Zombie Aqua)	Live/Dead (Zombie Aqua)
TCRβ- PeCy7	CD45- BV785	CD45- BV785
CD4- PerCPCy5.5	TCRβ- PeCy7	CD11b- PB
CD8- e450	CD4- PerCPCy5.5	LY6G- APC-Cy7
CD62L- PE	CD41- APC	CD45- FITC
CD44- FITC	IL4- PE-Dazzle	LY6C- BV605
CD19- APC-Cy7	IL10- PE	SIGLECF- e710
CD45- BV785	IFNγ- FITC	CD64- PE
CD41- APC		MHCII- A700
		iNOS- PE-e610
		RELMα (rabbit anti-RELMα, goat anti-rabbit A647)
		YM1 (biotin-YM1, Srcp PE-Cy7)

2.8 RNA sequencing

2.8.1 Sample validation and preparation

For our long-read Oxford Nanopore Technologies (ONT) RNA sequencing experiments, RNA was extracted and prepared including DNase I treatment as described previously, from *WT* and *Malat1*$^{-/-}$ female naïve CD4^{+} T cells and cells at day 2 of Th2 differentiation. Initial RNA concentration and purity was assessed via nanodrop. A small portion of RNA (5 µl) was then used for cDNA synthesis and qRTPCR as a quality check. Th2 marker *Gata*3, T cell activation markers *Cd69* and *Il2ra*, and *Malat1* were assessed to ensure the T cells had differentiated correctly and that there was no cross contamination between *WT* and *Malat1*$^{-/-}$ samples. Samples failing quality checks were excluded and not sent for sequencing. Samples were then analysed via the Agilent 2100 bioanalyzer by Lesley Gilbert (York University Technology facility). RNA integrity numbers (RINs) for all samples were between 8.8-10.

2.8.2 Library preparation and long-read ONT sequencing

Minimum 300 ng RNA in 10 ul were provided for sequencing. Full length cDNA libraries were prepared by Sally James at the York University Technology Facility using the ONT cDNA-PCR Sequencing V14 – Barcoding kit (SQK-PCB114.24). cDNA RT adapters were ligated to 3' ends (polyA tails) of transcripts, prior to strand switching cDNA synthesis and a 13 cycle PCR reaction with barcoded primers, labelling each cDNA sample with a unique DNA barcode. Barcoded cDNAs were pooled at equimolar ratios before final adapter ligation and sequencing on R10.4.1 flowcells in ONT PromethION sequencer (8 samples per flow cell). Live superaccuracy basecalling and barcode

demultiplexing were performed in MinKNOW software (version 24.06.10) at the time of the run. We acquired 0.745-1.121 million reads per sample, with 604-840 bases mean read length. Demultiplexed reads were analyzed through the workflow transcriptomes from Epi2Me^{TM} application, specifically designed by ONT. The Viking cluster, provided by the University of York, was used for the analyses.

2.8.3 RNAseq data analysis

Long-read Oxford Nanopore Technology (ONT) sequencing then analysis was performed by Sally James and Fabiano Pais at the Genomics Lab and Data Science Hub respectively, in the University of York Bioscience Technology Facility. The Epi2Me workflow (available at https://github.com/epi2me-labs/wf-transcriptomes) was used to generate differential gene expression (DGE) data with edgeR (Robinson et al., 2009), and differential transcript usage (DTU) data with Dexseq (Anders et al., 2012), using a reference transcriptome. CSV files generated from this and from pre-existing short-read sequencing (performed previously by Katie West) were analysed using python, Microsoft Excel, and R version 4.2.2. R package pheatmap version 1.0.12 was used to generate heatmaps. GSEA analyses (Subramanian et al., 2005) were performed using R package clusterprofiler version 4.16.0, and the GSEA website (available at https://www.gsea-msigdb.org/gsea/index.jsp). Cluster analysis was performed via STRING db (Szklarczyk et al., 2023) (accessible through https://string-db.org/) with k means clustering.

2.9 Data availability

Raw data are available upon request. RNAseq data have been deposited in the National Center for Biotechnology Gene Expression Omnibus database

at https://www.ncbi.nlm.nih.gov/geo/. Accession numbers are GSE279185 for Illumina RNAseq and GSE278413 for Oxford Nanopore Technologies RNAseq data.

2.10 Diagrams and schematics

All schematics for pathways, treatments or models were generated using either Powerpoint (Microsoft Office), Biorender software available at https://biorender.com/, or NIH BioART

2.11 Statistical analyses

All results, unless specified otherwise, were plot and analysed using GraphPad Prism 9 or 10 (GraphPad Software). In instances where multiple experiments have been merged, each experiment is represented via the symbols used for each data point- circles are experiment 1, squares experiment 2, triangles experiment 3 etc. Appropriate statistical methods, as detailed below, were used to compensate for experimental variability.

For comparison of just two samples, unpaired or paired T-tests were used as appropriate for the experiment. For comparison of multiple groups with lower n ($n<9$), one-way ANOVAs were used for statistical testing, followed by Sidak's multiple comparisons test for comparison of samples with biological relevance (most often comparing *WT* female to *Malat1*$^{-/-}$ female, *WT* male to *Malat1*$^{-/-}$ male, and *WT* female to *WT* male). Confidence levels were set to 0.05 for significance. In data with larger n ($n>10$), consensus between Anderson-Darling, Shapiro-Wilk and D'Agostino & Pearson tests were used to determine normality. If all samples proved normally distributed either T-tests or one-way ANOVAs were performed as previously described. If one or more

samples proved to not follow a normal distribution, then Mann-Whitney U or Kruskal-Wallis tests followed by Dunn's multiple comparison tests were used to identify significance, with confidence levels of 0.05. Analysis of data between two differing time points, or when sample number was unequal between replicates, resulted in use of a two-way ANOVA with Sidak's post-hoc test for significance ($p<0.05$). P values in graphs are displayed as asterisks representing P value classification, where * ≤ 0.05, ** ≤ 0.01, ***≤ 0.001 and **** ≤ 0.0001. In relevant places (e.g. p value is borderline non-significant) the raw p value will be shown instead.

3. *Malat1* Regulates End-Stage Th2 Differentiation in a Sex-Specific Manner

3.1 Introduction

3.1.1 Statement

Some of the work presented in this chapter is also featured in the publication:

Gwynne M, West KA, van Dongen S, Kourtzelis I, Coverley D, Teichmann SA, James KR, Hewitson JP, Lagos D. *Malat1* regulates female Th2 cell cytokine expression through controlling early differentiation and response to IL-2. J Immunol. 2025 Aug 28:vkaf177. doi: 10.1093/jimmun/vkaf177. Epub ahead of print. PMID: 40865984.

3.1.2 *Malat1* and IL10 expression

Previous work in the Lagos lab group from Dr. James Hewitson and Dr. Katie West was performed on investigating the role of *Malat1* in $CD4^+$ T cell differentiation (Hewitson et al., 2020). Initial bulk RNA-seq experiments identified that *Malat1* was rapidly downregulated during the first 24 hours of T cell differentiation. This downregulation was anti-correlated with an increase in expression of genes involved in RNA binding, ribosomal function, metabolism, and cellular structure/localization. *In vitro* T cell differentiation experiments were then performed, revealing that *Malat1* loss in Th1, Th2, and Th17 cells caused a significant downregulation of cytokine IL10. These results were also confirmed at the RNA level by qRTPCR. Further exploration identified that transcription factor *Maf* correlated with *Malat1* and was downregulated following *Malat1* loss. Investigating the effects of *Malat1* loss *in vivo*, during *L. donovani* infection *Malat1* loss led to a decrease in IL10 expression, increase in neutrophil iNOS expression, and improved parasite clearance. During *Plasmodium chabaudi chabaudi AS* infection, the experiment was terminated early due to an increased rate of weight loss. IL10 expression was again significantly decreased, along with a small decrease in IFNγ expression.

Together, these results clearly demonstrated that *Malat1* was core to Th cell differentiation, particularly impacting the expression of IL10.

Dr. Katie West performed further experiments for her PhD thesis (not shown here) investigating differences between female and male $CD4^+$ T cells. Initial experiments indicated that, during Th2 differentiation, the impact of *Malat1* loss on IL10 expression in Th2 cells was seen to only occur in females, with *Malat1* loss in males leaving IL10 expression unaffected. Proteomics analyses using RNA antisense purification coupled with mass spectrometry (RAP-MS) (McHugh & Guttman, 2018), then identified that *Malat1* had distinct RBP binding partners based on sex, with RBPs such as MBNL1, ALDOA and TIAL1 bound more in females, and SRSF1, SRSF10 and PUF60 bound more in males (unpublished). This initial work provided a strong case that *Malat1* may be involved in different pathways between female and male $CD4^+$ T cells, warranting further investigation.

3.1.3 Chapter hypothesis and aims

Previous work in T helper cells has suggested that *Malat1* may differentially regulate female and male Th2 differentiation, with a particularly strong impact on IL10 expression. In this chapter, we aimed to test the hypothesis that *Malat1* has distinct effects on female and male Th2 differentiation. We aimed to fully characterise the effect of *Malat1* loss on end-stage Th2 differentiation and response to exogenous levels of IL2 in both female and male $CD4^+$ T cells, using *in vitro* and *in vivo* models of Th2 differentiation.

The aims of this chapter were to:

- Identify the effects of *Malat1* deficiency on cytokine expression in female and male Th2 cells.
- Assess the impact of *Malat1* deficiency on the transcriptome during Th2 differentiation.
- Determine whether Th cell activation strength modulates the effects of *Malat1* loss on Th2 cell differentiation.
- Investigate how *Malat1* loss affects Th2 differentiation *in vivo*.

3.2 Results

3.2.1 *Malat1* loss downregulates Th2 cell cytokine expression in females

To investigate the impact of *Malat1* loss in male and female $CD4^+$ T cells, we began by performing *in vitro* Th2 cell differentiations of naïve $CD4^+$ T cells obtained from *WT* and *Malat1*$^{-/-}$ mice, of both female and male sex. Levels of cytokines IL10 and IL4 were then measured in endpoint differentiated Th2 cells by intracellular cytokine staining (flow cytometry) and qRTPCR. A schematic of this is shown in *Figure 3.1*. *Malat1*$^{-/-}$ mice were generated by the Prasanth laboratory (Nakagawa et al., 2012), via insertion of a *LacZ* gene and polyadenylation signal downstream of the transcriptional start site of *Malat1* (*Figure 3.2 A*). *Malat1* knock-out in both naïve and Th2 cells was confirmed via qRTPCR, (*Figure 3.2 B*). Some residual *Malat1* RNA expression was still detectable via qRTPCR at around 0.02% of normal *WT* levels. Residual expression was previously observed by Nakagawa *et al.* in brain tissue, and was hypothesized to be caused by the presence of an internal promoter (Nakagawa et al., 2012). We still chose to proceed with this model, as the vast majority of *Malat1* expression is ablated and it has proven a reliable platform for analysing the effects of *Malat1* loss on $CD4^+$ T cells previously.

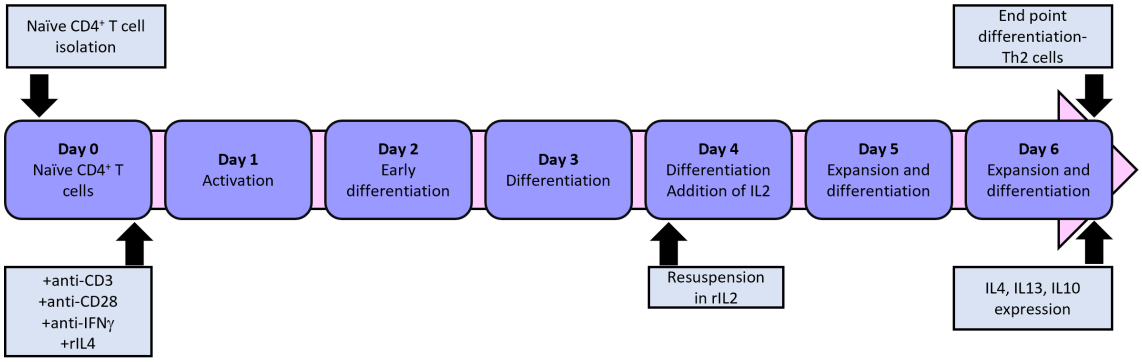

Figure 3.1 *In vitro* Th cell differentiation schematic

Schematic representation of the stages of Th cell differentiation *in vitro*, including Th cell activation, early differentiation, and the response to IL2.

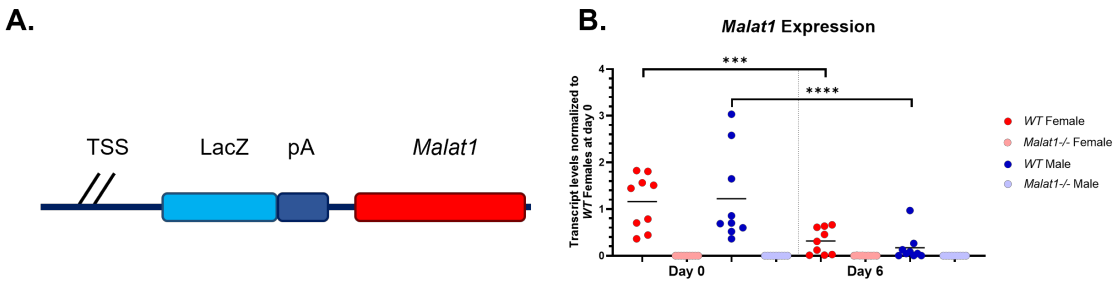

Figure 3.2 LacZ *Malat1* knock-out model and *Malat1* knock-out efficiency

A. Schematic representation of *Malat1* knock-out via lacZ and poly-A site insertion. **B.** Relative levels of *Malat1* RNA expression detected by qRTPCR in naïve and Th2 cells, for female and male WT and *Malat1*$^{-/-}$ samples (n=9).

When investigating cytokine expression at end-point differentiation (*Figure 3.3 A*), we observed that the percentage of IL10 expressing cells was significantly downregulated in *Malat1*$^{-/-}$ females when compared to *WT* females, with around a 50% decrease in expression (*Figure 3.3 B*). However, in males *Malat1* loss did not appear to impact IL10 expression. Similar results were observed for IL4 (*Figure 3.3* C) and IL10 IL4 double positive cells (*Figure 3.3 D*), although the decrease in expression seen was less than that of IL10. *WT* male cytokine expression in this *in vitro* model was also significantly lower than *WT* female expression, at a similar level to that of *Malat1*$^{-/-}$ females (*Figure 3.3 B, C*). Transcript expression of *Il10*, *Il4* and *Maf* were assessed by qRTPCR, revealing significant decreases in both *Il10* and *Il4* transcripts in *Malat1*$^{-/-}$ females (*Figure 3.3 E, F*), and non-significant (p=0.3069) downwards trend for *Maf* expression (*Figure 3.3 G*). No statistically significant changes were seen in males.

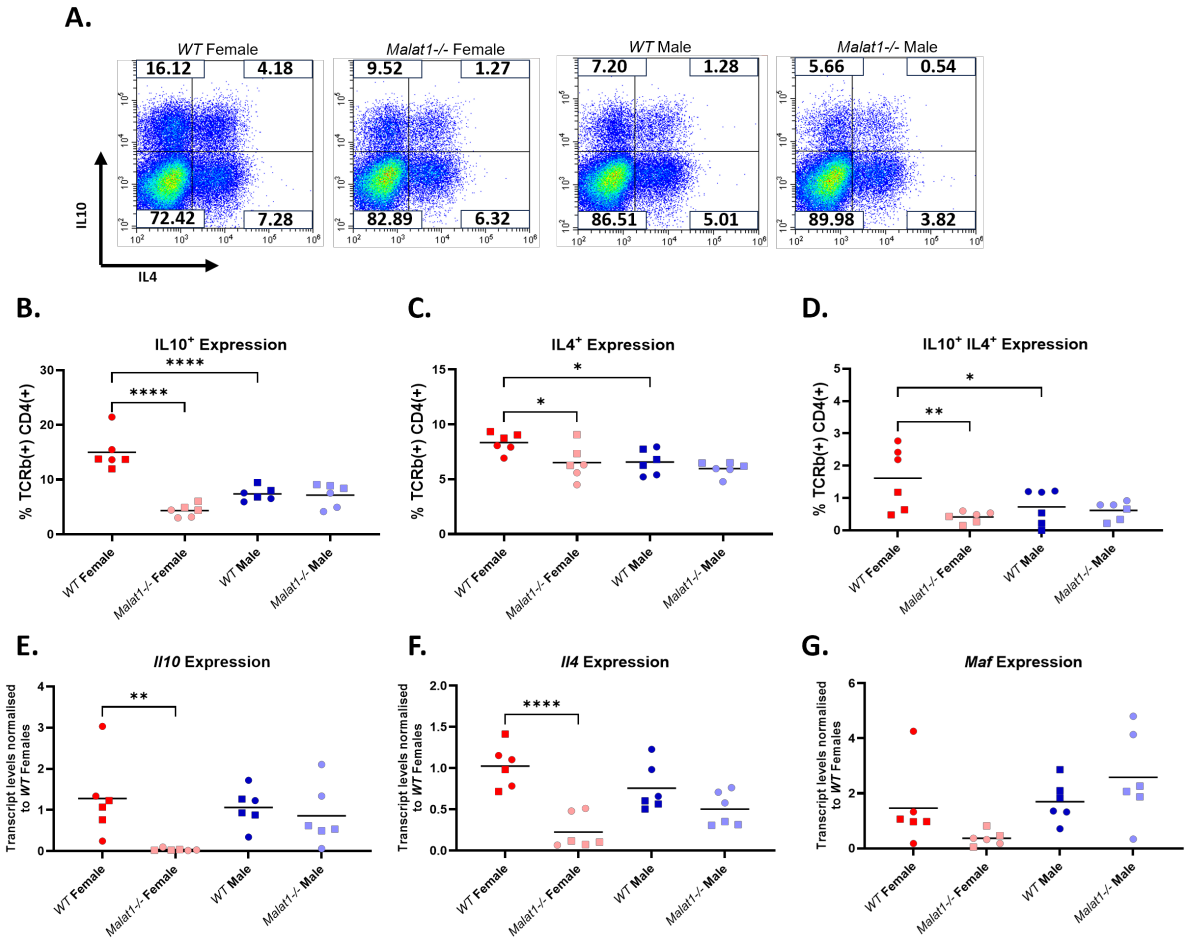

Figure 3.3 *Malat1* loss suppresses cytokine expression during Th2 differentiation

A. Representative FACS plots of IL10 and IL4 expression in *WT* and *Malat1*$^{-/-}$ female and male *in vitro* differentiated Th2 cells, at end point differentiation. **B.** Percentage IL10 expression in *WT* or *Malat1*$^{-/-}$ CD4^{+} T cells from mice of both sexes at day 6 of *in vitro* Th2 differentiation (experimental end-point). Levels determined by flow cytometry with intracellular cytokine staining (n=6 per condition, data from 2 experiments of n=3, appropriate statistics as detailed in the methods were used to compensate for experimental variability.). **C.** As in B. but for IL4 expressing cells. **D.** As in B. but for IL10^{+} IL4^{+} double positive expression. **E.** *Il10* transcript levels in *in vitro* differentiated Th2 cells at day 6, determined by qRTPCR. Levels normalised to U6 and average levels of WT females (n=6, data from 2 experiments of n=3). **F.** As in E. but for *Il4*. **G.** As in E. but for *Maf*.

3.2.2 The effect of *Malat1* loss on cytokine expression is enhanced upon inhibiting IL10 signalling

As IL10 is a potent anti-inflammatory cytokine, we theorised that high expression in *WT* female Th2 cells may suppress levels of other Th2 cytokines, in turn obscuring differences in cytokine expression resulting from *Malat1* loss. To assess this, we performed Th2 *in vitro* differentiation experiments in the presence of an anti-IL10 receptor antibody or an IgG control. Cytokine expression was then investigated by flow cytometry. We also assessed levels of another Th2 cytokine, IL13, in these experiments.

Anti-IL10R treatment in females did not impact the percentage of cells expressing IL10, although we did observe the sex-specific decrease in *Malat1*$^{-/-}$ females in both IgG and anti-IL10R treated samples (*Figure 3.4 A*). However, anti-IL10R treatment enhanced expression of both IL4 and IL13 (*Figure 3.4 B, C*) in *WT* females. While no significant changes were observed on *Malat1* loss for either IL4 and IL13 in the IgG treated samples, significant decreases in both cytokines were observed in response to IL10R blockade in *Malat1*$^{-/-}$ females. Again, no changes were observed following *Malat1* loss in males. The female specific decrease in expression from *Malat1* loss was observed in anti-IL10R treated samples for both IL4/IL13 and IL10/IL4 double positive cells as well (*Figure 3.4 D, E*). This demonstrated that the sex-specific decrease in IL10 compensates for the effects of *Malat1* on other Th2 cytokines.

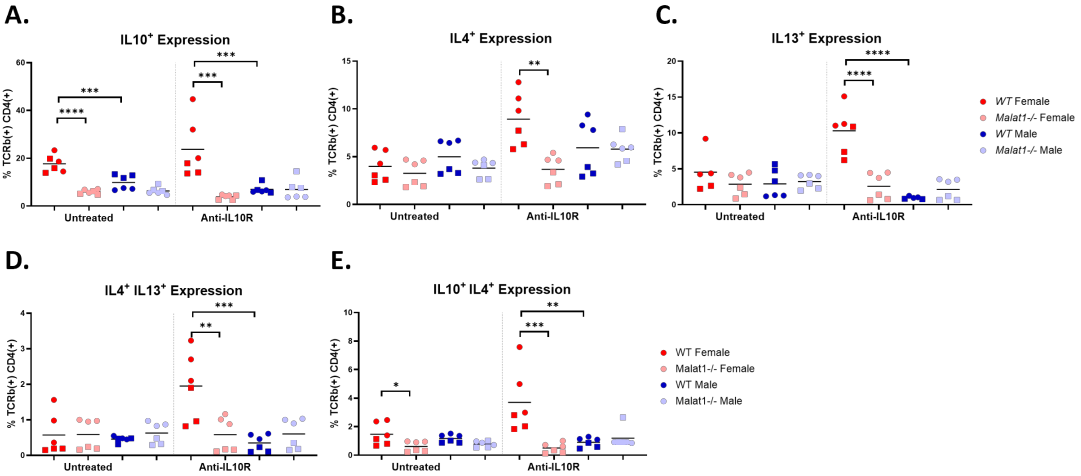

Figure 3.4 IL10R blockade enhances the effects of *Malat1* loss on pro-inflammatory cytokine expression

A. Percentage IL10 expression from $CD4^+$ T cells derived from *WT* or *Malat1*$^{-/-}$ mice of both sexes at day 6 (experimental end-point) of *in vitro* Th2 differentiation, with or without 10 µg/ml anti-IL10 receptor antibody treatment. Levels determined by flow cytometry with intracellular cytokine staining (n=6 per condition, data pooled from two experiments of n=3, appropriate statistics as detailed in the methods were used to compensate for experimental variability). **B.** As in A. but for IL4 expressing cells. **C.** As

3.2.3 *Malat1* causes a transcriptional blunting of the Th2 differentiation programme

To identify whether the sex-specific effects of *Malat1* loss were affecting overall Th2 differentiation or just limited to cytokine expression, we examined an Illumina short-read RNA-seq dataset for transcriptomic changes resulting from *Malat1* loss. This dataset was originally created by Dr. Katie West and involved sequencing of *WT* and *Malat1*$^{-/-}$ females and males, in both naïve and Th2 cells.

Sequencing results identified few significant changes resulting from *Malat1* loss in both naïve and Th2 cells. Assessment of core Th2 genes (*Table 3.1 A, B*) revealed that, as expected, *Il10, Il4* and *Maf* levels were downregulated following *Malat1* loss in Th2 cells in females and not males. However, none of these reached statistical significance in this dataset following multiple correction testing. This suggested this RNA-seq dataset represented a conservative estimate of the effects of *Malat1* loss.

To further examine this dataset, we opted to investigate differences in DEGs between naïve and Th2 cells for each of the samples. Similar numbers of genes were significantly upregulated (~1000) and downregulated (~1500) during Th2 differentiation in all samples, with few changes resulting from *Malat1* loss (*Figure 3.5*). Assessment of core Th2 genes (*Table 3.2 A-D*) displayed upregulation in all samples between naïve and Th2 cells, suggesting correct Th2 differentiation had occurred. Assessment of core Th2 genes revealed *WT* females displayed a stronger upregulation of *Il10, IL4* and *Maf* when compared to *Malat1*$^{-/-}$ females (*Table 3.2 A-D*), confirming our previous results on the protein and RNA level (*Figure 3.3*), although *Gata3* and *IL13* were upregulated slightly in *Malat1*$^{-/-}$ females.

Table 3.1 Differentially expressed Th2 genes between *WT* and *Malat1*$^{-/-}$ female and males in Th2 cells

A. WT female vs Malat1-/- female

Gene	LogFC	FDR
Il10	-0.88159	0.768832
Il4	-0.21435	0.829595
Il13	0.099604	0.950121
Gata3	-0.09551	0.934452
Maf	-0.71583	0.768832

B. WT male vs Malat1-/- male

Gene	LogFC	FDR
Il10	0.029131	0.999682
Il4	-0.25019	0.999682
Il13	0.750531	0.999682
Gata3	-0.04888	0.999682
Maf	0.062207	0.999682

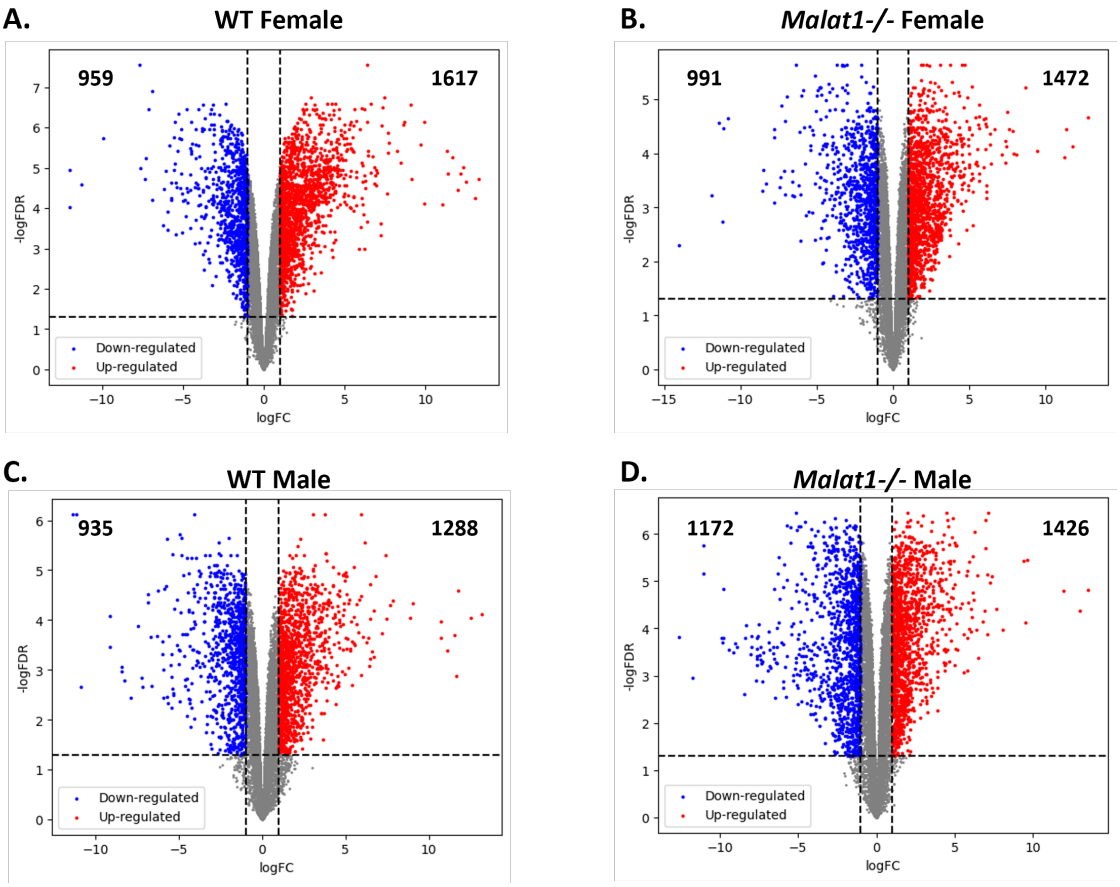

Figure 3.5 Similar numbers of DEGs occur during Th2 differentiation following *Malat1* loss

A. Volcano plots comparing transcriptome-wide gene expression changes during *in vitro* Th2 differentiation of *WT* female $CD4^+$ T cells, with numbers of significantly upregulated and downregulated (FDR<0.05, LFC<-1 and >1) genes highlighted. Data derived from our short-read RNA-seq dataset. **B.** As in A. but for *Malat1*$^{-/-}$ females. **C.** As in A. but for *WT* males. **D.** As in A. but for *Malat1*$^{-/-}$ males.

Table 3.2 Core Th2 genes are significantly upregulated during Th2 differentiation, and to a lesser degree in *Malat1*$^{-/-}$ females and males

A. *WT* female

Gene	logFC	FDR
Il10	5.129468	1.89E-06
Il4	3.015039	1.55E-05
Il13	5.381014	9.92E-05
Gata3	1.683893	3.41E-06
Maf	3.96995	1.46E-06

B. *Malat1-/-* female

Gene	logFC	FDR
Il10	3.324636	0.000494
Il4	2.787815	6.51E-05
Il13	6.155055	3.14E-05
Gata3	1.768407	0.000291
Maf	2.769489	0.000271

C. *WT* male

Gene	logFC	FDR
Il10	2.572077	0.002395
Il4	2.740746	6.84E-05
Il13	4.682792	0.000133
Gata3	1.097253	0.002
Maf	3.581782	1.90E-05

D. *Malat1-/-* male

Gene	logFC	FDR
Il10	1.332278	0.010306
Il4	2.708547	1.71E-05
Il13	5.567838	0.000136
Gata3	1.222885	0.000393
Maf	3.563569	5.61E-07

We assessed effects of *Malat1* loss on the transcriptome during Th2 differentiation by comparing the LFC of all (FDR<0.01) or the top 500 DEGs during Th2 differentiation with the LFC of these same genes resulting from *Malat1* loss in Th2 cells. Here, we observed a transcriptome-wide blunting effect on Th2 gene expression in females (*Figure 3.6 A*), with genes upregulated during Th2 differentiation upregulated to a lesser extent from *Malat1* loss, with a similar effect on downregulated genes. This effect was not seen from *Malat1* loss in males (*Figure 3.6 B*). Taking a stricter threshold for DEGs than previously between Th2 and naïve $CD4^+$ T cells from *WT* and *Malat1*$^{-/-}$ female mice (FDR<0.001, LFC>2 or <-2), we found 524 DEGs from both *WT* and *Malat1*$^{-/-}$ females, 469 DEGs only in *WT*, and 139 DEGs only in *Malat1*$^{-/-}$ Th2 cells. Both common and *WT* only DEGs were primarily up-regulated during Th2 differentiation, whereas *Malat1*$^{-/-}$ only DEGs were primarily down-regulated.

We then performed GeneSet Enrichment Analysis (GSEA) using the Gene Ontology- Biological Processes (GO-BP) genesets, aiming to identify the activated and suppressed genesets during Th2 differentiation. Genes involved in mitosis and cell division were generally upregulated during Th2 differentiation (*Figure 3.7, Figure 3.8*). Significantly downregulated genesets in *WT* females, mainly IFNβ signalling and protein folding (*Figure 3.7 A*), were not present in *Malat1*$^{-/-}$ females (*Figure 3.7 B*). Downregulated genesets were involved in immune cell activation, immune processes, and adaptive immunity, suggesting potential defects occurring in cell activation. Genesets were similar between *WT* and *Malat1*$^{-/-}$ males (*Figure 3.8 A, B*), however downregulated genesets from both *WT* and *Malat1*$^{-/-}$ males were involved in immune effector processes and defence responses, potentially suggested decreased Th cell responses compared to females. Overall, these results suggest that *Malat1* loss in females impairs transcriptional changes that occur during Th2 differentiation across the transcriptome.

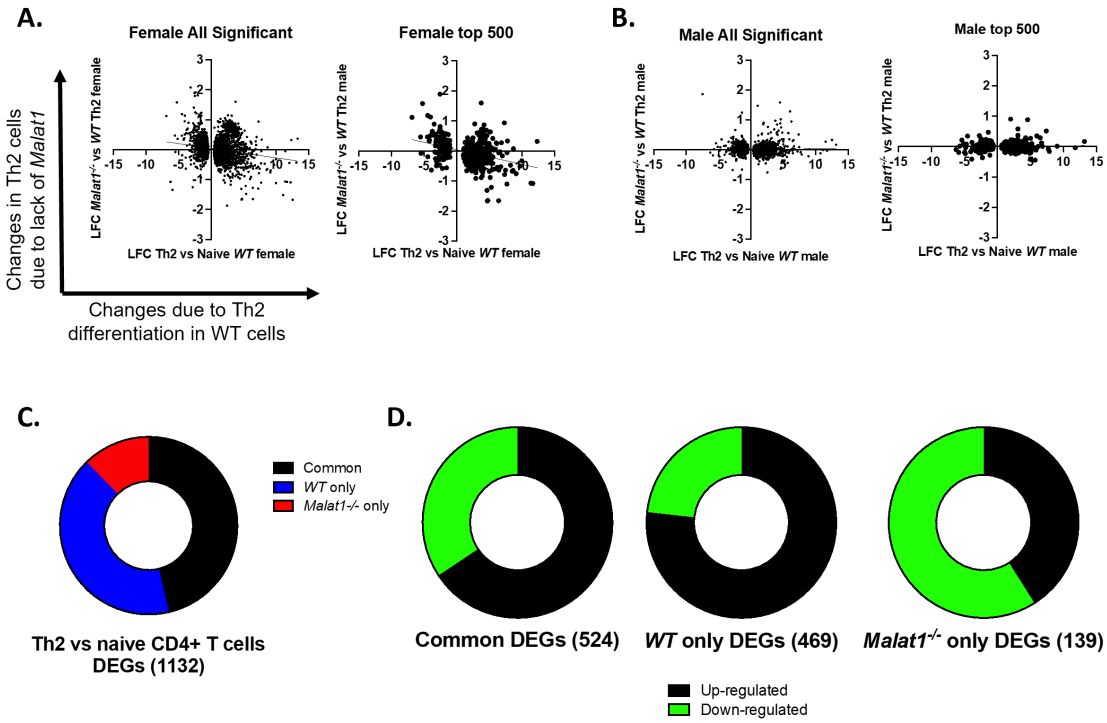

Figure 3.6 *Malat1* loss in females blunts transcriptional changes that occur during Th2 differentiation

A. Effects of *Malat1* loss on gene expression trajectories during Th2 differentiation. LFC in gene expression during *in vitro* Th2 differentiation in females (y axis) plot against LFC in gene expression between fully differentiated *WT* and *Malat1*$^{-/-}$ female Th2 cells (x axis). Skew from x axis represents effect of *Malat1* loss on transcriptome-wide gene expression. Data acquired from previously mentioned short-read RNA-seq experiment, and is shown for all significant (FDR<0.01) or the top 500 most significant DEGs between Th2 and naïve CD4+ T cells in females. **B.** As in A. but for *WT* and *Malat1*$^{-/-}$ males. **C.** Pie chart displaying proportions of significant DEGs between naïve and *in vitro* differentiated Th2 cells from the short-read RNA-seq dataset. Data shown for both *WT* and *Malat1*$^{-/-}$ cells (black), *WT* only (blue), and *Malat1*$^{-/-}$ only (red). **D.** Pie charts displaying percentages of up- and down-regulated DEGs during *in vitro* Th2 differentiation in our short-read RNA-seq dataset. Data shown for both *WT* and *Malat1*$^{-/-}$, *WT* only, or *Malat1*$^{-/-}$ only cells.

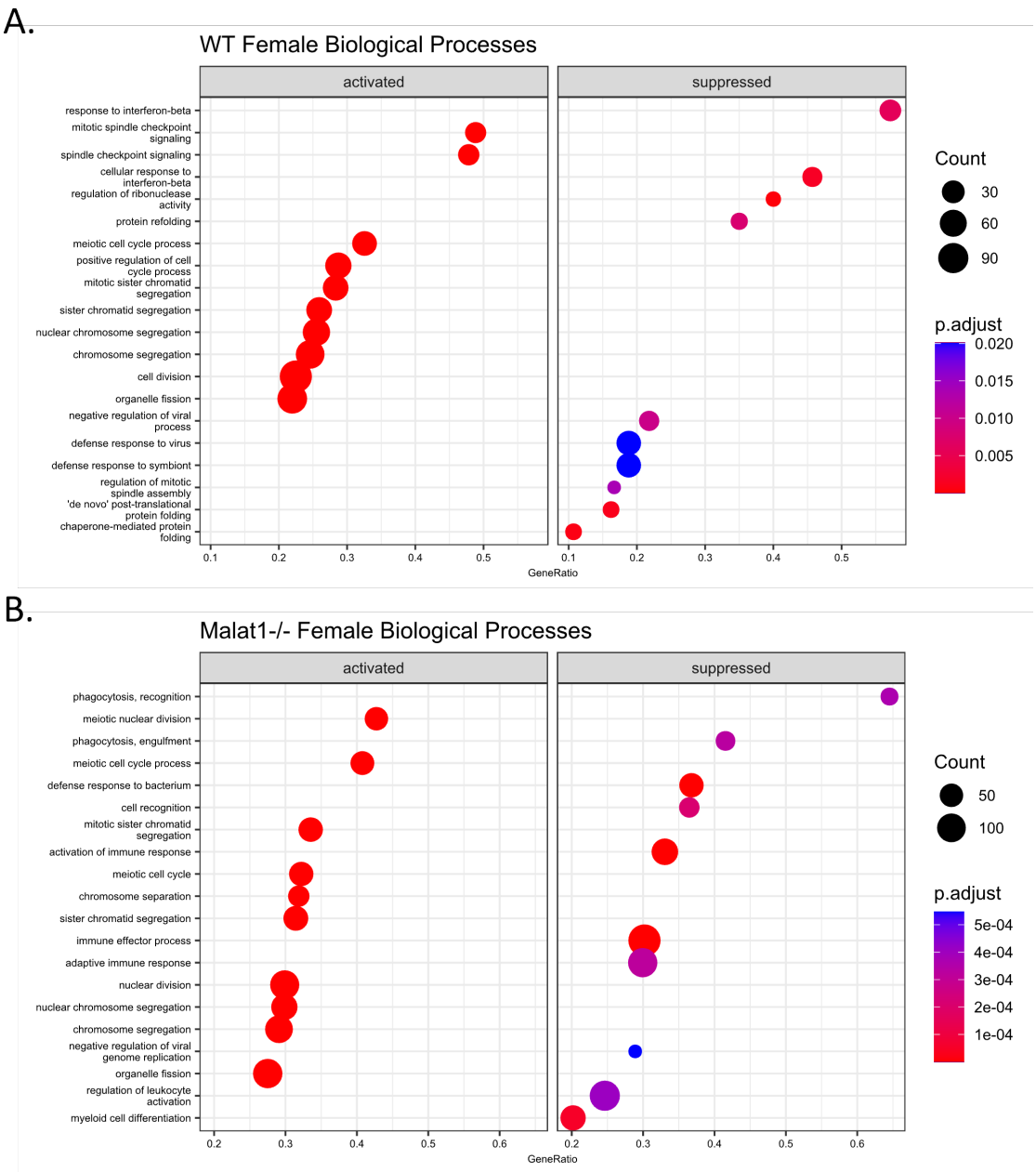

Figure 3.7 GSEA analysis of DEGs during Th2 differentiation in *WT* and *Malat1*$^{-/-}$ females

A. GSEA for gene ontology-biological process (GO:BP) genesets, of DEGs during Th2 differentiation in *WT* females. Significance, gene count and gene ratio are shown for the top 10 significantly activated and suppressed genesets during Th2 differentiation. Data from our short-read RNA-seq dataset. **B.** As in A. but for *Malat1*$^{-/-}$ females.

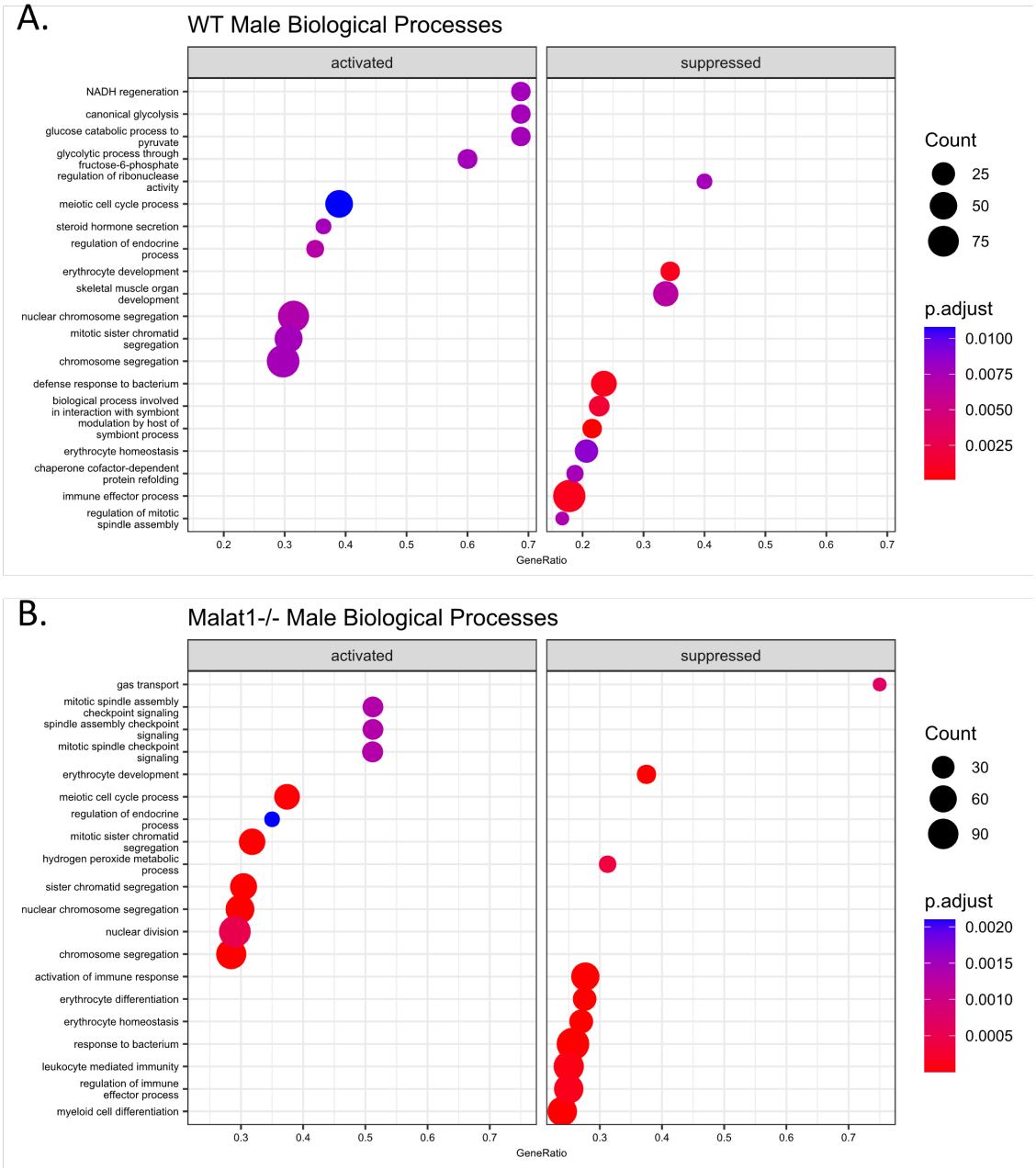

Figure 3.8 GSEA analysis of DEGs during Th2 differentiation in *WT* and *Malat1*$^{-/-}$ males

A. GSEA GO:BP analysis of DEGs during Th2 differentiation in *WT* males. Significance, gene count and gene ratio are shown for the top 10 significantly activated and suppressed genesets. **B.** As in A. but for *Malat1*$^{-/-}$ males.

3.2.4 The sex-specific effect of *Malat1* loss is activation strength independent

As male cell *in vitro* Th2 differentiation was typically weaker than that observed in female cells, we next tested whether *Malat1* deficiency affected Th2 differentiation under weaker activation conditions. To achieve this, we varied the levels of anti-CD3 used during Th2 differentiation, using 2 μg/ml as weaker activation condition, and assessed cytokine expression and cell numbers at end-point differentiation. We also treated cells with anti-IL10R again at the weaker activation condition, to assess the impact of *Malat1* loss on IL4 and IL13.

As expected, at standard conditions (10 μg/ml) IL10 displayed significantly decreased expression in *Malat1*$^{-/-}$ and *WT* males, while the decrease in IL4 was borderline non-significant (*Figure 3.9 A, B*). At weaker conditions, both IL4 and IL10 levels in *WT* females were lower than during standard differentiation, suggesting that we had successfully reduced differentiation strength. Cell numbers also did not increase between day 4 and day 6 (*Figure 3.9 C, D*), while numbers typically doubled at standard polarising conditions. *Malat1*$^{-/-}$ cells still displayed lower IL10 expression with suboptimal differentiation, while IL4 levels were not significantly affected. IL10R blockade at weaker activation conditions slightly upregulated expression of IL4 in *WT* females, however this did not enhance decreases in IL4 and IL13 from *Malat1* loss in females. This may be due to low expression of these cytokines under these conditions.

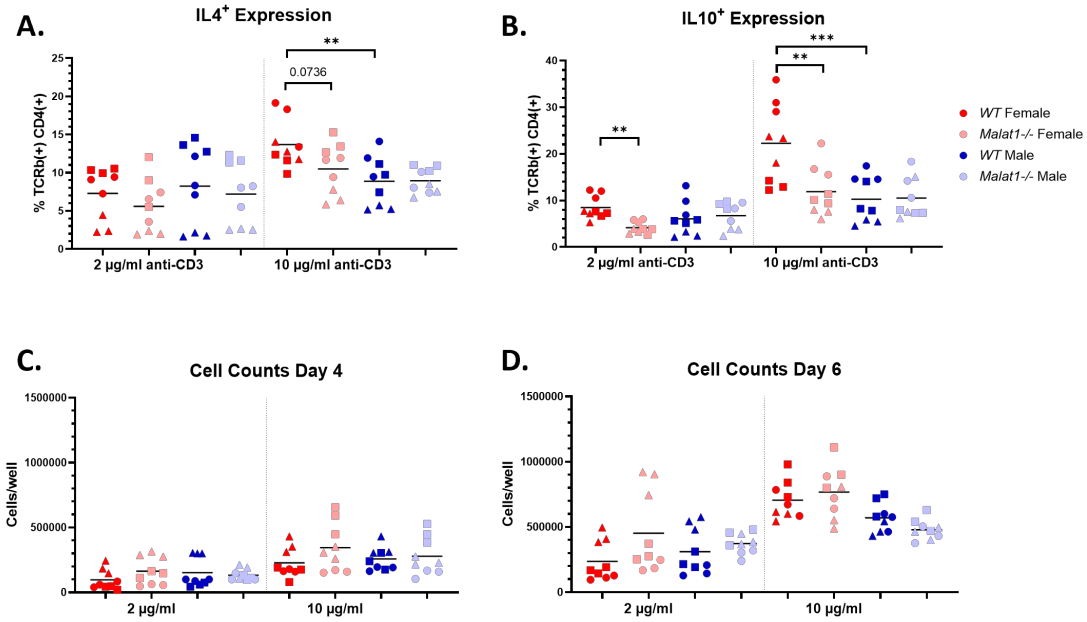

Figure 3.9 *Malat1* loss affects IL10 expression in females independent of differentiation strength

A. Percentage IL4^{+} expression in *WT* or *Malat1*$^{-/-}$ *in vitro* differentiated Th2 cells derived from female and male mice, with 10 µg/ml or 2 µg/ml levels of anti-CD3 antibody. Levels determined by flow cytometry with intracellular cytokine staining (n=9, data from 3 experiments of n=3, appropriate statistics as detailed in the methods were used to compensate for experimental variability). **B.** As in A. but for IL10^{+} cells. **C.** Cell counts at day 4 of Th2 *in vitro* differentiation of *WT* or *Malat1*$^{-/-}$ cells derived from female and male mice, with 10 µg/ml or 2 µg/ml concentration of anti-CD3 antibody (n=9). **D.** as in C. but at day 6 of differentiation.

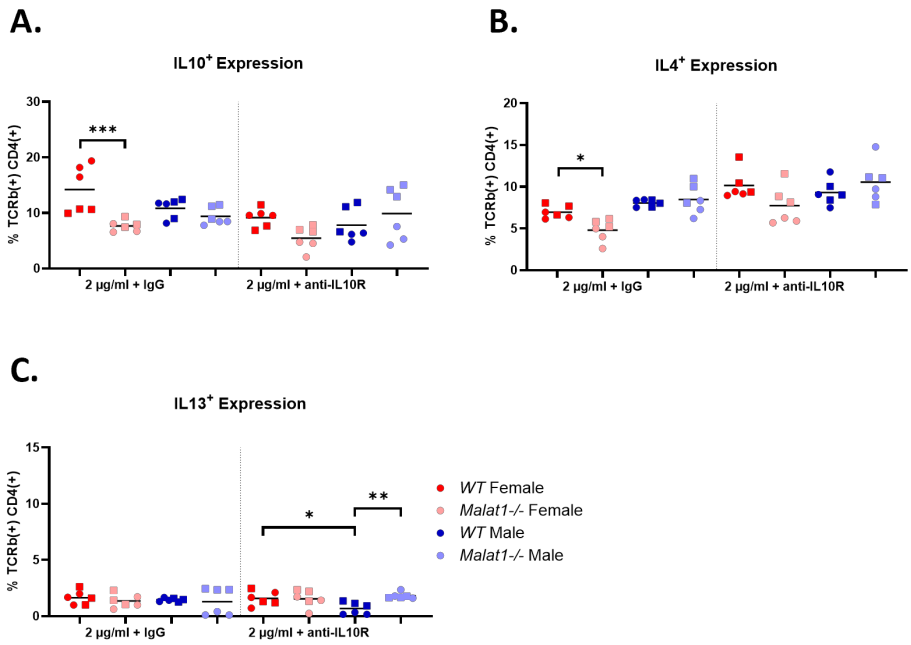

Figure 3.10 IL10R blockade during weaker T cell activation does not enhance the effects of *Malat1* loss on IL4 and IL13

A. Percentage IL10 expression in *WT* or *Malat1*$^{-/-}$ *in vitro* differentiated Th2 cells derived from female and male mice. Samples were treated with 2 µg/ml of anti-CD3 at activation, with and without treatment with an anti-IL10 receptor antibody. Levels determined by flow cytometry with intracellular cytokine staining (n=6, from 2 experiments of n=3, appropriate statistics as detailed in the methods were used to compensate for experimental variability). **B.** As in A. but for IL4^{+} cells. **C.** As in A. but for IL13^{+} cells.

3.2.5 *Malat1* loss is required during early Th2 differentiation

Knock-out models have previously been seen to disrupt the genomic loci, potentially causing phenotypes unrelated to the lncRNA transcript (Eisener-Dorman et al., 2008). To confirm effects on cytokine expression were due to loss of the *Malat1* RNA, we utilised alternate *Malat1* knock-down of *Malat1* during Th2 differentiation via anti-sense oligonucleotide GapmeRs. We treated cells with control or *Malat1* targeting GapmeRs either at experimental start (day 0) or prior to resuspension in IL2 (day 4), to assess whether *Malat1* is required from the start or only during the IL2 response.

Assessment of GapmeR knock-down efficiency (*Figure 3.11 A*) showed an average 70-80% knock-down throughout polarisation. Treatment of female naïve $CD4^+$ T cells (day 0) with *Malat1*-targeting GapmeRs mimicked results seen in *Malat1*$^{-/-}$ cells, displaying significantly reduced IL10 expression compared to non-targeting control (NTC) treated females (*Figure 3.11 B*). However, GapmeR treatment at day 4 did not result in any changes to IL10 expression, suggesting that *Malat1* loss is required for correct differentiation from the start of differentiation. In males, GapmeR treatment did not significantly change IL10 expression at day 0 or day 4. No significant effects were seen from *Malat1* loss in females or males in terms of IL4 or IL10 IL4 double positive cells, although non-significant downwards trends were seen in GapmeR treated females (*Figure 3.11 C, D*).

GapmeR treated cells were also co-treated with IgG or anti-IL10R, to assess the effect of *Malat1* loss on other cytokine expression. IL10R blockade here again enhanced the effect of *Malat1* loss on IL4, leading to a sex-specific significant decrease in expression in *Malat1*$^{-/-}$ females (*Figure 3.12 A, B*). However, no effect was seen on IL13 during IL10R blockade (*Figure 3.12 C*). This lack of impact on IL13 may be due to overall lower levels of IL13 seen under both GapmeR treated and NTC treated conditions

(when compared to *Figure 3.4 C*). These results confirmed the sex specific effects of *Malat1* loss on IL10 and IL4 expression via an alternate knock-down method and suggested that *Malat1* is required during early differentiation for correct Th2 differentiation.

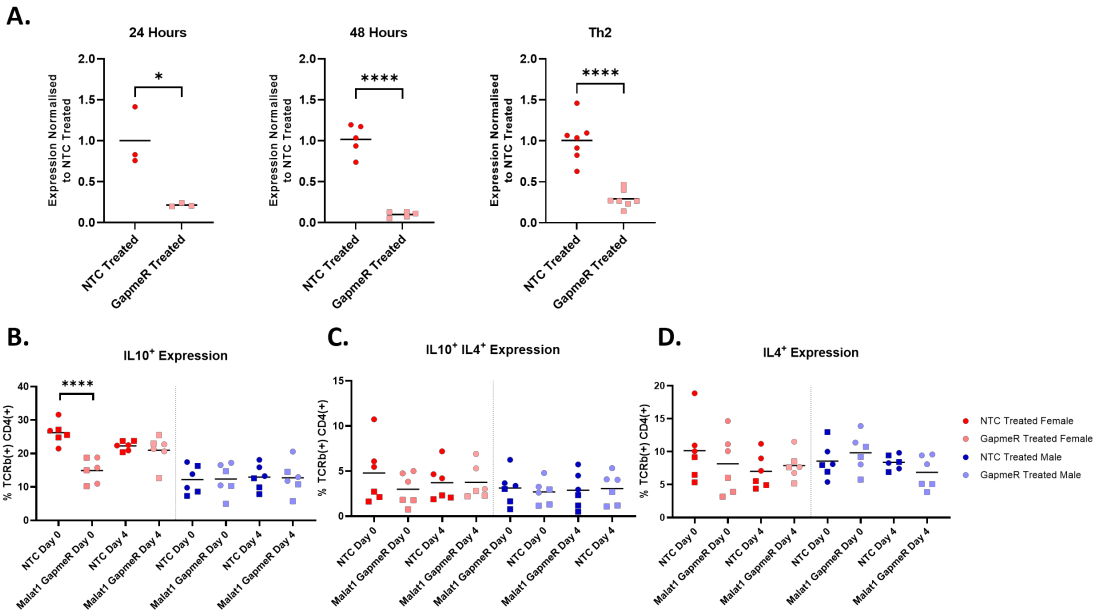

Figure 3.11 The effect of *Malat1* depletion on IL10 expression occurs during early stages of differentiation

A. *Malat1* RNA levels at days 1, 2 and 6 (end-point) of *in vitro* Th2 differentiation, following treatment with NTC or *Malat1* targeting GapmeRs on day 0. Levels determined by qRTPCR and normalised to U6 and average levels of NTC treated GapmeRs. **B.** Percentage of $IL10^+$ expression in *in vitro* differentiated *WT* Th2 cells derived from female and male mice, treated with either non-targeting control (NTC) GapmeRs or *Malat1* targeting GapmeRs at day 0 or day 4 of differentiation. Levels determined by flow cytometry with intracellular cytokine staining (n=6, from 2 experiments of n=3, appropriate statistics as detailed in the methods were used to compensate for experimental variability). **C.** As in B. but for $IL10^+$ $IL4^+$ double positive cells. **D.** As in B. but for $IL4^+$ cells.

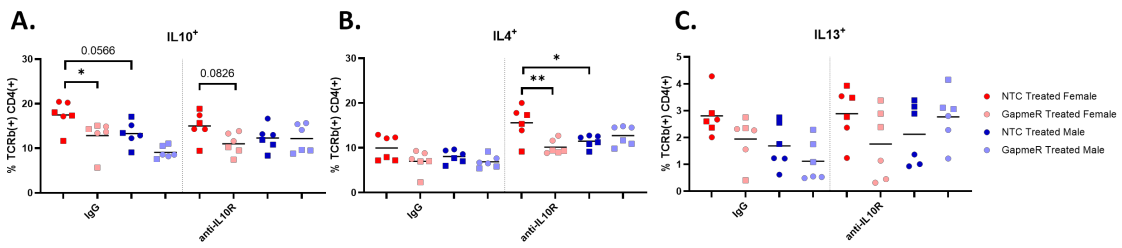

Figure 3.12 Anti-IL10R blockade enhances the effects of *Malat1* GapmeR treatment on IL4 but not IL13

A. Percentage of IL10^{+} expression in *in vitro* differentiated Th2 cells, derived from *WT* female and male mice treated with non-targeting control (NTC) or *Malat1* targeting GapmeRs during differentiation. Cells were further treated with or without anti-IL10 receptor antibody during differentiation. Levels determined by flow cytometry with intracellular cytokine staining (n=6, from 2 experiments of n=3, appropriate statistics as detailed in the methods were used to compensate for experimental variability). **B.** As in A. but for IL4^{+} cells. **C.** As in A. but for IL13^{+} cells.

3.2.6 Differentiating Th2 cells respond to IL2 in a sex-specific manner *in vitro*

As we saw that *Malat1* loss was required from the start of differentiation, we hypothesised that this might affect IL2 receptor expression by day 4 of T cell differentiation, which in turn would affect the response to IL2. We next investigated how T cells respond to IL2 during late-stage differentiation, and if the IL2 response was disrupted from *Malat1* deficiency. We differentiated cells from naïve to Th2 cells, assessing cytokine expression at day 4 (just prior to resuspension in rIL2) and day 6 (end-point differentiation).

Prior to rIL2 treatment, IL10 expression was similar between WT and *Malat1*$^{-/-}$ cells in both females and males. rIL2 treatment in females caused a large significant increase in IL10 expression in *WT* females, however *Malat1* loss suppressed this increase (*Figure 3.13 A*). Males also displayed a reduced increase in IL10 in response to rIL2, at similar levels to the *Malat1*$^{-/-}$ females. Sex-specific responses to IL2 in *Malat1*$^{-/-}$ female mice were also seen for IL4 and IL4 IL10 co-expression (*Figure 3.13 B, C*). Further investigation of IL4^{+} IL10^{-} cells revealed no significant changes from *Malat1* loss (*Figure 3.13 D*), suggesting that the increase in IL4^{+} cells was likely driven by increasing numbers of double positive cells. qRTPCR analysis of RNA samples taken between days 4 and 6 also revealed that *Malat1* levels in *WT* females significantly increased following IL2 treatment, with no change occurring in males (*Figure 3.13 E*). This may reflect the general hypo-responsiveness of *WT* males to IL2 in our *in vitro* polarisation conditions.

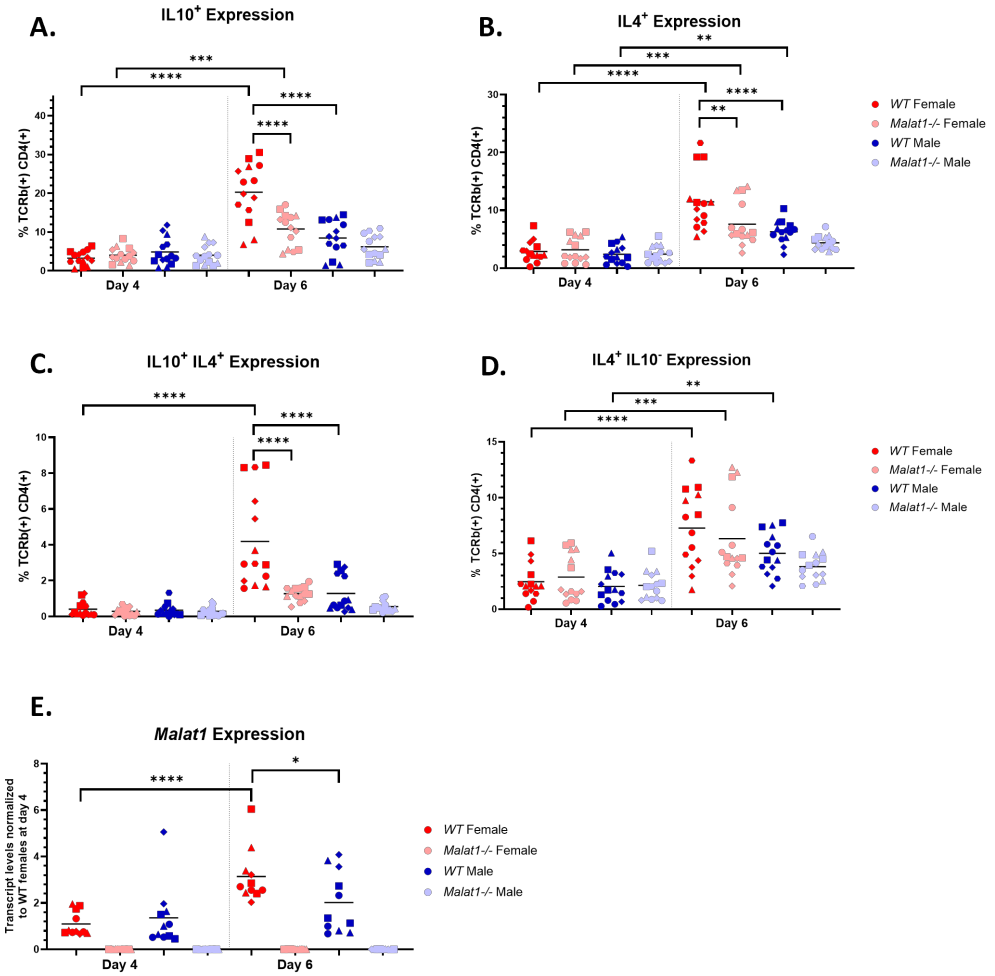

Figure 3.13 Cytokine expression in response to rIL2 is disrupted following *Malat1* loss in females

A. Percentage IL10 expression in *WT* or *Malat1*$^{-/-}$ CD4^{+} T cells at days 4 (prior to exogenous IL2 addition) and day 6 (experimental end-point) of *in vitro* Th2 differentiation. Levels determined by flow cytometry with intracellular cytokine staining (n=14 per condition, 4 experiments of n=3, 1 experiment of n=2, , appropriate statistics as detailed in the methods used to compensate for experimental variability). **B.** As in A., but for IL4^{+} cells. **C.** As in A., but for IL10^{+} IL4^{+} double positive cells. **D.** As in A., but for IL4^{+} IL10^{-} cells. **E.** *Malat1* levels in in vitro differentiated Th2 cells at day 4 (prior to resuspension in IL2) and at day 6 (experimental end point), determined by qRTPCR. Levels normalised to U6 and average levels of *WT* females at day 4 (n=11).

3.2.7 *Malat1* loss suppresses expression of the IL2 receptor

We then performed Th2 differentiation experiments with *WT* and *Malat1*$^{-/-}$ mice, and assessed expression of the IL2 receptor by flow cytometry at day 4 (just prior to resuspension in rIL2). We opted to investigate expression of two subunits of the IL2R. These were IL2Rα and IL2Rγ. IL2Rα is a conventional marker of T cell activation (Belot et al., 2018), and is required for the high affinity form of the IL2 receptor (Ross & Cantrell, 2018). IL2Rγ forms part of the medium affinity IL2 receptor but is capable of signalling. IL2Rγ is X-linked (Puck et al., 1993), so differences in expression could explain the sex-specific effects seen during Th2 differentiation.

IL2Rα expression was significantly suppressed in *Malat1*$^{-/-}$ females at day 4, with a small decrease from ~90% of cells expressing IL2Rα to ~75% in *Malat1*$^{-/-}$ females (*Figure 3.14 A, B*). In *Malat1*$^{-/-}$ males a similar but non-significant downwards trend was also observed. IL2Rγ expression was significantly decreased in both *Malat1*$^{-/-}$ females and males (*Figure 3.14 C, D*). GapmeR-mediated *Malat1* knockdown also resulted in significant decreases in IL2Rα and IL2Rγ in female cells (*Figure 3.14 E, F*), while there were no significant changes seen in male-derived cells. Interestingly, assessment of IL2Rα and IL2Rγ expression via qRTPCR revealed no significant changes resulting from *Malat1* loss (*Figure 3.15 A, B*). This demonstrated that *Malat1* loss in females disrupts expression of the IL2R, and these changes may be at the translational level, or transcriptional changes may be occurring at earlier time points.

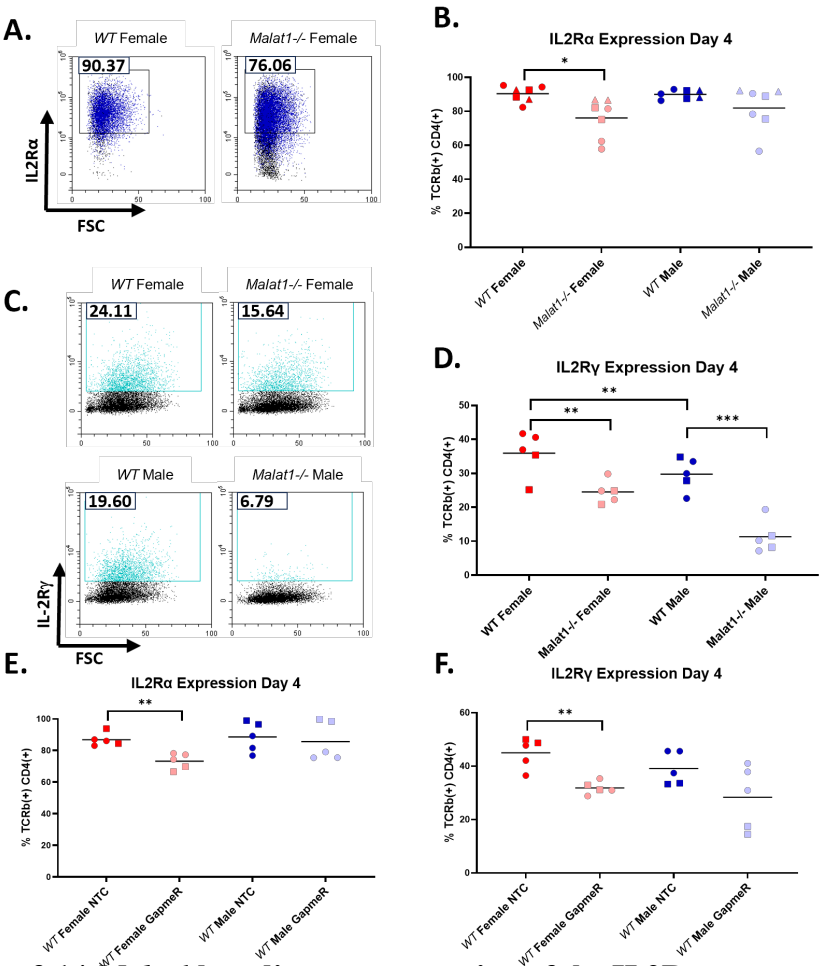

Figure 3.14 *Malat1* loss disrupts expression of the IL2R

A. Representative dot plots displaying IL2Rα expression in *WT* and *Malat1*$^{-/-}$ female mice at day 4 of Th2 *in vitro* differentiation. **B.** Percentage IL2Rα expression in *WT* or *Malat1*$^{-/-}$ CD4^{+} T cells from mice of both sexes at day 4 of *in vitro* Th2 differentiation. Levels determined by flow cytometry (n=7, pooled from 1 experiment of n=3, and 2 of n=2, appropriate statistics as detailed in the methods used to compensate for experimental variability). **C.** As in A. but for IL2Rγ expression. **D.** As in B. but for IL2Rγ^{+} expression (n=5, pooled from one experiment of n=3, and one of n=2). **E.** Percentage IL2Rα expression in CD4^{+} T cells from *WT* mice, at day 4 of *in vitro* Th2 differentiation. Cells were treated with either non-targeting control (NTC) or *Malat1* targeting GapmeRs. (n=5, one experiment of n=3 one of n=2). **F.** As in E. but for IL2Rγ^{+} cells.

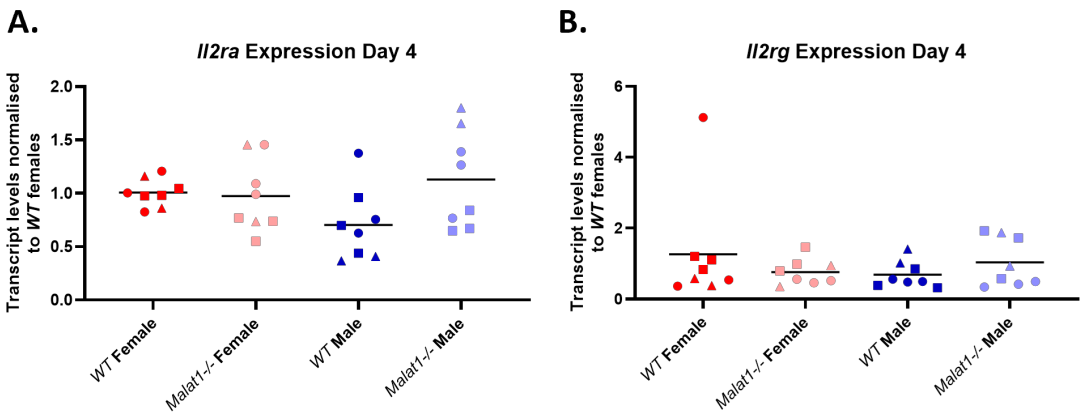

Figure 3.15 *Il2ra* and *Il2rg* transcript levels are not disrupted at day 4 following *Malat1* loss

A. *Il2ra* transcript levels in *WT* or *Malat1*$^{-/-}$ CD4^{+} T cells derived from male or female mice at day 4 of *in vitro* Th2 differentiation of. Expression determined by qRTPCR. Levels normalized to U6 and average levels of *WT* females (n=8, 2 experiments of n=3, 1 of n=2, appropriate statistics as detailed in the methods used to compensate for experimental variability). **B.** As in A. but for *Il2rg*.

3.2.8 Male differentiating Th2 cells are less sensitive to IL2 treatment

The response to rIL2 in *Figure 3.13* caused a larger upregulation of cytokine expression in females than males, suggesting a difference in responsiveness to IL2. We investigated this by performing titrations of different rIL2 levels during Th2 differentiation of *WT* females and males. We varied rIL2 concentrations at day 4 between 2-20 U/ml and measured cytokine expression and cell numbers at end-point differentiation.

Increasing concentrations of rIL2 up to 10 U/ml caused increases in both IL10 and IL4 in female cells (*Figure 3.16 A, B*), however in male cells this increase did not occur to a similar degree. Male cells also demonstrated significantly lower IL10 expression than female cells at all concentrations of IL2, and significantly lower levels of both IL4 and IL10/IL4 double positives at standard rIL2 levels (10 U/ml) (*Figure 3.16 A-C*). While female cell numbers at day 6 increased along with rIL2 concentration, male cells were able to expand effectively even at the lowest rIL2 concentration (*Figure 3.16 D*). To account for experiment-experiment differences, we also normalised IL10, IL4 and IL10/IL4 expression between experiments (*Figure 3.16 E-G*), which confirmed difference in IL2 responsiveness between females and males. Overall, this suggests that male Th2 cells may be less sensitive to differences in IL2 levels in terms of for cell expansion, and do not upregulate cytokine expression to the same extent as in females.

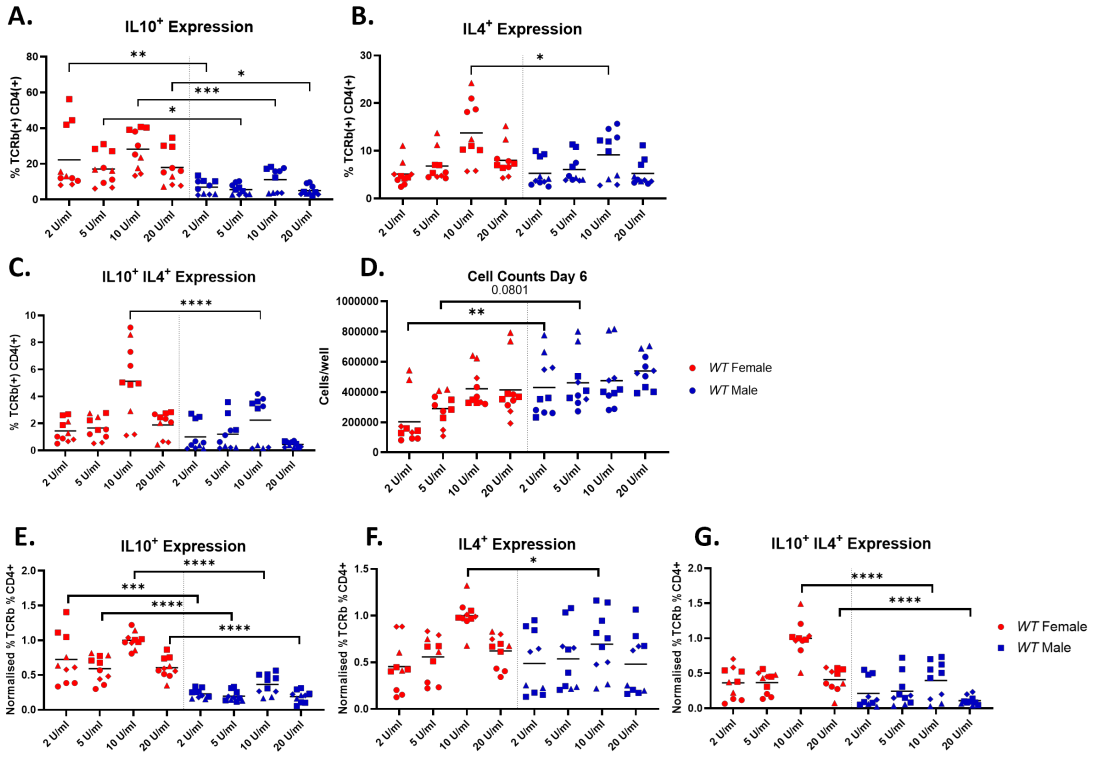

Figure 3.16 Male CD4$^+$ T cells display lower sensitivity to exogenous IL2 levels

A. Percentage IL10 expression in CD4$^+$ T cells from *WT* or *Malat1*$^{-/-}$ mice of both sexes, at day 6 of *in vitro* Th2 differentiation. Cells were resuspended at day 4 of *in vitro* differentiation in the indicated concentrations of rIL2. Levels determined by intracellular staining (n=10 per condition, 2 experiments of n=2, 2 experiments of n=3, appropriate statistics as detailed in the methods used to compensate for experimental variability). **B.** As in A. but for IL4 expression. **C.** As in A. but for IL10$^+$ IL4$^+$ double positive expression. **D.** As in A. but for total numbers of live cells (as determined by trypan blue staining and haemocytometer counts) at day 6 of *in vitro* Th2 differentiation. **E.** As in A. but with IL10 expression normalised to 10 U/ml. **F.** As in E. but for IL4 expression. **G.** As in E. but for IL10$^+$ IL4$^+$ cells.

3.2.9 *Malat1* loss causes a sex-specific decrease in IL10 expression in an *in vivo* model of lung inflammation

To identify whether the *Malat1* loss affected Th2 differentiation and cytokine expression profile *in vivo*, we used the *S. mansoni* egg-injection model in *WT* and *Malat1* to stimulate lung inflammation. A schematic for this model is shown in *Figure 3.17 A* and in section 2.7.1 of this thesis. We analysed immune cell responses in the lung as the primary site of inflammation, and the spleen to identify systemic effects. As this experiment required a large number of mice and required staining of multiple flow cytometry panels per organ, we opted to split processing of females and males on different days.

While total mouse weight did not significantly change (*Figure 3.17 B*), lung weights significantly increased in size in all samples upon egg injection, and spleen weights increased in all bar *Malat1*$^{-/-}$ males (*Figure 3.17 C, D*. Total lung immune cells also increased, although this only reached significance in *WT* females and *Malat1*$^{-/-}$ males (*Figure 3.17 E, F*).

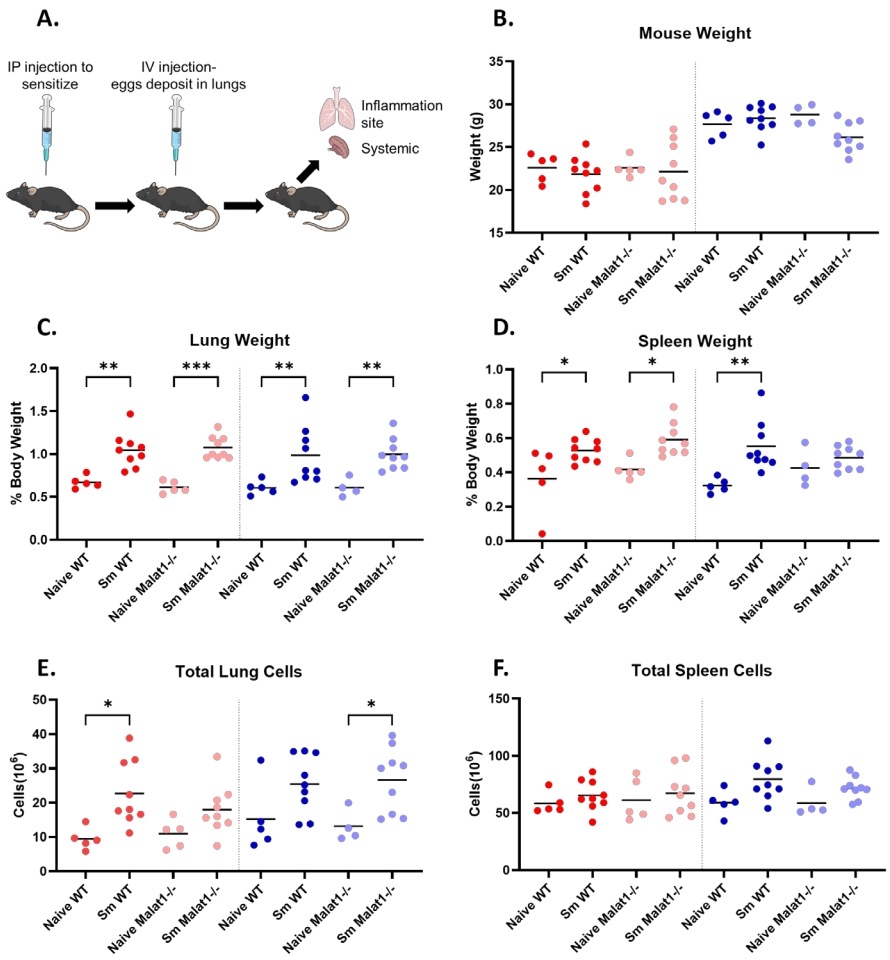

Figure 3.17 *S. mansoni* egg-injection triggered immune responses in both the lung and the spleen

A. Schematic of S. mansoni egg injection experiment. 5,000 dead S. mansoni eggs were injected IP into mice, then after a week the injection was repeated IV via the tail vein. After another week, lungs and spleens were harvested and processed for FACS. **B.** Total weight of naïve and *S. mansoni* egg injected (*Sm*) *WT* or *Malat1*$^{-/-}$ mice of both sexes (n=4 for *Malat1*$^{-/-}$ male naïve, n=5 for all other naïve, n=9 for egg injected mice). **C.** Dry lung weight as a percentage of body weight for naïve and *Sm* egg injected *WT* or *Malat1*$^{-/-}$ mice of both sexes. **D.** As in C. but for dry spleen weight. **E.** Total cell numbers in lungs of naive and *Sm* egg injected *WT* or *Malat1*$^{-/-}$ mice of both sexes. **F.** As in E, but for total splenic cell numbers.

We first analysed granulocyte and monocyte responses in the lungs via flow cytometry, to confirm the generation of a localised type 2 inflammatory response. As expected, percentages of eosinophils ($CD45^+$ $CD11b^+$ $SIGLECF^+$) and eosinophil cell numbers both increased dramatically upon infection in all samples, as did eosinophil activation (RELMα expression) (*Figure 3.18 A, D*). Interestingly, *Malat1*$^{-/-}$ females displayed a slight decrease in eosinophil cell numbers (*Figure 3.18 B*), although this did not reach significance. Neutrophil percentages significantly decreased in females in response to egg injection, although cell numbers did not change (*Figure 3.18 E, F*), suggesting that this change was likely due to expansion of other cell subsets. Neutrophil cell numbers were elevated in both *WT* and *Malat1*$^{-/-}$ males compared to females, however *Malat1*$^{-/-}$ males displayed a significant decrease on infection, while *WT* males did not. Bone marrow derived ($Ly6C^{hi}$) monocyte ($CD11b^+$ $CD64^+$) percentages were significantly reduced on egg-injection in all samples bar *Malat1*$^{-/-}$ males, although cell numbers were unaffected, again suggesting that this was due to expansion of other cell types (*Figure 3.19 A, B*). Local patrolling ($Ly6C^{lo}$) monocyte percentages were unchanged in response to infection, however numbers increased in all samples bar *Malat1*$^{-/-}$ females (*Figure 3.19 C, D*). Both $Ly6C^{hi}$ and $Ly6C^{lo}$ monocytes displayed significantly increased RELMα expression upon infection, suggesting an increase in alternative (type 2) activation (*Figure 3.19 E, F*).

After confirming that we had generated robust alternative monocyte and eosinophil activation, we assessed lymphocyte cells via a lymphocyte surface panel. B ($CD19^+$ $CD45^+$) cell percentages were significantly reduced in both *WT* and *Malat1*$^{-/-}$ females and not in males in the lung on egg-injection (*Figure 3.20 A*), however numbers for all samples in both the lung (*Figure 3.20 A, B*) and the spleen were unaffected on infection (*Figure 3.20 C, D*) suggesting this was caused by expansion of another cell type.

Lung $CD4^+$ T cell ($CD45^+$ $CD4^+$ $TCR\beta^+$) percentages were significantly increased only in *WT* females and *Malat1*$^{-/-}$ males, while cell numbers only significantly increased in *WT* females (*Figure 3.21 A, B*). Splenic $CD4^+$ T cell percentages were unaffected by infection, while cell numbers did slightly increase in *Malat1*$^{-/-}$ males (*Figure 3.21 C, D*). $CD4^+$ T cell activation ($CD44^{hi}$ $CD62L^{lo}$) in the lungs was significantly increased on infection for both percentages and cell numbers in all samples (*Figure 3.21 E, F*). Borderline non-significant downwards trends in $CD44^{hi}$ $CD62L^{lo}$ cells were observed resulting from *Malat1* loss in females and not males, suggesting *Malat1* loss may be impacting T cell activation. No significant changes were seen in splenic $CD4^+$ T cells on infection, bar an increase in *Malat1*$^{-/-}$ male cell numbers on infection (*Figure 3.21 G, H*).

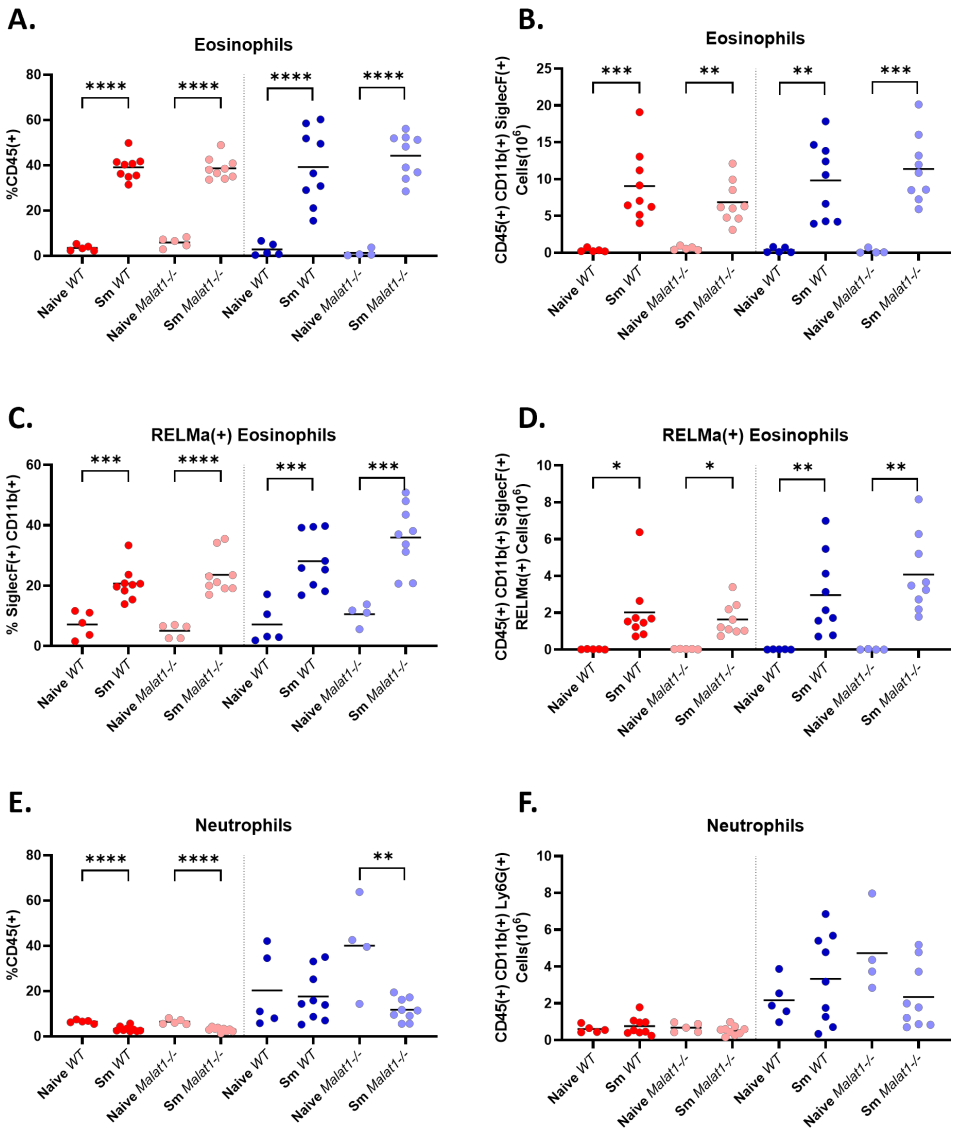

Figure 3.18 Egg-injection generates robust eosinophil responses in the lung

A. Percentages of eosinophils ($CD45^+$, $CD11b^+$, $SIGLECF^+$) in lungs of naïve or *Sm* egg injected *WT* or *Malat1*$^{-/-}$ mice of both sexes. Levels determined by surface staining (n=4 for *Malat1*$^{-/-}$ male naïve, n=5 for all other naïve, n=9 for egg injected mice). **B.** As in A. but for total eosinophil cell numbers. **C.** Percentages of RELMα expressing lung eosinophils. **D.** Total cell numbers of $RELM\alpha^+$ eosinophils. **E.** As in A. but for the percentage of neutrophils ($CD45^+$, $CD11b^+$, $Ly6G^+$) in the lungs. **F.** Total neutrophil cell numbers.

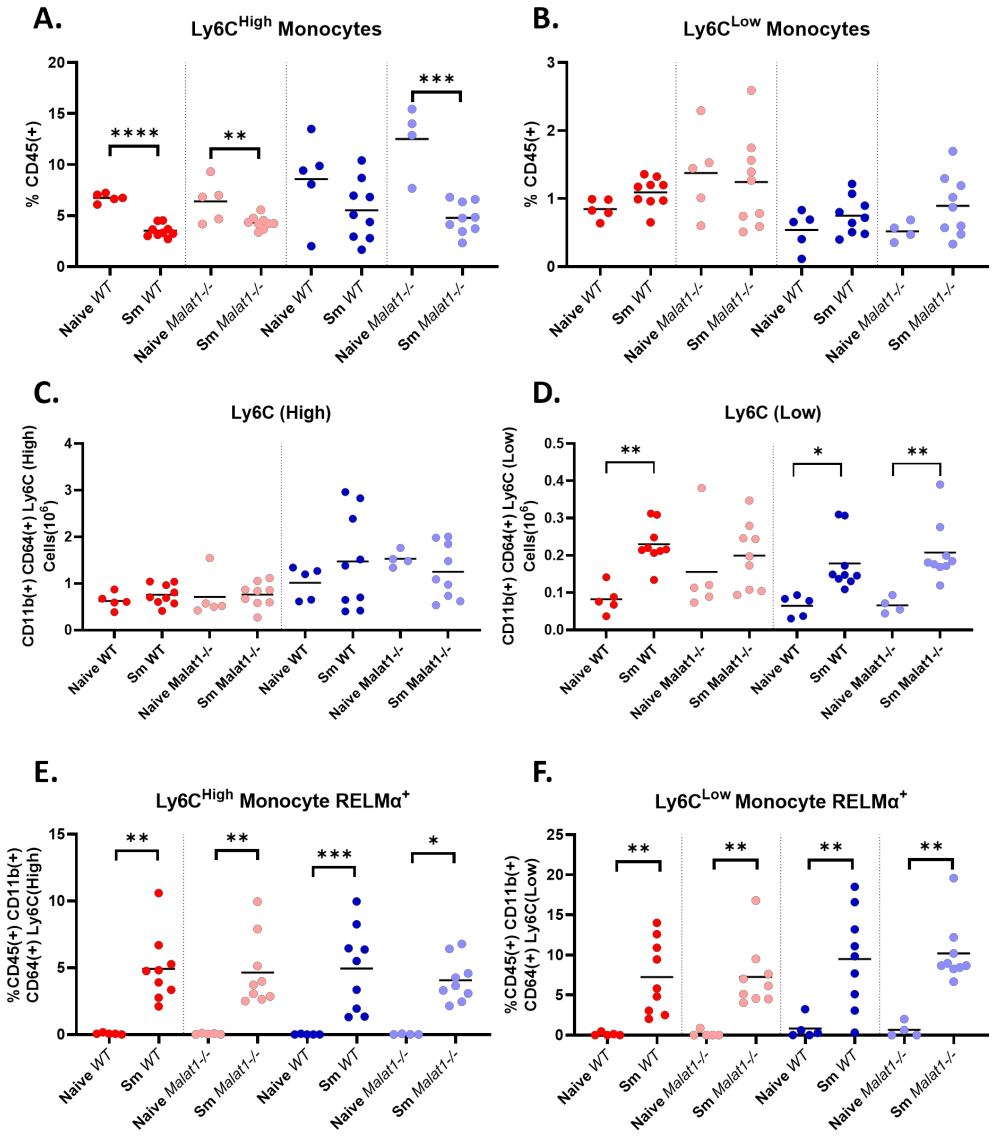

Figure 3.19 Egg-injection triggers monocyte alternative activation

A. Percentages of Ly6C^{high} monocytes (CD45^{+}, CD11b^{+}, CD64^{+}, Ly6C^{high}) in lungs of naïve or *Sm* egg injected *WT* or *Malat1*$^{-/-}$ mice of both sexes. Levels determined by surface staining (n=4 for *Malat1*$^{-/-}$ male naïve, n=5 for all other naïve, n=9 for egg injected mice). **B.** As in A. but for Ly6C^{low} monocytes. **C.** Total lung ly6C^{high} monocyte cell numbers. **D.** Total lung Ly6C^{low} monocyte cell numbers. **E.** Percentage of RELMα expressing Ly6C^{high} monocytes in the lung. **F.** As in E. but for Ly6C^{low} monocytes.

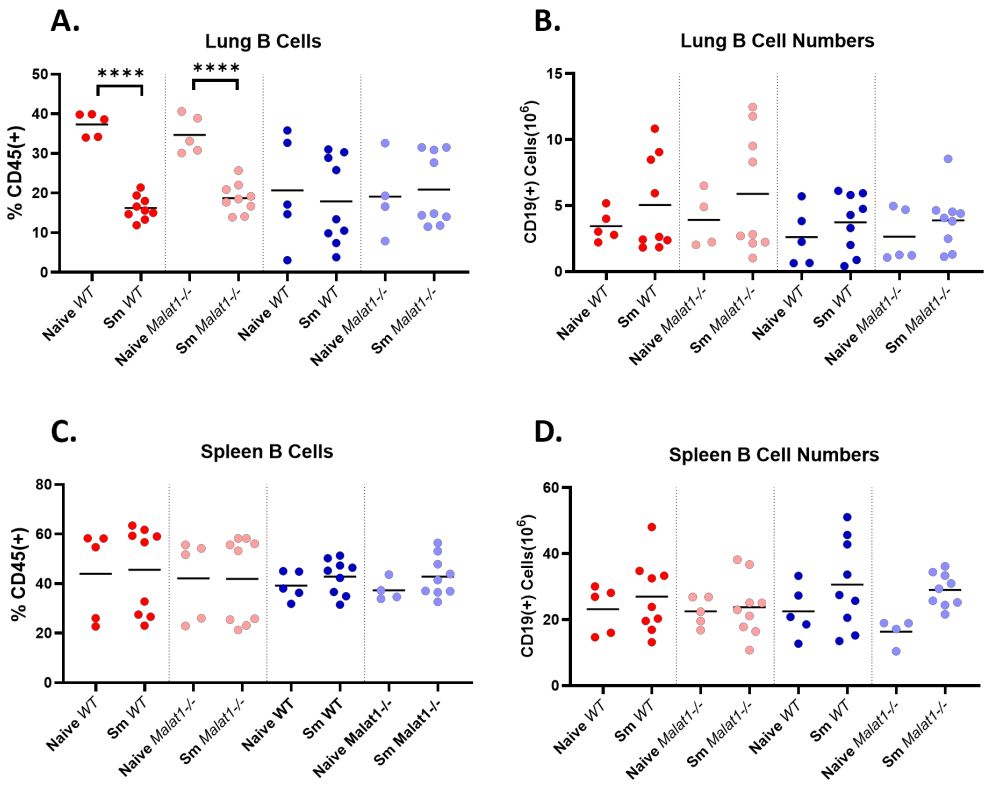

Figure 3.20 B cells are unaffected by *Malat1* loss

A. Percentages of B cells ($CD45^+$, $CD19^+$) in lungs of naïve or *Sm* egg injected, *WT* or *Malat1*$^{-/-}$, female or male mice. Levels determined by surface staining (n=4 for *Malat1*$^{-/-}$ male naïve, n=5 for all other naïve, n=9 for egg injected mice). **B.** Total lung B cell numbers. **C.** Percentages of B cells in the spleens. **D.** Total splenic B cell numbers.

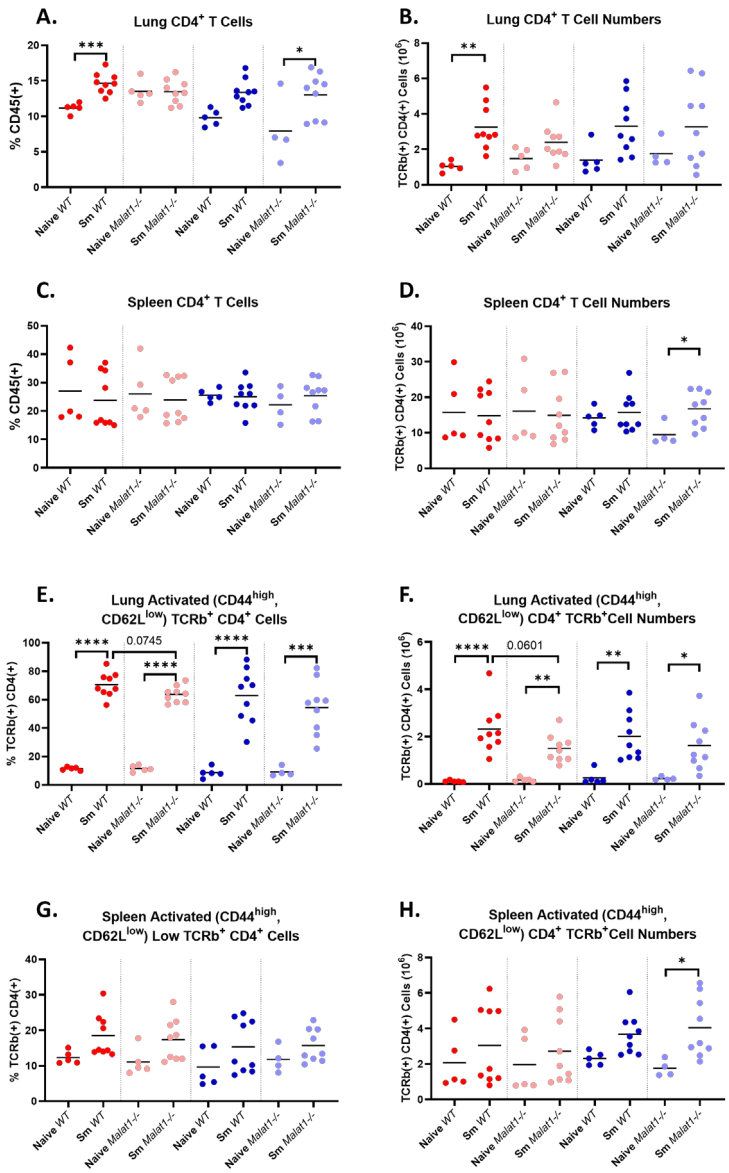

Figure 3.21 *Malat1* loss may impact CD4$^+$ T cell activation in the lung

A. Percentages of CD4$^+$ T cells (TCRβ$^+$ CD4$^+$) cells in lungs of naïve or *Sm* egg injected *WT* or *Malat1*$^{-/-}$ mice of both sexes. Levels determined by surface staining (n=4 for *Malat1*$^{-/-}$ male naïve, n=5 for all other naïve, n=9 for egg injected mice). **B.** Total lung CD4$^+$ T cell numbers. **C.** Percentages of CD4$^+$ T cells in the spleen. **D.** Total splenic CD4$^+$ T cell numbers. **E.** Percentage of activated (CD44^{high} CD62L^{low}) CD4$^+$ T cells in the lung. **F.** Total activated lung CD4$^+$ T cell numbers. **G.** Percentages of splenic activated CD4$^+$ T cells. **H.** Activated splenic CD4$^+$ T cell numbers.

We then assessed $CD4^+$ T cell cytokine expression using an intra-cellular cytokine staining flow cytometry panel. In agreement with *in vitro* data, IL10 expression in the lung was significantly decreased in *Malat1*$^{-/-}$ females when compared to *WT* females, both in terms of percentage of $CD4^+$ cells expressing IL10 and total cell numbers (*Figure 3.22 A-C*). No significant changes were seen resulting from *Malat1* loss in males. Similar results were also observed in the spleen, where IL10 was again significantly decreased in *Malat1*$^{-/-}$ females and not males (*Figure 3.22 D, E*). IL4 expression was not affected by *Malat1* loss in either the lungs or the spleen, although splenic $IL4^+$ cell numbers did increase in *Malat1*$^{-/-}$ males on infection (*Figure 3.23 A-D*). IFNγ expression in terms of cell numbers was significantly decreased in lung *Malat1*$^{-/-}$ females, while the percentage of cells in the spleen expressing IFNγ was significantly increased in *Malat1*$^{-/-}$ males (*Figure 3.23 E-H*). When investigating double positive cells, the percentage of IL10/IL4 double positive cells was significantly decreased in *Malat1*$^{-/-}$ females in both the lung and the spleen (*Figure 3.24 A-D*), although this did not reach significance in lung cell numbers. *Malat1*$^{-/-}$ males displayed the opposite of this, with significantly increased percentages of IL10 IL4 double positives in the spleen. IL10 IFNγ double positives were also significantly decreased in *Malat1*$^{-/-}$ females in the lung (*Figure 3.24 E, F*), although this result was not seen in the spleen (*Figure 3.24 G, H*). Overall, these results demonstrated that the sex-specific effects of *Malat1* loss on cytokine expression, especially on IL10 and IL10 IL4 cells, are also observed in *in vivo* generated Th2 cells.

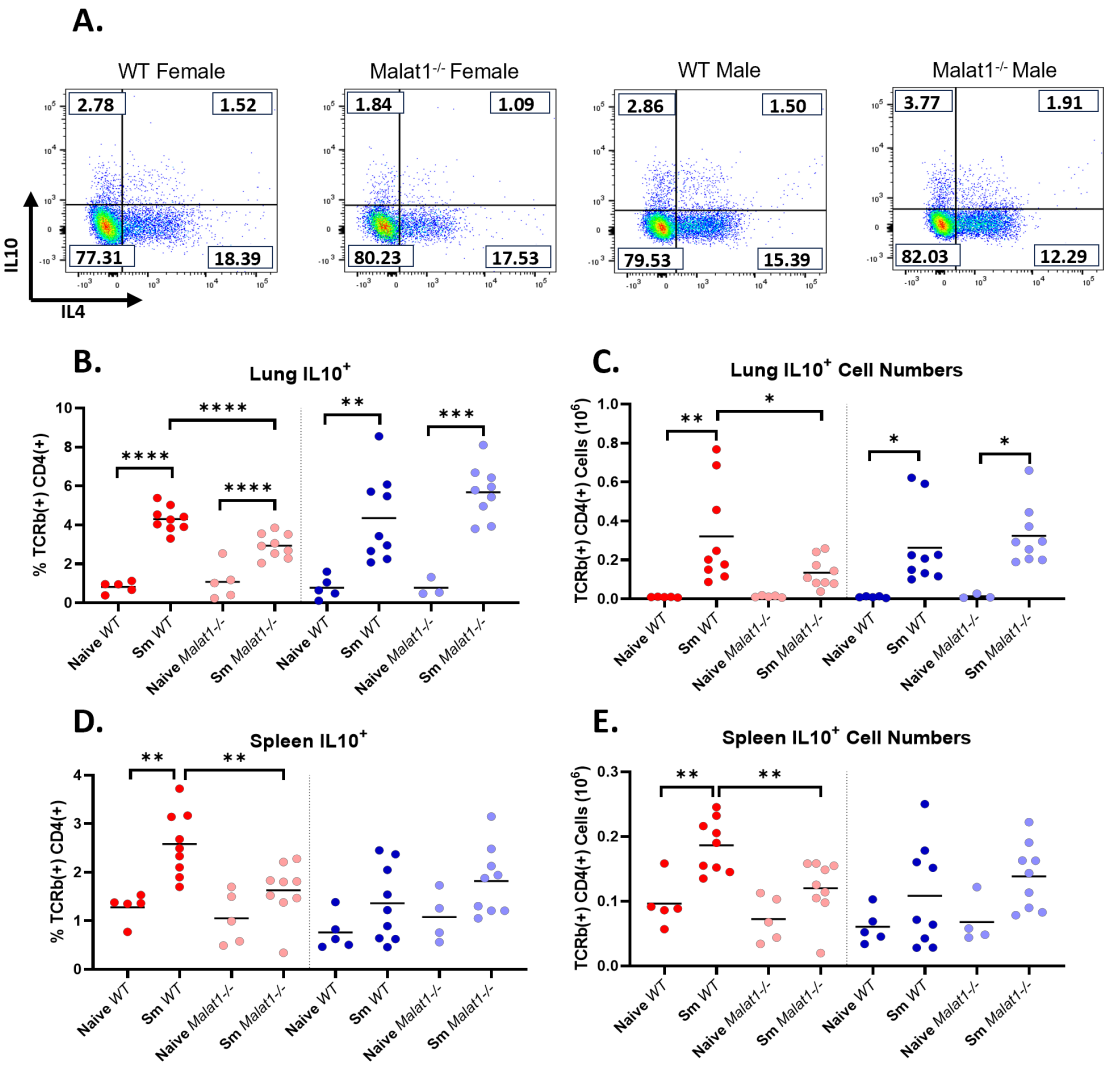

Figure 3.22 *In vivo* loss of *Malat1* disrupts IL10 expression in females

A. Representative FACS plots of IL10 and IL4 expression in lung CD4+ TCRβ+ cells from *Sm* egg-injected *WT* or *Malat1*$^{-/-}$ mice of both sexes. **B.** Percentages of lung IL10 expressing TCRβ^{+} CD4^{+} cells derived from naïve or *Sm* egg injected *WT* or *Malat1*$^{-/-}$ mice of both sexes. Levels determined by intracellular staining (n=4 for *Malat1*$^{-/-}$ male naïve, n=5 for all other naïve, n=9 for egg injected mice). **C.** Total numbers of lung IL10 expressing TCRβ^{+} CD4^{+} cells. **D.** As in B. but for splenic IL10 expressing TCRβ^{+} CD4^{+} cells. **E.** Total numbers of splenic IL10 expressing TCRβ^{+} CD4^{+} cells.

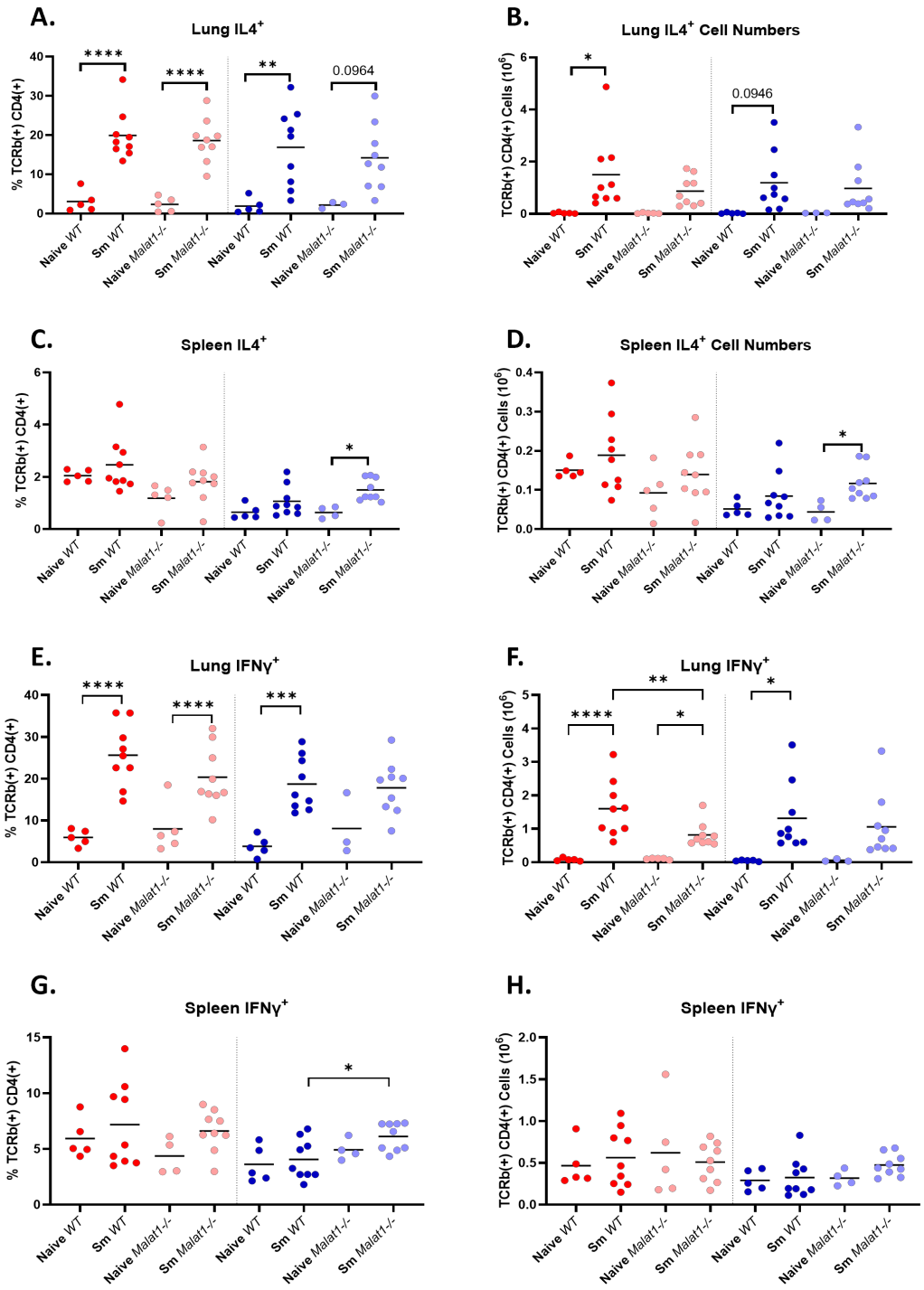
A.
Lung IL4+
% TCRb(+) CD4(+)
****
****
**
0.0964
B.
Lung IL4+ Cell Numbers
TCRb(+) CD4(+) Cells (10^6)
*
0.0946
C.
Spleen IL4+
% TCRb(+) CD4(+)
*
D.
Spleen IL4+ Cell Numbers
TCRb(+) CD4(+) Cells (10^6)
*
E.
Lung IFNγ+
% TCRb(+) CD4(+)
****
****
***
F.
Lung IFNγ+
TCRb(+) CD4(+) Cells (10^6)
**
*
****
*
G.
Spleen IFNγ+
% TCRb(+) CD4(+)
*
H.
Spleen IFNγ+
TCRb(+) CD4(+) Cells (10^6)
Naive WT
Sm WT
Naive Malat1-/-
Sm Malat1-/-

Figure 3.23 *Malat1* loss does not affect IL4 or IFNγ expression *in vivo*

A. Percentages of lung IL4 expressing TCRβ$^+$ CD4$^+$ cells derived from naïve or *Sm* egg injected *WT* or *Malat1*$^{-/-}$ mice of both sexes. Levels determined by intracellular staining (n=4 for *Malat1*$^{-/-}$ male naïve, n=5 for all other naïve, n=9 for egg injected mice). **B.** Total numbers of lung IL4 expressing TCRβ$^+$ CD4$^+$ cells. **C.** Percentages of splenic IL4 expressing TCRβ$^+$ CD4$^+$ cells. **D.** Total numbers of splenic IL4 expressing TCRβ$^+$ CD4$^+$ cells. **E.** Percentages of lung IFNγ expressing TCRβ$^+$ CD4$^+$ cells. **F.** Total numbers of lung IFNγ expressing TCRβ$^+$ CD4$^+$ cells. **G.** Percentages of splenic IFNγ$^+$ expressing TCRβ$^+$ CD4$^+$ cells. **H.** Total numbers of splenic IFNγ$^+$ expressing TCRβ$^+$ CD4$^+$ cells.

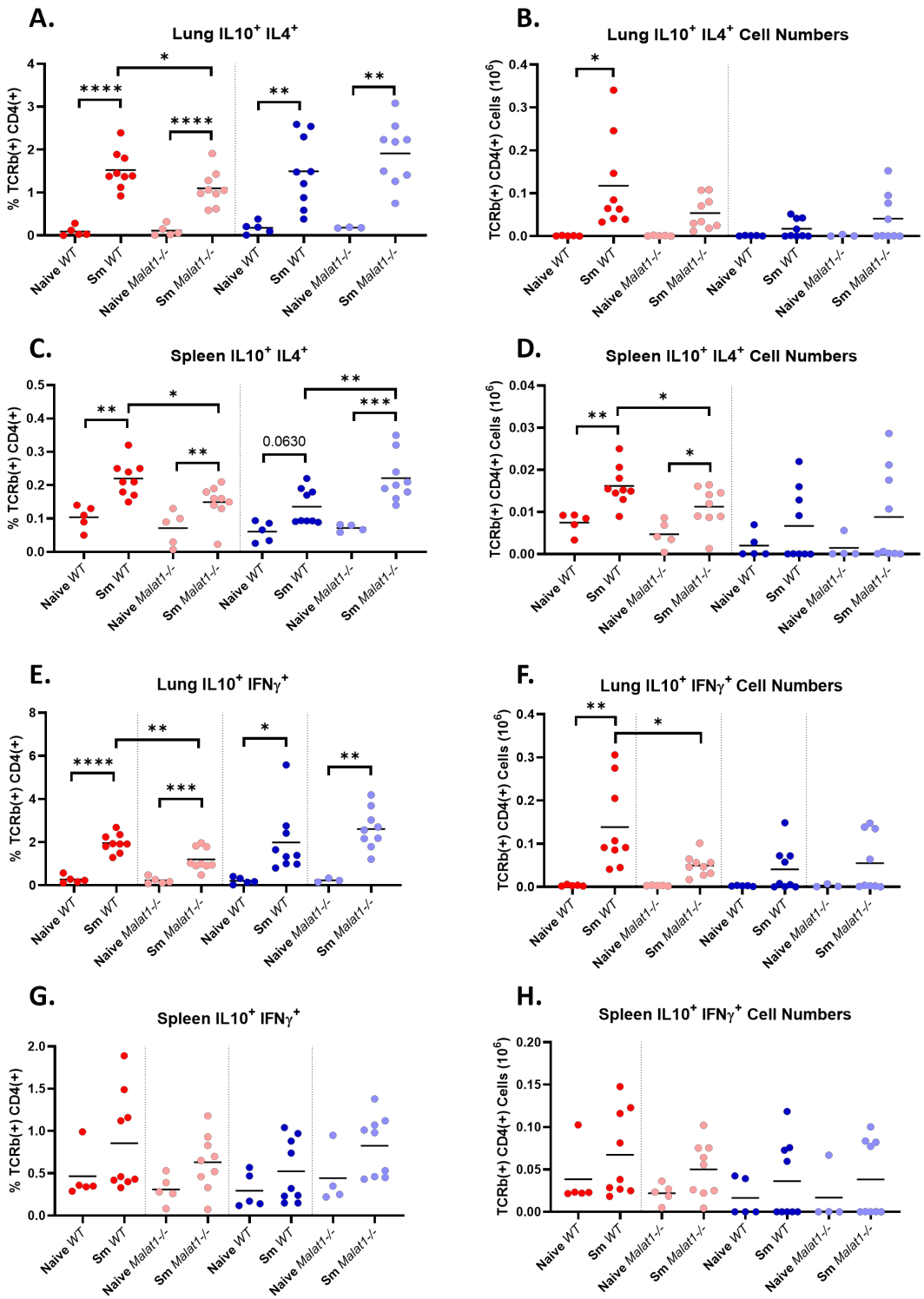
A.
Lung IL10+ IL4+
% TCRb(+) CD4(+)
B.
Lung IL10+ IL4+ Cell Numbers
TCRb(+) CD4(+) Cells (10^6)
C.
Spleen IL10+ IL4+
0.0630
D.
Spleen IL10+ IL4+ Cell Numbers
E.
Lung IL10+ IFNγ+
F.
Lung IL10+ IFNγ+ Cell Numbers
G.
Spleen IL10+ IFNγ+
H.
Spleen IL10+ IFNγ+ Cell Numbers
Naive WT
Sm WT
Naive Malat1-/-
Sm Malat1-/-

Figure 3.24 *Malat1* loss disrupts IL10$^+$ IL4$^+$ and IL10$^+$ IFNγ$^+$ cells *in vivo*

A. Percentages of lung IL10$^+$ IL4$^+$ double positive TCRβ$^+$ CD4$^+$ cells derived from naïve or *Sm* egg injected *WT* or *Malat1*$^{-/-}$ mice of both sexes. Levels determined by intracellular staining (n=4 for *Malat1*$^{-/-}$ male naïve, n=5 for all other naïve, n=9 for egg injected mice). **B.** Total numbers of lung IL10$^+$ IL4$^+$ double positive TCRβ$^+$ CD4$^+$ cells. **C.** Percentages of splenic IL10$^+$ IL4$^+$ double positive TCRβ$^+$ CD4$^+$ cells. **D.** Total numbers of splenic IL10$^+$ IL4$^+$ double positive TCRβ$^+$ CD4$^+$ cells. **E.** Percentages of lung IL10$^+$ IFNγ$^+$ double positive TCRβ$^+$ CD4$^+$ cells. **F.** Total numbers of lung IL10$^+$ IFNγ$^+$ double positive TCRβ$^+$ CD4$^+$ cells. **G.** Percentages of splenic IL10$^+$ IFNγ$^+$ double positive TCRβ$^+$ CD4$^+$ cells. **H.** Total numbers of splenic IL10$^+$ IFNγ$^+$ double positive TCRβ$^+$ CD4$^+$ cells.

Following confirmation that the egg-injection experiment triggered type 2 inflammation in the lung, and that we observed sex-specific effects on cytokine expression in Th cells *in vivo*, we performed a second *in vivo* egg injection experiment. In this experiment females and males were processed on the same days, allowing for more direct comparisons. Due to the changes seen *in vitro* on the IL2 receptor, we investigated IL2Rα and IL2Rγ in the T cell surface receptor panel. We also added IL13 in the $CD4^+$ T cell intra-cellular cytokine panel to allow for identification Th2 cells, via expression of both IL4 and IL13. Full exploration of this experiment is shown in the appendix of this thesis, but only relevant figures will be shown in text (these include eosinophil activation, IL2R staining and parts of the cytokine panel). Of note, the immune response generated in this experiment was weaker than previously, as eosinophil numbers and RELMα expression (*Figure 3.25A-C*) were decreased compared to the previous experiment (*Figure 3.19*).

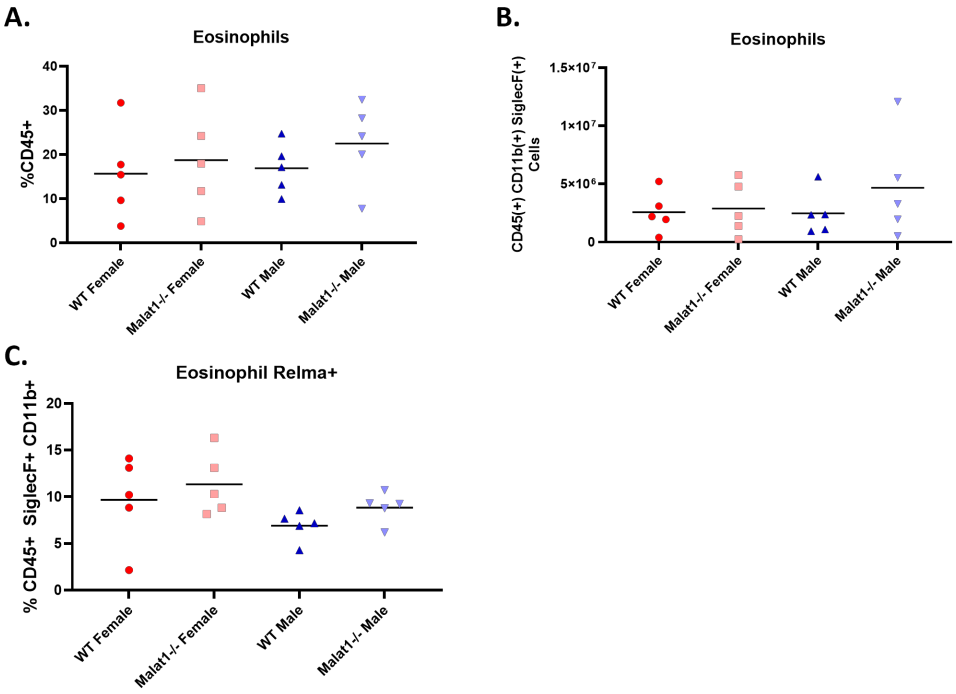

Figure 3.25 The repeated egg-injection experiment generated a weaker type 2 response

A. Percentages of eosinophils ($CD45^+$, $CD11b^+$, $SIGLECF^+$) in lungs of *Sm* egg injected *WT* or *Malat1*$^{-/-}$ mice of both sexes. Levels determined by surface staining (n=5). **B.** Eosinophil lung cell numbers. **C.** Percentages RELMα expressing eosinophils in lungs of *S. mansoni* egg injected, *WT* or *Malat1*$^{-/-}$ mice of both sexes.

When investigating IL2R expression, overall IL2R expression in $CD4^+$ T cells was lower *in vivo* than our *in vitro* experiments. IL2Rα expression was decreased in *Malat1*$^{-/-}$ females in both the lung and the spleen, although this only reached significance in the spleen (*Figure 3.26 A, B*). Interestingly, IL2Rα was significantly affected in *Malat1*$^{-/-}$ males, upregulated in the lung and downregulated in the spleen. IL2Rγ was unaffected by *Malat1* loss in the lung but decreased in *Malat1*$^{-/-}$ females and *WT* males in the spleen, with no difference resulting from *Malat1* loss in males (*Figure 3.26 C, D*). IL2Rα IL2Rγ double positive cells were unaffected in the lung but downregulated in *WT* males and upregulated in *Malat1*$^{-/-}$ males in the spleen (*Figure 3.26 E, F*).

We further investigated IL2R expression within activated ($CD44^{hi}$ $CD62L^{lo}$) cells, as we reasoned these may be similar to the activated Th cells we generate *in vitro*. Here, IL2Rα expression was decreased in *Malat1*$^{-/-}$ females only in the lung, while in the spleen IL2Rα expression was increased in *Malat1*$^{-/-}$ males only (*Figure 3.27 A, B*). IL2Rγ was significantly decreased again only in the spleen for both *Malat1*$^{-/-}$ females and *WT* males (*Figure 3.27 C, D*), while IL2Rα IL2Rγ double positives displayed little change, with only a significant increase in *Malat1*$^{-/-}$ males in the spleen (*Figure 3.27 E, F*). Overall, these results suggest that *Malat1* loss affects IL2R expression *in vivo*.

In terms of cytokine expression in this experiment, the percentage of cells expressing IL10 displayed a borderline non-significant decrease in *Malat1*$^{-/-}$ females in both the lungs and the spleen (*Figure 3.28 A-D*). The lack of significance was potentially due to the overall weaker immune response. No significant results were seen for other cytokine expression, including IL13. However, when using IL4 and IL13 to gate for Th2 cells ($CD4^+$ $TCR\beta^+$ $IL4^+$ $IL13^+$), *Malat1* loss in females caused a large and significant decrease in IL10 within this population (*Figure 3.28 E, F*), again confirming the sex-specific effects of *Malat1* loss on cytokine expression *in vivo*.

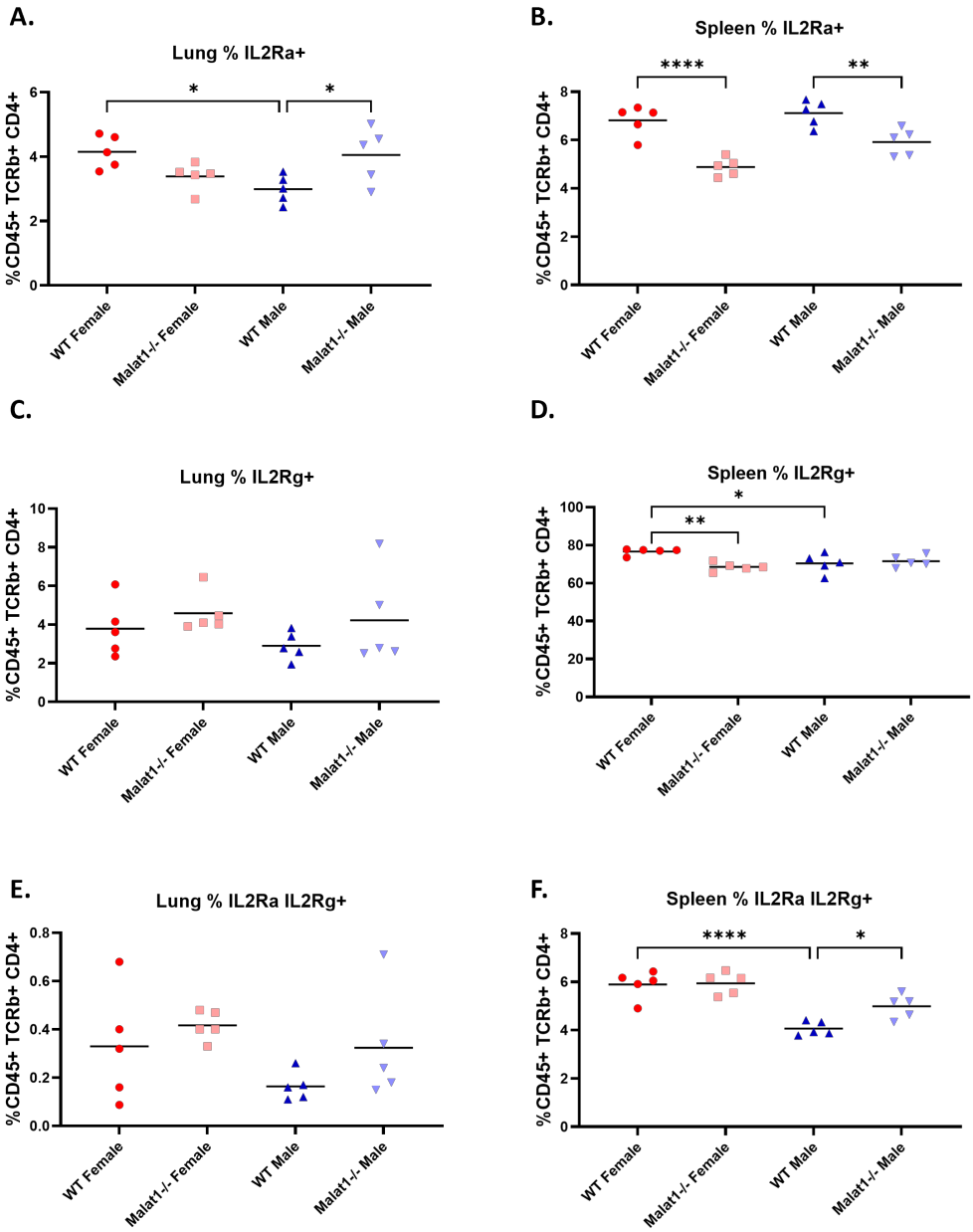

Figure 3.26 *Malat1* loss impacts the expression of the IL2R *in vivo*

A. Percentages of lung IL2Rα expressing TCRβ$^+$ CD4$^+$ cells from the lungs of *Sm* egg injected *WT* or *Malat1*$^{-/-}$ mice of both sexes. Levels determined by intracellular staining (n=5). **B.** Percentages of splenic IL2Rα expressing TCRβ$^+$ CD4$^+$ cells. **C.** Percentages of lung IL2Rγ expressing TCRβ$^+$ CD4$^+$ cells. **D.** Percentages of splenic IL2Rγ expressing TCRβ$^+$ CD4$^+$ cells. **E.** Percentages of lung IL2Rα$^+$ IL2Rγ$^+$ double positive TCRβ$^+$ CD4$^+$ cells. **F.** Percentages of splenic IL2Rα$^+$ IL2Rγ$^+$ double positive TCRβ$^+$ CD4$^+$ cells.

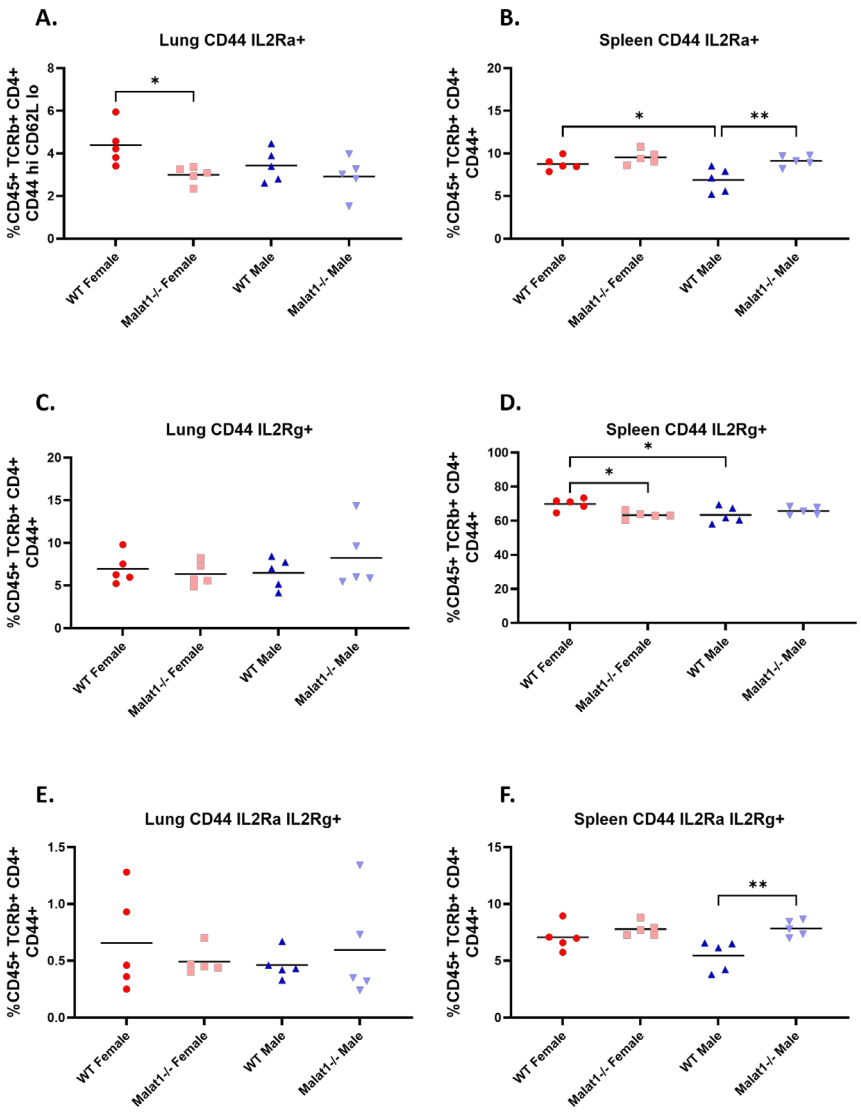

Figure 3.27 *Malat1* loss impacts the expression of the IL2R in activated CD4$^+$ T cells *in vivo*

A. Percentages of lung activated (CD44^{hi} CD62L^{lo}) TCRβ$^+$ CD4$^+$ cells expressing IL2Rα$^+$ from *Sm* egg injected *WT* or *Malat1*$^{-/-}$ mice of both sexes. Levels determined by intracellular staining (n=5). **B.** Percentages of splenic IL2Rα$^+$ expressing activated TCRβ$^+$ CD4$^+$ cells. **C.** Percentages of lung activated TCRβ$^+$ CD4$^+$ cells expressing IL2Rγ$^+$. **D.** Percentages of splenic IL2Rγ$^+$ expressing activated TCRβ$^+$ CD4$^+$ cells. **E.** Percentages of lung activated TCRβ$^+$ CD4$^+$ cells expressing both IL2Rα$^+$ IL2Rγ$^+$. **F.** Percentages of splenic IL2Rα$^+$ IL2Rγ$^+$ expressing activated TCRβ$^+$ CD4$^+$ cells.

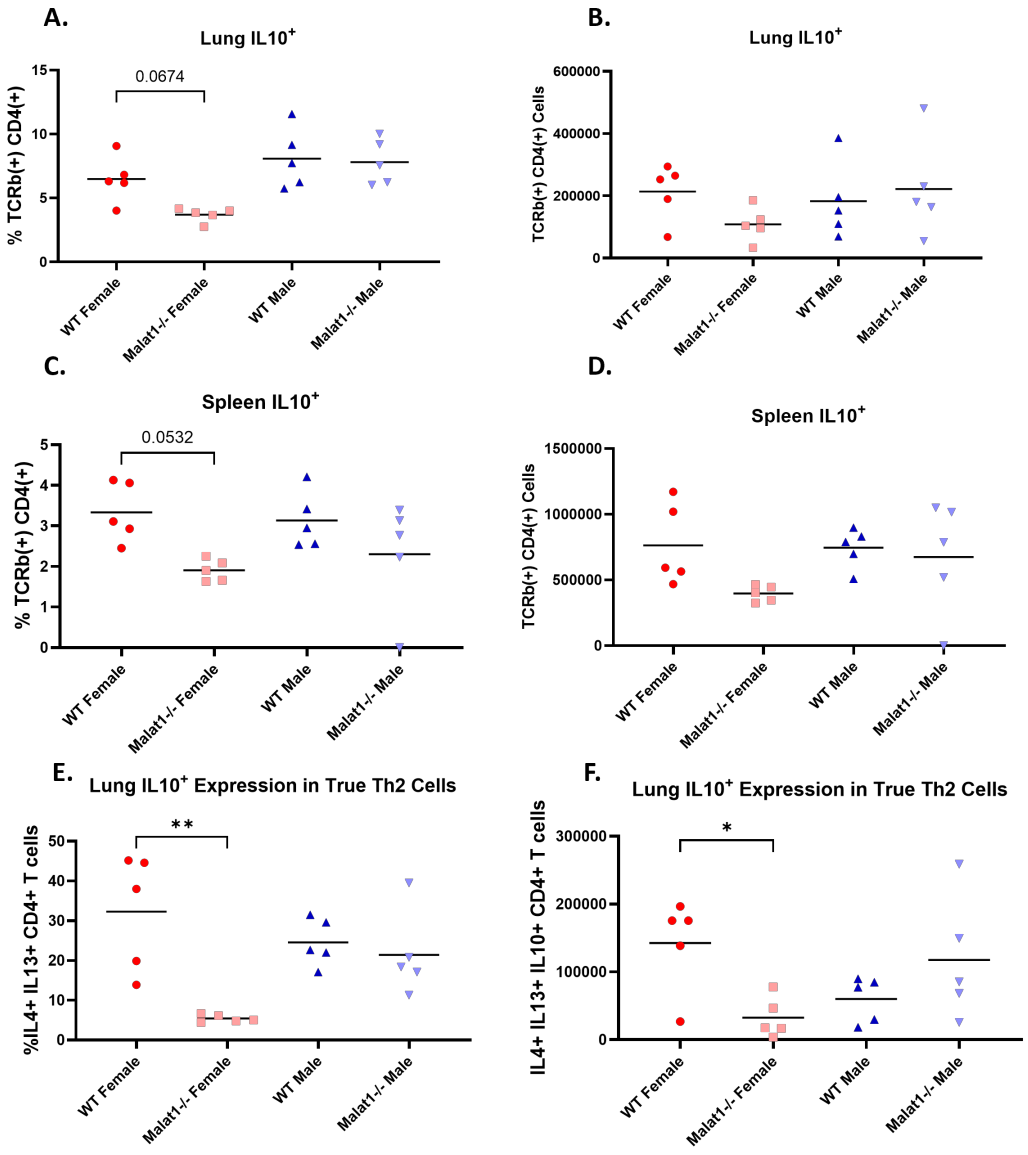

Figure 3.28 *Malat1* loss in females affects IL10 expression in IL4$^+$ IL13$^+$ Th2 cells

A. Percentages of lung IL10 expressing TCRβ$^+$ CD4$^+$ cells from *Sm* egg injected *WT* or *Malat1*$^{-/-}$ mice from both sexes. Levels determined by intracellular staining (n=5). **B.** Total numbers of lung IL10 expressing TCRβ$^+$ CD4$^+$ cells. **C.** Percentages of splenic IL10 expressing TCRβ$^+$ CD4$^+$ cells. **D.** Total numbers of splenic IL10 expressing TCRβ$^+$ CD4$^+$ cells. **E.** Percentages of IL10$^+$ expressing cells within lung Th2 (IL4$^+$ IL13$^+$ TCRβ$^+$ CD4$^+$) cells. **F.** Total numbers of IL10$^+$ expressing Th2 (IL4$^+$ IL13$^+$ TCRβ$^+$ CD4$^+$) cells.

3.3 Discussion

In this chapter, we demonstrated that lncRNA *Malat1* controls Th2 differentiation in a sex-specific manner, with *Malat1* loss in females affecting not just expression of cytokine IL10, but also impacting expression of other Th2 cytokines and blunting transcriptomic changes that occur during Th2 differentiation. We discovered that *Malat1* controls expression of the IL2 receptor, with loss leading to a blunted response to rIL2, likely causing the cytokine and transcriptomic changes seen. We also identified that *WT* male cells display reduced sensitivity to IL2, potentially explaining why *Malat1* loss does not impact cytokine expression in males. Finally, we validated the effects of *Malat1* loss in an *in vivo* model of type 2 lung inflammation, identifying sex-specific decreases in cytokine expression, particularly affecting IL10 and IL10 IL4 expression, and limited effects from *Malat1* loss on the IL2 receptor.

Our results demonstrate that *Malat1* is a novel cell intrinsic and sex-specific regulator of Th2 differentiation, with effects of *Malat1* loss seen both *in vivo* and in an *in vitro* assay. Identifying novel cell intrinsic mediators of sexual dimorphism in T cells is critical to addressing differences in incidence and severity of immunopathologies such as autoimmune disorders or allergies between females and males (Conrad et al., 2023; Gutiérrez-Brito et al., 2024). Known sex-specific drivers of T cell differentiation are predominantly related to the X chromosome or hormonal regulation. However, *Malat1* is not X-linked, and the effects of *Malat1* loss were seen in an *in vitro* assay performed in a hormone-independent environment suggesting that the sex differences were not a result of hormonal regulation. Previous literature has also not suggested that *Malat1* plays a role in hormonal regulation either, although this does not rule out potential hormonal priming of naïve $CD4^+$ T cells, which could result in differing intracellular organisation between females and males. Oestrogen has previously been shown to alter thymic T cell

development (Rijhsinghani et al., 1996), potentially suggesting differences in T cell intracellular organisation following maturation, although this was primarily shown to affect T cell numbers. Cell-intrinsic drivers of T cell sexual dimorphism so far have primarily been linked to X chromosome inactivation escape (Forsyth, Toothacre, et al., 2024), or to direct interactions with *Xist* (R. Y. Guo et al., 2022). However, no research has suggested that *Malat1* can affect X chromosome inactivation or bind to *Xist*.

Malat1 loss here was particularly seen to affect the expression of cytokine IL10 in females, and IL10 signalling blockade was seen to enhance the impact of *Malat1* loss on other Th2 cytokines, revealing decreases in expression of both IL4 and IL13. This combined with the RNA-seq data identifying suppression of transcriptomic changes suggests that *Malat1* loss is inhibiting overall Th2 differentiation. IL10 is highly produced by Th2 cells with expression levels similar to those of IL4, IL5 and IL13 (Saraiva & O'Garra, 2010), although IL10 expression is not Th2 specific and can be expressed by all Th cells later during differentiation (Jankovic et al., 2010; Yssel et al., 1992). IL10 has previously been shown to suppress both Th1 and Th2 differentiation (Akdis & Blaser, 2001), suggesting that the high level of IL10 produced in *in vitro* differentiated Th2 cells masked the effects on other cytokine expression. However, this effect may be context dependent, as IL10 expression during intestinal inflammation is involved more in suppressing Th1 and promoting Th2 responses (Webster et al., 2022). IL10 expression in Th2 cells is directly regulated by transcription factor MAF (Saraiva & O'Garra, 2010), which has previously been shown to be disrupted from *Malat1* loss in Th1 cells (Hewitson et al., 2020), although this was only investigated in female mice. In Th2 cells both MAF and IL10 lie downstream of GATA3 and STAT6 signalling (Saraiva & O'Garra, 2010; Shoemaker et al., 2006) suggesting disruption to the core Th2 signalling from *Malat1* loss in females, which would explain the further effects on IL4, IL13 and the Th2

transcriptome seen, although confirmation would require further investigation of these pathways.

IL10 is known to be a major driver of immune sexual dimorphism, with both expression levels and the cellular effects varying between sexes. IL10 expression can be directly induced in male $CD4^+$ T cells via testosterone signalling, potentially explaining the lower expression levels in our *in vitro* model compared to *in vivo* (Liva & Voskuhl, 2001), while oestrogen instead promotes a more general pro-inflammatory cytokine expression (Mohammad et al., 2018). Interestingly, some sex differences have also been observed in IL10 signalling, such as a heightened STAT3 activation from IL10 signalling in male blood leukocytes (Islam et al., 2022), suggesting stronger intracellular regulation of IL10. This increased intracellular signalling may explain the higher IL10 levels seen in *WT* females seen here.

The effect on differentiation in female *Malat1*$^{-/-}$ cells is likely to be caused, at least in part, by the disrupted response to IL2. IL2 signalling via STAT5 in Th2 cells promotes the expression of IL4Rα and IL4, and therefore disruption to IL2 signalling could inhibit transcriptional changes from IL4 signalling (Liao et al., 2008; Wohlfert et al., 2011). *Malat1* in humans has been linked to both IL4 and GATA3 expression in Th2 differentiation previously, with *Malat1* knock-down disrupting both IL4 and GATA3 expression in a model of ovalbumin induced Th2 differentiation (Liang & Tang, 2020). Disruption to IL4 signalling would likely impact GATA3 levels however, and no differences were seen in *Gata3* transcript expression from *Malat1* loss in our RNA-seq data, although again this could be caused by the compensatory mechanism from the increased IL10 levels in *WT* females. IL10 expression is also in part regulated by downstream IL2R activation and IL2 signalling. IL2 signalling in Th cells promotes

expression of transcription factors such as BLIMP-1 and MAF, both of which promote IL10 expression in Th cells (Rani et al., 2011; Shouse et al., 2024).

Malat1 loss in females specifically was able to impact expression of both IL2Rγ and IL2Rα *in vitro*. *In vivo Malat1* loss had a modest effect on IL2R expression, particularly affecting IL2Rα levels in activated lung T cells, and IL2Rγ levels in splenic T cells. However, levels of these two IL2R subunits were extremely variable between *in vitro* and *in vivo* differentiated Th2 cells, and the T cells *in vivo* were likely at differing stages of activation. Expression dynamics also differ between the IL2R subunits in Th cell differentiation, as IL2Rα is expressed relatively quickly following T cell activation and is commonly used as a marker of Th cell activation and differentiation (Belot et al., 2018), while IL2Rγ is expressed constitutively instead. The disruption to IL2Rα expression may hint at impacts from *Malat1* loss at earlier time points during the Th2 differentiation procedure, such as during initial T cell activation. This is also consistent with our GapmeR knockdown experiments revealing that *Malat1* was required at the early stages of differentiation and could also explain the fact that *Malat1* loss does not impact the *Il2ra* and *Il2rg* transcripts at day 4, as the RNA levels may be disrupted in prior time points.

IL2Rα expression in $CD4^+$ T cells is associated with the development of Tcm cells (Dooms et al., 2007). Interestingly, in $CD8^+$ T cells, *Malat1* was shown to regulate memory cell formation and to affect cell proliferation and IL2 expression, likely via targeting of PRC2 (Kanbar et al., 2022). Memory cell formation in CD8 T cells is also heavily linked to IL2 signalling, with IL2 shown to rescue CD8s from death following cell contraction and to promote differentiation to effector memory cells. (Boyman et al., 2010). *Malat1* has been demonstrated to associate with EZH2 and PRC2 in a number of

different cell types, also including a T cell lymphoma line and embryonic stem cells (S. H. Kim et al., 2017), with knock-down shown to dysregulate H3K27me3 patterns. During T cell differentiation subset specific genes and cytokines are demethylated to upregulate expression, which is particularly important for core Th2 cytokine IL4 (D. U. Lee et al., 2002), while active methylation occurs to suppress alternate Th cell subsets transcription factor and cytokine expression (Yano et al., 2003). This could suggest that *Malat1* is regulating similar pathways between $CD4^+$ and $CD8^+$ T cells via its known association with PRC2, although further research into histone methylation and whether *Malat1* associates with PRC2 during Th2 differentiation would be required to investigate this. However, more recent research have shown that direct interactions between PRC2 and lncRNA such as *Malat1* may be an experimental artifact,. CLIP and RIP experiments performed with denaturing conditions have failed to identify PRC2 binding to lncRNAs (J. K. Guo et al., 2024), while RNase A degradation during CLIP (previously used to show that RNA was required for PRC2 occupancy on chromatin) in fact lead to non-specific chromatin precipitation, suggesting that it is not directly regulated by lncRNAs (Hall Hickman & Jenner, 2024; Healy et al., 2024). However, regulation of PRC2 by *Malat1* may still occur via regulation of an intermediate RBP, or as a result of *Malat1* regulating other processes.

Malat1 has also been shown to affect alternative splicing, via its interactions with SR and HNRNP splicing factors (Miao et al., 2022; Tripathi et al., 2010). Changes in alternative splicing events are core to T cell activation (Ip et al., 2007), and play further roles in regulating T cell differentiation, proliferation and apoptotic signalling (Banerjee et al., 2023). *Malat1* loss affecting the function of its associated splicing factors could cause the observed effects on differentiation. Some *Malat1* RBP binding partners are already known to regulate parts of T cell differentiation. SRSF1 is a regulator of Treg

cells, with knock-down causing aberrant expression of proinflammatory cytokines such as IL17 (Katsuyama & Moulton, 2021). Meanwhile, SRSF2 has been shown to be upregulated in and linked to exhausted T cells, where it regulates H3K27 acetylation (Z. Wang et al., 2020). In terms of other cellular roles, *Malat1* has been shown to localise to actively transcribing chromatin and aid in the targeting of transcription factors and transcriptional repressors (Aslanzadeh et al., 2024), disruption of which could also explain the general impacts on Th2 differentiation.

While IL2Rα was disrupted only in *Malat1*$^{-/-}$ females, IL2Rγ expression was disrupted in both *Malat1*$^{-/-}$ females and males *in vitro* and in some T cell subsets *in vivo*. This discrepancy could be explained by the high affinity receptor mediating the majority of the biological effects of IL2 (Ross & Cantrell, 2018). However, we also observed a differential sensitivity to IL2 observed between females and males. IL2 activation of STAT5 is suggested to be critical for Th2 differentiation, promoting the expression of Th2 cytokines such as IL4 (Cote-Sierra et al., 2004), although our results suggest IL2 may be more critical for Th2 differentiation in females than males, and therefore disruption to the IL2 receptor would not cause the same level of disruption in males. Increased sensitivity to IL2 in females has been noted previously in other immune cell types. Female ILC2s demonstrate increased proliferation and cytokine expression in response to IL2 (Cephus et al., 2017), while female NK cells produce higher levels of IFNγ than males in response to increasing levels of IL2 (Menees et al., 2021). This may suggest that generally IL2 signalling is altered in males, or that males are less sensitive to IL2.

As part of T cell differentiation, IL2 signalling in activated Th cells promotes CD4^{+} T cell expansion through the mTORC pathway (Katzen et al., 1985; Ross & Cantrell, 2018), however despite the effects on cytokine expression no differences were noted in cell numbers resulting from *Malat1* loss. This could suggest that *Malat1* loss

affects specific signalling pathways, and proliferation is unaffected. This result could also be in part due to a high amount of cell death occurring during the contraction phase of Th cell differentiation (Garrod et al., 2012; McKinstry et al., 2010), which could act as a compensatory mechanism. *Malat1* has also previously been linked to cell proliferation in cancers, with knockdown of inhibiting ovarian cancer cell progression (Gordon et al., 2019) and hepatocellular carcinoma proliferation (Malakar et al., 2016), suggesting that further experiments may identify differences here, and future experiments should trial methods such as CFSE staining for assessing whether cell division is impacted.

The effect on IL10 expression *in vivo* may hint at real consequences in infection if *Malat1* is mutated or its expression is altered. IL10 *in vivo* is critical for a number of infections and diseases, generally preventing tissue damage during acute levels of inflammation by inhibiting activity of Th cells, NK cells and macrophages (Couper et al., 2008). Th2 cytokine expression, particularly IL10, is also known to be an important determinant of full *Schistosoma* worm infection outcomes in mice. Neutralisation or knock-out of IL10 during *S. mansoni* infection was seen to enhance Th1 responses and increase granuloma size (Flores Villanueva et al., 1993; Sadler et al., 2003). Failure to properly set up Th2 responses in *Schistosoma* infection in mice is suggested to increase mortality (MacDonald et al., 2002). Therefore, it would be interesting to perform further exploration investigating *Malat1* loss in full *S. mansoni* infection. Due to the IL10R blockade *in vitro* enhancing the effects of *Malat1* loss on Th2 differentiation, future experiments investigating IL10R blockade *in vivo* may enhance differences on other Th cell cytokines and in other cell types. However, IL10 levels in this *in vivo* model are lower than *in vitro* (5% compared to 20%), while the inverse occurs for IL4 expression (20% to 10%), therefore the impact of IL10R blockade on IL4 and IL13 may not occur to the same extent. IL10 expression from $CD4^+$ T cells is also critical in developing immune tolerance

to allergens (Akdis & Akdis, 2014), and therefore further validation of *Malat1* loss on Th2 differentiation in alternative *in vivo* models of allergic inflammation, such using the HDM allergen (Woo et al., 2018), may provide additional context for the role of *Malat1* in allergy and autoimmunity.

While we identified similar trends for the effects of *Malat1* loss on IL10 in females both *in vivo* and *in vitro*, we also observed a number of differences in our *in vivo* model compared to our *in vitro* model for Th2 cell generation. Malat1 *loss in* vivo in males generally displayed enhanced immune responses to egg-injection, more similar to those observed in *WT* females. Neutrophil and $Ly6C^{High}$ monocyte percentages significantly decreased on egg-injection in *Malat1*$^{-/-}$ males similar to those seen in females, while $CD4^+$ T cell percentages significantly increased similar to those seen in WT females. Meanwhile, in the spleen both total and activated splenic $CD4^+$ T cell numbers significantly increased only in *Malat1*$^{-/-}$ males. In terms of the Th2 differentiation, we observed a significant decrease in $IL10^+$ expression and $IL10^+$ $IL4^+$ expression in *Malat1*$^{-/-}$ females, consistent with our *in vitro* data, as well as a significant decrease in $IL10^+$ $IFN\gamma^+$ cells. However, we did not observe significant decreases in IL4 and IL13 expression from *Malat1* loss, although this was inconsistent in our *in vitro* dataset without treatment with anti-IL10R blocking antibody, which was not used in our *in vivo* experiments. We also did not observe a significant increase in IL10 and IL4 expression in *WT* females compared to *WT* males *in vivo*, with consistent cytokine levels seen between both *WT* male and females. We also observed changes in the IL2R in *Malat1*$^{-/-}$ females *in vivo*, with decreased IL2Rα and IL2Rγ expression in *Malat1*$^{-/-}$ females both overall and in activated ($CD44^+$) cells, consistent with our results *in vitro*. However, expression levels of IL2Rα were greatly decreased *in vivo* (3-5%) compared to *in vitro* (70-80% expression), which is likely a consequence of the Th cells *in vivo* being at differing stages

of differentiation. IL2Rγ expression also differed between the lung (6% expression) and spleen (70% expression), suggesting that IL2Rγ levels may be more tissue specific *in vivo* and therefore less comparable to our *in vitro* data.

we also observed differences in *Malat1*$^{-/-}$ males not seen *in vitro*, such as significant increases in splenic IL4^{+} on injection not seen in other samples, significant increases in IFNγ^{+} and IL10^{+} IL4^{+} cells compared to *WT* males, and significant decreases in splenic IL2Rγ^{+} cells compared to *WT* males. We also observed that *in vivo* Th2 cells displayed lower IL10 expression compared to our *in vitro* models and, higher IL4 and IL13 expression. These *in* vivo results in males may suggest that *Malat1* loss enhances the overall immune response in males, particularly highlighting the sex-specific effects of *Malat1* loss, and may suggest that *Malat1* is affecting different intracellular pathways between females and males. However, none of the changes in cytokine expression in males were seen in our *in vitro* assays, potentially suggesting that these could be induced from *Malat1* loss in other immune cell types or from hormonal regulation.

Th cell differentiation in our *in vitro* model was seen to differ between males and females. *In vitro*, males generally displayed lower cytokine expression than females, and RNA-seq data in males displayed a suppression in immune effector genesets and an overall smaller upregulation of core Th2 genes. However, the differences in cytokine expression are not seen in our *in vivo* model, with roughly similar levels of IL10, IL4 and IL13 expression between females and males. This may suggest that supplementary factors are missing from the *in vitro* polarisation assays, particularly in males. Testosterone in particular is linked to heightened expression of IL10 in Th cells (Liva & Voskuhl, 2001), potentially suggesting that male CD4^{+} T cells require this for the heightened expression seen in females. Alternatively, oestrogen can promote inflammatory cytokine expression, potentially limiting IL10 expression in females *in vivo* (Mohammad et al., 2018), and

phenol red in media may have weak oestrogenic activity (Berthois et al., 1986). Future experiments investigating how hormones affect Th cell differentiation *in vitro* may provide useful information, alongside investigating Th cell differentiation in hormone free media.

Sex differences have also been previously reported in full *Schistosoma* worm infections. In humans, males are more likely to be re-infected with *Schistosoma* following praziquantel treatment than females, and the prevalence of infections is known to be higher in males (Trienekens et al., 2020). However, the differences in humans may be at least in part due to an increased exposure rate, which could explain the increased infection rates when compared to females (Ayabina et al., 2021). In mice, testosterone has been identified as a regulator of *S. mansoni* infection, with males displaying reduced numbers of adult worms than females as a result of testosterone signalling (Nakazawa et al., 1997). Meanwhile, infected female mice display an overall stronger inflammatory response to *S. mansoni* infection (Eloi-Santos et al., 1992). This may warrant future investigation on the role of *Malat1* in full *Schistosoma* infection, and whether it could act as a driver for sexual dimorphism in the immune response here.

To conclude, the work presented in this chapter suggests that *Malat1* is a critical sex-specific regulator of end-stage Th2 differentiation. *Malat1* loss has wide ranging impacts in females on Th cell differentiation, impacting expression of the IL2R, Th2 subset cytokines, and transcriptional changes during Th2 differentiation, with effects seen both *in vivo* and *in vitro*. This provides an exciting platform for investigating novel lncRNA regulators of sexual dimorphism in $CD4^+$ T cells.

4. *Malat1* Regulates the Th2 Gene Programme During Early Differentiation via Repression of a Type-I Interferon Inducible Geneset

4.1 Introduction

4.1.1 Statement

Some of the work presented in this chapter is also featured in the publications:

Gwynne M, West KA, van Dongen S, Kourtzelis I, Coverley D, Teichmann SA, James KR, Hewitson JP, Lagos D. Malat1 regulates female Th2 cell cytokine expression through controlling early differentiation and response to IL-2. J Immunol. 2025 Aug 28:vkaf177. doi: 10.1093/jimmun/vkaf177. Epub ahead of print. PMID: 40865984.

4.1.2 $CD4^+$ T cell activation (markers CD69, IL2Rα, CD44)

As previously mentioned, during T cell activation a major transcriptional and translational burst occurs in the first 24 hours, leading to the expression of a number of key T cell activation genes. Several cell surface receptor genes, due to their relative low expression in naïve T cells and direct links to TCR stimulation, are commonly used as marker of activation. These include CD69, IL2Rα, and CD44. CD69 expression is triggered via TCR stimulation, via activation-associated transcription factors such as AP-1 causing rapid transcriptional upregulation (Cibrián & Sánchez-Madrid, 2017). In terms of its expression kinetics, *Cd69* mRNA becomes detectable under an hour post-activation. Transcript levels then peak at around 2-3 hours and begin to decrease after 4-6 hours (Cibrián & Sánchez-Madrid, 2017). Interestingly, CD69 protein expression is not directly coupled to that of the transcript. CD69 protein is first detectable at low levels on the cell surface at 2-3 hours post-activation, when *Cd69* transcript expression peaks. The protein levels then increase from here until 12 hours post-activation, remaining at stable levels for 24 hours, while the transcript levels decrease after the 3 hour peak (M. Wang et al., 2008).

Despite its high expression levels during *in vitro* activation, CD69 binding to its ligand Gal-1 on DCs modulates T cell activation via interacting with the Jak3/Stat5 pathway. Early activation of this pathway is used to attenuate Th cell activation, enhancing Treg differentiation to limit and prevent T cell overactivation (Cibrián & Sánchez-Madrid, 2017). CD69, through its interaction with Gal1, has previously been shown to negatively regulate IL17 and IFNγ expression in Th1 and Th17, cells and promote IL10 expression in Tr1 cells (Fuente et al., 2014). CD69 may also be involved in regulating Th2 cell differentiation too, as CD69 knock-out has been shown to enhance Th2 cytokine expression in asthma models (Fuente et al., 2014).

In comparison to CD69, both IL2Rα and CD44 are used as markers of later activation. While both IL2Rα and CD44 expression is also triggered following TCR-stimulation and via activation of AP-1 and NF-kB pathways, expression is delayed in comparison to CD69. In terms of these receptors, expression is first detectable at 24 hours post-activation, reaching maximal expression at 48 hours post activation. Also unlike CD69, IL2Rα and CD44 expression remains high during the remainder of Th cell differentiation (Fuente et al., 2014; Moran et al., 2016).

4.1.3 Type-I IFN signalling in $CD4^+$ T cells

Type-I IFNs are primarily produced in response to viral infection, with the aim of inducing antiviral states in surrounding cells. The most well studied of these include the IFNα cluster, consisting of 13 separate *Ifna* genes, and IFNβ. Less well studied type-I IFNs include IFN ε, κ, ω, δ and τ. Type-I IFNs signal via the IFNα receptor (IFNAR), comprised of subunits IFNAR1 and IFNAR2 (Kuka et al., 2019).

In terms of type-I IFN impacts on Th cells, signalling during initial Th cell activation has shown to inhibit T cell expansion (Dondi et al., 2003). However, signalling during differentiation primarily pushes cells towards a Th1 phenotype, but can also help cause Tfh cell differentiation (Kuka et al., 2019). Type I IFN signalling aids in upregulating expression of TBET (Nakayamada et al., 2014), and IFN signalling during Th1 differentiation promotes IFNγ expression. This in turn triggers M1 macrophage activation and enhances cytotoxic T cell responses, mediating infected cell apoptosis and viral clearance. In terms of the Tfh response, type-I IFN signalling in $CD4^+$ T cells is required for initial Tfh activation. IFN signalling results in increased expression of Tfh master regulator BCL6, and of Tfh surface markers CXCR5 and PD-1 (Nakayamada et al., 2014). However, end-point differentiated Tfh cell expression of cytokines such as IL21 is unaffected by IFN signalling (Dondi et al., 2003).

In vivo type-I IFN signalling shows slightly differing and contrasting responses to those *in vitro*. Type-I IFNs *in vivo* in both humans and mice are primarily produced by DCs, acting to modulate T cell responses. During acute infection, type I IFNs have been suggested to promote $CD4^+$ T cell differentiation, clonal expansion, and survival similar to that identified *in vitro*. However, in contrast to this type-I IFNs may also aid in the creation of an immunosuppressive environment (Kuka et al., 2019), and have been shown to stimulate IL10 expression in some Th cell subsets such as Th17 cells in mice (L. Zhang et al., 2011). Type-I IFN signalling during chronic infection has also been suggested to increase expression T cell exhaustion markers PD-1, TIM-3 and TIGIT in humans (Sumida et al., 2022). In some specific conditions, $CD4^+$ T cells are also able to produce type-I IFNs, likely in the context of antitumour immunity in humans. Here, tumour infiltrating $CD4^+$ T cells are suggested to utilise type-I IFNs to upregulate class-I MHC

expression, enhancing $CD8^+$ T cell cytotoxicity and improving patient outcomes (Lei, de Groot, et al., 2024).

Type-I IFN signalling may also play a role in priming naïve T cells for responses. While there is limited research in this area, recent research into naïve $CD4^+$ T cells suggests they display significant heterogeneity, forming distinct sub-populations. One subpopulation in mice is characterised by increased expression of type-I IFN responsive genes and was suggested to be IFN primed (Deep et al., 2024). This type-I IFN primed cluster of cells is suggested to be both infection and commensal independent and is present even in both germ free and specific pathogen free mice (Even et al., 2024). This cluster of IFN primed cells is linked to diminished TCR signalling and a preference to differentiate towards memory cells over effector cells, suggesting that type-I IFN signalling in naïve CD4+ T cells may aid in priming cells towards Tcm fate (Deep et al., 2024). Interestingly, subsequent research investigating naïve cell cytokine priming identified that helminth *Nippostrongylus brasiliensis* infection altered the differing subpopulations of naïve cells, resulting in an IL4 responsive naive subpopulation. This subpopulation, when transferred to uninfected mice, resulted in reduced responses to immunisation (Even et al., 2024).

4.1.4 Nanopore long-read RNA sequencing

The majority of published RNA-sequencing data uses next generation short-read Illumina RNA sequencing (Stark et al., 2019). For short-read sequencing, cDNA libraries are generated, where input RNA is enriched for mRNA via oligo(dT) capture, fragmented into short (<300 bp) sequences, then reverse transcribed. cDNA libraries are then loaded onto the flow cell, where fragments are then sequenced by DNA polymerase, which

incorporates fluorescently tagged nucleotides into its complimentary sequence, allowing for accurate base identification (Goodwin et al., 2016). However, the fragmented sequences required for Illumina sequencing are much shorter than a typical mRNA, meaning that accurate identification of different splice variants or repetitive regions of transcripts is not possible with this technology (Castaldi et al., 2022).

To overcome the limitations of Illumina sequencing, long-read sequencing methods such as Oxford Nanopore Technology (ONT) or PacBio sequencing were developed. The ONT sequencing method involves applying a constant voltage across a membrane-embedded pore and helicase protein, which passes single stranded nucleic acids through the pore in a step wise manner. Alterations in current caused by differing charges in single stranded nucleic acids passing through the pore allows for accurate real-time base calling (Y. Wang et al., 2021). ONT RNA sequencing can involve generation of cDNA libraries and limited PCR-amplification (PCR-cDNA sequencing) or direct-RNA sequencing, which overcomes limitations associated with reverse-transcription and also allows for identification of post-transcriptional nucleotide modifications, such as methylation (Jain et al., 2022).

Unlike short-read sequencing, ONT sequencing does not require RNA fragmentation, allowing for significantly longer reads. Reads are able to span multiple exons and can cover the full transcript length, allowing for more precise identification of different transcript isoforms and better identification of transcript co-dependencies (H. Wu et al., 2023). The fragmentation step also introduces biases towards certain major isoforms seen in short-read sequencing, which are avoided in long-read sequencing (H. Wu et al., 2023). In terms of comparability to Illumina sequencing for analysing gene expression, recent benchmarking has revealed that ONT direct RNA and PCR-cDNA sequencing perform similarly to short-read sequencing in terms of identifying differential

gene expression (Y. Chen et al., 2025), making the ONT sequencing method extremely useful for analysing gene expression, alternative splicing, post-transcriptional modifications, and polyA length from the same sequencing run.

4.1.5 Hypothesis and aims

Results in chapter 3 of this thesis indicated that *Malat1* loss was required during early Th2 differentiation to affect end-point Th2 differentiation. In this chapter, we tested the hypothesis that *Malat1* loss affects gene expression in early differentiating Th2 cells. We aimed to determine how *Malat1* loss affects the transcriptome of differentiating Th2 cells *in vitro* using long-read RNA sequencing.

The aims of this chapter were to:

- Investigate the effects of *Malat1* loss on naïve CD4+ T cell activation and early Th2 cell differentiation
- Investigate transcriptomic changes resulting from *Malat1* loss at day 2 of differentiation via long-read ONT RNA sequencing.
- Identify *Malat1*-dependent pathways that are associated with Th2 differentiation and explore whether their disruption phenocopies the impact of *Malat1* loss on Th2 differentiation.

4.2 Results

4.2.1 *Malat1* loss causes a sex-specific increase in the early activation marker CD69

To identify if *Malat1* loss disrupted early T cell activation, we performed *in vitro* Th2 cell differentiations of naïve $CD4^+$ T cells from *WT* and *Malat1*$^{-/-}$ mice, of both female and male sex. We investigated the expression of early activation marker CD69 during the first 24 hours by flow cytometry and qRTPCR. *Cd69* mRNA expression peaks at 3 hours post-activation (Cibrián & Sánchez-Madrid, 2017), and the protein level becomes detectable at later time points, peaking at around 24 hours (M. Wang et al., 2008). Therefore, we opted to take samples for analysis at 3- , 7- and 24-hours post-activation.

When investigating receptor expression (*Figure 4.1 A, B*), we observed increasing expression of CD69 during activation, reaching the maximum expression levels at 24 hours. The kinetics of CD69 expression were shifted as a result of *Malat1* loss in females, with the percentage of cells expressing CD69 increasing at 3 hours following activation, the effect reaching statistical significance at the 7-hour mark. However, at 24 hours CD69 expression was significantly decreased in *Malat1*$^{-/-}$ females instead, suggesting that the dynamics of CD69 expression were shifted slightly earlier. *WT* males displayed similar trends to *Malat1*$^{-/-}$ females, with a significant increase at 3 hours post-activation, however no changes were seen between *WT* and *Malat1*$^{-/-}$ males.

We next assessed transcript levels at these time points by qRTPCR. Consistent with previous literature, we observed that *Malat1* levels in both males and females were rapidly downregulated by the 24-hour mark of activation, at <10% of the levels in naïve cells (*Figure 4.2 A*). When assessing *Cd69* expression (*Figure 4.2 B*), we identified

differing kinetics compared to the receptor expression, with *Cd69* transcript expression peaking at 3 hours post-activation, then decreasing back to naïve cell levels by 24 hours. Here, at 3 hours post-activation, we observed a significant increase in the *Malat1*$^{-/-}$ females, consistent with the results at the protein level. For comparison, we investigated expression of a second activation marker IL2Rα (also known as CD25) at these time points by flow cytometry (*Figure 4.2 C*), however IL2Rα only began to be upregulated at 24 hours, providing little comparison at earlier time points, and no significant differences were identified here. Overall, these results indicated that *Malat1* loss affects the kinetics of T cell activation in females.

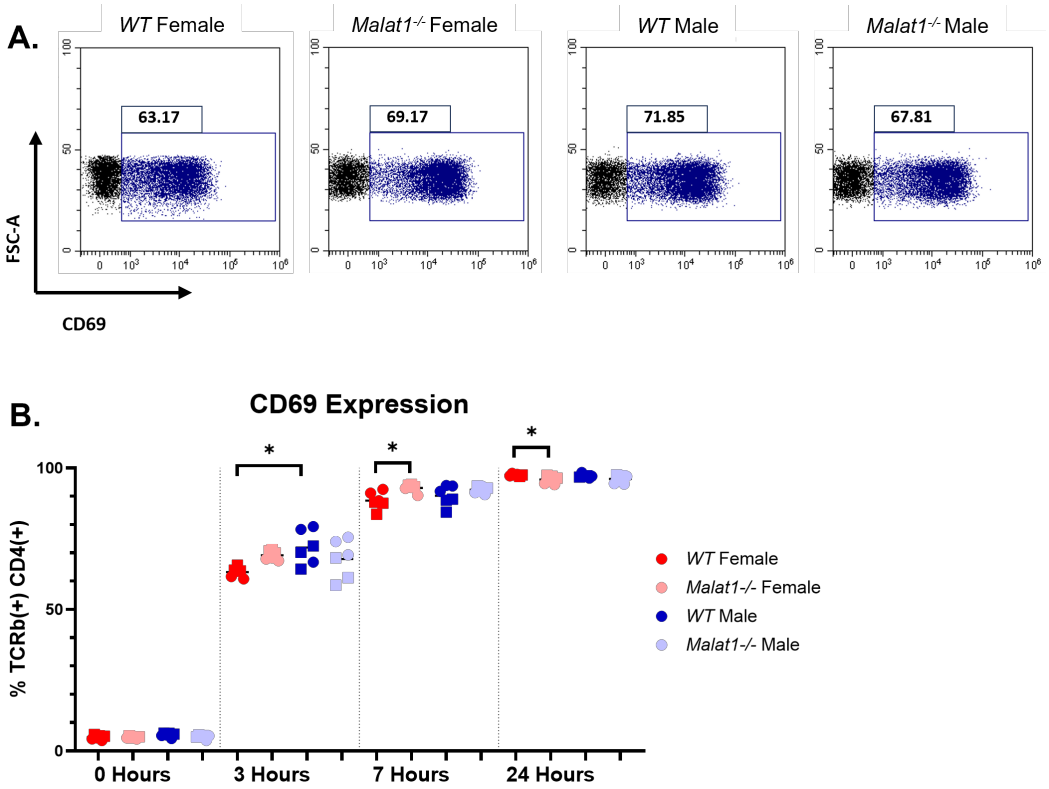

Figure 4.1 *Malat1* loss affects CD69 expression and kinetics

A. Representative FACS plots displaying CD69 expression in *WT* and *Malat1*$^{-/-}$ female and male in vitro differentiated Th2 cells, at 3 hours post-activation. **B.** Percentage CD69^{+} expression in CD4^{+} T cells from *WT* or *Malat1*$^{-/-}$ cells of both sexes, at 0-, 3-, 7- and 24-hours into Th2 *in vitro* differentiation. Levels determined by flow cytometry (n=6, 2 experiments of n=3, appropriate statistics as detailed in the methods used to compensate for experimental variability).

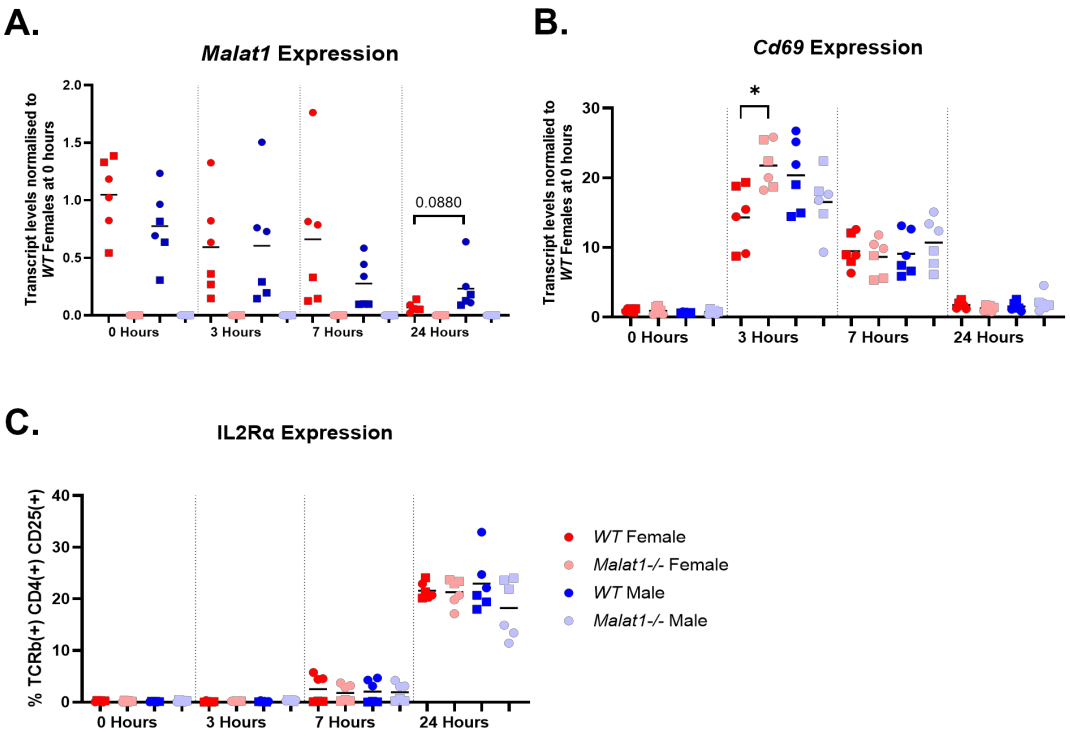

Figure 4.2 *Malat1* loss affects CD69 mRNA levels

A. *Malat1* transcript levels in *WT* and *Malat1*$^{-/-}$ CD4^{+} T cells of both sexes, at 0-, 3-, 7- and 24-hours of *in vitro* Th2 differentiation. Levels determined by qRTPCR, and normalised to U6 and the average levels of WT females at 0 hours (n=6, data from 2 experiments of n=3, appropriate statistics as detailed in the methods used to compensate for experimental variability). **B.** As in A. but for *Cd69* transcript expression. **C.** Percentage of IL2Rα expression in CD4^{+} T cells from *WT* or *Malat1*$^{-/-}$ mice of both sexes, at 0-, 3-, 7- and 24-hours of *in vitro* Th2 differentiation. Levels determined by flow cytometry (n=6, 2 experiments of n=3).

4.2.2 Time course experiments of Th2 differentiation identifies disruption of key Th2 genes at 2 days post-activation

Following the above findings on CD69 expression during the first 24 hours of activation, we explored whether the altered activation kinetics affected expression of core Th cell differentiation genes. We therefore performed an exploratory time-course experiment, collecting RNA between days 1-4 of Th2 differentiation, and exploring gene expression by qRTPCR.

We first assessed *Malat1* and *Xist* as quality controls (*Figure 4.3 A, B*), observing downregulation of *Malat1* in *WT* males compared to *WT* females between days 1-3, and *Xist* downregulation in *Malat1*$^{-/-}$ females at day 2. Due to effects previously seen on the IL2R (*Figure 3.14*), we then assessed expression of the IL2 receptor and IL2 (*Figure 4.3 C-E*), observing consistent suppression of *Il2ra, Il2rg* and *Il2* transcripts in *Malat1*$^{-/-}$ females beginning at day 2. No changes were observed at day 4 of differentiation, consistent with our previous data displaying no differences in *Il2Ra* and *Il2Rg* transcript levels at day 4 of differentiation (*Figure 3.15*). We also assessed expression of key transcription factors involved in Th2 differentiation. These included Th2 transcription factor *Gata3*, Th1 transcription factor *Tbet*, and IL10 controlling factor *Maf* (*Figure 4.4 A-C*). Both *Gata3* and *Tbet* levels were again suppressed in *Malat1*$^{-/-}$ females at day 2 post-activation, similar to effects seen on IL2/IL2R and *Xist*. No changes were observed to *Maf* levels at these early time points. We performed further validation by qRTPCR at 2 days post-activation, with a larger sample size for greater statistical power (*Figure 4.5 A-D*). Here, we observed significant suppression of *Il2ra, Il2rg, Gata3* and *Xist* in *Malat1*$^{-/-}$ females , consistent with results of our exploratory experiment, (*Figures 4.3, Figure 4.4*), however we also observed non-significant downwards trends in *Malat1*$^{-/-}$ males for *Gata3*, *Il2ra* and *Il2rg*, suggesting a level of disruption to males resulting from *Malat1*

loss during early differentiation. This suggested that *Malat1* loss caused major disruption to Th2 gene expression profiles in early differentiating cells (day 2 post-activation).

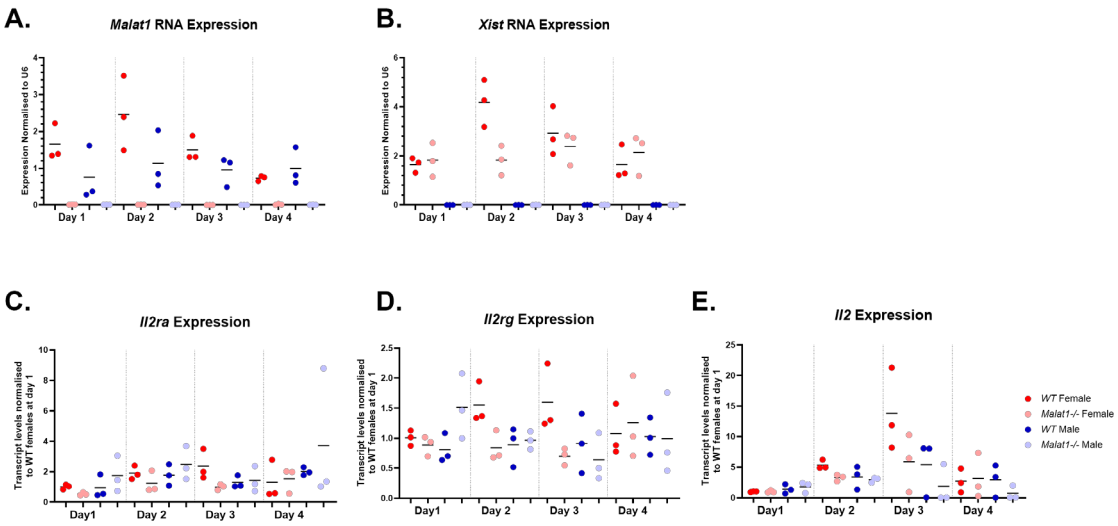

Figure 4.3 *Malat1* loss impairs *Il2* receptor and cytokine transcript expression during early differentiation

A. *Malat1* transcript levels in *WT* and *Malat1*$^{-/-}$ CD4^{+} T cells of both sexes at days 1-4 of *in vitro* Th2 differentiation, determined by qRTPCR. Levels normalised to U6 and average levels of *WT* females at day 1 (n=3). **B.** As in A. but for *Xist* transcript expression. **C.** As in A. but for *Il2ra* transcript expression. **D.** As in A. but for *Il2rg* transcript expression. **E.** As in A. but for *Il2* transcript expression.

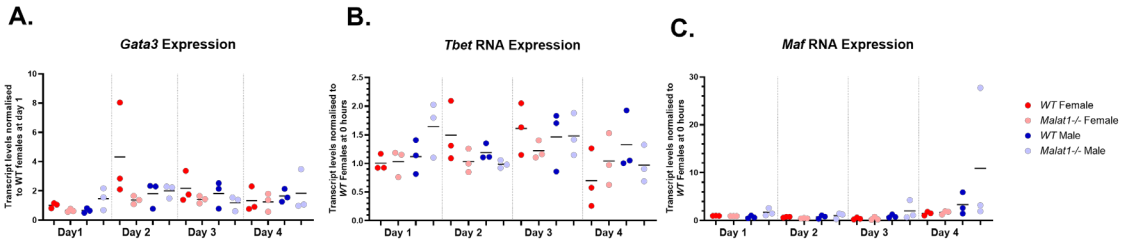

Figure 4.4 *Malat1* loss impairs *Gata3* transcript expression during early differentiation

A. *Gata3* transcript levels in *WT* and *Malat1*$^{-/-}$ CD4^{+} T cells of both sexes at days 1-4 of *in vitro* Th2 differentiation, determined by qRTPCR. Levels normalised to U6 and average levels of WT females at day 1 (n=3). **B.** As in A. but for *Tbet* transcript expression. **C.** As in A. but for *Maf* transcript expression.

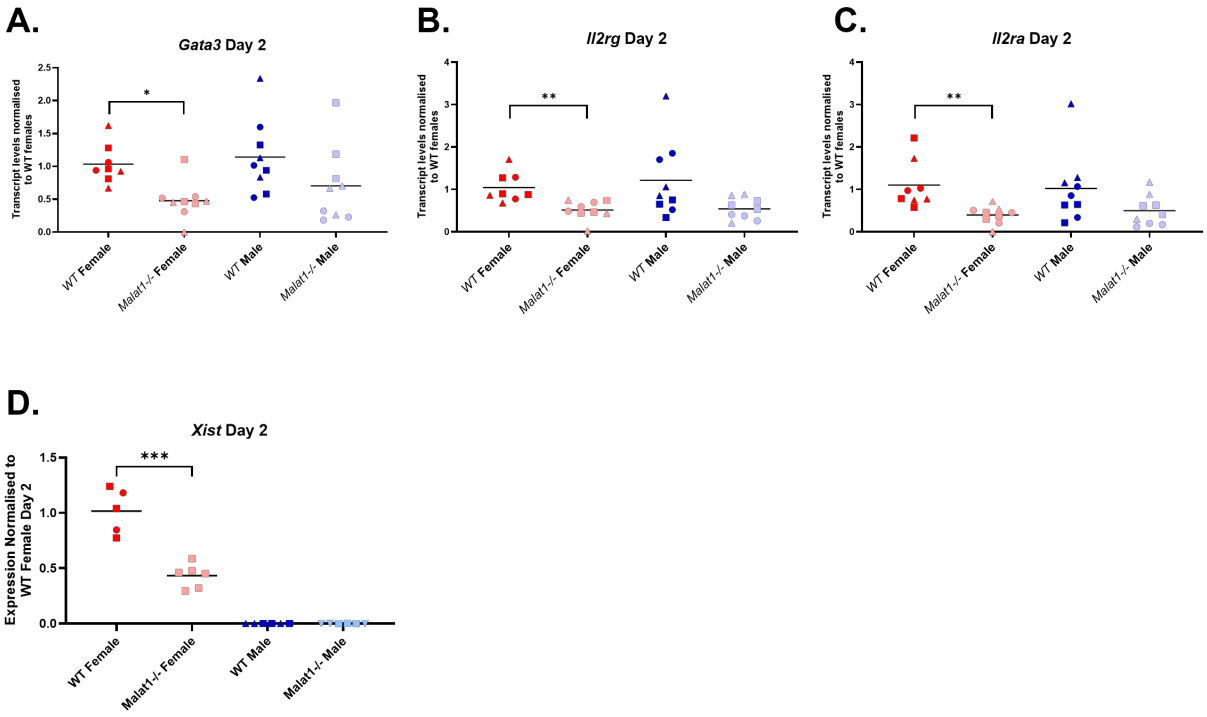

Figure 4.5 *Malat1* loss impairs early Th2 differentiation at day 2 of *in vitro* differentiation

A. *Gata3* transcript levels in $CD4^+$ T cells from *WT* and *Malat1*$^{-/-}$ mice of both sexes, at day 2 of *in vitro* Th2 differentiation, determined by qRTPCR. Levels normalised to U6 and average levels of WT females (n=8 for *WT* females, n=9 for all other conditions, data from 3 experiments of n=3, appropriate statistics as detailed in the methods used to compensate for experimental variability). **B.** As in A. but for *Il2rg* transcript expression. **C.** As in A. but for *Il2ra* transcript expression. **D.** As in A. but for *Xist* transcript expression (n=6, 2 experiments of n=6).

4.2.3 GATA3 expression is disrupted following *Malat1* loss in both females and males

We next assessed whether GATA3 protein levels were disrupted following *Malat1* loss. We reasoned that disruption to GATA3 may explain the overall disruption to Th2 differentiation and end-point cytokine expression. We performed Th2 differentiations experiments collecting samples for flow cytometry analysis from *WT* and*Malat1*$^{-/-}$ naïve and day 2 differentiated cells.

As a result of Th2 differentiation, GATA3 expression drastically increased between naïve and day 2 differentiated cells (*Figure 4.6 A, B*). Consistent with the RNA results, at day 2 both the percentage of cells expressing GATA3 and the GATA3 median fluorescence intensity (MFI) were significantly decreased in females following *Malat1* loss (*Figure 4.6 C, D*). However, despite no significant changes to transcript levels, GATA3 expression was significantly reduced in *Malat1*$^{-/-}$ males, suggesting the impact *of* Malat1 loss on Th2 differentiation could not be explained by its effect on GATA3 levels, as this was not sex-specific.

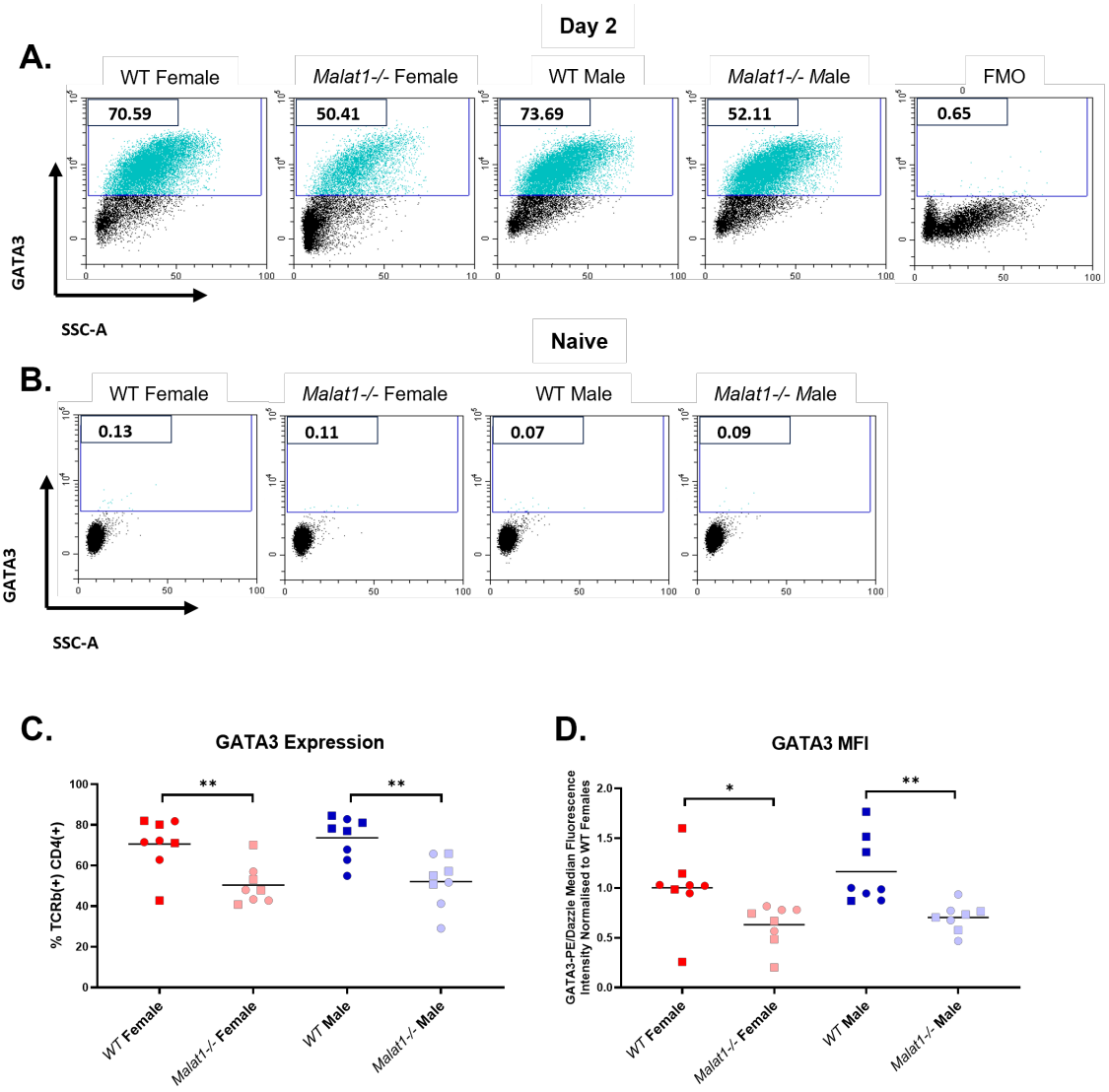

Figure 4.6 *Malat1* loss suppresses GATA3 expression at day 2 of *in vitro* Th2 differentiation

A. Representative FACS plots of GATA3 expression in *WT* and *Malat1*$^{-/-}$ CD4^{+} T cells of both sexes at day 2 of *in vitro* Th2 differentiation. **B.** As in A. but for naïve CD4^{+} T cells. **C.** Percentage of GATA3^{+} expression in CD4^{+} T cells from *WT* or *Malat1*$^{-/-}$ mice of both sexes, at day 2 of *in vitro* Th2 differentiation (n=8 per condition, 2 experiments of n=4, appropriate statistics as detailed in the methods used to compensate for experimental variability). **D.** As in C. but for GATA3 median fluorescence intensity (MFI).

4.2.4 *Malat1* loss suppresses the downregulation of a type-I interferon responsive geneset

Following identification that *Malat1* loss affected gene expression at day 2 of differentiation, we performed RNA-seq analysis of *WT* and *Malat1*$^{-/-}$ female cells, both in naïve CD4+ T cells and at day 2 of differentiation. As *Malat1* is linked to alternative splicing events, we chose to perform long-read nanopore RNA-seq to accurately identify differing RNA isoforms (H. Wu et al., 2023). The protocol for this is listed in greater detail in the methods section of this thesis.

Prior to sequencing, samples were validated via qRTPCR to ensure that Th2 differentiation had occurred correctly, *Malat1* was correctly suppressed in the *Malat1*$^{-/-}$ females, and to identify if similar trends were seen on early gene expression as in *Figure 4.5*. Here, *Il2ra, Il2rg* and *Gata3* (*Figure 4.7 A-C*) were upregulated at day 2, suggesting correct Th2 differentiation, and *Malat1* was also confirmed to not be expressed in the *Malat1*$^{-/-}$ females (*Figure 4.7 D*). Downwards trends at day 2 were identified for *Il2ra, Il2rg, Gata3* and *Xist* (*Figure 4.7 A-E*) in *Malat1*$^{-/-}$ female samples, suggesting that these samples were representative of the effects of *Malat1* loss and were appropriate for RNA-seq analysis.

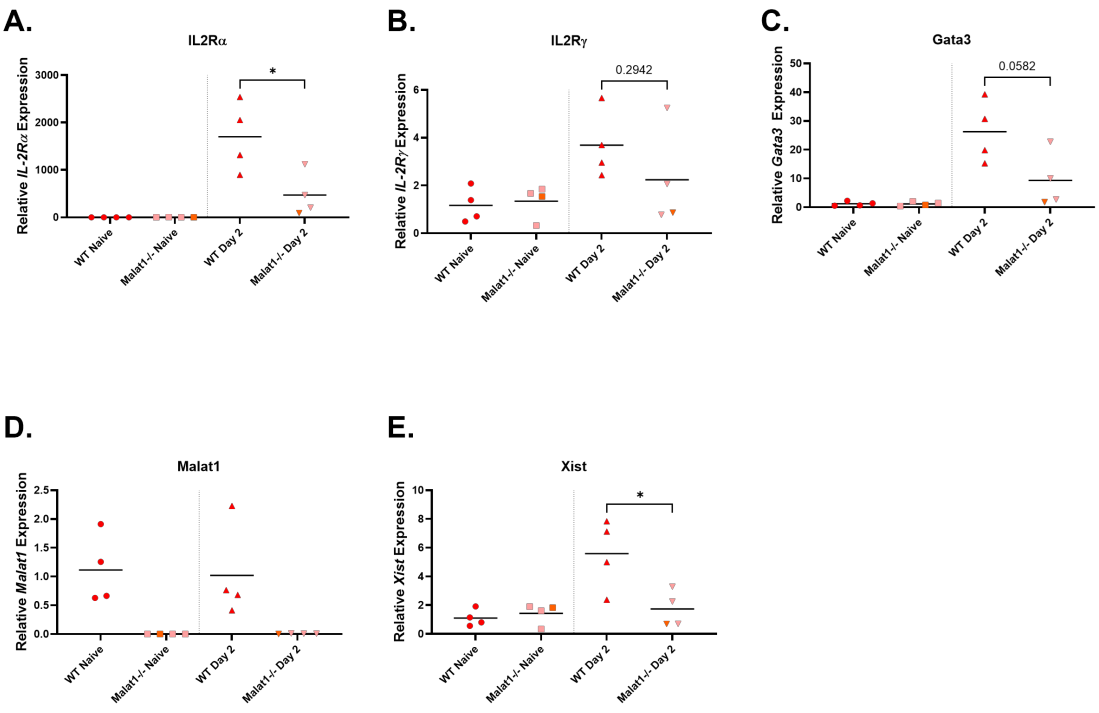

Figure 4.7 Long-read sequencing sample validation

A. *Il2ra* transcript expression in $CD4^+$ T cells chosen for long read RNA-seq from *WT* and *Malat1*$^{-/-}$ mice of both sexes, at days 0 and 2 of *in vitro* Th2 differentiation. Levels determined by qRTPCR. Levels normalised to U6 and average levels of WT females at day 0 (n=4). **B.** As in A. but for *Il2rg* transcript expression. **C.** As in A. but for *Gata3* transcript expression. **D.** As in A. but for *Malat1* transcript expression. **E.** As in A. but for *Xist* transcript expression.

From our sequencing data, we initially investigated DEGs between *WT* and *Malat1*$^{-/-}$ female samples. Similar to our previous short-read sequencing results, naïve cells displayed few differences between *WT* and *Malat1*$^{-/-}$ females, with 16 DEGs at FDR<0.1 (*Figure 4.8 A*, *Table 4.1*). However, at day 2, 239 DEGs were identified at FDR<0.1, of which 199 were upregulated resulting from *Malat1* loss (*Figure 4.8 B, Figure 4.9*). GSEA hallmark analysis revealed strong significant upregulation of IFNα and IFNγ response genesets, while downregulated genesets including hypoxia and glycolysis only showed reached modest statistical significance. While downwards trends were identified in this dataset for both *Il2ra* and *Gata3* (*Il2ra* LFC = −0.589 and *Gata3* LFC = −0.401) neither reached significance, suggesting that IFN responsive gene upregulation may be the most prominent feature of *Malat1* loss at this time point.

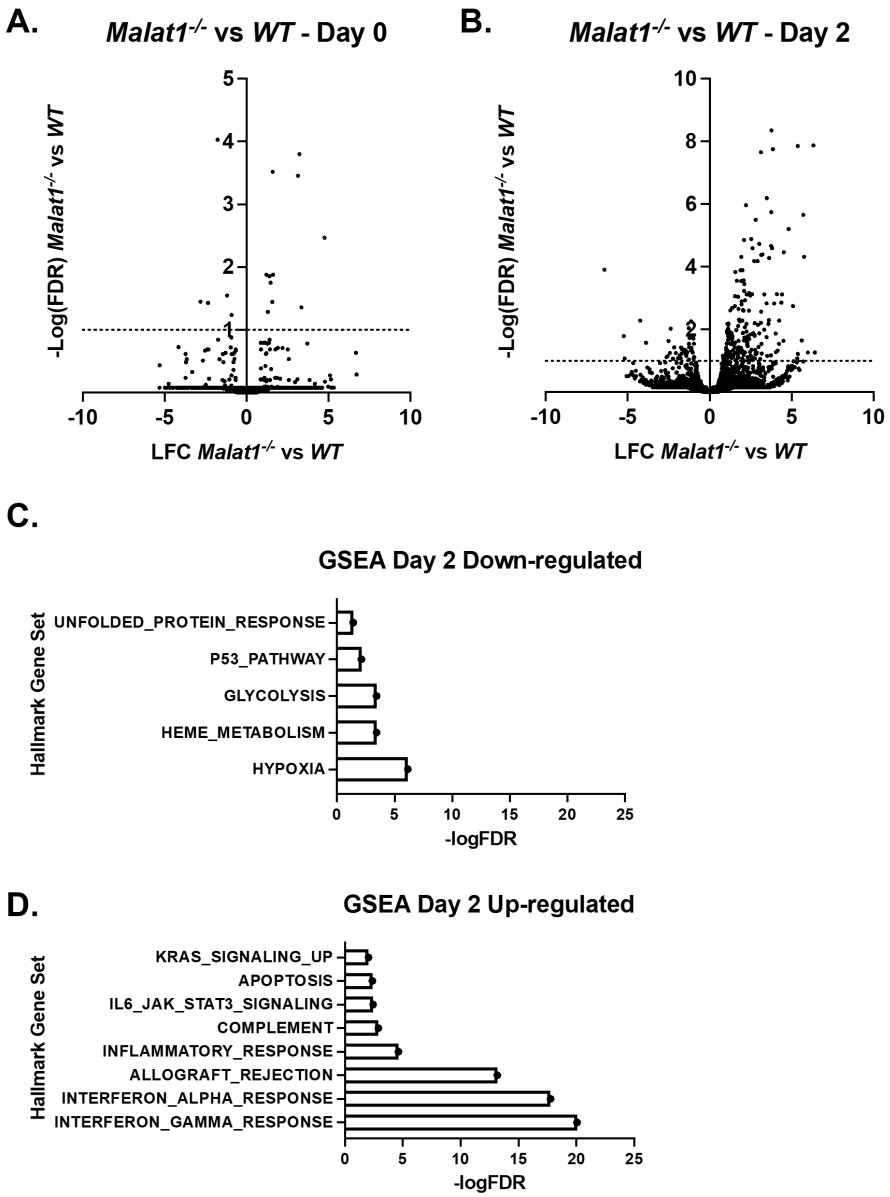

Figure 4.8 *Malat1* loss triggers upregulation of a large number of transcripts during early differentiation

A. Volcano plot displaying LFC in gene expression between WT and Malat1$^{-/-}$ female cells, against -logFDR at day 0 of *in vitro* Th2 differentiation. Data derived from our nanopore long-read RNAseq dataset (n=4 per group). **B.** As in A. but for day 2 of *in vitro* Th2 differentiation. **C.** GSEA hallmark gene sets significantly enriched (-logFDR shown) within significantly downregulated genes in *Malat1*$^{-/-}$ cells at day 2 of *in vitro* differentiation. **D.** As in C. but for day 2 of *in vitro* differentiation.

Table 4.1 Differentially expressed genes (FDR<0.1) between WT and Malat1$^{-/-}$ naïve CD4+ T cells from Nanopore long-read RNA-seq

Gene name	LFC	FDR
Snf8	-1.7590961	9.33E-05
Hspa1b	3.22754044	0.00015885
Gm47283	1.59401137	0.00030269
Hspa1a	3.14048541	0.00035047
Gm35279	4.76290568	0.00340621
Gm42427	1.6221625	0.01321738
Dnajb1	1.21454344	0.01322504
Gm10524	1.39790094	0.01398078
Gm33887	1.46744881	0.01767938
Cndp2	-1.1846287	0.02825061
n-R5s125	-2.805354	0.03544061
Camk2b	1.56841857	0.03578047
Gng11	-2.3471341	0.03727618
Gm20481	3.35471598	0.04366374
Gm4316	1.2984562	0.05152143
Trdc	-0.9081753	0.05791964

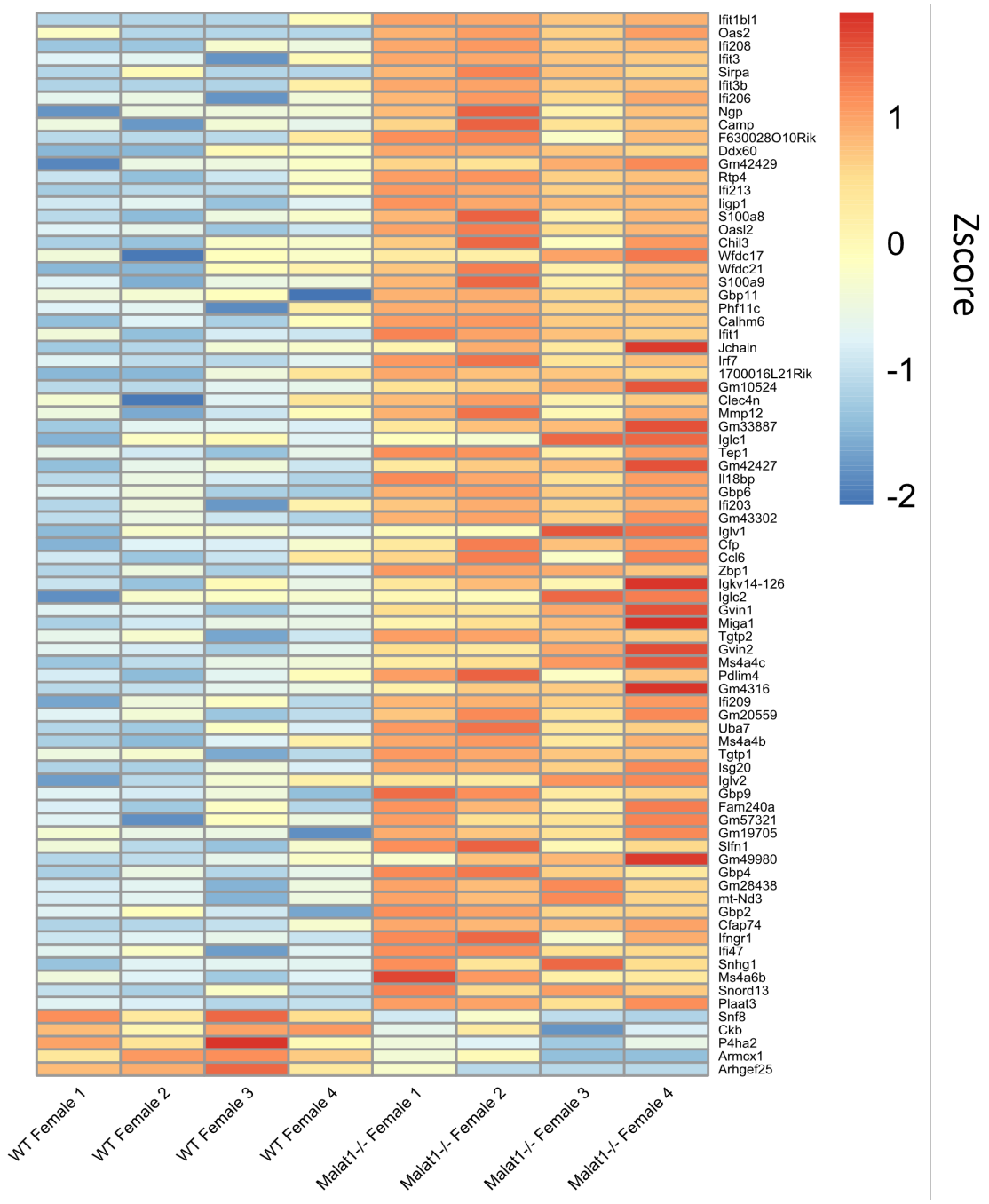

Figure 4.9 *Malat1* loss upregulates expression of IFN stimulated genes

Heatmap displaying Z scored log2CPM for significant DEGs (FDR<0.01) between *WT* and *Malat1*$^{-/-}$ cells at day 2 of *in vitro* differentiation. Data from our nanopore long-read RNA-seq dataset. Genes presented in descending order of LFC.

Further investigation of upregulated genes at day 2 was performed via STRING analysis and k-means clustering (k=9). Here, we identified a major cluster of typical interferon stimulated genes (ISGs), including *Ifit1bl1, Ifit3, Ifit1*, *Ifngr1, Oas2, Iigp1* and many others, that were upregulated as a result of *Malat1* loss at day 2. This gene module also contained important type-I IFN responsive transcription factors, including *Stat1, Irf1* and *Irf7* (*4.10* and *Table 4.2*). Interestingly, while *Ifngr1* was significantly upregulated as part of this gene modules, *Ifng* itself was unaffected, consistent with our previous results exploring *Tbet* expression (*Figure 4.4 B*). Of note, in other clusters cytokine genes such as *Il9, Il1b* and *Il12a*, chemokine pathway genes *Ccl6, Ccl9, Ccr9* and *Ccl2,* and expression of X-linked PRR *Tlr7* were found to be upregulated resulting from *Malat1* loss.

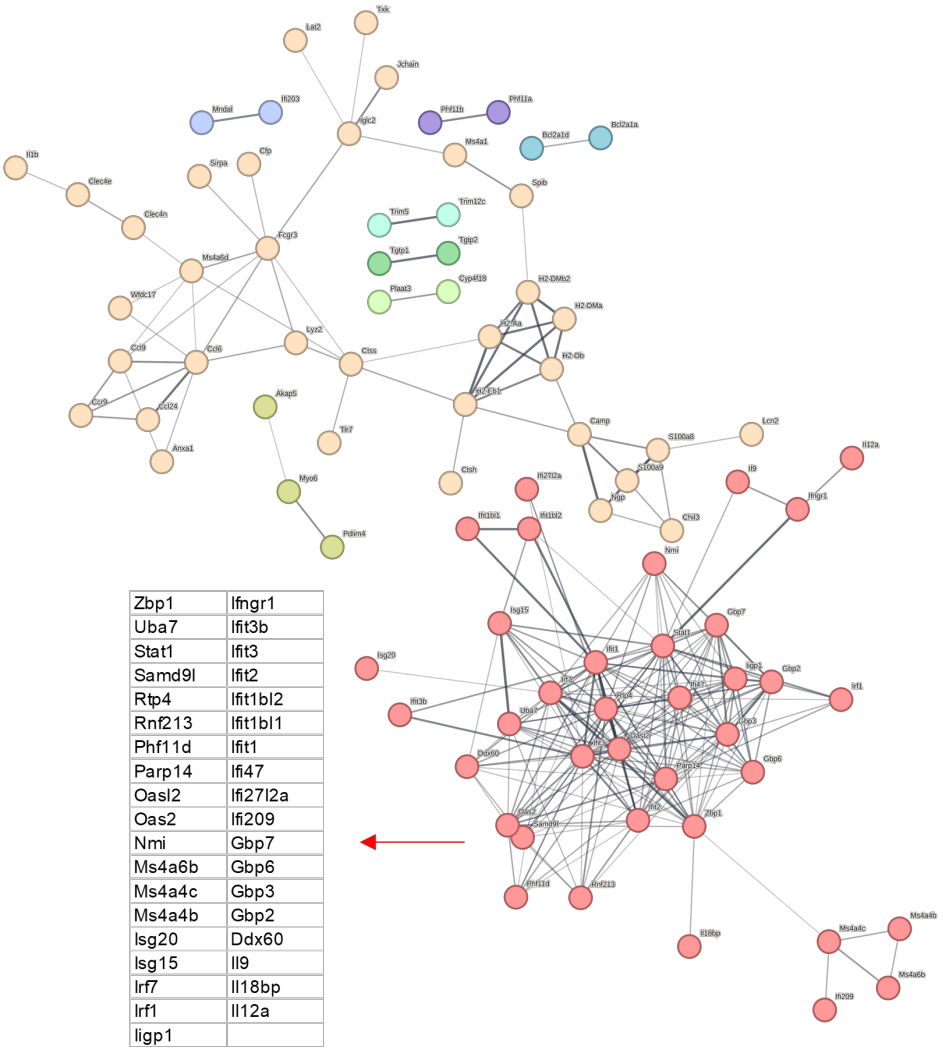

Figure 4.10 STRING analysis identifies a cluster of type-I ISGs and transcription factors resulting from *Malat1* loss

STRING network of significantly up-regulated genes in *Malat1*$^{-/-}$ cells at day 2 of *in vitro* Th2 differentiation. Data derived from our nanopore long read RNA-seq dataset. Clusters identified by k-means clustering (k=9).

Table 4.2 Gene clusters and genes identified by K-means clustering among up-regulated DEGs in day 2 *Malat1*$^{-/-}$ cells

Cluster number	Cluster color	Protein name
1	Red	Ddx60
1	Red	Gbp2
1	Red	Gbp3
1	Red	Gbp6
1	Red	Gbp7
1	Red	Ifi209
1	Red	Ifi27l2a
1	Red	Ifi47
1	Red	Ifit1
1	Red	Ifit1bl1
1	Red	Ifit1bl2
1	Red	Ifit2
1	Red	Ifit3
1	Red	Ifit3b
1	Red	Ifngr1
1	Red	Iigp1
1	Red	Il12a
1	Red	Il18bp
1	Red	Il9
1	Red	Irf1
1	Red	Irf7
1	Red	Isg15
1	Red	Isg20
1	Red	Ms4a4b
1	Red	Ms4a4c
1	Red	Ms4a6b
1	Red	Nmi
1	Red	Oas2
1	Red	Oasl2
1	Red	Parp14
1	Red	Phf11d
1	Red	Rnf213
1	Red	Rtp4
1	Red	Samd9l
1	Red	Stat1
1	Red	Uba7
1	Red	Zbp1
3	Dark Golden Rod	Akap5
3	Dark Golden Rod	Myo6
3	Dark Golden Rod	Pdlim4
4	Green	Cyp4f18
4	Green	Plaat3
2	Brown	Camp
2	Brown	Ccl24
2	Brown	Ccl6
2	Brown	Ccl9
2	Brown	Ccr9
2	Brown	Cfp
2	Brown	Chil3
2	Brown	Clec4e
2	Brown	Clec4n
2	Brown	Ctsh
2	Brown	Ctss
2	Brown	Fcgr3
2	Brown	H2-Aa
2	Brown	H2-DMa
2	Brown	H2-DMb2
2	Brown	H2-Eb1
2	Brown	H2-Ob
2	Brown	Iglc2
2	Brown	Il1b
2	Brown	Jchain
2	Brown	Lat2
2	Brown	Lcn2
2	Brown	Lyz2
2	Brown	Ms4a1
2	Brown	Ms4a6d
2	Brown	Ngp
2	Brown	S100a8
2	Brown	S100a9
2	Brown	Sirpa
2	Brown	Spib
2	Brown	Tlr7
2	Brown	Txk
2	Brown	Wfdc17
5	Green 2	Trim12c
5	Green 2	Trim5
6	Cyan	Tgtp1
6	Cyan	Tgtp2
7	Dark Cyan	Bcl2a1a
7	Dark Cyan	Bcl2a1d
8	Blue	Phf11a
8	Blue	Phf11b
9	Medium Blue	Ifi203
9	Medium Blue	Mndal

We next investigated how *Malat1*-associated DEGs were regulated during differentiation. The majority of DEGs were significantly downregulated between naïve and day 2 cells (*Figure 4.11 A*), suggesting that these DEGs may require suppression for correct Th2 differentiation. *Malat1* loss was seen to skew this effect, inhibiting their downregulation. We further investigated expression of these day 2 DEGs between naïve and end-point differentiated Th2 cells, using our previously mentioned short-read sequencing data. Here, we observed similar downregulation during differentiation and resultant skew from *Malat1* loss (*Figure 11 B*). When investigating the ISG module (*Figure 11 C, D*), this effect was further pronounced, with all bar two genes downregulated during differentiation. Again, a failure to properly downregulate these genes was seen resulting from *Malat1* loss. Further analysis of all transcriptomic changes between naïve and day 2 cells revealed that, as in our short-read sequencing data between naïve and Th2 cells, *Malat1* loss also displayed transcriptome-wide impacts on Th2 differentiation, with a general suppression of transcriptomic changes occurring during differentiation (*Figure 11 E, F*). Overall, these analyses demonstrated that *Malat1* is necessary for early Th2 differentiation, with a role in suppressing IFN responsive gene expression.

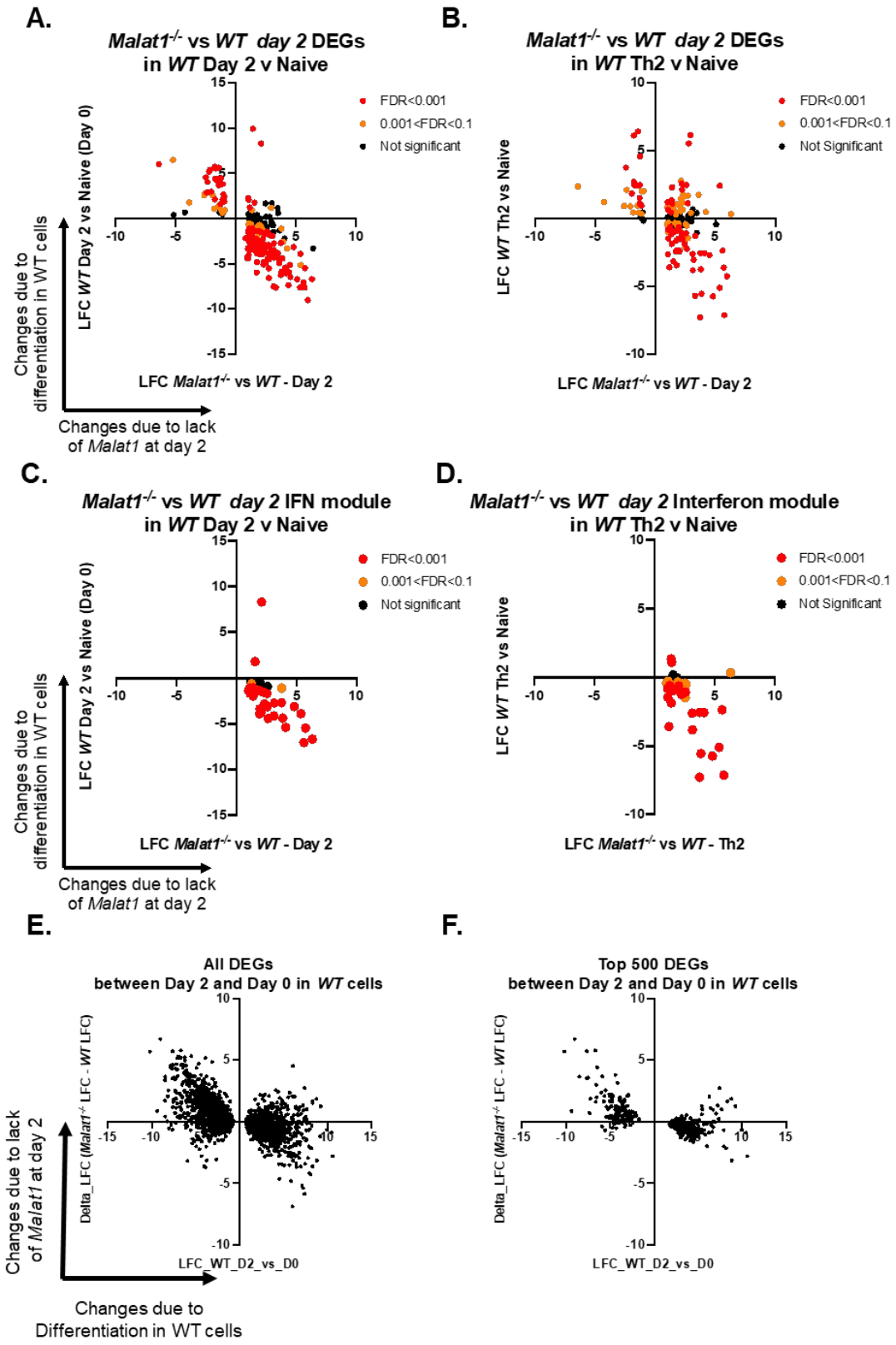
A.
Malat1-/- vs WT day 2 DEGs in WT Day 2 v Naive
FDR<0.001
0.001<FDR<0.1
Not significant
LFC WT Day 2 vs Naive (Day 0)
LFC Malat1-/- vs WT - Day 2
Changes due to differentiation in WT cells
Changes due to lack of Malat1 at day 2
B.
Malat1-/- vs WT day 2 DEGs in WT Th2 v Naive
FDR<0.001
0.001<FDR<0.1
Not Significant
LFC WT Th2 vs Naive
LFC Malat1-/- vs WT - Day 2
C.
Malat1-/- vs WT day 2 IFN module in WT Day 2 v Naive
FDR<0.001
0.001<FDR<0.1
Not significant
LFC WT Day 2 vs Naive (Day 0)
LFC Malat1-/- vs WT - Day 2
Changes due to differentiation in WT cells
Changes due to lack of Malat1 at day 2
D.
Malat1-/- vs WT day 2 Interferon module in WT Th2 v Naive
FDR<0.001
0.001<FDR<0.1
Not Significant
LFC WT Th2 vs Naive
LFC Malat1-/- vs WT - Th2
E.
All DEGs between Day 2 and Day 0 in WT cells
Delta_LFC (Malat1-/- LFC - WT LFC)
LFC_WT_D2_vs_D0
Changes due to lack of Malat1 at day 2
Changes due to Differentiation in WT cells
F.
Top 500 DEGs between Day 2 and Day 0 in WT cells
Delta_LFC (Malat1-/- LFC - WT LFC)
LFC_WT_D2_vs_D0

Figure 4.11 *Malat1* loss suppresses downregulation of an IFN-stimulated geneset

A. The effects of *Malat1* loss on gene expression trajectories during the first two days of Th2 differentiation. LFC in gene expression in *WT* female $CD4^+$ T cells during the first 2 days of *in vitro* differentiation (y axis), plot against LFC between *WT* and *Malat1*$^{-/-}$ female cells at day 2 of *in vitro* Th2 differentiation (x axis). Data from our nanopore long read RNA-seq dataset, shown for all statistically significant DEGs between WT and *Malat1*$^{-/-}$ cells at day 2. Colours indicate the level of significance in differential expression when comparing day 2 vs naïve $CD4^+$ T cells **B.** Tracking the trajectories of genes affected by *Malat1* loss at day 2 throughout Th2 differentiation. LFC in gene expression in *WT* female $CD4^+$ T cells during full *in vitro* Th2 differentiation (from our short-read RNA-seq dataset) plot against LFC between *WT* and *Malat1*$^{-/-}$ female cells at day 2 of *in vitro* Th2 differentiation (nanopore long-read dataset). Data shown for all statistically significant DEGs between WT and *Malat1*$^{-/-}$ cells at day 2 of *in vitro* Th2 differentiation. **C.** As in A., but with data filtered to only show the IFN gene module identified at day 2 in Figure 4.10. **D.** As in B., but with data again filtered for the IFN gene module. **E.** As in A., but with data shown for all significant DEGs between naïve and day 2 of *in vitro* Th2 differentiation in *WT* female $CD4^+$ T cells. **F.** As in E, but only for the top 500 DEGs by significance.

4.2.5 DEGs resulting from *Malat1* loss are enriched on chromosome 19

Due to disrupted *Xist* expression identified from qRTPCR analysis at day 2, and upregulation of X-linked *Tlr7* in our RNA-seq dataset, we performed further analysis of chromosomal enrichment within DEGs (FDR<0.1) as seen in *Figure 4.12 A*. This revealed that the X chromosome was underrepresented in this dataset, instead with enrichment of chromosomes 2, 3, 5, 7, 11 and 19. When normalising for gene number per chromosome (*Figure 4.12 B*) the X chromosome remained under-represented, however chromosome 19 (where *Malat1* resides in the mouse genome) became the most highly enriched, with chromosome 11 in second. Further investigation of DEGs present on chromosome 19 (*Figure 4.12 C*) revealed the presence of the IFIT family of genes (*Ifit1, Ifit2, Ifit3, Ifit1bl1, Ifit1bl2* and *Ifit3b*), which were all significantly (FDR<0.05) upregulated following *Malat1* loss.

When investigating the IFNα and IFNγ response hallmark genesets for comparison of normalised chromosomal enrichment (*Figure 4.12 D, E*), chromosome 19 remained slightly enriched but not to the same extent. Instead, these genesets displayed highest enrichment for chromosomes 16 and 17 respectively. To test for significant enrichment of these genes within our dataset, GSEA analysis for mouse positional genesets in the day 2 *Malat1*$^{-/-}$ DEGs confirmed significant enrichment of chromosome 19 band C1, which contains the 6 mouse *Ifit* genes (*Figure 4.12 F, Table 4.3*). Interestingly, chromosomal bands 1H3, 16A3 and 5E5 were all also significantly enriched, due to of IFN inducible clusters of *Ifi*, *Iglc* and *Gbp* gene families respectively present on these bands.

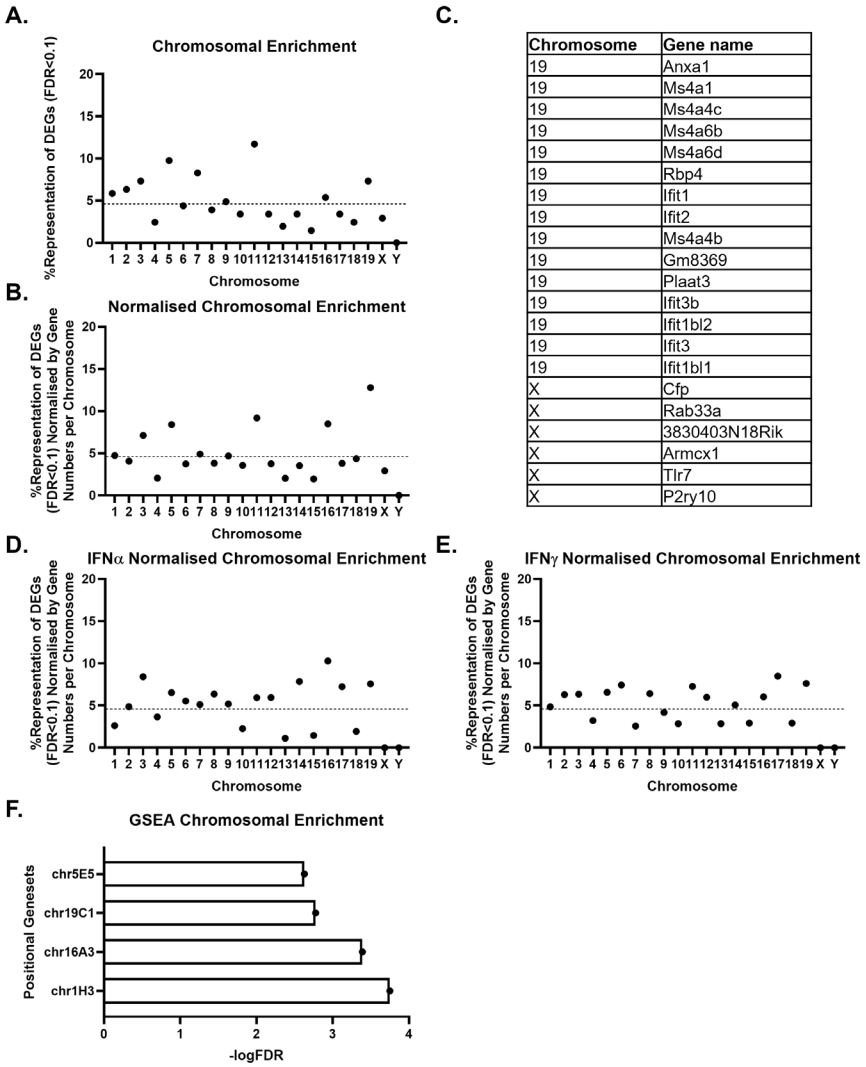

Chromosome	Gene name
19	Anxa1
19	Ms4a1
19	Ms4a4c
19	Ms4a6b
19	Ms4a6d
19	Rbp4
19	Ifit1
19	Ifit2
19	Ms4a4b
19	Gm8369
19	Plaat3
19	Ifit3b
19	Ifit1bl2
19	Ifit3
19	Ifit1bl1
X	Cfp
X	Rab33a
X	3830403N18Rik
X	Armcx1
X	Tlr7
X	P2ry10

Figure 4.12 DEGs resultant from *Malat1* loss are enriched on chromosome 19

A. Percentages of DEGs (FDR<0.1) from our long read RNA-seq dataset in *Malat1*$^{-/-}$ cells at day 2 of *in vitro* differentiation, present on each chromosome in the mouse genome. **B.** Percentages of DEGs in *Malat1*$^{-/-}$ female cells on each chromosome, normalised to total gene numbers per chromosome. **C.** List of DEGs present on chromosome 19 and the X chromosome. **D.** Percentages of interferon alpha response genes from the hallmark GSEA set present on each chromosome, normalised to total gene numbers per chromosome. **E.** As in D. but for interferon gamma response genes from the hallmark GSEA set. **F.** GSEA chromosome positional gene set terms enriched within DEGs in *Malat1*$^{-/-}$ cells at day 2 of *in vitro* differentiation.

Table 4.3 Significantly enriched genes and corresponding chromosome bands in *Malat1*$^{-/-}$ DEGs at day 2 of differentiation

Gene name	Chromosome band
Ifi208	1H3
Mndal	1H3
Ifi206	1H3
Fcgr3	1H3
Ifi203	1H3
Ifi209	1H3
Ifi214	1H3
Ifi213	1H3
2010309G21Rik	16A3
Iglv2	16A3
Iglc1	16A3
Iglc2	16A3
Iglc3	16A3
Iglv1	16A3
Iglv3	16A3
Ifit1bl2	19C1
Ifit1	19C1
Ifit2	19C1
Ifit3	19C1
Ifit3b	19C1
Ifit1bl1	19C1
Gbp6	5E5
Gbp4	5E5
Gbp9	5E5
Gbp10	5E5
Gbp11	5E5

4.2.6 Upregulation of the type-I IFN responsive geneset can be validated by qRTPCR

We next performed validation of the RNA-seq results via qRTPCR. We aimed to confirm the suppression of ISGs during differentiation as well as the upregulation at day 2 following *Malat1* loss and identify whether similar trends occurred in males. We performed Th2 differentiations, collecting RNA from naïve and day 2 of differentiation. We then selected a set of the most highly upregulated ISGs from *Malat1* loss (*Ifit1bl1, Ifit3b, Iigp1* and *Ifit1*) and three major transcription factors (*Stat1, Irf1* and *Irf7*) for analysis.

When comparing naïve to day 2 differentiated cells (*Figure 4.13*), we identified significant downregulation of *Ifit1bl1, Ifit1*, *Irf7* and *Stat1* for *WT* females. This significant downregulation was seen in these genes for all samples (*WT* and *Malat1*$^{-/-}$ of both sexes) bar *Stat1*, which was significantly downregulated only in *WT* females. Downwards trends were also observed for *Iigp1, Ifit3b* and *Irf1*, although these did not reach significance. When investigating expression of these genes at day 2 (*Figure 4.14*), we identified that *Ifit1bl1, Ifit1, Iigp1*, *Ifit3b* and *Irf7* were all significantly upregulated from *Malat1* loss in females, confirming the *Malat1* dependent inhibition of the ISG module seen in the RNA-seq data. Transcription factors *Irf1* and *Stat1* did not reach significance here, although upwards trends were still seen. Interestingly, ISG expression was also elevated in *WT* males, reaching significance for *Ifit1bl1, Ifit3b* and *Irf7* when compared to *WT* females, however no significant impacts were seen from *Malat1* loss in males.

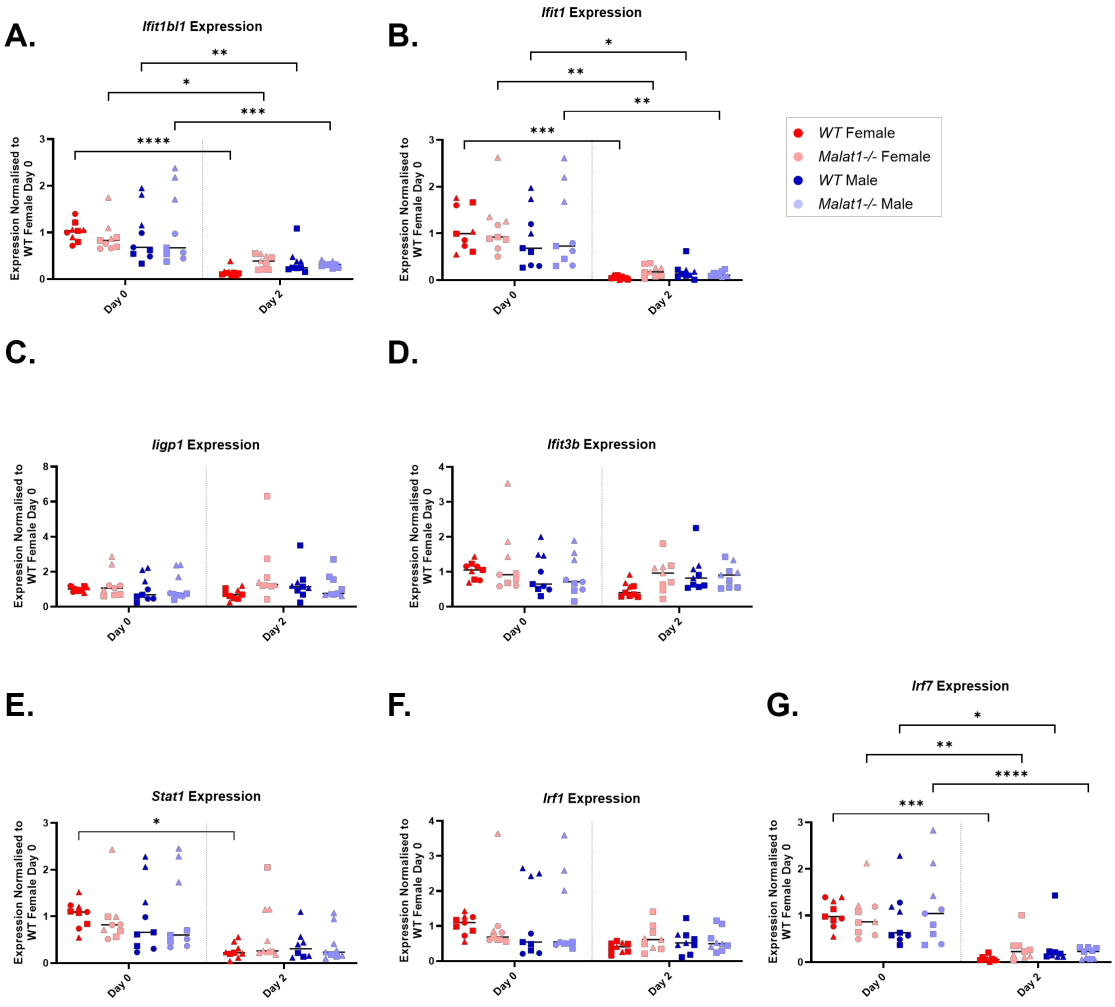

Figure 4.13 qRTPCR validates downregulation of IFN-stimulated genes during Th2 differentiation

A. *Ifit1bl1* transcript expression in *WT* and *Malat1*$^{-/-}$ CD4^{+} T cells from both sexes, at days 0 and 2 of *in vitro* Th2 differentiation. Determined by qRTPCR and normalised to *U6* and average levels of *WT* cells from female mice at day 0 (n=9, 3 experiments of n=3, appropriate statistics as detailed in the methods used to compensate for experimental variability). **B.** As in A. but for *Ifit1*. **C.** As in A. but for *Iigp1*. **D.** As in A. but for *Ifit3b*. **E.** As in A. but for *Stat1*. **F.** As in A. but for *Irf1*. **G.** As in A. but for *Irf7*.

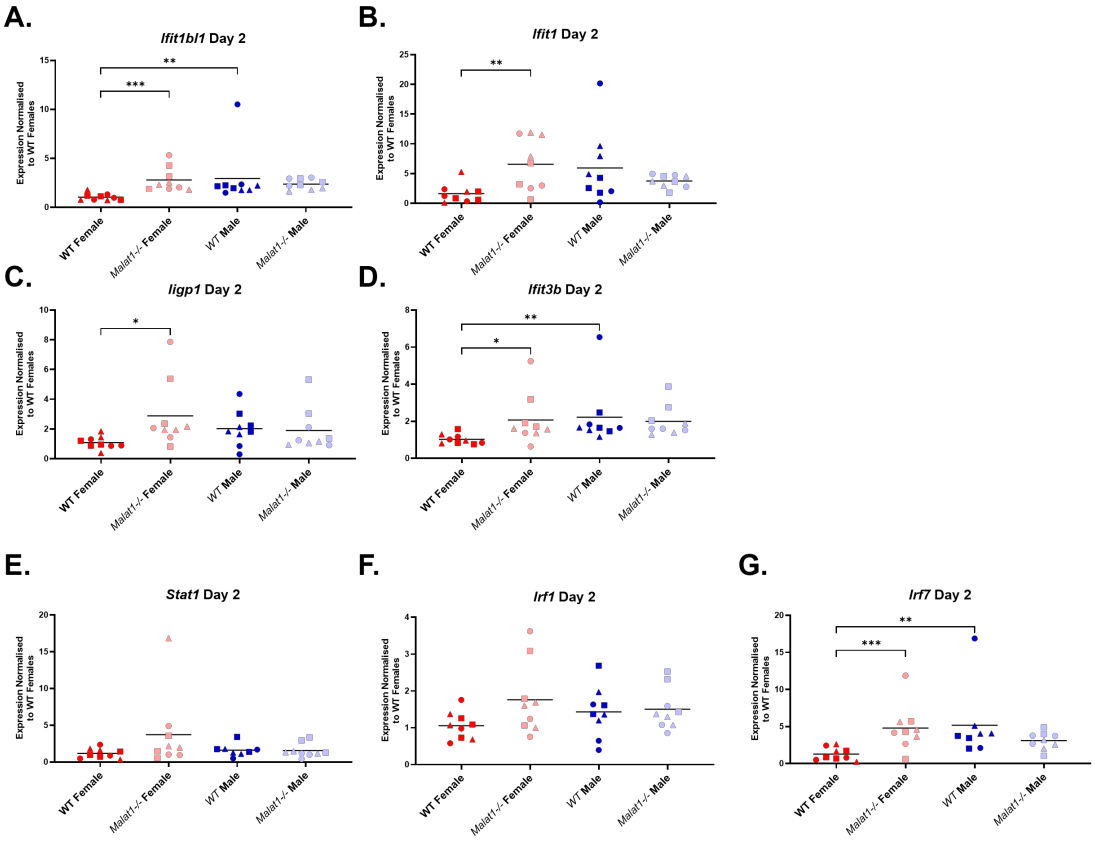

Figure 4.14 qRTPCR confirms significant upregulation of IFN-stimulated genes at day 2 of differentiation from *Malat1* loss

A. *Ifit1bl1* transcript expression in *WT* and *Malat1*$^{-/-}$ CD4^{+} T cells from both sexes, at day 2 of *in vitro* Th2 differentiation. Levels determined by qRTPCR (n=9, 3 experiments of n=3, appropriate statistics as detailed in the methods used to compensate for experimental variability) and normalised to *U6* and average levels of *WT* cells from female mice. **B.** As in A. but for *Ifit1*. **C.** As in A. but for *Iigp1*. **D.** As in A. but for *Ifit3b*. **E.** As in A. but for *Stat1*. **F.** As in A. but for *Irf1*. **G.** As in A. but for *Irf7*.

4.2.7 Type-I Interferon treatment disrupts Th2 differentiation in a sex-specific manner

We next explored the link between early IFN stimulated gene expression and end-point Th2 differentiation. We performed Th2 differentiations of *WT* female and male cells, combined with treatment of 5000 U/ml of IFNβ. Samples were collected on day 2 to assess upregulation of the IFN stimulated gene module via qRTPCR, day 4 to assess IL2R expression via flow cytometry, and day 6 to assess cytokine expression. We also performed this experiment with IL10R blockade, to assess impacts on IL4 and IL13.

At day 2, IFNβ treatment caused significant upregulation of ISGs *Ifit1bl1* and *Ifit3b Irf7* and *Stat1*, with a borderline non-significant upregulation of *Irf1* (*Figure 4.15 A*). No change was seen for *Iigp1* or *Ifit1* as a result of IFNβ treatment, and no significant changes were identified in IFNβ treated males (*Figure 4.15 B*). Some differences were observed between IFNβ treatment and *Malat1* loss, as *Iigp1 and Ifit1* were not significantly upregulated from IFNβ treatment, while stronger effects were seen from IFNβ treatment on *Stat1* and *Irf1*.

When assessing cytokine expression in differentiated Th2 cells, IFNβ treatment caused significant downregulation of cytokine IL10 in females, phenocopying the impact of *Malat1* loss (*Figure 4.16 A*). However, IL4 was unaffected (*Figure 4.16 B*). IL10R blockade alongside IFNβ treatment was able to enhance the effects on IL13 resulting in a significant decrease in expression, however IL4 expression remained unaffected (*Figure 4.17*). When assessing IL2R expression at day 4 of differentiation, IFNβ treatment in females caused a non-significant downward trend in IL2Rα expression (*Figure 4.18 A*), and a strong significant decrease in IL2Rγ expression (*Figure 4.18 B*), again similar to the impacts of *Malat1* loss. No differences were seen in males. Overall, these results

suggest that activation of ISGs during early Th2 differentiation can partially replicate the effects of *Malat1* loss.

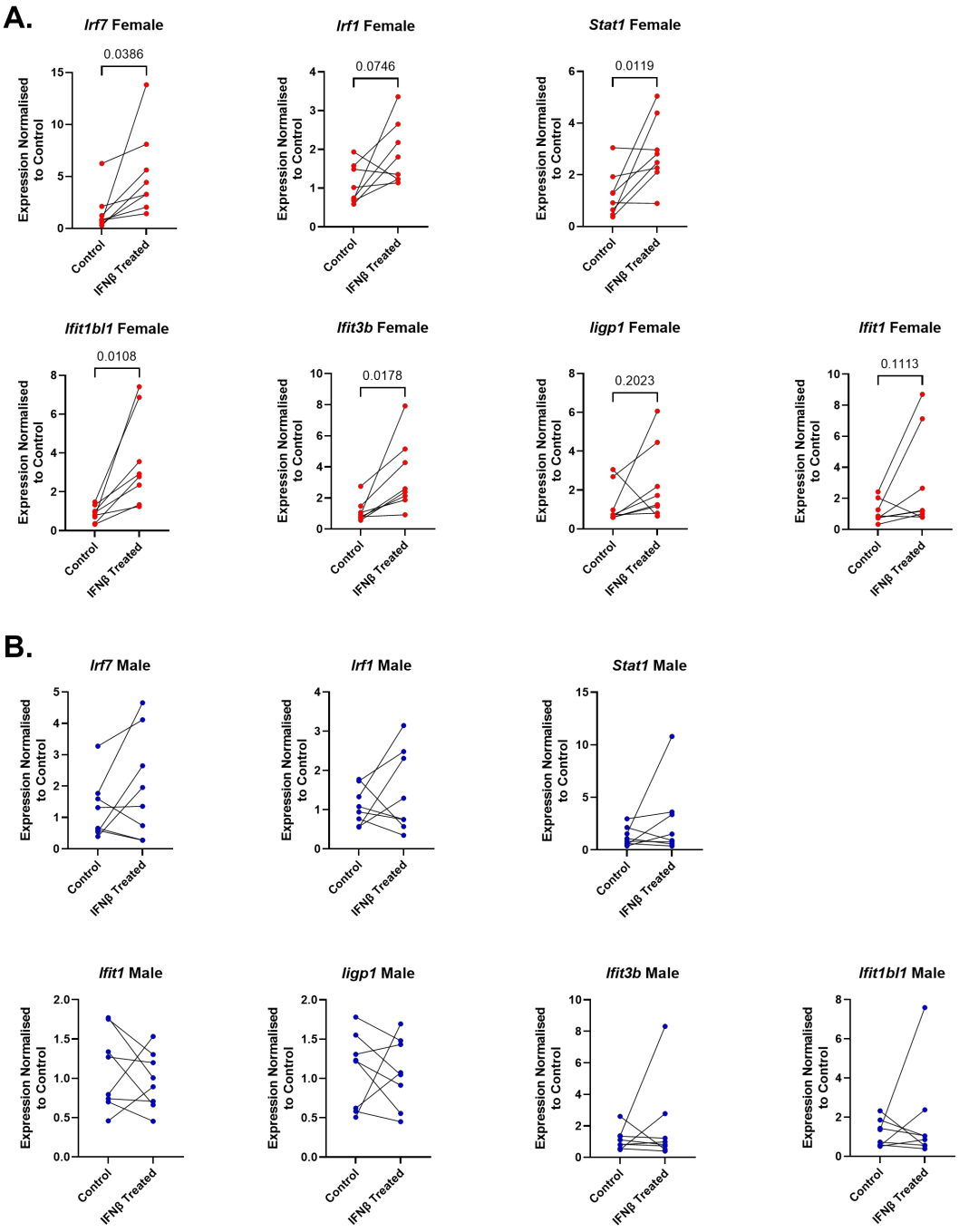

Figure 4.15 IFNβ treatment upregulates IFN-stimulated genes in females

A. Transcript levels of interferon induced transcription factors (*Stat1, Irf1, Irf7*) and genes (*Ifit1bl1*, *Ifit3b*, *Iigp1*, *Ifit1*) in *WT* female CD4$^+$ T cells at day 2 of *in vitro* Th2 differentiation, with treatment of 0 or 5000 U/ml IFNβ. mRNA levels determined by qRTPCR (n=7) and normalised to *U6* and average levels for the 0 U/ml treatment. **B.** as in A. but for *WT* male Th2 cells.

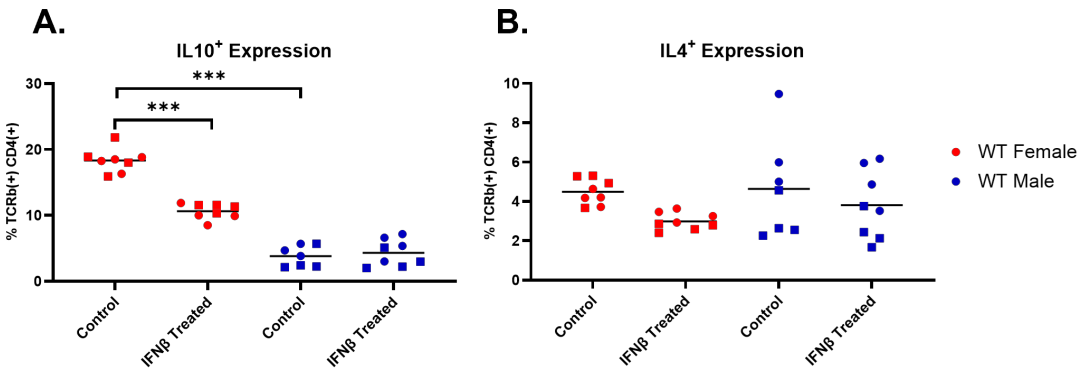

Figure 4.16 IFNβ treatment phenocopies the sex-specific impacts of *Malat1* loss on IL10 expression

A. Percentages of IL10 expression in *WT* CD4$^+$ T cells at day 6 of *in vitro* Th2 differentiation. Samples were also treated with 0 or 5000 U/ml IFNβ during initial activation. Levels determined by flow cytometry with intracellular cytokine staining (n=8 for all conditions except for 0 U/ml treated *WT* male which is n=7, from two experiments of n=4). **B.** As in A. but for IL4 expressing cells.

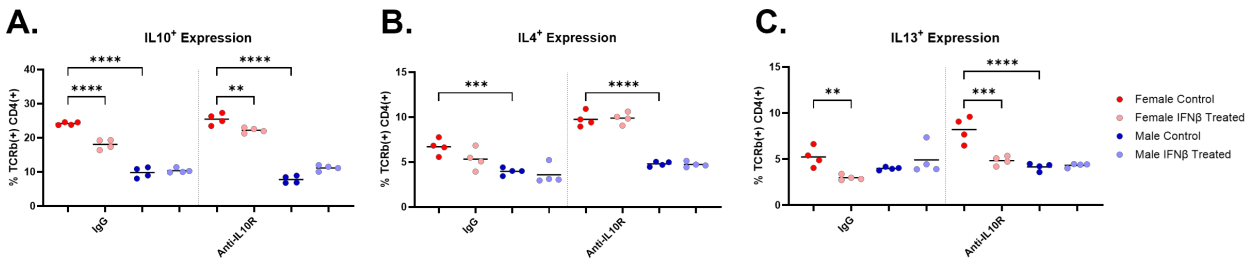

Figure 4.17 IL10R blockade reveals IFNβ treatment suppresses IL10 and IL13 expression in females

A. Percentages of IL10 expressing *WT* TCRβ^{+} CD4^{+} cells from mice of both sexes at day 6 of *in vitro* Th2 differentiation. Cells were treated with 0 or 5000 U/ml IFNβ, and with either IgG control or anti-IL10R antibody. Levels determined by flow cytometry with intracellular cytokine staining (n=4). **B.** As in A. but for IL4 expressing cells. **C.** As in A. but for IL13 expressing cells.

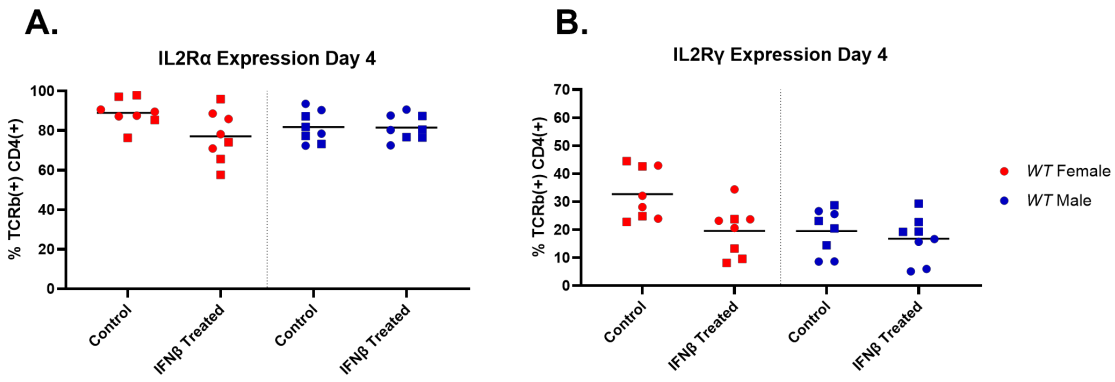

Figure 4.18 IFNβ treatment impacts IL2R levels in females

A. Percentage of IL2Rα expression in *WT* $CD4^+$ T cells from both sexes, at day 4 of *in vitro* Th2 differentiation. Cells were treated with 0 (control) or 5000 U/ml IFNβ. Levels determined by flow cytometry with surface staining (n=8, from 2 experiments of n=4, appropriate statistics as detailed in the methods used to compensate for experimental variability). **B.** As in A. but for IL2Rγ expressing cells.

4.2.8 *Malat1* loss does not affect type-I IFN expression during Th2 differentiation

We next investigated whether Th2 cells were either expressing or responding to type-I IFNs during early differentiation. We aimed to assess general type-I IFN cytokine *Ifna* and *Ifnb* expression, as well as isoform *Ifna4* which was lowly detectable in our RNA-seq dataset, and *Ifnar1* and *Ifnar2* expression. We performed Th2 differentiations, collecting samples on day 0 and day 2 for qRTPCR analysis of type-I IFN expression, and for flow-cytometry analysis of IFNAR1 expression.

Type-I IFNs were not detectable in naïve cells by qRTPCR but were expressed at low levels at day 2 (Ct values of 30-33). No differences resulting from *Malat1* loss were observed in RNA levels of *Ifna, Ifnb, Ifna4, Ifnar1* or *Ifnar2* at this time point, either in females or males (*Figure 4.19*). In terms of IFN receptor expression by flow cytometry, both the percentage of cells expressing IFNAR1 and IFNAR1 MFI increased between naïve and cells at day 2 of differentiation (*Figure 4.20*). Again, no significant changes were seen in *Malat1*$^{-/-}$ females, although a small significant increase was seen in *Malat1*$^{-/-}$ male naïve cells. This suggests that the increased expression of ISGs in *Malat1*$^{-/-}$ females was not a result of increased type-I IFN signalling occurring during differentiation of Th2 cells.

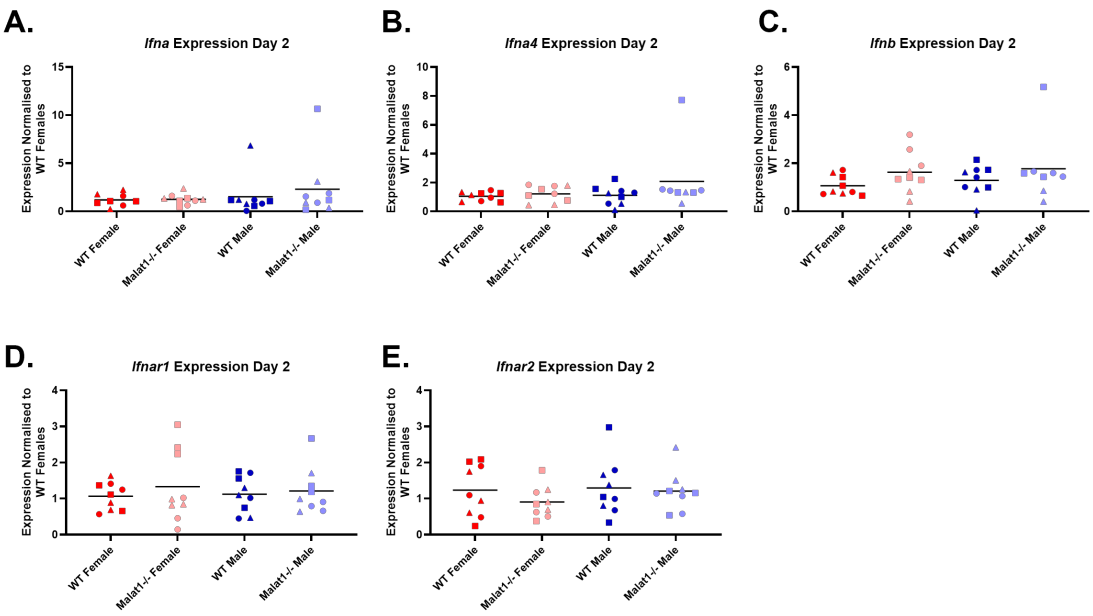

Figure 4.19 *Malat1* loss during Th2 differentiation does not affect type-I IFN cytokine or receptor transcript expression

A. *Ifna* transcript expression in $CD4^+$ T cells from *WT* and *Malat1*$^{-/-}$ mice of both sexes at day 2 of *in vitro* Th2 differentiation, determined by qRTPCR (n=9, 3 experiments of n=3, appropriate statistics as detailed in the methods used to compensate for experimental variability). Levels normalised to U6 and average levels of *WT* females. **B.** as in A. but for *Ifna4* transcript expression. **C.** As in A. but for *Ifnb* transcript expression. **D.** As in A. but for *Ifnar1* transcript expression. **E.** As in A. but for *Ifnar2* transcript expression.

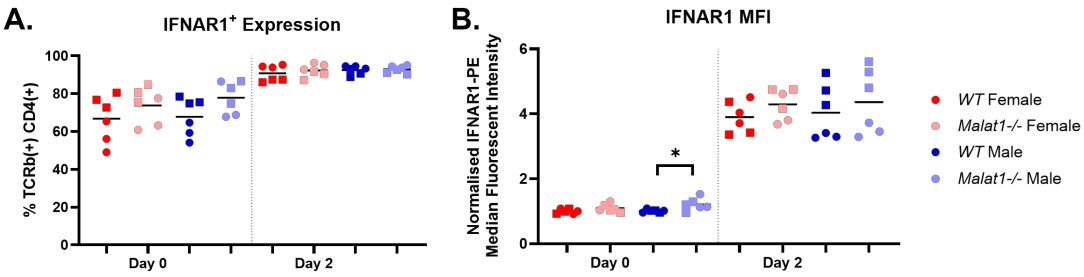

Figure 4.20 *Malat1* loss during Th2 differentiation does not affect IFNAR1 expression

A. Percentage of IFNAR1^{+} expression in CD4^{+} T cells from *WT* or *Malat1*$^{-/-}$ mice of both sexes at day 0 and day 2 of *in vitro* differentiation. Levels determined by flow cytometry with surface staining (n=6, data pooled from two experiments of n=3, appropriate statistics as detailed in the methods used to compensate for experimental variability). **B.** As in A. but for IFNAR1 MFI.

4.2.9 *Malat1* loss has limited effects on alternative splicing

Malat1 has previously been reported to associate with SR and HNRNP splicing factors (Miao et al., 2022), and shown to affect alternative splicing events (Tripathi et al., 2010). Therefore, we proceeded to analyse DTU via Dexseq in our long-read RNA-seq dataset to identify whether *Malat1* loss affected splicing during early differentiation.

Malat1 loss in females displayed only a modest effect on DTU, significantly impacting 25 genes at FDR<0.1 (*Table 4.4*). Genes affected included cytokines, such as *Il21, Il24* and core Th2 cytokine *Il4*, histone demethylase *Kdm2a,* and lncRNA *Gas5*. When looking DTU patterns between naïve and day 2 cells, a portion of significant genes such as *Il4, Il24, Kdm2a* and *Trim12a* demonstrated isoform usage changes due to *Malat1* loss that showed opposing patterns to those induced during differentiation (*Figure 4.21*), suggesting that *Malat1* loss may inhibit changes in alternative splicing events that occur during Th2 differentiation. However, other significant genes such as *Ndufs6* and *Snf8* did not follow this trend, and the overall percentage changes for significant isoforms remained small.

Table 4.4 Genes demonstrating DTU (FDR<0.05) between WT and Malat1$^{-/-}$ cells on day 2 of CD4+ T cell differentiation

FDR_DTU	Gene name	Number of isoforms	Number of differentially expressed isoforms (KO vs WT)
0.00076427	2310001H17Rik	38	3
0.03906294	Clec12a	2	2
1.43E-11	Dnajc7	19	7
0.01076268	Fntb	5	1
0.00168573	Gas5	149	5
0.01403486	Gimap4	6	1
0.01762127	Gimap5	4	2
0.03129099	Gstt1	2	2
0.00026601	Il21	2	2
0.00927377	Il24	4	2
0.03329888	Il4	4	1
0.02890363	Kdm2a	5	1
0.09584018	Lsm6	4	3
0	Ndufs6	5	3
0.08244566	Phkg2	9	1
0.08639127	Plaat3	3	2
0.04679064	Prr13	5	1
0.01584275	Snf8	5	3
0	Snhg1	26	13
0.09778325	Snhg17	74	1
0.00047815	Snx6	5	2
0.00077081	Trim12a	6	2
0.0116619	Usp53	3	2
0.0018117	Xaf1	5	1
0.0398128	Xpo7	4	0

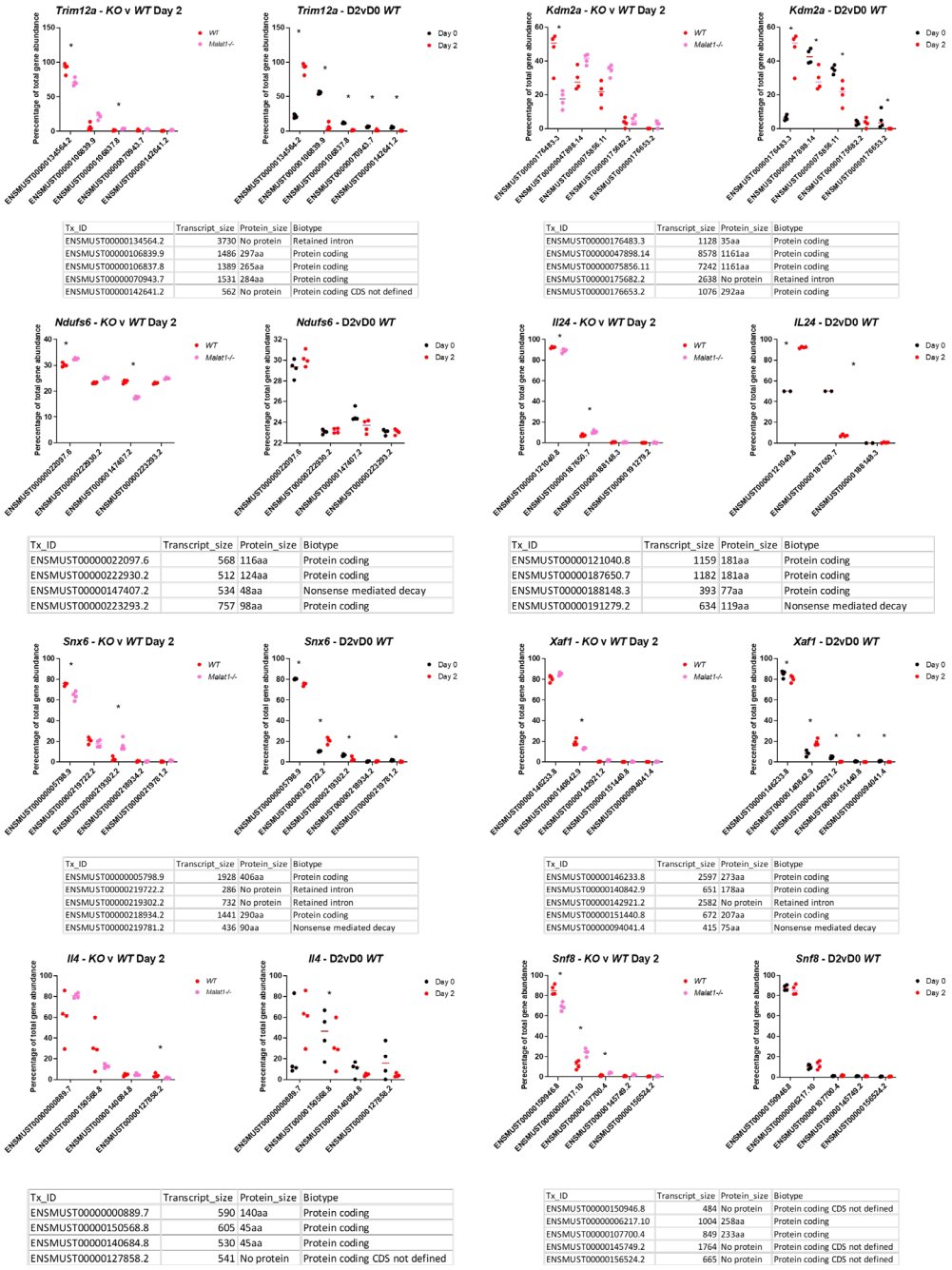

Tx_ID	Transcript_size	Protein_size	Biotype
ENSMUST00000134564.2	3730	No protein	Retained intron
ENSMUST00000106839.9	1486	297aa	Protein coding
ENSMUST00000106837.8	1389	265aa	Protein coding
ENSMUST00000070943.7	1531	284aa	Protein coding
ENSMUST00000142641.2	562	No protein	Protein coding CDS not defined

Tx_ID	Transcript_size	Protein_size	Biotype
ENSMUST00000176483.3	1128	35aa	Protein coding
ENSMUST00000047898.14	8578	1161aa	Protein coding
ENSMUST00000075856.11	7242	1161aa	Protein coding
ENSMUST00000175682.2	2638	No protein	Retained intron
ENSMUST00000176653.2	1076	292aa	Protein coding

Tx_ID	Transcript_size	Protein_size	Biotype
ENSMUST00000022097.6	568	116aa	Protein coding
ENSMUST00000222930.2	512	124aa	Protein coding
ENSMUST00000147407.2	534	48aa	Nonsense mediated decay
ENSMUST00000223293.2	757	98aa	Protein coding

Tx_ID	Transcript_size	Protein_size	Biotype
ENSMUST00000121040.8	1159	181aa	Protein coding
ENSMUST00000187650.7	1182	181aa	Protein coding
ENSMUST00000188148.3	393	77aa	Protein coding
ENSMUST00000191279.2	634	119aa	Nonsense mediated decay

Tx_ID	Transcript_size	Protein_size	Biotype
ENSMUST00000005798.9	1928	406aa	Protein coding
ENSMUST00000219722.2	286	No protein	Retained intron
ENSMUST00000219302.2	732	No protein	Retained intron
ENSMUST00000218934.2	1441	290aa	Protein coding
ENSMUST00000219781.2	436	90aa	Nonsense mediated decay

Tx_ID	Transcript_size	Protein_size	Biotype
ENSMUST00000146233.8	2597	273aa	Protein coding
ENSMUST00000140842.9	651	178aa	Protein coding
ENSMUST00000142921.2	2582	No protein	Retained intron
ENSMUST00000151440.8	672	207aa	Protein coding
ENSMUST00000094041.4	415	75aa	Nonsense mediated decay

Tx_ID	Transcript_size	Protein_size	Biotype
ENSMUST00000000889.7	590	140aa	Protein coding
ENSMUST00000150568.8	605	45aa	Protein coding
ENSMUST00000140684.8	530	45aa	Protein coding
ENSMUST00000127858.2	541	No protein	Protein coding CDS not defined

Tx_ID	Transcript_size	Protein_size	Biotype
ENSMUST00000150946.8	484	No protein	Protein coding CDS not defined
ENSMUST00000006217.10	1004	258aa	Protein coding
ENSMUST00000107700.4	849	233aa	Protein coding
ENSMUST00000145749.2	1764	No protein	Protein coding CDS not defined
ENSMUST00000156524.2	665	No protein	Protein coding CDS not defined

Figure 4.21 *Malat1* loss has modest effects on differential transcript usage

Transcript usage as a percentage of total gene abundance for indicated genes that demonstrated statistically significant DTU in our long read RNA-seq dataset. Levels shown between *WT* and *Malat1*$^{-/-}$ female CD4^{+} T cells at day 2 of *in vitro* differentiation (left graphs) or between day 0 and day 2 in *WT* female cells (right graphs). Levels determined by Dexseq (n=4 per condition). Tables indicate isoforms. Stars indicate significance.

4.3 Discussion

In this chapter we investigated the impacts of *Malat1* loss on early differentiation. We discovered that *Malat1* loss initially enhances early activation, identified via earlier CD69 expression dynamics. Further exploration however revealed that by day 2 of differentiation *Malat1* loss had disrupted the expression of important Th cell differentiation genes such as *Gata3, Il2ra* and *Il2rg*, as well as X-chromosome inactivation lncRNA *Xist*. RNA-seq and qRTPCR at this time point identified that *Malat1* loss inhibited the suppression of a type-I IFN stimulated geneset present in naïve $CD4^+$ T cells. Activation of ISG signalling during differentiation via IFNβ treatment partially phenocopied the effects of *Malat1* loss on cytokine expression and the IL2R, linking the impacts seen from *Malat1* loss during early activation to the effects on end-point differentiation.

Despite suppressing overall Th2 differentiation, *Malat1* loss in females enhanced expression of T cell activation marker CD69 at early time points. CD69 expression displayed a stronger initial but shorter-lived expression. Increased TCR engagement and activation signalling has previously been shown to bias differentiation towards Th1 cells and inhibit Th2 differentiation (Tao et al., 1997), potentially linking this to effects seen on end-point differentiation from *Malat1* loss. *WT* male cells here also displayed similar CD69 expression dynamics to that of *Malat1*$^{-/-}$ females, with increased expression at early time points. As *Malat1* levels are depleted during this same 24-hour period that CD69 is upregulated, *Malat1* may have an inhibitory effect on initial Th cell activation. Previous literature has shown that *Malat1* knock-down delocalises SR proteins and transcript processing factors from nuclear speckles to the rest of the nucleus (Tripathi et al., 2010), which could suggest its downregulation during Th cell differentiation is required for the

release of transcript processing factors. However, further experiments identifying *Malat1* binding partners in Th2 cells and their localisation would be required to confirm this.

We identified day 2 as a critical moment for *Malat1* in Th cell differentiation. The sex-specific downregulation of *Il2ra* and *Il2rg* transcripts seen here from *Malat1* loss potentially explains the disruption to IL2R protein levels seen at day 4 of differentiation, and the further inhibition of *Gata3* expression both at the protein and transcript level can partially explain the impacts of *Malat1* loss on overall differentiation. However, GATA3 protein expression was disrupted in both *Malat1*$^{-/-}$ females and males, therefore this could not be the sole cause of the sex-specific decrease in Th2 differentiation. Interestingly, *Xist* expression was significantly downregulated in *Malat1*$^{-/-}$ females alongside core Th2 genes in our qRTPCR data, and X-linked gene *Tlr7* was significantly upregulated in our RNA-seq data. This could suggest a reduced level of X chromosome inactivation resulting from *Malat1* loss, although X-linked gene *Il2rg* expression was decreased from *Malat1* loss, and the X chromosome was underrepresented in DEGs. Further experiments investigating allele specific expression of X-linked genes via techniques such as allele specific qRTPCR would also be required to determine whether and how *Malat1* loss affects X inactivation (Papp et al., 2003).

Despite a decrease in GATA3 expression at day 2, *Malat1*$^{-/-}$ male end-point Th2 differentiation is not disrupted when compared to *WT* males. This may suggest that, similar to the IL2R, male cells are less sensitive to levels of GATA3 than female cells. However, given the importance of GATA3 in Th2 differentiation, there may be compensatory mechanisms at play to also explain this result. GATA3^{-} cells may represent inactivated cells, which could die during the contraction period of Th cell differentiation while the GATA3^{+} cells still expand as normal in response to IL2, acting as a compensatory mechanism (McKinstry et al., 2010). Male *Malat1*$^{-/-}$ CD4^{+} T cells in our *in*

vivo model also displayed slightly increased cytokine expression in response to egg-injection, in both the spleen and the lung. This could suggest that *Malat1* loss in males enhances Th2 cell differentiation, potentially by upregulating downstream signalling such as increased STAT6 activation, offsetting the GATA3 decrease in early differentiation. However, further investigation of Th2 signalling pathways would be required in males to confirm this.

Despite previous literature on *Malat1* and splicing regulation (Miao et al., 2022), we observed only 25 genes with significant DTU from *Malat1* loss at day 2. Some small changes were observed in cytokine mRNAs, including IL4, IL21 and IL24, and in histone demethylase *Kdm2a* potentially hinting at defects in transcriptional repression (L. Liu et al., 2021). Effect sizes of significantly affected transcripts were also comparatively small to the ISG upregulation seen at the same time point. This is in agreement with some previous research in mouse brainstems and livers which also did not identify differences from *Malat1* loss in alternative splicing (B. Zhang et al., 2012), suggesting a role for *Malat1* in other cellular processes. However, while DTU provides the percentages of each mature transcript variant detected and is representative of alternatively spliced isoforms (Anders et al., 2012), it does not necessarily represent overall splicing efficiency, which could be affected here instead. Further analysis of our RNA-seq dataset via investigation of processes such as intron inclusion could provide an idea of how *Malat1* affects splicing efficiency. Splicing in eukaryotes also occurs co-transcriptionally, and our cDNA synthesis step involving adapter ligation to the 3' poly-A tail of completely transcribed mRNAs. Therefore, future analysis using alternate techniques like RNA polymerase II ChIP-seq may provide more information on whether splicing efficiency is affected (Titus et al., 2024).

The major impact of *Malat1* loss on early activation appeared to be the failure to suppress the ISG module. Th1 transcription factor *Tbet* and cytokine *Ifng* were not significantly upregulated following *Malat1* loss in our RNA-seq data, suggesting that this defect in ISG suppression was not due to nor caused a shift from Th2 to Th1 differentiation, with only disrupted Th2 differentiation seen. Activation of this ISG module via IFNβ treatment resulted in similar impacts on Th2 differentiation as *Malat1* loss, suggesting that suppression of this module is required for correct Th2 cell differentiation, although ISG expression and impacts on end-point differentiation did vary slightly between *Malat1* loss and IFNβ treatment. The upregulated ISG module contained three major type-I IFN signalling transcription factors: *Irf1*, *Stat1* and *Irf7*. All these factors were significantly upregulated as a result of *Malat1* loss in our long-read RNA-seq data. However, only *Irf7* remaining significant in our qRTPCR validation, although *Stat1* was significantly downregulated during differentiation only in *WT* females by qRTPCR. *Irf1*, *Stat1* and *Irf7* are linked to viral immune responses and expression of type I IFNs. However, *Irf1* and *Stat1* have previously been linked to regulating Type-I immunity and differentiation, which could explain the inhibition of Th2 differentiation seen with their upregulation. IRF1, along with BATF, is a major transcription factor required for differentiation of Th1 cells to Tr1 cells (Giang & La Cava, 2017), while STAT1 is required alongside STAT4 for typical Th1 polarisation in response to viruses, promoting expression of IFNγ and TBET (Finn et al., 2023).

IRF7 is the master regulator of type-I IFN gene expression and ISGs (W. Ma et al., 2023). IRF7 expression is triggered via activation of pattern recognition receptors (PRRs) in the cytoplasm, with activation allowing translocation to the nucleus for its transcription factor activity. However, the function of IRF7 in T cells has not been well reported on. In $CD8^+$ T cells, decreased expression of IRF7 was previously shown to

disrupt responses to specific viral epitopes, suggesting it may play a role in suppressing viral infection (S. Zhou et al., 2012). In $CD4^+$ T cells, IRF7 may be involved in Th1 immune responses like IRF1 and STAT1, with IRF7 shown to affect type-I IFN expression in Th1/Th17 cells in the context of antitumour Th cell activity (Lei, Xiao, et al., 2024). However, no changes in type-I IFN production directly were seen in our Th2 cells by qRTPCR and while IFNAR1 expression did increase during activation, again no changes were seen from *Malat1* loss, suggesting its effects are primarily on intracellular signalling. IRF7 is also known to play a role in other lymphocyte cells too, with involvement in B cell germinal centre formation and IgG class switching (Fike et al., 2025), and in promoting ILC2 type 2 cytokine expression and encouraging cell expansion (He et al., 2019).

ISG module expression, specifically IFIT proteins, IRF7, and STAT1 but not IFNγ, has been previously identified in aberrant Th2 cells in the context of asthma and allergy, linking to the disrupted Th2 differentiation seen here. Human Th cells stimulated with house dust mite antigen developed a type-I IFN responsive subset, which was seen to restrain allergic Th2 responses (Seumois et al., 2020). A similar subset of type-I IFN responsive Th cells was also identified in mice, again containing similar ISGs to those seen from *Malat1* loss (Tibbitt et al., 2019). Consistent with the restrained Th2 response in allergy and our IFNβ treated cells, type-I IFN signalling has been shown to disrupt Th2 differentiation, with IFNβ signalling specifically shown to disrupt GATA3 expression (Huber et al., 2010). This could link expression of the ISG module to our observed downregulation of the IL2R and GATA3, and eventual suppression of end-stage Th2 differentiation. However, *Malat1* loss affected GATA3 levels in both sexes, although we did not identify any changes in ISG expression in males, suggesting that this could only partially explain the effects of *Malat1* loss.

When investigating chromosomal representation in the ISG module, we identified enrichment of chromosome 19, where *Malat1* resides. This enrichment was likely due to the increased expression of *Ifit* family genes, which are present on chromosome 19 on band C1 and highly upregulated from *Malat1* loss. *Ifit* gene expression is triggered following type-I IFN signalling and viral infection, with IFIT proteins forming a complex providing broad spectrum antiviral immunity. This complex is involved in viral RNA sensing and binding to eIF3 to inhibit cap-dependent protein translation (Diamond & Farzan, 2013). This translational inhibition ability from the IFIT complex could also explain why *Gata3* and *Il2r* transcript levels are not significantly differentially expressed in our RNA-seq dataset, but we detected changes in the protein level. In terms of chromosomal gene regulation, both *Malat1* and *Neat1* in humans, which reside on chromosome 11 instead of 19, have been shown to bind to actively transcribing chromatin across chromosome 11 (West et al., 2014), suggesting that *Malat1* may aid in regulating gene expression along its chromosome of residence. Adding to this, *Malat1* loss in mice has also been shown to upregulate expression of neighbouring genes on chromosome 19 via *in cis* interaction, (B. Zhang et al., 2012), although the IFIT proteins enriched in our data are not present near to the *Malat1* gene locus (location 19qA in mice).

Expression of this ISG module is also downregulated during Th2 differentiation, potentially linking this to the ISG expressing subset previously identified in naïve cells (Deep et al., 2024). The 50 gene signature that defines these ISG expressing naïves shows substantial overlap (26/50) with the ISG module identified here from *Malat1* loss, including expression of both *Irf7* and *Stat1*. These ISG expressing naïves demonstrate impaired TCR stimulation, and were suggested to favour differentiation towards Tcm cells. Our results may suggest that *Malat1* aids in transcriptional repression of this lineage during Th2 differentiation. *Malat1* has been shown to regulate specific genesets

previously during immune cell activation and differentiation, via its interactions with RNA processing and transcription factors. In macrophages *Malat1* has been seen to inhibit type-I IFN responses via inhibition of TDP-43 cleavage and IRF3 signalling (W. Liu et al., 2020), potentially warranting further exploration of this as a mechanism behind ISG expression in Th2 cells. However, despite the activation of similar pathways, *Malat1* loss in macrophages mainly affected type-I IFN cytokine expression with little overlap of ISGs identified here, and investigated ISGs STAT1 and IFIT1 expression were unaffected.

As previously mentioned, *Malat1* has been shown to affect PRC2 function in a number of cell types (Arratia et al., 2023; Kanbar et al., 2022; S. H. Kim et al., 2017), which could help explain the failure to suppress the ISG module. *Malat1* regulation of PRC2 inhibited expression of memory cell associated genes via association with component EZH2 (Kanbar et al., 2022). This could suggest that *Malat1* may be more generally involved in transcriptional repression of memory cell formation in T cells. A subset of genes affected by *Malat1* loss in $CD8^+$ T cells overlap with our RNA-seq dataset, including transcription factor *Stat1* and *Ifit* family genes. Further adding to this, STAT1 expression in $CD8^+$ T cells has been identified as a major regulator of memory cell formation (Quigley et al., 2008), suggesting *Malat1* may regulate somewhat similar pathways between $CD4^+$ and $CD8^+$ T cells. However, the majority of genes affected by *Malat1* loss differ between our RNA-seq dataset and $CD8^+$ T cells, and transcription factors *Irf1* and *Irf7* expression are unaffected by *Malat1* loss in $CD8^+$ T cells. Further investigation of H3K27me3 levels via immunofluorescence staining or chromatin immunoprecipitation (ChIP) (Young et al., 2011), and investigation of interaction between *Malat1* and PRC2 components by RNA immunoprecipitation (Ye et al., 2020) would likely be required to confirm whether the effects seen on the ISG module are PRC dependent.

We identified sex-differences between females and males in terms of ISG expression and type-I IFN responsiveness. A portion of the ISG module, including *Irf7*, *Ifit1bl1* and *Ifit3b* were expressed significantly higher in *WT* males than females. Furthermore, male ISG expression was unaffected by *Malat1* loss, and males were less responsive to the levels of IFNβ utilised in our experiment. This increased expression of the ISG module could be representative of decreased differentiation strength seen in our *in vitro* model. Alternatively, this may suggest that male Th cells are less sensitive to type-I IFN treatment than females. Previous research has identified that the X chromosome is involved in promoting the response to type-I IFNs. Some cell types, such as pDCs, are more responsive to type-I IFNs in females than males, with links to increased expression of X-linked proteins such as TLR7 (Webb et al., 2019). Sex differences in type-I IFN signalling have also been previously identified in CD4 T cell responses. In HIV-1 infected individuals, females express significantly higher levels of type-I IFNs and ISGs in $CD4^+$ T cells, including expression of genes seen in our dataset, such as IFIT genes, IRF7, IRF1, and STAT1. This increased expression was also correlated with a lower viral load than males, potentially suggesting that female $CD4^+$ T cells may be more responsive to type-I IFN signalling (El-Badry et al., 2024).

The work presented in this chapter suggests that *Malat1* is a crucial sex-specific determinant of early Th cell differentiation in females. *Malat1* controls the suppression of a set of ISGs, which are potentially involved in Tcm cell differentiation, at day 2 of *in vitro* differentiation. Increased expression of this ISG module phenocopied the effects of *Malat1* loss on Th2 differentiation, resulting in disruption of the IL2 response and end-point cytokine expression. However, the mechanism behind the *Malat1* regulated suppression of ISGs is still unknown, and is likely not caused by any effects of *Malat1* loss on alternative splicing. Males constitutively express higher ISG levels than females

and are unaffected by *Malat1* loss, potentially explaining the decreased level of end-point differentiation in *WT* males and the lack of effect seen from *Malat1* loss *in vitro*.

5. *Malat1* Regulates Nuclear Speckle Function and X Chromosome Inactivation During Th Cell Differentiation

5.1 Introduction

5.1.1 Nuclear speckle function and their role in Th cell differentiation

Nuclear speckles are sub-nuclear membrane-less compartments that form in interchromosomal regions. Nuclear speckles are formed via association of core speckle proteins SON and SRRM2, and contain a number of pre-mRNA splicing factors, spliceosome RNA components, other non-coding RNAs, and inactive RNA polymerase II (Spector & Lamond, 2011; Xie et al., 2006). In terms of their function, the phosphorylation state of speckle-associated pre-mRNA splicing factors regulates their localisation between speckles and areas of active splicing (Aubol et al., 2018; Brown et al., 2008). This regulation of splicing factor localisation is thought to generate concentration gradients of splicing efficiency surrounding speckles, leading to increased rates of splicing in their proximity (Bhat et al., 2024). Previous research has also suggested that speckles may regulate transcription. DNA loci present in proximity to nuclear speckles display amplified transcript levels compared to those further away, and actively transcribed genes have also previously been identified to cluster around nuclear speckles (Brown et al., 2008; J. Kim et al., 2020).

Malat1 is a core ncRNA component of nuclear speckles, and has been shown previously to localise there in a number of different cell types (Fei et al., 2017; Tripathi et al., 2010). While initial knock-out models suggested that *Malat1* was dispensable for speckle formation (B. Zhang et al., 2012), recent studies demonstrated that *Malat1* instead plays a role in intra-speckle organisation. In the majority of speckles, *Malat1* localises specifically to the speckle periphery along with other spliceosomal RNAs, while SON, SRRM2 and other pre-mRNA splicing factors localising to the speckle centre. Depletion of *Malat1* instead caused a reduction in the total amount of SON present within speckles,

and resulted in SON, SRRM2 and pre-mRNA splicing factor presence in the speckle periphery (Fei et al., 2017). Alongside its speckle organisational role, interactions between *Malat1* and speckle-associated splicing factors have previously been shown to regulate both their phosphorylation state and activity in terms of alternative splicing (Miao et al., 2022). Furthermore, *Malat1* knock-down has been shown to reduce splicing factor association with speckles (Tripathi et al., 2010).

While nuclear speckles in T cells have not been well studied, some prior research has suggested that speckles are linked to both T cell activation, in both $CD4^+$ and $CD8^+$ T cells. TCR stimulation of cells derived from whole blood resulted in drastic increases in both speckle numbers and size (Dow et al., 2010; McCuaig et al., 2015). However, no detailed research has been performed on how speckles change during early T cell activation, or between human or murine naïve and differentiated cells.

5.1.2 X chromosome inactivation during Th cell differentiation

Prior research into X chromosome inactivation in lymphocytes suggests that T and B cells display altered Xi dynamics when compared to regular somatic cells (Syrett et al., 2019; J. Wang et al., 2016). Naïve T and B cells from female mice and humans do not display *Xist* cloud localisation present over the Xi, and also display reduced H3K27me3 suppression marks, suggesting that the Xi is not fully suppressed in this state. *Xist* localisation and Xi inactivation as a whole is lost during T cell maturation in the thymus, with only around 10% of mature thymocytes containing regular *Xist* marks on the Xi. During T cell activation, both *Xist* localisation and H3K27me3 marks return to the Xi, with *in vitro* stimulation followed by FISH identified that full *Xist* clouds completely return to T cells at around 2 days post activation (Syrett et al., 2019). TCR signalling via

the NF-kB pathway was identified as the direct cause for *Xist* and other inactivation marks to reappear on Xi, and this re-inactivation was seen for several different types of Th cell differentiation, including Treg, Th1 and CD8 T cells (Forsyth, Toothacre, et al., 2024; Huret et al., 2024). Interestingly, while *Xist* does not associate with the Xi in naïve cells, the Xi itself remains primarily transcriptionally silent in unstimulated T cells and some H3K27me3 levels still remain (Forsyth, Toothacre, et al., 2024).

Reduced *Xist* and silencing complex localisation to the Xi is thought to allow for increased X-linked gene escape during T cell activation. Several genes have previously been shown to escape the X re-inactivation during T cell differentiation, including *Il2rg*, *Kdm6a*, *Cd40l, Cxcr3*, *Tlr7* and *Tlr8* (Forsyth, Toothacre, et al., 2024; Youness et al., 2023). In SLE, a disease displaying heavy sex bias towards females (Christou et al., 2018), peripheral T cells from pediatric patients display mislocalised *Xist* patterns (J. Wang et al., 2016) and increased expression of X-linked genes (Q. Lu et al., 2007; Syrett et al., 2019), suggesting increased Xi escape may even contribute towards disease progression.

5.1. Chapter aims

In the previous chapter, we identified that *Malat1* loss disrupts gene expression changes during early Th2 differentiation in a sex specific manner, specifically enhancing expression of an ISG module. *Malat1* is known to localise to nuclear speckles and interact with speckle-localised splicing components, and disruption to speckle function could provide a mechanism for how *Malat1* loss affects Th cells. However nuclear speckles are not well researched in $CD4^+$ T cells. In this chapter, we aimed to investigate how nuclear speckles change during early Th2 differentiation and whether *Malat1* loss affects their function, via immunofluorescence imaging and analysis. We also tested the hypothesis that *Malat1* affected X chromosome inactivation during early Th2 differentiation, as a possible explanation for the sex-specific effects seen on Th2 differentiation.

The aims of this chapter were to:

- Identify how nuclear speckles change during both mouse and human Th cell differentiation
- Investigate whether *Malat1* loss affects nuclear speckle formation and function during early Th2 differentiation.
- Investigate the effects of *Malat1* loss on X chromosome inactivation during early Th2 differentiation.
- Investigate whether *Malat1* affects H3K27me3 deposition during early Th2 differentiation.

5.2 Results

5.2.1 Nuclear speckles increase in both number and size during T cell differentiation

As *Malat1* localises to nuclear speckles and plays a role in speckle organisation, we aimed to investigate whether *Malat1* loss disrupted nuclear speckle formation and function during early differentiation. To first investigate this, we performed *in vitro* Th2 differentiation experiments of *WT* females, collecting, fixing and permeabilising at naïve and day 2 Th2 cells. Resultant slides were then stained for DAPI and core speckle marker SON. We chose SON as a marker, as previous research had identified no localisation of SON to nuclear bodies other than speckles, and that there was little diffuse nuclear signal from staining (A. Sharma et al., 2010). We also opted to use the LSM880 microscope with airyscan processing for high resolution imaging of cells, taking tilescan Z-stack images. For image analysis we investigated both nuclear speckle numbers and size, as prior literature has linked nuclear speckle numbers to global changes in splicing, and size to unspliced RNA buildup within the speckles (O'Keefe et al., 1994; J. Wu et al., 2024). Images were analysed via ImageJ as detailed in methods chapter 2.6.5.In brief, z-stack images were converted into maximum intensity projections, and a cell mask was generated from the DAPI layer. The mask was then applied to the SON layer, then auto-thresholding and particle analysis were performed in each cell to estimate SON particle size and number. We reasoned that this automated analysis provided a more unbiased analysis of nuclear speckle number and size compared to manual approaches. Click or tap here to enter text.

From our images, we were able to identify distinct clusters of SON staining (*Figure 5.1 A+B, Supplementary Figures 13+14*) present within interchromatin regions

(dim DAPI staining) in the cell nucleus, similar to previous literature that had performed immunofluorescence staining for nuclear speckles (Ilık et al., 2020; A. Sharma et al., 2010; J. Wu et al., 2024). Interestingly, speckle size and number as indicated by SON staining in these images appeared to visually increase during the first two days of Th2 differentiation. This was confirmed after performing image analysis, as we identified that nuclear speckle dramatically increase between days 0 and 2 in *WT* female-derived cells from around 25 speckles in naïve cells to around 50 by day 2 of differentiation (*Figure 5.1 C*), alongside an increase in average nuclear speckle area (*Figure 5.1 D*) from ~0.2 to ~0.4 μm^2. This measured speckle size, while at the low end, also falls within currently published estimates of nuclear speckle sizes at 0.3-3 μm in diameter (Bhat et al., 2024), giving confidence that our speckle analysis method was able to correctly identify nuclear speckles.

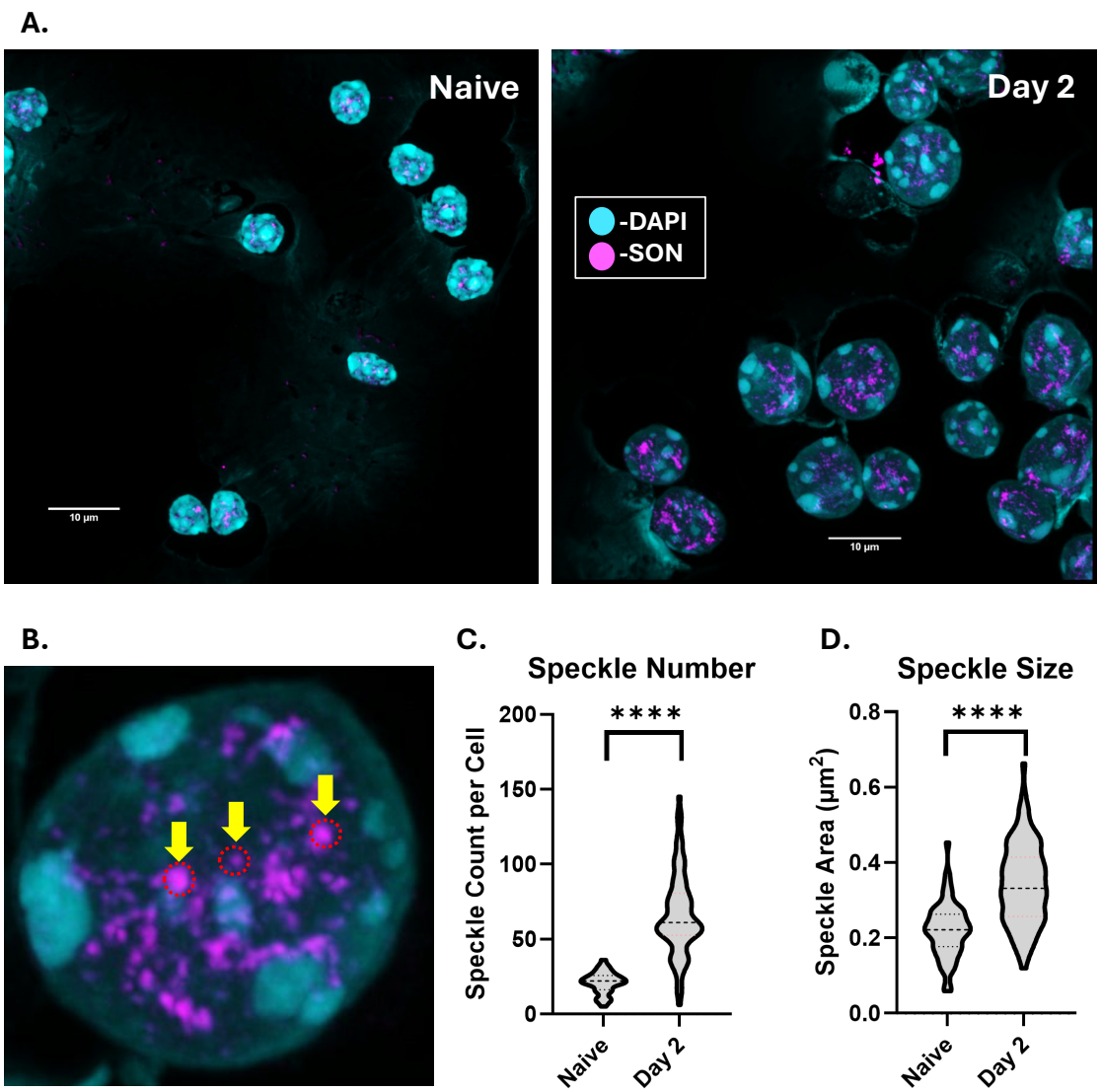

Figure 5.1 Nuclear speckle numbers and size increase during Th differentiation

A. Representative 63x images from SON and DAPI staining of *in vitro* differentiated *WT* female CD4$^+$ T cells, at naïve and 48 hours post-activation. Brightness and contrast were increased by 20% on all images. **B.** Representative cell from A. at 48 hours of *in vitro* Th2 differentiation, with example speckles highlighted by red circles with yellow arrows. **C.** Violin plot displaying nuclear speckle count per cell nucleus of *WT* female CD4$^+$ T cells during *in vitro* Th2 differentiation, at naïve and 48 hours post-activation. Minimum 30 cells were counted from two tilescan images at each condition, and results were merged between 2 biological replicates (Naïve total n=64, day 2 n=145). **D.** As in C. but for speckle area (um^2).

5.2.2 *Malat1* loss disrupts nuclear speckle numbers during differentiation

We next investigated whether nuclear speckles differ when *Malat1* is lost at day 2 of differentiation. To confirm this, we performed Th2 *in vitro* polarisations of WT and *Malat1*$^{-/-}$ female- and male-derived cells, collecting slides on days 0 and 2 of differentiation for immunofluorescence staining with DAPI and SON. Images were again acquired on the LSM-880 with airyscan processing and analysed by ImageJ for speckle number and size.

At day 2, visibly lower numbers of speckles could be seen resulting from *Malat1* loss in females (*Figure 5.2 A, Supplementary Figures 15+16*), and this decrease was further confirmed by the previously used image analysis (*Figure 5.2 B*). Interestingly, while *Malat1* loss did not significantly affect nuclear speckle numbers in males, *WT* males had significantly lower numbers than females. Nuclear speckle size (*Figure 5.2 C*) was unaffected by *Malat1* loss in females or males. However, *WT* males also displayed significantly lower speckle sizes when compared to *WT* females. When performing image analysis investigating change in speckles between days 0 and 2, both speckle numbers and size significantly increased for all samples (*Figure 5.3 A, B*).

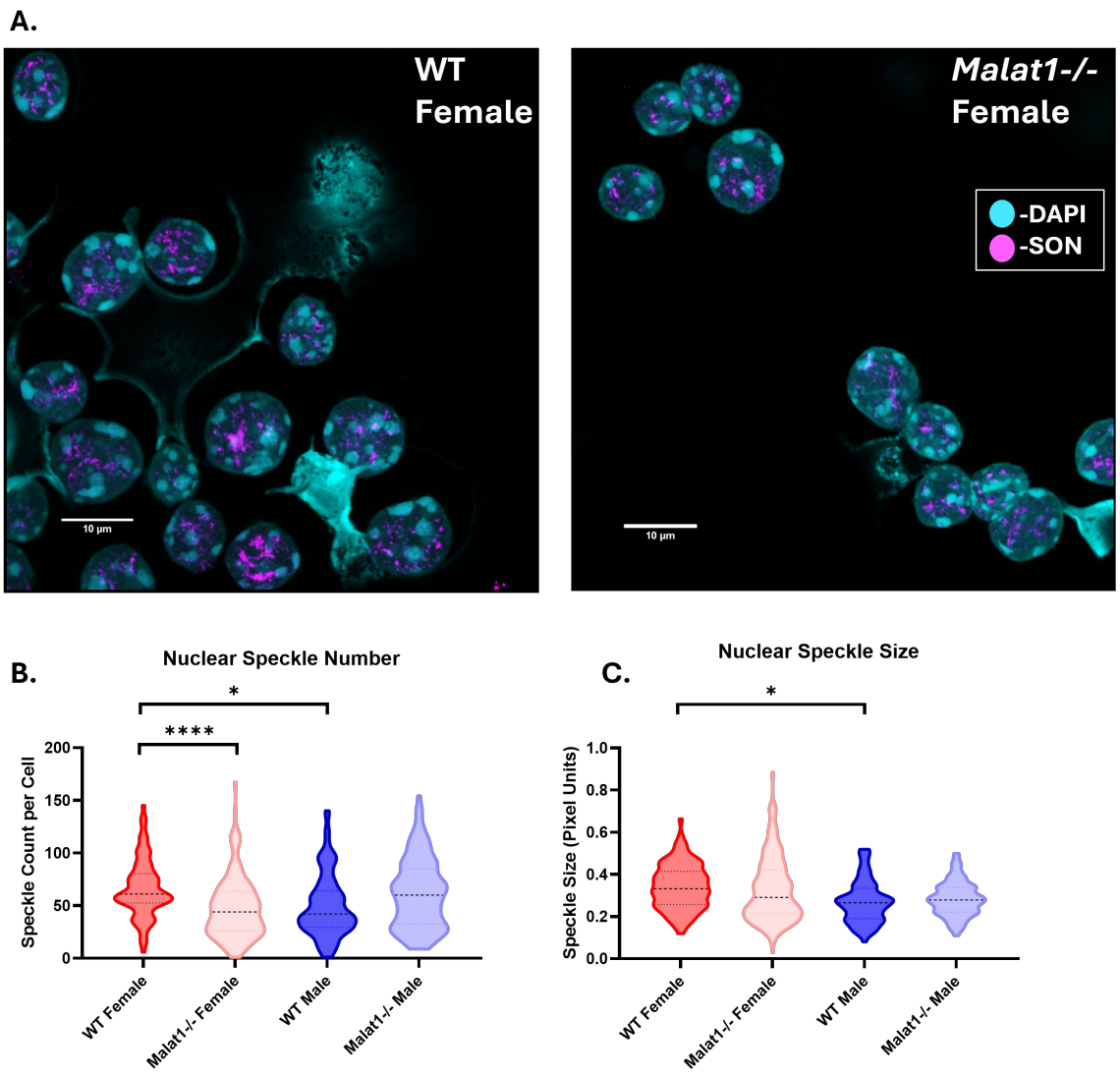

Figure 5.2 Nuclear speckle numbers and size increase during Th2 differentiation

A. Representative 63x images from SON and DAPI staining of *in vitro* differentiated *WT* and *Malat1*$^{-/-}$ female CD4^{+} T cells, at 48 hours post-activation. Brightness and contrast were increased by 20% on all images. **B.** Violin plot displaying nuclear speckle count per cell nucleus of *WT* and *Malat1*$^{-/-}$ female and male CD4^{+} T cells during *in vitro* Th2 differentiation, at 48 hours post-activation. Minimum 30 cells were counted from two tilescan images at each condition, and results were merged between 2 biological replicates (total *WT* female n=98, *Malat1*$^{-/-}$ female n=192, *WT* male n=110, *Malat1*$^{-/-}$ male n=141). **C.** As in B. but for nuclear speckle area (um^{2}).

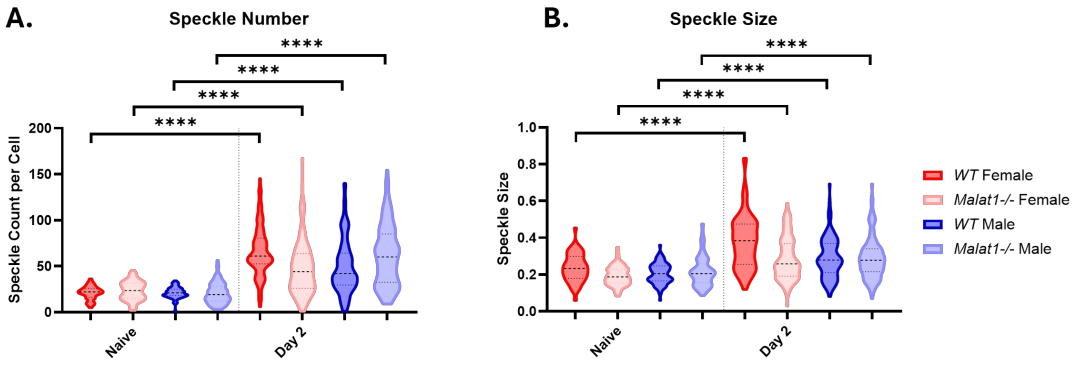

Figure 5.3 Nuclear speckle numbers and size increase during Th2 differentiation

A. Violin plot displaying nuclear speckle count per cell nucleus of *WT* and *Malat1*$^{-/-}$ female and male CD4^{+} T cells at days 0 and 2 of *in vitro* Th2 differentiation. Minimum 30 cells were counted from two tilescan images at each condition, and results were merged between 2 biological replicates (day 2 cell numbers as listed in *Figure 5.*2, naïve numbers: total *WT* female n=64, *Malat1*$^{-/-}$ female n=85, *WT* male n=65, *Malat1*$^{-/-}$ male n=106). **C.** As in B. but for nuclear speckle area (um^{2}).

As previous literature had suggested that *Malat1* loss could disrupt SON expression (Fei et al., 2017), we also investigated whether core speckle components *Son* and *Srrm2* transcript levels were disrupted during T cell differentiation. We performed *in vitro* Th2 differentiation of *WT* and *Malat1*$^{-/-}$ female and male CD4^{+} T cells, collected RNA at days 0 and 2 of *in vitro* Th2 differentiation, and investigated transcript levels by qRTPCR.

Neither *Son* nor *Srrm2* levels significantly changed between day 0 and 2 of differentiation (*Figure 5.4 A, B*). However, both transcripts displayed a downwards trend upon *Malat1* loss in females at day 2 of differentiation, although this change remained non-significant. Overall, these results suggest that *Malat1* may regulate nuclear speckle formation in a sex-specific manner, without significantly affecting core speckle protein transcript levels.

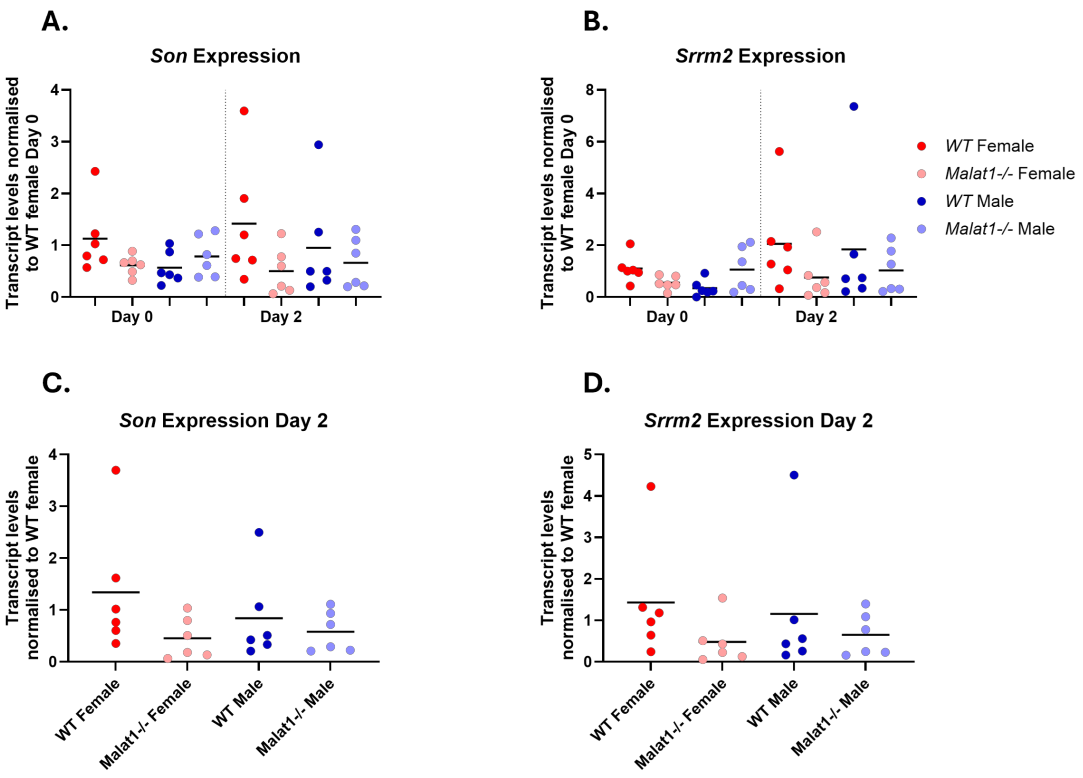

Figure 5.4 *Son* and *Srrm2* transcript levels are not significantly affected by *Malat1* loss

A. *Son* transcript expression in *WT* and *Malat1*$^{-/-}$ *in vitro* differentiated female or male cells at day 0 and day 2 of differentiation. mRNA levels determined by qRT-PCR (n=6) and normalised to *U6* and average levels of *WT* cells from female mice at day 0. **B.** As in A. but for *Srrm2* expression. **C.** *Son* expression in *WT* and *Malat1*$^{-/-}$ *in vitro* differentiated female or male cells at day 2 of differentiation. **D.** As in C. but for *Srrm2* expression.

5.2.3 *Malat1* loss affects SR protein phosphorylation during differentiation

Following identification of a significant decrease in nuclear speckle numbers resulting from *Malat1* loss in females, we next aimed to measure if nuclear speckle activity was disrupted, via investigation of SR protein phosphorylation. SR protein phosphorylation causes SR protein localisation out of speckles to the nucleoplasm, where they are then able to engage the spliceosome and participate in splicing regulation (Aubol et al., 2018; Long et al., 2019). We reasoned that changes in phospho-SR intensity could imply changes in SR protein activation, and a build-up of phosphorylated SR proteins in speckles and could imply disruption to SR protein localisation. To assess this, we again collected slides from *WT* and *Malat1*$^{-/-}$ females and males on day 0 and 2 of *in vitro* Th2 differentiation, staining for DAPI, SON, and phospho-SR proteins via an anti-phosphoepitope-SR antibody.

Phosphorylated SR protein staining visibly increased in *WT* females during differentiation alongside the previously identified increase in nuclear speckles, suggesting that speckle activity increased during differentiation (*Figure 5.5 A+B, Supplementary Figures 17-20*). While phospho-SR foci did not overlap with nuclear speckles, phospho-SR foci were predominantly positioned in proximity to nuclear speckles (*Figure 5.5 B*), consistent with their localisation out of speckles to aid with nearby transcript splicing (Aubol et al., 2018). SR protein phosphorylation was further confirmed by image analysis with ImageJ, where we identified a significant increase in mean phospho-SR protein staining between days 0 and 2 (*Figure 5.5 C*).

When comparing *WT* and *Malat1*$^{-/-}$ cell images at day 2, we did not observe any visible changes in phospho-SR protein localisation from *Malat1* loss or any overlap

between phospho-SR foci and nuclear speckles (*Figure 5.5 B+D, Supplementary Figures 19-22*). Analysis with ImageJ identified a significant decrease in mean phospho-SR intensity resulting from *Malat1* loss in females and not males, suggesting a sex-specific decrease in SR protein activation occurred from *Malat1* loss (*Figure 5.5 E*). *WT* males also displayed significantly lower phospho-SR staining than *WT* females, with no *Malat1*-dependent effects observed. Overall, these data suggest that *Malat1* loss disrupts SR protein activation and therefore nuclear speckle function in a sex-specific manner.

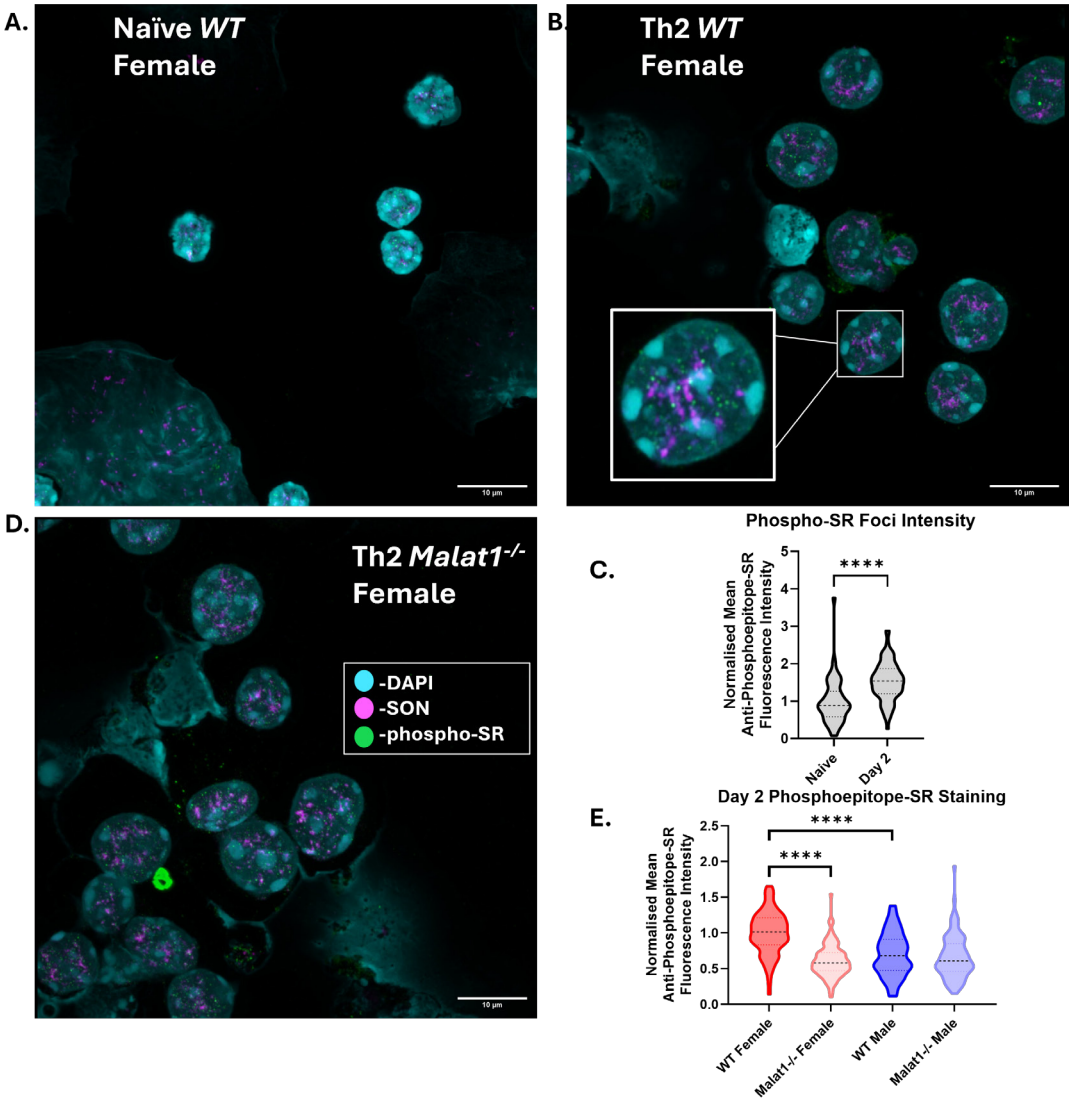

Figure 5.5 SR protein phosphorylation is disrupted following *Malat1* loss

A. Representative 63x images of phospho-SR, SON and DAPI staining of naïve *WT* female CD4$^+$ T cells. Brightness and contrast increased by 20% on all images. **B.** As in A. but at day 2 of Th2 *in vitro* differentiation. **C.** Violin plot of the change in mean phospho-SR nuclear intensity during the first 2 days of *in vitro* Th2 differentiation (total naïve n=52, day 2 n=86). **D.** As in A. but for *Malat1*$^{-/-}$ female CD4$^+$ T cells at day 2 of Th2 *in vitro* differentiation. **E.** Mean nuclear intensity of *WT* and *Malat1*$^{-/-}$ CD4$^+$ T cells of both sexes at day 2 of *in vitro* Th2 differentiation. Data merged between 2 biological replicates (total *WT* female n=86, *Malat1*$^{-/-}$ female n=125, *WT* male n=97, *Malat1*$^{-/-}$ male n=101).

5.2.4 *Malat1* loss affects Xi complex formation in females

Due to the observed *Malat1*-dependent sex-specific differences in gene expression and nuclear speckle formation at day 2 of differentiation, a time window coinciding with X chromosome re-inactivation (J. Wang et al., 2016), we performed preliminary experiments with Professor Dawn Coverley, investigating whether *Malat1* loss affected X chromosome inactivation. Here, we performed Th2 differentiation of *WT* and *Malat1*$^{-/-}$ female cells and collected slides for immunofluorescence staining at differing time points during the initial 48 hours of T cell differentiation. We investigated at 2-, 6-, 24- and 48-hours post-activation, as we had previously identified changed to CD69 expression from *Malat1* loss during early activation, and the 24- and 48-hour time points would line up with transcriptomic and speckle differences seen at days 1 and 2 of differentiation. Cells were fixed, permeabilised, and investigated by immunofluorescence staining. To investigate Xi formation, we used two antibodies targeting the nuclear protein CIZ1, a core part of the X inactivation complex which can be used as a marker of Xi patch formation (Sofi & Coverley, 2023). CIZ1 strongly associates with *Xist* in the nucleus, aiding in anchoring the X inactivation complex to the Xi. We used two antibodies for studying CIZ1, the CIZ1-1794 Ab which targets the CIZ1 N terminal region, and the CIZ1-87 Ab which targets the CIZ1 C terminal region, both provided by the Coverley lab group. Slides were investigated and imaged on the Coverley lab group's Zeiss Axiovert 200M, with Zen Blue.

When investigating *WT* naïve cells (*Figure 5.6 A, Supplementary Figures 27-30*), we identified little to no CIZ1 staining on the Xi patch in the majority of cells, only small delocalised CIZ1 foci, suggesting that no Xi patch was present at this time point. Following T cell activation, we visually identified an increase in CIZ1-1794 foci formation in *WT* cells, starting in some cells as early as 6 hours post-activation. This

became clearly visible in nearly all cells by 24 hours. At 48 hours, a clear large Xi patch had formed in most cells, suggesting that Xi formation was completed by this time point. When comparing *WT* and *Malat1*$^{-/-}$ mice, we identified that the Xi patches appeared smaller at 48 hours in *Malat1*$^{-/-}$ females (*Figure 5.6 B, Supplementary Figures 31+32*), although no differences were easily visible in naïve cells (*Figure 5.6 C, Supplementary Figures 33+34*). Interestingly, while the CIZ1-1794 antibody was detectable on the Xi at earlier time points, the CIZ1-87 Ab did not appear to localise well to the Xi until nearly 48 hours, instead staining the periphery of the nucleus. While this may represent different CIZ1 domains interacting with differing areas, the CIZ1-1794 Ab had been previously shown to co-localise well with *Xist* (Sofi & Coverley, 2023), and we therefore opted to use this antibody for following analyses.

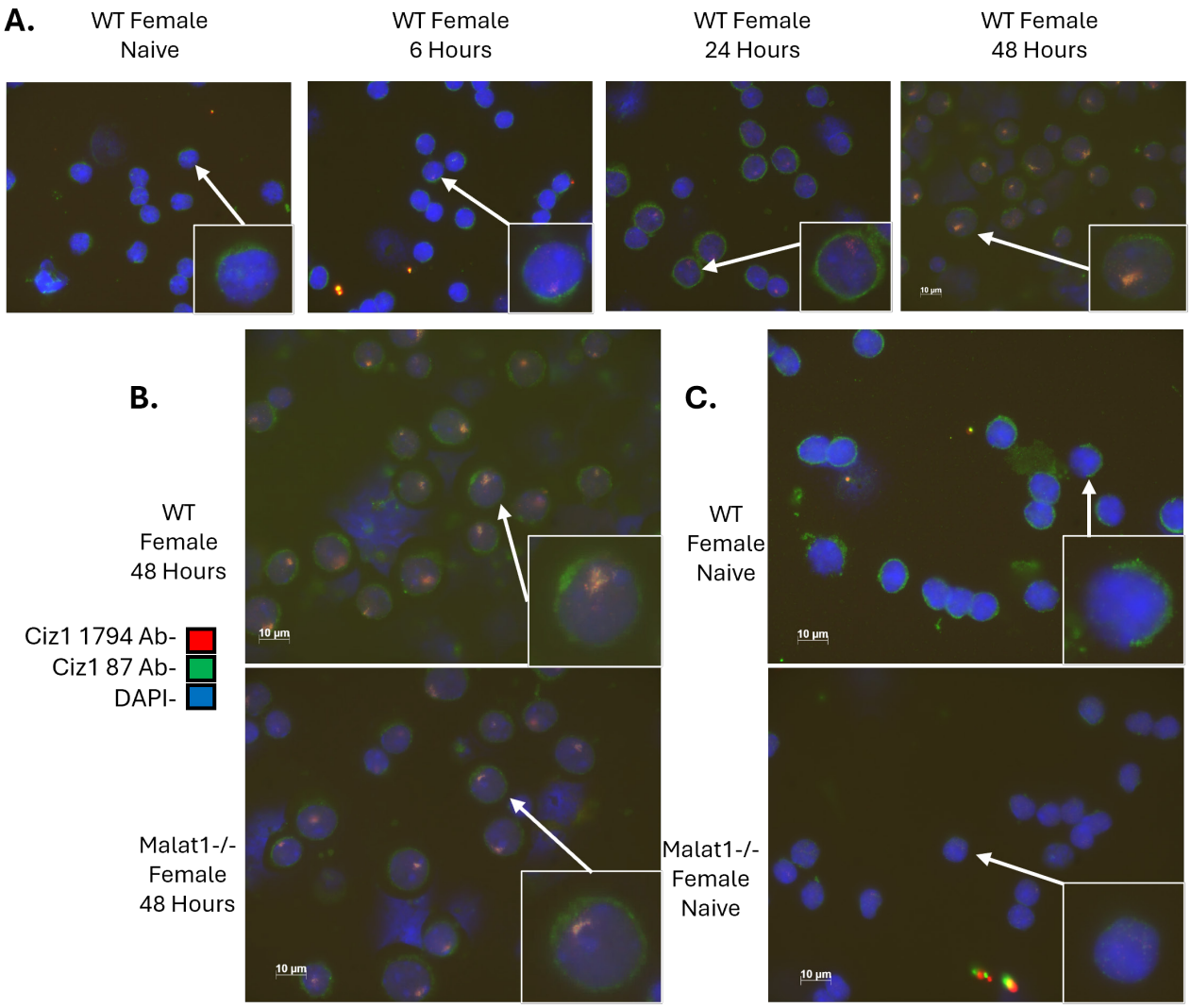

Figure 5.6 CIZ1 localises to the X chromosome during CD4$^+$ T cell differentiation

A. Representative 40x images with DAPI and CIZ1 (both N terminal 87 and C terminal 1794 antibodies) staining of *WT* female CD4$^+$ T cells in naïve cells, 6 hours, 24 hours and 48 hours post-activation. **B.** Representative 40x images of *WT* and *Malat1*$^{-/-}$ female CD4$^+$ T cells at 48 hours post-activation, stained with DAPI and CIZ1 (87 and 1794 Abs). **C.** As in B. but for naïve cells. Brightness and contrast of all images shown in this figure were increased by 20%, for ease of viewing.

We next investigated Xi inactivation progress during Th2 *in vitro* differentiation. To assess this, we determined four categories representing stages of Xi formation, based on previous literature which had categorised *Xist* patch assemblies on the X chromosome during T cell maturation in the thymus (Syrett et al., 2019; J. Wang et al., 2016). These categories were no Xi (N, represented by no CIZ1 staining on the Xi), dispersed CIZ1 foci within a nuclear area (D), a clear Xi focal point (F), and a clear large Xi patch (P). Examples of each category are shown in *Figure 5.7 A*. Slides were investigated under a microscope, and cells within each category were visibly counted within two focal areas at 63x magnification. Slides were randomised to reduce bias, and counts were verified by Dawn Coverley.

Categorisation of cells from all time-points in the first replicate (*Figure 5.7 B*) revealed that *WT* female cells progressed through each category during *in vitro* Th2 differentiation. The majority of naive cells displayed the N category, intermediate time points displayed a mixture of D, F and P categories, and at 48 hours the majority displayed P category. Interestingly, a significant decrease in P formation in *Malat1*$^{-/-}$ females was seen at both 24 and 48 hours, suggesting that Xi patch formation had been partially disrupted from *Malat1* loss. During early differentiation (naïve and 2 hours), we observed a slight increase in cells displaying the D category in *Malat1*-deficient cells at early time points. Repetition of this experiment (*Figure 5.7 C*) confirmed these results, with similar increases in D category at early time points (although no significance was seen in this replicate), and suppression of P categories at 48 hours, suggesting that the dynamics of Xi formation are disrupted from *Malat1* loss.

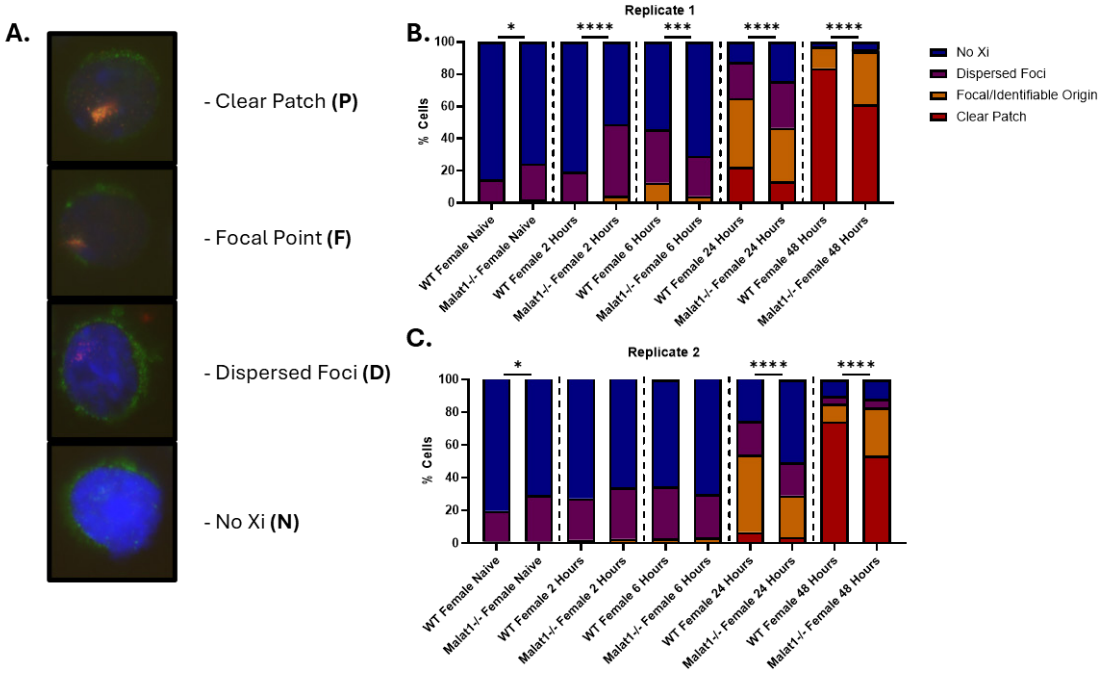

Figure 5.7 *Malat1* loss affects Xi patch formation during differentiation

A. Representative images for Xi patch identification and categorisation from CIZ1 staining, including no Xi, dispersed CIZ1 foci, Xi focal point and clear Xi patch. **B.** Xi patch categorisation from one *WT* and one *Malat1*$^{-/-}$ mouse of CD4^{+} T cells during *in vitro* differentiation. Between 90 and 130 total cells were counted and categorised from three-5 static focal planes per sample. Time points include naïve, 2 hours, 6 hours, 24 hours and 48 hours post-activation. Chi-square tests were performed to identify changes in each category. **C.** Replicate of Xi patch identification performed in B.

From images captured at each time point, we next investigated CIZ1-1794 staining intensity per nucleus via ImageJ to attempt to quantify changes in Xi patch formation. We reasoned that mean and maximum intensity measurements may correspond to the strength of the Xi patch, and allow for quantification of differences resulting from *Malat1* loss. CIZ1 maximum intensity was significantly decreased following *Malat1* loss, confirming disruption of the Xi patch. no significant changes were seen at other time points resulting from Malat1 loss (*Figure 5.8 A*). When investigating mean intensity, we identified a modest significant downregulation resulting from *Malat1* loss at 24 and 48 hours, similar to that seen with maximum intensity (*Figure 5.8 B*). However, we also identified a statistically significant increase at 6 hours, potentially consistent with the increase in patch formation seen in *Figure 5.7*, although this was at an earlier time point. Overall, these results suggest that *Malat1* loss disrupts X inactivation kinetics and Xi patch formation during $CD4^+$ T cell differentiation.

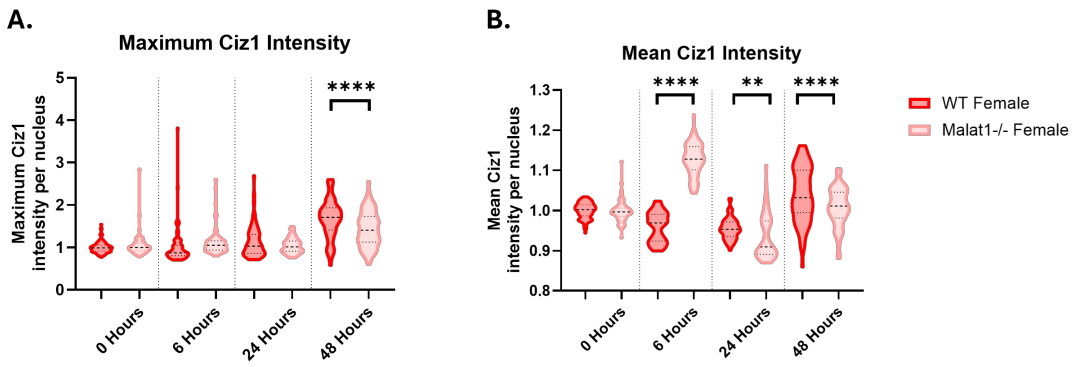

Figure 5.8 *Malat1* loss impacts CIZ1 intensity during T cell differentiation

A. Violin plot displaying maximum CIZ1-1794 intensity per cell nucleus of *WT* and *Malat1*$^{-/-}$ female CD4^{+} T cells during *in vitro* Th2 differentiation, at naïve, 6 hours, 24 hours and 48 hours post-activation. Cells were counted from 5 images at each condition and merged between 2 biological replicates (total cells 0 hours *WT* n=109 *Malat1*$^{-/-}$ n=105, 6 hours *WT* n=83 *Malat1*$^{-/-}$ n=86, 24 hours *WT* n=70 *Malat1*$^{-/-}$ n=94, 48 hours *WT* n=83 *Malat1*$^{-/-}$ n= 104). **B.** As in A. but for mean CIZ1-1794 expression.

5.2.5 *Malat1* affects X-linked gene expression during Th2 differentiation

Due to the identified disruption to Xi patch formation, we re-analysed our day 0 against day 2 long-read RNA-seq dataset, specifically to identify expression patterns of X-linked genes and whether these are affected by deletion of *Malat1*. As previously mentioned, at day 2 only 6 DEGs between *WT* and *Malat1*$^{-/-}$ females were X-linked, with four of them upregulated following *Malat1* loss (*Figure 5.9 A*). Included in this set was gene *Tlr7*, which has previously been shown to escape X inactivation in T cells (Souyris et al., 2018) and *Cfp*, which is involved in complement activation.

When comparing naïve to day2 cells, there were total 193 significant (FDR<0.05) X-linked activation-associated DEG. Of these, 99 genes were upregulated in *WT* females with 23 common between *WT* and *Malat1*$^{-/-}$ females, and 94 downregulated with 16 in common and 2 downregulated only in *Malat1*$^{-/-}$ females (*Figure 5.9 B*), suggesting an inhibition of transcriptional changes of X-linked during differentiation resulting from *Malat1* loss, consistent with our results investigating the whole transcriptome (*Figure 4.11 A*). When investigating how *Malat1* affects changes in expression of these X-linked DEGs at day 2 (*Figure 5.9 C*), *Malat1* loss visually appeared to have a stronger effect in regards to LFC on X-linked genes suppressed during differentiation. When setting a LFC cutoff of >1 between *WT* and *Malat1*$^{-/-}$ females at day 2 we identified 20 genes downregulated during differentiation but upregulated due to *Malat1* loss and only 4 genes upregulated during differentiation and downregulated from *Malat1* loss (*Figure 5.9 D*), suggesting that *Malat1* loss may affect specifically the suppression of X-linked genes, although many of these changes were non-significant. Downregulated genes with increased LFC resulting from *Malat1* loss included immune genes such as *Btk, Gata1, Tlr7* and *Cfp*, although of these only *Tlr7* and *Cfp* were significantly differentially expressed between *WT* and *Malat1*$^{-/-}$ females.

Following this, we investigated whether components of X chromosome inactivation were disrupted from *Malat1* loss. Of the lncRNAs involved in X inactivation (*Table 5.1 A*) only *Xist* was significantly (FDR<0.05) upregulated between day 0 and day 2 in *WT* females. *Xist* was also downregulated resulting from *Malat1* loss at day 2 consistent with our qRTPCR results, although this did not reach significance in our RNA-seq data. Of *Xist* interacting RBPs (list compiled from Da Rocha & Heard, 2017; McHugh et al., 2015), *Tardbp* (TDP-43), *Ezh2, Hnrnpc, Hnrnpk, Matr3 Ptbp1* and *Pcgf5* were significantly (FDR<0.05) upregulated during differentiation (*Table 5.1 B*), consistent with the increased rate of Xi patch formation. *Malat1* loss did not significantly affect expression of any of *Xist* interacting RBPs at day 2 of differentiation, and effect sizes were still relatively weak, with only *Rybp* displaying a LFC>1 from *Malat1* loss.

A.

Day 2 Significant X-Linked DEGs

Log Fold Change	Gene name
2.549378	Tlr7
2.408698	3830403N18Rik
2.26518	Cfp
1.040437	P2ry10
-2.50734	Rab33a
-4.23622	Armcx1

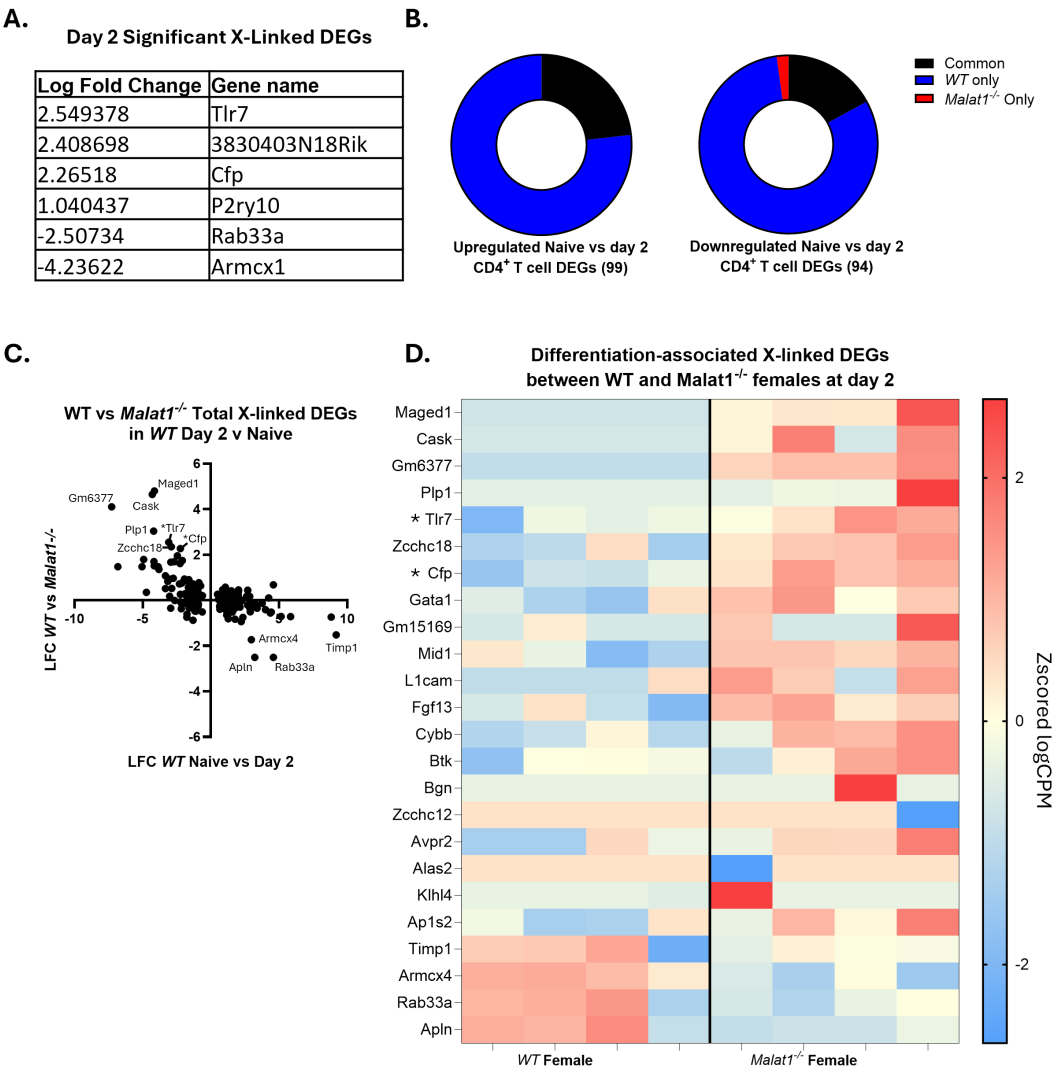

Figure 5.9 *Malat1* loss affects expression of X-linked genes

A. List of significant (FDR<0.05) X-linked DEGs between *WT* and *Malat1*$^{-/-}$ females at day 2 of *in vitro* Th2 differentiation. **B.** Significant (FDR<0.05) upregulated and downregulated DEGs between naïve and *in vitro* differentiated Th2 cells at day 2 for both *WT* and *Malat1*$^{-/-}$ cells (black), only *WT* (blue), and only *Malat1*$^{-/-}$ (red). **C.** LFC for significant X-linked DEGs between *WT* female naïve and day 2 *in vitro* differentiated Th2 cells against LFC between *WT* and *Malat1*$^{-/-}$ female cells at day 2. Significant DEGs at day 2 labelled with *. **D.** Heatmap displaying Z scored log2CPM of differentiation-associated DEGs at day 2 of differentiation (LFC>1 between *WT* and *Malat1*$^{-/-}$ cells at day 2). Genes ordered by decreasing LFC.

Table 5.1 Table of X chromosome inactivation lncRNAs and *Xist* interacting RBPs between day 0 and day 2 of *in vitro* Th2 differentiation

A. LncRNAs involved in Xi formation

Gene	LFC *WT* Day 0 vs Day 2	FDR *WT* Day 0 vs Day 2	LFC *WT* vs *Malat1-/-* Day 2	FDR *WT* vs *Malat1-/-* Day 2	Chromosome
Xist	1.272991292	0.000766	-0.811	0.3706	X
Firre	0.664050946	0.589912	0.9048	0.7052	X
Tsix	-0.014150625	0.989639	-0.559	0.7052	X

B. *Xist interacting RBPs*

Gene	LFC *WT* Day 0 vs Day 2	FDR *WT* Day 0 vs Day 2	LFC *WT* vs *Malat1-/-* Day 2	FDR *WT* vs *Malat1-/-* Day 2	Chromosome
Rybp	-1.196347782	0.187341	1.09008	0.70522	6
Myef2	0.748141092	0.121774	0.679383	0.688485	2
Tardbp	1.89843577	9.58E-07	0.36997	0.70522	4
Rbm15	-0.081776213	0.924083	0.35547	0.79339	3
Raly	-0.21138752	0.594563	0.318016	0.705224	2
Celf1	-0.262371658	0.408763	0.29427	0.70522	2
Ezh2	1.893112755	2.27E-05	0.26796	0.70544	6
Spen	-0.934218042	0.058301	0.20998	0.89069	4
Hnrnpu	0.176763472	0.589041	0.12966	0.89006	1
Hnrnpm	0.534434272	0.051395	0.114028	0.898568	17
Hnrnpc	1.02707862	0.0001	0.050681	0.966616	14
Lbr	-0.284934513	0.397148	-0.0409	0.966616	1
Hnrnpk	0.376618176	0.093979	-0.07438	0.946671	13
Hnrnpa0	-0.213059213	0.502842	-0.17355	0.844866	13
Matr3	1.623436008	9.98E-06	-0.1814	0.82401	18
Hnrnpl	0.336885584	0.191503	-0.23912	0.705224	7
Ptbp1	0.78729868	0.001561	-0.2667	0.70522	10
Pcgf5	1.486865532	1.87E-05	-0.2724	0.70522	19
Ciz1	-0.591627777	0.072218	-0.4197	0.70522	2

5.2.6 Inhibition of Xi formation may disrupt Th2 differentiation

To assess whether inhibition of Xi patch formation affected Th2 differentiation, we compared *WT* and *Ciz1*$^{-/-}$ mice. We isolated naïve CD4^{+} T cells from *WT* and *Ciz1*$^{-/-}$ female mice, then performed *in vitro* Th2 differentiation. Cell numbers and cytokine expression (IL10 and IL4) were then assessed as markers of activation in terminally differentiated cells.

Cell numbers resulting from *Ciz1* loss were not significantly affected when compared to *WT* cells, although there was a small downwards trend seen in the *Ciz1*$^{-/-}$ mice (*Figure 5.10 A*). Cytokine expression in a majority of *Ciz1*$^{-/-}$ samples displayed non-significant downwards trends for IL10^{+}, IL4^{+} and IL10^{+} IL4^{+} double positive cells (*Figure 5.10 B*). However, one outlier *Ciz1*$^{-/-}$ mouse (as determined by Grubbs test alpha=0.05 for IL10^{+}, IL4^{+} and IL10^{+} IL4^{+} expression) instead displayed increased cytokine expression compared to *WT* samples. Removal of this outlier sample (*Figure 5.10 C*) resulted in a significant downregulation of IL10^{+} and IL10^{+} IL4^{+} double positive cells with a non-significant downwards trend for IL4^{+} cells, similar to the effects of *Malat1* loss (*Figure 3.3 A*). This suggests that inhibition of X chromosome inactivation may suppress Th2 differentiation, potentially consistent with increased type I inflammatory and Th1 associated genes from Xi escape in females (Huret et al., 2024; Itoh et al., 2019; Souyris et al., 2018), although further replicates and investigation of the effects of *Ciz1* loss in males will be required to confirm this result.

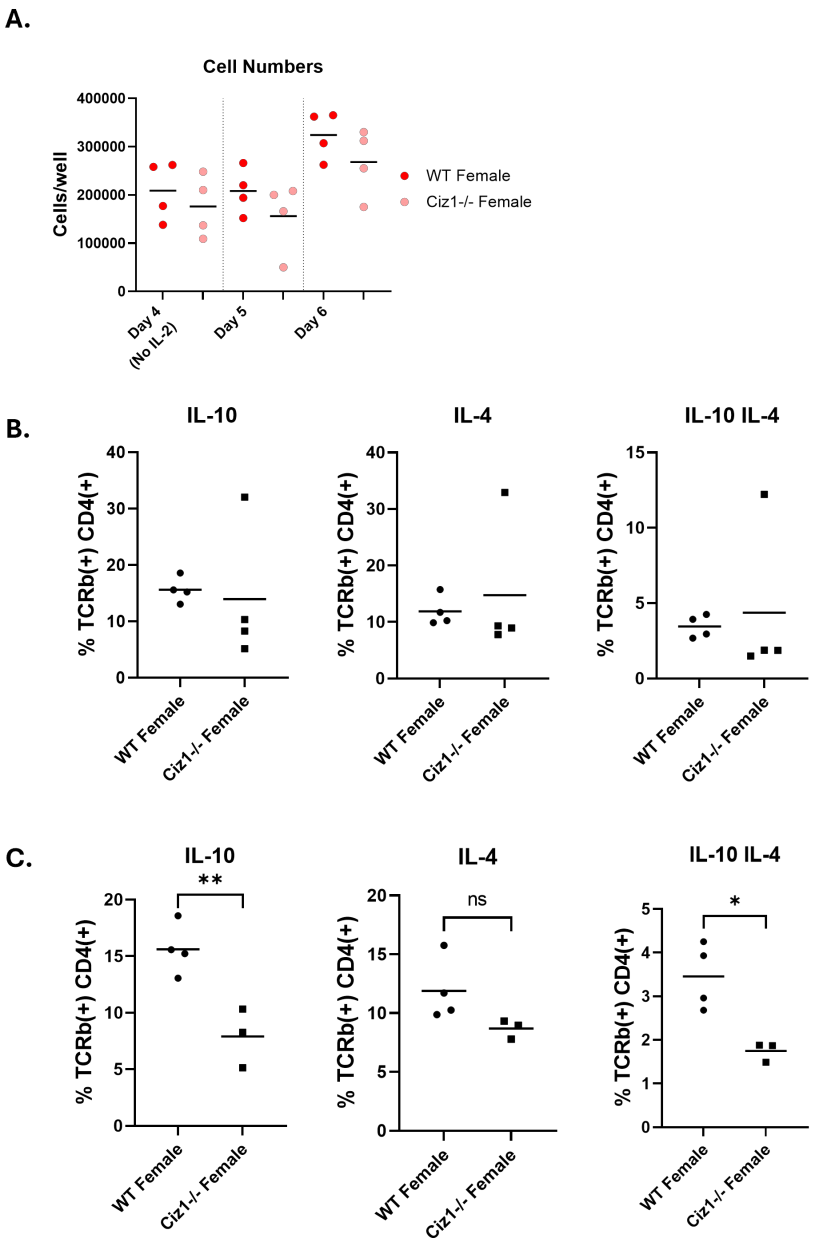

Figure 5.10 *Ciz1* loss may disrupt CD4$^+$ T cell differentiation

A. Cell counts at end-point Th2 *in vitro* differentiation of *WT* or *Ciz1*$^{-/-}$ female cells. **B.** Percentage of IL10$^+$ live TCRβ$^+$ CD4$^+$ *WT* or *Ciz1*$^{-/-}$ *in vitro* differentiated Th2 cells derived from female mice at day 6 (experimental end-point). Levels determined by intracellular cytokine staining (n=4 per condition). **C.** As in B. but with the potential outlier *Ciz1*$^{-/-}$ mouse sample removed.

5.2.7 *Malat1* loss affects H3K27me3 deposition during early Th cell differentiation

In chapter 4.2.3, we identified that *Malat1* loss in females during early differentiation caused $CD4^+$ T cells to fail to suppress an ISG module. We speculated that this may be caused by the potential regulation of PRC2 by *Malat1* (Arratia et al., 2023; S. H. Kim et al., 2017), although direct interactions between *Malat1* and PRC2 has more recently been disputed. Furthermore, Xi patch formation triggers the deposition of repressive histone marks such as H3K27me3 on the X chromosome via PRC2 (Tjalsma et al., 2021), and alteration to this may explain the previously observed decrease in Xi patch formation. To investigate whether PRC2 function was altered following *Malat1* loss in females, we performed immunofluorescence staining of *WT* and *Malat1*$^{-/-}$ female slides collected for Xi patch analysis at day 2 of differentiation. Slides were stained with DAPI and an anti-H3K27me3 antibody and imaged on the Zeiss Axiovert 200M provided by the Coverley lab, with Zen Blue.

We identified a decrease in H3K27me3 deposition between *WT* and *Malat1*$^{-/-}$ females at 48 hours post-differentiation (*Figure 5.11 A, Supplementary Figures 35+36*), in both the whole nucleus and on the Xi specifically. Further image analysis was then performed via ImageJ, to quantify differences in H3K27me3 maximum and mean intensity. Both maximum (*Figure 5.11 B*) and mean (*Figure 5.11 C*) H3K27me3 intensity were significantly reduced resulting from *Malat1* loss, with a near 50% decrease in maximum H3K27me3 intensity, potentially suggesting that H3K27me3 deposition was disrupted at day 2 of Th2 differentiation.

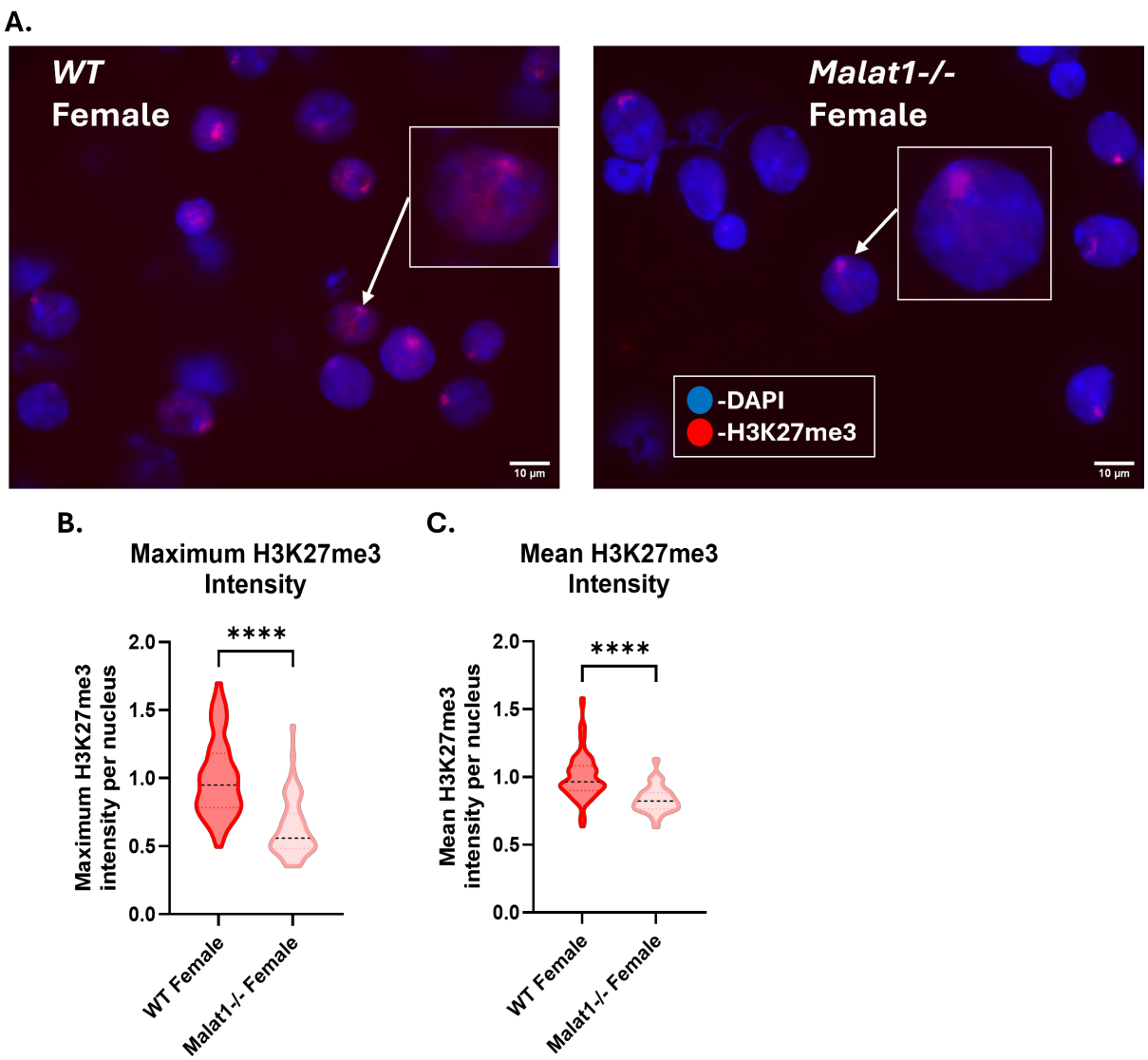

Figure 5.11 *Malat1* loss impacts nuclear H3K27me3 intensity during differentiation

A. Representative 40x images with DAPI and H3K27me3 staining of *in vitro* differentiated *WT* and *Malat1*$^{-/-}$ female CD4^{+} T cells at 48 hours post-activation. Brightness and contrast were increased by 40% on all images. **B.** Violin plot displaying maximum H3K27me3 intensity per cell nucleus of *WT* and *Malat1*$^{-/-}$ female CD4^{+} T cells during *in vitro* Th2 differentiation, at 48 hours post-activation. Results merged from two mice per condition. Cells were counted from 5 images at each condition and merged between 2 biological replicates (*WT* female n=100, *Malat1*$^{-/-}$ female n=85). **C.** as in B. but for mean H3K27me3 intensity.

Due to the significant change in maximum intensity, we next investigated whether total H3K27me3 levels were disrupted from *Malat1* loss. To assess this, we performed *in vitro* Th2 differentiations of *WT* and *Malat1*$^{-/-}$ cells, collecting protein samples at day 2 for western blot analysis of H3K27me3 and total H3 levels. We investigated both female and male samples, to identify if H3K27me3 levels differed between sexes.

Despite the changes to mean and maximum intensity in *Figure 5.16#1*, no clear differences were seen in band strength resulting from *Malat1* loss in either females or males (*Figure 5.12 A*), suggesting that total H3K27me3 levels were not disrupted. Densitometry analysis (*Figure 5.12 B*) identified a slight downwards trend for both *Malat1*$^{-/-}$ females and males consistent with the small decrease in mean H3K27me3 intensity seen, however this was not statistically significant. This could suggest that total H3K27me3 levels are relatively unaffected from *Malat* loss while targeted H3K27me3 deposition to specific areas may instead be disrupted, although this would require further investigation.

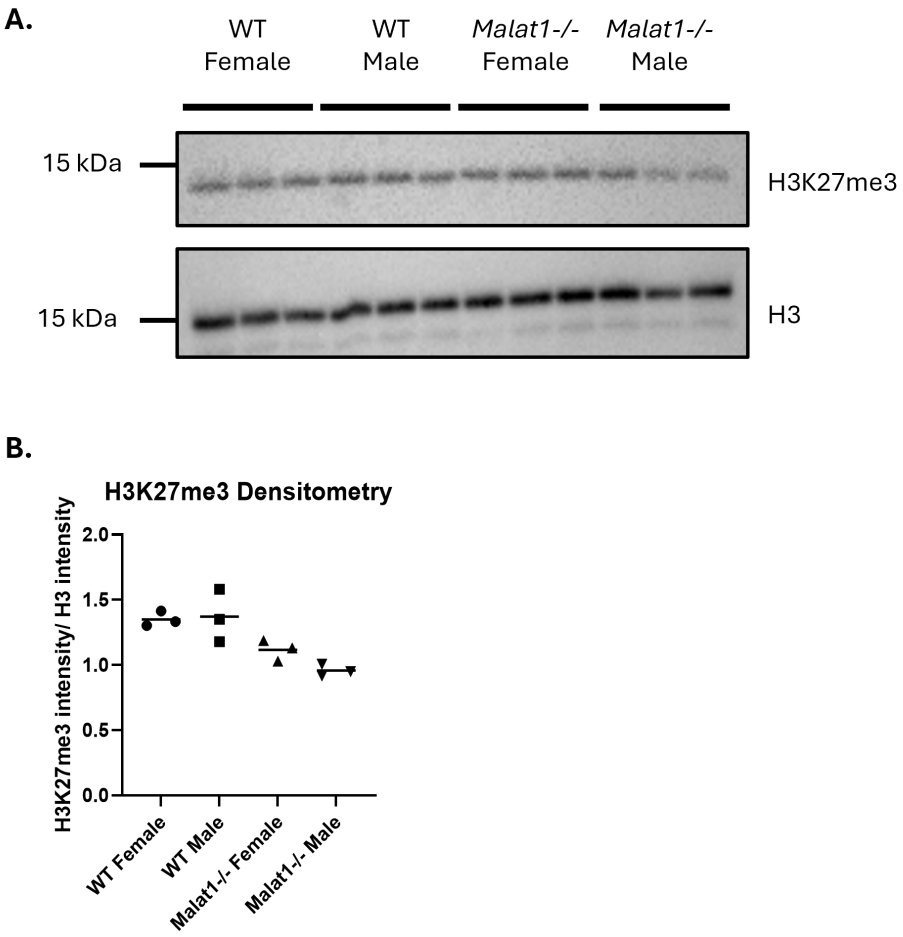

Figure 5.12 *Malat1* loss does not change overall H3K27me3 levels

A. Western blot displaying H3K27me3 and total H3 levels in *WT* and *Malat1*$^{-/-}$ females and males, in *in vitro* differentiated CD4^{+} T cells at 48 hours post-activation (n=3). **B.** Densitometry of A. with normalisation of H3K27me3 levels to total H3 levels, then to the average of *Malat1*$^{-/-}$ males.

5.2.7 *MALAT1* is downregulated during human T cell *in vitro* differentiation

Finally, we aimed to investigate *MALAT1* and nuclear speckles in the context of *in vitro* differentiation of human cells. We specifically investigated whether the hallmark downregulation of *MALAT1* and increase in nuclear speckle numbers and size occurred during $CD4^+$ T cell differentiation. Total $CD4^+$ T cells were provided by Dr. Dave Boucher after purification from whole blood of 4 donors (*Figure 5.13 A*). We isolated between 5-10 million cells per 10 ml of blood from each donor total (*Figure 5.13 B*). To assess T cell differentiation, we performed both Th0 (no addition of subset specific cytokines) and Th2 *in vitro* differentiation assays, with 100,000 total $CD4^+$ T cells per well. After 3 days cell numbers were counted to assess whether T cell expansion had occurred, RNA samples were collected for qRTPCR, and slides were collected for immunofluorescence staining. Extra Th0 cells following slide and RNA sample collection were resuspended in IL2 and expanded, with overall differentiation assessed by flow cytometry at day 8. Unfortunately, not enough Th2 cells remained after RNA and slide collection, and *in vitro* Th2 differentiation was assessed by qRTPCR at day 3 instead.

By day 3, cell numbers had doubled for all donors, for both Th0 and Th2 *in vitro* differentiation (*Figure 5.13 C, D*). For assessing *in vitro* Th0 differentiation, cell numbers had increased by day 8 (*Figure 5.14 A*), and cells produced high levels of IFNγ (20-40%) (*Figure 5.14 B*) and lower levels of IL4 (3-9%) (*Figure 5.14 C*), suggesting that cells had activated and differentiation had occurred. For assessing *in vitro* Th2 differentiation, RNA levels of *Il4* and *Il13* were assessed at day 3 by qRTPCR. *In vitro* Th2 differentiated samples displayed significant upregulation of both *Il4* (*Figure 5.15 A*) and *Il13* (*Figure 5.15 B*), again confirming that Th2 differentiation had occurred. Following confirmation of *in vitro* differentiation, we investigated *MALAT1* levels at day 0 and day 3 by qRTPCR

(*Figure 5.15* C) and observed significant downregulation of *MALAT1* during both Th0 and Th2 *in vitro* differentiation, confirming that this is a hallmark of both mouse and human $CD4^+$ T cells.

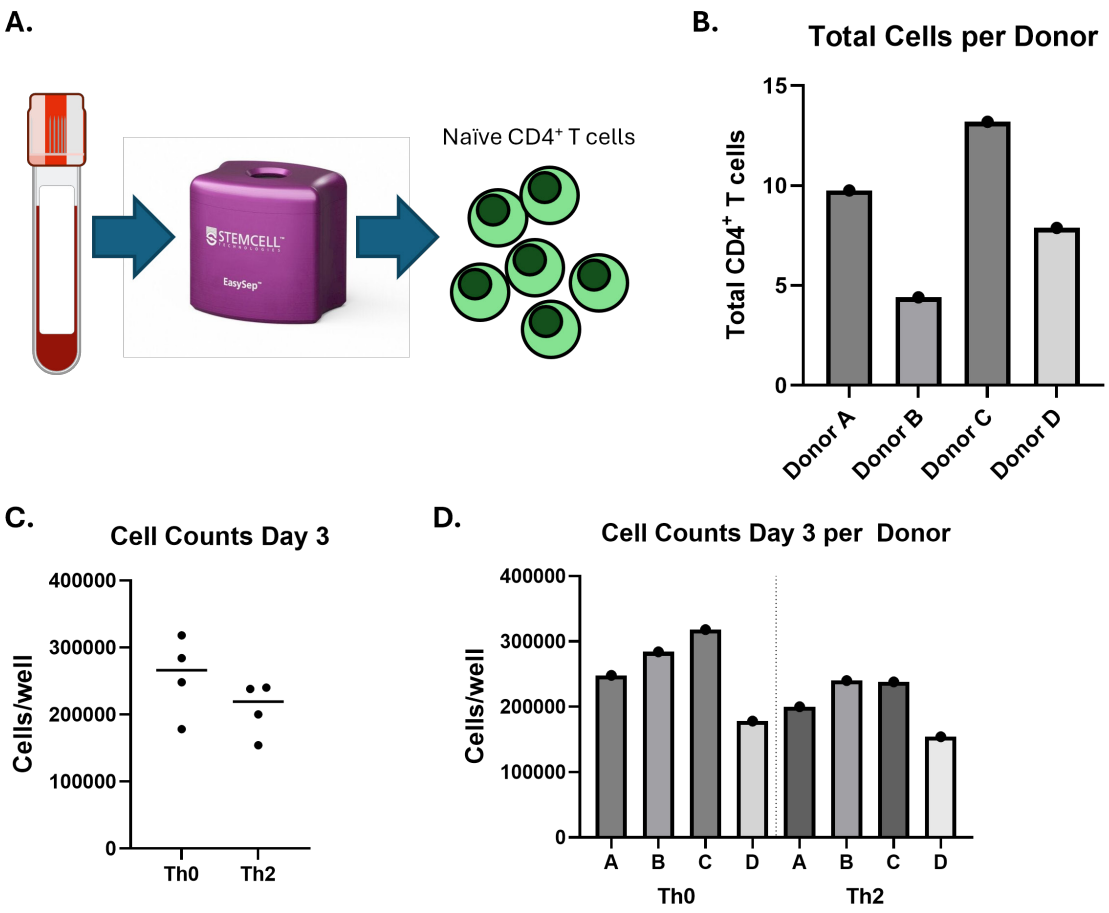

Figure 5.13 Isolation of total CD4⁺ T cells from human blood

A. Schematic displaying isolation of total CD4⁺ T cells from human blood. **B.** Total CD4⁺ T cells isolated per donor. **C.** CD4⁺ T cell counts following 3 days of either Th0 or Th2 *in vitro* differentiation (n=4). **D.** As in C. but split by individual donor.

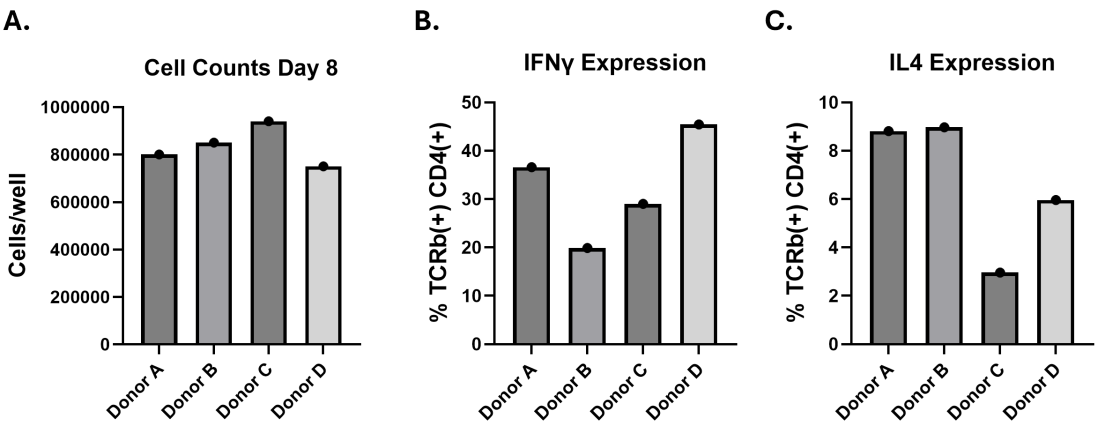

Figure 5.14 Human Th0 cell cytokine expression following *in vitro* differentiation

A. Human $CD4^+$ T cell counts per donor following 8 days of Th0 *in vitro* differentiation. **B.** Percentage of $CD4^+$ $TCR\beta^+$ cells expressing IFNγ in *in vitro* differentiated T cells. Results split per donor. **C.** As in B. but for IL4 expressing cells.

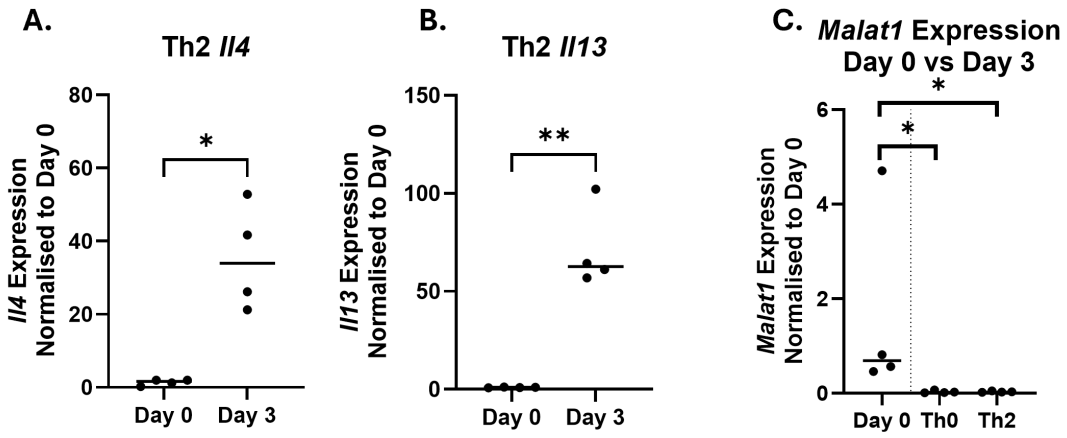

Figure 5.15 *Malat1* levels decrease following human T cell activation

A. *Il4* transcript levels normalised to *U6* at days 0 and 3 of Th2 *in vitro* differentiation of human $CD4^+$ T cells. **B.** As in A. but for *Il13*. **C.** *Malat1* transcript levels normalised to *U6* at day 0 and day 3 of Th0 or Th2 *in vitro* differentiation of human $CD4^+$ T cells.

5.2.8 Nuclear speckles increase in numbers and size during human *in vitro* differentiation

We next investigated whether nuclear speckle numbers and size changed during human Th cell differentiation, via immunofluorescence staining of slides collected at days 0 and 3 of *in vitro* Th0 and Th2 differentiation. Slides were stained with both DAPI and anti-SON antibodies.

Similar to murine $CD4^+$ T cells, both nuclear speckle numbers and size visibly increased during Th cell differentiation (*Figure 5.16 A+B* and *Supplementary Figures 23-26*). Image analysis revealed significant increases for both speckle numbers and size for Th2 (*Figure 5.17 A, B*) and Th0 (*Figure 5.17 C, D*) *in vitro* Th2 differentiations. Interestingly, numbers at both day 0 and day 3 are lower than speckle numbers in mice, with around 20 speckles seen at day 3, compared to around 50 at day 2 in murine $CD4^+$ T cells. Nuclear speckle sizes were also increased in humans compared to mice, with an area of around 0.7 um^2 at day 3 compared to an area of around 0.4 um^2 in murine $CD4^+$ T cells. Overall, this confirms that an increase in speckle numbers and size occurs during both murine and human Th cell differentiation, although there are large differences in speckle size and number.

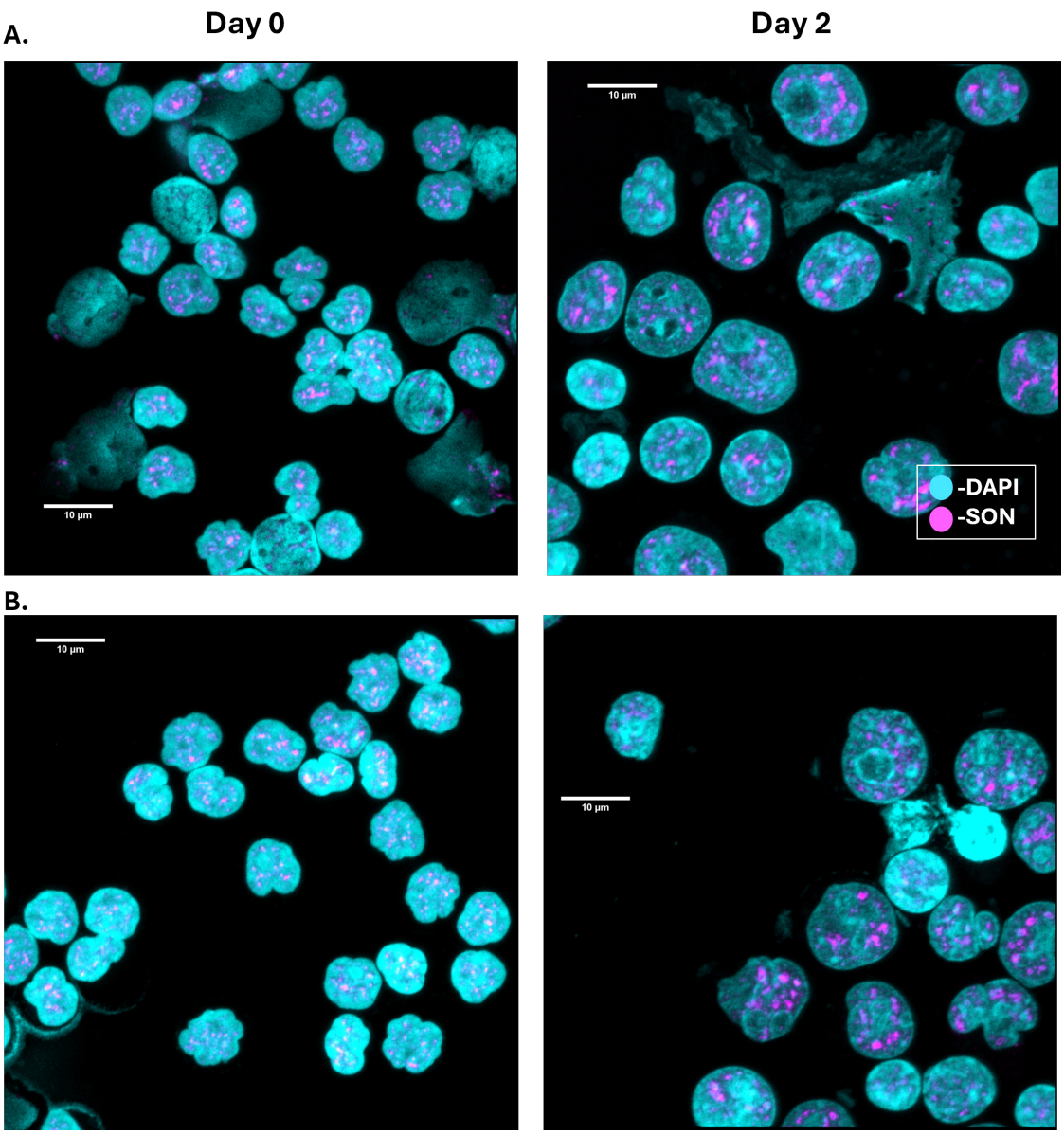

Figure 5.16 SON staining of human CD4$^+$ T cells

A. Representative images of SON and DAPI staining of human CD4$^+$ T cells from donor A. at days 0 and 3 of Th2 *in vitro* differentiation. Brightness and contrast were increased by 20% on all images. **B.** As in A. but for donor C.

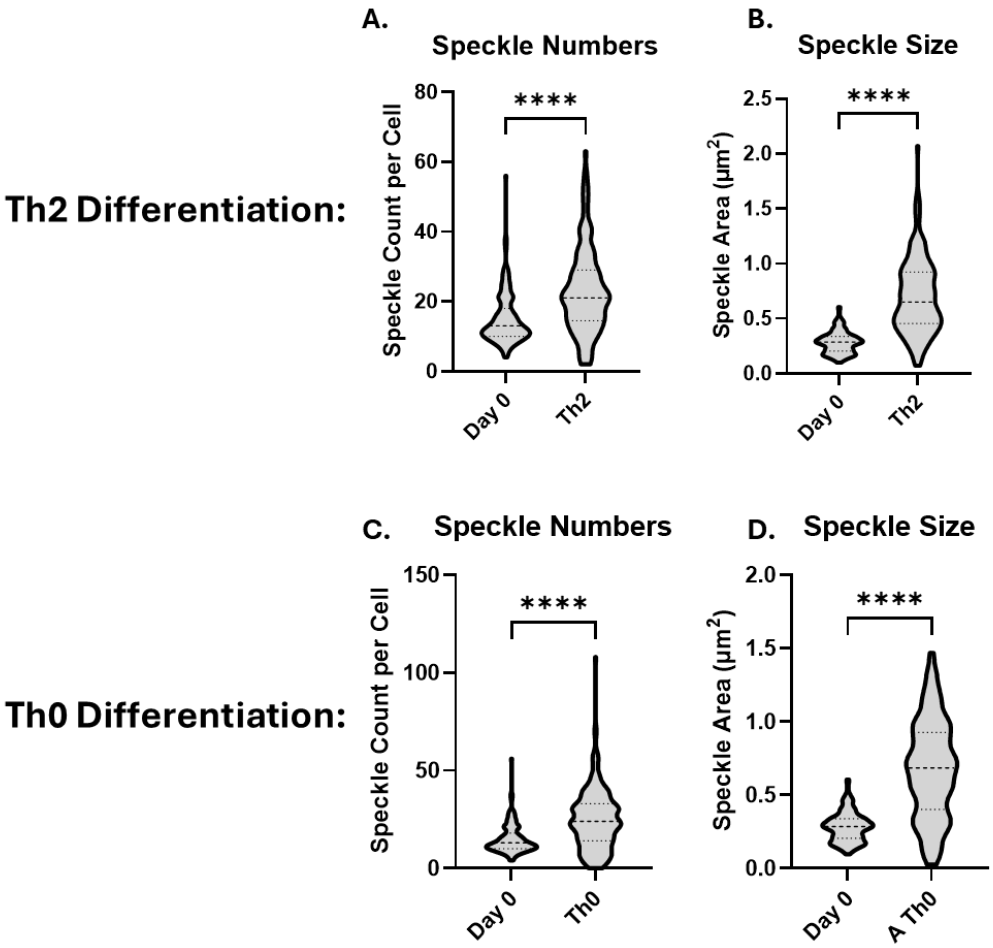

Figure 5.17 Speckle numbers and size increase during human CD4$^+$ T cell differentiation

A. Violin plot displaying nuclear speckle count per cell nucleus of human CD4$^+$ T cell, at both day 0 and day 3 *in vitro* Th2 differentiation. Results merged from 4 donors. **B.** As in A. but for nuclear speckle area (um^2). **C.** Violin plot displaying nuclear speckle count per cell nucleus of human CD4$^+$ T cell, at both day 0 and day 3 *in vitro* Th0 differentiation. Results merged from 4 donors. **D.** As in C. but for nuclear speckle area (um^2).

5.3 Discussion

In this chapter, we investigated whether *Malat1* affected changes in nuclear architecture, including nuclear speckles, the inactive X chromosome, and H3K27me3 deposition. We identified sex-specific effects on both nuclear speckle formation and Xi patch formation resulting from *Malat1* loss, providing a novel link between these core nuclear processes. We identified that both nuclear speckle numbers and size significantly increased during Th cell differentiation in both humans and mice, and *Malat1* loss here disrupted nuclear speckle numbers and activity (determined by SR protein phosphorylation) in a sex-specific manner. Preliminary work also revealed that *Malat1* loss disrupted localisation of Xi component CIZ1 to the inactive X chromosome, and further investigation with a model of Xi disruption (*Ciz1*$^{-/-}$ mice) caused similar trends to cytokine expression in fully differentiated cells to those of *Malat1* loss. H3K27me3 maximum and mean staining intensity were also significantly decreased following *Malat1* loss in females, however overall protein levels were unaffected, suggesting that targeting of H3K27me3 deposition may instead be altered.

We identified that nuclear speckle numbers and size increase drastically during *in vitro* T cell differentiation in murine CD4^{+} T cells, with preliminary data suggesting that similar effects are also seen with human CD4^{+} T cells. However, the results in human cells used comparatively few donors, and we did not have any donor information to identify sex or ensure that patients were healthy, likely requiring further investigation in future experiments. During T cell activation a major transcriptional burst occurs, with levels of thousands of transcripts increasing (Conley et al., 2016). As speckles regulate pre-mRNA splicing efficiency (Bhat et al., 2024) the increase in speckle numbers and activity likely coincides with increased demand for mRNA processing and splicing in activated T cells. The increase in speckle numbers and activity at day 2 also coincides

with the completion of Xi patch formation, potentially suggesting that these processes may be regulated by similar signalling pathways in T cells. X chromosome inactivation in $CD4^+$ T cell differentiation is controlled via TCR stimulation in an NF-kB pathway dependent manner (Forsyth, Toothacre, et al., 2024), and while NF-kB signalling has not been shown to affect speckle formation some NF-kB signalling pathway proteins are known to localise to speckles (D. Wang et al., 2023), providing an avenue for further exploration.

Interestingly, this increase in speckle function occurs alongside a decrease in *Malat1* levels (*Figure 3.2 C, Figure 4.2 A*) This could suggest speckles in activated Th cells contain lower amounts of *Malat1,* which may affect speckle function. Alongside the decrease in *Malat1* and increase in speckle numbers, SR protein phosphorylation was also seen to increase. *Malat1* has previously been shown to regulate SR protein phosphorylation (Tripathi et al., 2010), potentially suggesting that *Malat1* downregulation is required for their activation in Th cells. As an alternative explanation, *Malat1* here may inhibit SR protein mobility instead, as previously mentioned *Malat1* knockdown has previously been shown to trigger de-localisation of SR proteins from nuclear speckles to the nucleoplasm (Tripathi et al., 2010), therefore lower *Malat1* levels may also aid in movement of SR proteins to sites of active transcription.

Despite previous literature suggesting that *Malat1* does not affect speckle formation (B. Zhang et al., 2012), complete *Malat1* loss caused a significant sex-specific decrease in both nuclear speckle numbers and SR-protein phosphorylation, at day 2 of *in vitro* differentiation. This effect occurs despite the downregulation of *Malat1* that occurs during Th2 differentiation, suggesting that some amount of *Malat1* present may be critical for correct speckle formation. However, this could also suggest that the effects of *Malat1* loss only become relevant when its levels are both limiting to cell activation (as seen from

our CD69 results) and required for nuclear speckle biogenesis. Interestingly, previous work of *Malat1* and nuclear speckles did not investigate them in immune cells, which could suggest that *Malat1* is also involved in differing intracellular pathways in different cell types. As $CD4^+$ T cells are required to undergo rapid major changes in intracellular organisation during differentiation, they may be less resilient to the effects *Malat1* loss via any compensatory mechanisms or redundancy. Previous research suggesting that *Malat1* loss did not affect nuclear speckles also did not investigate either core-speckle markers or total SR protein phosphorylation, instead investigating phosphorylation of only SRSF1-6 by western blots as readout of nuclear speckle function (B. Zhang et al., 2012). This could suggest that *Malat1* may have a more specific effect on SON localisation in speckle formation, or on activation and phosphorylation of other speckle-associated proteins such as HNRNP proteins or PTBP1. Further adding to this, disruption to *SON* levels and localisation has been identified previously from *Malat1* loss (Fei et al., 2017), although transcript levels of both core speckle proteins *Son* and *Srrm2* were not significantly disrupted here.

In our preliminary imaging work, we confirmed that X chromosome inactivation occurred during the first 2 days of T cell differentiation, transitioning from little to no Xi patch formation in naïve cells, to full Xi patch formation by day 2 of differentiation. *Malat1* loss here partially disrupted this process, suggesting that *Malat1* may affect X chromosome inactivation and potentially providing a link to why *Malat1* loss has sex-specific effects on Th2 differentiation. This would also link to the downregulation of *Xist* transcript levels identified in the previous chapter. However, further super resolution microscopy experiments would be required for confirmation that repression of the Xi itself is disrupted, and other experiments such as RNA-FISH would likely be required to ensure that the effect is on *Xist* and Xi localisation and not just on CIZ1. Literature so far

has not suggested that *Malat1* interacts with *Xist* or is involved in X inactivation, providing little context for how *Malat1* loss here can affect Xi patch formation. However, some HNRNP and SRSF splicing proteins, such as SRSF1, SRSF2, HNRNPU and HNRNPK, are known to bind to both *Malat1* and *Xist*, and may play dual roles in the regulation of X chromosome inactivation and splicing (Agostini et al., 2012; Z. Lu et al., 2020; Malakar et al., 2016; Navarro-Cobos et al., 2022; Nguyen et al., 2019; Tripathi et al., 2010). HNRNPK and HNRNPU, two proteins that have previously been shown to interact with *Malat1* (Aslan et al., 2023; Nguyen et al., 2019), play critical roles in X chromosome inactivation, with HNRNPK mediating *Xist* recruitment of PRC1/2, and HNRNPU aiding in anchoring *Xist* to the Xi (Hasegawa et al., 2010; Nakamoto et al., 2020). Disruption to phosphorylation of these splicing factors from *Malat1* loss would likely affect their activity, potentially explaining the effects on Xi patch formation. Alternatively, *Malat1* loss could alter mobility of these proteins, preventing localisation to the Xi. *WT* female and male $CD4^+$ T cells also displayed differences in nuclear speckle numbers, size, and SR protein phosphorylation, which were significantly decreased in *WT* males compared to females. As X inactivation occurs in tandem with the increase in speckle numbers during T cell differentiation, this could suggest increased speckle numbers and activity in females may be due to an increased demand for SR proteins involved in X inactivation, a demand not required in males. Further identification of *Malat1* and *Xist* RBP binding partners during Th2 differentiation via techniques such as RAP-MS, and investigation of their localisation via immunofluorescence staining would provide more information on how these processes could be linked in the future (McHugh & Guttman, 2018).

We identified trends suggesting that *Malat1* loss primarily inhibits suppression of X-linked genes at day 2 of differentiation, suggesting increased rates of Xi escape in

Malat1$^{-/-}$ females, potentially linking this to the decreased Xi patch formation seen. *Ciz1*$^{-/-}$ mice also displayed similar trends in disrupted cytokine expression as those from *Malat1* loss in females, suggesting that inhibition of X chromosome inactivation may also inhibit Th2 differentiation, linking to the effects of *Malat1* loss. Interestingly, Xi escape in T cells has previously been shown to promote Th1 responses via *Kdm6a* and *Tlr7* expression, which upregulate type-I IFNs and cytokines IFNγ and IL17 (Huret et al., 2024; Itoh et al., 2019). *Tlr7* was present in our RNA-seq data (*Table 4.2*) and was one of two significantly upregulated X-linked genes at day 2 alongside complement protein *Cfp*. TLR7 activity lies directly upstream of IRF7 signalling (Ning et al., 2011), therefore increased *Tlr7* escape from the Xi could explain the upregulation of IRF7 and ISGs seen when *Malat1* is lost.

However, the results using *Ciz1*$^{-/-}$ mice were not fully conclusive, with one potential outlier displaying significantly increased end-point cytokine expression instead. Furthermore, X-linked gene *Il2rg* (*Figure 4.5*) decreased in expression by qRTPCR at day 2 when increased Xi escape should enhance expression levels, and analysis via regular qRTPCR and RNA-seq cannot identify whether expression is specifically increased from the Xi over the autosomal X. Complete assessment of Xi escape would require experiments such as allele-specific qRTPCR (Vasques & Pereira, 2001) to confirm if this is the case. CIZ1 is also not solely involved in X chromosome inactivation, with roles in cell cycle regulation via interactions with CDC6 and CDK2 (Pauzaite et al., 2016), providing an opportunity for non-specific effects. Therefore, alternate methods of inhibiting Xi patch formation such as *Xist* targeting anti-sense oligonucleotides (Bauer et al., 2021) or small molecules (Nickbarg et al., 2023) may be required to confirm the effects on Th2 differentiation.

During early activation (~2 hours post-activation), Xi patch formation was partially enhanced by *Malat1* loss. This small increase could reflect the stronger early activation dynamics identified in *Figure 4.1* from CD69 expression, as Xi patch formation in $CD4^+$ T cells is known to be directly tied to TCR stimulation via the NF-kB signalling pathway (Forsyth, Toothacre, et al., 2024). The connection between T cell differentiation and X chromosome inactivation may suggest that the decrease in Xi patch formation in *Malat1*$^{-/-}$ females at later time points could also reflect the general decrease in Th cell differentiation strength seen there, instead of representing a direct effect of *Malat1* in Xi formation. This could also suggest that nuclear speckle biogenesis is regulated by a similar pathway in $CD4^+$ T cells, potentially explaining why both occur during a similar timeframe, although further work would be required to identify whether this is the case.

At day 2 of differentiation *Malat1* loss was also seen to decrease H3K27me3 intensity in females, suggesting that H3K27me3 deposition in the nucleus may be disrupted. However, total H3K27me3 levels as identified by western blot were not significantly affected from *Malat1* loss, although there was a slight downwards trend, which could reflect the small significant decrease in mean intensity seen from *Malat1* loss. As mentioned previously, *Malat1* has been linked to H3K27me3 deposition via PRC2, and previous research has suggested that *Malat1* may affect PRC2 targeting (Arratia et al., 2023; S. H. Kim et al., 2017), which could explain the differences in H3K27me3 intensity without largely affecting overall levels. Alternatively, the disruption to overall differentiation from *Malat1* loss and the high levels of H3K27me3 seen in naïve cells may act as a compensatory mechanism (Wei et al., 2009), where any decrease in methylation levels from *Malat1* loss is offset by the amount remaining from the less differentiated state of the cell. Regulation of PRC2 by *Malat1* could also explain multiple effects seen from *Malat1* loss during early differentiation, including both the upregulation

of the ISG module, and the decrease in Xi patch formation. During Th cell differentiation, deposition of H3K27me3 on genes from alternate Th cell subsets is critical for their repression (Wei et al., 2009). Meanwhile *Xist* recruitment of PRC2 is required for deposition of repressive H3K27me3 marks on the Xi (Bousard et al., 2019), aiding in the formation of a transcriptionally repressive state. The large decrease in maximum H3K27me3 could aso reflect the decrease in Xi patch formation. However, while we have seen overall changes in H3K27me3 levels in females, repetition of this experiment would be required in males to identify whether *Malat1* loss only affects H3K27me3 levels in females alone. Furthermore, the lack of H3K27me3 level change via western blot may require investigation from techniques such as ChIP-seq (Young et al., 2011) to identify if methylation of ISGs or the Xi is disrupted from *Malat1* loss.

To conclude, *Malat1* is core to nuclear speckle formation in Th2 cells, with *Malat1* downregulation core to both human and murine T cell activation, and complete *Malat1* loss inhibiting both speckle formation and function during Th2 differentiation in a sex-specific manner. In murine $CD4^+$ T cells *Malat1* loss has further ranging effects on other aspects of nuclear architecture, affecting H3K27me3 deposition during T cell differentiation and X chromosome inactivation, potentially providing some explanation for how *Malat1* affects Th cell differentiation in a sex-specific manner.

6 Concluding Discussion

6.1 *Malat1* in Th cell differentiation

Previous work attempting to identify roles of *Malat1* in Th cell differentiation were often conflicting, with some studies suggesting no function (Yao et al., 2018), some suggesting that *Malat1* inhibited Th cell differentiation (Masoumi et al., 2019), and others suggesting that *Malat1* promoted Th differentiation (Xue et al., 2022). Furthermore, not all studies investigated how *Malat1* regulated Th cells *in vivo*, and prior studies either did not report investigating sex or only investigated female cells. In this thesis, we have determined that *Malat1* is a critical cell-intrinsic and sex-specific regulator of both early and late Th2 cell differentiation, and that it may act as a novel molecular co-ordinator of differentiation-associated nuclear processes including nuclear speckle formation and X inactivation. Impacts of *Malat1* loss on cytokine expression, particularly IL10 expression, were seen both *in vitro* (Chapter 3. Aim 1. Identify the effects of *Malat1* deficiency on cytokine expression in female and male Th2 cells) and *in vivo* (Chapter 3. Aim 4. Investigate how *Malat1* loss affects Th2 differentiation *in vivo*) during Th2 differentiation, with transcriptome-wide effects on overall differentiation identified via RNA-seq experiments (Chapter 3. Aim 2. Assess the impact of *Malat1* deficiency on the transcriptome during Th2 differentiation.)

Our work investigating end-point Th cell differentiation in females broadly agreed with previous work, where *Malat1* loss in female cells disrupted cytokine IL10 expression in Th1 and Th2 cells via an effect on *Maf* (Hewitson et al., 2020), and where *Malat1* loss affected GATA3 expression in Th2 cells (X. H. Wu et al., 2022). However, we did not identify effects on end-point cytokine expression from *Malat1* loss in males, although some effects such as a decrease in IL2Rγ and GATA3 levels were seen in both *Malat1*$^{-/-}$ females and males. Further expanding on this, we identified that the high IL10 levels produced in female Th2 cells over males masked effects from *Malat1* loss on other

cytokines. The broader effect on Th cell differentiation in females was likely caused by a general disruption to IL2R levels following *Malat1* loss, and the sex differences in part by decreased sensitivity to IL2 in male cells (Chapter 3. Aim 3. Determine whether Th cell activation strength modulates the effects of *Malat1* loss on Th2 cell differentiation). Biological sex has been implicated in IL10 expression and signalling previously, as IL10 is responsive to testosterone, and its expression in $CD4^+$ T cells can be directly stimulated by testosterone (Liva & Voskuhl, 2001). However, IL10 signalling may be constitutively stronger in females, as female blood leukocytes showed increased STAT3 activation and upregulated TNFα expression in response to IL10 signalling compared to males (Warren et al., 2017), suggesting that the positive feedback loop that regulates IL10 expression is enhanced in females. Complete IL10 loss in mice is also known to cause increased rates of inflammatory bowel diseases in females (Casado-Bedmar et al., 2023), suggesting that female Th cells may induce higher levels of anti-inflammatory signalling to compensate for an enhanced inflammatory immune environment, resulting in the increased IL10 levels seen in *WT* females here.

In terms of the effects of *Malat1* on early Th cell activation and differentiation, *Malat1* is downregulated during the first 24 hours of Th cell differentiation, which may be linked to the transcriptional burst at this time point (Dey et al., 2023; Hewitson et al., 2020). Consistent with this, we identified enhanced early activation resulting from *Malat1* loss (Chapter 4. Aim 1. Investigate the effects of *Malat1* loss on naïve CD4+ T cell activation and early Th2 cell differentiation), suggesting that high *Malat1* levels are inhibitory for initial Th cell activation. However, complete *Malat1* loss suppressed early Th cell differentiation in females by day 2, via impaired suppression of an ISG module, which has previously been associated with naïve cells and disrupted Th2 differentiation (Chapter 4. Aim 2. Investigate transcriptomic changes resulting from *Malat1* loss at day

2 of differentiation via long-read ONT RNA sequencing). Increased ISG expression in female immune cells has been identified in response to viral infection previously (J. J. Chang et al., 2013; Pujantell & Altfeld, 2022), and this is thought to be linked to the pro-inflammatory effects of oestrogen signalling and Xi escape of pro-inflammatory genes such as *Tlr7* (Laffont et al., 2014; Seillet et al., 2012). In contrast to this, *WT* male differentiating Th2 cells here displayed higher ISG expression during early activation than *WT* females. This could suggest that Th2 differentiation in males is more permissive to low level ISG signalling, potentially due to the lack of inflammatory X-linked genes, or that ISG expression may require more dedicated suppression in *WT* females. This could also explain how ISG levels in *Malat1*$^{-/-}$ females are similar to those seen in *WT* males and yet only disrupt IL2R and cytokine expression in females. ISG activation in females partially phenocopied the effects of *Malat1* loss, suggesting that activation of the ISGs affected IL2R expression and end-point cytokine expression, linking the effects of *Malat1* loss on early and late Th cell differentiation. (Chapter 4. Aim 3. Identify *Malat1*-dependent pathways that are associated with Th2 differentiation and explore whether their disruption phenocopies the impact of *Malat1* loss on Th2 differentiation).

We also identified here that *WT* males displayed decreased sensitivity to differing levels of IL2 when compared to females. Sex has previously been shown to affect IL2 signalling in other cell types. Similar to our work in Th cells, female ILC2s respond stronger to IL2 signalling than males suggesting that females overall may be more sensitive to IL2 levels, although this mostly affected ILC2s in females (Warren et al., 2017). STAT5 signalling downstream of IL2 has also been shown to differ between females and males as well, with knockout of STAT5A causing disruption to liver cell function and gene expression in females but not males, potentially suggesting that STAT5 signalling targets different genesets between sexes (Park et al., 1999). Alternatively, as

cytokine expression *in vivo* was more similar between *WT* females and males, other components may be missing from our *in vitro* experiments that modulate IL2 signalling, such as cell surface receptor signalling from other immune cell types of hormonal signalling.

Despite an effect from *Malat1* loss on expression of Th2 transcription factor GATA3, no effects on end-point cytokine expression or the Th2 transcriptome were seen in males. While sex differences in GATA3 expression have been identified previously, they mostly suggest that GATA3 is responsive to oestrogen and upregulated in cancers in females (H.-W. Lee et al., 2013), which would not explain our results in a hormone independent environment. Our results could suggest that males may be less sensitive to GATA3 levels than females, similar to the effects seen for IL2. However, another explanation for this could lie in the contraction phase of T cell differentiation (McKinstry et al., 2010), where $GATA3^-$ cells die and lead to underrepresentation of the $GATA3^-$ cells later in differentiation. We also identified slightly increased levels of cytokine production in $Malat1^{-/-}$ males *in vivo*, suggesting that *Malat1* could repress downstream signalling of GATA3 in males, which rescues the effects of GATA3 loss, while other sex-specific effects such as the decrease in IL2Rα expression and increased ISG expression still inhibit female differentiation. Further adding to this explanation, chromatin remodelling in $CD8^+$ T cells has been shown to affect whether GATA3 can access and promote expression of some genes (Eeckhoute et al., 2007), potentially suggesting that the disruption to H3K27me3 deposition in males could act as a compensatory mechanism for the decreased GATA3 levels in males.

We identified a sex-specific decrease in IL10 expression due to *Malat1* loss both *in vitro* and in a model of type 2 lung inflammation *in vivo*, consistent with decreased IL10 expression seen from *L. donovani* and *Plasmodium chabaudi chabaudi* infection.

This could suggest real consequences from *Malat1* dysregulation in infection as IL10 is critical to regulating the immune response in a number of diseases (Carlini et al., 2023; Schopf et al., 2002). These sex-specific effects of *Malat1* loss on Th2 cytokine expression could improve our overall understanding of sex differences in autoimmunity and type 2 immunopathologies. Outside of its initial links to cancer, *Malat1* is known to be upregulated and linked to inflammatory pathways, with links in mice to experimental autoimmune encephalitis (Masoumi et al., 2019), and in human clinical data to rheumatoid arthritis (Chatterjee et al., 2020), SLE (Gao et al., 2020; H. Yang et al., 2017), and multiple sclerosis (Shaker et al., 2019). Furthermore, in type 2 immunity *Malat1* expression has been linked to atopic dermatitis and allergic rhinitis, promoting T cell differentiation and type 2 inflammatory cytokine production here (Ruiz-Ojeda et al., 2024; X. H. Wu et al., 2022). The sex-specific effects of *Malat1* seen here could also partially explain how high levels of *Malat1* could trigger disease progression in females and not males (Conrad et al., 2023; Dunn et al., 2024), although further work would likely need to investigate whether *Malat1* directly affects these conditions.

6.2 Nuclear architecture in T cell/lymphocyte development

We discovered that *Malat1* plays a novel role in regulating nuclear architecture in a sex-specific manner during early Th cell differentiation, specifically that *Malat1* affects deposition of repressive marker H3K27me3 (Chapter 5. Aim 2. Investigate whether *Malat1* affects H3K27me3 deposition during early Th2 differentiation) and that *Malat1* loss partially disrupts Xi complex localisation during Th cell differentiation (Chapter 5. Aim 1. Investigate the effects of *Malat1* loss on X chromosome inactivation during early Th2 differentiation). Spatial organisation of nuclei is known to be critical for function.

Genes of similar function on different chromosomes cluster together into specific genomic compartments, and actively expressed genes typically localise to areas with increased inter-chromosomal contacts in the nuclear interior. Repressed genes meanwhile typically localising near the nuclear periphery in nuclear lamina-associated domains (Meldi & Brickner, 2011). Genomic organisation is also known to differ greatly between cell types, likely due to differing gene expression requirements. For chromatin organisation, DNA in the nucleus is supercoiled and wrapped around histones, which comprise of two histone H3-H4, H2a-H2b dimers, and are separated by a linker H1. In transcriptionally active areas, histones are loosely packed together to allow for physical access of transcription associated machinery to required genes. Meanwhile, in transcriptionally repressive areas histones are tightly compressed together, preventing physical access. As mentioned previously, transcriptionally active area histones are typically associated with H3K27ac and H3K4me marks, while repressive areas are associated with H3K27me3 and H3K9me3 marks (Hübner et al., 2012).

Biological sex has previously been shown to affect nuclear architecture in differing cell types, although outside of studies on the X chromosome most papers reporting on nuclear architecture do not include sex as a variable (Fischer & Riddle, 2017). In germline cells, following DNA demethylation cells are seen undergo repressive histone modification remodelling from PRC2 component EZH2, resulting in sex-specific histone signatures (T. C. Huang et al., 2021). Investigation into female and male muscle fibers also identified differences in chromatin accessibility between sexes, suggesting that nuclear architecture may generally differ between females and males (Hanks et al., 2025). Nuclear bodies other than nuclear speckles and the X chromosome may also be affected by sex. Both expression of *Neat1* and paraspeckle formation are known to be oestrogen sensitive (Chakravarty et al., 2014), and paraspeckles and their associated lncRNA *Neat1*

have been linked to pregnancy, with loss affecting both corpus luteum and progesterone expression during pregnancy (Pisani & Baron, 2019).

Regulation of nuclear architecture is known to be important for Th cell differentiation. Major changes in nuclear architecture including widespread chromatin and transcriptional remodelling occur as a result of TCR stimulation, cytokine signalling and co-stimulatory signalling. Naïve cells display a highly compact chromatin structure, with differentiation inducing wide scale chromatin de-condensation to allow for enhanced gene expression. Th cell transcription factors play a role in this, with activation induced AP-1 and IL2 induced STAT5 mediating long-range chromatin interactions (B. Wang & Bian, 2025). Alongside this, wide-scale histone demethylation and acetylation occurs, and the nuclear envelope is disrupted to reduce gene association with the nuclear lamina (Xu et al., 2024). However, some level of H3K27me3 deposition is still required during Th cell differentiation, to allow for repression of transcription factors from other Th cell subsets and enforcing Th cell subset commitment (Wei et al., 2009).

While some research has suggested that *Malat1* is not involved in regulating nuclear architecture (Eißmann et al., 2012), more recent research has identified that *Malat1* affects the function of complexes involved in chromatin structure and transcriptional regulation (M. Huang et al., 2018; Kanbar et al., 2022; S. H. Kim et al., 2017; L. Yang et al., 2011). *Malat1* and neighbouring paraspeckle lincRNA *Neat1* have also been shown to interact with areas of active transcription via RNA-RNA interactions, potentially suggesting that it may be involved in co-ordinating localisation of factors involved in transcriptional regulation or transcript processing to actively transcribing genes (West et al., 2014). Regulation of transcriptional and chromatin machinery by *Malat1* could link between both the observed change in H3K27me3 deposition and ISG upregulation when *Malat1* is lost during Th cell differentiation. Knock-out of PRC2

catalytic component EZH2, which *Malat1* has been shown to interact with (D. Wang et al., 2015; X. Wang et al., 2016), has also previously shown mixed impacts on Th cell differentiation, displaying a perceived Th1 skew and enhanced IFNγ expression during differentiation, potentially linking the changes in H3K27me3 deposition and increased ISG expression from *Malat1* loss (Karantanos et al., 2016). However, EZH2 knock-out also enhanced IL10 expression in Th2 cells (Y. Zhang et al., 2014), suggesting that a decrease in H3K27me3 levels alone is likely not the cause of IL10 suppression. IL10 has also been shown to be particularly responsive to the epigenetic landscape of the cell, with knock-out of chromatin remodelling enzymes such as CTCF causing disruption to IL10 expression in Th cells previously (Ribeiro de Almeida et al., 2009; H. Zhang & Kuchroo, 2019), potentially linking disrupted chromatin architecture from *Malat1* loss to the effects seen on end-point Th cell differentiation.

Malat1 has also been shown to associate with PRC2 component EZH2 in $CD8^+$ T cells and is involved in targeting PRC2 to suppress genes involved in memory cell formation (Kanbar et al., 2022). Due to overlap between memory cells and ISG expression this could suggest that *Malat1* is performing similar roles between CD4 and CD8 T cells, and disruption to targeting of PRC2 may explain the changes seen in H3K27me3 staining, while not affecting overall levels. ISG expression in naïve $CD4^+$ T cells has also been previously linked to central memory cell formation (Deep et al., 2024), which could suggest regulation of similar memory associated genesets between $CD4^+$ and $CD8^+$ T cells. Tcm cells display limited cytokine production capabilities when compared to effector or effector memory subsets (Berard & Tough, 2002), potentially explaining the suppressed cytokine expression in end-point differentiation, although further research on identifying specific effector and memory subsets via flow cytometry would be required to investigate this in $CD4^+$ T cells.

The X chromosome inactivation process involves significant transcriptional repression and genomic rearrangement. *Xist* recruits repressive complexes to modify the chromatin of the inactive X chromosome, leading to transcriptional repression, chromatin condensation and Xi localisation to the nuclear periphery (Augui et al., 2011; Loda et al., 2022), while *Firre* is involved in anchoring the Xi at the nuclear periphery via interchromosomal contacts (Fang et al., 2020). Consistent with our work, previous literature has shown altered Xi states in naive lymphocytes, with the Xi complex only re-localising to the Xi following cell activation (Syrett et al., 2019; J. Wang et al., 2016). X chromosome inactivation is also intrinsically linked to TCR stimulation and T cell differentiation (Forsyth, Toothacre, et al., 2024), and while the disruption to Xi patch localisation from *Malat1* loss could represent indirect differences in Th cell activation, the effect on Xi patch formation from *Malat1* loss could only occur in females, potentially explaining the causes of the female-specific effects seen throughout *in vitro* and *in vivo* Th cell differentiation.

In terms of the effects of *Malat1* loss, disrupted Xi patch formation from *Malat1* loss would likely affect H3K27me3 deposition on the X chromosome. The inter-chromosomal contacts formed via lncRNA *Firre* would also likely be disrupted from an overall decrease in X inactivation. This disruption could cause a general disruption to overall nuclear architecture and cause global impacts on transcription, although would require further investigation. Disrupted X inactivation or Xi escape has not been directly linked to modified IL10 expression in differentiated Th cells previously, although Xi skew (bias in Xi formation towards one X chromosome) has been linked to decreased IL10 levels (Roberts et al., 2022), providing some link between altered Xi states and the decrease in IL10 expression seen here. While links between Xi patch formation on Th2 differentiation have also not been identified previously, it has also been linked to

increased ISG expression and a skew towards type-I IFN cytokine expression via the escape of X-linked genes, particularly *Kdm6a* and *Tlr7*. While *Kdm6a* is unaffected in our RNA-seqs dataset, *Tlr7* is upregulated resulting from *Malat1* loss at day 2 and lies upstream of IRF7 activation, potentially explaining the increased ISG expression only in females, which could then link to the disrupted end-point Th2 differentiation (Huret et al., 2024; Itoh et al., 2019).

6.3 Nuclear speckle function in T cells

Here, we discovered that speckle numbers, size and activity all drastically increase during Th cell differentiation (Chapter 5. Aim 3. Identify how nuclear speckles change during both mouse and human Th cell differentiation), consistent with previous results identifying changes in speckle numbers during T cell activation (Dow et al., 2010; McCuaig et al., 2015). This increase in number and activity suggests an increase in splicing and mRNA processing, likely due to the increased transcript processing requirements from the Th cell transcriptional burst (Conley et al., 2016). Interestingly, this event occurs parallel to a decrease in *Malat1* levels, suggesting that differing *Malat1* level within speckles could affect their function. *Malat1* in lung fibroblast cells regulates speckle intracellular organisation; splicing factors and proteins such as SON and SRRM2 typically localise to the speckle core, while *Malat1* and other RNAs localise to the speckle periphery (Fei et al., 2017; Shinn et al., 2025). Loss of *Malat1* is thought to cause a more mixed phenotype of protein and RNA content, a decrease in overall SON levels, and a decrease in speckle SR protein localisation to the speckles (Fei et al., 2017). In our work, *Malat1* was shown to be inhibitory for initial Th cell activation via expression of marker CD69, suggesting that low levels of *Malat1* in speckles may be important for cell

activation or differentiation processes, potentially via the release of speckle-localised splicing factors. However, despite the decrease in *Malat1* levels during activation, complete *Malat1* loss in females partially disrupted both speckle formation and function, suggesting that *Malat1* plays a non-redundant role in speckle function when both its levels are limiting and novel speckle biogenesis is occurring (Chapter 5. Aim 4. Investigate whether *Malat1* loss affects nuclear speckle formation and function during early Th2 differentiation).

Consistent with our results, *Malat1* is known to interact with and affect the function of speckle-associated proteins involved in splicing and pre-mRNA processing (Z. Y. Hu et al., 2016; Malakar et al., 2016; Tripathi et al., 2010). This could suggest global disruption to splicing or transcript processing occurring from *Malat1* loss in Th cells, which would explain the transcriptomic blunting effect seen in females. While alternative splicing events were unaffected in our RNA-seq dataset, we did not investigate whether splicing efficiency (un-spliced vs fully spliced transcripts) or transcript processing were affected by *Malat1* loss instead (Sánchez-Escabias et al., 2022). Previous work has suggested that speckles localise in proximity to areas of active transcription, and regulate transcript splicing efficiency (Bhat et al., 2024). As an alternate explanation, disruption to genomic architecture from *Malat1* loss could affect speckle and actively transcribed localisation, again delaying transcript processing. Disruption to speckles has previously been linked to a reduction in chromatin interactions (S. Hu et al., 2019), suggesting potential knock-on effects of speckle disruption on overall genome arrangement, which could also affect repression of the Xi. Analysis of un-spliced transcripts via investigating intron retention in our long-read ONT-seq dataset could be performed to investigate whether splicing is affected by *Malat1* loss, however as splicing occurs co-transcriptionally further experiments such as ChrRNA-seq (Sánchez-Escabias

et al., 2022) or RNA polymerase II ChIP seq may also be required to fully explore this (Titus et al., 2024).

Neither *Malat1* nor nuclear speckles have been shown to interact with the X chromosome inactivation previously, although some speckle component proteins (such as HNRNPU, HNRNPK, SRSF1 and SRSF2) are also core to the Xi complex and can interact with both *Malat1* and *Xist* (Agostini et al., 2012; Z. Lu et al., 2020; Malakar et al., 2016; Navarro-Cobos et al., 2022; Nguyen et al., 2019; Tripathi et al., 2010), providing some links between these processes. Disruption of SR protein phosphorylation from *Malat1* loss could affect their activity and ability to localise to the Xi, causing the reduction in X inactivation seen in our preliminary data. Splicing of *Xist* has also previously been shown to affect its expression and function. Efficient *Xist* intron removal by PTBP1 is required for its expression in embryonic stem cells (Stork et al., 2018), and differences in *Xist* splicing is also linked to a reduced Xi heritability (Matsuura et al., 2021). Previous research identified that *Malat1* can interact with PTBP1 to regulate alternative splicing events (Miao et al., 2022) providing some links between *Malat1* and *Xist*, and consistent with altered *Xist* splicing we observed significant downregulation of *Xist* transcript levels from *Malat1* loss by qRTPCR at day 2 of differentiation. Some *Malat1* and *Xist* RBP interactors have also been shown to play a role in Th cell differentiation (J. W. Chang et al., 2009; Luo et al., 2025), providing potential bridges between disruption to these two nuclear processes and overall Th cell differentiation and cytokine expression.

Alongside speckles, other nuclear condensates such as paraspeckles may also change during Th cell differentiation. Paraspeckle lincRNA *Neat1* is downregulated during Th cell activation (Hewitson et al., 2020), suggesting an effect on paraspeckle formation during T cell differentiation. The processes of nuclear condensate formation, X

inactivation and chromatin remodelling all occur within a similar timeframe of the first few days of Th cell differentiation, suggesting major co-ordination of nuclear re-arrangements during Th cell differentiation, which ultimately controls cell progression through to end-point differentiation and cytokine expression. Coordination of nuclear processes is critical for correct cell differentiation and involves complex regulation and dynamic interplay from a number of different nuclear factors (Cha, 2024). Crosstalk between nuclear condensates (both speckles and paraspeckles) under differing conditions have also previously been shown to be important for chromatin architecture and intra-chromosomal contact formation (Hsu et al., 2025; S. Hu et al., 2019; K. Li & Wang, 2021), cementing the inter-linked nature of these different nuclear processes. As *Malat1* loss has been shown to affect a number of these processes, this may imply that *Malat1* aids in co-ordinating these processes during Th cell differentiation, although further identifying direct RBP interactors with *Malat1* would be required to investigate this further. While the regulation of speckle and paraspeckle biogenesis during Th cell differentiation is not known and requires further investigation, X inactivation and chromatin remodelling are directly regulated by NF-κB signalling from TCR engagement (Forsyth, Toothacre, et al., 2024; L. Zhang et al., 2019), a pathway that *Malat1* has also previously been shown to affect (Juan et al., 2018; Shi et al., 2021; G. Zhao et al., 2016; H. J. Zhou et al., 2018).

6.4 Future work

6.4.1 Investigating *Malat1* interacting RBPs during Th cell differentiation

While we have identified disruptions caused by *Malat1* loss to Xi patch formation, H3K27me3 deposition, and speckle formation in female Th cells, we have not identified direct interactions with RBPs to link *Malat1* to these processes, and also have not identified direct interactions between these pathways. Therefore, future experiments should be involved in investigating the *Malat1* interactome in differentiating or differentiated Th cells, and how it may differ between females and males. Previous techniques involving cross-linking of RNA and RBPs and then purification of resultant complexes, such as RAP-MS (McHugh & Guttman, 2018), HyPR-MS (Spiniello et al., 2018) and CHART-MS (Davis & West, 2015) have been utilised to identify RBP interactomes of lncRNAs previously, including *Malat1*. More targeted techniques such as RIP-seq could also be used to identify whether known *Malat1* binding RBPs (Ye et al., 2020), such as EZH2 or SRSF1, interact with *Malat1* during Th2 differentiation. Further experiments could also be performed on *Xist*, to identify common RBP binding partners with *Malat1* that could explain the differences seen in X inactivation.

Previous results have shown that *Malat1* loss leads to the delocalisation of SR proteins such as SRSF1 from the speckles and the nucleus, and reduced targeting of EZH2 to specific genes (Kanbar et al., 2022; Tripathi et al., 2010; X. Wang et al., 2016). Further immunofluorescence experiments investigating the localisation of some of these factors may identify whether this is dysregulated when *Malat1* is lost, and this could be combined with FISH experiments to identify *Malat1* localisation in *WT* cells. The interaction

between *Malat1* and PRC2 could also be further investigated by ChIP-seq experiments, which could identify genes differentially methylated when *Malat1* is lost (Young et al., 2011).

6.4.2 Further characterising the effects of *Malat1* loss in type 2 immunity and Th cell differentiation

Despite effects *in vivo*, our model of type 2 immunity still displays a number of limitations. These include the fact that *Malat1*$^{-/-}$ could also affect other cell types and not just CD4^{+} T cells, potentially obscuring or enhancing certain effects we identified. A conditional CD4^{+} T cell knock-out of *Malat1* may therefore be beneficial to investigating T cell specific effects *in vivo*, and how this affects overall type 2 responses (Gubin et al., 2014; Shui et al., 2006). Further adding to this, our experimental model of type 2 lung inflammation using *S. mansoni* eggs is not representative of type 2 immunopathologies such as asthma or dermatitis, and effects between type 2 mouse models may differ. Therefore, future experiments could investigate whether *Malat1* affects mouse models such as the HDM allergen model of lung inflammation.

Some further questions remain unanswered about how *Malat1* loss affects Th cell differentiation, specifically whether *Malat1* loss affects Tcm and Tem differentiation, and whether the sex-specific effects can be identified in other Th cell subsets. Further FACS investigation of markers such as IL7Rα, CD44 and CD62L in both *in vitro* and *in vivo* models of Th2 differentiation would allow for identification of naïve, effector, effector memory and central memory cells, and specific Th1, Th17 and Treg differentiation models could be used to identify whether *Malat1* loss disrupts differentiation and cytokine expression in each subset.

6.4.3 Investigating sex-differences in Th cell differentiation

During Th2 differentiation we identified a number of sex differences inherent to *WT* Th cells and as a result of *Malat1* loss, such as a decreased IL2 sensitivity in *WT* males, and the sex specific decrease in cytokine expression resultant from *Malat1* loss. As our *in vitro* studies were performed in a hormone independent manner, we concluded that the impacts on Th cell differentiation are cell intrinsic. However, cytokine levels in our *in vivo* model were more similar between females and males than our *in vitro* model, suggesting some factors may be missing *in vitro* for correct Th cell differentiation. It may prove useful to investigate how hormones modulate Th2 differentiation and whether this affects *Malat1*, potentially *in vitro* via treatment of both male and female cells with sex hormones, or *in vivo* via the use of castrated mice or hormonal replacement.

The sex-specific effects resulting from *Malat1* loss here have also only been observed in mouse Th cells. Mouse and human immune systems are known to differ (Mestas & Hughes, 2004), and lncRNA function has also previously been shown to differ between mouse and humans (C. J. Guo et al., 2020). Furthermore, identifying sex-specific disruption to Th differentiation from *Malat1* loss in human cells would have more direct impacts on human health. As performed in this study, human $CD4^+$ T cells can be isolated from whole blood, however knockout of *MALAT1* in this context is not possible. Pilot studies investigating *MALAT1* knockdown via methods such as antisense oligonucleotides or siRNA treatment (Amodio et al., 2018) during Th cell differentiation would allow for study of how *MALAT1* affects human Th cells. As an alternative option, humanised mouse models such as the Hu-BLT model could also be used to investigate the impact of human *MALAT1* loss on immune cells (Karpel et al., 2015).

6.5 Concluding remarks

To conclude, despite its high expression and strong conservation, the role of *Malat1* in immune cells is not well understood. Here, we identified that *Malat1* regulates Th2 differentiation in a sex-specific manner. *Malat1* loss disrupts cytokine expression and general transcriptomic changes that occur during differentiation in females, via aberrant upregulation of an ISG module during early differentiation, which disrupts IL2R expression and the response to extrinsic levels IL2. When investigating the mechanism of *Malat1* loss we identified disruption to nuclear architecture in females during early time points, identifying that nuclear speckle numbers and activity increase during Th cell differentiation. We Identified similar disruption from *Malat1* loss on X chromosome inactivation and H3K27me3 deposition, identifying novel potential connections between *Malat1*, nuclear speckles, polycomb and Xi formation. Overall, these results show that *Malat1* is a critical sex-specific and cell-intrinsic regulator of Th cell differentiation with roles in co-ordinating differentiation-associated changes in nuclear architecture and X inactivation, and potential relevance in explaining sex-differences in autoimmunity and type 2 immunopathologies.

Acronyms

Acronym	Abbreviation
ACK	ammonium-chloride-potassium
ARG1	arginase 1
ASO	anti-sense oligonucleotide
BCA	bicinchoninic assay
BSA	bovine serum albumin
CCR	C-C chemokine receptor
CD	cluster of differentiation
cDNA	complimentary DNA
CHART	capture hybridisation analysis of RNA targets
ChIP	chromatin immunoprecipitation
CIZ1	Cip1-interacting zinc finger protein
CLIP	crosslinking immunoprecipitation
Ct	cycle threshold
DC	dendritic cells
DEG	differentially expressed gene
DMSO	dimethyl sulphoxide
DNA	deoxyribonucleic acid
DTU	differential transcript usage
EDTA	ethylenediaminetetraacetic acid
FACS	fluorescence activated cell sorting
FBS	foetal bovine serum
FDR	false discover rate
FIRRE	functional intergenic repeating RNA element
FOXP3	forkhead box protein P3
FSC	forward scatter
GATA	GATA binding protein
GSEA	geneset enrichment analysis
HDM	house dust mite
HNRNP	heterogenous nuclear ribonuclear proteins
IFN	interferon

IFNAR	IFNa receptor
Ig	Immunoglobulin
IL	interleukin
IL10R	IL10 receptor
IL2R	interleukin 2 receptor
IL4R	interleukin 4 receptor
ILC	innate lymphoid cells
iNOS	inducible nitric oxide synthase
IP	interperitoneal
ISG	interferon stimulated gene
IV	intravenous
LFC	log2 fold change
lincRNA	long intergenic non-coding RNA
lncRNA	long non-coding RNA
MAF	avian musculoaponeurotic fibrosarcoma oncogene homolog
MALAT1	metastasis associated lung adenocarcinoma transcript 1
mascRNA	*MALAT1*-associated small cytoplasmic RNA
MHC	major histocompatibility complex
MFI	median fluorescence intensity
miRNA	micro-RNA
mRNA	messenger RNA
MS	mass spectrometry
ncRNA	non-coding RNA
NEAT1	nuclear enriched abundant transcript 1
NEAT2	nuclear enriched transcript 2
NET	neutrophil extracellular traps
NFAT	nuclear factor of activated T cells
NK	natural killer
NTC	non-targeting control
nTreg	thymic derived Treg
ONT	Oxford nanopore technology
PBS	phosphate-buffered saline

piRNA	PIWI-interacting RNA
PRC	polycomb repressive complex
PRR	pattern recognition receptor
pTreg	peripheral Treg
qRTPCR	quantitative real-time polymerase chain reaction
RAP	RNA-antisense purification
RBP	RNA-binding protein
RELMα	resistin-like molecule alpha
RIN	RNA integrity number
RIP	RNA immunoprecipitation
RNA	ribonucleic acid
RNA-seq	RNA sequencing
RPMI	roswell park memorial institute
SDS-PAGE	sodium dodecyl sulfate polyacrylamide gel electrophoresis
SLE	systemic lupus erythematosus
Sm	*S. mansoni*
SNP	single nucleotide polymorphism
snRNA	small nuclear RNA
SR	serine/arginine
SRRM2	serine/arginine repetitive matrix protein 2
SRSF	serine and arginine-rich splicing factor
SSC	side scatter
STAT	signal transducer and actovator of transcription
TBET	T-box transcription factor
Tcm	T central memory
TCR	T cell receptor
Tem	T effector memory
Tfh	T follicular helper
TGF	transforming growth factor
Th	T helper
TNF	tumour necrosis factor
Tr1	T regulatory 1

Treg	Regulatory T cell
WT	wild-type
Xa	active X chromosome
Xi	inactive X chromosome
XIST	X-inactive specific transcript
TLR	toll-like receptor

References

Agostini, F., Cirillo, D., Bolognesi, B., & Tartaglia, G. G. (2012). X-inactivation: quantitative predictions of protein interactions in the Xist network. *Nucleic Acids Research*, *41*(1), e31. https://doi.org/10.1093/NAR/GKS968

Ahmad, I., Naqvi, R. A., Valverde, A., & Naqvi, A. R. (2023). LncRNA MALAT1/microRNA-30b axis regulates macrophage polarization and function. *Frontiers in Immunology*, *14*, 1214810. https://doi.org/10.3389/FIMMU.2023.1214810/BIBTEX

Akdis, C. A., & Akdis, M. (2014). Mechanisms of immune tolerance to allergens: role of IL-10 and Tregs. *The Journal of Clinical Investigation*, *124*(11), 4678. https://doi.org/10.1172/JCI78891

Akdis, C. A., Arkwright, P. D., Brüggen, M. C., Busse, W., Gadina, M., Guttman-Yassky, E., Kabashima, K., Mitamura, Y., Vian, L., Wu, J., & Palomares, O. (2020). Type 2 immunity in the skin and lungs. *Allergy: European Journal of Allergy and Clinical Immunology*, *75*(7), 1582–1605. https://doi.org/10.1111/ALL.14318;SUBPAGE:STRING:FULL

Akdis, C. A., & Blaser, K. (2001). Mechanisms of interleukin-10-mediated immune suppression. *Immunology*, *103*(2), 131. https://doi.org/10.1046/J.1365-2567.2001.01235.X

Amodio, N., Raimondi, L., Juli, G., Stamato, M. A., Caracciolo, D., Tagliaferri, P., & Tassone, P. (2018). MALAT1: A druggable long non-coding RNA for targeted anti-cancer approaches. *Journal of Hematology and Oncology*, *11*(1), 1–19. https://doi.org/10.1186/S13045-018-0606-4/TABLES/2

Anders, S., Reyes, A., & Huber, W. (2012). Detecting differential usage of exons from RNA-seq data. *Genome Research*, *22*(10), 2008. https://doi.org/10.1101/GR.133744.111

Annunziato, F., Romagnani, C., & Romagnani, S. (2015). The 3 major types of innate and adaptive cell-mediated effector immunity. *Journal of Allergy and Clinical Immunology*, *135*(3), 626–635. https://doi.org/10.1016/J.JACI.2014.11.001/ASSET/016F9877-77C0-4842-AFF8-7535194A53B5/MAIN.ASSETS/GR4.JPG

Arab, K., Karaulanov, E., Musheev, M., Trnka, P., Schäfer, A., Grummt, I., & Niehrs, C. (2019). GADD45A binds R-loops and recruits TET1 to CpG island promoters. *Nature Genetics 2019 51:2*, *51*(2), 217–223. https://doi.org/10.1038/s41588-018-0306-6

Arratia, F., Fierro, C., Blanco, A., Fuentes, S., Nahuelquen, D., Montecino, M., Rojas, A., & Aguilar, R. (2023). Selective Concurrence of the Long Non-Coding RNA MALAT1 and the Polycomb Repressive Complex 2 to Promoter Regions of Active Genes in MCF7 Breast Cancer Cells. *Current Issues in Molecular Biology*, *45*(6), 4735–4748. https://doi.org/10.3390/CIMB45060301/S1

Arun, G., Aggarwal, D., & Spector, D. L. (2020). MALAT1 Long Non-Coding RNA: Functional Implications. *Non-Coding RNA*, *6*(2). https://doi.org/10.3390/NCRNA6020022

Arun, G., Diermeier, S., Akerman, M., Chang, K. C., Wilkinson, J. E., Hearn, S., Kim, Y., MacLeod, A. R., Krainer, A. R., Norton, L., Brogi, E., Egeblad, M., & Spector, D. L. (2016). Differentiation of mammary tumors and reduction in metastasis upon

Malat1 lncRNA loss. *Genes & Development*, *30*(1), 34. https://doi.org/10.1101/GAD.270959.115

Aslan, G. S., Jaé, N., Manavski, Y., Fouani, Y., Shumliakivska, M., Kettenhausen, L., Kirchhof, L., Günther, S., Fischer, A., Luxán, G., & Dimmeler, S. (2023). Malat1 deficiency prevents neonatal heart regeneration by inducing cardiomyocyte binucleation. *JCI Insight*, *8*(5). https://doi.org/10.1172/JCI.INSIGHT.162124

Aslanzadeh, M., Stanicek, L., Tarbier, M., Mármol-Sánchez, E., Biryukova, I., & Friedländer, M. R. (2024). Malat1 affects transcription and splicing through distinct pathways in mouse embryonic stem cells. *NAR Genomics and Bioinformatics*, *6*(2), 45. https://doi.org/10.1093/NARGAB/LQAE045

Aubol, B. E., Keshwani, M. M., Fattet, L., & Adams, J. A. (2018). Mobilization of A Splicing Factor Through A Nuclear Kinase-Kinase Complex. *The Biochemical Journal*, *475*(3), 677. https://doi.org/10.1042/BCJ20170672

Augui, S., Nora, E. P., & Heard, E. (2011). Regulation of X-chromosome inactivation by the X-inactivation centre. *Nature Reviews Genetics 2011 12:6*, *12*(6), 429–442. https://doi.org/10.1038/nrg2987

Ayabina, D. V., Clark, J., Bayley, H., Lamberton, P. H. L., Toor, J., & Hollingsworth, T. D. (2021). Gender-related differences in prevalence, intensity and associated risk factors of Schistosoma infections in Africa: A systematic review and meta-analysis. *PLoS Neglected Tropical Diseases*, *15*(11), e0009083. https://doi.org/10.1371/JOURNAL.PNTD.0009083

Baban, B., Chandler, P. R., Sharma, M. D., Pihkala, J., Koni, P. A., Munn, D. H., & Mellor, A. L. (2009). IDO activates regulatory T cells and blocks their conversion

into TH17-like T cells. *Journal of Immunology (Baltimore, Md. : 1950)*, *183*(4), 2475. https://doi.org/10.4049/JIMMUNOL.0900986

Banerjee, S., Galarza-Muñoz, G., & Garcia-Blanco, M. A. (2023). Role of RNA Alternative Splicing in T Cell Function and Disease. *Genes*, *14*(10), 1896. https://doi.org/10.3390/GENES14101896/S1

Bauer, M., Vidal, E., Zorita, E., Üresin, N., Pinter, S. F., Filion, G. J., & Payer, B. (2021). Chromosome compartments on the inactive X guide TAD formation independently of transcription during X-reactivation. *Nature Communications 2021 12:1*, *12*(1), 1–21. https://doi.org/10.1038/s41467-021-23610-1

Belot, M. P., Castell, A. L., Le Fur, S., & Bougnères, P. (2018). Dynamic demethylation of the IL2RA promoter during in vitro CD4+ T cell activation in association with IL2RA expression. *Epigenetics*, *13*(5), 459. https://doi.org/10.1080/15592294.2018.1469893

Berard, M., & Tough, D. F. (2002). Qualitative differences between naïve and memory T cells. *Immunology*, *106*(2), 127. https://doi.org/10.1046/J.1365-2567.2002.01447.X

Berletch, J. B., Yang, F., Xu, J., Carrel, L., & Disteche, C. M. (2011). Genes that escape from X inactivation. *Human Genetics*, *130*(2), 237. https://doi.org/10.1007/S00439-011-1011-Z

Bernstein, J. A., Bernstein, J. S., Makol, R., Ward, S., A Bernstein, O. J., Bernstein, J. S., & Author, C. (2024). Allergic Rhinitis: A Review. *JAMA*, *331*(10), 866–877. https://doi.org/10.1001/JAMA.2024.0530

Berthois, Y., Katzenellenbogen, J. A., & Katzenellenbogen, B. S. (1986). Phenol red in tissue culture media is a weak estrogen: implications concerning the study of estrogen-responsive cells in culture. *Proceedings of the National Academy of Sciences of the United States of America*, *83*(8), 2496. https://doi.org/10.1073/PNAS.83.8.2496

Bhat, P., Chow, A., Emert, B., Ettlin, O., Quinodoz, S. A., Strehle, M., Takei, Y., Burr, A., Goronzy, I. N., Chen, A. W., Huang, W., Ferrer, J. L. M., Soehalim, E., Goh, S. T., Chari, T., Sullivan, D. K., Blanco, M. R., & Guttman, M. (2024). Genome organization around nuclear speckles drives mRNA splicing efficiency. *Nature 2024 629:8014*, *629*(8014), 1165–1173. https://doi.org/10.1038/s41586-024-07429-6

Bousard, A., Raposo, A. C., Żylicz, J. J., Picard, C., Pires, V. B., Qi, Y., Gil, C., Syx, L., Chang, H. Y., Heard, E., & da Rocha, S. T. (2019). The role of Xist -mediated Polycomb recruitment in the initiation of X-chromosome inactivation . *EMBO Reports*, *20*(10). https://doi.org/10.15252/EMBR.201948019,

Bousquet, J., Anto, J. M., Bachert, C., Baiardini, I., Bosnic-Anticevich, S., Walter Canonica, G., Melén, E., Palomares, O., Scadding, G. K., Togias, A., & Toppila-Salmi, S. (2020). Allergic rhinitis. *Nature Reviews Disease Primers*, *6*(1), 1–17. https://doi.org/10.1038/S41572-020-00227-0;SUBJMETA=1785,1807,1809,31,692,699;KWRD=ASTHMA,RESPIRATORY+SIGNS+AND+SYMPTOMS

Boyman, O., Cho, J. H., & Sprent, J. (2010). The Role of Interleukin-2 in Memory CD8 Cell Differentiation. *Advances in Experimental Medicine and Biology*, *684*, 28–41. https://doi.org/10.1007/978-1-4419-6451-9_3

Brajic, A., Franckaert, D., Burton, O., Bornschein, S., Calvanese, A. L., Demeyer, S., Cools, J., Dooley, J., Schlenner, S., & Liston, A. (2018). The long non-coding RNA Flatr anticipates Foxp3 expression in regulatory T cells. *Frontiers in Immunology*, *9*(SEP), 1989. https://doi.org/10.3389/FIMMU.2018.01989/FULL

Brooks-Asplund, E. M., Tupper, C. E., Daun, J. M., Kenney, W. L., & Cannon, J. G. (2002). HORMONAL MODULATION OF INTERLEUKIN-6, TUMOR NECROSIS FACTOR AND ASSOCIATED RECEPTOR SECRETION IN POSTMENOPAUSAL WOMEN. *Cytokine*, *19*(4), 193–200. https://doi.org/10.1006/CYTO.2002.1963

Brown, J. M., Green, J., Neves, R. P. Das, Wallace, H. A. C., Smith, A. J. H., Hughes, J., Gray, N., Taylor, S., Wood, W. G., Higgs, D. R., Iborra, F. J., & Buckle, V. J. (2008). Association between active genes occurs at nuclear speckles and is modulated by chromatin environment. *The Journal of Cell Biology*, *182*(6), 1083. https://doi.org/10.1083/JCB.200803174

Bunders, M. J., & Altfeld, M. (2020). Implications of Sex Differences in Immunity for SARS-CoV-2 Pathogenesis and Design of Therapeutic Interventions. *Immunity*, *53*(3), 487–495. https://doi.org/10.1016/j.immuni.2020.08.003

Bupp, M. R. G., & Jorgensen, T. N. (2018). Androgen-Induced Immunosuppression. *Frontiers in Immunology*, *9*(APR), 794. https://doi.org/10.3389/FIMMU.2018.00794

Cardamone, G., Paraboschi, E. M., Soldà, G., Cantoni, C., Supino, D., Piccio, L., Duga, S., & Asselta, R. (2019). Not only cancer: the long non-coding RNA MALAT1 affects the repertoire of alternatively spliced transcripts and circular RNAs in

multiple sclerosis. *Human Molecular Genetics*, *28*(9), 1414–1428. https://doi.org/10.1093/HMG/DDY438

Carlini, V., Noonan, D. M., Abdalalem, E., Goletti, D., Sansone, C., Calabrone, L., & Albini, A. (2023). The multifaceted nature of IL-10: regulation, role in immunological homeostasis and its relevance to cancer, COVID-19 and post-COVID conditions. *Frontiers in Immunology*, *14*, 1161067. https://doi.org/10.3389/FIMMU.2023.1161067/FULL

Casado-Bedmar, M., Roy, M., & Viennois, E. (2023). The Effect of Sex-Specific Differences on IL-10−/− Mouse Colitis Phenotype and Microbiota. *International Journal of Molecular Sciences*, *24*(12), 10364. https://doi.org/10.3390/IJMS241210364

Castaldi, P. J., Abood, A., Farber, C. R., & Sheynkman, G. M. (2022). Bridging the splicing gap in human genetics with long-read RNA sequencing: finding the protein isoform drivers of disease. *Human Molecular Genetics*, *31*(R1), R123–R136. https://doi.org/10.1093/HMG/DDAC196

Cephus, J. Y., Stier, M. T., Fuseini, H., Yung, J. A., Toki, S., Bloodworth, M. H., Zhou, W., Goleniewska, K., Zhang, J., Garon, S. L., Hamilton, R. G., Poloshukin, V. V., Boyd, K. L., Peebles, R. S., & Newcomb, D. C. (2017). Testosterone attenuates group 2 innate lymphoid cell-mediated airway inflammation. *Cell Reports*, *21*(9), 2487. https://doi.org/10.1016/J.CELREP.2017.10.110

Cha, H. J. (2024). Nuclear structures and their emerging roles in cell differentiation and development. *BMB Reports*, *57*(9), 381. https://doi.org/10.5483/BMBREP.2024-0101

Chakraborty, B., Byemerwa, J., Krebs, T., Lim, F., Chang, C. Y., & McDonnell, D. P. (2023). Estrogen Receptor Signaling in the Immune System. *Endocrine Reviews*, *44*(1), 117–141. https://doi.org/10.1210/ENDREV/BNAC017

Chakravarty, D., Sboner, A., Nair, S. S., Giannopoulou, E., Li, R., Hennig, S., Mosquera, J. M., Pauwels, J., Park, K., Kossai, M., Macdonald, T. Y., Fontugne, J., Erho, N., Vergara, I. A., Ghadessi, M., Davicioni, E., Jenkins, R. B., Palanisamy, N., Chen, Z., … Rubin, M. A. (2014). The oestrogen receptor alpha-regulated lncRNA NEAT1 is a critical modulator of prostate cancer. *Nature Communications*, *5*, 5383. https://doi.org/10.1038/NCOMMS6383

Chan, W. F., Coughlan, H. D., Iannarella, N., Smyth, G. K., Johanson, T. M., Keenan, C. R., & Allan, R. S. (2021). Identification and characterization of the long noncoding RNA Dreg1 as a novel regulator of Gata3. *Immunology and Cell Biology*, *99*(3), 323–332. https://doi.org/10.1111/IMCB.12408;JOURNAL:JOURNAL:14401711A;WGROUP:STRING:PUBLICATION

Chang, J. J., Woods, M., Lindsay, R. J., Doyle, E. H., Griesbeck, M., Chan, E. S., Robbins, G. K., Bosch, R. J., & Altfeld, M. (2013). Higher Expression of Several Interferon-Stimulated Genes in HIV-1-Infected Females After Adjusting for the Level of Viral Replication. *The Journal of Infectious Diseases*, *208*(5), 830. https://doi.org/10.1093/INFDIS/JIT262

Chang, J. W., Koike, T., & Iwashima, M. (2009). hnRNP-K is a nuclear target of TCR-activated ERK and required for T-cell late activation. *International Immunology*, *21*(12), 1351. https://doi.org/10.1093/INTIMM/DXP106

Chaplin, D. D. (2010). Overview of the Immune Response. *The Journal of Allergy and Clinical Immunology*, *125*(2 Suppl 2), S3. https://doi.org/10.1016/J.JACI.2009.12.980

Chatterjee, S., Bhattcharjee, D., Misra, S., Saha, A., Bhattacharyya, N. P., & Ghosh, A. (2020). Increase in MEG3, MALAT1, NEAT1 Significantly Predicts the Clinical Parameters in Patients With Rheumatoid Arthritis. *Personalized Medicine*, *17*(6), 445–457. https://doi.org/10.2217/PME-2020-0009

Chen, J., Guan, L., Tang, L., Liu, S., Zhou, Y., Chen, C., He, Z., & Xu, L. (2019). T Helper 9 Cells: A New Player in Immune-Related Diseases. *DNA and Cell Biology*, *38*(10), 1040. https://doi.org/10.1089/DNA.2019.4729

Chen, L. L., & Kim, V. N. (2024). Small and long non-coding RNAs: Past, present, and future. *Cell*, *187*(23), 6451–6485. https://doi.org/10.1016/J.CELL.2024.10.024

Chen, S., Wang, J., Zhang, K., Ma, B., Li, X., Wei, R., & Nian, H. (2023). LncRNA Neat1 targets NonO and miR-128-3p to promote antigen-specific Th17 cell responses and autoimmune inflammation. *Cell Death & Disease 2023 14:9*, *14*(9), 1–11. https://doi.org/10.1038/s41419-023-06132-0

Chen, Y., Davidson, N. M., Wan, Y. K., Yao, F., Su, Y., Gamaarachchi, H., Sim, A., Patel, H., Low, H. M., Hendra, C., Wratten, L., Hakkaart, C., Sawyer, C., Iakovleva, V., Lee, P. L., Xin, L., Ng, H. E. V., Loo, J. M., Ong, X., … Göke, J. (2025). A systematic benchmark of Nanopore long-read RNA sequencing for transcript-level analysis in human cell lines. *Nature Methods*, *22*(4), 801–812. https://doi.org/10.1038/S41592-025-02623-4;SUBJMETA=114,337,631;KWRD=COMPUTATIONAL+BIOLOGY+AND+BIOINFORMATICS,MOLECULAR+BIOLOGY

Chowdhury, N. U., Guntur, V. P., Newcomb, D. C., & Wechsler, M. E. (2021). Sex and gender in asthma. *European Respiratory Review*, *30*(162), 210067. https://doi.org/10.1183/16000617.0067-2021

Christou, E. A. A., Banos, A., Kosmara, D., Bertsias, G. K., & Boumpas, D. T. (2018). Sexual dimorphism in SLE: above and beyond sex hormones. *Lupus*, *28*(1), 3. https://doi.org/10.1177/0961203318815768

Cibrián, D., & Sánchez-Madrid, F. (2017). CD69: from activation marker to metabolic gatekeeper. *European Journal of Immunology*, *47*(6), 946–953. https://doi.org/10.1002/EJI.201646837

Collier, S. P., Henderson, M. A., Tossberg, J. T., & Aune, T. M. (2014). Regulation of the Th1 Genomic Locus from Ifng through Tmevpg1 by T-bet. *The Journal of Immunology*, *193*(8), 3959–3965. https://doi.org/10.4049/JIMMUNOL.1401099

Conley, J. M., Gallagher, M. P., & Berg, L. J. (2016). T cells and gene regulation: The switching on and turning up of genes after T cell receptor stimulation in CD8 T cells. *Frontiers in Immunology*, *7*(FEB), 182769. https://doi.org/10.3389/FIMMU.2016.00076/BIBTEX

Conrad, N., Misra, S., Verbakel, J. Y., Verbeke, G., Molenberghs, G., Taylor, P. N., Mason, J., Sattar, N., McMurray, J. J. V., McInnes, I. B., Khunti, K., & Cambridge, G. (2023). Incidence, prevalence, and co-occurrence of autoimmune disorders over time and by age, sex, and socioeconomic status: a population-based cohort study of 22 million individuals in the UK. *The Lancet*, *401*(10391), 1878–1890. https://doi.org/10.1016/S0140-6736(23)00457-9

Cote-Sierra, J., Foucras, G., Guo, L., Chiodetti, L., Young, H. A., Hu-Li, J., Zhu, J., & Paul, W. E. (2004). Interleukin 2 plays a central role in Th2 differentiation.

Proceedings of the National Academy of Sciences of the United States of America, *101*(11), 3880. https://doi.org/10.1073/PNAS.0400339101

Couper, K. N., Blount, D. G., & Riley, E. M. (2008). IL-10: The Master Regulator of Immunity to Infection. *The Journal of Immunology*, *180*(9), 5771–5777. https://doi.org/10.4049/JIMMUNOL.180.9.5771

Crotty, S. (2019). T follicular helper cell biology: A decade of discovery and diseases. *Immunity*, *50*(5), 1132. https://doi.org/10.1016/J.IMMUNI.2019.04.011

Cuddapah, S., Barski, A., & Zhao, K. (2010). Epigenomics of T cell activation, differentiation and memory. *Current Opinion in Immunology*, *22*(3), 341. https://doi.org/10.1016/J.COI.2010.02.007

Cui, H., Banerjee, S., Guo, S., Xie, N., Ge, J., Jiang, D., Zörnig, M., Thannickal, V. J., & Liu, G. (2019). Long noncoding RNA Malat1 regulates differential activation of macrophages and response to lung injury. *JCI Insight*, *4*(4). https://doi.org/10.1172/JCI.INSIGHT.124522

Cui, L., Shao, X., Sun, W., Zheng, F., Dong, J., Li, J., Wang, H., & Li, J. (2022). Anti-inflammatory effects of progesterone through NF-κB and MAPK pathway in lipopolysaccharide- or Escherichia coli-stimulated bovine endometrial stromal cells. *PLoS ONE*, *17*(4), e0266144. https://doi.org/10.1371/JOURNAL.PONE.0266144

Da Rocha, S. T., & Heard, E. (2017). Novel players in X inactivation: Insights into Xist-mediated gene silencing and chromosome conformation. *Nature Structural and Molecular Biology*, *24*(3), 197–204. https://doi.org/10.1038/NSMB.3370;SUBJMETA

Davis, C. P., & West, J. A. (2015). Purification of specific chromatin regions using oligonucleotides: capture hybridization analysis of RNA targets (CHART). *Methods in Molecular Biology (Clifton, N.J.)*, *1262*, 167–182. https://doi.org/10.1007/978-1-4939-2253-6_10

De Kleer, I., Willems, F., Lambrecht, B., & Goriely, S. (2014). Ontogeny of myeloid cells. *Frontiers in Immunology*, *5*(AUG), 110421. https://doi.org/10.3389/FIMMU.2014.00423/XML

De Vries, J. E. (1998). The role of IL-13 and its receptor in allergy and inflammatory responses. *Journal of Allergy and Clinical Immunology*, *102*(2), 165–169. https://doi.org/10.1016/S0091-6749(98)70080-6

Deaton, A. M., Cook, P. C., De Sousa, D., Phythian-Adams, A. T., Bird, A., & Macdonald, A. S. (2014). A unique DNA methylation signature defines a population of IFN-γ/IL-4 double-positive T cells during helminth infection. *European Journal of Immunology*, *44*(6), 1835. https://doi.org/10.1002/EJI.201344098

Deep, D., Gudjonson, H., Brown, C. C., Rose, S. A., Sharma, R., Paucar Iza, Y. A., Hong, S., Hemmers, S., Schizas, M., Wang, Z. M., Chen, Y., Wesemann, D. R., Pascual, V., Pe'er, D., & Rudensky, A. Y. (2024). Precursor central memory versus effector cell fate and naïve CD4+ T cell heterogeneity. *Journal of Experimental Medicine*, *221*(10). https://doi.org/10.1084/JEM.20231193/276993

Dey, S., Ashwin, H., Milross, L., Hunter, B., Majo, J., Filby, A. J., Fisher, A. J., Kaye, P. M., & Lagos, D. (2023). Downregulation of MALAT1 is a hallmark of tissue and peripheral proliferative T cells in COVID-19. *Clinical and Experimental Immunology*, *212*(3), 262. https://doi.org/10.1093/CEI/UXAD034

Diamond, M. S., & Farzan, M. (2013). The broad-spectrum antiviral functions of IFIT and IFITM proteins. *Nature Reviews Immunology*, *13*(1), 46–57. https://doi.org/10.1038/NRI3344;SUBJMETA=247,254,256,262;KWRD=INFECTION,INFLAMMATION,INNATE+IMMUNITY

Diederichs, S. (2014). The four dimensions of noncoding RNA conservation. *Trends in Genetics*, *30*(4), 121–123. https://doi.org/10.1016/j.tig.2014.01.004

Djebali, S., Davis, C. A., Merkel, A., Dobin, A., Lassmann, T., Mortazavi, A., Tanzer, A., Lagarde, J., Lin, W., Schlesinger, F., Xue, C., Marinov, G. K., Khatun, J., Williams, B. A., Zaleski, C., Rozowsky, J., Röder, M., Kokocinski, F., Abdelhamid, R. F., … Gingeras, T. R. (2012). Landscape of transcription in human cells. *Nature*, *488*. https://doi.org/10.1038/nature11233

Dondi, E., Rogge, L., Lutfalla, G., Uzé, G., & Pellegrini, S. (2003). Down-Modulation of Responses to Type I IFN Upon T Cell Activation. *The Journal of Immunology*, *170*(2), 749–756. https://doi.org/10.4049/JIMMUNOL.170.2.749,

Dooms, H., Wolslegel, K., Lin, P., & Abbas, A. K. (2007). Interleukin-2 enhances CD4+ T cell memory by promoting the generation of IL-7Rα–expressing cells. *The Journal of Experimental Medicine*, *204*(3), 547. https://doi.org/10.1084/JEM.20062381

Dou, D. R., Zhao, Y., Belk, J. A., Zhao, Y., Casey, K. M., Chen, D. C., Li, R., Yu, B., Srinivasan, S., Abe, B. T., Kraft, K., Hellström, C., Sjöberg, R., Chang, S., Feng, A., Goldman, D. W., Shah, A. A., Petri, M., Chung, L. S., … Chang, H. Y. (2024). Xist ribonucleoproteins promote female sex-biased autoimmunity. *Cell*, *187*(3), 733-749.e16. https://doi.org/10.1016/J.CELL.2023.12.037

Dow, E. C., Liu, H., & Rice, A. P. (2010). T-Loop Phosphorylated Cdk9 Localizes to Nuclear Speckle Domains Which May Serve as Sites of Active P-TEFb Function and Exchange Between the Brd4 and 7SK/HEXIM1 Regulatory Complexes. *Journal of Cellular Physiology*, *224*(1), 84. https://doi.org/10.1002/JCP.22096

du Sert, N. P., Ahluwalia, A., Alam, S., Avey, M. T., Baker, M., Browne, W. J., Clark, A., Cuthill, I. C., Dirnagl, U., Emerson, M., Garner, P., Holgate, S. T., Howells, D. W., Hurst, V., Karp, N. A., Lazic, S. E., Lidster, K., MacCallum, C. J., Macleod, M., … Würbel, H. (2020). Reporting animal research: Explanation and elaboration for the ARRIVE guidelines 2.0. *PLOS Biology*, *18*(7), e3000411. https://doi.org/10.1371/JOURNAL.PBIO.3000411

Dunn, S. E., Perry, W. A., & Klein, S. L. (2024). Mechanisms and consequences of sex differences in immune responses. *Nature Reviews Nephrology*, *20*(1), 37–55. https://doi.org/10.1038/S41581-023-00787-W

Edwards, C. L., Ng, S. S., de Labastida Rivera, F., Corvino, D., Engel, J. A., de Oca, M. M., Bukali, L., Frame, T. C. M., Bunn, P. T., Chauhan, S. B., Singh, S. S., Wang, Y., Na, J., Amante, F. H., Loughland, J. R., Soon, M. S. F., Waddell, N., Mukhopadhay, P., Koufariotis, L. T., … Engwerda, C. R. (2023). IL-10-producing Th1 cells possess a distinct molecular signature in malaria. *The Journal of Clinical Investigation*, *133*(1), e153733. https://doi.org/10.1172/JCI153733

Eeckhoute, J., Keeton, E. K., Lupien, M., Krum, S. A., Carroll, J. S., & Brown, M. (2007). Positive Cross-Regulatory Loop Ties GATA-3 to Estrogen Receptor α Expression in Breast Cancer. *Cancer Research*, *67*(13), 6477–6483. https://doi.org/10.1158/0008-5472.CAN-07-0746

Eisener-Dorman, A. F., Lawrence, D. A., & Bolivar, V. J. (2008). Cautionary Insights on Knockout Mouse Studies: The Gene or Not the Gene? *Brain, Behavior, and Immunity*, *23*(3), 318. https://doi.org/10.1016/J.BBI.2008.09.001

Eißmann, M., Gutschner, T., Hämmerle, M., Günther, S., Caudron-Herger, M., Groß, M., Schirmacher, P., Rippe, K., Braun, T., Zörnig, M., & Diederichs, S. (2012). Loss of the abundant nuclear non-coding RNA MALAT1 is compatible with life and development. *RNA Biology*, *9*(8), 1076. https://doi.org/10.4161/RNA.21089

El-Badry, E., Chen, L., Ghneim, K., Li, Z., Brooks, K., Rhodes, J., Sekaly, R., Kilembe, W., Allen, S., Wu, H., & Hunter, E. (2024). Heightened expression of type I interferon signaling genes in CD4+ T cells from acutely HIV-1–infected women is associated with lower viral loads. *Frontiers in Immunology*, *15*, 1507530. https://doi.org/10.3389/FIMMU.2024.1507530/BIBTEX

Eldash, S., Sanad, E. F., Nada, D., & Hamdy, N. M. (2023). The Intergenic Type LncRNA (LINC RNA) Faces in Cancer with In Silico Scope and a Directed Lens to LINC00511: A Step toward ncRNA Precision. *Non-Coding RNA*, *9*(5), 58. https://doi.org/10.3390/NCRNA9050058

Eloi-Santos, S., Olsen, N. J., Correa-Oliveira, R., & Colley, D. G. (1992). Schistosoma mansoni: Mortality, pathophysiology, and susceptibility differences in male and female mice. *Experimental Parasitology*, *75*(2), 168–175. https://doi.org/10.1016/0014-4894(92)90176-B

Engreitz, J. M., Sirokman, K., McDonel, P., Shishkin, A. A., Surka, C., Russell, P., Grossman, S. R., Chow, A. Y., Guttman, M., & Lander, E. S. (2014). RNA-RNA Interactions Enable Specific Targeting of Noncoding RNAs to Nascent Pre-

mRNAs and Chromatin Sites. *Cell*, *159*(1), 188. https://doi.org/10.1016/J.CELL.2014.08.018

Even, Z., Meli, A. P., Tyagi, A., Vidyarthi, A., Briggs, N., de Kouchkovsky, D. A., Kong, Y., Wang, Y., Waizman, D. A., Rice, T. A., De Kumar, B., Wang, X., Palm, N. W., Craft, J., Basu, M. K., Ghosh, S., & Rothlin, C. V. (2024). The amalgam of naive CD4+ T cell transcriptional states is reconfigured by helminth infection to dampen the amplitude of the immune response. *Immunity*, *57*(8), 1893-1907.e6. https://doi.org/10.1016/J.IMMUNI.2024.07.006/ASSET/8EF94CD2-77D7-4539-B31D-3E6F0BF3A7AD/MAIN.ASSETS/GR6.JPG

Ezkurdia, I., Juan, D., Rodriguez, J. M., Frankish, A., Diekhans, M., Harrow, J., Vazquez, J., Valencia, A., & Tress, M. L. (2014). Multiple evidence strands suggest that there may be as few as 19 000 human protein-coding genes. *Human Molecular Genetics*, *23*(22), 5866–5878. https://doi.org/10.1093/HMG/DDU309

Fang, H., Bonora, G., Lewandowski, J. P., Thakur, J., Filippova, G. N., Henikoff, S., Shendure, J., Duan, Z., Rinn, J. L., Deng, X., Noble, W. S., & Disteche, C. M. (2020). Trans- and cis-acting effects of Firre on epigenetic features of the inactive X chromosome. *Nature Communications*, *11*(1), 6053. https://doi.org/10.1038/S41467-020-19879-3

Fei, J., Jadaliha, M., Harmon, T. S., Li, I. T. S., Hua, B., Hao, Q., Holehouse, A. S., Reyer, M., Sun, Q., Freier, S. M., Pappu, R. V, Prasanth, K. V, & Ha, T. (2017). *Quantitative analysis of multilayer organization of proteins and RNA in nuclear speckles at super resolution*. https://doi.org/10.1242/jcs.206854

Femoe, U. M., Jatsa, H. B., Greigert, V., Brunet, J., Cannet, C., Kenfack, M. C., Feussom, N. G., Fassi, J. B. K., Nkondo, E. T., Abou-Bacar, A., Pfaff, A. W., Dimo,

T., Kamtchouing, P., & Tchuenté, L. A. T. (2022). Pathological and immunological evaluation of different regimens of praziquantel treatment in a mouse model of Schistosoma mansoni infection. *PLOS Neglected Tropical Diseases*, *16*(4), e0010382. https://doi.org/10.1371/JOURNAL.PNTD.0010382

Fike, A. J., Bricker, K. N., Gonzalez, M. V., Maharjan, A., Bui, T., Nuon, K., Emrich, S. M., Weber, J. L., Luckenbill, S. A., Choi, N. M., Sauteraud, R., Liu, D. J., Olsen, N. J., Caricchio, R., Trebak, M., Chodisetti, S. B., & Rahman, Z. S. M. (2025). IRF7 controls spontaneous autoimmune germinal center and plasma cell checkpoints. *The Journal of Experimental Medicine*, *222*(7). https://doi.org/10.1084/JEM.20231882/277976

Finn, C. M., Dhume, K., Prokop, E., Strutt, T. M., & McKinstry, K. K. (2023). STAT1 controls the functionality of influenza-primed CD4 T cells but therapeutic STAT4 engagement maximizes their antiviral impact. *Journal of Immunology (Baltimore, Md. : 1950)*, *210*(9), 1292. https://doi.org/10.4049/JIMMUNOL.2200407

Fischer, K. E., & Riddle, N. C. (2017). Sex Differences in Aging: Genomic Instability. *The Journals of Gerontology Series A: Biological Sciences and Medical Sciences*, *73*(2), 166. https://doi.org/10.1093/GERONA/GLX105

Fischinger, S., Boudreau, C. M., Butler, A. L., Streeck, H., & Alter, G. (2018). Sex differences in vaccine-induced humoral immunity. *Seminars in Immunopathology*, *41*(2), 239. https://doi.org/10.1007/S00281-018-0726-5

Flores Villanueva, P. O., Chikunguwo, S. M., Harris, T. S., & Stadecker, M. J. (1993). Role of IL-10 on antigen-presenting cell function for schistosomal egg-specific monoclonal T helper cell responses in vitro and in vivo. *The Journal of Immunology*, *151*(6), 3192–3198. https://doi.org/10.4049/JIMMUNOL.151.6.3192

Forsyth, K. S., Jiwrajka, N., Lovell, C. D., Toothacre, N. E., & Anguera, M. C. (2024). The conneXion between sex and immune responses. *Nature Reviews Immunology*, *24*(7), 487–502. https://doi.org/10.1038/S41577-024-00996-9

Forsyth, K. S., Toothacre, N. E., Jiwrajka, N., Driscoll, A. M., Shallberg, L. A., Cunningham-Rundles, C., Barmettler, S., Farmer, J., Verbsky, J., Routes, J., Beiting, D. P., Romberg, N., May, M. J., & Anguera, M. C. (2024). Maintenance of X chromosome inactivation after T cell activation requires NF-κB signaling. *Science Immunology*, *9*(100), 398. https://doi.org/10.1126/SCIIMMUNOL.ADO0398/SUPPL_FILE/SCIIMMUNOL.ADO0398_MDAR_REPRODUCIBILITY_CHECKLIST.PDF

Fuente, H. de la, Cruz-Adalia, A., Hoyo, G. M. del, Cibrián-Vera, D., Bonay, P., Pérez-Hernández, D., Vázquez, J., Navarro, P., Gutierrez-Gallego, R., Ramirez-Huesca, M., Martín, P., & Sánchez-Madrid, F. (2014). The Leukocyte Activation Receptor CD69 Controls T Cell Differentiation through Its Interaction with Galectin-1. *Molecular and Cellular Biology*, *34*(13), 2479. https://doi.org/10.1128/MCB.00348-14

Gabryšová, L., Alvarez-Martinez, M., Luisier, R., Cox, L. S., Sodenkamp, J., Hosking, C., Pérez-Mazliah, D., Whicher, C., Kannan, Y., Potempa, K., Wu, X., Bhaw, L., Wende, H., Sieweke, M. H., Elgar, G., Wilson, M., Briscoe, J., Metzis, V., Langhorne, J., … O'Garra, A. (2018). c-Maf controls immune responses by regulating disease-specific gene networks and repressing IL-2 in CD4+ T cells. *Nature Immunology*, *19*(5), 497. https://doi.org/10.1038/S41590-018-0083-5

Gao, F., Tan, Y., & Luo, H. (2020). MALAT1 is involved in type I IFNs-mediated systemic lupus erythematosus by up-regulating OAS2, OAS3, and OASL.

Brazilian Journal of Medical and Biological Research, *53*(5), e9292. https://doi.org/10.1590/1414-431X20209292

Garrod, K. R., Moreau, H. D., Garcia, Z., Lemaître, F., Bouvier, I., Albert, M. L., & Bousso, P. (2012). Dissecting T Cell Contraction In Vivo Using a Genetically Encoded Reporter of Apoptosis. *Cell Reports*, *2*(5), 1438–1447. https://doi.org/10.1016/J.CELREP.2012.10.015

Gasper, D. J., Tejera, M. M., & Suresh, M. (2014). CD4 T-Cell Memory Generation and Maintenance. *Critical Reviews in Immunology*, *34*(2), 121. https://doi.org/10.1615/CRITREVIMMUNOL.2014010373

Gayen, S., Maclary, E., Buttigieg, E., Hinten, M., & Kalantry, S. (2015). A Primary Role for the Tsix lncRNA in Maintaining Random X-Chromosome Inactivation. *Cell Reports*, *11*(8), 1251–1265. https://doi.org/10.1016/J.CELREP.2015.04.039

Gazzinelli-Guimaraes, P. H., & Nutman, T. B. (2018). Helminth parasites and immune regulation. *F1000Research*, *7*, F1000 Faculty Rev-1685. https://doi.org/10.12688/F1000RESEARCH.15596.1

Giang, S., & La Cava, A. (2017). IRF1 and BATF: key drivers of type 1 regulatory T-cell differentiation. *Cellular and Molecular Immunology*, *14*(8), 652. https://doi.org/10.1038/CMI.2017.38

Gibbons, H. R., Shaginurova, G., Kim, L. C., Chapman, N., Spurlock, C. F., & Aune, T. M. (2018). Divergent lncRNA GATA3-AS1 Regulates GATA3 Transcription in T-Helper 2 Cells. *Frontiers in Immunology*, *9*, 365395. https://doi.org/10.3389/FIMMU.2018.02512/BIBTEX

Gierlikowska, B., Stachura, A., Gierlikowski, W., & Demkow, U. (2021). Phagocytosis, Degranulation and Extracellular Traps Release by Neutrophils—The Current Knowledge, Pharmacological Modulation and Future Prospects. *Frontiers in Pharmacology*, *12*, 666732. https://doi.org/10.3389/FPHAR.2021.666732

Gilhar, A., Reich, K., Keren, A., Kabashima, K., Steinhoff, M., & Paus, R. (2021). Mouse models of atopic dermatitis: a critical reappraisal. *Experimental Dermatology*, *30*(3), 319–336. https://doi.org/10.1111/EXD.14270

Girón-González, J. A., Moral, F. J., Elvira, J., García-Gil, D., Guerrero, F., Gavilán, I., & Escobar, L. (2000). Consistent production of a higher T(H)1:T(H)2 cytokine ratio by stimulated T cells in men compared with women. *European Journal of Endocrinology*, *143*(1), 31–36. https://doi.org/10.1530/EJE.0.1430031,

Goodwin, S., McPherson, J. D., & McCombie, W. R. (2016). Coming of age: ten years of next-generation sequencing technologies. *Nature Reviews. Genetics*, *17*(6), 333. https://doi.org/10.1038/NRG.2016.49

Gordon, M. A., Babbs, B., Cochrane, D. R., Bitler, B. G., & Richer, J. K. (2019). The long non-coding RNA MALAT1 promotes ovarian cancer progression by regulating RBFOX2-mediated alternative splicing. *Molecular Carcinogenesis*, *58*(2), 196–205. https://doi.org/10.1002/MC.22919,

Gray, J. I., Westerhof, L. M., & MacLeod, M. K. L. (2018). The roles of resident, central and effector memory CD4 T-cells in protective immunity following infection or vaccination. *Immunology*, *154*(4), 574. https://doi.org/10.1111/IMM.12929

Gubin, M. M., Techasintana, P., Magee, J. D., Dahm, G. M., Calaluce, R., Martindale, J. L., Whitney, M. S., Franklin, C. L., Besch-Williford, C., Hollingsworth, J. W., Abdelmohsen, K., Gorospe, M., & Atasoy, U. (2014). Conditional knockout of the

RNA-binding protein HuR in CD4+ T cells reveals a gene dosage effect on cytokine production. *Molecular Medicine*, *20*(1), 93–108. https://doi.org/10.2119/MOLMED.2013.00127/FIGURES/7

Guo, C. J., Ma, X. K., Xing, Y. H., Zheng, C. C., Xu, Y. F., Shan, L., Zhang, J., Wang, S., Wang, Y., Carmichael, G. G., Yang, L., & Chen, L. L. (2020). Distinct Processing of lncRNAs Contributes to Non-conserved Functions in Stem Cells. *Cell*, *181*(3), 621-636.e22. https://doi.org/10.1016/j.cell.2020.03.006

Guo, J. K., Blanco, M. R., Walkup, W. G., Bonesteele, G., Urbinati, C. R., Banerjee, A. K., Chow, A., Ettlin, O., Strehle, M., Peyda, P., Amaya, E., Trinh, V., & Guttman, M. (2024). Denaturing purifications demonstrate that PRC2 and other widely-reported chromatin proteins do not appear to bind directly to RNA in vivo. *Molecular Cell*, *84*(7), 1271. https://doi.org/10.1016/J.MOLCEL.2024.01.026

Guo, R. Y., Zhang, L., Wang, X., Yin, B. W., Song, S., Jia, Z., Li, B., & Guo, L. (2022). LncRNA Xist may regulate Th17 cell differentiation through TDP43-IRF3 pathway in neuromyelitis optica spectrum disorders. *Medical Hypotheses*, *165*, 110894. https://doi.org/10.1016/J.MEHY.2022.110894

Gutiérrez-Brito, J. A., Lomelí-Nieto, J. Á., Muñoz-Valle, J. F., Oregon-Romero, E., Corona-Angeles, J. A., & Hernández-Bello, J. (2024). Sex hormones and allergies: exploring the gender differences in immune responses. *Frontiers in Allergy*, *5*, 1483919. https://doi.org/10.3389/FALGY.2024.1483919/XML

Gutschner, T., Hämmerle, M., & Diederichs, S. (2013). MALAT1 - A paradigm for long noncoding RNA function in cancer. *Journal of Molecular Medicine*, *91*(7), 791–801. https://doi.org/10.1007/S00109-013-1028-Y/TABLES/2

Gyawali, B., Georas, S. N., & Khurana, S. (2025). Biologics in severe asthma: a state-of-the-art review. *European Respiratory Review*, *34*(175), 240088. https://doi.org/10.1183/16000617.0088-2024

Hall Hickman, A., & Jenner, R. G. (2024). Apparent RNA bridging between PRC2 and chromatin is an artifact of non-specific chromatin precipitation upon RNA degradation. *Cell Reports*, *43*(3), 113856. https://doi.org/10.1016/j.celrep.2024.113856

Hanks, S. C., Mauger, A. S., Varshney, A., Ciotlos, D. L., Manickam, N., Narisu, N., Shumway, A. J., Orchard, P., Erdos, M. R., Sweeney, M. D., Okamoto, J., Jackson, A. U., Stringham, H. M., Bonnycastle, L. L., Zhou, X., Lakka, T. A., Mohlke, K. L., Tuomilehto, J., Laakso, M., … Scott, L. J. (2025). Extensive differential gene expression and regulation by sex in human skeletal muscle. *Cell Genomics*, *5*(8), 100915. https://doi.org/10.1016/J.XGEN.2025.100915

Hasegawa, Y., Brockdorff, N., Kawano, S., Tsutui, K., Tsutui, K., & Nakagawa, S. (2010). The matrix protein hnRNP U is required for chromosomal localization of xist RNA. *Developmental Cell*, *19*(3), 469–476. https://doi.org/10.1016/j.devcel.2010.08.006

Hassoun, D., Malard, O., Barbarot, S., Magnan, A., & Colas, L. (2021). Type 2 immunity-driven diseases: Towards a multidisciplinary approach. *Clinical and Experimental Allergy*, *51*(12), 1538. https://doi.org/10.1111/CEA.14029

He, J., Yang, Q., Xiao, Q., Lei, A., Li, X., Zhou, P., Liu, T., Zhang, L., Shi, K., Yang, Q., Dong, J., & Zhou, J. (2019). IRF-7 Is a Critical Regulator of Type 2 Innate Lymphoid Cells in Allergic Airway Inflammation. *Cell Reports*, *29*(9), 2718-2730.e6. https://doi.org/10.1016/J.CELREP.2019.10.077

Healy, E., Zhang, Q., Gail, E. H., Agius, S. C., Sun, G., Bullen, M., Pandey, V., Das, P. P., Polo, J. M., & Davidovich, C. (2024). The apparent loss of PRC2 chromatin occupancy as an artifact of RNA depletion. *Cell Reports*, *43*(3), 113858. https://doi.org/10.1016/j.celrep.2024.113858

Henze, L., Will, N., Lee, D., Haas, V., Casar, C., Meyer, J., Stein, S., Mangler, F., Steinmann, S., Poch, T., Krause, J., Fuss, J., Schröder, J., Kulle, A. E., Holterhus, P. M., Bonn, S., Altfeld, M., Huber, S., Lohse, A. W., … Schramm, C. (2025). Testosterone affects female CD4+ T cells in healthy individuals and autoimmune liver diseases. *JCI Insight*, *10*(8), e184544. https://doi.org/10.1172/JCI.INSIGHT.184544

Hewitson, J. P., West, K. A., James, K. R., Rani, G. F., Dey, N., Romano, A., Brown, N., Teichmann, S. A., Kaye, P. M., & Lagos, D. (2020). Malat1 Suppresses Immunity to Infection through Promoting Expression of Maf and IL-10 in Th Cells . *The Journal of Immunology*, *204*(11), 2949–2960. https://doi.org/10.4049/JIMMUNOL.1900940/-/DCSUPPLEMENTAL

Hirahara, K., Kokubo, K., Aoki, A., Kiuchi, M., & Nakayama, T. (2021). The Role of CD4+ Resident Memory T Cells in Local Immunity in the Mucosal Tissue – Protection Versus Pathology –. *Frontiers in Immunology*, *12*, 616309. https://doi.org/10.3389/FIMMU.2021.616309/XML

Hoeffel, G., & Ginhoux, F. (2015). Ontogeny of tissue-resident macrophages. *Frontiers in Immunology*, *6*(SEP), 162667. https://doi.org/10.3389/FIMMU.2015.00486/XML

Hoffman, W., Lakkis, F. G., & Chalasani, G. (2016). B cells, antibodies, and more. *Clinical Journal of the American Society of Nephrology*, *11*(1), 137–154. https://doi.org/10.2215/CJN.09430915,

Howell, I., Howell, A., & Pavord, I. D. (2023). Type 2 inflammation and biological therapies in asthma: Targeted medicine taking flight. *The Journal of Experimental Medicine*, *220*(7), e20221212. https://doi.org/10.1084/JEM.20221212

Hsu, C.-I., Mei, S., Demmerle, J., Prakash, A., Ruttenberg, S., Sahn, M., & Yu, J.-R. (2025). Paraspeckle protein NONO regulates active chromatin by allosterically stimulating NSD1. *Cell Reports*, *44*(9), 116247. https://doi.org/10.1016/J.CELREP.2025.116247

Hu, G., Lou, Z., & Gupta, M. (2014). The Long Non-Coding RNA GAS5 Cooperates with the Eukaryotic Translation Initiation Factor 4E to Regulate c-Myc Translation. *PLoS ONE*, *9*(9), e107016. https://doi.org/10.1371/JOURNAL.PONE.0107016

Hu, S., Lv, P., Yan, Z., & Wen, B. (2019). Disruption of nuclear speckles reduces chromatin interactions in active compartments. *Epigenetics and Chromatin*, *12*(1), 1–12. https://doi.org/10.1186/S13072-019-0289-2/FIGURES/5

Hu, Z. Y., Wang, X. Y., Guo, W. Bin, Xie, L. Y., Huang, Y. Q., Liu, Y. P., Xiao, L. W., Li, S. N., Zhu, H. F., Li, Z. G., & Kan, H. (2016). Long non-coding RNA MALAT1 increases AKAP-9 expression by promoting SRPK1-catalyzed SRSF1 phosphorylation in colorectal cancer cells. *Oncotarget*, *7*(10), 11733–11743. https://doi.org/10.18632/ONCOTARGET.7367,

Huang, M., Wang, H., Hu, X., & Cao, X. (2018). lncRNA MALAT1 binds chromatin remodeling subunit BRG1 to epigenetically promote inflammation-related

hepatocellular carcinoma progression. *Oncoimmunology*, *8*(1), e1518628. https://doi.org/10.1080/2162402X.2018.1518628

Huang, T. C., Wang, Y. F., Vazquez-Ferrer, E., Theofel, I., Requena, C. E., Hanna, C. W., Kelsey, G., & Hajkova, P. (2021). Sex-specific chromatin remodelling safeguards transcription in germ cells. *Nature*, *600*(7890), 737–742. https://doi.org/10.1038/S41586-021-04208-5;TECHMETA

Huber, J. P., Ramos, H. J., Gill, M. A., & Farrar, J. D. (2010). Cutting Edge: Type I IFN Reverses Human Th2 Commitment and Stability by Suppressing GATA3. *The Journal of Immunology*, *185*(2), 813–817. https://doi.org/10.4049/JIMMUNOL.1000469,

Hübner, M. R., Eckersley-Maslin, M. A., & Spector, D. L. (2012). Chromatin Organization and Transcriptional Regulation. *Current Opinion in Genetics & Development*, *23*(2), 89. https://doi.org/10.1016/J.GDE.2012.11.006

Hung, T., Wang, Y., Lin, M. F., Koegel, A. K., Kotake, Y., Grant, G. D., Horlings, H. M., Shah, N., Umbricht, C., Wang, P., Wang, Y., Kong, B., Langerød, A., Børresen-Dale, A. L., Kim, S. K., Van De Vijver, M., Sukumar, S., Whitfield, M. L., Kellis, M., … Chang, H. Y. (2011). Extensive and coordinated transcription of noncoding RNAs within cell-cycle promoters. *Nature Genetics*, *43*(7), 621–629. https://doi.org/10.1038/NG.848;SUBJMETA=144,208,2489,337,384,572,631,68;KWRD=CANCER+GENETICS,NON-CODING+RNAS,TRANSCRIPTION

Huret, C., Ferrayé, L., David, A., Mohamed, M., Valentin, N., Charlotte, F., Savignac, M., Goodhardt, M., Guéry, J. C., Rougeulle, C., & Morey, C. (2024). Altered X-chromosome inactivation predisposes to autoimmunity. *Science Advances*, *10*(18), 6537.

https://doi.org/10.1126/SCIADV.ADN6537/SUPPL_FILE/SCIADV.ADN6537_TABLES_S1_TO_S5.ZIP

Hussain, M., & Liu, G. (2024). Eosinophilic Asthma: Pathophysiology and Therapeutic Horizons. *Cells*, *13*(5), 384. https://doi.org/10.3390/CELLS13050384

Hwang, J. R., Byeon, Y., Kim, D., & Park, S. G. (2020). Recent insights of T cell receptor-mediated signaling pathways for T cell activation and development. *Experimental & Molecular Medicine 2020 52:5*, *52*(5), 750–761. https://doi.org/10.1038/s12276-020-0435-8

Ilık, İ. A., Malszycki, M., Lübke, A. K., Schade, C., Meierhofer, D., & Aktaş, T. (2020). SON and SRRM2 are essential for nuclear speckle formation. *ELife*, *9*, e60579. https://doi.org/10.7554/ELIFE.60579

Ip, J. Y., Tong, A., Pan, Q., Topp, J. D., Blencowe, B. J., & Lynch, K. W. (2007). Global analysis of alternative splicing during T-cell activation. *RNA*, *13*(4), 563–572. https://doi.org/10.1261/RNA.457207

Islam, H., Jackson, G. S., Yoon, J. S. J., Cabral-Santos, C., Lira, F. S., Mui, A. L., & Little, J. P. (2022). Sex differences in IL-10's anti-inflammatory function: Greater STAT3 phosphorylation and stronger inhibition of TNF-α production in male blood leukocytes ex vivo. *American Journal of Physiology - Cell Physiology*, *322*(6), C1095–C1104. https://doi.org/10.1152/AJPCELL.00091.2022/ASSET/IMAGES/LARGE/AJPCELL.00091.2022_F006.JPEG

Itoh, Y., Golden, L. C., Itoh, N., Matsukawa, M. A., Ren, E., Tse, V., Arnold, A. P., & Voskuhl, R. R. (2019). The X-linked histone demethylase Kdm6a in CD4+ T

lymphocytes modulates autoimmunity. *The Journal of Clinical Investigation*, *129*(9), 3852–3863. https://doi.org/10.1172/JCI126250

Jain, M., Abu-Shumays, R., Olsen, H. E., & Akeson, M. (2022). Advances in nanopore direct RNA sequencing. *Nature Methods*, *19*(10), 1160–1164. https://doi.org/10.1038/S41592-022-01633-W;SUBJMETA=1058,1949,350,514,61,631;KWRD=NANOPORES,RNA+SEQUENCING

Jankovic, D., Kugler, D. G., & Sher, A. (2010). IL-10 production by CD4+ effector T cells: a mechanism for self-regulation. *Mucosal Immunology*, *3*(3), 239. https://doi.org/10.1038/MI.2010.8

Jeskey, J., Kurien, C., Blunk, H., Sehmi, K., Areti, S., Nguyen, D., & Hostoffer, R. (2024). Atopic Dermatitis: A Review of Diagnosis and Treatment. *The Journal of Pediatric Pharmacology and Therapeutics : JPPT*, *29*(6), 587. https://doi.org/10.5863/1551-6776-29.6.587

Ji, P., Diederichs, S., Wang, W., Böing, S., Metzger, R., Schneider, P. M., Tidow, N., Brandt, B., Buerger, H., Bulk, E., Thomas, M., Berdel, W. E., Serve, H., & Müller-Tidow, C. (2003). MALAT-1, a novel noncoding RNA, and thymosin beta4 predict metastasis and survival in early-stage non-small cell lung cancer. *Oncogene*, *22*(39), 8031–8041. https://doi.org/10.1038/SJ.ONC.1206928

Jiang, R., Tang, J., Chen, Y., Deng, L., Ji, J., Xie, Y., Wang, K., Jia, W., Chu, W. M., & Sun, B. (2017). The long noncoding RNA lnc-EGFR stimulates T-regulatory cells differentiation thus promoting hepatocellular carcinoma immune evasion. *Nature Communications 2017 8:1*, *8*(1), 1–15. https://doi.org/10.1038/ncomms15129

Jin, H., He, R., Oyoshi, M., & Geha, R. S. (2009). Animal models of atopic dermatitis. *The Journal of Investigative Dermatology*, *129*(1), 31. https://doi.org/10.1038/JID.2008.106

Johnsson, P., Lipovich, L., Grandér, D., & Morris, K. V. (2014). Evolutionary conservation of long noncoding RNAs; sequence, structure, function. *Biochimica et Biophysica Acta*, *1840*(3), 1063. https://doi.org/10.1016/J.BBAGEN.2013.10.035

Joyce, K. L., Morgan, W., Greenberg, R., & Nair, M. G. (2012). Using Eggs from Schistosoma mansoni as an In vivo Model of Helminth-induced Lung Inflammation. *Journal of Visualized Experiments : JoVE*, (64), 1. https://doi.org/10.3791/3905

Juan, C., Mao, Y., Wang, Q., Cao, Q., Chen, Y., & Zhou, G. (2018). The LncRNA MALAT1 regulates CD80 transcription via the NF-κB signaling pathway in the A549 cell line. *Biochemical and Biophysical Research Communications*, *503*(3), 1674–1681. https://doi.org/10.1016/J.BBRC.2018.07.098

Kak, G., Raza, M., & Tiwari, B. K. (2018). Interferon-gamma (IFN-γ): Exploring its implications in infectious diseases. *Biomolecular Concepts*, *9*(1), 64–79. https://doi.org/10.1515/BMC-2018-0007/ASSET/GRAPHIC/J_BMC-2018-0007_FIG_002.JPG

Kanbar, J. N., Ma, S., Kim, E. S., Kurd, N. S., Tsai, M. S., Tysl, T., Widjaja, C. E., Limary, A. E., Yee, B., He, Z., Hao, Y., Fu, X.-D., Yeo, G. W., Huang, W. J., & Chang, J. T. (2022). The long noncoding RNA Malat1 regulates CD8+ T cell differentiation by mediating epigenetic repression. *The Journal of Experimental Medicine*, *219*(6). https://doi.org/10.1084/JEM.20211756

Kanda, A., Yun, Y., Bui, D. Van, Nguyen, L. M., Kobayashi, Y., Suzuki, K., Mitani, A., Sawada, S., Hamada, S., Asako, M., & Iwai, H. (2021). The multiple functions and subpopulations of eosinophils in tissues under steady-state and pathological conditions. *Allergology International*, *70*(1), 9–18. https://doi.org/10.1016/J.ALIT.2020.11.001

Karakas, D., & Ozpolat, B. (2021). The Role of LncRNAs in Translation. *Non-Coding RNA*, *7*(1), 16. https://doi.org/10.3390/NCRNA7010016

Karantanos, T., Chistofides, A., Barhdan, K., Li, L., & Boussiotis, V. A. (2016). Regulation of T Cell Differentiation and Function by EZH2. *Frontiers in Immunology*, *7*(MAY), 172. https://doi.org/10.3389/FIMMU.2016.00172

Karpel, M. E., Boutwell, C. L., & Allen, T. M. (2015). BLT Humanized Mice as a Small Animal Model of HIV Infection. *Current Opinion in Virology*, *13*, 75. https://doi.org/10.1016/J.COVIRO.2015.05.002

Karpuzoglu-Sahin, E., Zhi-Jun, Y., Lengi, A., Sriranganathan, N., & Ansar Ahmed, S. (2001). Effects of long-term estrogen treatment on IFN-γ, IL-2 and IL-4 gene expression and protein synthesis in spleen and thymus of normal C57BL/6 mice. *Cytokine*, *14*(4), 208–217. https://doi.org/10.1006/cyto.2001.0876

Katsuyama, T., & Moulton, V. R. (2021). Splicing factor SRSF1 is indispensable for regulatory T cell homeostasis and function. *Cell Reports*, *36*(1), 109339. https://doi.org/10.1016/J.CELREP.2021.109339

Katzen, D., Chu, E., Terhost, C., Leung, D. Y., Gesner, M., Miller, R. A., & Geha, R. S. (1985). Mechanisms of human T cell response to mitogens: IL 2 induces IL 2 receptor expression and proliferation but not IL 2 synthesis in PHA-stimulated T

cells. *The Journal of Immunology*, *135*(3), 1840–1845. https://doi.org/10.4049/JIMMUNOL.135.3.1840

Keegan, A. D., Leonard, W. J., & Zhu, J. (2021). Recent advances in understanding the role of IL-4 signaling. *Faculty Reviews*, *10*, 71. https://doi.org/10.12703/R/10-71

Kim, J., Venkata, N. C., Gonzalez, G. A. H., Khanna, N., & Belmont, A. S. (2020). Gene expression amplification by nuclear speckle association. *Journal of Cell Biology*, *219*(1). https://doi.org/10.1083/JCB.201904046/VIDEO-6

Kim, S. H., Kim, S. H., Yang, W. I., Kim, S. J., & Yoon, S. O. (2017). Association of the long non-coding RNA MALAT1 with the polycomb repressive complex pathway in T and NK cell lymphoma. *Oncotarget*, *8*(19), 31305. https://doi.org/10.18632/ONCOTARGET.15453

Kirk, J. M., Kim, S. O., Inoue, K., Smola, M. J., Lee, D. M., Schertzer, M. D., Wooten, J. S., Baker, A. R., Sprague, D., Collins, D. W., Horning, C. R., Wang, S., Chen, Q., Weeks, K. M., Mucha, P. J., & Calabrese, J. M. (2018). Functional classification of long non-coding RNAs by k-mer content. *Nature Genetics 2018 50:10*, *50*(10), 1474–1482. https://doi.org/10.1038/s41588-018-0207-8

Klein, S. L., & Flanagan, K. L. (2016). Sex differences in immune responses. *Nature Reviews Immunology*, *16*(10), 626–638. https://doi.org/10.1038/NRI.2016.90;SUBJMETA=2152,250,262,631;KWRD=ADAPTIVE+IMMUNITY,INNATE+IMMUNITY

Koh, B. H., Hwang, S. S., Kim, J. Y., Lee, W., Kang, M. J., Lee, C. G., Park, J. W., Flavell, R. A., & Lee, G. R. (2010). Th2 LCR is essential for regulation of Th2 cytokine genes and for pathogenesis of allergic asthma. *Proceedings of the National Academy of Sciences of the United States of America*, *107*(23), 10614–

10619. https://doi.org/10.1073/PNAS.1005383107/SUPPL_FILE/PNAS.201005383SI.PDF

Kołat, D., Hammouz, R., Bednarek, A. K., & Płuciennik, E. (2019). Exosomes as carriers transporting long non-coding RNAs: Molecular characteristics and their function in cancer. *Molecular Medicine Reports*, *20*(2), 851. https://doi.org/10.3892/MMR.2019.10340

Kopp, F., & Mendell, J. T. (2018). Functional Classification and Experimental Dissection of Long Noncoding RNAs. *Cell*, *172*(3), 393–407. https://doi.org/10.1016/J.CELL.2018.01.011

Kratofil, R. M., Kubes, P., & Deniset, J. F. (2017). Monocyte conversion during inflammation and injury. *Arteriosclerosis, Thrombosis, and Vascular Biology*, *37*(1), 35–42. https://doi.org/10.1161/ATVBAHA.116.308198/SUPPL_FILE/308198.PDF

Krol, J. (2017). Paraspeckles: nuclear nests helping to raise mature miRNAs. *Nature Structural & Molecular Biology 2017 24:10*, *24*(10), 783–784. https://doi.org/10.1038/nsmb.3479

Krystel-Whittemore, M., Dileepan, K. N., & Wood, J. G. (2016). Mast cell: A multi-functional master cell. *Frontiers in Immunology*, *6*(JAN), 165675. https://doi.org/10.3389/FIMMU.2015.00620/XML

Kubelkova, K., & Macela, A. (2019). Innate Immune Recognition: An Issue More Complex Than Expected. *Frontiers in Cellular and Infection Microbiology*, *9*, 241. https://doi.org/10.3389/FCIMB.2019.00241/BIBTEX

Kuka, M., De Giovanni, M., & Iannacone, M. (2019). The role of type I interferons in CD4+ T cell differentiation. *Immunology Letters*, *215*, 19. https://doi.org/10.1016/J.IMLET.2019.01.013

Laffont, S., Rouquié, N., Azar, P., Seillet, C., Plumas, J., Aspord, C., & Guéry, J.-C. (2014). X-Chromosome Complement and Estrogen Receptor Signaling Independently Contribute to the Enhanced TLR7-Mediated IFN-α Production of Plasmacytoid Dendritic Cells from Women. *The Journal of Immunology*, *193*(11), 5444–5452. https://doi.org/10.4049/JIMMUNOL.1303400

Lakshmikanth, T., Consiglio, C., Sardh, F., Forlin, R., Wang, J., Tan, Z., Barcenilla, H., Rodriguez, L., Sugrue, J., Noori, P., Ivanchenko, M., Piñero Páez, L., Gonzalez, L., Habimana Mugabo, C., Johnsson, A., Ryberg, H., Hallgren, Å., Pou, C., Chen, Y., … Brodin, P. (2024). Immune system adaptation during gender-affirming testosterone treatment. *Nature 2024 633:8028*, *633*(8028), 155–164. https://doi.org/10.1038/s41586-024-07789-z

Lamond, A. I., & Earnshaw, W. C. (1998). Structure and function in the nucleus. *Science*, *280*(5363), 547–553. https://doi.org/10.1126/SCIENCE.280.5363.547/ASSET/DAB6DADB-DF48-4116-BAF0-77BF2A59EADC/ASSETS/GRAPHIC/SE1786457003.JPEG

Lamond, A. I., & Spector, D. L. (2003). Nuclear speckles: A model for nuclear organelles. *Nature Reviews Molecular Cell Biology*, *4*(8), 605–612. https://doi.org/10.1038/NRM1172;KWRD=LIFE+SCIENCES

Lee, D. U., Agarwal, S., & Rao, A. (2002). Th2 Lineage Commitment and Efficient IL-4 Production Involves Extended Demethylation of the IL-4 Gene. *Immunity*, *16*(5), 649–660. https://doi.org/10.1016/S1074-7613(02)00314-X

Lee, H.-W., Wang, H.-T., Weng, M.-W., Kuo, J., Huang, W. C., Donin, N., & Lepor, H. (2013). 1129 SEX HORMONES REGULATE GATA3 IN THE URINARY BLADDER: A POTENTIAL MECHANISM OF GENDER-SPECIFIC DIFFERENCE IN BLADDER CANCER INCIDENCE. *The Journal of Urology*, *189*(4S). https://doi.org/10.1016/J.JURO.2013.02.744

Lei, X., de Groot, D. C., Welters, M. J. P., de Wit, T., Schrama, E., van Eenennaam, H., Santegoets, S. J., Oosenbrug, T., van der Veen, A., Vos, J. L., Zuur, C. L., de Miranda, N. F. C. C., Jacobs, H., van der Burg, S. H., Borst, J., & Xiao, Y. (2024). CD4+ T cells produce IFN-I to license cDC1s for induction of cytotoxic T-cell activity in human tumors. *Cellular and Molecular Immunology*, *21*(4), 374–392. https://doi.org/10.1038/S41423-024-01133-1;SUBJMETA=133,1566,21,250,2504,580,631;KWRD=CELLULAR+IMMUNITY,DENDRITIC+CELLS,TUMOUR+IMMUNOLOGY

Lei, X., Xiao, R., Chen, Z., Ren, J., Zhao, W., Tang, W., Wen, K., Zhu, Y., Li, X., Ouyang, S., Xu, A., Hu, Y., & Bi, E. (2024). Augmenting antitumor efficacy of Th17-derived Th1 cells through IFN-γ-induced type I interferon response network via IRF7. *Proceedings of the National Academy of Sciences of the United States of America*, *121*(47), e2412120121. https://doi.org/10.1073/PNAS.2412120121/SUPPL_FILE/PNAS.2412120121.SAPP.PDF

Li, F., Li, X., Qiao, L., Liu, W., Xu, C., & Wang, X. (2019). MALAT1 regulates miR-34a expression in melanoma cells. *Cell Death & Disease 2019 10:6*, *10*(6), 389-. https://doi.org/10.1038/s41419-019-1620-3

Li, J., Tian, J., Lu, J., Wang, Z., Ling, J., Wu, X., Yang, F., & Xia, Y. (2020). LncRNA GAS5 inhibits Th17 differentiation and alleviates immune thrombocytopenia via promoting the ubiquitination of STAT3. *International Immunopharmacology*, *80*, 106127. https://doi.org/10.1016/J.INTIMP.2019.106127

Li, K., & Wang, Z. (2021). Speckles and paraspeckles coordinate to regulate HSV-1 genes transcription. *Communications Biology*, *4*(1), 1–10. https://doi.org/10.1038/S42003-021-02742-6;TECHMETA

Li, L., Chen, H., Gao, Y., Wang, Y. W., Zhang, G. Q., Pan, S. H., Ji, L., Kong, R., Wang, G., Jia, Y. H., Bai, X. W., & Sun, B. (2016). Long noncoding RNA MALAT1 promotes aggressive pancreatic cancer proliferation and metastasis via the stimulation of autophagy. *Molecular Cancer Therapeutics*, *15*(9), 2232–2243. https://doi.org/10.1158/1535-7163.MCT-16-0008,

Liang, Z., & Tang, F. (2020). The potency of lncRNA MALAT1/miR-155/CTLA4 axis in altering Th1/Th2 balance of asthma. *Bioscience Reports*, *40*(2). https://doi.org/10.1042/BSR20190397/221794

Liao, W., Lin, J. X., Wang, L., Li, P., & Leonard, W. J. (2011). Modulation of cytokine receptors by IL-2 broadly regulates differentiation into helper T cell lineages. *Nature Immunology 2011 12:6*, *12*(6), 551–559. https://doi.org/10.1038/ni.2030

Liao, W., Schones, D. E., Oh, J., Cui, Y., Cui, K., Roh, T. Y., Zhao, K., & Leonard, W. J. (2008). Priming for T helper type 2 differentiation by interleukin 2-mediated induction of IL-4 receptor α chain expression. *Nature Immunology*, *9*(11), 1288. https://doi.org/10.1038/NI.1656

Lin, A., & Loré, K. (2017). Granulocytes: New members of the antigen-presenting cell family. *Frontiers in Immunology*, *8*(DEC), 319852. https://doi.org/10.3389/FIMMU.2017.01781/BIBTEX

Lin, H., Mosmann, T. R., Guilbert, L., Tuntipopipat, S., & Wegmann, T. G. (1993). Synthesis of T helper 2-type cytokines at the maternal-fetal interface. *The Journal of Immunology*, *151*(9), 4562–4573. https://doi.org/10.4049/JIMMUNOL.151.9.4562

Liu, L., Liu, J., & Lin, Q. (2021). Histone demethylase KDM2A: Biological functions and clinical values (Review). *Experimental and Therapeutic Medicine*, *22*(1), 723. https://doi.org/10.3892/ETM.2021.10155

Liu, W., Wang, Z., Liu, L., Yang, Z., Liu, S., Ma, Z., Liu, Y., Ma, Y., Zhang, L., Zhang, X., Jiang, M., & Cao, X. (2020). LncRNA Malat1 inhibition of TDP43 cleavage suppresses IRF3-initiated antiviral innate immunity. *Proceedings of the National Academy of Sciences of the United States of America*, *117*(38), 23695–23706. https://doi.org/10.1073/PNAS.2003932117/-/DCSUPPLEMENTAL

Liva, S. M., & Voskuhl, R. R. (2001). Testosterone Acts Directly on CD4+ T Lymphocytes to Increase IL-10 Production. *The Journal of Immunology*, *167*(4), 2060–2067. https://doi.org/10.4049/JIMMUNOL.167.4.2060,

Loda, A., Collombet, S., & Heard, E. (2022). Gene regulation in time and space during X-chromosome inactivation. *Nature Reviews Molecular Cell Biology 2022 23:4*, *23*(4), 231–249. https://doi.org/10.1038/s41580-021-00438-7

Long, Y., Sou, W. H., Yung, K. W. Y., Liu, H., Wan, S. W. C., Li, Q., Zeng, C., Law, C. O. K., Chan, G. H. C., Lau, T. C. K., & Ngo, J. C. K. (2019). Distinct mechanisms govern the phosphorylation of different SR protein splicing factors. *Journal of*

Biological Chemistry, *294*(4), 1312–1327. https://doi.org/10.1074/JBC.RA118.003392

Lu, Q., Wu, A., Tesmer, L., Ray, D., Yousif, N., & Richardson, B. (2007). Demethylation of CD40LG on the Inactive X in T Cells from Women with Lupus. *The Journal of Immunology*, *179*(9), 6352–6358. https://doi.org/10.4049/JIMMUNOL.179.9.6352

Lu, X., Huang, J., Wu, S., Zheng, Q., Liu, P., Feng, H., Su, X., Fu, H., Xi, Q., & Wang, G. (2020). The tRNA-like small noncoding RNA mascRNA promotes global protein translation. *EMBO Reports*, *21*(12), e49684. https://doi.org/10.15252/EMBR.201949684

Lu, Z., Guo, J. K., Wei, Y., Dou, D. R., Zarnegar, B., Ma, Q., Li, R., Zhao, Y., Liu, F., Choudhry, H., Khavari, P. A., & Chang, H. Y. (2020). Structural modularity of the XIST ribonucleoprotein complex. *Nature Communications*, *11*(1), 1–14. https://doi.org/10.1038/S41467-020-20040-3;TECHMETA=100,41,42,45,90,91;SUBJMETA=114,2401,45,500,631;KWRD=DATA+INTEGRATION,RNA

Luckheeram, R. V., Zhou, R., Verma, A. D., & Xia, B. (2012). CD4+T Cells: Differentiation and Functions. *Clinical and Developmental Immunology*, *2012*, 925135. https://doi.org/10.1155/2012/925135

Luo, Y., Vermeer, M., Linssen, M. M., de Bie, F. J., Pijnacker-Verspuij, M., Brouwers, C., Claassens, J., de Gruijl, F. R., Hohenstein, P., & Tensen, C. P. (2025). A novel knockout mouse model to assess the impact of one-copy loss of Hnrnpk in CD4 + T cells in chronically inflamed skin as a prelude to CTCL. *Scientific Reports*, *15*(1), 1–11. https://doi.org/10.1038/S41598-025-98640-6;SUBJMETA

Ma, W., Huang, G., Wang, Z., Wang, L., & Gao, Q. (2023). IRF7: role and regulation in immunity and autoimmunity. *Frontiers in Immunology*, *14*, 1236923. https://doi.org/10.3389/FIMMU.2023.1236923/XML

Ma, Y., Shi, L., Zhao, K., & Zheng, C. (2022). lncRNA FR215775 Regulates Th2 Differentiation in Murine Allergic Rhinitis. *Journal of Immunology Research*, *2022*, 7783481. https://doi.org/10.1155/2022/7783481

MacDonald, A. S., Patton, E. A., La Flamme, A. C., Araujo, M. I., Huxtable, C. R., Bauman, B., & Pearce, E. J. (2002). Impaired Th2 Development and Increased Mortality During Schistosoma mansoni Infection in the Absence of CD40/CD154 Interaction. *The Journal of Immunology*, *168*(9), 4643–4649. https://doi.org/10.4049/JIMMUNOL.168.9.4643

Mace, E. M. (2022). Human natural killer cells: form, function, and development. *The Journal of Allergy and Clinical Immunology*, *151*(2), 371. https://doi.org/10.1016/J.JACI.2022.09.022

Maizels, R. M., Balic, A., Gomez-Escobar, N., Nair, M., Taylor, M. D., Allen, J. E., Babayan, S., Dresser, D., Finney, C., Gilmour, K., Graham, A., Gregory, B., Harris, A., Harcus, Y., Lamb, T., Murray, J., Nicol, G., Prieto-Lafuente, L., & Schabussova, I. (2004). Helminth parasites – masters of regulation. *Immunological Reviews*, *201*(1), 89–116. https://doi.org/10.1111/J.0105-2896.2004.00191.X

Maizels, R. M., & Gause, W. C. (2023). Targeting helminths: The expanding world of type 2 immune effector mechanisms. *The Journal of Experimental Medicine*, *220*(10), e20221381. https://doi.org/10.1084/JEM.20221381

Malakar, P., Shilo, A., Mogilevsky, A., Stein, I., Pikarsky, E., Nevo, Y., Benyamini, H., Elgavish, S., Zong, X., Prasanth, K. V., & Karni, R. (2016). Long noncoding RNA

MALAT1 promotes hepatocellular carcinoma development by SRSF1 up-regulation and mTOR activation. *Cancer Research*, *77*(5), 1155. https://doi.org/10.1158/0008-5472.CAN-16-1508

Manuel, R. S. J., & Liang, Y. (2021). Sexual Dimorphism in Immunometabolism and Autoimmunity: Impact on Personalized Medicine. *Autoimmunity Reviews*, *20*(4), 102775. https://doi.org/10.1016/J.AUTREV.2021.102775

Marshall, J. S., Warrington, R., Watson, W., & Kim, H. L. (2018). An introduction to immunology and immunopathology. *Allergy, Asthma and Clinical Immunology*, *14*(2), 1–10. https://doi.org/10.1186/S13223-018-0278-1/TABLES/4

Martinez, F. O., & Gordon, S. (2014). The M1 and M2 paradigm of macrophage activation: Time for reassessment. *F1000Prime Reports*, *6*. https://doi.org/10.12703/P6-13,

Martinez-Terroba, E., Plasek-Hegde, L. M., Chiotakakos, I., Li, V., de Miguel, F. J., Robles-Oteiza, C., Tyagi, A., Politi, K., Zamudio, J. R., & Dimitrova, N. (2024). Overexpression of Malat1 drives metastasis through inflammatory reprogramming of the tumor microenvironment. *Science Immunology*, *9*(96), eadh5462. https://doi.org/10.1126/SCIIMMUNOL.ADH5462

Masoumi, F., Ghorbani, S., Talebi, F., Branton, W. G., Rajaei, S., Power, C., & Noorbakhsh, F. (2019). Malat1 long noncoding RNA regulates inflammation and leukocyte differentiation in experimental autoimmune encephalomyelitis. *Journal of Neuroimmunology*, *328*, 50–59. https://doi.org/10.1016/J.JNEUROIM.2018.11.013

Matsuura, R., Nakajima, T., Ichihara, S., & Sado, T. (2021). Ectopic Splicing Disturbs the Function of Xist RNA to Establish the Stable Heterochromatin State. *Frontiers*

in Cell and Developmental Biology, *9*, 751154. https://doi.org/10.3389/FCELL.2021.751154/BIBTEX

Matveishina, E., Antonov, I., & Medvedeva, Y. A. (2020). Practical Guidance in Genome-Wide RNA:DNA Triple Helix Prediction. *International Journal of Molecular Sciences*, *21*(3), 830. https://doi.org/10.3390/IJMS21030830

McCuaig, R. D., Dunn, J., Li, J., Masch, A., Knaute, T., Schutkowski, M., Zerweck, J., & Rao, S. (2015). PKC-theta is a novel SC35 splicing factor regulator in response to T cell activation. *Frontiers in Immunology*, *6*(NOV), 159659. https://doi.org/10.3389/FIMMU.2015.00562/BIBTEX

McHugh, C. A., Chen, C. K., Chow, A., Surka, C. F., Tran, C., McDonel, P., Pandya-Jones, A., Blanco, M., Burghard, C., Moradian, A., Sweredoski, M. J., Shishkin, A. A., Su, J., Lander, E. S., Hess, S., Plath, K., & Guttman, M. (2015). The Xist lncRNA directly interacts with SHARP to silence transcription through HDAC3. *Nature*, *521*(7551), 232. https://doi.org/10.1038/NATURE14443

McHugh, C. A., & Guttman, M. (2018). RAP-MS: A Method to Identify Proteins that Interact Directly with a Specific RNA Molecule in Cells. *Methods in Molecular Biology*, *1649*, 473–488. https://doi.org/10.1007/978-1-4939-7213-5_31

McKinstry, K. K., Strutt, T. M., & Swain, S. L. (2010). Regulation of CD4+ T-cell contraction during pathogen challenge. *Immunological Reviews*, *236*(1), 110–124. https://doi.org/10.1111/J.1600-065X.2010.00921.X;CSUBTYPE:STRING:SPECIAL;PAGE:STRING:ARTICLE/CHAPTER

McSorley, H. J., & Maizels, R. M. (2012). Helminth Infections and Host Immune Regulation. *Clinical Microbiology Reviews*, *25*(4), 585–608. https://doi.org/10.1128/CMR.05040-11

Meldi, L., & Brickner, J. H. (2011). Compartmentalization of the nucleus. *Trends in Cell Biology*, *21*(12), 701. https://doi.org/10.1016/J.TCB.2011.08.001

Menees, K. B., Earls, R. H., Chung, J., Jernigan, J., Filipov, N. M., Carpenter, J. M., & Lee, J. K. (2021). Sex- and age-dependent alterations of splenic immune cell profile and NK cell phenotypes and function in C57BL/6J mice. *Immunity and Ageing*, *18*(1), 1–13. https://doi.org/10.1186/S12979-021-00214-3/FIGURES/6

Mestas, J., & Hughes, C. C. W. (2004). Of Mice and Not Men: Differences between Mouse and Human Immunology. *The Journal of Immunology*, *172*(5), 2731–2738. https://doi.org/10.4049/JIMMUNOL.172.5.2731

Miao, H., Wu, F., Li, Y., Qin, C., Zhao, Y., Xie, M., Dai, H., Yao, H., Cai, H., Wang, Q., Song, X., & Li, L. (2022). MALAT1 modulates alternative splicing by cooperating with the splicing factors PTBP1 and PSF. *Science Advances*, *8*(51). https://doi.org/10.1126/SCIADV.ABQ7289/SUPPL_FILE/SCIADV.ABQ7289_TABLES_S1_AND_S2.ZIP

Min, B., Brown, M. A., & Legros, G. (2012). Understanding the roles of basophils: breaking dawn. *Immunology*, *135*(3), 192. https://doi.org/10.1111/J.1365-2567.2011.03530.X

Mohammad, I., Starskaia, I., Nagy, T., Guo, J., Yatkin, E., Väänänen, K., Watford, W. T., & Chen, Z. (2018). Estrogen receptor contributes to T cell–mediated autoimmune inflammation by promoting T cell activation and proliferation. *Science Signaling*, *11*(526), 9415. https://doi.org/10.1126/SCISIGNAL.AAP9415,

Montes de Oca, M., Kumar, R., de Labastida Rivera, F., Amante, F. H., Sheel, M., Faleiro, R. J., Bunn, P. T., Best, S. E., Beattie, L., Ng, S. S., Edwards, C. L., Muller, W., Cretney, E., Nutt, S. L., Smyth, M. J., Haque, A., Hill, G. R., Sundar, S., Kallies, A., & Engwerda, C. R. (2016). Blimp-1-Dependent IL-10 Production by Tr1 Cells Regulates TNF-Mediated Tissue Pathology. *PLoS Pathogens*, *12*(1), e1005398. https://doi.org/10.1371/JOURNAL.PPAT.1005398

Moran, A. E., Polesso, F., & Weinberg, A. D. (2016). Immunotherapy expands and maintains the function of high affinity tumor infiltrating CD8 T cells in situ. *Journal of Immunology (Baltimore, Md. : 1950)*, *197*(6), 2509. https://doi.org/10.4049/JIMMUNOL.1502659

Mosmann, T. R., & Coffman, R. L. (1989). TH1 and TH2 cells: Different patterns of lymphokine secretion lead to different functional properties. *Annual Review of Immunology*, *7*(Volume 7, 1989), 145–173. https://doi.org/10.1146/ANNUREV.IY.07.040189.001045/CITE/REFWORKS

Naganuma, T., Nakagawa, S., Tanigawa, A., Sasaki, Y. F., Goshima, N., & Hirose, T. (2012). Alternative 3′-end processing of long noncoding RNA initiates construction of nuclear paraspeckles. *The EMBO Journal*, *31*(20), 4020. https://doi.org/10.1038/EMBOJ.2012.251

Nakagawa, S., Ip, J. Y., Shioi, G., Tripathi, V., Zong, X., Hirose, T., & Prasanth, K. V. (2012). Malat1 is not an essential component of nuclear speckles in mice. *RNA*, *18*(8), 1487–1499. https://doi.org/10.1261/RNA.033217.112

Nakamoto, M. Y., Lammer, N. C., Batey, R. T., & Wuttke, D. S. (2020). hnRNPK recognition of the B motif of Xist and other biological RNAs. *Nucleic Acids Research*, *48*(16), 9320–9335. https://doi.org/10.1093/NAR/GKAA677

Nakayamada, S., Poholek, A. C., Lu, K. T., Takahashi, H., Kato, M., Iwata, S., Hirahara, K., Cannons, J. L., Schwartzberg, P. L., Vahedi, G., Sun, H., Kanno, Y., & O'Shea, J. J. (2014). Type I Interferon induces binding of STAT1 to Bcl6: Divergent Roles of STAT-family transcription factors in the TFH cell genetic program. *Journal of Immunology (Baltimore, Md. : 1950)*, *192*(5), 2156. https://doi.org/10.4049/JIMMUNOL.1300675

Nakazawa, M., Fantappie, M. R., Freeman, G. L., Eloi-Santos, S., Olsen, N. J., Kovacs, W. J., Secor, W. E., & Colley, D. G. (1997). Schistosoma mansoni:Susceptibility Differences between Male and Female Mice Can Be Mediated by Testosterone during Early Infection. *Experimental Parasitology*, *85*(3), 233–240. https://doi.org/10.1006/EXPR.1997.4148

Navarro-Cobos, M. J., Morales-Guzman, S. I., Baldry, S. E. L., & Brown, C. J. (2022). Derivation of a minimal functional XIST by combining human and mouse interaction domains. *Human Molecular Genetics*, *32*(8), 1289. https://doi.org/10.1093/HMG/DDAC285

Nelwan, M. L. (2019). Schistosomiasis: Life Cycle, Diagnosis, and Control. *Current Therapeutic Research, Clinical and Experimental*, *91*, 5. https://doi.org/10.1016/J.CURTHERES.2019.06.001

Neumann, C., Heinrich, F., Neumann, K., Junghans, V., Mashreghi, M. F., Ahlers, J., Janke, M., Rudolph, C., Mockel-Tenbrinck, N., Kühl, A. A., Heimesaat, M. M., Esser, C., Im, S. H., Radbruch, A., Rutz, S., & Scheffold, A. (2014). Role of Blimp-1 in programing Th effector cells into IL-10 producers. *The Journal of Experimental Medicine*, *211*(9), 1807. https://doi.org/10.1084/JEM.20131548

Nguyen, T. M., Kabotyanski, E. B., Reineke, L. C., Shao, J., Xiong, F., Lee, J. H., Dubrulle, J., Johnson, H., Stossi, F., Tsoi, P. S., Choi, K. J., Ellis, A. G., Zhao, N., Cao, J., Adewunmi, O., Ferreon, J. C., Ferreon, A. C. M., Neilson, J. R., Mancini, M. A., … Rosen, J. M. (2019). The SINEB1 element in the long non-coding RNA Malat1 is necessary for TDP-43 proteostasis. *Nucleic Acids Research*, *48*(5), 2621. https://doi.org/10.1093/NAR/GKZ1176

Nickbarg, E. B., Spencer, K. B., Mortison, J. D., & Lee, J. T. (2023). Targeting RNA with small molecules: lessons learned from Xist RNA. *RNA*, *29*(4), 463. https://doi.org/10.1261/RNA.079523.122

Ning, S., Pagano, J. S., & Barber, G. N. (2011). IRF7: activation, regulation, modification and function. *Genes and Immunity*, *12*(6), 399. https://doi.org/10.1038/GENE.2011.21

Ogulur, I., Mitamura, Y., Yazici, D., Pat, Y., Ardicli, S., Li, M., D'Avino, P., Beha, C., Babayev, H., Zhao, B., Zeyneloglu, C., Giannelli Viscardi, O., Ardicli, O., Kiykim, A., Garcia-Sanchez, A., Lopez, J. F., Shi, L. L., Yang, M., Schneider, S. R., … Akdis, C. A. (2025). Type 2 immunity in allergic diseases. *Cellular & Molecular Immunology 2025 22:3*, *22*(3), 211–242. https://doi.org/10.1038/s41423-025-01261-2

O'Keefe, R. T., Mayeda, A., Sadowski, C. L., Krainer, A. R., & Spector, D. L. (1994). Disruption of pre-mRNA splicing in vivo results in reorganization of splicing factors. *Journal of Cell Biology*, *124*(3), 249–260. https://doi.org/10.1083/JCB.124.3.249

Page, S. T., Plymate, S. R., Bremner, W. J., Matsumoto, A. M., Hess, D. L., Lin, D. W., Amory, J. K., Nelson, P. S., & Wu, J. D. (2006). Effect of medical castration on

CD4+CD25+ T cells, CD8+ T cell IFN-γ expression, and NK cells: A physiological role for testosterone and/or its metabolites. *American Journal of Physiology - Endocrinology and Metabolism*, *290*(5), 856–863. https://doi.org/10.1152/AJPENDO.00484.2005/ASSET/IMAGES/LARGE/ZH100506448300004.JPEG

Panning, B. (2008). X-chromosome inactivation: The molecular basis of silencing. *Journal of Biology*, *7*(8), 1–4. https://doi.org/10.1186/JBIOL95/FIGURES/2

Papapavlou, G., Hellberg, S., Raffetseder, J., Brynhildsen, J., Gustafsson, M., Jenmalm, M. C., & Ernerudh, J. (2021). Differential effects of estradiol and progesterone on human T cell activation in vitro. *European Journal of Immunology*, *51*(10), 2430–2440. https://doi.org/10.1002/EJI.202049144;WEBSITE:WEBSITE:PERICLES;WGROUP:STRING:PUBLICATION

Papp, A. C., Pinsonneault, J. K., Cooke, G., & Sadée, W. (2003). Single Nucleotide Polymorphism Genotyping Using Allele-Specific PCR and Fluorescence Melting Curves. *BioTechniques*, *34*(5), 1068–1072. https://doi.org/10.2144/03345DD03

Park, S. H., Liu, X., Hennighausen, L., Davey, H. W., & Waxman, D. J. (1999). Distinctive Roles of STAT5a and STAT5b in Sexual Dimorphism of Hepatic P450 Gene Expression: IMPACT OF Stat5a GENE DISRUPTION. *Journal of Biological Chemistry*, *274*(11), 7421–7430. https://doi.org/10.1074/JBC.274.11.7421

Pauzaite, T., Thacker, U., Tollitt, J., & Copeland, N. A. (2016). Emerging Roles for Ciz1 in Cell Cycle Regulation and as a Driver of Tumorigenesis. *Biomolecules*, *7*(1), 1. https://doi.org/10.3390/BIOM7010001

Pelaia, C., Paoletti, G., Puggioni, F., Racca, F., Pelaia, G., Canonica, G. W., & Heffler, E. (2019). Interleukin-5 in the Pathophysiology of Severe Asthma. *Frontiers in Physiology*, *10*, 1514. https://doi.org/10.3389/FPHYS.2019.01514

Pisani, G., & Baron, B. (2019). Nuclear paraspeckles function in mediating gene regulatory and apoptotic pathways. *Non-Coding RNA Research*, *4*(4), 128. https://doi.org/10.1016/J.NCRNA.2019.11.002

Pratt, A. J., & MacRae, I. J. (2009). The RNA-induced Silencing Complex: A Versatile Gene-silencing Machine. *The Journal of Biological Chemistry*, *284*(27), 17897. https://doi.org/10.1074/JBC.R900012200

Puck, J. M., Deschenes, S. M., Porter, J. C., Dutra, A. S., Brown, C. J., Willard, H. F., & Henthorn, P. S. (1993). The interleukin-2 receptor γ chain maps to Xq13.1 and is mutated in X-linked severe combined immunodeficiency, SCIDX1. *Human Molecular Genetics*, *2*(8), 1099–1104. https://doi.org/10.1093/HMG/2.8.1099

Pujantell, M., & Altfeld, M. (2022). Consequences of sex differences in Type I IFN responses for the regulation of antiviral immunity. *Frontiers in Immunology*, *13*, 986840. https://doi.org/10.3389/FIMMU.2022.986840

Quigley, M., Huang, X., & Yang, Y. (2008). STAT1 Signaling in CD8 T Cells Is Required for Their Clonal Expansion and Memory Formation Following Viral Infection In Vivo. *The Journal of Immunology*, *180*(4), 2158–2164. https://doi.org/10.4049/JIMMUNOL.180.4.2158,

Radhouani, M., & Starkl, P. (2024). Adjuvant-independent airway sensitization and infection mouse models leading to allergic asthma. *Frontiers in Allergy*, *5*, 1423938. https://doi.org/10.3389/FALGY.2024.1423938/XML

Raghupathy, R., & Szekeres-Bartho, J. (2022). Progesterone: A Unique Hormone with Immunomodulatory Roles in Pregnancy. *International Journal of Molecular Sciences*, *23*(3), 1333. https://doi.org/10.3390/IJMS23031333

Rainard, P., Cunha, P., Martins, R. P., Gilbert, F. B., Germon, P., & Foucras, G. (2020). Type 3 immunity: a perspective for the defense of the mammary gland against infections. *Veterinary Research*, *51*(1), 1–8. https://doi.org/10.1186/S13567-020-00852-3/FIGURES/1

Raju, G. S. R., Pavitra, E., Bandaru, S. S., Varaprasad, G. L., Nagaraju, G. P., Malla, R. R., Huh, Y. S., & Han, Y. K. (2023). HOTAIR: a potential metastatic, drug-resistant and prognostic regulator of breast cancer. *Molecular Cancer 2023 22:1*, *22*(1), 1–15. https://doi.org/10.1186/S12943-023-01765-3

Rani, A., Afzali, B., Kelly, A., Tewolde-Berhan, L., Hackett, M., Kanhere, A. S., Pedroza-Pacheco, I., Bowen, H., Jurcevic, S., Jenner, R. G., Cousins, D. J., Ragheb, J. A., Lavender, P., & John, S. (2011). IL-2 REGULATES EXPRESSION OF C-MAF IN HUMAN CD4 T CELLS. *Journal of Immunology (Baltimore, Md. : 1950)*, *187*(7), 3721. https://doi.org/10.4049/JIMMUNOL.1002354

Ranzani, V., Rossetti, G., Panzeri, I., Arrigoni, A., Bonnal, R. J. P., Curti, S., Gruarin, P., Provasi, E., Sugliano, E., Marconi, M., De Francesco, R., Geginat, J., Bodega, B., Abrignani, S., & Pagani, M. (2015). LincRNA landscape in human lymphocytes highlights regulation of T cell differentiation by linc-MAF-4. *Nature Immunology*, *16*(3), 318. https://doi.org/10.1038/NI.3093

Ratchataswan, T., Banzon, T. M., Thyssen, J. P., Weidinger, S., Guttman-Yassky, E., & Phipatanakul, W. (2021). Biologics for Treatment of Atopic Dermatitis: Current

Status and Future Prospect. *The Journal of Allergy and Clinical Immunology. In Practice*, *9*(3), 1053. https://doi.org/10.1016/J.JAIP.2020.11.034

Ray, A., & Kolls, J. K. (2017). Neutrophilic Inflammation in Asthma and Association with Disease Severity. *Trends in Immunology*, *38*(12), 942. https://doi.org/10.1016/J.IT.2017.07.003

Ribeiro de Almeida, C., Heath, H., Krpic, S., Dingjan, G. M., van Hamburg, J. P., Bergen, I., van de Nobelen, S., Sleutels, F., Grosveld, F., Galjart, N., & Hendriks, R. W. (2009). Critical Role for the Transcription Regulator CCCTC-Binding Factor in the Control of Th2 Cytokine Expression. *The Journal of Immunology*, *182*(2), 999–1010. https://doi.org/10.4049/JIMMUNOL.182.2.999

Ridings-Figueroa, R., Stewart, E. R., Nesterova, T. B., Coker, H., Pintacuda, G., Godwin, J., Wilson, R., Haslam, A., Lilley, F., Ruigrok, R., Bageghni, S. A., Albadrani, G., Mansfield, W., Roulson, J. A., Brockdorff, N., Ainscough, J. F. X., & Coverley, D. (2017). The nuclear matrix protein CIZ1 facilitates localization of Xist RNA to the inactive X-chromosome territory. *Genes and Development*, *31*(9), 876–888. https://doi.org/10.1101/GAD.295907.117/-/DC1

Rijhsinghani, A. G., Thompson, K., Bhatia, S. K., & Waldschmidt, T. J. (1996). Estrogen blocks early T cell development in the thymus. *American Journal of Reproductive Immunology*, *36*(5), 269–277. https://doi.org/10.1111/J.1600-0897.1996.TB00176.X;WGROUP:STRING:PUBLICATION

Roberts, A. L., Morea, A., Amar, A., Zito, A., Moustafa, J. S. E. S., Tomlinson, M., Bowyer, R. C. E., Zhang, X., Christiansen, C., Costeira, R., Steves, C. J., Mangino, M., Bell, J. T., Wong, C. C. Y., Vyse, T. J., & Small, K. S. (2022). Age acquired

skewed X chromosome inactivation is associated with adverse health outcomes in humans. *ELife*, *11*. https://doi.org/10.7554/ELIFE.78263

Robinson, M. D., McCarthy, D. J., & Smyth, G. K. (2009). edgeR: a Bioconductor package for differential expression analysis of digital gene expression data. *Bioinformatics*, *26*(1), 139. https://doi.org/10.1093/BIOINFORMATICS/BTP616

Ross, S. H., & Cantrell, D. A. (2018). Signaling and Function of Interleukin-2 in T Lymphocytes. *Annual Review of Immunology*, *36*, 411. https://doi.org/10.1146/ANNUREV-IMMUNOL-042617-053352

Rosser, E. C., & Mauri, C. (2015). Regulatory B Cells: Origin, Phenotype, and Function. *Immunity*, *42*(4), 607–612. https://doi.org/10.1016/j.immuni.2015.04.005

Roth, D. B. (2014). V(D)J Recombination: Mechanism, Errors, and Fidelity. *Microbiology Spectrum*, *2*(6), 10.1128/microbiolspec.MDNA3-0041–2014. https://doi.org/10.1128/MICROBIOLSPEC.MDNA3-0041-2014

Ruan, X., Li, P., Chen, Y., Shi, Y., Pirooznia, M., Seifuddin, F., Suemizu, H., Ohnishi, Y., Yoneda, N., Nishiwaki, M., Shepherdson, J., Suresh, A., Singh, K., Ma, Y., Jiang, C. fei, & Cao, H. (2020). In vivo functional analysis of non-conserved human lncRNAs associated with cardiometabolic traits. *Nature Communications 2020 11:1*, *11*(1), 1–13. https://doi.org/10.1038/s41467-019-13688-z

Ruiz-Ojeda, D., Guzmán-Martín, C. A., Bojalil, R., Balderas, X. F., Paredes-González, I. S., González-Ramírez, J., Torres-Rasgado, E., Hernández-DíazCouder, A., Springall, R., & Sánchez-Muñoz, F. (2024). Long noncoding RNA MALAT1 in dermatologic disorders: a comprehensive review. *Biomarkers in Medicine*, *18*(19), 853. https://doi.org/10.1080/17520363.2024.2369044

Sadler, C. H., Rutitzky, L. I., Stadecker, M. J., & Wilson, R. A. (2003). IL-10 is crucial for the transition from acute to chronic disease state during infection of mice with Schistosoma mansoni. *European Journal of Immunology*, *33*(4), 880–888. https://doi.org/10.1002/EJI.200323501;SUBPAGE:STRING:FULL

Sallusto, F., Geginat, J., & Lanzavecchia, A. (2004). Central memory and effector memory T cell subsets: Function, generation, and maintenance. *Annual Review of Immunology*, *22*, 745–763. https://doi.org/10.1146/ANNUREV.IMMUNOL.22.012703.104702,

Sánchez-Escabias, E., Guerrero-Martínez, J. A., & Reyes, J. C. (2022). Co-transcriptional splicing efficiency is a gene-specific feature that can be regulated by TGFβ. *Communications Biology*, *5*(1), 1–13. https://doi.org/10.1038/S42003-022-03224-Z;TECHMETA

Sanders, V. M. (2006). Epigenetic regulation of Th1 and Th2 cell development. *Brain, Behavior, and Immunity*, *20*(4), 317–324. https://doi.org/10.1016/J.BBI.2005.08.005

Saraiva, M., & O'Garra, A. (2010). The regulation of IL-10 production by immune cells. *Nature Reviews Immunology 2010 10:3*, *10*(3), 170–181. https://doi.org/10.1038/nri2711

Saraiva, M., Vieira, P., & O'Garra, A. (2019). Biology and therapeutic potential of interleukin-10. *The Journal of Experimental Medicine*, *217*(1), e20190418. https://doi.org/10.1084/JEM.20190418

Schopf, L. R., Hoffmann, K. F., Cheever, A. W., Urban, J. F., & Wynn, T. A. (2002). IL-10 is critical for host resistance and survival during gastrointestinal helminth

infection. *Journal of Immunology (Baltimore, Md. : 1950)*, *168*(5), 2383–2392. https://doi.org/10.4049/JIMMUNOL.168.5.2383

Seillet, C., Laffont, S., Trémollières, F., Rouquié, N., Ribot, C., Arnal, J. F., Douin-Echinard, V., Gourdy, P., & Guéry, J. C. (2012). The TLR-mediated response of plasmacytoid dendritic cells is positively regulated by estradiol in vivo through cell-intrinsic estrogen receptor α signaling. *Blood*, *119*(2), 454–464. https://doi.org/10.1182/BLOOD-2011-08-371831

Seumois, G., Ramírez-Suástegui, C., Schmiedel, B. J., Liang, S., Peters, B., Sette, A., & Vijayanand, P. (2020). Single-cell transcriptomic analysis of allergen-specific T cells in allergy and asthma. *Science Immunology*, *5*(48). https://doi.org/10.1126/SCIIMMUNOL.ABA6087/SUPPL_FILE/ABA6087_TABLE_S5.XLSX

Shaker, O. G., Mahmoud, R. H., Abdelaleem, O. O., Ibrahem, E. G., Mohamed, A. A., Zaki, O. M., Abdelghaffar, N. K., Ahmed, T. I., Hemeda, N. F., Ahmed, N. A., & Mansour, D. F. (2019). LncRNAs, MALAT1 and lnc-DC as potential biomarkers for multiple sclerosis diagnosis. *Bioscience Reports*, *39*(1), BSR20181335. https://doi.org/10.1042/BSR20181335

Sharma, A., Takata, H., Shibahara, K. I., Bubulya, A., & Bubulya, P. A. (2010). Son Is Essential for Nuclear Speckle Organization and Cell Cycle Progression. *Molecular Biology of the Cell*, *21*(4), 650. https://doi.org/10.1091/MBC.E09-02-0126

Sharma, S., Findlay, G. M., Bandukwala, H. S., Oberdoerffer, S., Baust, B., Li, Z., Schmidt, V., Hogan, P. G., Sacks, D. B., & Rao, A. (2011). Dephosphorylation of the nuclear factor of activated T cells (NFAT) transcription factor is regulated by an RNA-protein scaffold complex. *Proceedings of the National Academy of Sciences*

of the United States of America, *108*(28), 11381–11386. https://doi.org/10.1073/PNAS.1019711108/SUPPL_FILE/PNAS.1019711108_SI.PDF

Shevyrev, D., & Tereshchenko, V. (2020). Treg Heterogeneity, Function, and Homeostasis. *Frontiers in Immunology*, *10*, 495736. https://doi.org/10.3389/FIMMU.2019.03100/XML

Shi, Z., Zheng, Z., Lin, X., & Ma, H. (2021). Long Noncoding RNA MALAT1 Regulates the Progression of Atherosclerosis by miR-330-5p/NF-kB Signal Pathway. *Journal of Cardiovascular Pharmacology*, *78*(2), 235–246. https://doi.org/10.1097/FJC.0000000000001061

Shih, C. H., Chuang, L. L., Tsai, M. H., Chen, L. H., Chuang, E. Y., Lu, T. P., & Lai, L. C. (2021). Hypoxia-Induced MALAT1 Promotes the Proliferation and Migration of Breast Cancer Cells by Sponging MiR-3064-5p. *Frontiers in Oncology*, *11*, 658151. https://doi.org/10.3389/FONC.2021.658151/BIBTEX

Shinn, M. K., Tomares, D. T., Liu, V., Pant, A., Qiu, Y., Song, Y. J., Ayala, Y., Strout, G. W., Ruff, K. M., Lew, M. D., Prasanth, K. V, Pappu, R. V, & Louis, S. (2025). Nuclear speckle proteins form intrinsic and MALAT1-dependent microphases. *BioRxiv*, 2025.02.26.640430. https://doi.org/10.1101/2025.02.26.640430

Shoemaker, J., Saraiva, M., & O'Garra, A. (2006). GATA-3 Directly Remodels the IL-10 Locus Independently of IL-4 in CD4+ T Cells . *The Journal of Immunology*, *176*(6), 3470–3479. https://doi.org/10.4049/JIMMUNOL.176.6.3470,

Shouse, A. N., LaPorte, K. M., & Malek, T. R. (2024). Interleukin-2 signaling in the regulation of T cell biology in autoimmunity and cancer. *Immunity*, *57*(3), 414–428. https://doi.org/10.1016/J.IMMUNI.2024.02.001

Shui, J.-W., Hu, M. C.-T., & Tan, T.-H. (2006). Conditional Knockout Mice Reveal an Essential Role of Protein Phosphatase 4 in Thymocyte Development and Pre-T-Cell Receptor Signaling. *Molecular and Cellular Biology*, *27*(1), 79. https://doi.org/10.1128/MCB.00799-06

Sirey, T. M., Roberts, K., Haerty, W., Bedoya-Reina, O., Granados, S. R., Tan, J. Y., Li, N., Heather, L. C., Carter, R. N., Cooper, S., Finch, A. J., Wills, J., Morton, N. M., Marques, A. C., & Ponting, C. P. (2019). The long non-coding RNA Cerox1 is a post transcriptional regulator of mitochondrial complex I catalytic activity. *ELife*, *8*, e45051. https://doi.org/10.7554/ELIFE.45051

Sofi, S., & Coverley, D. (2023). CIZ1 in Xist seeded assemblies at the inactive X chromosome. *Frontiers in Cell and Developmental Biology*, *11*, 1296600. https://doi.org/10.3389/FCELL.2023.1296600

Song, P., Adeloye, D., Salim, H., Dos Santos, J. P., Campbell, H., Sheikh, A., & Rudan, I. (2022). Global, regional, and national prevalence of asthma in 2019: a systematic analysis and modelling study. *Journal of Global Health*, *12*, 04052. https://doi.org/10.7189/JOGH.12.04052

Souyris, M., Cenac, C., Azar, P., Daviaud, D., Canivet, A., Grunenwald, S., Pienkowski, C., Chaumeil, J., Mejía, J. E., & Guéry, J. C. (2018). TLR7 escapes X chromosome inactivation in immune cells. *Science Immunology*, *3*(19). https://doi.org/10.1126/SCIIMMUNOL.AAP8855/SUPPL_FILE/AAP8855_MOVIE_S1.AVI

Spector, D. L., & Lamond, A. I. (2011). Nuclear Speckles. *Cold Spring Harbor Perspectives in Biology*, *3*(2), a000646. https://doi.org/10.1101/CSHPERSPECT.A000646

Spellberg, B., & Edwards, J. E. (2001). Type 1/Type 2 Immunity in Infectious Diseases. *Clinical Infectious Diseases*, *32*(1), 76–102. https://doi.org/10.1086/317537

Spiniello, M., Knoener, R. A., Steinbrink, M. I., Yang, B., Cesnik, A. J., Buxton, K. E., Scalf, M., Jarrard, D. F., & Smith, L. M. (2018). HyPR-MS for Multiplexed Discovery of MALAT1, NEAT1, and NORAD lncRNA Protein Interactomes. *Journal of Proteome Research*, *17*(9), 3022–3038. https://doi.org/10.1021/ACS.JPROTEOME.8B00189

Stark, R., Grzelak, M., & Hadfield, J. (2019). RNA sequencing: the teenage years. *Nature Reviews Genetics 2019 20:11*, *20*(11), 631–656. https://doi.org/10.1038/s41576-019-0150-2

Statello, L., Guo, C. J., Chen, L. L., & Huarte, M. (2020). Gene regulation by long non-coding RNAs and its biological functions. *Nature Reviews Molecular Cell Biology 2020 22:2*, *22*(2), 96–118. https://doi.org/10.1038/s41580-020-00315-9

Stork, C., Li, Z., Lin, L., & Zheng, S. (2018). Developmental Xist induction is mediated by enhanced splicing. *Nucleic Acids Research*, *47*(3), 1532. https://doi.org/10.1093/NAR/GKY1198

Subramanian, A., Tamayo, P., Mootha, V. K., Mukherjee, S., Ebert, B. L., Gillette, M. A., Paulovich, A., Pomeroy, S. L., Golub, T. R., Lander, E. S., & Mesirov, J. P. (2005). Gene set enrichment analysis: A knowledge-based approach for interpreting genome-wide expression profiles. *Proceedings of the National Academy of Sciences of the United States of America*, *102*(43), 15545–15550. https://doi.org/10.1073/PNAS.0506580102/SUPPL_FILE/06580FIG7.JPG

Sumida, T. S., Dulberg, S., Schupp, J. C., Lincoln, M. R., Stillwell, H. A., Axisa, P. P., Comi, M., Unterman, A., Kaminski, N., Madi, A., Kuchroo, V. K., & Hafler, D. A.

(2022). Type I interferon transcriptional network regulates expression of coinhibitory receptors in human T cells. *Nature Immunology 2022 23:4*, *23*(4), 632–642. https://doi.org/10.1038/s41590-022-01152-y

Syrett, C. M., Paneru, B., Sandoval-Heglund, D., Wang, J., Banerjee, S., Sindhava, V., Behrens, E. M., Atchison, M., & Anguera, M. C. (2019). Altered X-chromosome inactivation in T cells may promote sex-biased autoimmune diseases. *JCI Insight*, *4*(7). https://doi.org/10.1172/JCI.INSIGHT.126751

Szklarczyk, D., Kirsch, R., Koutrouli, M., Nastou, K., Mehryary, F., Hachilif, R., Gable, A. L., Fang, T., Doncheva, N. T., Pyysalo, S., Bork, P., Jensen, L. J., & Von Mering, C. (2023). The STRING database in 2023: protein–protein association networks and functional enrichment analyses for any sequenced genome of interest. *Nucleic Acids Research*, *51*(D1), D638–D646. https://doi.org/10.1093/NAR/GKAC1000

Taiana, E., Ronchetti, D., Todoerti, K., Nobili, L., Tassone, P., Amodio, N., & Neri, A. (2020). LncRNA NEAT1 in Paraspeckles: A Structural Scaffold for Cellular DNA Damage Response Systems? *Non-Coding RNA*, *6*(3), 26. https://doi.org/10.3390/NCRNA6030026

Tao, X., Constant, S., Jorritsma, P., & Bottomly, K. (1997). Strength of TCR signal determines the costimulatory requirements for Th1 and Th2 CD4+ T cell differentiation. *The Journal of Immunology*, *159*(12), 5956–5963. https://doi.org/10.4049/JIMMUNOL.159.12.5956

Tian, J., Zhang, D., Yang, Y., Huang, Y., Wang, L., Yao, X., & Lu, Q. (2023). Global epidemiology of atopic dermatitis: a comprehensive systematic analysis and

modelling study. *British Journal of Dermatology*, *190*(1), 55–61. https://doi.org/10.1093/BJD/LJAD339

Tian, W., Du, Y., Ma, Y., Gu, L., Zhou, J., & Deng, D. (2018). MALAT1–miR663a negative feedback loop in colon cancer cell functions through direct miRNA–lncRNA binding. *Cell Death and Disease*, *9*(9), 1–12. https://doi.org/10.1038/S41419-018-0925-Y;TECHMETA=106,109,13,38,42,44,61,77,89;KWRD=LIFE+SCIENCES

Tibbitt, C. A., Stark, J. M., Martens, L., Ma, J., Mold, J. E., Deswarte, K., Oliynyk, G., Feng, X., Lambrecht, B. N., De Bleser, P., Nylén, S., Hammad, H., Arsenian Henriksson, M., Saeys, Y., & Coquet, J. M. (2019). Single-Cell RNA Sequencing of the T Helper Cell Response to House Dust Mites Defines a Distinct Gene Expression Signature in Airway Th2 Cells. *Immunity*, *51*(1), 169-184.e5. https://doi.org/10.1016/J.IMMUNI.2019.05.014

Titus, K. R., Simandi, Z., Chandrashekar, H., Paquet, D., & Phillips-Cremins, J. E. (2024). Cell-type-specific loops linked to RNA polymerase II elongation in human neural differentiation. *Cell Genomics*, *4*(8), 100606. https://doi.org/10.1016/J.XGEN.2024.100606

Tjalsma, S. J. D., Hori, M., Sato, Y., Bousard, A., Ohi, A., Raposo, A. C., Roensch, J., Saux, A. Le, Nogami, J., Maehara, K., Kujirai, T., Handa, T., Bagés-Arnal, S., Ohkawa, Y., Kurumizaka, H., Rocha, S. T. da, Żylicz, J. J., Kimura, H., & Heard, E. (2021). H4K20me1 and H3K27me3 are concurrently loaded onto the inactive X chromosome but dispensable for inducing gene silencing. *EMBO Reports*, *22*(3), e51989. https://doi.org/10.15252/EMBR.202051989

Trienekens, S. C. M., Faust, C. L., Meginnis, K., Pickering, L., Ericssonid, O., Nankasi, A., Moses, A., Tukahebwa, E. M., & Lamberton, P. H. L. (2020). Impacts of host gender on Schistosoma mansoni risk in rural Uganda—A mixed-methods approach. *PLOS Neglected Tropical Diseases*, *14*(5), e0008266. https://doi.org/10.1371/JOURNAL.PNTD.0008266

Trinchieri, G. (2007). Interleukin-10 production by effector T cells: Th1 cells show self control. *Journal of Experimental Medicine*, *204*(2), 239–243. https://doi.org/10.1084/JEM.20070104

Tripathi, V., Ellis, J. D., Shen, Z., Song, D. Y., Pan, Q., Watt, A. T., Freier, S. M., Bennett, C. F., Sharma, A., Bubulya, P. A., Blencowe, B. J., Prasanth, S. G., & Prasanth, K. V. (2010). The Nuclear-Retained Noncoding RNA MALAT1 Regulates Alternative Splicing by Modulating SR Splicing Factor Phosphorylation. *Molecular Cell*, *39*(6), 925. https://doi.org/10.1016/J.MOLCEL.2010.08.011

Tripathi, V., Shen, Z., Chakraborty, A., Giri, S., Freier, S. M., Wu, X., Zhang, Y., Gorospe, M., Prasanth, S. G., Lal, A., & Prasanth, K. V. (2013). Long Noncoding RNA MALAT1 Controls Cell Cycle Progression by Regulating the Expression of Oncogenic Transcription Factor B-MYB. *PLOS Genetics*, *9*(3), e1003368. https://doi.org/10.1371/JOURNAL.PGEN.1003368

Trotman, J. B., A Braceros, K. C., Cherney, R. E., Murvin, M. M., Mauro Calabrese, J., Mauro Calabrese, C. J., Y W O R D S Airn, K. E., & Keean A Braceros, X. C. (2021). The control of polycomb repressive complexes by long noncoding RNAs. *Wiley Interdisciplinary Reviews: RNA*, *12*(6), e1657. https://doi.org/10.1002/WRNA.1657

Tsagakis, I., Douka, K., Birds, I., & Aspden, J. L. (2020). Long non-coding RNAs in development and disease: conservation to mechanisms. In *Journal of Pathology* (Vol. 250, Number 5, pp. 480–495). John Wiley and Sons Ltd. https://doi.org/10.1002/path.5405

Tsymala, I., & Kuchler, K. (2023). Innate lymphoid cells—Underexplored guardians of immunity. *PLOS Pathogens*, *19*(10), e1011678. https://doi.org/10.1371/JOURNAL.PPAT.1011678

Vasques, L. R., & Pereira, L. V. (2001). Allele-specific X-linked gene activity in normal human cells assayed by expressed single nucleotide polymorphisms (cSNPs). *DNA Research*, *8*(4), 173–177. https://doi.org/10.1093/DNARES/8.4.173,

Voehringer, D., Reese, T. A., Huang, X., Shinkai, K., & Locksley, R. M. (2006). Type 2 immunity is controlled by IL-4/IL-13 expression in hematopoietic non-eosinophil cells of the innate immune system. *The Journal of Experimental Medicine*, *203*(6), 1435. https://doi.org/10.1084/JEM.20052448

Voruganti, A., & Bowness, P. (2020). New developments in our understanding of ankylosing spondylitis pathogenesis. *Immunology*, *161*(2), 94. https://doi.org/10.1111/IMM.13242

Wainer Katsir, K., & Linial, M. (2019). Human genes escaping X-inactivation revealed by single cell expression data. *BMC Genomics*, *20*(1), 1–17. https://doi.org/10.1186/S12864-019-5507-6/FIGURES/6

Wang, B., & Bian, Q. (2025). Regulation of 3D genome organization during T cell activation. *The FEBS Journal*, *292*(8), 1833–1852. https://doi.org/10.1111/FEBS.17211

Wang, D., Ding, L., Wang, L., Zhao, Y., Sun, Z., Karnes, R. J., Zhang, J., & Huang, H. (2015). LncRNA MALAT1 enhances oncogenic activities of EZH2 in castration-resistant prostate cancer. *Oncotarget*, *6*(38), 41045. https://doi.org/10.18632/ONCOTARGET.5728

Wang, D., Zheng, X., Chai, L., Zhao, J., Zhu, J., Li, Y., Yang, P., Mao, Q., & Xia, H. (2023). FAM76B regulates NF-κB-mediated inflammatory pathway by influencing the translocation of hnRNPA2B1. *ELife*, *12*, e85659. https://doi.org/10.7554/ELIFE.85659

Wang, J., Syrett, C. M., Kramer, M. C., Basu, A., Atchison, M. L., & Anguera, M. C. (2016). Unusual maintenance of X chromosome inactivation predisposes female lymphocytes for increased expression from the inactive X. *Proceedings of the National Academy of Sciences of the United States of America*, *113*(14), E2029–E2038. https://doi.org/10.1073/PNAS.1520113113/SUPPL_FILE/PNAS.201520113SI.PDF

Wang, J. Z., Xiang, J. J., Wu, L. G., Bai, Y. Sen, Chen, Z. W., Yin, X. Q., Wang, Q., Guo, W. H., Peng, Y., Guo, H., & Xu, P. (2017). A genetic variant in long non-coding RNA MALAT1 associated with survival outcome among patients with advanced lung adenocarcinoma: A survival cohort analysis. *BMC Cancer*, *17*(1), 1–8. https://doi.org/10.1186/S12885-017-3151-6/FIGURES/2

Wang, M., Windgassen, D., & Papoutsakis, E. T. (2008). Comparative analysis of transcriptional profiling of CD3+, CD4+ and CD8+ T cells identifies novel immune response players in T-Cell activation. *BMC Genomics*, *9*(1), 1–16. https://doi.org/10.1186/1471-2164-9-225/FIGURES/9

Wang, X., Sehgal, L., Jain, N., Khashab, T., Mathur, R., & Samaniego, F. (2016). LncRNA MALAT1 promotes development of mantle cell lymphoma by associating with EZH2. *Journal of Translational Medicine*, *14*(1), 346. https://doi.org/10.1186/S12967-016-1100-9

Wang, Y., Zhao, Y., Bollas, A., Wang, Y., & Au, K. F. (2021). Nanopore sequencing technology, bioinformatics and applications. *Nature Biotechnology 2021 39:11*, *39*(11), 1348–1365. https://doi.org/10.1038/s41587-021-01108-x

Wang, Z., Li, K., Chen, W., Wang, X., Huang, Y., Wang, W., Wu, W., Cai, Z., & Huang, W. (2020). Modulation of SRSF2 expression reverses the exhaustion of TILs via the epigenetic regulation of immune checkpoint molecules. *Cellular and Molecular Life Sciences*, *77*(17), 3441–3452. https://doi.org/10.1007/S00018-019-03362-4/FIGURES/6

Warren, K. J., Sweeter, J. M., Pavlik, J. A., Nelson, A. J., Devasure, J. M., Dickinson, J. D., Sisson, J. H., Wyatt, T. A., & Poole, J. A. (2017). Sex differences in activation of lung-related type 2 innate lymphoid cells in experimental asthma. *Annals of Allergy, Asthma & Immunology*, *118*(2), 233–234. https://doi.org/10.1016/J.ANAI.2016.11.011

Webb, K., Peckham, H., Radziszewska, A., Menon, M., Oliveri, P., Simpson, F., Deakin, C. T., Lee, S., Ciurtin, C., Butler, G., Wedderburn, L. R., & Ioannou, Y. (2019). Sex and pubertal differences in the type 1 interferon pathway associate with both X chromosome number and serum sex hormone concentration. *Frontiers in Immunology*, *10*(JAN), 3167. https://doi.org/10.3389/FIMMU.2018.03167/FULL

Webster, H. C., Gamino, V., Andrusaite, A. T., Ridgewell, O. J., McCowan, J., Shergold, A. L., Heieis, G. A., Milling, S. W. F., Maizels, R. M., & Perona-Wright, G.

(2022). Tissue-based IL-10 signalling in helminth infection limits IFNγ expression and promotes the intestinal Th2 response. *Mucosal Immunology 2022 15:6*, *15*(6), 1257–1269. https://doi.org/10.1038/s41385-022-00513-y

Wei, G., Wei, L., Zhu, J., Zang, C., Hu-Li, J., Yao, Z., Cui, K., Kanno, Y., Roh, T. Y., Watford, W. T., Schones, D. E., Peng, W., Sun, H. wei, Paul, W. E., O'Shea, J. J., & Zhao, K. (2009). Global Mapping of H3K4me3 and H3K27me3 Reveals Specificity and Plasticity in Lineage Fate Determination of Differentiating CD4+ T Cells. *Immunity*, *30*(1), 155–167. https://doi.org/10.1016/J.IMMUNI.2008.12.009

West, J. A., Davis, C. P., Sunwoo, H., Simon, M. D., Sadreyev, R. I., Wang, P. I., Tolstorukov, M. Y., & Kingston, R. E. (2014). The Long Noncoding RNAs NEAT1 and MALAT1 Bind Active Chromatin Sites. *Molecular Cell*, *55*(5), 791–802. https://doi.org/10.1016/J.MOLCEL.2014.07.012

Wilusz, J. E., Freier, S. M., & Spector, D. L. (2008). 3′ End Processing of a Long Nuclear-Retained Noncoding RNA Yields a tRNA-like Cytoplasmic RNA. *Cell*, *135*(5), 919–932. https://doi.org/10.1016/J.CELL.2008.10.012

Wilusz, J. E., JnBaptiste, C. K., Lu, L. Y., Kuhn, C. D., Joshua-Tor, L., & Sharp, P. A. (2012). A triple helix stabilizes the 3′ ends of long noncoding RNAs that lack poly(A) tails. *Genes & Development*, *26*(21), 2392. https://doi.org/10.1101/GAD.204438.112

Wohlfert, E. A., Grainger, J. R., Bouladoux, N., Konkel, J. E., Oldenhove, G., Ribeiro, C. H., Hall, J. A., Yagi, R., Naik, S., Bhairavabhotla, R., Paul, W. E., Bosselut, R., Wei, G., Zhao, K., Oukka, M., Zhu, J., & Belkaid, Y. (2011). GATA3 controls Foxp3+ regulatory T cell fate during inflammation in mice. *The Journal of Clinical Investigation*, *121*(11), 4503. https://doi.org/10.1172/JCI57456

Woo, L. N., Guo, W. Y., Wang, X., Young, A., Salehi, S., Hin, A., Zhang, Y., Scott, J. A., & Chow, C. W. (2018). A 4-Week Model of House Dust Mite (HDM) Induced Allergic Airways Inflammation with Airway Remodeling. *Scientific Reports 2018 8:1*, *8*(1), 1–11. https://doi.org/10.1038/s41598-018-24574-x

Wright, J. E., Werkman, M., Dunn, J. C., & Anderson, R. M. (2018). Current epidemiological evidence for predisposition to high or low intensity human helminth infection: a systematic review. *Parasites & Vectors*, *11*(1), 65. https://doi.org/10.1186/S13071-018-2656-4

Wu, G. Y., & Halim, M. H. (2000). Schistosomiasis: progress and problems. *World Journal of Gastroenterology*, *6*(1), 12. https://doi.org/10.3748/WJG.V6.I1.12

Wu, H., Lu, Y., Duan, Z., Wu, J., Lin, M., Wu, Y., Han, S., Li, T., Fan, Y., Hu, X., Xiao, H., Feng, J., Lu, Z., Kong, D., & Li, S. (2023). Nanopore long-read RNA sequencing reveals functional alternative splicing variants in human vascular smooth muscle cells. *Communications Biology 2023 6:1*, *6*(1), 1–12. https://doi.org/10.1038/s42003-023-05481-y

Wu, J., Xiao, Y., Liu, Y., Wen, L., Jin, C., Liu, S., Paul, S., He, C., Regev, O., & Fei, J. (2024). Dynamics of RNA localization to nuclear speckles are connected to splicing efficiency. *Science Advances*, *10*(42), eadp7727. https://doi.org/10.1126/SCIADV.ADP7727

Wu, J., Zhang, H., Zheng, Y., Jin, X., Liu, M., Li, S., Zhao, Q., Liu, X., Wang, Y., Shi, M., Zhang, S., Tian, J., Sun, Y., Zhang, M., & Yu, B. (2018). The long noncoding RNA MALAT1 induces tolerogenic dendritic cells and regulatory T cells via miR155/dendritic cell-specific intercellular adhesion molecule-3 grabbing

nonintegrin/IL10 axis. *Frontiers in Immunology*, *9*(AUG), 1847. https://doi.org/10.3389/FIMMU.2018.01847/BIBTEX

Wu, X. H., Zhao, S. J., Huang, W. Q., Huang, L. H., Luo, X. Y., & Long, S. L. (2022). Long non-coding RNA MALAT1 promotes Th2 differentiation by regulating microRNA-135b-5p/GATA-3 axis in children with allergic rhinitis. *Kaohsiung Journal of Medical Sciences*, *38*(10), 971–980. https://doi.org/10.1002/KJM2.12587;WGROUP:STRING:PUBLICATION

Xiao, J., Lin, L., Luo, D., Shi, L., Chen, W., Fan, H., Li, Z., Ma, X., Ni, P., Yang, L., & Xu, Z. (2020). Long noncoding RNA TRPM2-AS acts as a microRNA sponge of miR-612 to promote gastric cancer progression and radioresistance. *Oncogenesis*, *9*(3), 29. https://doi.org/10.1038/S41389-020-0215-2

Xie, S. Q., Martin, S., Guillot, P. V., Bentley, D. L., & Pombo, A. (2006). Splicing Speckles Are Not Reservoirs of RNA Polymerase II, but Contain an Inactive Form, Phosphorylated on Serine2 Residues of the C-Terminal Domain. *Molecular Biology of the Cell*, *17*(4), 1723. https://doi.org/10.1091/MBC.E05-08-0726

Xu, J., Sun, X., Chen, Z., Ma, H., & Liu, Y. (2024). Super-resolution imaging of T lymphocyte activation reveals chromatin decondensation and disrupted nuclear envelope. *Communications Biology*, *7*(1), 1–11. https://doi.org/10.1038/S42003-024-06393-1;TECHMETA

Xue, Y., Ke, J., Zhou, X., Chen, Q., Chen, M., Huang, T., Lin, F., & Chen, F. (2022). Knockdown of LncRNA MALAT1 Alleviates Coxsackievirus B3-Induced Acute Viral Myocarditis in Mice via Inhibiting Th17 Cells Differentiation. *Inflammation 2021 45:3*, *45*(3), 1186–1198. https://doi.org/10.1007/S10753-021-01612-X

YaliChe, Y. C., Liu, J., Zhang, X., Zhu, H., Wang, Y., Li, Z., Liu, Y., Liu, S., Liu, S., Li, N., Chen, K., & Cao, X. (2022). lncRNA-GM targets Foxo1 to promote T cell–mediated autoimmunity. *Science Advances*, *8*(31), eabn9181. https://doi.org/10.1126/SCIADV.ABN9181

Yáñez, A., Bono, C., & Goodridge, H. S. (2022). Heterogeneity and origins of myeloid cells. *Current Opinion in Hematology*, *29*(4), 201. https://doi.org/10.1097/MOH.0000000000000716

Yang, H., Liang, N., Wang, M., Fei, Y., Sun, J., Li, Z., Xu, Y., Guo, C., Cao, Z., Li, S., Jiao, Y., Yang, H., Liang, N., Wang, M., Fei, Y., Sun, J., Li, Z., Xu, Y., Guo, C., … Jiao, Y. (2017). Long noncoding RNA MALAT-1 is a novel inflammatory regulator in human systemic lupus erythematosus. *Oncotarget*, *8*(44), 77400–77406. https://doi.org/10.18632/ONCOTARGET.20490

Yang, L., Lin, C., Liu, W., Zhang, J., Ohgi, K. A., Grinstein, J. D., Dorrestein, P. C., & Rosenfeld, M. G. (2011). NcRNA- and Pc2 methylation-dependent gene relocation between nuclear structures mediates gene activation programs. *Cell*, *147*(4), 773–788. https://doi.org/10.1016/j.cell.2011.08.054

Yang, X., Bam, M., Becker, W., Nagarkatti, P. S., & Nagarkatti, M. (2020). lncRNA AW112010 promotes the differentiation of inflammatory T cells by suppressing IL10 expression through histone demethylation. *Journal of Immunology (Baltimore, Md. : 1950)*, *205*(4), 987. https://doi.org/10.4049/JIMMUNOL.2000330

Yano, S., Ghosh, P., Kusaba, H., Buchholz, M., & Longo, D. L. (2003). Effect of Promoter Methylation on the Regulation of IFN-γ Gene During In Vitro Differentiation of Human Peripheral Blood T Cells into a Th2 Population. *The*

Journal of Immunology, *171*(5), 2510–2516. https://doi.org/10.4049/JIMMUNOL.171.5.2510

Yao, Y., Guo, W., Chen, J., Guo, P., Yu, G., Liu, J., Wang, F., Liu, J., You, M., Zhao, T., Kang, Y., Ma, X., & Yu, S. (2018). Long noncoding RNA Malat1 is not essential for T cell development and response to LCMV infection. *RNA Biology*, *15*(12), 1477. https://doi.org/10.1080/15476286.2018.1551705

Ye, M., Xie, L., Zhang, J., Liu, B., Liu, X., He, J., Ma, D., & Dong, K. (2020). Determination of long non-coding RNAs associated with EZH2 in neuroblastoma by RIP-seq, RNA-seq and ChIP-seq. *Oncology Letters*, *20*(4). https://doi.org/10.3892/OL.2020.11862

Yoon, J. H., Abdelmohsen, K., Srikantan, S., Yang, X., Martindale, J. L., De, S., Huarte, M., Zhan, M., Becker, K. G., & Gorospe, M. (2012). LincRNA-p21 Suppresses Target mRNA Translation. *Molecular Cell*, *47*(4), 648–655. https://doi.org/10.1016/J.MOLCEL.2012.06.027

Youness, A., Cenac, C., Faz-López, B., Grunenwald, S., Barrat, F. J., Chaumeil, J., Mejía, J. E., & Guéry, J. C. (2023). TLR8 escapes X chromosome inactivation in human monocytes and CD4+ T cells. *Biology of Sex Differences*, *14*(1), 60. https://doi.org/10.1186/S13293-023-00544-5

Youness, A., Miquel, C. H., & Guéry, J. C. (2021). Escape from X Chromosome Inactivation and the Female Predominance in Autoimmune Diseases. *International Journal of Molecular Sciences*, *22*(3), 1114. https://doi.org/10.3390/IJMS22031114

Young, M. D., Willson, T. A., Wakefield, M. J., Trounson, E., Hilton, D. J., Blewitt, M. E., Oshlack, A., & Majewski, I. J. (2011). ChIP-seq analysis reveals distinct

H3K27me3 profiles that correlate with transcriptional activity. *Nucleic Acids Research*, *39*(17), 7415. https://doi.org/10.1093/NAR/GKR416

Yssel, H., De Waal Malefyt, R., Roncarolo, M. G., Abrams, J. S., Lahesmaa, R., Spits, H., & de Vries, J. E. (1992). IL-10 is produced by subsets of human CD4+ T cell clones and peripheral blood T cells. *The Journal of Immunology*, *149*(7), 2378–2384. https://doi.org/10.4049/JIMMUNOL.149.7.2378

Zemmour, D., Pratama, A., Loughhead, S. M., Mathis, Di., & Benoist, C. (2017). Flicr, a long noncoding RNA, modulates Foxp3 expression and autoimmunity. *Proceedings of the National Academy of Sciences of the United States of America*, *114*(17), E3472–E3480. https://doi.org/10.1073/PNAS.1700946114/-/DCSUPPLEMENTAL

Zhang, B., Arun, G., Mao, Y. S., Lazar, Z., Hung, G., Bhattacharjee, G., Xiao, X., Booth, C. J., Wu, J., Zhang, C., & Spector, D. L. (2012). The lncRNA Malat1 is dispensable for mouse development but its transcription plays a cis-regulatory role in the adult. *Cell Reports*, *2*(1), 111. https://doi.org/10.1016/J.CELREP.2012.06.003

Zhang, H., & Kuchroo, V. (2019). Epigenetic and transcriptional mechanisms for the regulation of IL-10. *Seminars in Immunology*, *44*, 101324. https://doi.org/10.1016/J.SMIM.2019.101324

Zhang, K., Chen, L., Zhu, C., Zhang, M., & Liang, C. (2023). Current Knowledge of Th22 Cell and IL-22 Functions in Infectious Diseases. *Pathogens*, *12*(2), 176. https://doi.org/10.3390/PATHOGENS12020176

Zhang, L., Xiao, X., Arnold, P. R., & Li, X. C. (2019). Transcriptional and epigenetic regulation of immune tolerance: roles of the NF-κB family members. *Cellular and Molecular Immunology*, *16*(4), 315. https://doi.org/10.1038/S41423-019-0202-8

Zhang, L., Yuan, S., Cheng, G., & Guo, B. (2011). Type I IFN Promotes IL-10 Production from T Cells to Suppress Th17 Cells and Th17-Associated Autoimmune Inflammation. *PLoS ONE*, *6*(12), e28432. https://doi.org/10.1371/JOURNAL.PONE.0028432

Zhang, N., & Bevan, M. J. (2011). CD8+ T Cells: Foot Soldiers of the Immune System. *Immunity*, *35*(2), 161–168. https://doi.org/10.1016/j.immuni.2011.07.010

Zhang, Y., Kinkel, S., Maksimovic, J., Bandala-Sanchez, E., Tanzer, M. C., Naselli, G., Zhang, J. G., Zhan, Y., Lew, A. M., Silke, J., Oshlack, A., Blewitt, M. E., & Harrison, L. C. (2014). The polycomb repressive complex 2 governs life and death of peripheral T cells. *Blood*, *124*(5), 737–749. https://doi.org/10.1182/BLOOD-2013-12-544106

Zhao, G., Su, Z., Song, D., Mao, Y., & Mao, X. (2016). The long noncoding RNA MALAT1 regulates the lipopolysaccharide-induced inflammatory response through its interaction with NF-κB. *FEBS Letters*, *590*(17), 2884–2895. https://doi.org/10.1002/1873-3468.12315

Zhao, Y., Ning, J., Teng, H., Deng, Y., Sheldon, M., Shi, L., Martinez, C., Zhang, J., Tian, A., Sun, Y., Nakagawa, S., Yao, F., Wang, H., & Ma, L. (2024). Long noncoding RNA Malat1 protects against osteoporosis and bone metastasis. *Nature Communications 2024 15:1*, *15*(1), 2384-. https://doi.org/10.1038/s41467-024-46602-3

Zheremyan, E. A., Kon, N. R., Ustiugova, A. S., Stasevich, E. M., Bogomolova, E. A., Murashko, M. M., Uvarova, A. N., Demin, D. E., Kuprash, D. V., & Korneev, K. V. (2025). The half-century odyssey of regulatory B cells: from Breg discovery to emerging frontiers. *Frontiers in Immunology*, *16*, 1681082. https://doi.org/10.3389/fimmu.2025.1681082

Zhong, H., Gui, X., Hou, L., Lv, R., & Jin, Y. (2022). From Inflammation to Fibrosis: Novel Insights into the Roles of High Mobility Group Protein Box 1 in Schistosome-Induced Liver Damage. *Pathogens*, *11*(3), 289. https://doi.org/10.3390/PATHOGENS11030289

Zhou, H. J., Wang, L. Q., Wang, D. B., Yu, J. B., Zhu, Y., Xu, Q. S., Zheng, X. J., & Zhan, R. Y. (2018). Long noncoding RNA MALAT1 contributes to inflammatory response of microglia following spinal cord injury via the modulation of a miR-199b/IKKβ/NF-κB signaling pathway. *Https://Doi.Org/10.1152/Ajpcell.00278.2017*, *315*(1), C52–C61. https://doi.org/10.1152/AJPCELL.00278.2017

Zhou, S., Cerny, A. M., Fitzgerald, K. A., Kurt-Jones, E. A., & Finberg, R. W. (2012). Role of Interferon Regulatory Factor 7 in T Cell Responses during Acute Lymphocytic Choriomeningitis Virus Infection. *Journal of Virology*, *86*(20), 11254. https://doi.org/10.1128/JVI.00576-12

Zhu, J., Cote-Sierra, J., Guo, L., & Paul, W. E. (2003). Stat5 Activation Plays a Critical Role in Th2 Differentiation. *Immunity*, *19*(5), 739–748. https://doi.org/10.1016/S1074-7613(03)00292-9

Zitzmann, M., Erren, M., Kamischke, A., Simoni, M., & Nieschlag, E. (2005). Endogenous Progesterone and the Exogenous Progestin Norethisterone Enanthate

Are Associated with a Proinflammatory Profile in Healthy Men. *The Journal of Clinical Endocrinology & Metabolism*, *90*(12), 6603–6608. https://doi.org/10.1210/JC.2005-0847

Zuk, M., & McKean, K. A. (1996). Sex differences in parasite infections: Patterns and processes. *International Journal for Parasitology*, *26*(10), 1009–1024. https://doi.org/10.1016/S0020-7519(96)80001-4

Appendix

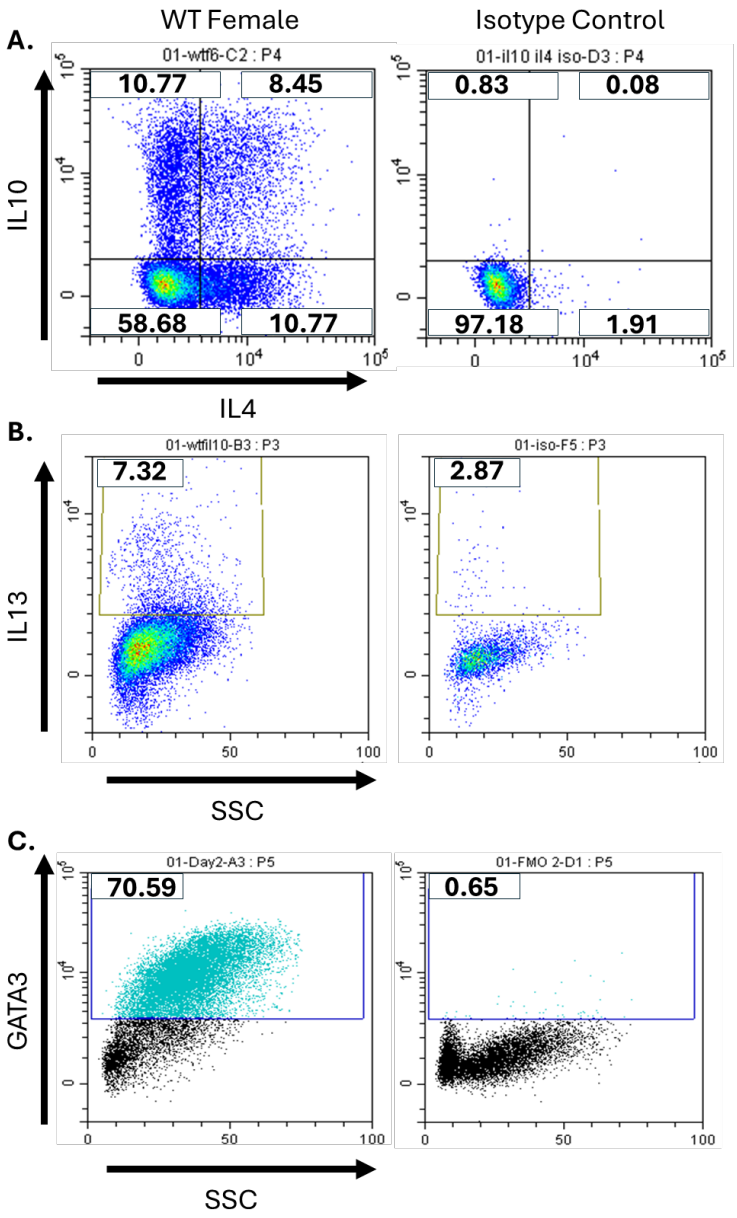

Supplementary Figure 1 Representative Isotype and FMO Control FACS Plots

A. Representative flow cytometry plots displaying IL10 and IL4 and isotype control staining in *WT* female CD4$^+$ T cells. Data from day 6 of a Th2 *in vitro* polarisation (*Figure 3.13*). **B.** Representative flow cytometry plots displaying IL13 and isotype control staining in anti-IL10R treated *WT* female CD4$^+$ T cells. Data from day 6 of a Th2 *in vitro* polarisation (*Figure 3.4*). **C.** Representative flow cytometry plots displaying GATA3 staining and FMO control. Data from day 2 of Th2 *in vitro* polarisation (*Figure 4.6*).

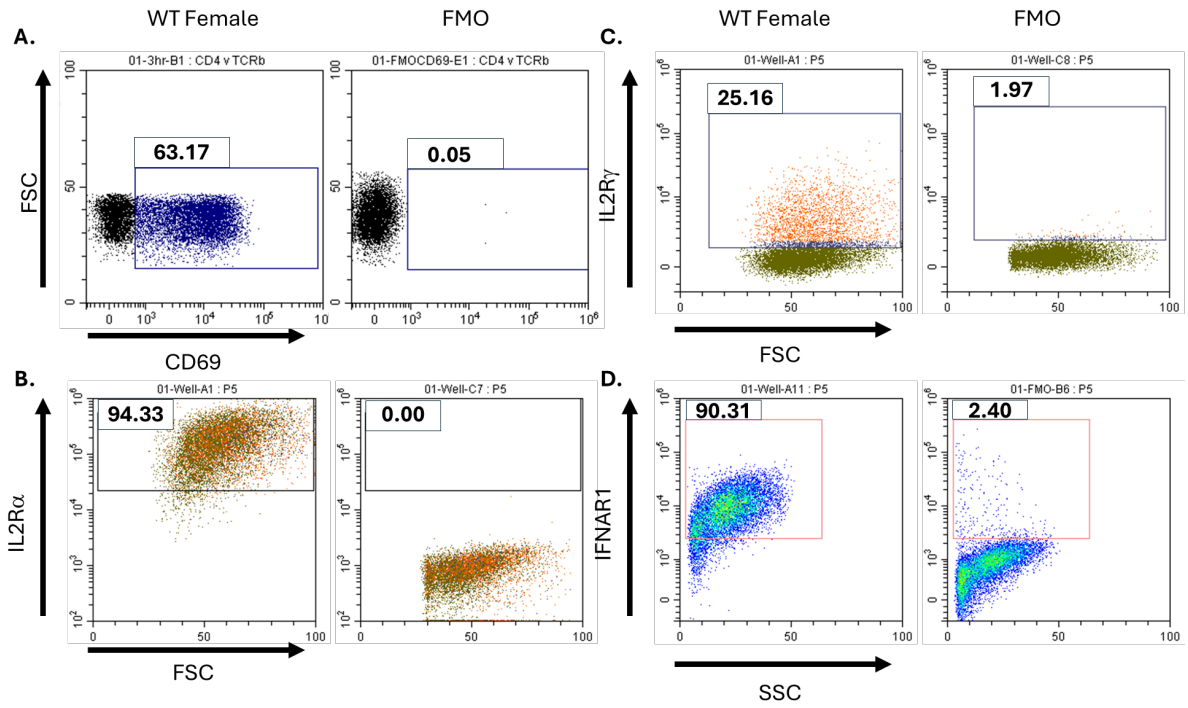

Supplementary Figure 2 Representative Isotype and FMO Control FACS Plots

A. Representative flow cytometry plots displaying CD69 staining and FMO control in *WT* female $CD4^+$ T cells. Data from 3 hours post-Th2 *in vitro* polarisation (*Figure 4.1*). **B.** Representative flow cytometry plots displaying IL2Rα staining and FMO control in *WT* female $CD4^+$ T cells. Data from day 4 of a Th2 *in vitro* polarisation (*Figure 3.14*). **C.** Representative flow cytometry plots displaying IL2Rγ staining and FMO control in *WT* female $CD4^+$ T cells. Data from day 4 of a Th2 *in vitro* polarisation (*Figure 3.14*). **D.** Representative flow cytometry plots displaying IFNAR1 staining and FMO control in *WT* female $CD4^+$ T cells. Data from day 2 of a Th2 *in vitro* polarisation (*Figure 4.20*).

A. Naive

Gene	logFC	FDR
Cndp2	-1.240032	0.000454
Gm5898	-3.291868	0.001807
Fads1	1.19895	0.00201
Malat1	-11.26106	0.00201
Gm10036	-4.162046	0.002132
Gm28438	4.30336	0.002953
Gpatch11	-0.742926	0.004139
ENSMUSG00000095041	-0.595316	0.004139
Ncmap	-1.710909	0.010851
Tshz3	1.8364	0.02564
Sytl1	-0.876711	0.033108
Cep85	1.0779	0.044972
Gm11223	4.20187	0.044972
Plaat3	0.58129	0.044972

B. Th2

Gene	logFC	FDR
Malat1	-11.29672	0.005308
Gm28438	7.03649	0.011726
Cndp2	-1.056563	0.039465

C. Naive

Gene	logFC	FDR
Malat1	-11.35063	0.026848
Cndp2	-1.209576	0.04155
Gm28438	5.02301	0.04155

D. Th2

Gene	logFC	FDR
Malat1	-12.69944	1.09E-07
Gpatch11	-0.944893	2.95E-05
Prnp	-1.45588	0.000322
Gm11223	3.28933	0.000588
Gm28438	5.76003	0.000588
Camk2b	1.34887	0.000689
4930453N24Rik	0.60784	0.000913
Fads1	0.663	0.003151
Mmrn1	11.4162	0.007798
Cndp2	-1.059343	0.007883
Zdhhc24	0.7807	0.007964
Mid1-ps1	3.86712	0.011652
Eps8l1	1.24674	0.012254
Gm43305	1.47009	0.014905
Carns1	-0.665576	0.029599
Gm10505	0.90448	0.032395
Nthl1	0.80666	0.038291

Supplementary Table 1. Significantly differentially expressed genes between *WT* and *Malat1*$^{-/-}$ female and males in naïve and Th2 cells

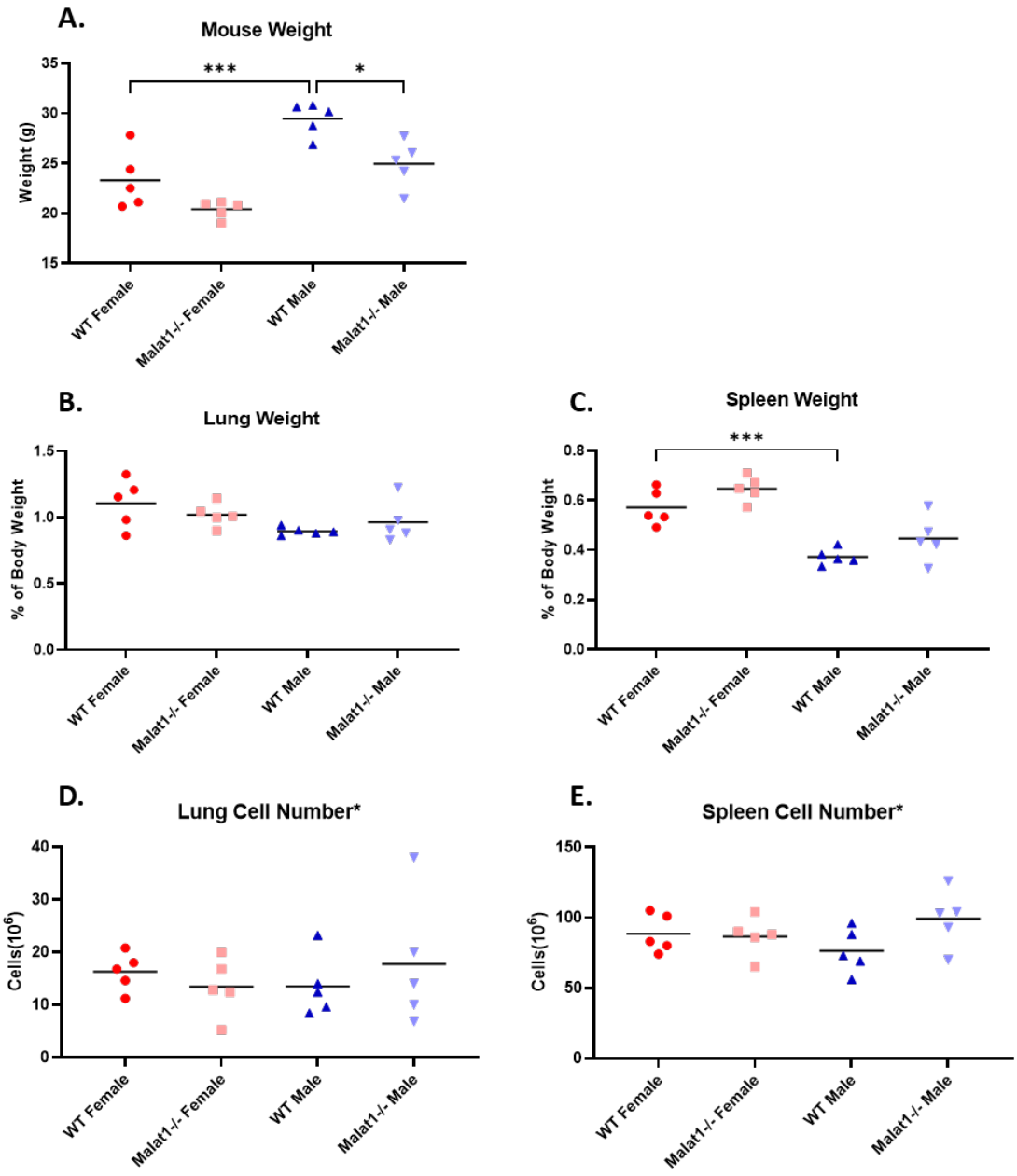

Supplementary Figure 3 *S. mansoni* egg-injection repeat responses in both the lung and the spleen.

A. Total weight of *S. mansoni* egg injected (*Sm*) *WT* or *Malat1*$^{-/-}$, female or male mice (n=5). **B.** As in A. but for lung weight as a % of body weight. **C.** As in A, but for spleens. **D.** Total cell numbers in lungs of *S. mansoni* egg injected (*Sm*) *WT* or *Malat1*$^{-/-}$, female or male mice (n=5). E**.** As in D, but for splenic cell numbers.

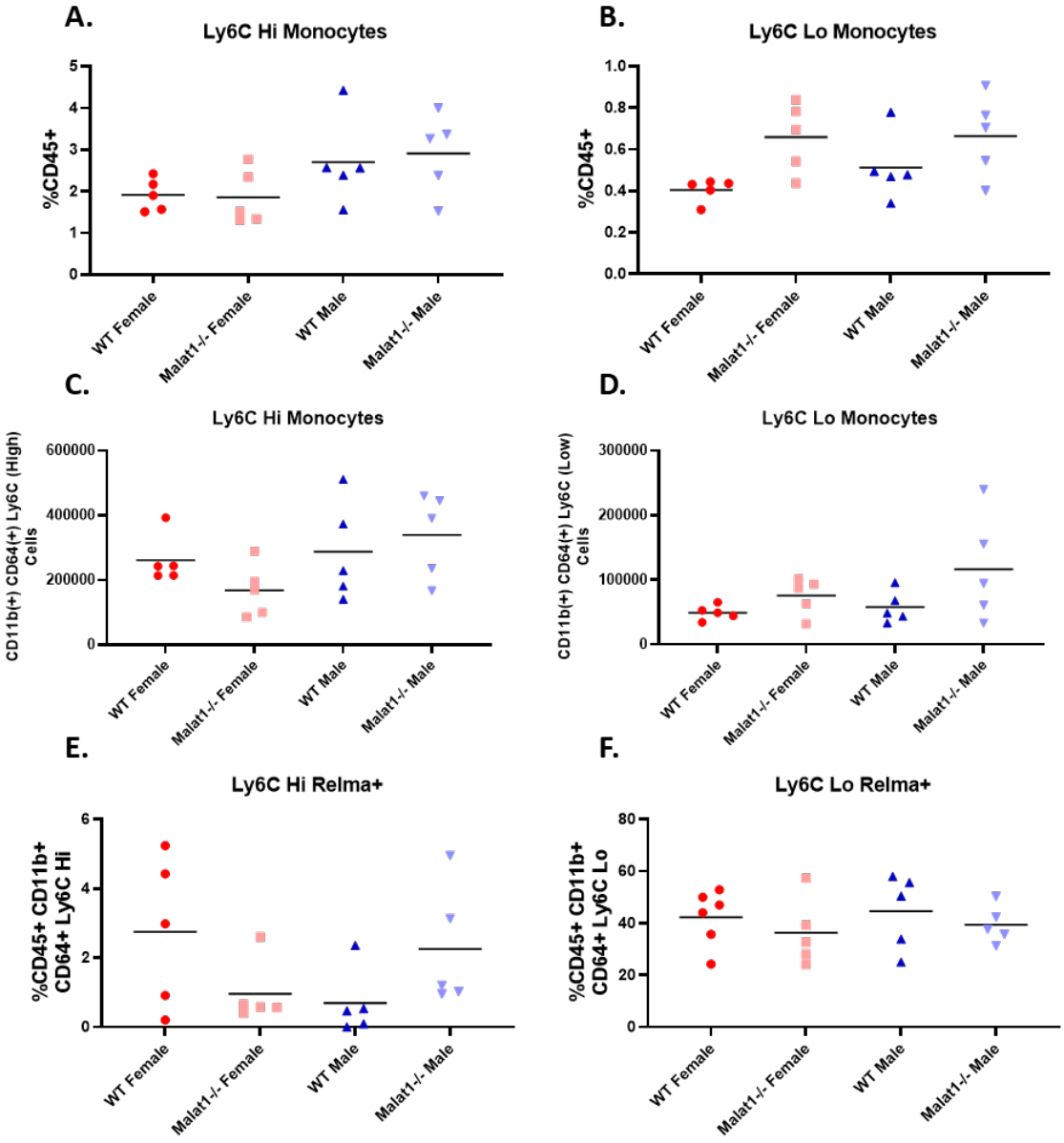

Supplementary Figure 4 *S. mansoni* egg-injection repeat monocyte responses

A. Percentages of Ly6C^{high} monocytes (CD45^{+}, CD11b^{+}, CD64^{+}) in lungs of *S. mansoni* egg injected, *WT* or *Malat1*$^{-/-}$, female or male mice. Levels determined by surface staining (n=5). **B.** As in A. but for Ly6C^{low} monocytes. **C.** Lung Ly6C^{high} monocyte cell numbers. **D.** Lung Ly6C^{low} monocyte cell numbers. **E.** Percentage of Ly6C^{high} monocytes in the lung expressing RELMα. **F.** As in E. but for Ly6C^{low} monocytes.

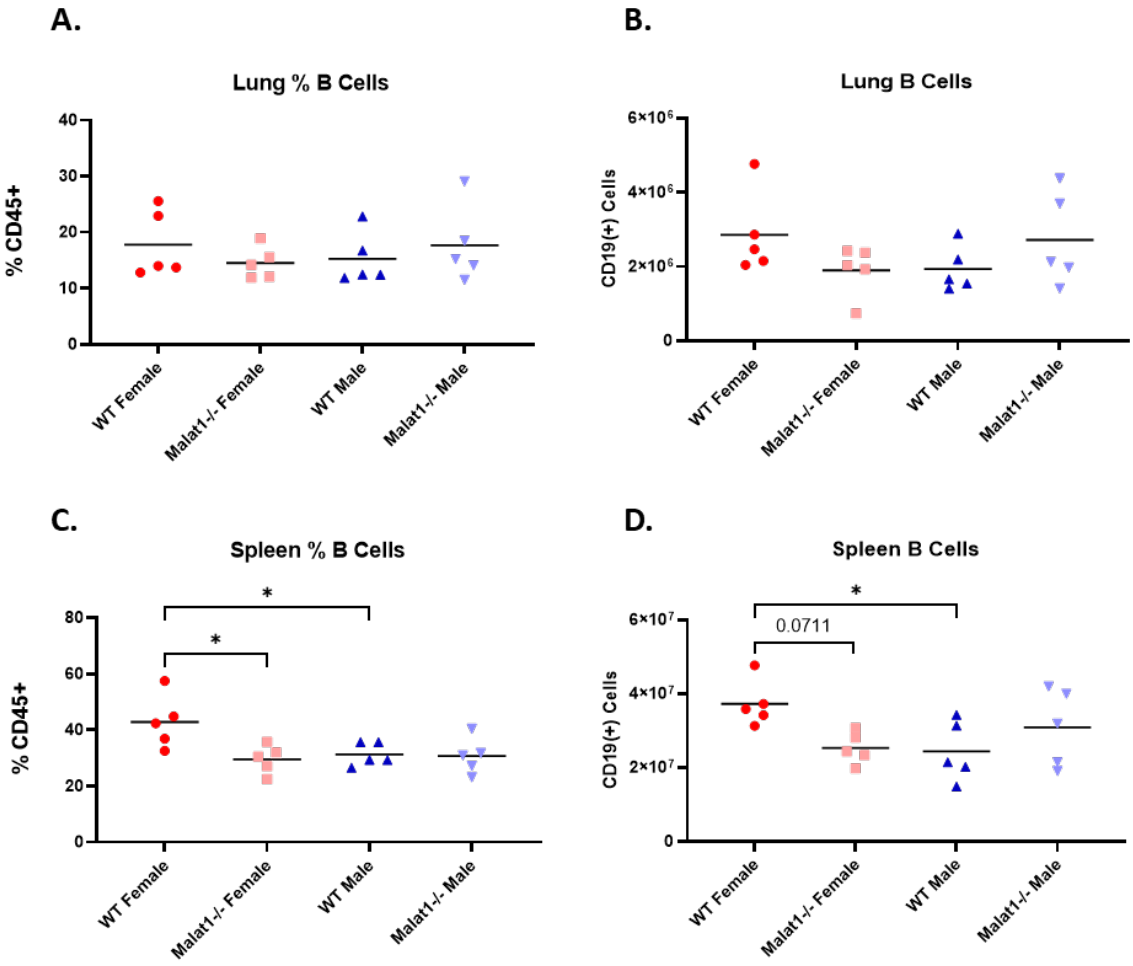

Supplementary Figure 5 *S. mansoni* egg-injection repeat B cell responses

A. Percentages of B cells ($CD45^+$, $CD19^+$) in lungs of *S. mansoni* egg injected, *WT* or *Malat1*$^{-/-}$, female or male mice. Levels determined by surface staining (n=5). **B.** Lung B cell numbers. **C.** Percentages of B cells in the spleens. **D.** Splenic B cell numbers.

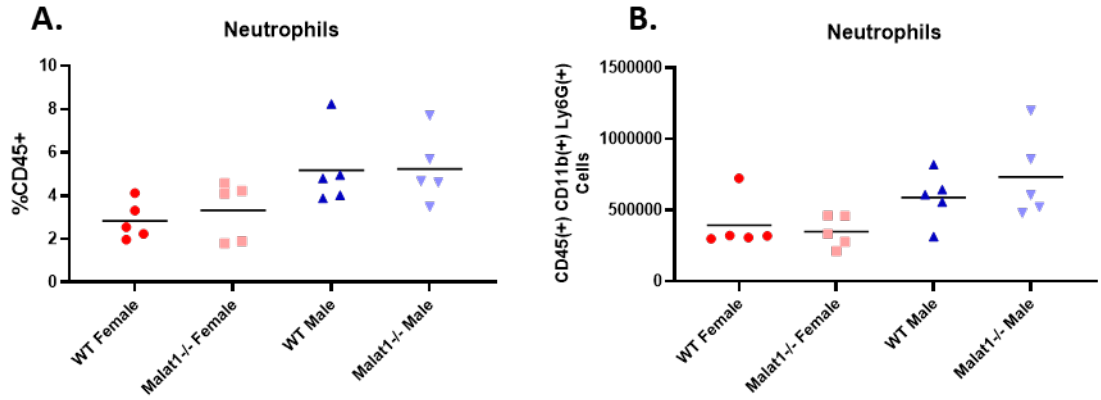

Supplementary Figure 6 *S. mansoni* egg-injection repeat Neutrophil responses

E. Percentages of neutrophils ($CD45^+$, $CD11b^+$, $Ly6G^+$) in the lungs of *S. mansoni* egg injected, *WT* or *Malat1*$^{-/-}$, female or male mice. Levels determined by surface staining (n=5). **F.** Neutrophil cell numbers.

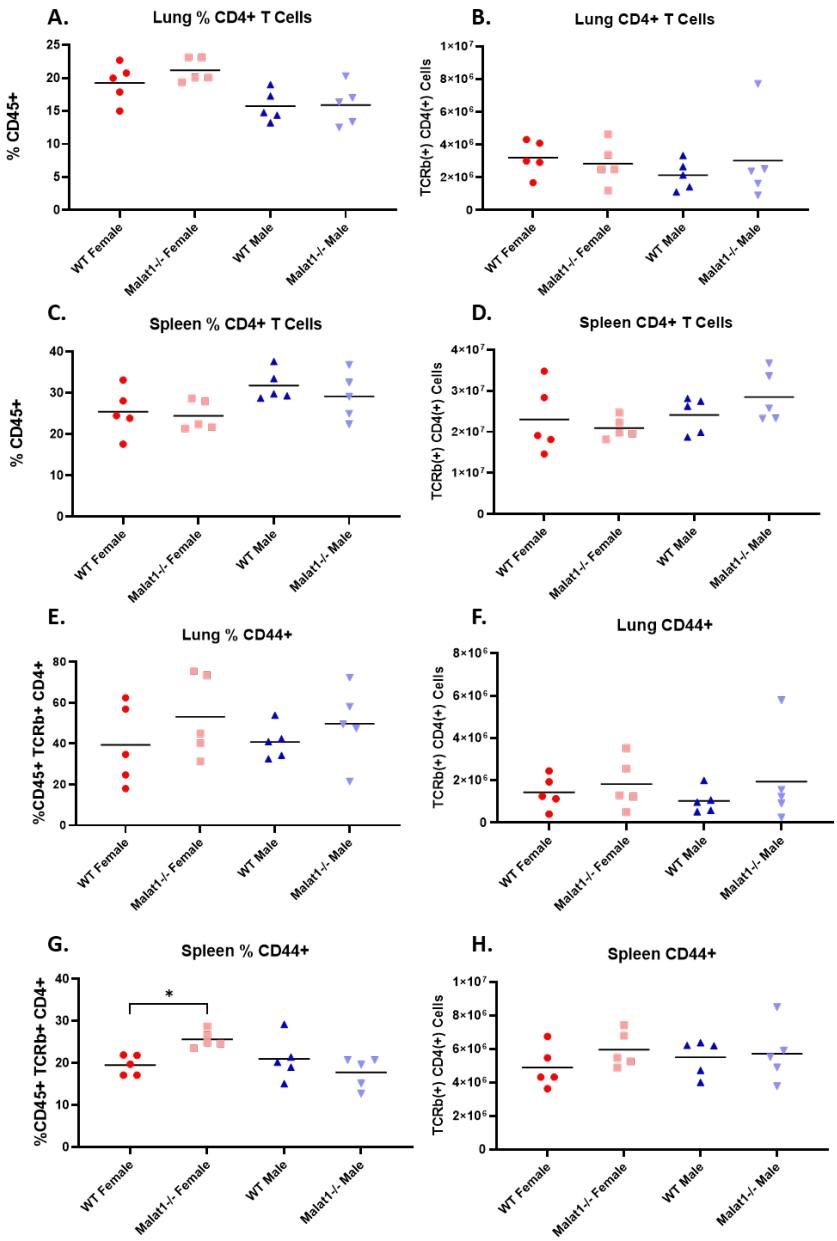

Supplementary Figure 7 *S. mansoni* egg-injection repeat T cell activation

A. Percentages of $CD4^+$ T cells ($TCR\beta^+$ $CD4^+$) cells in lungs of *S. mansoni* egg injected, *WT* or *Malat1*$^{-/-}$, female or male mice. Levels determined by surface staining (n=5). **B.** Lung $CD4^+$ T cell numbers. **C.** Percentages of $CD4^+$ T cells in the spleen. **D.** Splenic $CD4^+$ T cell numbers. **E.** Percentages of activated ($CD44^{high}$ $CD62L^{low}$) $CD4^+$ T cells in the lung. **F.** Activated lung $CD4^+$ T cell numbers. **G.** Percentages of activated $CD4^+$ T cells in the spleen. **H.** Activated splenic $CD4^+$ T cell numbers.

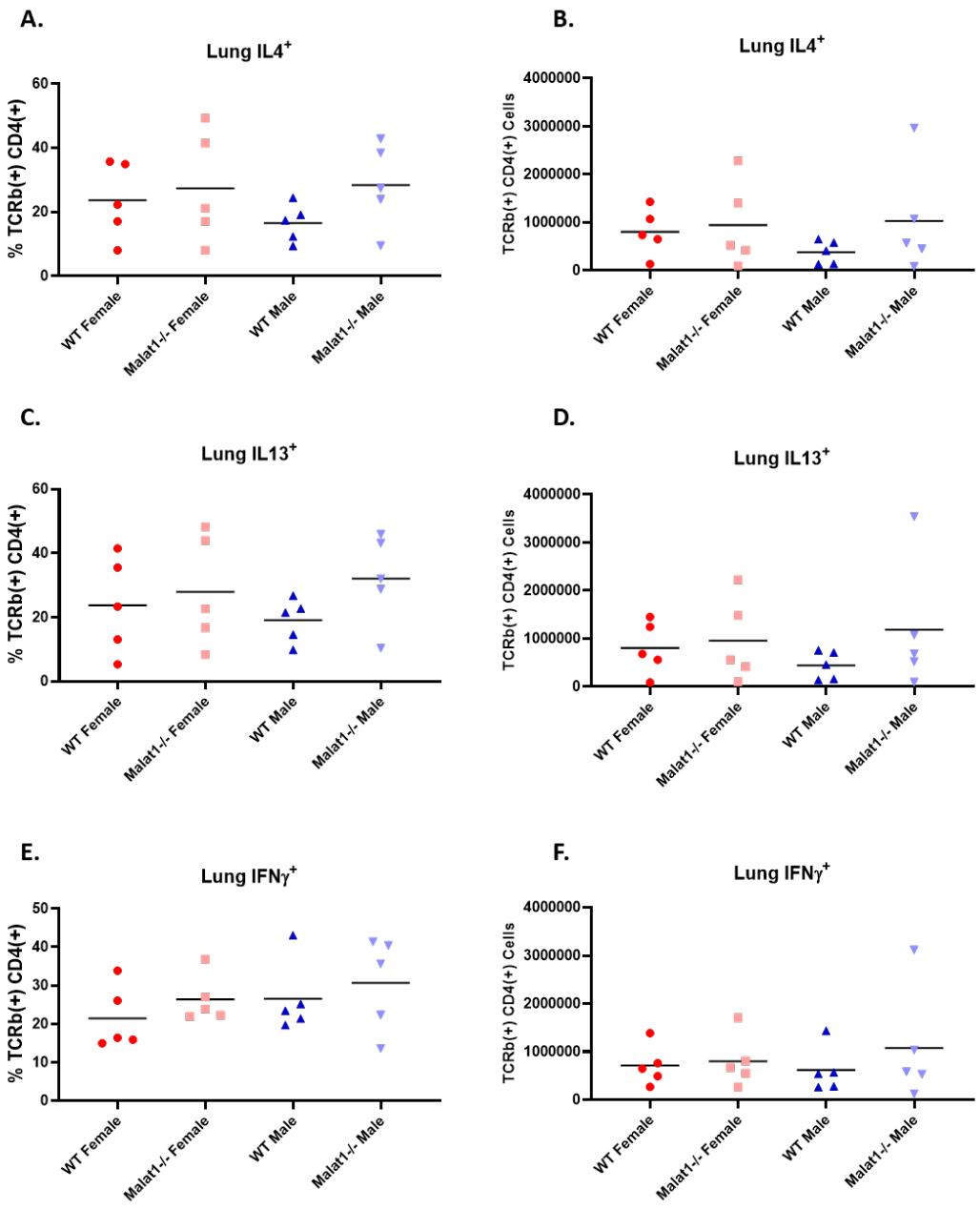

Supplementary Figure 8 *S. mansoni* egg-injection repeat lung T cell IL4, IL13 and IFNγ responses

A. Percentages of lung IL4$^+$ TCRβ$^+$ CD4$^+$ cells derived from *S. mansoni* egg injected (*Sm*) *WT* or *Malat1*$^{-/-}$, female and male mice. Levels determined by intracellular staining (n=5). **B.** Numbers of lung IL4$^+$ TCRβ$^+$ CD4$^+$ cells. **C.** As in A. but for IL13$^+$ TCRβ$^+$ CD4$^+$ cells. **D.** Numbers of lung IL13$^+$ TCRβ$^+$ CD4$^+$ cells. **E.** As in A. but for lung IFNγ$^+$ TCRβ$^+$ CD4$^+$ cells. **F.** Numbers of lung IFNγ$^+$ TCRβ$^+$ CD4$^+$ cells.

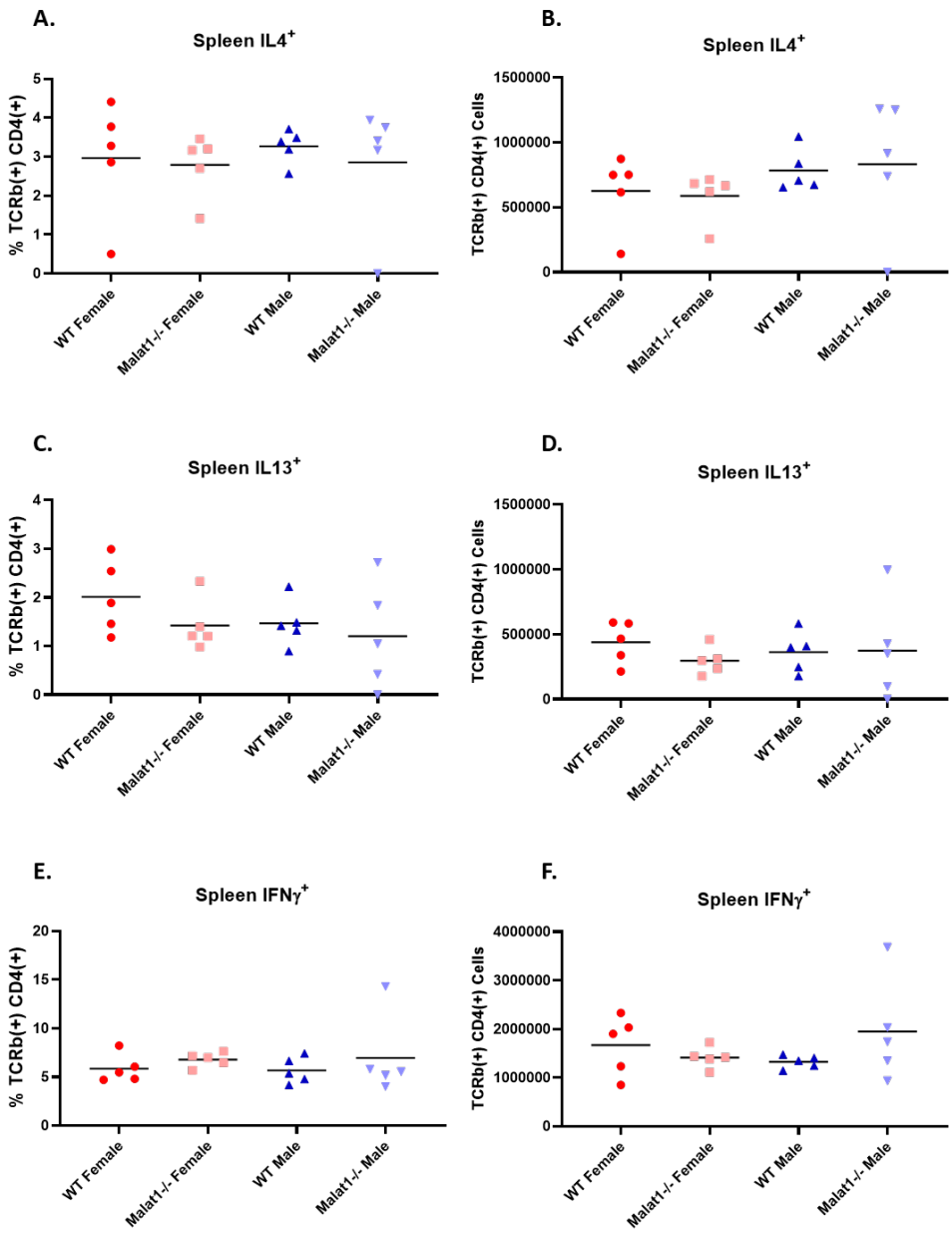

Supplementary Figure 9 *S. mansoni* egg-injection repeat spleen T cell IL4, IL13 and IFNγ responses

A. Percentages of splenic IL4$^+$ TCRβ$^+$ CD4$^+$ cells derived from *S. mansoni* egg injected (*Sm*) *WT* or *Malat1*$^{-/-}$, female and male mice. Levels determined by intracellular staining (n=5). **B.** Numbers of splenic IL4$^+$ TCRβ$^+$ CD4$^+$ cells. **C.** As in A. but for IL13$^+$ TCRβ$^+$ CD4$^+$ cells. **D.** Numbers of splenic IL13$^+$ TCRβ$^+$ CD4$^+$ cells. **E.** As in A. but for splenic IFNγ$^+$ TCRβ$^+$ CD4$^+$ cells. **F.** Numbers of splenic IFNγ$^+$ TCRβ$^+$ CD4$^+$ cells.

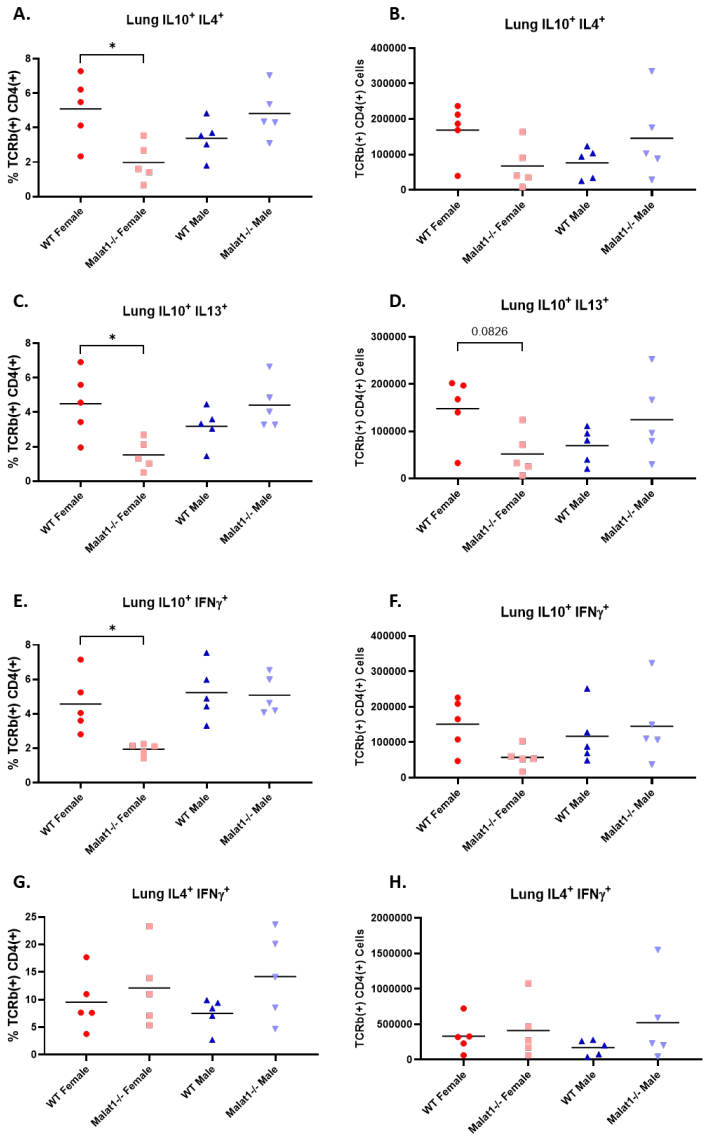

Supplementary Figure 10 *S. mansoni* egg-injection repeat lung T cell double positive cytokine responses

A. Percentages of lung IL10$^+$ IL4$^+$ TCRβ$^+$ CD4$^+$ cells derived from *S. mansoni* egg injected (*Sm*) *WT* or *Malat1*$^{-/-}$, female and male mice. Levels determined by intracellular staining (n=5). **B.** Numbers of lung IL10$^+$ IL4$^+$ TCRβ$^+$ CD4$^+$ cells. **C.** As in A. but for IL10$^+$ IL13$^+$ TCRβ$^+$ CD4$^+$ cells. **D.** Numbers of lung IL10$^+$ IL13$^+$ TCRβ$^+$ CD4$^+$ cells. **E.** As in A. but for lung IL10$^+$ IFNγ$^+$ TCRβ$^+$ CD4$^+$ cells. **F.** Numbers of lung IL10$^+$ IFNγ$^+$ TCRβ$^+$ CD4$^+$ cells. **G.** As in A. but for lung IL4$^+$ IFNγ$^+$ TCRβ$^+$ CD4$^+$ cells. **H.** Numbers of lung IL4$^+$ IFNγ$^+$ TCRβ$^+$ CD4$^+$ cells.

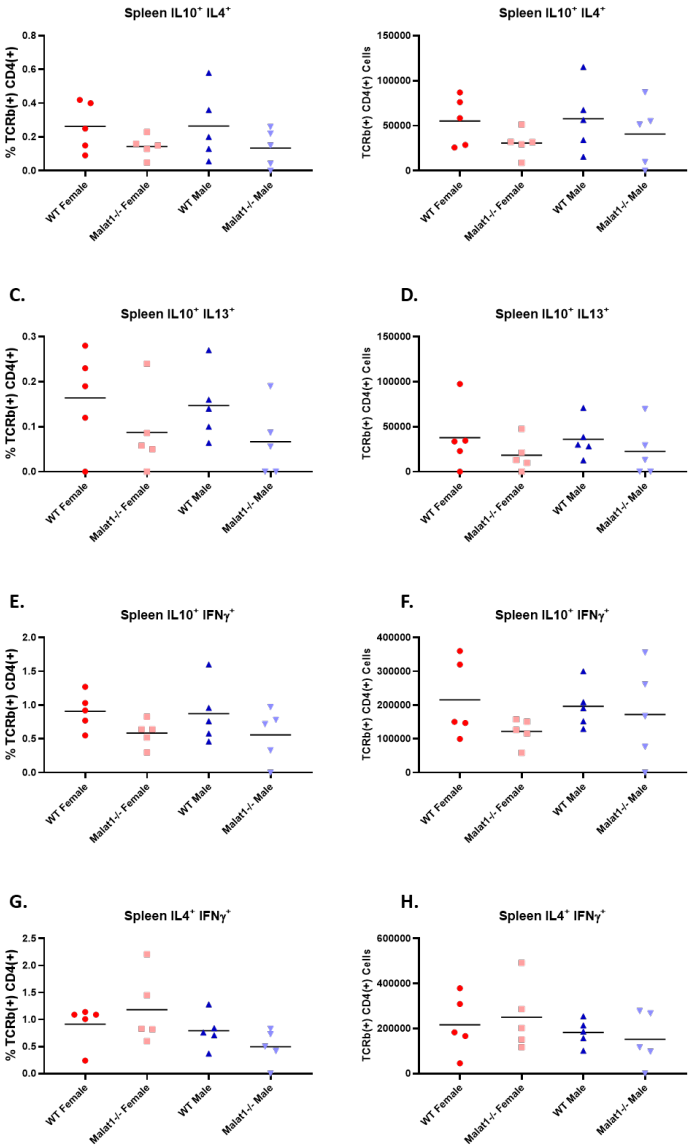

Supplementary Figure 11 *S. mansoni* egg-injection repeat spleen T cell double positive responses

A. Percentages of splenic IL10$^+$ IL4$^+$ TCRβ$^+$ CD4$^+$ cells derived from *S. mansoni* egg injected (*Sm*) *WT* or *Malat1*$^{-/-}$, female and male mice. Levels determined by intracellular staining (n=5). **B.** Numbers of splenic IL10$^+$ IL4$^+$ TCRβ$^+$ CD4$^+$ cells. **C.** As in A. but for IL10$^+$ IL13$^+$ TCRβ$^+$ CD4$^+$ cells. **D.** Numbers of splenic IL10$^+$ IL13$^+$ TCRβ$^+$ CD4$^+$ cells. **E.** As in A. but for splenic IL10$^+$ IFNγ$^+$ TCRβ$^+$ CD4$^+$ cells. **F.** Numbers of splenic IL10$^+$ IFNγ$^+$ TCRβ$^+$ CD4$^+$ cells. **G.** As in A. but for IL4$^+$ IFNγ$^+$ TCRβ$^+$ CD4$^+$ cells. **H.** Numbers of splenic IL4$^+$ IFNγ$^+$ TCRβ$^+$ CD4$^+$ cells.

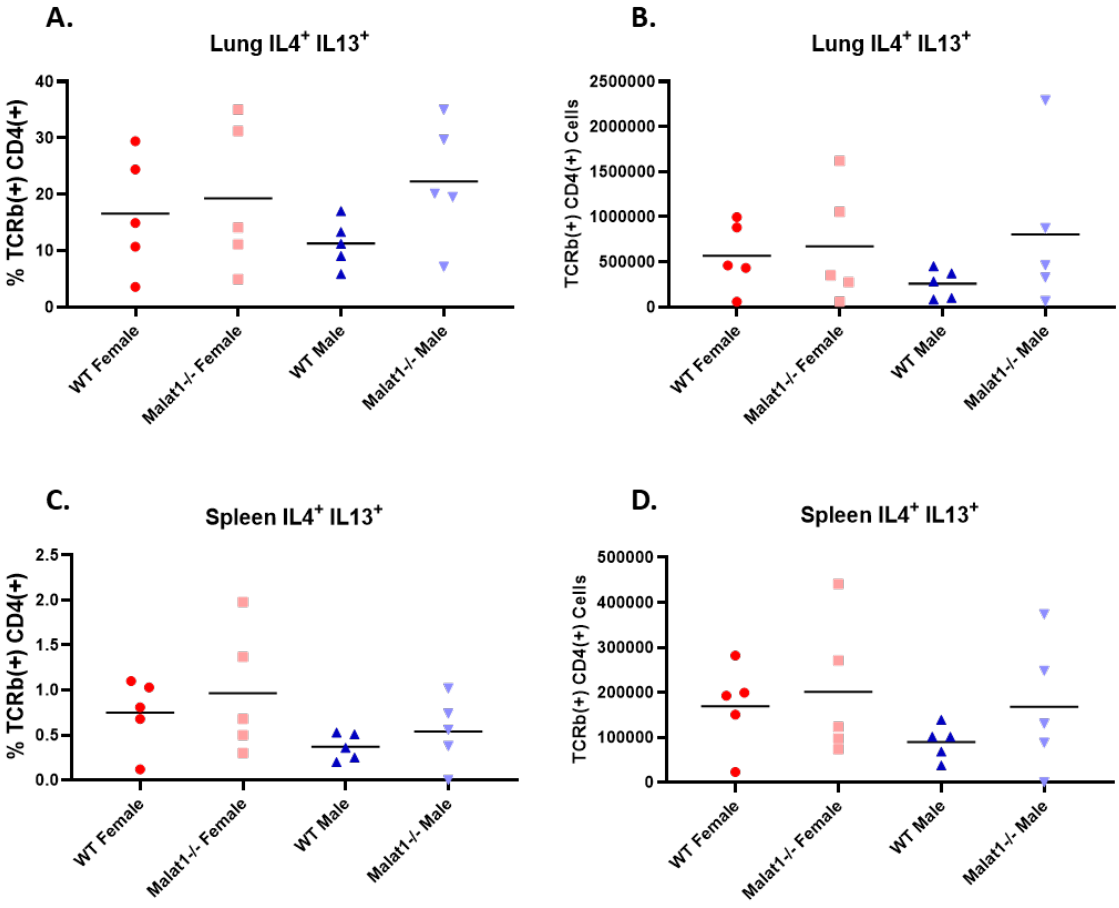

Supplementary Figure 12 *S. mansoni* egg-injection repeat lung T cell IL4 IL13 double positive responses

A. Percentages of lung IL4$^+$ IL13$^+$ TCRβ$^+$ CD4$^+$ cells derived from *S. mansoni* egg injected (*Sm*) *WT* or *Malat1*$^{-/-}$, female and male mice. Levels determined by intracellular staining (n=5). **B.** Numbers of lung IL4$^+$ IL13$^+$ TCRβ$^+$ CD4$^+$ cells. **C.** As in A. but for splenic IL4$^+$ IL13$^+$ TCRβ$^+$ CD4$^+$ cells. **D.** Numbers of splenic IL4$^+$ IL13$^+$ TCRβ$^+$ CD4$^+$ cells.

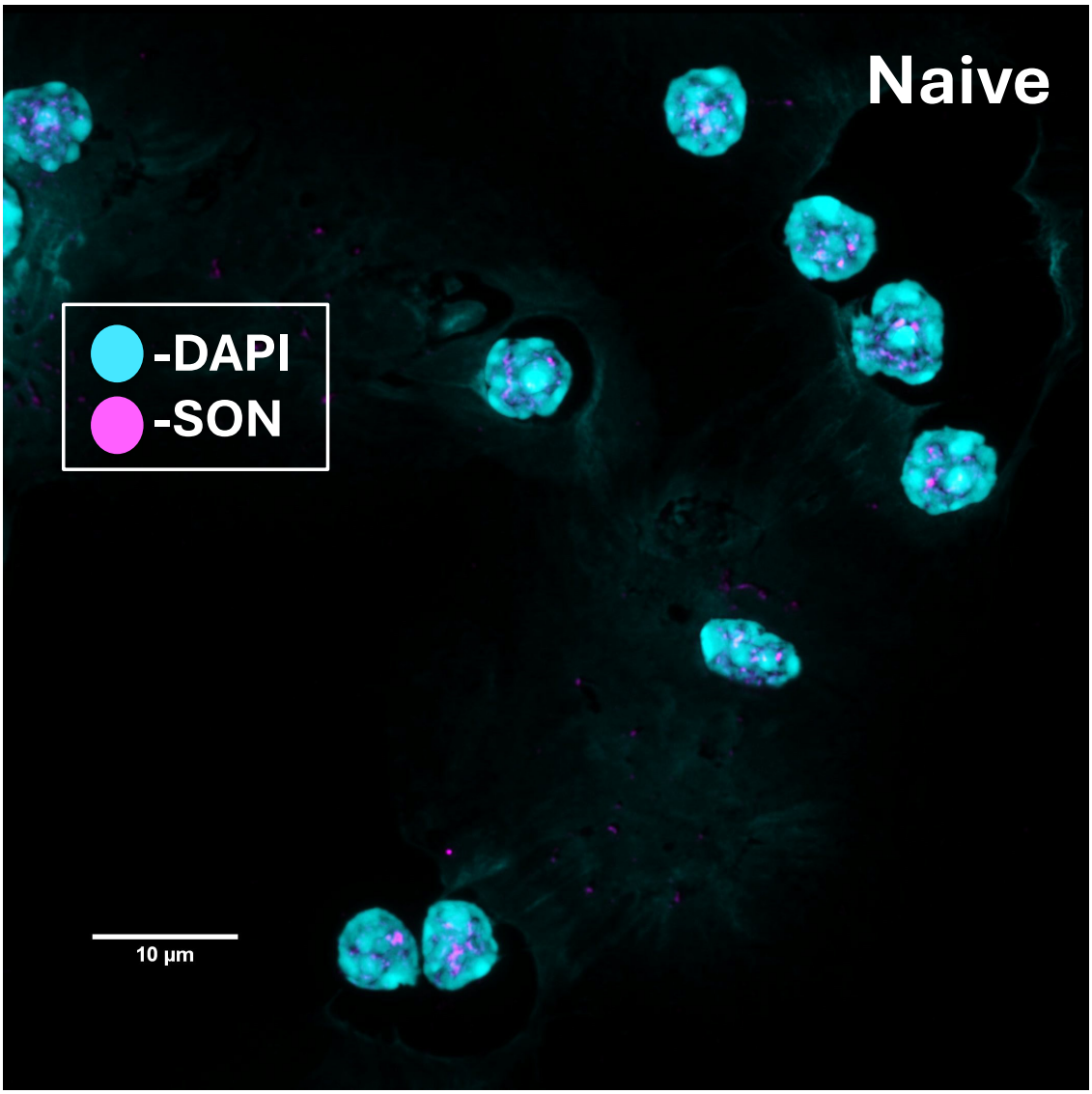

Supplementary Figure 13

Representative 63x images from SON and DAPI staining naïve *WT* female $CD4^+$ T cells. Brightness and contrast were increased by 20%.

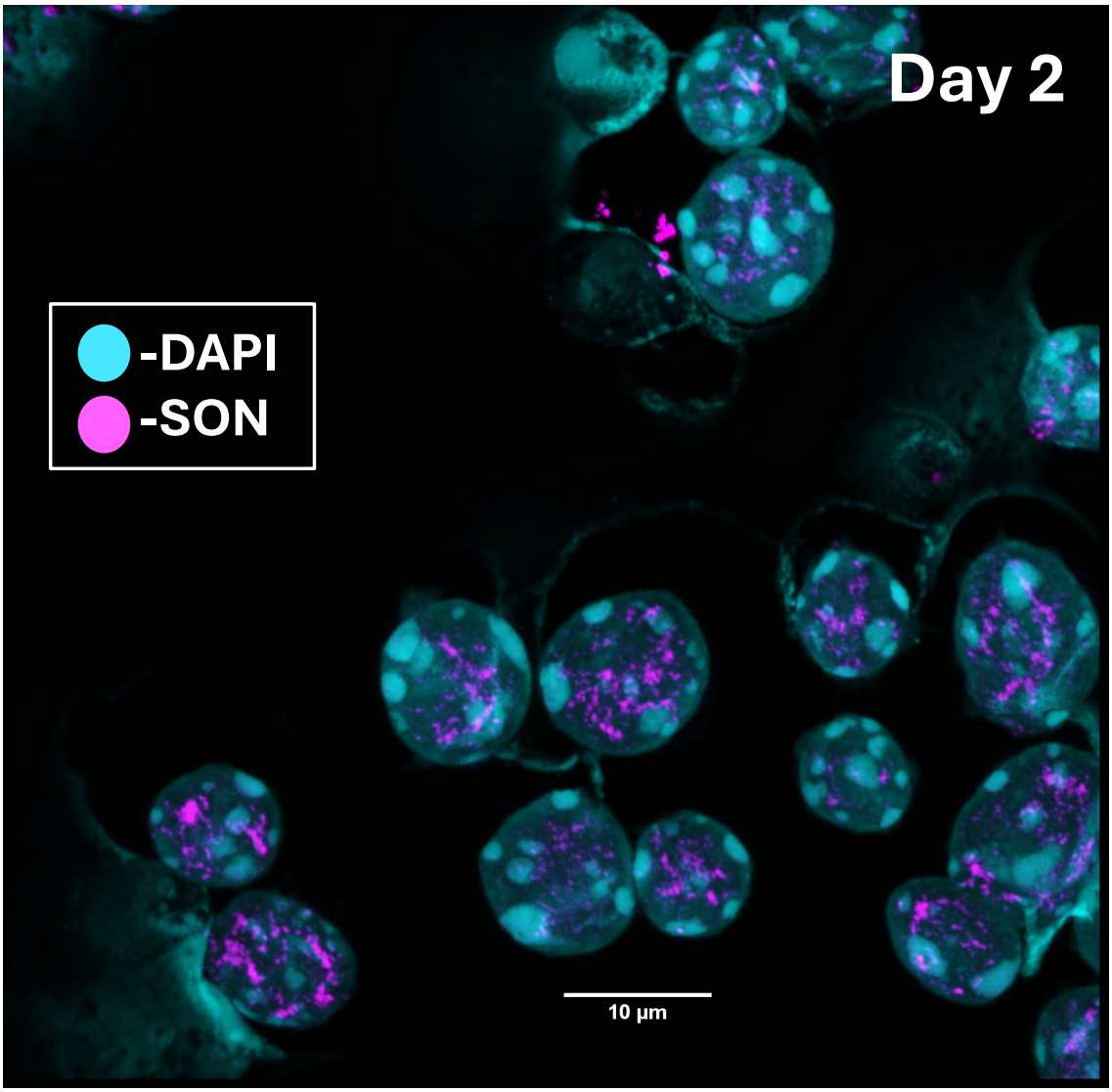

Supplementary Figure 14

Representative 63x images from SON and DAPI staining *in vitro* differentiated *WT* female $CD4^+$ T cells at day 2 of differentiation. Brightness and contrast were increased by 20%.

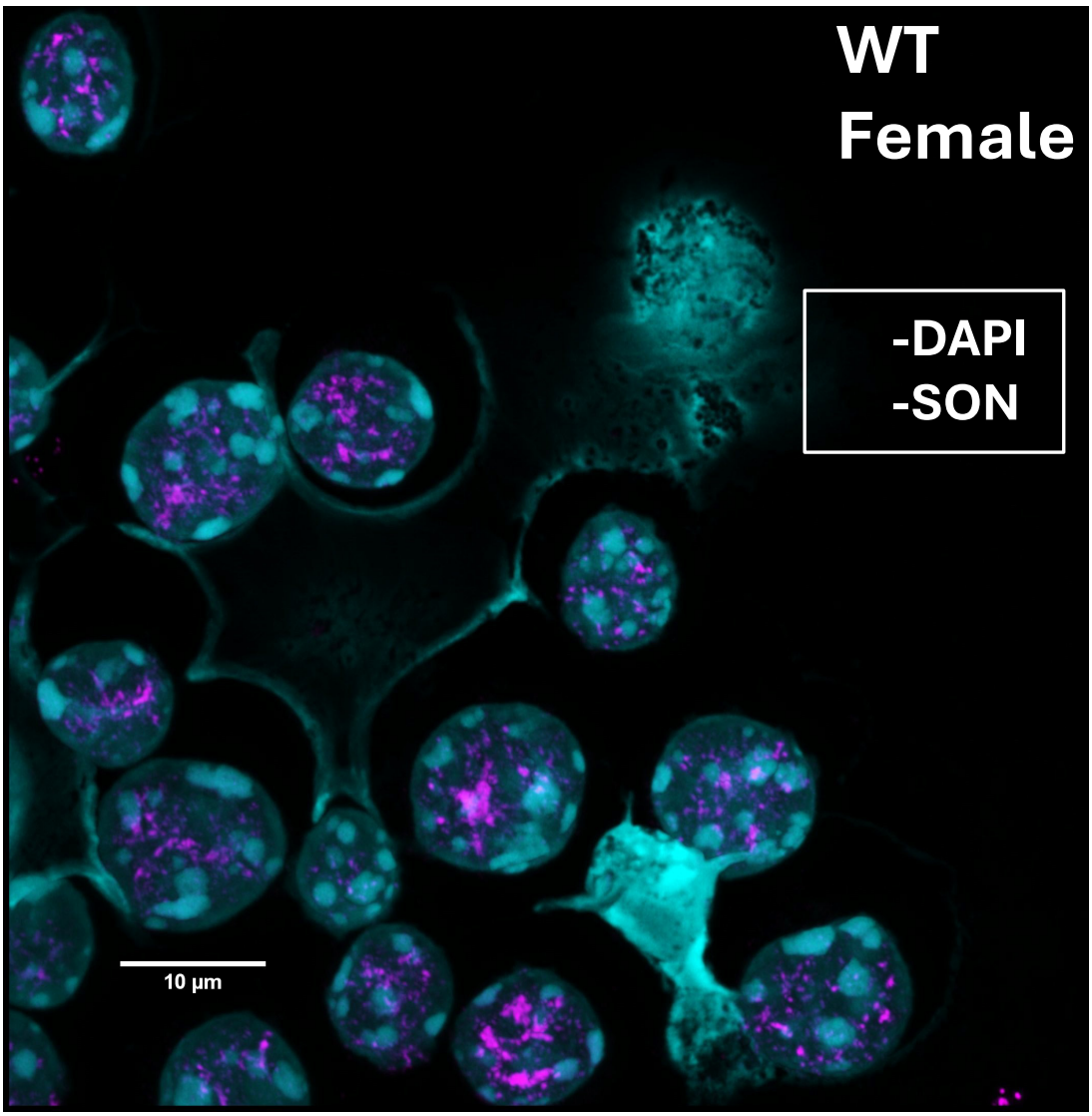

Supplementary Figure 15

Representative 63x images from SON and DAPI staining *in vitro* differentiated *WT* female $CD4^+$ T cells at day 2 of differentiation. Brightness and contrast were increased by 20%.

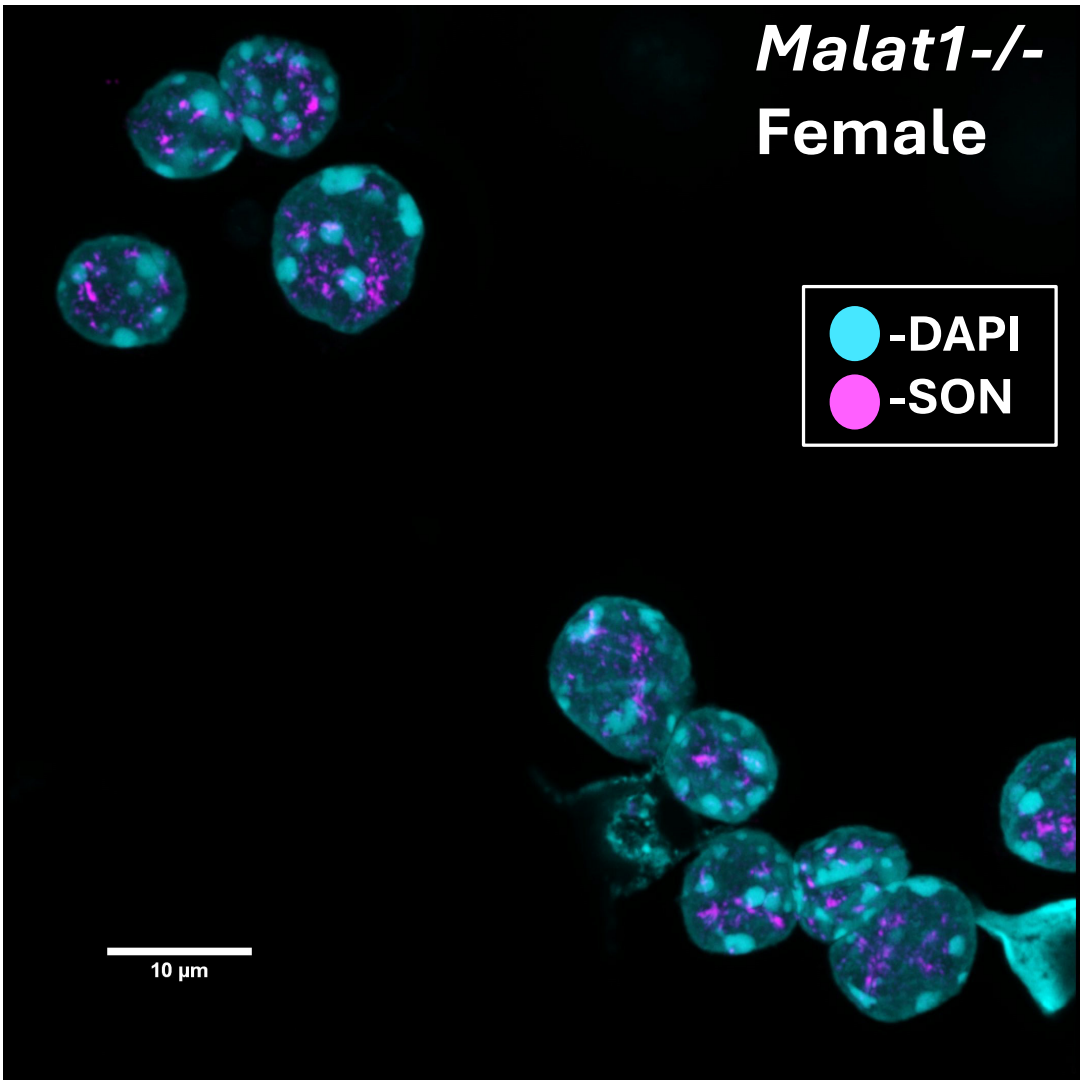

Supplementary Figure 16

Representative 63x images from SON and DAPI staining *in vitro* differentiated *Malat1*$^{-/-}$ female CD4^{+} T cells at day 2 of differentiation. Brightness and contrast were increased by 20%.

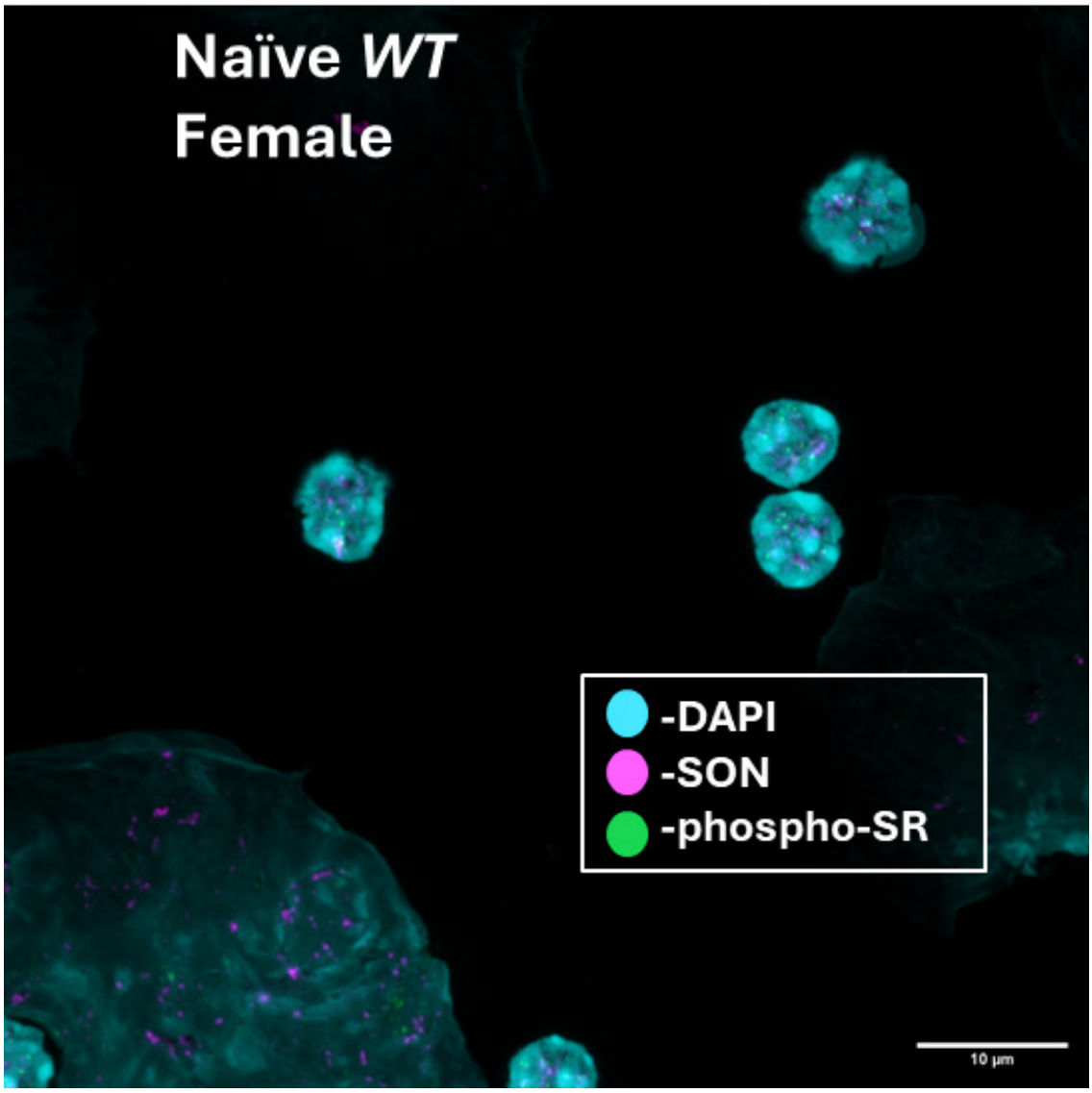

Supplementary Figure 17

Representative 63x images of phospho-SR, SON and DAPI staining of naïve *WT* female $CD4^+$ T cells. Brightness and contrast increased by 20%.

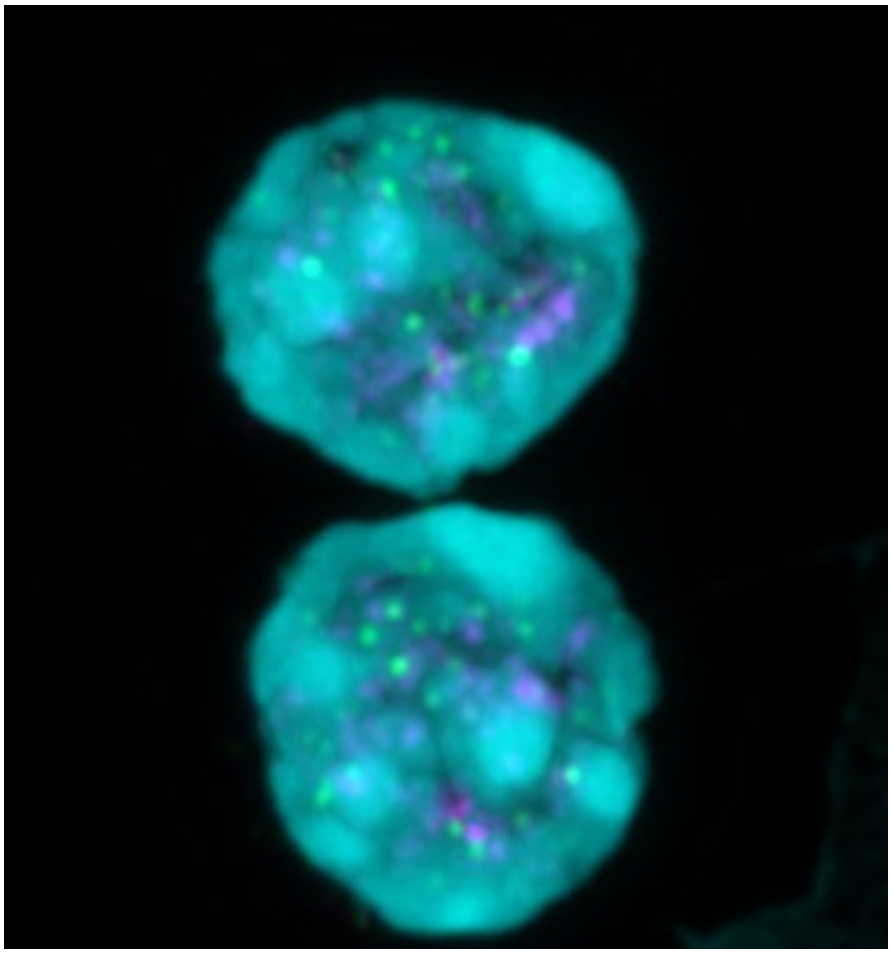

Supplementary Figure 18

Representative cell image of phospho-SR, SON and DAPI staining of naïve *WT* female $CD4^+$ T cells. Brightness and contrast increased by 20%.

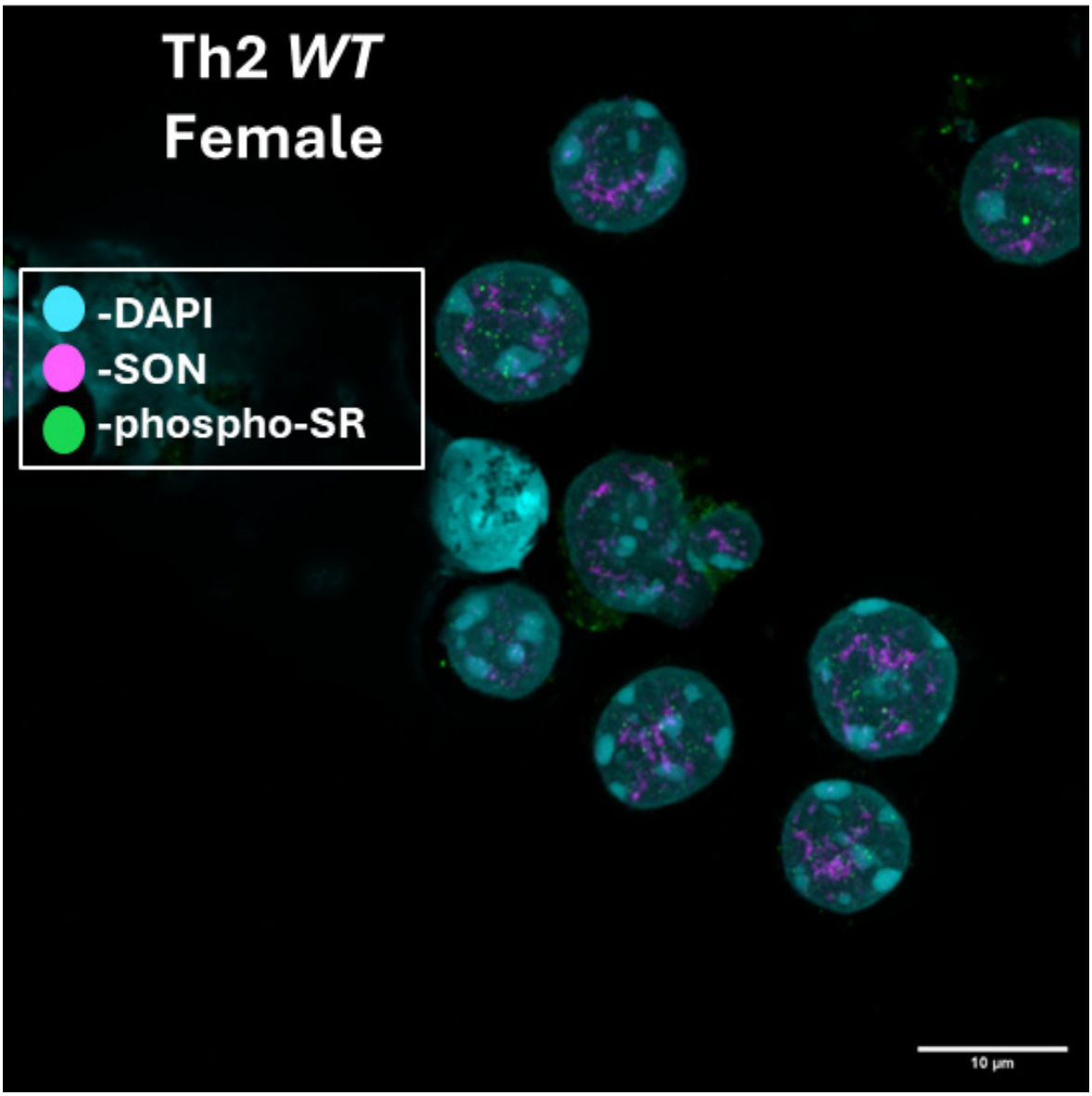

Supplementary Figure 19

Representative 63x images of phospho-SR, SON and DAPI staining of *WT* female $CD4^+$ T cells at day 2 of *in vitro* Th2 differentiation. Brightness and contrast increased by 20%.

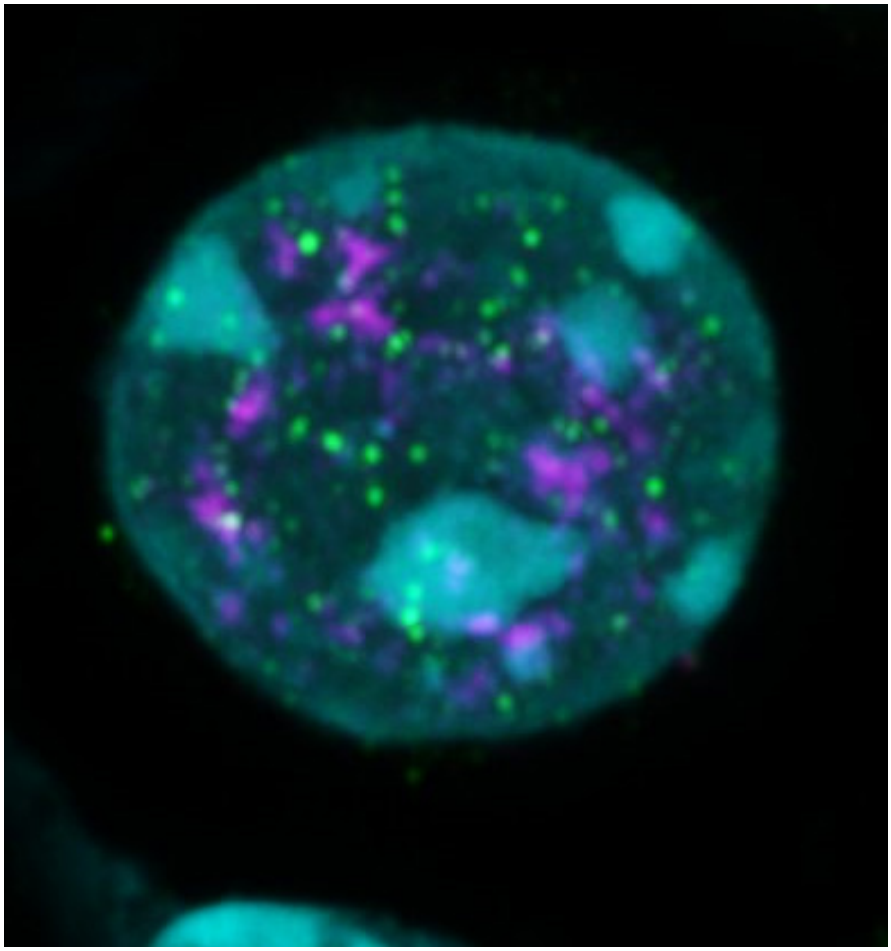

Supplementary Figure 20

Representative cell image of phospho-SR, SON and DAPI staining of *WT* female $CD4^+$ T cells at day 2 of *in vitro* Th2 differentiation. Brightness and contrast increased by 20%.

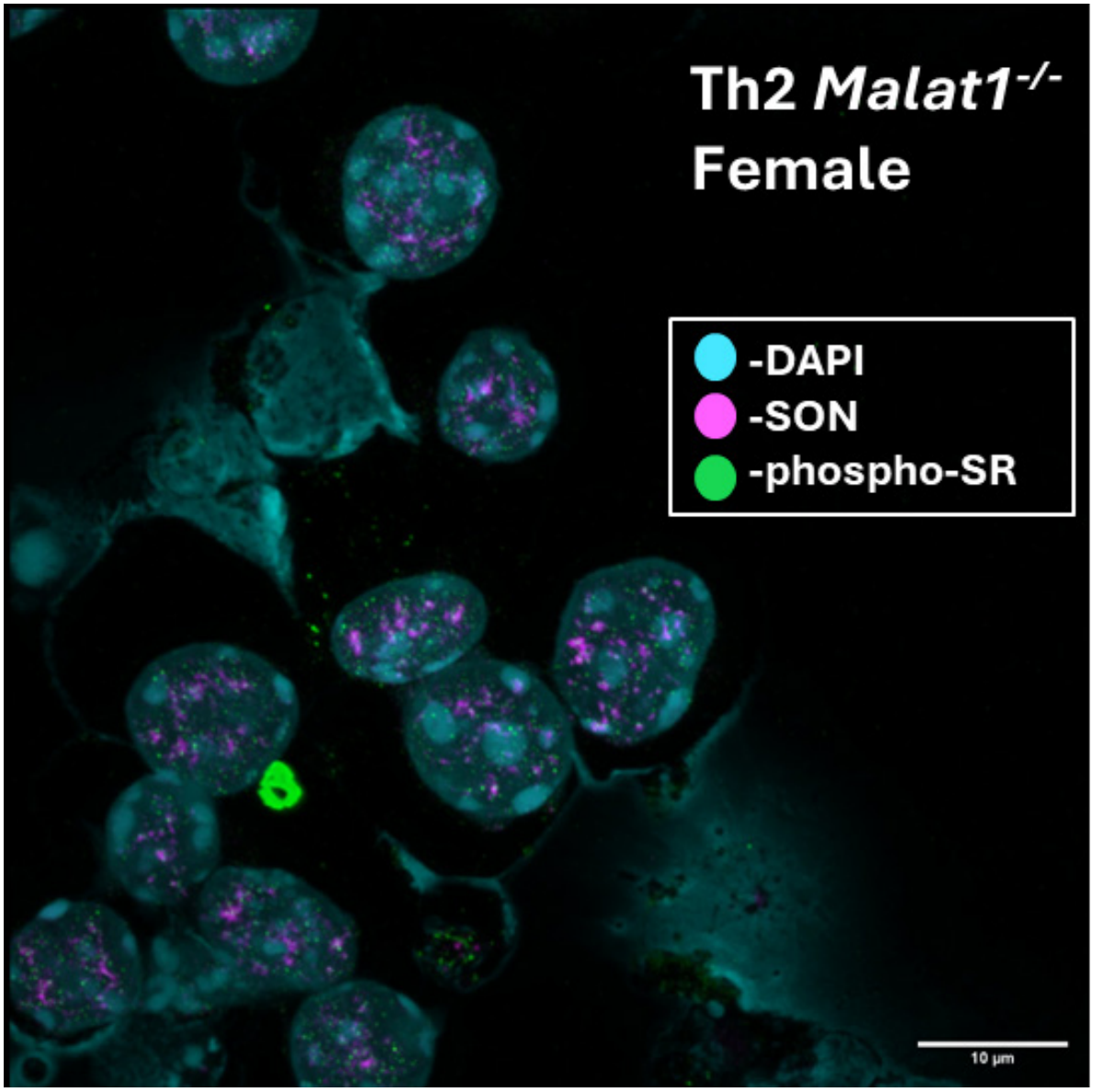

Supplementary Figure 21

Representative 63x images of phospho-SR, SON and DAPI staining of *Malat1*$^{-/-}$ female CD4^{+} T cells at day 2 of *in vitro* Th2 differentiation. Brightness and contrast increased by 20%.

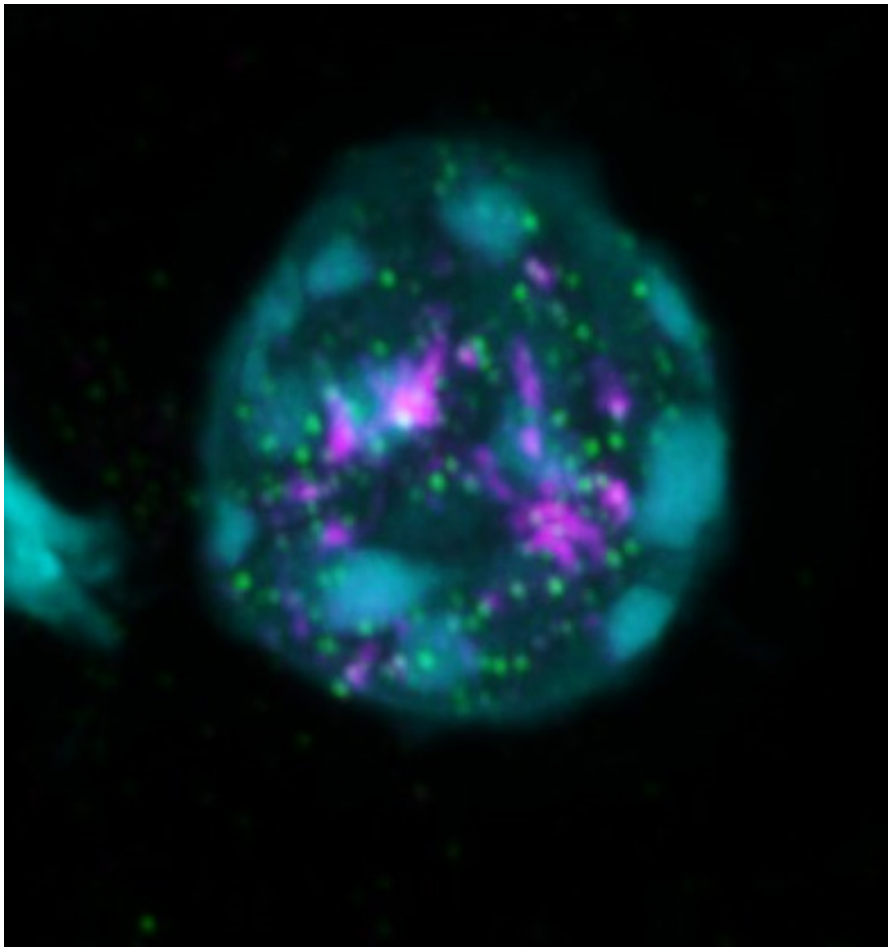

Supplementary Figure 22

Representative cell image of phospho-SR, SON and DAPI staining of *Malat1*$^{-/-}$ female CD4^{+} T cells at day 2 of *in vitro* Th2 differentiation. Brightness and contrast increased by 20%.

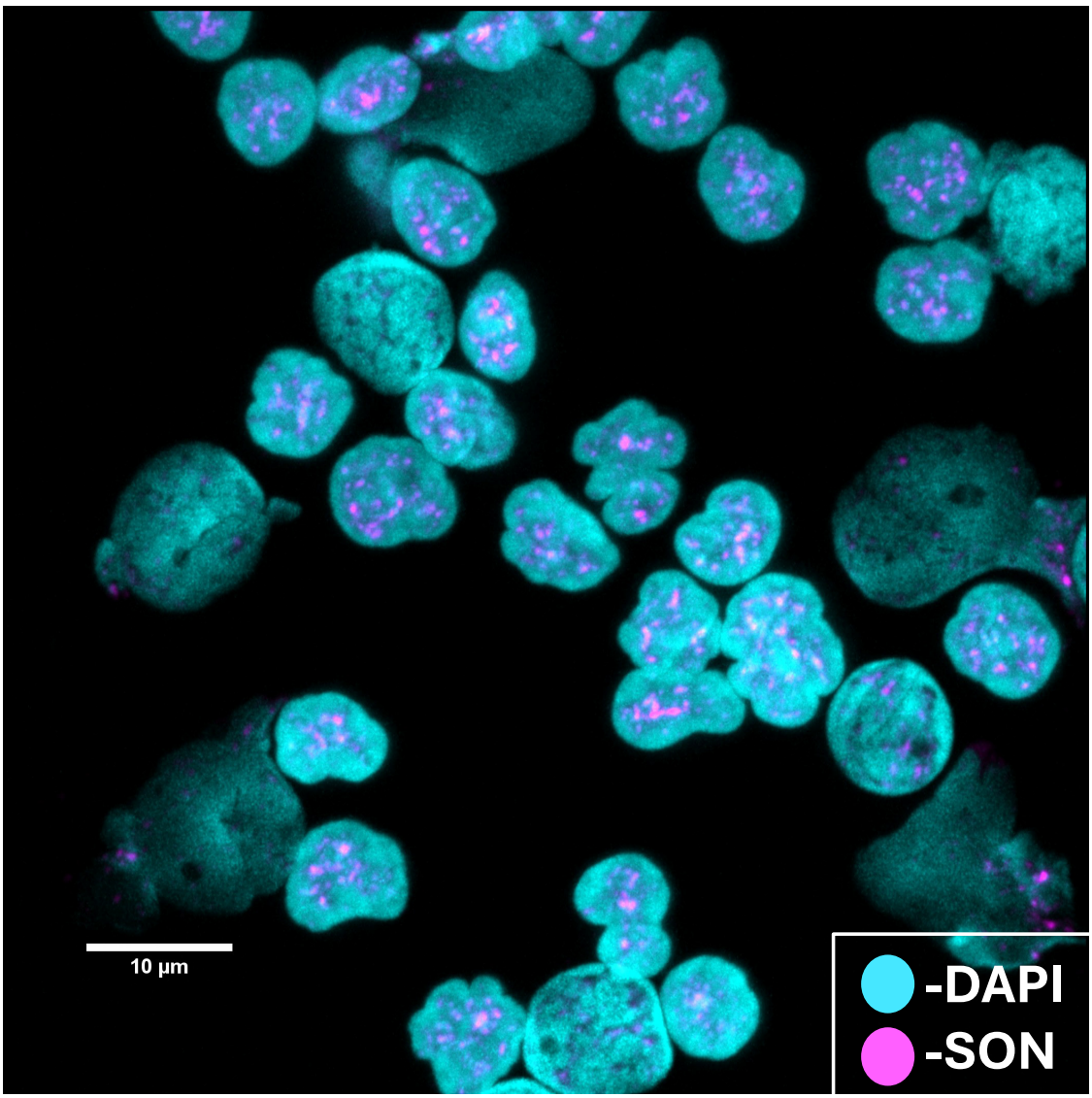

Supplementary Figure 23

Representative images of SON and DAPI staining of human $CD4^+$ T cells from donor A. at day 0 of Th2 *in vitro* differentiation. Brightness and contrast were increased by 20%.

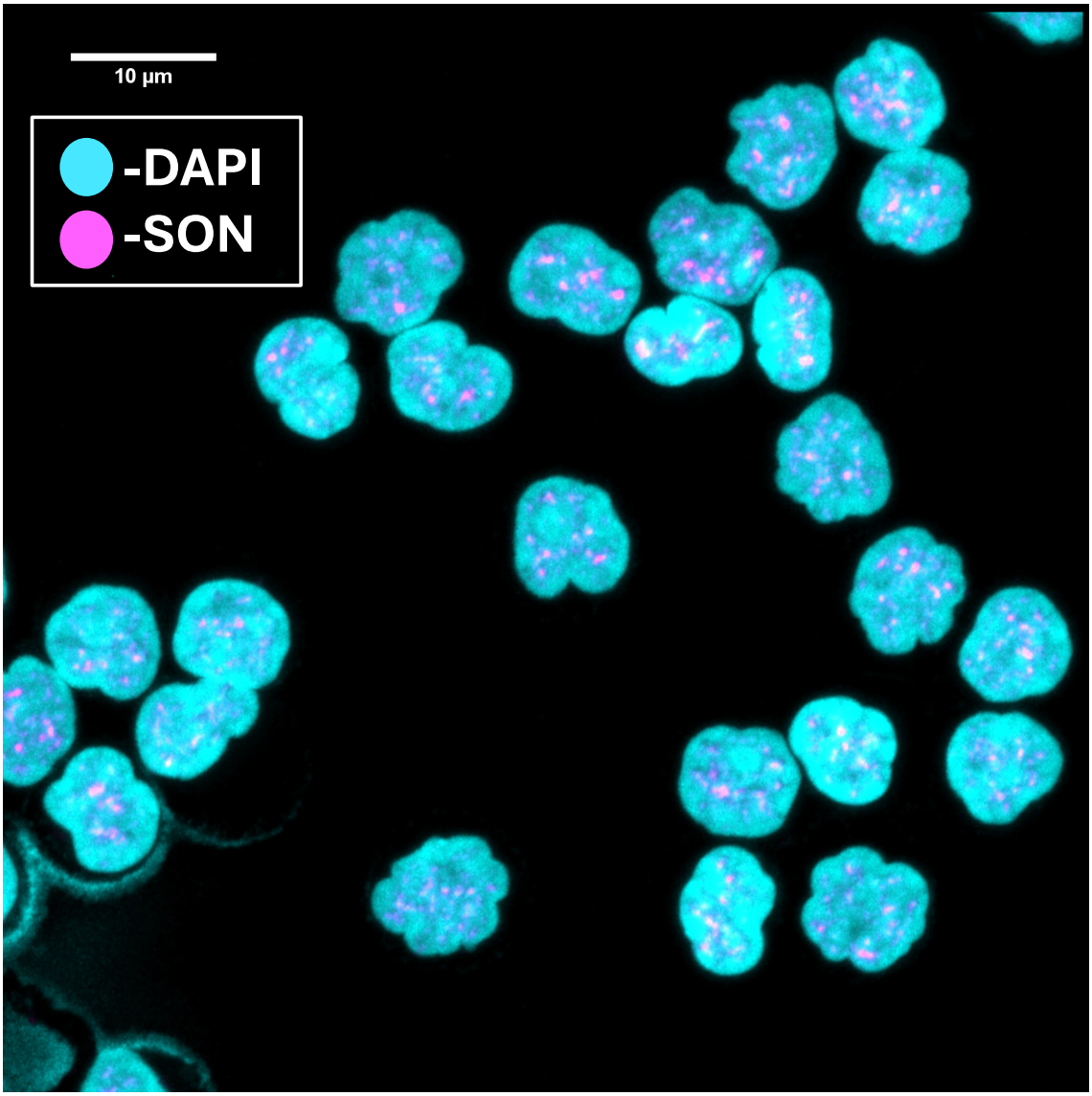

Supplementary Figure 24

Representative images of SON and DAPI staining of human $CD4^+$ T cells from donor C. at day 0 of Th2 *in vitro* differentiation. Brightness and contrast were increased by 20%.

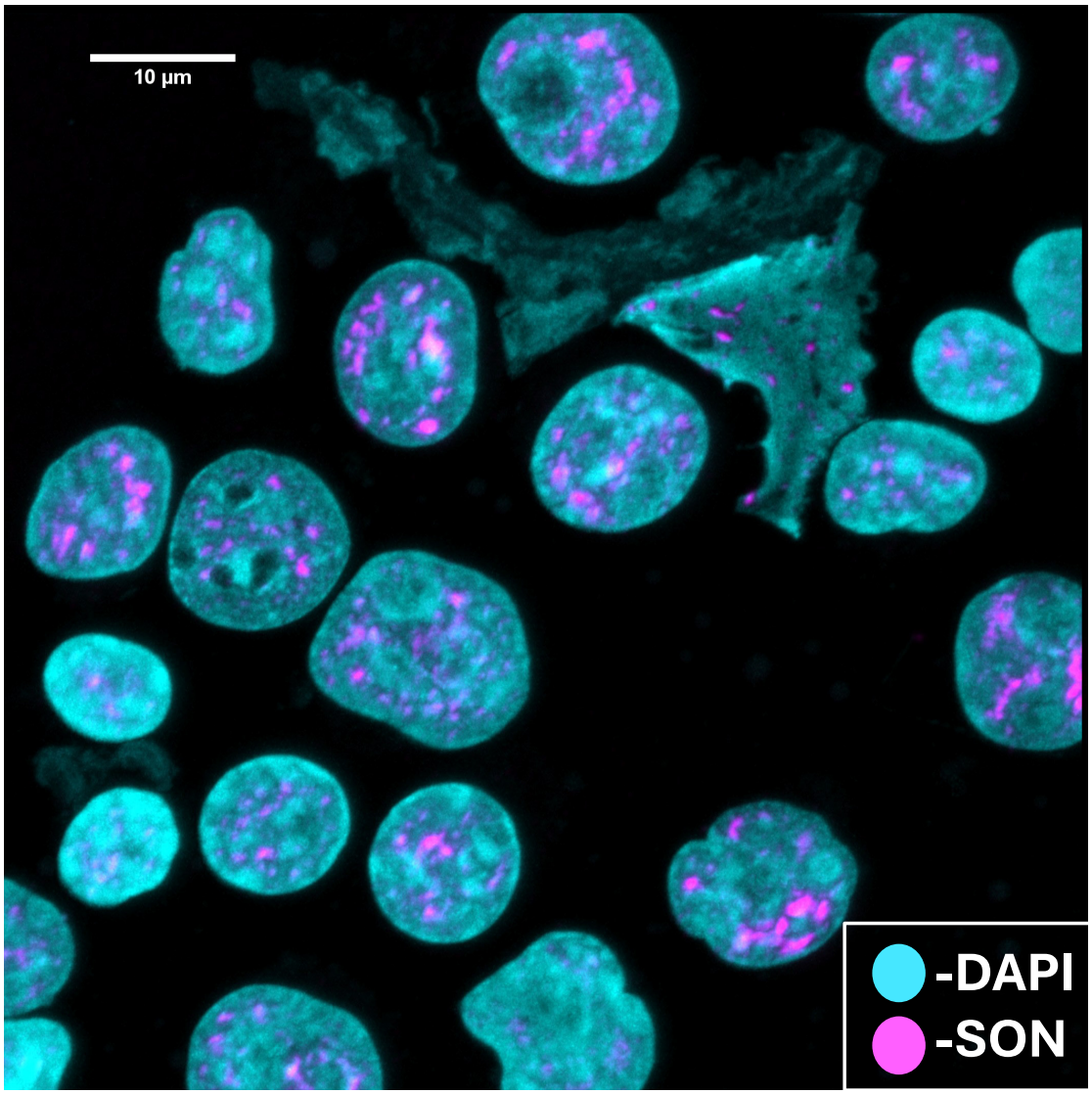

Supplementary Figure 25

Representative images of SON and DAPI staining of human $CD4^+$ T cells from donor A. at day 3 of Th2 *in vitro* differentiation. Brightness and contrast were increased by 20%.

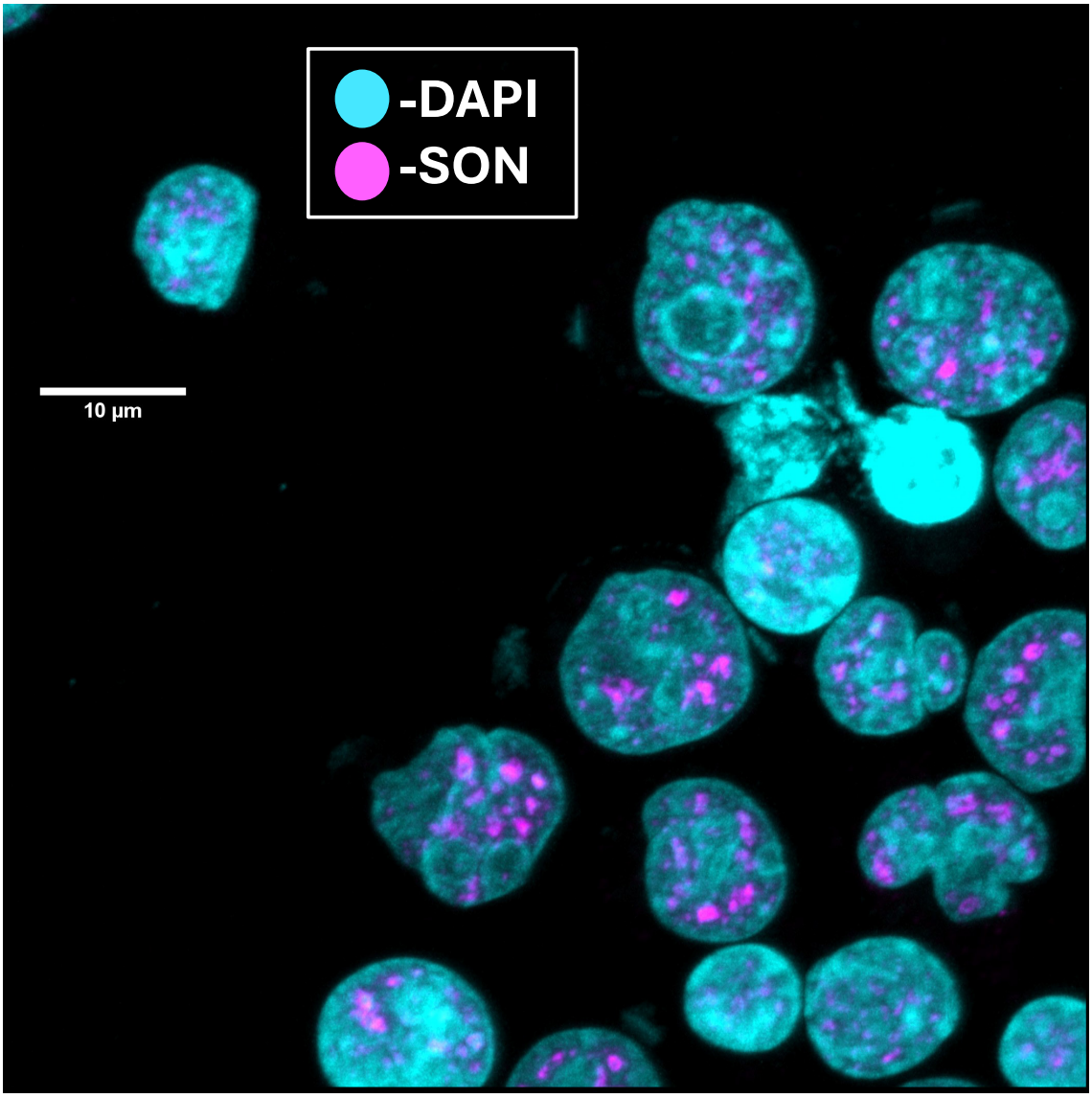

Supplementary Figure 26

Representative images of SON and DAPI staining of human $CD4^+$ T cells from donor C. at day 3 of Th2 *in vitro* differentiation. Brightness and contrast were increased by 20%.

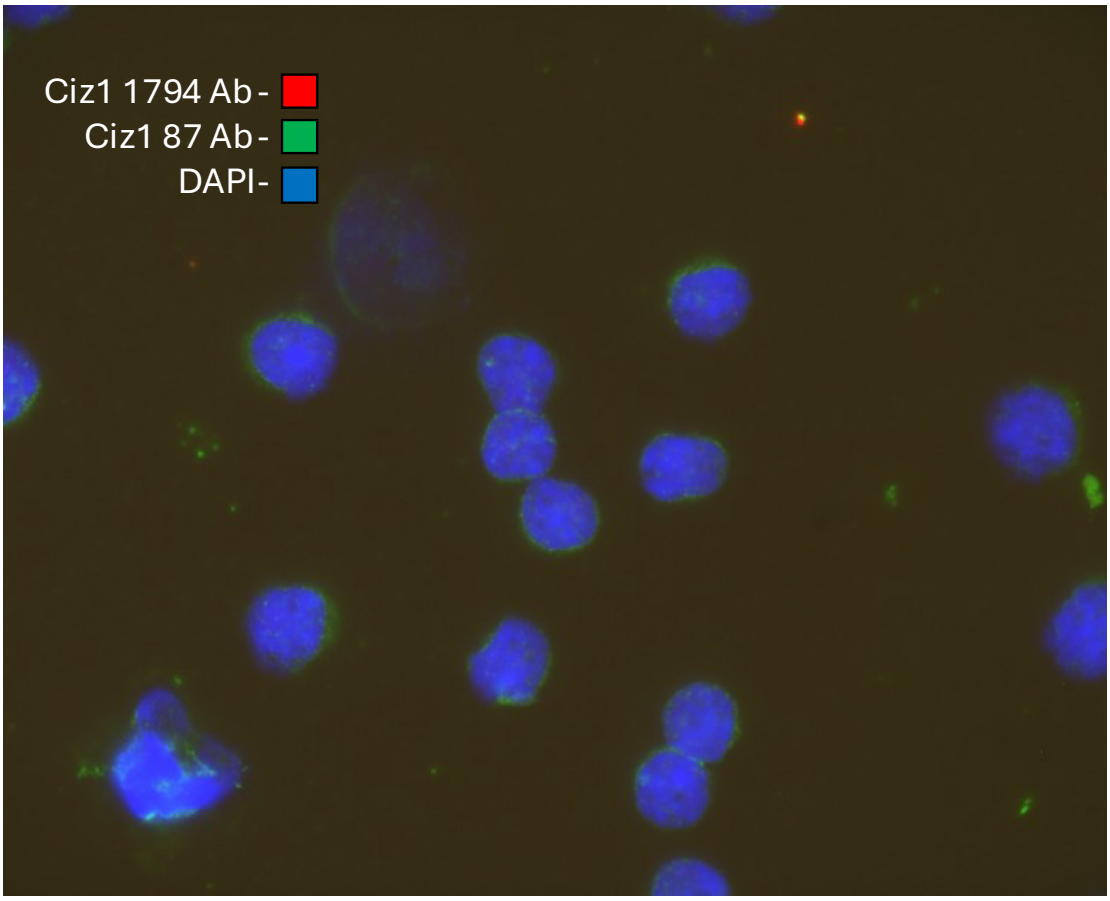

Supplementary Figure 27

Representative 43x images with DAPI and CIZ1 (both N terminal 87 and C terminal 1794 antibodies) staining of naïve *WT* female $CD4^+$ T cells. Brightness and contrast were increased by 20%.

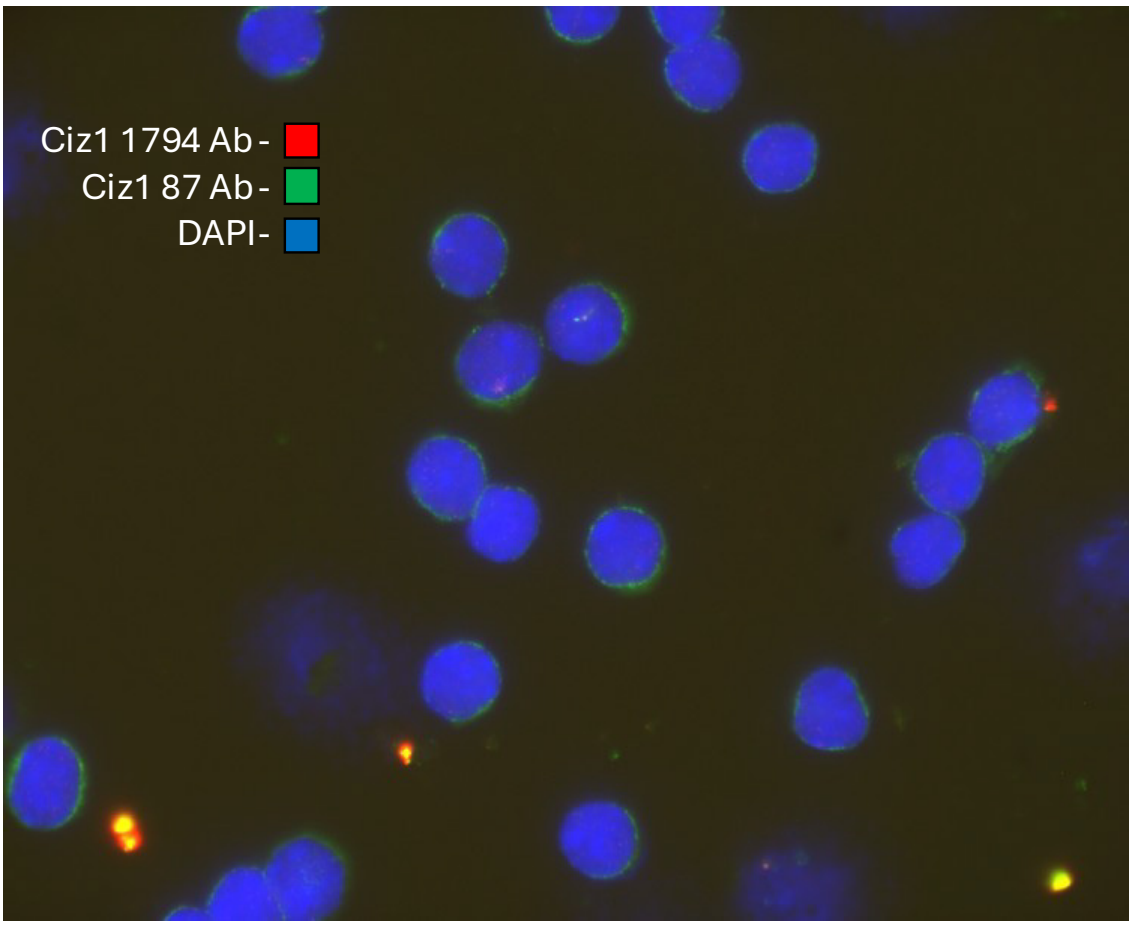

Supplementary Figure 28

Representative 43x images with DAPI and CIZ1 (both N terminal 87 and C terminal 1794 antibodies) staining of *WT* female $CD4^+$ T cells 6 hours post-activation. Brightness and contrast were increased by 20%.

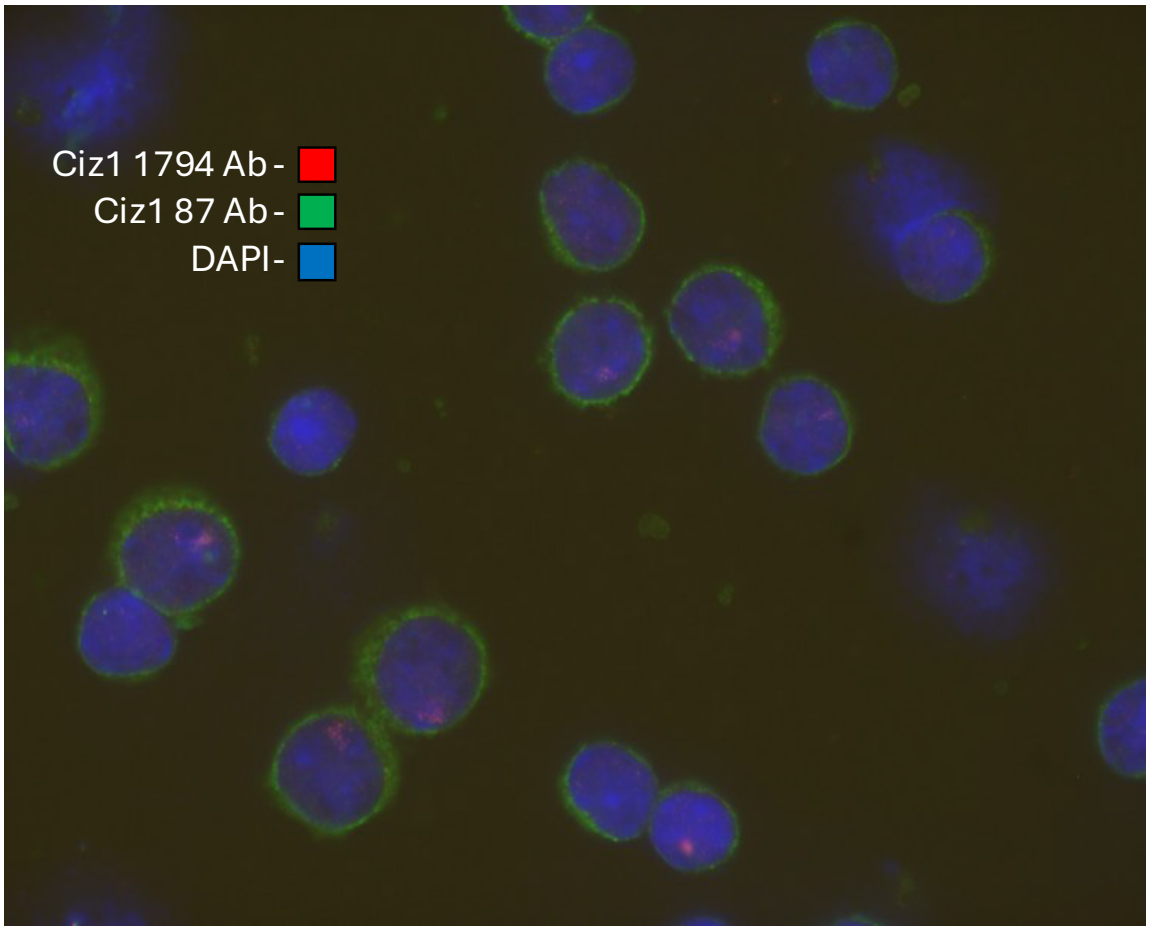

Supplementary Figure 29

Representative 43x images with DAPI and CIZ1 (both N terminal 87 and C terminal 1794 antibodies) staining of *WT* female $CD4^+$ T cells 24 hours post-activation. Brightness and contrast were increased by 20%.

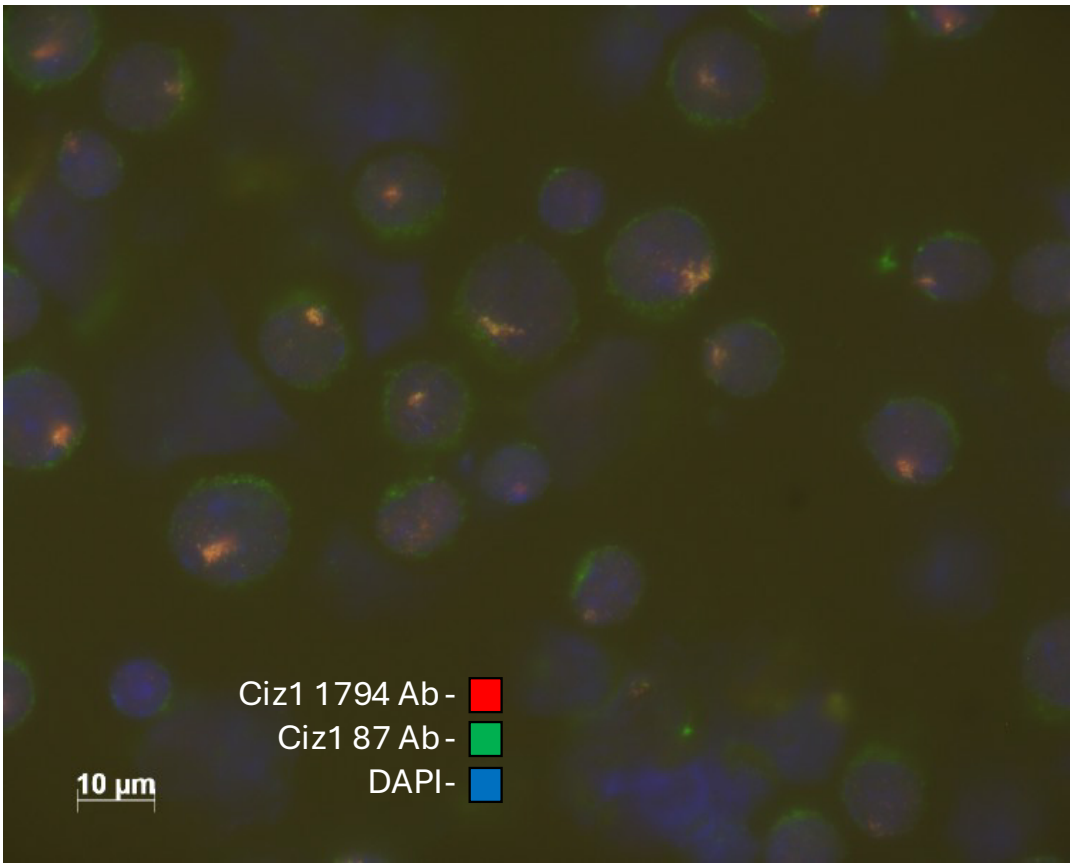

Supplementary Figure 30

Representative 43x images with DAPI and CIZ1 (both N terminal 87 and C terminal 1794 antibodies) staining of *WT* female $CD4^+$ T cells 48 hours post-activation. Brightness and contrast were increased by 20%.

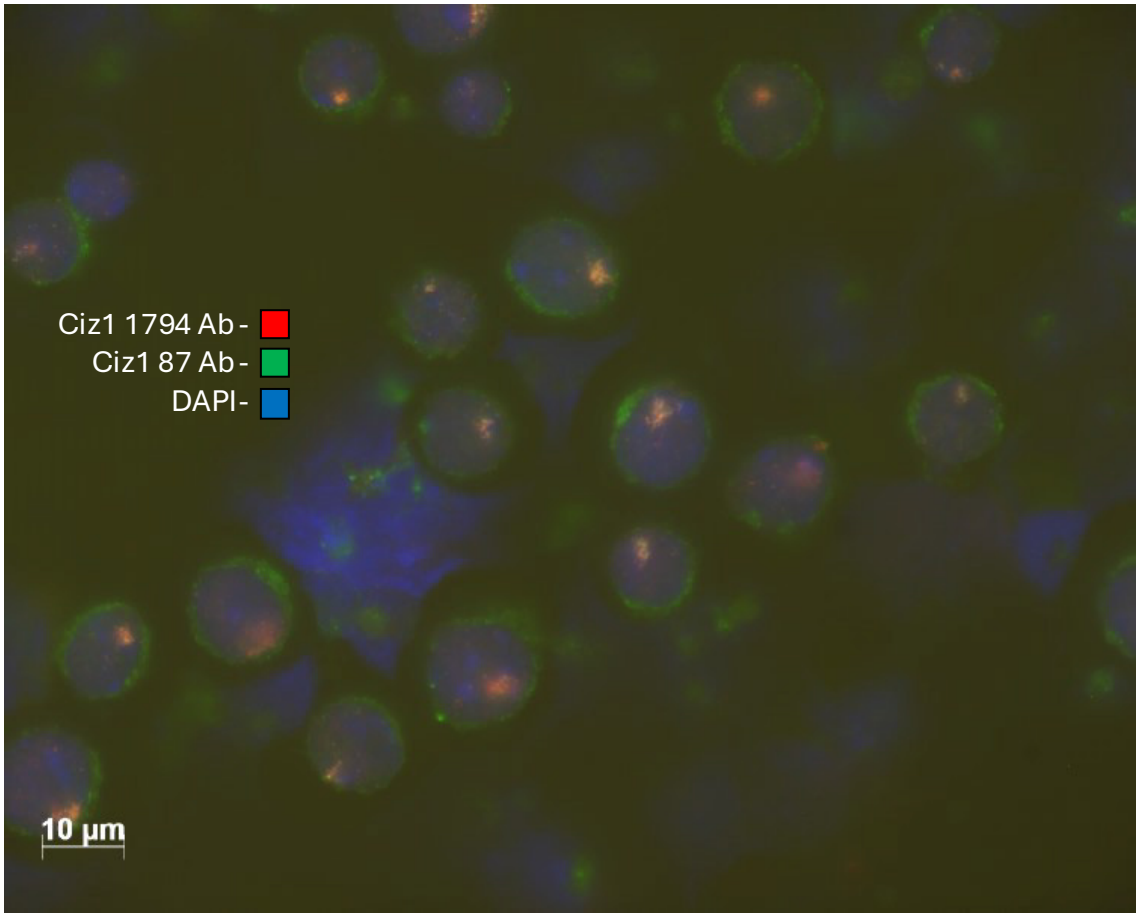

Supplementary Figure 31

Representative 43x images with DAPI and CIZ1 (both N terminal 87 and C terminal 1794 antibodies) staining of *WT* female $CD4^+$ T cells 48 hours post-activation. Brightness and contrast were increased by 20%.

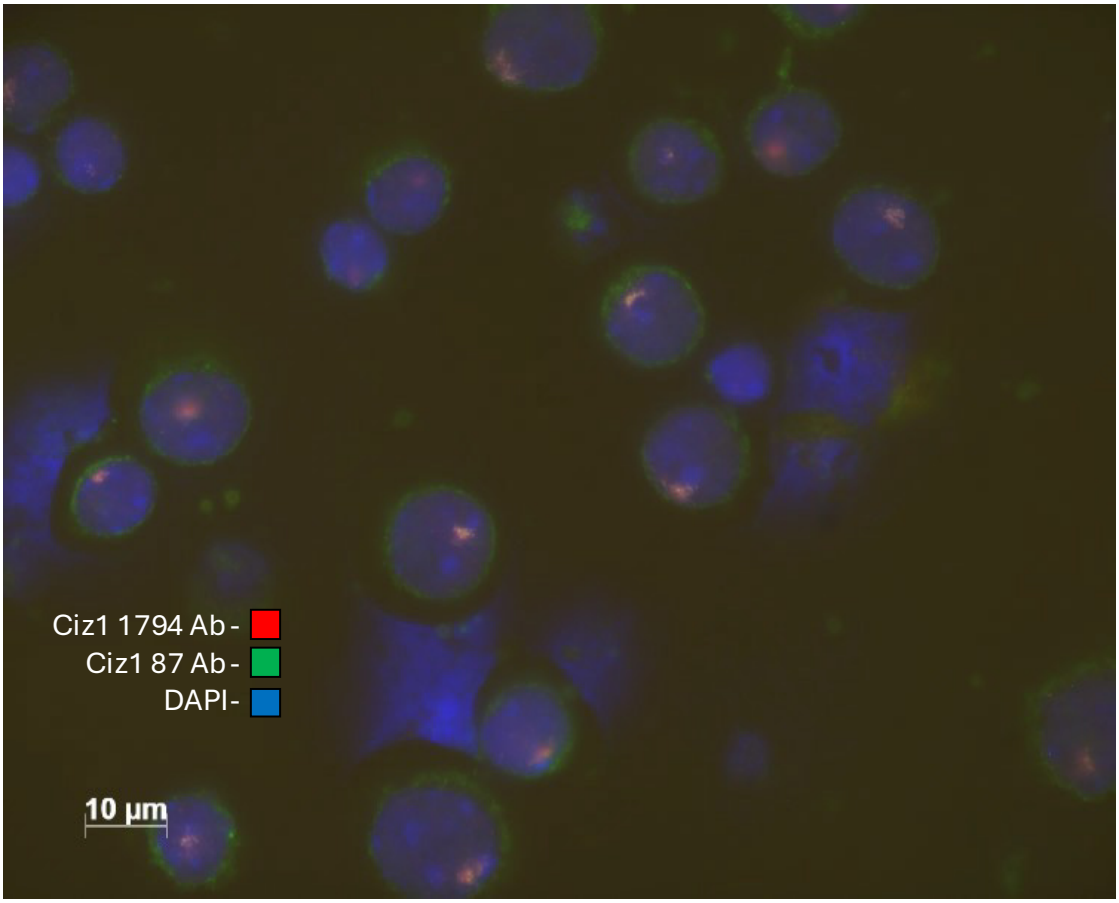

Supplementary Figure 32

Representative 43x images with DAPI and CIZ1 (both N terminal 87 and C terminal 1794 antibodies) staining of *Malat1*$^{-/-}$ female CD4^{+} T cells 48 hours post-activation. Brightness and contrast were increased by 20%.

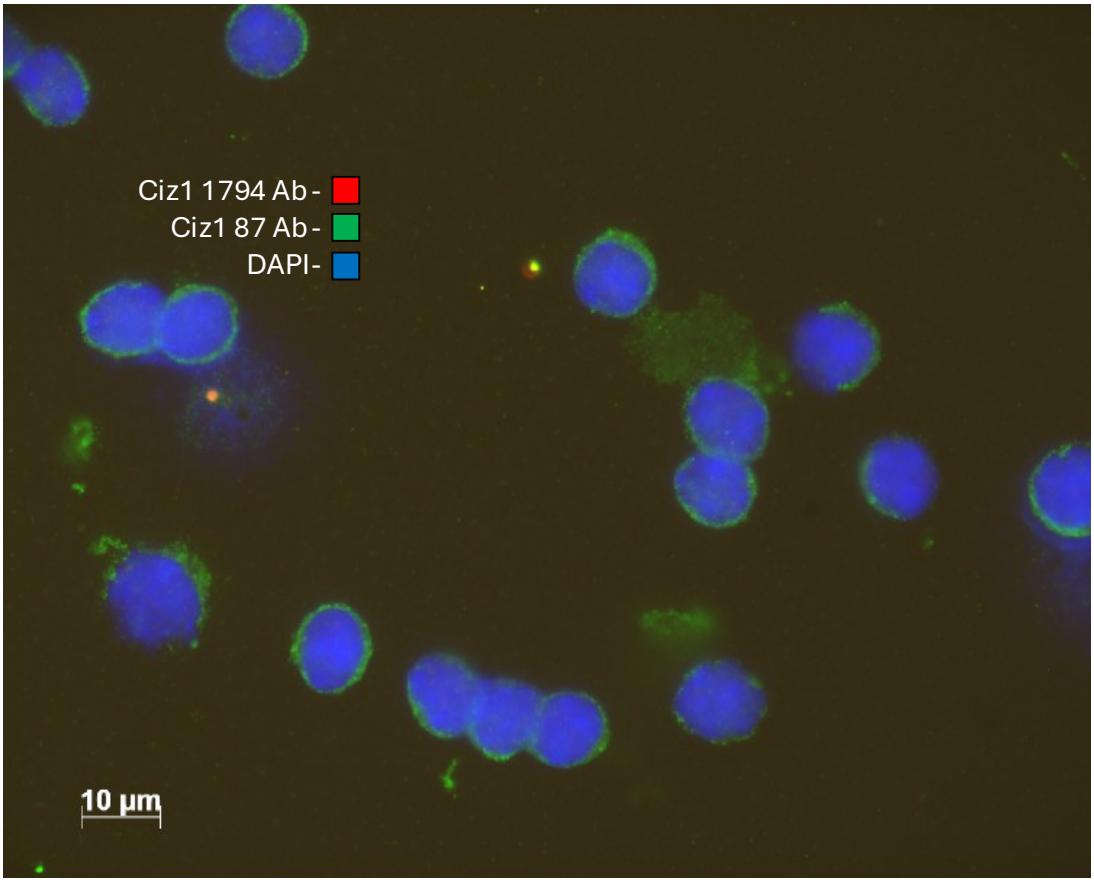

Supplementary Figure 33

Representative 43x images with DAPI and CIZ1 (both N terminal 87 and C terminal 1794 antibodies) staining of naïve *WT* female $CD4^+$ T cells. Brightness and contrast were increased by 20%.

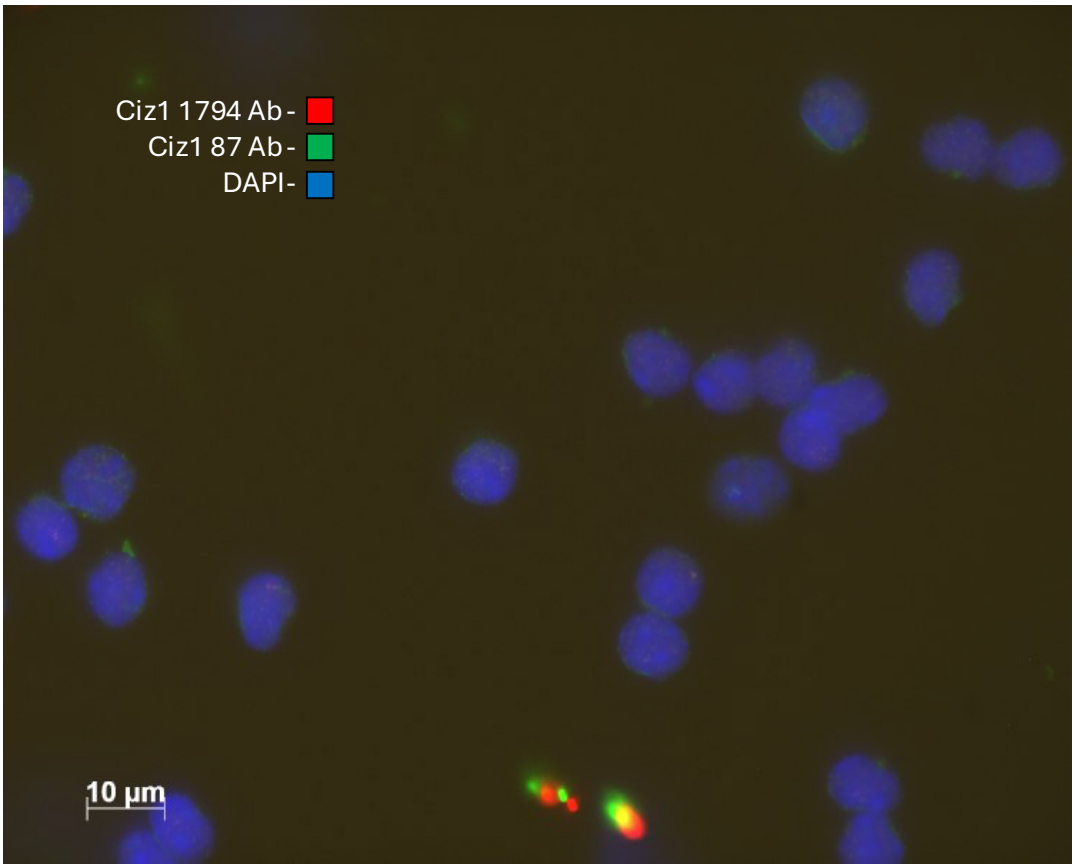

Supplementary Figure 34

Representative 43x images with DAPI and CIZ1 (both N terminal 87 and C terminal 1794 antibodies) staining of naïve *Malat1*$^{-/-}$ female CD4^{+} T cells. Brightness and contrast were increased by 20%.

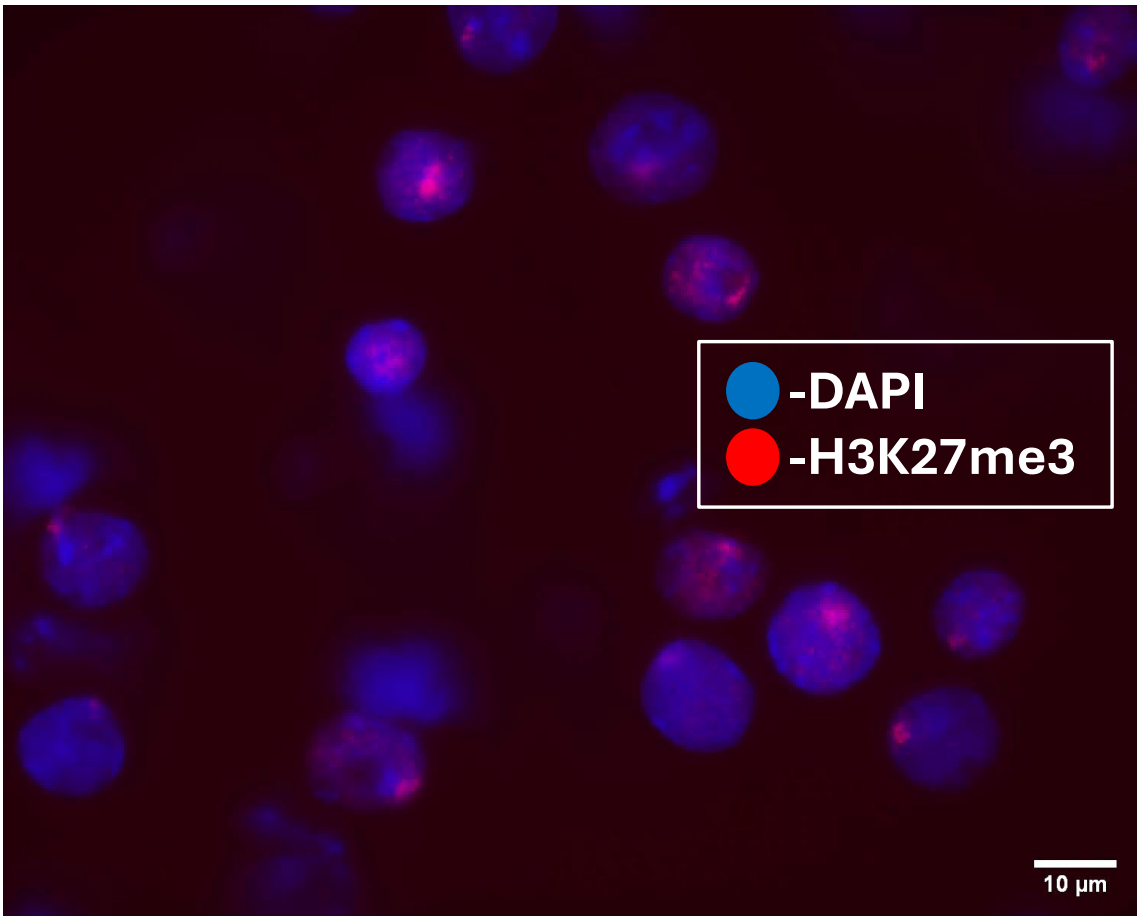

Supplementary Figure 35

Representative 40x images with DAPI and H3K27me3 staining of *in vitro* differentiated *WT* female $CD4^+$ T cells at 48 hours post-activation. Brightness and contrast were increased by 40%.

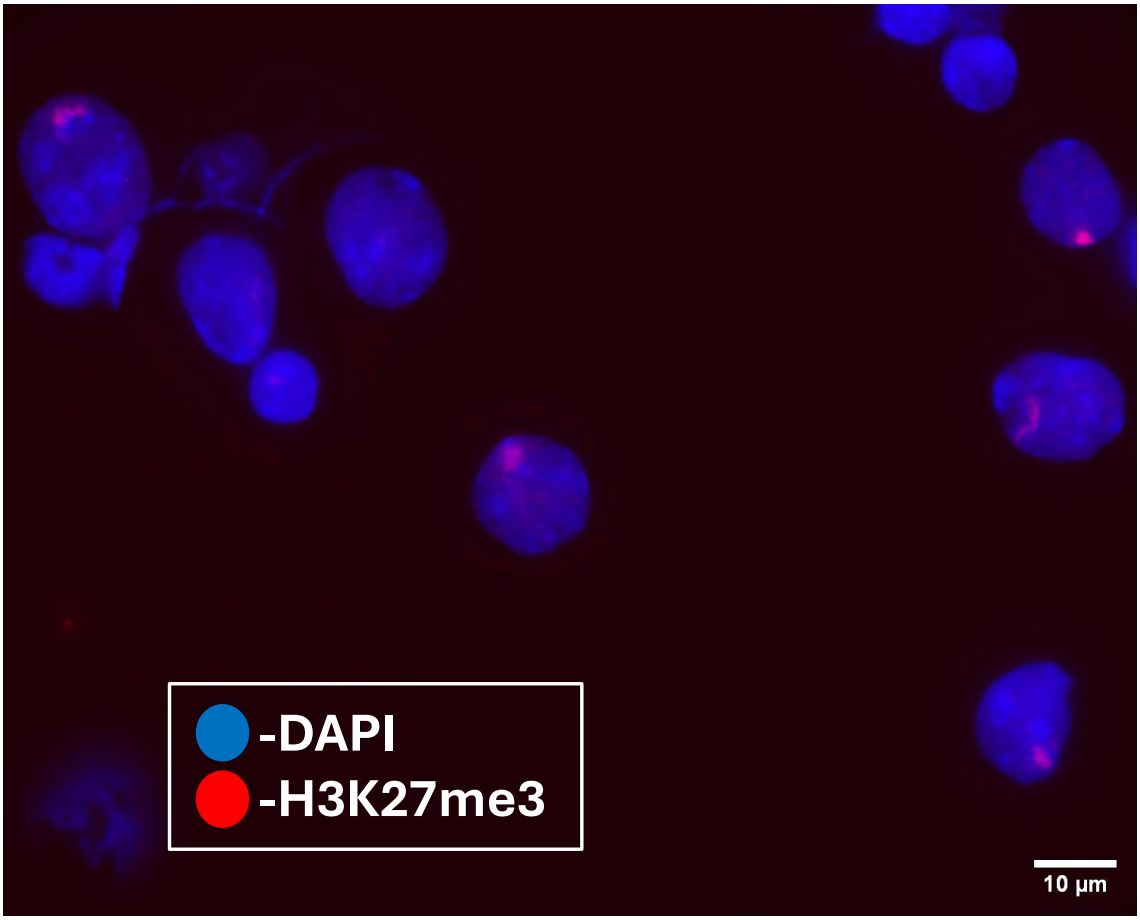

Supplementary Figure 36

Representative 40x images with DAPI and H3K27me3 staining of *in vitro* differentiated *Malat1*$^{-/-}$ female CD4^{+} T cells at 48 hours post-activation. Brightness and contrast were increased by 40%.